AFCRL-66-182

7133-3-T = RL-2148

7133-3-T

Copy ____

THE UNIVERSITY OF MICHIGAN

COLLEGE OF ENGINEERING

DEPARTMENT OF ELECTRICAL ENGINEERING

Radiation Laboratory

Studies in Radar Cross Sections L - Diffraction and Scattering by Regular Bodies IV: The Circular Cylinder

O. EINARSSON

R. E. KLEINMAN

P. LAURIN

P.L.E. USLENGHI

February, 1966

Scientific Report No. 3

Contract No. AF 19(628)-4328

Project 5635

Task 563502

Contract With: Air Force Cambridge Research Laboratories
Office of Aerospace Research
United States Air Force
Bedford, Massachusetts

Administered through:

OFFICE OF RESEARCH ADMINISTRATION • ANN ARBOR

THE UNIVERSITY OF MICHIGAN

7133-3-T

AFCRL-66-182

STUDIES IN RADAR CROSS SECTIONS L - DIFFRACTION AND SCATTERING BY REGULAR BODIES IV: THE CIRCULAR CYLINDER

by

O. Einarsson
R.E. Kleinman
P. Laurin
P.L.E. Uslenghi

Scientific Report No. 3

Contract AF 19(628)-4328
Project 5635
Task 563502

February 1966

Prepared for

AIR FORCE CAMBRIDGE RESEARCH LABORATORIES
OFFICE OF AEROSPACE RESEARCH
UNITED STATES AIR FORCE
BEDFORD, MASSACHUSETTS

Unclassified

Security Classification

DOCUMENT CONTROL DATA - R&D

(Security classification of title, body of abstract and indexing annotation must be entered when the overall report is classified)

1. ORIGINATING ACTIVITY *(Corporate author)*
The University of Michigan
Department of Electrical Engineering
The Radiation Laboratory

2a. REPORT SECURITY CLASSIFICATION
Unclassified

2b GROUP

3. REPORT TITLE
Studies in Radar Cross Sections L - Diffraction and Scattering by Regular Bodies IV: The Circular Cylinder

4. DESCRIPTIVE NOTES *(Type of report and inclusive dates)*
Scientific Report No. 3

5. AUTHOR(S) *(Last name, first name, initial)*
Einarsson, Olov
Kleinman, Ralph E.
Laurin, Pushpamala
Uslenghi, Piergiorgio L.E.

6. REPORT DATE	7a. TOTAL NO. OF PAGES	7b. NO. OF REFS
February 1966	323	168

8a. CONTRACT OR GRANT NO.
AF 19(628)-4328

b. PROJECT NO
5635

c.
Task 563502

d.

9a. ORIGINATOR'S REPORT NUMBER(S)
7133-3-T

9b. OTHER REPORT NO(S) *(Any other numbers that may be assigned this report)*
AFCRL-66-182

10. AVAILABILITY/LIMITATION NOTICES
Distribution of this document is unlimited.

11. SUPPLEMENTARY NOTES

12. SPONSORING MILITARY ACTIVITY
Air Force Cambridge Research Laboratories
Office of Aerospace Research, USAF
Bedford, Massachusetts

13. ABSTRACT

A survey of electromagnetic and acoustical scattering by a circular cylinder is performed. Theoretical methods and results for infinite and semi-infinite cylinders, and experimental ones for finite cylinders, are included. Only time-harmonic fields are considered, and dielectric cylinders are not taken into account.

DD FORM 1 JAN 64 1473

Unclassified

Security Classification

14. KEY WORDS	LINK A		LINK B		LINK C	
	ROLE	WT	ROLE	WT	ROLE	WT
Electromagnetic Acoustical Scattering Circular cylinders Theoretical Experimental						

INSTRUCTIONS

1. ORIGINATING ACTIVITY: Enter the name and address of the contractor, subcontractor, grantee, Department of Defense activity or other organization *(corporate author)* issuing the report.

2*a*. REPORT SECURITY CLASSIFICATION: Enter the overall security classification of the report. Indicate whether "Restricted Data" is included. Marking is to be in accordance with appropriate security regulations.

2*b*. GROUP: Automatic downgrading is specified in DoD Directive 5200.10 and Armed Forces Industrial Manual. Enter the group number. Also, when applicable, show that optional markings have been used for Group 3 and Group 4 as authorized.

3. REPORT TITLE: Enter the complete report title in all capital letters. Titles in all cases should be unclassified. If a meaningful title cannot be selected without classification, show title classification in all capitals in parenthesis immediately following the title.

4. DESCRIPTIVE NOTES: If appropriate, enter the type of report, e.g., interim, progress, summary, annual, or final. Give the inclusive dates when a specific reporting period is covered.

5. AUTHOR(S): Enter the name(s) of author(s) as shown on or in the report. Enter last name, first name, middle initial. If military, show rank and branch of service. The name of the principal author is an absolute minimum requirement.

6. REPORT DATE: Enter the date of the report as day, month, year; or month, year. If more than one date appears on the report, use date of publication.

7*a*. TOTAL NUMBER OF PAGES: The total page count should follow normal pagination procedures, i.e., enter the number of pages containing information.

7*b*. NUMBER OF REFERENCES: Enter the total number of references cited in the report.

8*a*. CONTRACT OR GRANT NUMBER: If appropriate, enter the applicable number of the contract or grant under which the report was written.

8*b*, 8*c*, & 8*d*. PROJECT NUMBER: Enter the appropriate military department identification, such as project number, subproject number, system numbers, task number, etc.

9*a*. ORIGINATOR'S REPORT NUMBER(S): Enter the official report number by which the document will be identified and controlled by the originating activity. This number must be unique to this report.

9*b*. OTHER REPORT NUMBER(S): If the report has been assigned any other report numbers *(either by the originator or by the sponsor)*, also enter this number(s).

10. AVAILABILITY/LIMITATION NOTICES: Enter any limitations on further dissemination of the report, other than those imposed by security classification, using standard statements such as:

(1) "Qualified requesters may obtain copies of this report from DDC."

(2) "Foreign announcement and dissemination of this report by DDC is not authorized."

(3) "U. S. Government agencies may obtain copies of this report directly from DDC. Other qualified DDC users shall request through _____."

(4) "U. S. military agencies may obtain copies of this report directly from DDC. Other qualified users shall request through _____."

(5) "All distribution of this report is controlled. Qualified DDC users shall request through _____."

If the report has been furnished to the Office of Technical Services, Department of Commerce, for sale to the public, indicate this fact and enter the price, if known.

11. SUPPLEMENTARY NOTES: Use for additional explanatory notes.

12. SPONSORING MILITARY ACTIVITY: Enter the name of the departmental project office or laboratory sponsoring *(paying for)* the research and development. Include address.

13. ABSTRACT: Enter an abstract giving a brief and factual summary of the document indicative of the report, even though it may also appear elsewhere in the body of the technical report. If additional space is required, a continuation sheet shall be attached.

It is highly desirable that the abstract of classified reports be unclassified. Each paragraph of the abstract shall end with an indication of the military security classification of the information in the paragraph, represented as *(TS)*, *(S)*, *(C)*, or *(U)*.

There is no limitation on the length of the abstract. However, the suggested length is from 150 to 225 words.

14. KEY WORDS: Key words are technically meaningful terms or short phrases that characterize a report and may be used as index entries for cataloging the report. Key words must be selected so that no security classification is required. Identifiers, such as equipment model designation, trade name, military project code name, geographic location, may be used as key words but will be followed by an indication of technical context. The assignment of links, rules, and weights is optional.

ABSTRACT

A survey of electromagnetic and acoustical scattering by a circular cylinder is performed. Theoretical methods and results for infinite and semi-infinite cylinders, and experimental ones for finite cylinders, are included. Only time-harmonic fields are considered, and dielectric cylinders are not taken into account.

MISSING
PAGE

TABLE OF CONTENTS

Table of Contents (cont'd)

I
INTRODUCTION

1.1 Preliminary Remarks

This is the fourth in a series of reports on electromagnetic and acoustical scattering by selected bodies of simple shape. The previous reports dealt with the sphere (Goodrich et al, 1961), the cone (Kleinman and Senior, 1963) and the prolate spheroid (Sleator, 1964). The choice of the circular cylinder was dictated by various considerations. Firstly, the large number of theoretical and experimental results which have been published on this shape during the last one hundred years is in itself sufficient to justify the writing of the present report. Secondly, the circular cylinder has often been used for the development and testing of approximation methods of general applicability, in both the low and high frequency limits. Finally, it is a shape of considerable interest in practical applications such as scattering by the central part of a missile and radiation and scattering by cylindrical antennas.

In this report, the emphasis is placed on scattering rather than on radiation problems, i.e. the source is usually located off the surface of the cylinder. Radiating slots and gaps in the cylinder surface are not considered, and the interested reader should consult the various excellent monographs on this subject, such as the books by King (1956) and by Wait (1959). Although the case of an electric dipole on the surface of the cylinder is examined, the problem of the equivalence of dipoles and slots is not discussed.

Only the case of time harmonic fields is considered explicitly. This choice is justified by the fact that an arbitrary field can always be decomposed into the sum of monochromatic waves by Fourier analysis, and that most of the literature does indeed consider time harmonic fields only. However, there exist a few works on diffraction of pulses by circular cylinders, for example Friedlander's (1954) and Barakat's (1965) in which a Laplace transform method is adopted. The propagation of

acoustic pulses from a circular cylinder has been investigated by Barakat (1961). Useful information is also contained in a book by Friedlander (1958).

Chapters II, III and IV are devoted to exact solutions, low and high frequency approximations for a cylinder of infinite length. Special emphasis has been given the equivalence between acoustical and electromagnetic boundary value problems. Wherever possible, the case of an impedance boundary condition has been considered, and the results for soft, hard and perfectly conducting cylinders have been derived as limiting cases. In Chapter V, the scattering by a semi-infinite circular cylinder is investigated. Chapter VI is devoted to a brief survey of measurement techniques and experimental results. It seemed reasonable to include such measurements on (necessarily) finite cylinders, even though a theoretical chapter on finite cylinders does not appear in this report. The principal reason for the exclusion of such a chapter is that a satisfactory theory for a cylinder of finite length does not yet exist; most works on this subject deal with the two limiting cases of a thin long cylinder (a wire) and of a short fat cylinder (a disc), and a comprehensive treatment of either one of these two cases would require a separate book. A brief outline of the main existing works on scattering by a finite cylinder is given in section 1.3.

A considerable effort has been made to take into account all relevant contributions to the subject of this report and to give due credit to bibliographical sources. However, a complete bibliographical listing has not been attempted. The authors are indebted to their colleagues of the Radiation Laboratory for criticism and comment. This report has been typewritten by Miss C. Rader, and the figures have been drawn by Mr. A. Antones.

1.2 Brief Historical Survey

Some of the following historical remarks are taken from a recent paper by Logan (1965). They illustrate the principal studies on scattering by circular cylinders until the beginning of World War II. The numerous contributions which have

appeared in the technical literature during the last twenty-five years are adequately described in the following chapters of this report, and therefore will not be mentioned in this section.

The first important study on the scattering of waves by a circular cylinder is contained in section 343 of Rayleigh's Theory of Sound (Strutt, 1945), which was completed in the Spring of 1877. In that section, Rayleigh showed how to separate the wave equation in circular cylindrical coordinates, and carried out the analysis explicitly for the case of a plane sound wave normally incident on a cylinder of gas of given density and compressibility and with radius small compared to the wavelength. Four years later, Rayleigh published a paper (Strutt, 1881) in which, on the basis of Maxwell's theory of electromagnetism, he solved exactly the problem of the scattering of electromagnetic waves by a dielectric cylinder; he reconsidered this problem almost thirty years later (Strutt, 1918). Rayleigh's solution is valid for normal incidence (the case of oblique incidence has been investigated only recently by Wait (1955)), and it is known that for this case the acoustical and electromagnetic problems are essentially equivalent, as Rayleigh showed in 1897. A few years earlier, the first study of the scattering of plane waves by a perfectly conducting infinite circular cylinder had been published by J.J. Thomson in his Recent Researches in Electricity and Magnetism (1893).

In 1905 and 1906, Seitz published two papers on diffraction by a metal cylinder, which contain various numerical results. In those same years, Debye (1908) succeeded in proving that the exact solution for the circular cylinder leads to results consistent with the predictions of geometrical optics. Also, Nicholson (1912) published an interesting work on the pressure exerted on a perfectly conducting cylinder by an incident electromagnetic wave, and Bromwich (1919) discussed the separability of Maxwell's equations in orthogonal curvilinear coordinates, of which the circular cylindrical coordinates are a special case. Bromwich's paper is especially interesting because he does not restrict himself to harmonic time dependence.

It was not until the advent of the radar that a new series of studies on scattering by cylinders began. In 1941, the well-known book by Stratton appeared, and in that same year a theoretical report by Moullin and Reynolds was distributed, in which the case of plane waves normally incident on infinite circular cylinders was considered, and the numerical data obtained from the exact solution were displayed in a number of graphs.

1.3 Scattering from Finite Cylinders

The purpose of this section is to provide the reader with some bibliographical references on scattering and radiation by finite cylinders. Although these two problems are closely related, the latter has received much more attention in the literature owing to its importance in antenna applications. Hallén (1938) was the first to obtain an approximate solution for a thin cylindrical antenna, i.e. for values of the cylinder radius much smaller than the wavelength. He derived an integral equation for the unknown current distribution on the surface of the cylinder, and solved it approximately by an iteration technique.

Since Hallén's attempt, several authors have introduced modifications in the integral equation: Van Vleck, Bloch and Hammermesh (1947), King and Middleton (1946), Gray (1944), Duncan and Hinchey (1960), Kapitsa, Fock and Wainshtein (1960), among others. Van Vleck, Bloch and Hammermesh (1947) presented two independent methods for deriving approximations to radar back scattering from thin cylinders. In solving for the current induced on the thin cylinder, they assumed that this current consists of four trigonometric functions, two of which correspond to forced terms, that is, to the voltage impressed by the incident wave, whereas the remaining two were attributed to resonant parts, i.e. to the current present on the cylinder at the resonant frequencies. In the first of their two methods, the end-condition is imposed for choosing two of the parameters in the expression for the current, viz., the current vanishes at the ends of the cylinder. The other two parameters are determined by imposing the conservation of energy. In the second

method, two of the parameters are found by equating the terms in Hallén's equations corresponding to the voltage impressed by the incident wave and the other two are determined using the end-condition with an iterative procedure. The reader is referred to the original paper for details and for a discussion of the advantages of both methods.

Storer (1951) and Tai (1951) have independently applied variational methods for calculating the scattering cross section. Tai expressed the back scattering cross section as a function of the unknown current on the cylinder. This function is transformed with the help of Hallén's integral equation into one which is stationary in the unknown current function. By substituting various trial functions for the current into the stationary functional and then determining the free parameters by the Rayleigh-Ritz method, the back scattering cross section is estimated. The trial function used by Tai is a linear combination of the currents on the cylinder at the first and second resonant frequencies, and it had been previously adopted by Van Vleck et al (1947).

Williams (1956) has used an extension of the Wiener-Hopf technique for calculating the scattering of a plane sound wave by a finite cylinder. Williams' method is parallel to the method of Jones (1952); it involves the Laplace transformation of the differential equation before applying the boundary conditions and the reduction of the problem to the solution of two complex integral equations. Although these equations cannot be solved exactly, an approximate solution has been obtained under the assumption $k\ell \gg 1$ (ℓ = length of the cylinder). Williams has also obtained explicit expressions for the end-condition by taking into consideration the resonance of the system.

Wilcox (1955) has conducted a detailed study of scattering of electromagnetic radiation by finite cylindrical shells. He has used the integral equation method and has obtained approximations to the scattering cross sections in terms of the tangential electric field on the axial extension of the cylinder surface in a form which

is stationary with respect to variations about the correct values. The tangential component of the electric field due to scattering by a semi-infinite cylinder is used as a trial function in the stationary expression. Wilcox has also derived variational expressions for the far field in the thin cylinder approximation.

A high frequency asymptotic solution of scattering by a solid conducting finite cylinder is given by Kieburtz (1962). However, his results are incorrect except for the first order term, because they are based on an erroneous assumption concerning the locations of the singularities of the Fourier transforms of the field components*.

Numerical methods are available for calculating the current distribution from integral equations. Govorun (1962) has obtained numerical results for the symmetric part of the surface current on a solid cylinder excited by a plane wave at broadside incidence. The length to radius ratio varies from 6 to 65536 and the length from $\lambda/8$ to $7\lambda/4$. The paper also contains results for a cylindrical antenna with a circumferential gap of finite width. His solution converges quite rapidly for thin cylinders. Williams (1956) has included a few numerical results in his previously-mentioned paper.

Much of the work done in the area of finite cylinders has been devoted to thin cylinders in consideration of the practical applications to antennas. King (1956) has written a book which gives an extensive treatment of this subject.

*Kieburtz reports in a private communication that the method for construction of an asymptotic series expansion used in his recent paper (Kieburtz, 1965) can be applied to the cylinder problem.

II
EXACT SOLUTIONS FOR AN INFINITE CYLINDER

In this chapter, the boundary value problems of scattering of electromagnetic energy by an infinitely long circular cylinder are formulated and solved exactly. The relationship between vector and scalar problems is examined, and various types of sources are considered: plane waves, cylindrical waves, dipoles, and evanescent waves.

It is assumed that the cylinder is made of a perfectly conducting material. In some instances, however, the more general case is considered in which an impedance boundary condition may be applied at the surface of the cylinder.

The rationalized MKS system of units is employed throughout.*

2.1 Precise Formulation

This section deals with the problem of finding the electromagnetic field external to an infinitely long (perfectly conducting) circular cylinder embedded in a uniform, homogeneous and isotropic medium of electric permittivity ϵ, magnetic permeability μ and zero conductivity, which medium may be taken as free space.

The homogeneous Maxwell's equations

$$\nabla \wedge \underline{H} = \epsilon \frac{\partial \underline{E}}{\partial t} , \tag{2.1}$$

$$\nabla \wedge \underline{E} = -\mu \frac{\partial \underline{H}}{\partial t} , \tag{2.2}$$

govern the behavior of the electric field $\underline{E}$ and of the magnetic field $\underline{H}$ at all ordinary points in space, but do not describe the fields at the source points. By taking

* The following vector notation is used: vectors of arbitrary magnitude will be underlined, e.g. $\underline{E}$; unit vectors will be denoted by carets, e.g. $\hat{\rho}$; scalar products indicated by dots, e.g. $\hat{\rho} \cdot \underline{E}$; and vector products by wedges, e.g. $\nabla \wedge \underline{E}$.

the divergence of both sides of equations (2.1) and (2.2), and with the convention that at some time the fields may become solenoidal, which is certainly the case if, for example, $\underline{E}_{t=-\infty} = \underline{H}_{t=-\infty} = 0$, one finds the auxiliary equations

$$\nabla \cdot \underline{H} = \nabla \cdot \underline{E} = 0. \tag{2.3}$$

Equations (2.1), (2.2) and (2.3) are satisfied by the incident or primary fields $\underline{E}^i$ and $\underline{H}^i$, by the total (incident plus scattered) or diffracted field $\underline{E}$ and $\underline{H}$, and therefore also by the secondary or scattered fields $\underline{E}^s$ and $\underline{H}^s$, which represent the disturbance introduced in the primary fields by the infinite cylinder.

The presence of the cylinder is accounted for by requiring that on its surface the total electric and magnetic fields satisfy the impedance boundary condition:

$$\underline{E} - (\underline{E} \cdot \hat{\rho})\hat{\rho} = Z\hat{\rho} \wedge \underline{H}, \quad , \tag{2.4}$$

where Z is the surface impedance and $\hat{\rho}$ a unit vector perpendicular to the surface of the cylinder and directed from the surface into the surrounding medium. The case of perfect conductivity corresponds to $Z = 0$.

If the sources of the primary fields are specified, the surface impedance Z is given, and a radiation condition (which is necessary to ensure uniqueness) is assumed, then the boundary value problem is well set and may be formulated directly in terms of either the electric or the magnetic field. However, it is often advantageous to reformulate the problem in terms of auxiliary functions from which the field quantities may be derived through simple operations of differentiation.

Such auxiliary functions, or potentials, may be chosen in a variety of ways (see, for example, Stratton, 1941). Following the procedure adopted by Kleinman and Senior (1963), we define $\underline{E}$ and $\underline{H}$ in terms of a vector potential $\underline{A}$ through the relations:

$$\underline{E} = \nabla \wedge \nabla \wedge \underline{A} \ , \tag{2.5}$$

$$\underline{H} = \epsilon \frac{\partial}{\partial t} \nabla \wedge \underline{A} \ . \tag{2.6}$$

Maxwell's equations are satisfied by (2.5) and (2.6), provided that

$$\nabla \wedge \nabla \wedge \nabla \wedge \underline{A} + \epsilon\mu \nabla \wedge \frac{\partial^2 \underline{A}}{\partial t^2} = 0 \ , \tag{2.7}$$

that is,

$$\left(\nabla \wedge \nabla \wedge + \epsilon\mu \frac{\partial^2}{\partial t^2} \right) \underline{A} = \nabla f \ , \tag{2.8}$$

where f is an arbitrary scalar function of position and time. Formula (2.8) may be rewritten as

$$\left(\nabla^2 - \epsilon\mu \frac{\partial^2}{\partial t^2} \right) \underline{A} = \nabla f \ , \tag{2.9}$$

where ∇^2 operates on the Cartesian orthogonal components of $\underline{A}$. Any electromagnetic field can be derived from such a vector potential; in particular, there exists a potential which gives the field exterior to a conducting cylinder.

Instead of obtaining the fields $\underline{E}$ and $\underline{H}$ from (2.5) and (2.6), we may use the relations:

$$\underline{E} = -\mu \frac{\partial}{\partial t} \nabla \wedge \underline{A} \ , \tag{2.10}$$

$$\underline{H} = \nabla \wedge \nabla \wedge \underline{A} \ , \tag{2.11}$$

where $\underline{A}$ is still a solution of (2.9). It is then possible to express any electromagnetic field in the form:

$$\underline{E} = \nabla\wedge\nabla\wedge\underline{A}_1 - \mu \frac{\partial}{\partial t} \nabla\wedge\underline{A}_2 ,$$
$$\underline{H} = \nabla\wedge\nabla\wedge\underline{A}_2 + \epsilon \frac{\partial}{\partial t} \nabla\wedge\underline{A}_1 , \tag{2.12}$$

with $\underline{A}_1$ and $\underline{A}_2$ solutions of (2.9). Expressions (2.12) are obviously redundant, in the sense that a great freedom of choice is left for $\underline{A}_1$ and $\underline{A}_2$. Such freedom can be used to construct the vector potentials from scalar potentials. Let us set

$$\underset{2}{\underline{A}_1} = \psi_1 \underline{c} , \tag{2.13}$$

where $\underline{c}$ is a constant vector. It was proved by Whittaker (see, for example, Nisbet, 1955) that any electromagnetic field can be derived from (2.12) with the vector potentials restricted to the form (2.13), provided that the scalar functions ψ_1 and ψ_2 are two independent solutions of the wave equation

$$\left(\nabla^2 - \epsilon\mu \frac{\partial^2}{\partial t^2}\right)\psi = 0 . \tag{2.14}$$

The potentials $\underline{A}_1$ and $\underline{A}_2$ so determined are usually called electric and magnetic Hertz vectors, and denoted by $\underline{\Pi}_e$ and $\underline{\Pi}_m$ respectively.

The electric Hertz vector $\underline{\Pi}_e$ originates a field which is characterized by the absence of a component of $\underline{H}$ in the direction of $\underline{c}$ (transverse magnetic (TM) field), whereas the magnetic Hertz vector $\underline{\Pi}_m$ originates a field for which $\underline{E}\cdot\underline{c} = 0$ (transverse electric (TE) field).

Except when otherwise stated, in the following we shall consider the particular case of monochromatic radiation. The propagation constant k in the medium surrounding the cylinder is then given by

$$k = \omega\sqrt{\epsilon\mu} = \frac{2\pi}{\lambda} , \tag{2.15}$$

where ω is the angular frequency and λ the wavelength. In the preceding relations, the operator $\partial/\partial t$ is replaced by the multiplicative factor $-i\omega$. The time dependence factor $e^{-i\omega t}$ is suppressed throughout.

If rectangular Cartesian coordinates (x, y, z) and cylindrical polar coordinates (ρ, ϕ, z) connected by the relations $x = \rho\cos\phi$, $y = \rho\sin\phi$, $z = z$ are introduced (Fig. 2-1) so that $\underline{c} = \hat{i}_z$ is parallel to the axis z of the cylinder, then the field components defined by (2.12) are, in cylindrical coordinates:

$$E_\rho = \frac{\partial^2\psi_1}{\partial\rho\partial z} + \frac{i\omega\mu}{\rho}\frac{\partial\psi_2}{\partial\phi}\,, \qquad H_\rho = \frac{\partial^2\psi_2}{\partial\rho\partial z} - \frac{i\omega\epsilon}{\rho}\frac{\partial\psi_1}{\partial\phi}\,,$$

$$E_\phi = \frac{1}{\rho}\frac{\partial^2\psi_1}{\partial\phi\partial z} - i\omega\mu\frac{\partial\psi_2}{\partial\rho}\,, \qquad H_\phi = \frac{1}{\rho}\frac{\partial^2\psi_2}{\partial\phi\partial z} + i\omega\epsilon\frac{\partial\psi_1}{\partial\rho}\,, \qquad (2.16)$$

$$E_z = \frac{\partial^2\psi_1}{\partial z^2} + k^2\psi_1\,, \qquad H_z = \frac{\partial^2\psi_2}{\partial z^2} + k^2\psi_2\,.$$

Observe that if $\psi_1 \equiv 0$ then $E_z \equiv 0$ (TE case), while if $\psi_2 \equiv 0$ then $H_z \equiv 0$ (TM case).

The boundary conditions (2.4) at the surface $\rho = a$ of the cylinder now become:

$$E_z = ZH_\phi\,, \qquad E_\phi = -ZH_z\,, \qquad \text{at } \rho = a\,,$$

or also, by (2.16):

$$-i\omega\epsilon Z\frac{\partial\psi_1}{\partial\rho} + \frac{\partial^2\psi_1}{\partial z^2} + k^2\psi_1 = \frac{Z}{a}\frac{\partial^2\psi_2}{\partial\phi\partial z}\,,$$

$$-\frac{i\omega\mu}{Z}\frac{\partial\psi_2}{\partial\rho} + \frac{\partial^2\psi_2}{\partial z^2} + k^2\psi_2 = -\frac{1}{aZ}\frac{\partial^2\psi_1}{\partial\phi\partial z}\,, \qquad \text{at } \rho = a\,.$$

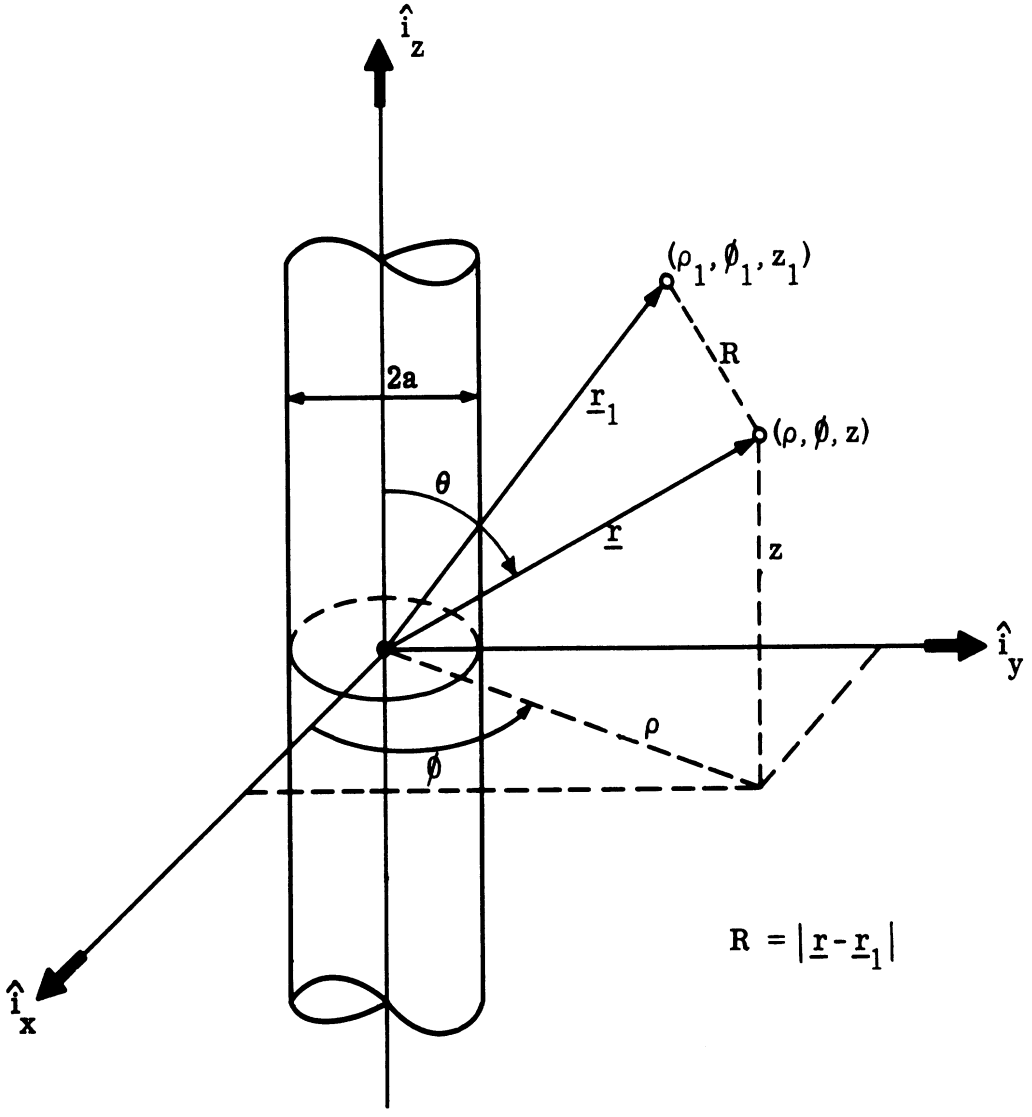

FIG. 2-1: GEOMETRY OF THE CIRCULAR CYLINDER

In order to satisfy these relations, in the case of perfect conductivity ($Z = 0$) it is sufficient to require that either

$$\psi_1 \equiv 0 \quad \text{and} \quad \left.\frac{\partial \psi_2}{\partial \rho}\right|_{\rho=a} = 0 ,$$

or

$$\psi_2 \equiv 0 , \quad \text{and} \quad \left.\psi_1\right|_{\rho=a} = 0 ,$$

whereas in the case in which $Z \neq 0$ both TE and TM fields must, in general, be present. However, if ψ_1 and ψ_2 are independent of z (two-dimensional problems, $\partial/\partial z \equiv 0$), then the boundary conditions can be satisfied by requiring that either

$$\psi_1 \equiv 0 , \quad \text{and} \quad \left(\frac{\partial}{\partial \rho} + ikZ\sqrt{\epsilon/\mu}\right)\psi_2\Big|_{\rho=a} = 0 ,$$

$$\psi_2 \equiv 0 , \quad \text{and} \quad \left(1 - \frac{i}{k} Z\sqrt{\epsilon/\mu}\,\frac{\partial}{\partial \rho}\right)\psi_1\Big|_{\rho=a} = 0 .$$

The scalar wave functions ψ_1 and ψ_2 can be represented by linear combinations of the elementary wave functions

$$\psi_{n,h} = \begin{matrix} J_n \\ H_n^{(1)} \end{matrix} \left(\rho\sqrt{k^2 - h^2}\right) e^{in\phi \pm ihz} , \qquad (2.17)$$

where n is a real integer ($n = 0, \pm 1, \pm 2$, etc), and h a parameter which is, in general, complex and whose values may cover a discrete set as well as a continuum spectrum. If h assumes only one value, as it happens, for example, when the primary source consists of a plane wave, then ψ_1 and ψ_2 are proportional to E_z and H_z, respectively.

In the case in which all primary sources are located within a finite distance from the origin $r = 0$ of the coordinate system, the fields $\underline{E}$ and $\underline{H}$ are required to satisfy the Silver-Müller radiation condition

$$\lim_{r\to\infty}\left\{\underline{r}\wedge(\nabla\wedge) + ikr\right\}\begin{matrix}\underline{E}\\ \underline{H}\end{matrix} = 0 \qquad \text{uniformly in } \hat{r}\ , \tag{2.18}$$

where $\underline{r} = r\hat{r} = x\hat{i}_x + y\hat{i}_y + z\hat{i}_z$, and the angle θ of Fig. 2-1 is restricted to the range $0<\delta\leqslant\theta\leqslant\pi-\delta$, with δ arbitrarily small and constant. From this condition and from Maxwell's equations it follows that the fields are of the form

$$\underline{f}(\hat{r})\,\frac{e^{ikr}}{r}\ , \qquad \text{as } r\to\infty\ .$$

If the primary source is a line source parallel to the cylinder axis, then the problem is two-dimensional and condition (2.18) is no longer valid. In such cases it is sufficient to require that

$$\lim_{\rho\to\infty}\rho^{1/2}\left(\frac{\partial}{\partial\rho} - ik\right)\begin{matrix}\psi_1\\ \psi_2\end{matrix} = 0 \qquad \text{uniformly in } \phi\ , \tag{2.19}$$

that is, ψ_1 and ψ_2 are of the form

$$\underline{f}(\phi)\,\frac{e^{ik\rho}}{\sqrt{\rho}}\ , \qquad \text{as } \rho\to\infty\ .$$

Finally, in the case of plane wave incidence it is necessary to separate incident from scattered fields; the scalar wave functions ψ_1^s and ψ_2^s which originate the scattered fields satisfy the two-dimensional radiation condition (2.19).

Two kinds of primary fields are of practical interest, and will be examined in detail in the following two sections of this report: plane waves, and sources located at a finite distance from the scatterer. The first kind is important in radar

scattering where the target is usually assumed to be illuminated by an incident plane wave. The second type is relevant to the case of an antenna mounted on the scatterer. The antenna may be taken to be a dipole, since more complicated sources can be considered as distributions of dipoles. On the other end, a plane wave is the limiting case of a dipole going to infinity in a direction perpendicular to its moment. From the strictly mathematical viewpoint, it is therefore sufficient to consider the simple case of a dipole source at a finite distance from the cylinder; the solution of the scattering problem for any given source distribution can subsequently be obtained by superposition.

In order to arrive at the definition of dipole, let us consider the scalar point source defined by

$$\psi_o = \frac{e^{ikR}}{R} ,$$

where

$$R = |\underline{r} - \underline{r}_1| = \left\{(\rho\cos\phi - \rho_1\cos\phi_1)^2 + (\rho\sin\phi - \rho_1\sin\phi_1)^2 + (z - z_1)^2\right\}^{1/2}$$

is the distance between the source point (ρ_1, ϕ_1, z_1) and the field or observation point (ρ, ϕ, z).

An electromagnetic source at the point (ρ_1, ϕ_1, z_1) can be derived from ψ_o in may ways. For instance, we may take either $\psi_1 = \psi_o$ and $\psi_2 = 0$ or $\psi_1 = 0$ and $\psi_2 = \psi_o$ in equations (2.16). In the first case the primary field components are those of an electric Hertz vector $\Pi_e = \frac{e^{ikR}}{R}\hat{i}_z$, whereas in the second case the fields are originated from a magnetic Hertz vector $\Pi_m = \frac{e^{ikR}}{R}\hat{i}_z$. In the notation of Stratton (1941), Π_e and Π_m represent electric and magnetic dipoles of moment $\underline{p}^{(1)} = 4\pi\epsilon\hat{i}_z$ and $\underline{m}^{(1)} = 4\pi\hat{i}_z$, respectively.

The components of the fields of an electric dipole (with moment $\underline{p}^{(1)} = 4\pi\epsilon\hat{i}_z$) are:

$$E_\rho^i = (z-z_1)\left[\rho-\rho_1\cos(\phi-\phi_1)\right]\left(-\frac{k^2}{R^3}-\frac{3ik}{R^4}+\frac{3}{R^5}\right)e^{ikR},$$

$$E_\phi^i = (z-z_1)\rho_1\sin(\phi-\phi_1)\left(-\frac{k^2}{R^3}-\frac{3ik}{R^4}+\frac{3}{R^5}\right)e^{ikR}, \qquad (2.20)$$

$$E_z^i = \left\{\frac{ik}{R^2}+\frac{k^2\left[\rho^2+\rho_1^2-2\rho\rho_1\cos(\phi-\phi_1)\right]-1}{R^3}-\frac{3ik(z-z_1)^2}{R^4}+\frac{3(z-z_1)^2}{R^5}\right\}e^{ikR},$$

$$H_\rho^i = -i\omega\epsilon\rho_1\sin(\phi-\phi_1)\left(\frac{ik}{R^2}-\frac{1}{R^3}\right)e^{ikR},$$

$$H_\phi^i = i\omega\epsilon\left[\rho-\rho_1\cos(\phi-\phi_1)\right]\left(\frac{ik}{R^2}-\frac{1}{R^3}\right)e^{ikR},$$

$$H_z^i = 0.$$

The components of the fields of a magnetic dipole (with moment $\underline{m}^{(1)} = 4\pi\hat{i}_z$) are obtained from (2.20) by replacing E with H, H with -E, and ϵ with μ.

The scattering of the electromagnetic field of an axially oriented electric dipole by a perfectly conducting infinite cylinder can be described by a scalar wave function ψ_1^s, which is single-valued and twice-differentiable in each of the quantities $\rho, \phi, z, \rho_1, \phi_1, z_1$, satisfies the wave equation

$$(\nabla^2+k^2)\psi_1^s = 0$$

and the boundary condition

$$\left(\frac{e^{ikR}}{R} + \psi_1^s\right)\Bigg|_{\rho=a} = 0 ,$$

and originates a diffracted electromagnetic field given by equations (2.16) with

$$\psi_1 = \frac{e^{ikR}}{R} + \psi_1^s \quad , \quad \psi_2 = 0 ,$$

which satisfies the radiation condition (2.18).

Similarly, the scattering of the electromagnetic field of an axially oriented magnetic dipole by a perfectly conducting cylinder can be described by a scalar wave function ψ_2^s, single-valued and twice differentiable in ρ, ϕ, z, ρ_1, ϕ_1, z_1, such that

$$(\nabla^2 + k^2)\psi_2^s = 0 , \qquad \frac{\partial}{\partial\rho}\left(\frac{e^{ikR}}{R} + \psi_2^s\right)\Bigg|_{\rho=a} = 0 ,$$

and that the diffracted field obtained by putting $\psi_1 = 0$ and $\psi_2 = e^{ikR}/R + \psi_2^s$ in (2.16) satisfies condition (2.18).

If the surface of the cylinder has a nonzero impedance, then two independent scalar wave functions are needed to describe the scattered field produced by an axially oriented dipole source.

In the general case of a dipole source arbitrarily oriented with respect to the cylinder axis, it is still possible to derive the solution of the scattering problem from two scalar wave functions ψ_1 and ψ_2, representing series of electric and magnetic multipoles oriented along the axis. An alternative but entirely equivalent approach consists in finding explicitly the Green's functions for the cylinder; such Green's functions are customarily grouped together into a dyadic Green's function, whose derivation for the case of a perfectly conducting cylinder is briefly outlined in section 2.3 of this report. The use of dyadic Green's functions is noteworthy

for its elegance, and has been particularly advocated by Schwinger (1943, 1950), Morse and Feshbach (1946, 1953), Tai (1953, 1954a, b) and van Bladel (1964), among others.

When the boundary value problem is two-dimensional, it is possible to formulate simultaneously both scalar and vector scattering problems. We shall limit our considerations to the case of a plane wave incident perpendicularly to the cylinder axis. A scalar or vector plane wave can be considered as a limiting case of a scalar point source or of a dipole removed to infinity. If we let $z_1 = 0$ and $\phi_1 = \pi$, then $R \sim \rho_1 + \rho\cos\phi$ when ρ_1 becomes very large, and

$$\frac{e^{ikR}}{R} \sim \frac{e^{ik\rho_1}}{\rho_1} e^{ikx} , \qquad \text{as} \qquad \rho_1 \to \infty ,$$

so that if the source strength is renormalized by neglecting the factor $e^{ik\rho_1}/\rho_1$, a scalar plane wave propagating in the $\hat{i}_x$ direction is obtained.

In the two-dimensional case, $\partial/\partial z \equiv 0$, and equations (2.16) simplify, becoming

$$E_\rho = \frac{i\omega\mu}{\rho}\frac{\partial\psi_2}{\partial\phi} , \qquad H_\rho = -\frac{i\omega\epsilon}{\rho}\frac{\partial\psi_1}{\partial\phi} ,$$

$$E_\phi = -i\omega\mu\frac{\partial\psi_2}{\partial\rho} , \qquad H_\phi = i\omega\epsilon\frac{\partial\psi_1}{\partial\rho} , \tag{2.21}$$

$$E_z = k^2\psi_1 , \qquad H_z = k^2\psi_2 .$$

By taking $\psi_1 = e^{ikx}$ and $\psi_2 = 0$ in relations (2.21), one finds that

$$E_z^i = k^2 e^{ik\rho\cos\phi} , \qquad E_\rho^i = E_\phi^i = H_z^i = 0 ,$$

$$H_\rho^i = -\sqrt{\epsilon/\mu}\,\sin\phi\, E_z^i\,, \qquad H_\phi^i = -\sqrt{\epsilon/\mu}\,\cos\phi\, E_z^i\,,$$

which are the components of an electromagnetic plane wave propagating in the direction of the positive x-axis with $\underline{E}^i = k^2 e^{ikx}\hat{i}_z$ and $\underline{H}^i = -\sqrt{\epsilon/\mu}\, k^2 e^{ikx}\hat{i}_y$. Alternatively, by making $\psi_1 = 0$ and $\psi_2 = e^{ikx}$ in (2.21), one obtains that

$$E_\rho^i = \sqrt{\mu/\epsilon}\,\sin\phi\, H_z^i\,, \qquad E_\phi^i = \sqrt{\mu/\epsilon}\,\cos\phi\, H_z^i\,,$$

$$E_z^i = H_\rho^i = H_\phi^i = 0\,, \qquad H_z^i = k^2 e^{ik\rho\cos\phi}\,,$$

which are the components of a plane wave propagating in the $\hat{i}_x$ direction with $\underline{E}^i = \sqrt{\mu/\epsilon}\, k^2 e^{ikx}\hat{i}_y$ and $\underline{H}^i = k^2 e^{ikx}\hat{i}_z$.

If a function $\psi_1^s(\rho,\phi)$ which is single-valued and twice-differentiable in both variables ρ and ϕ, can be found such that

$$(\nabla^2 + k^2)\psi_1^s = 0\,, \tag{2.22}$$

$$\left(1 - \frac{i}{k}\eta\frac{\partial}{\partial\rho}\right)(e^{ikx} + \psi_1^s)\Big|_{\rho=a} = 0\,, \tag{2.23}$$

$$\lim_{\rho\to\infty} \rho^{1/2}\left(\frac{\partial}{\partial\rho} - ik\right)\psi_1^s = 0 \qquad \text{uniformly in } \phi\,, \tag{2.24}$$

then:

(i) the acoustic velocity potential of the field scattered by a cylinder with $\eta = \zeta k/(\omega\delta)$ in the presence of the plane wave $\psi^i = e^{ikx}$ is given by ψ_1^s; here δ is the density (mass per unit volume) of the medium surrounding the cylinder and ζ is the normal acoustic impedance, i.e. the ratio of pressure to the normal component of the velocity at the surface of the cylinder (in particular, $\zeta = \eta = 0$ in the case of a perfectly soft cylinder);

(ii) the electromagnetic field diffracted by a cylinder with relative surface impedance $\eta = Z\sqrt{\epsilon/\mu}$ in the presence of the plane wave $E_z = -\sqrt{\mu/\epsilon}\, H_y = k^2 e^{ikx}$ is given by relations (2.21) with $\psi_1 = e^{ikx} + \psi_1^s$, $\psi_2 = 0$.

If a function $\psi_2^s(\rho, \phi)$ can be found which satisfies all requirements imposed on ψ_1^s except (2.23) which is replaced by

$$\left(\frac{\partial}{\partial\rho} + ik\tilde{\eta}\right)(e^{ikx} + \psi_2^s)\Big|_{\rho=a} = 0 , \tag{2.25}$$

then:

(i) the acoustic velocity potential of the field scattered by a cylinder with $\tilde{\eta} = \omega\delta/(\zeta k)$ in the presence of the plane wave $\psi^i = e^{ikx}$ is given by ψ_2^s (in particular, $\zeta^{-1} = \tilde{\eta} = 0$ in the case of a perfectly rigid cylinder);

(ii) the electromagnetic field diffracted by a cylinder with $\tilde{\eta} = Z\sqrt{\epsilon/\mu}$ in the presence of the plane wave $H_z = \sqrt{\epsilon/\mu}\, E_y = k^2 e^{ikx}$ is given by relations (2.21) with $\psi_1 = 0$, $\psi_2 = e^{ikx} + \psi_2^s$.

In closing this section, we point out that instead of dealing with the scattering problem from the point of view of differential equations, we could approach the problem from the equivalent viewpoint of integral equations. In the vector case, this approach would involve the use of dyadic Green's functions as previously mentioned. The introduction of dyadic Green's functions is avoided in the case in which one wants to determine only the electromagnetic field at the surface of the scatterer (Maue, 1949). Once the surface fields are known, the fields at any point in space may be obtained through an integration over the surface of the scattering body (Stratton, 1941). The use of Maue's integral equation in place of the differential (wave) equation usually represents a complication of the problem, which may be counterbalanced by two simplifications: (1) the number of independent variables is reduced by one and the introduction of a special space coordinate system is unnecessary, and (2) the integral equation is the only requirement imposed on the unknown

function, that is, the boundary conditions are automatically satisfied. Maue's integral equation formulation is therefore particularly useful when the scattering problem involves boundaries which are not coordinate surfaces in a system of coordinates for which the wave equation is separable, but obviously loses most of its interest in the simple case in which the scatterer is an infinite circular cylinder.

2.2 Plane Wave, Spherical Wave, and Line Source Incidence

In this section, the scattering of a plane electromagnetic wave by an infinite circular cylinder of radius a with relative surface impedance $\eta = Z\sqrt{\epsilon/\mu}$ is considered. The formulas which give the diffracted field components as infinite series of eigenfunctions are derived for the case of oblique incidence, and they are subsequently specialized to the case in which the incident wave propagates in a direction perpendicular to the axis of the cylinder. The transformation of the infinite series solutions into contour integrals in the complex plane is discussed.

Particular attention is devoted to the case of normal incidence on a perfectly conducting cylinder. The behavior of both near fields and far fields is investigated in detail, for the cases in which either the electric or the magnetic incident field is parallel to the cylinder axis. Finally, the scattering of cylindrical and spherical waves is also examined.

Let us consider the incident plane electromagnetic wave

$$\underline{E}^i = (-\cos\alpha\cos\beta\hat{i}_x + \sin\beta\hat{i}_y + \sin\alpha\cos\beta\hat{i}_z)\, e^{ik(x\sin\alpha + z\cos\alpha)},$$

$$\underline{H}^i = \sqrt{\epsilon/\mu}\,(-\cos\alpha\sin\beta\hat{i}_x - \cos\beta\hat{i}_y + \sin\alpha\sin\beta\hat{i}_z)\, e^{ik(x\sin\alpha + z\cos\alpha)}, \tag{2.26}$$

which propagates in the direction of the unit vector

$$\hat{k} = \frac{\underline{E}^i \wedge \underline{H}^i}{\left|\underline{E}^i \wedge \underline{H}^i\right|} = \sin\alpha\hat{i}_x + \cos\alpha\hat{i}_z \quad , \qquad (0 < \alpha < \pi) \ .$$

The incident electric field $\underline{E}^i$ forms the angle β with the (x, z) plane of Fig. 2-2. It is easily verified that, according to formulas (2.16), the scalar functions

$$\psi_1^i = \frac{E_z^i}{k^2 \sin^2\alpha} = \frac{\cos\beta}{k^2 \sin\alpha} e^{ik\rho \sin\alpha \cos\phi + ikz\cos\alpha},$$

$$\psi_2^i = \frac{H_z^i}{k^2 \sin^2\alpha} = \sqrt{\epsilon/\mu}\, \frac{\sin\beta}{k^2 \sin\alpha} e^{ik\rho \sin\alpha \cos\phi + ikz\cos\alpha}, \tag{2.27}$$

generate the incident fields (2.26).

The scattered fields $\underline{E}^s$ and $\underline{H}^s$ may be derived from two scalar functions ψ_1^s and ψ_2^s through formulas (2.16). The functions ψ_1^s and ψ_2^s are linear combinations of the elementary wave functions (2.17). Since the cylinder is assumed to be of infinite length, the dependence of the scattered fields on the coordinate z must be the same as for the incident fields, that is, both incident and scattered fields vary according to the factor $e^{ikz\cos\alpha}$. Hence $h = k\cos\alpha$, and only the plus sign is considered in the exponential of (2.17). Furthermore, the wave functions containing J_n do not satisfy the radiation condition (2.19), and must therefore be disregarded, so that we finally have:

$$\psi_1^s = \sum_{n=-\infty}^{\infty} a_n H_n^{(1)}(k\rho \sin\alpha)\, e^{in\phi + ikz\cos\alpha},$$

$$\psi_2^s = \sum_{n=-\infty}^{\infty} b_n H_n^{(1)}(k\rho \sin\alpha)\, e^{in\phi + ikz\cos\alpha}, \tag{2.28}$$

and therefore the scalar wave functions which generate the diffracted fields are given by:

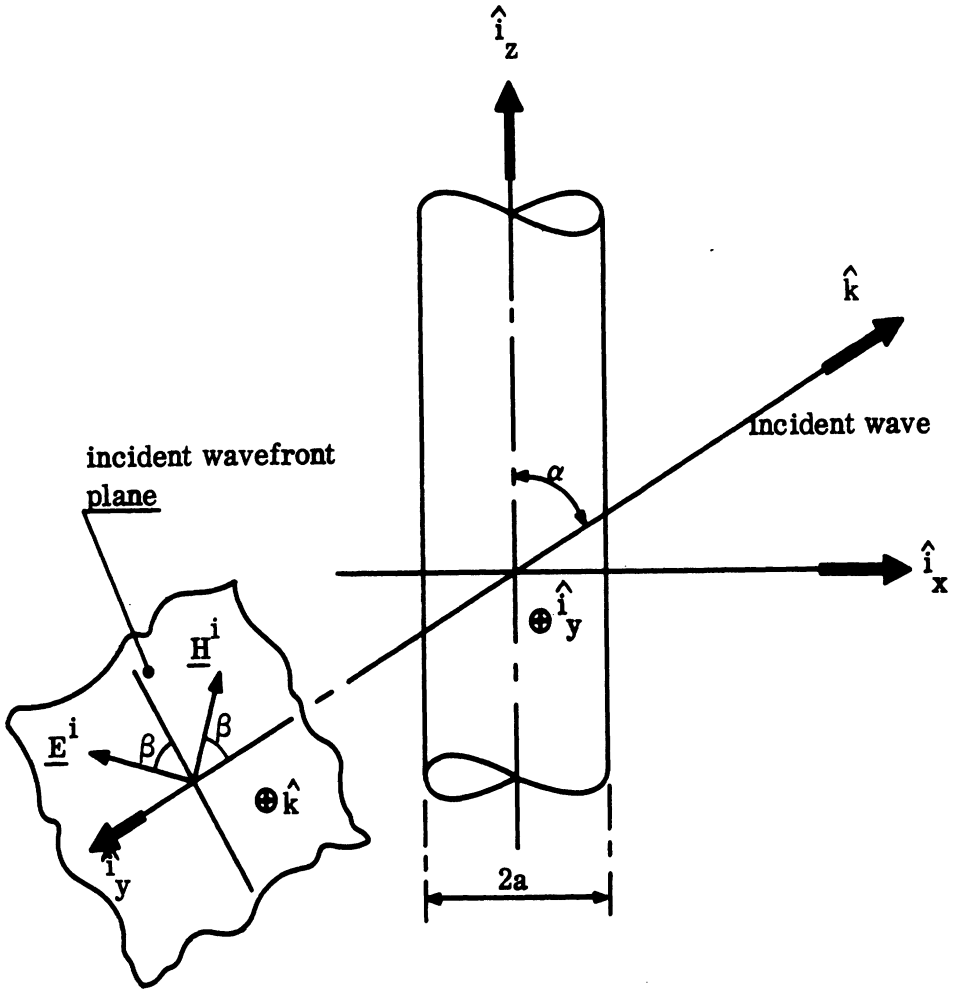

FIG. 2-2: GEOMETRY FOR PLANE WAVE INCIDENCE.

$$\psi_1 = \psi_1^i + \psi_1^s = \frac{e^{ikz\cos\alpha}}{k^2\sin\alpha}\left\{\cos\beta\, e^{ik\rho\sin\alpha\cos\phi} + \sum_{n=-\infty}^{\infty} i^n A_n H_n^{(1)}(k\rho\sin\alpha)\, e^{in\phi}\right\},$$

(2.29)

$$\psi_2 = \psi_2^i + \psi_2^s = \sqrt{\epsilon/\mu}\,\frac{e^{ikz\cos\alpha}}{k^2\sin\alpha}\left\{\sin\beta\, e^{ik\rho\sin\alpha\cos\phi} + \right.$$

$$\left. + \sum_{n=-\infty}^{\infty} i^n B_n H_n^{(1)}(k\rho\sin\alpha)\, e^{in\phi}\right\},$$

where we set, for convenience,

$$a_n = \frac{i^n}{k^2\sin\alpha} A_n, \qquad b_n = \sqrt{\epsilon/\mu}\,\frac{i^n}{k^2\sin\alpha} B_n. \tag{2.30}$$

The coefficients A_n and B_n are determined by imposing the boundary conditions at the surface of the cylinder. One finds that (Levy and Keller, 1959):

$$A_n = -\frac{1}{\Delta}\left[\cos\beta\left\{(J_n\sin\alpha - i\eta J_n')(\eta H_n^{(1)}\sin\alpha - iH_n^{(1)'}) + \eta J_n H_n^{(1)}\left(\frac{n\cos\alpha}{ka\sin\alpha}\right)^2\right\} + \right.$$

$$\left. + \sin\beta\,\frac{2n\eta\cos\alpha}{\pi(ka)^2\sin\alpha}\right],$$

(2.31)

$$B_n = -\frac{1}{\Delta}\left[\sin\beta\left\{(\eta J_n\sin\alpha - iJ_n')(H_n^{(1)}\sin\alpha - i\eta H_n^{(1)'}) + \eta J_n H_n^{(1)}\left(\frac{n\cos\alpha}{ka\sin\alpha}\right)^2\right\} - \right.$$

$$\left. - \cos\beta\,\frac{2n\eta\cos\alpha}{\pi(ka)^2\sin\alpha}\right],$$

where

$$\Delta = (H_n^{(1)}\sin\alpha - i\eta H_n^{(1)'})(\eta H_n^{(1)}\sin\alpha - i H_n^{(1)'}) + \eta\left(\frac{n\cos\alpha}{ka\sin\alpha} H_n^{(1)}\right)^2 , \qquad (2.32)$$

and the primes indicate the derivatives of the Bessel and Hankel functions with respect to the argument $ka\sin\alpha$. In deriving (2.31), the well known formula

$$e^{ik\rho\sin\alpha\cos\phi} = \sum_{n=-\infty}^{\infty} i^n J_n(k\rho\sin\alpha)\, e^{in\phi}$$

has been used. In particular, in the case of a perfectly conducting cylinder, one has that

$$(A_n)_{\eta=0} = -\frac{J_n(ka\sin\alpha)}{H_n^{(1)}(ka\sin\alpha)}\cos\beta , \quad (B_n)_{\eta=0} = -\frac{J_n'(ka\sin\alpha)}{H_n^{(1)'}(ka\sin\alpha)}\sin\beta . \qquad (2.33)$$

The components of the scattered fields are given by:

$$E_\rho^s = e^{ikz\cos\alpha}\sum_{n=-\infty}^{\infty} i^n e^{in\phi}\left\{iA_n\cos\alpha\, H_n^{(1)'} - \frac{nB_n}{k\rho\sin\alpha} H_n^{(1)}\right\} ,$$

$$E_\phi^s = -e^{ikz\cos\alpha}\sum_{n=-\infty}^{\infty} i^n e^{in\phi}\left\{\frac{nA_n\cos\alpha}{k\rho\sin\alpha} H_n^{(1)} + iB_n H_n^{(1)'}\right\} ,$$

$$E_z^s = e^{ikz\cos\alpha}\sin\alpha\sum_{n=-\infty}^{\infty} i^n A_n H_n^{(1)} e^{in\phi} , \qquad (2.34)$$

$$H_\rho^s = \sqrt{\epsilon/\mu}\; e^{ikz\cos\alpha}\sum_{n=-\infty}^{\infty} i^n e^{in\phi}\left\{\frac{nA_n}{k\rho\sin\alpha} H_n^{(1)} + iB_n\cos\alpha\, H_n^{(1)'}\right\},$$

$$H_{\phi}^{s} = \sqrt{\epsilon/\mu}\, e^{ikz\cos\alpha} \sum_{n=-\infty}^{\infty} i^{n} e^{in\phi} \left\{ iA_n H_n^{(1)'} - \frac{nB_n \cos\alpha}{k\rho \sin\alpha} H_n^{(1)} \right\} ,$$

$$H_{z}^{s} = \sqrt{\epsilon/\mu}\, e^{ikz\cos\alpha} \sin\alpha \sum_{n=-\infty}^{\infty} i^{n} B_n H_n^{(1)} e^{in\phi} ,$$

where the argument of the Bessel and Hankel functions and of their derivatives is $k\rho \sin\alpha$, and A_n and B_n are given by (2.31).

It is seen that if the cylinder is not perfectly conducting, then the z-component of the scattered electric (magnetic) field is different from zero, even if the z-component of the incident electric (magnetic) field is zero (see also Wait, 1955)*.

Formulas (2.34) become less complicated when the incident wave propagates in a direction perpendicular to the axis of the cylinder (normal incidence, $\alpha = \pi/2$). In such case, the function ψ_1^s generates a TM field and the function ψ_2^s a TE field, whose components are obtained through relations (2.21):

*In connection with this remark, it should be noted that the method given by Stöckel (1962) for deriving the diffracted electromagnetic field corresponding to oblique incidence from the field corresponding to normal incidence is valid only for perfectly conducting cylinders.

$$\left.\begin{aligned} E_z^s &= \cos\beta \sum_{n=-\infty}^{\infty} i^n \tilde{A}_n H_n^{(1)}(k\rho)\, e^{in\phi} , \\ H_\rho^s &= \sqrt{\epsilon/\mu}\, \frac{\cos\beta}{k\rho} \sum_{n=-\infty}^{\infty} n i^n \tilde{A}_n H_n^{(1)}(k\rho)\, e^{in\phi} , \\ H_\phi^s &= \sqrt{\epsilon/\mu}\, i\cos\beta \sum_{n=-\infty}^{\infty} i^n \tilde{A}_n H_n^{(1)'}(k\rho)\, e^{in\phi} , \end{aligned}\right\} \text{TM field}$$

(2.35)

$$\left.\begin{aligned} H_z^s &= \sqrt{\epsilon/\mu}\, \sin\beta \sum_{n=-\infty}^{\infty} i^n \tilde{B}_n H_n^{(1)}(k\rho)\, e^{in\phi} , \\ E_\rho^s &= -\frac{\sin\beta}{k\rho} \sum_{n=-\infty}^{\infty} n i^n \tilde{B}_n H_n^{(1)}(k\rho)\, e^{in\phi} , \\ E_\phi^s &= -i\sin\beta \sum_{n=-\infty}^{\infty} i^n \tilde{B}_n H_n^{(1)'}(k\rho)\, e^{in\phi} , \end{aligned}\right\} \text{TE field}$$

where we set:

$$\tilde{A}_n = -\frac{J_n(ka) - i\eta J_n'(ka)}{H_n^{(1)}(ka) - i\eta H_n^{(1)'}(ka)} , \qquad \tilde{B}_n = -\frac{J_n(ka) - i\eta^{-1} J_n'(ka)}{H_n^{(1)}(ka) - i\eta^{-1} H_n^{(1)'}(ka)} . \tag{2.36}$$

The scattered electromagnetic field for normal incidence is thus given by the superposition of a TM field proportional to $\cos\beta$ and a TE field proportional to $\sin\beta$; we can therefore limit our considerations to the particular cases $\beta = 0$ ($\underline{E}$ parallel to the cylinder axis) and $\beta = \pi/2$ ($\underline{H}$ parallel to the axis).

From formulas (2.35), one derives the following asymptotic expressions for the components of the far scattered field:

$$E_z^s \sim \sqrt{2/\pi}\, e^{-i\frac{\pi}{4}} \cos\beta \left\{ \sum_{n=0}^{\infty} \epsilon_n \tilde{A}_n \cos n\phi \right\} \frac{e^{ik\rho}}{\sqrt{k\rho}} \left[1+O(1/k\rho)\right],$$

$$H_\rho^s \sim \sqrt{\frac{2\epsilon}{\pi\mu}}\, e^{-i\frac{\pi}{4}} \cos\beta \left\{ \sum_{n=0}^{\infty} n\epsilon_n \tilde{A}_n \cos n\phi \right\} \frac{e^{ik\rho}}{(k\rho)^{3/2}} \left[1+O(1/k\rho)\right],$$

$$H_\phi^s \sim -\sqrt{\epsilon/\mu}\, E_z^s \left[1+O(1/k\rho)\right],$$

TM field for $k\rho \to \infty$;

$$H_z^s \sim \sqrt{\frac{2\epsilon}{\pi\mu}}\, e^{-i\frac{\pi}{4}} \sin\beta \left\{ \sum_{n=0}^{\infty} \epsilon_n \tilde{B}_n \cos n\phi \right\} \frac{e^{ik\rho}}{\sqrt{k\rho}} \left[1+O(1/k\rho)\right],$$

$$E_\rho^s \sim -\sqrt{2/\pi}\, e^{-i\frac{\pi}{4}} \sin\beta \left\{ \sum_{n=0}^{\infty} n\epsilon_n \tilde{B}_n \cos n\phi \right\} \frac{e^{ik\rho}}{(k\rho)^{3/2}} \left[1+O(1/k\rho)\right],$$

$$E_\phi^s \sim \sqrt{\mu/\epsilon}\, H_z^s \left[1+O(1/k\rho)\right],$$

TE field for $k\rho \to \infty$.

The infinite series solutions which have been obtained are of practical value as they stand only when the radius of the cylinder is not large compared to the wavelength. The number of terms of each series required to give a good approximation to the infinite sum is of the order of 2ka, so that numerical results are easily obtained only when ka is not very large compared to unity. The procedure commonly adopted in the case of large values of ka consists in replacing the infinite series

by contour integrals, which may be evaluated asymptotically*.

As an example, let us consider the case of a perfectly conducting cylinder ($\eta = 0$) with $\underline{E}$ parallel to the axis. From formulas (2.35) and (2.36) it follows that

$$E_z^s = -\sum_{n=0}^{\infty} \epsilon_n i^n \frac{J_n(ka)}{H_n^{(1)}(ka)} H_n^{(1)}(k\rho) \cos n\phi \ , \tag{2.37}$$

where $\epsilon_o = 1$ and $\epsilon_n = 2$ for $n \geqslant 1$. Treating the summation over n as a residue series, the summation is replaced by a contour integral C in the complex ν plane (Fig. 2-3) taken in the clockwise direction through the origin and around the poles at $\nu = 1, 2, \ldots$, giving:

$$E_z^s = -i \int_C \frac{J_\nu(ka)\, H_\nu^{(1)}(k\rho) \cos \nu\phi}{H_\nu^{(1)}(ka) \sin \nu\pi} e^{-i\nu\frac{\pi}{2}} d\nu \ . \tag{2.38}$$

Similarly, in the case of a perfectly conducting cylinder with $\underline{H}$ parallel to the axis, one has that

$$H_z^s = -\sqrt{\epsilon/\mu} \sum_{n=0}^{\infty} \epsilon_n i^n \frac{J_n'(ka)}{H_n^{(1)'}(ka)} H_n^{(1)}(k\rho) \cos n\phi \ , \tag{2.39}$$

which becomes:

$$H_z^s = -i\sqrt{\epsilon/\mu} \int_C \frac{J_\nu'(ka)\, H_\nu^{(1)}(k\rho) \cos \nu\phi}{H_\nu^{(1)'}(ka) \sin \pi\nu} e^{-i\nu\frac{\pi}{2}} d\nu \ . \tag{2.40}$$

* The contour integral solutions may also be introduced directly, without making use of the infinite series solutions (see, for example, Clemmow, 1959a).

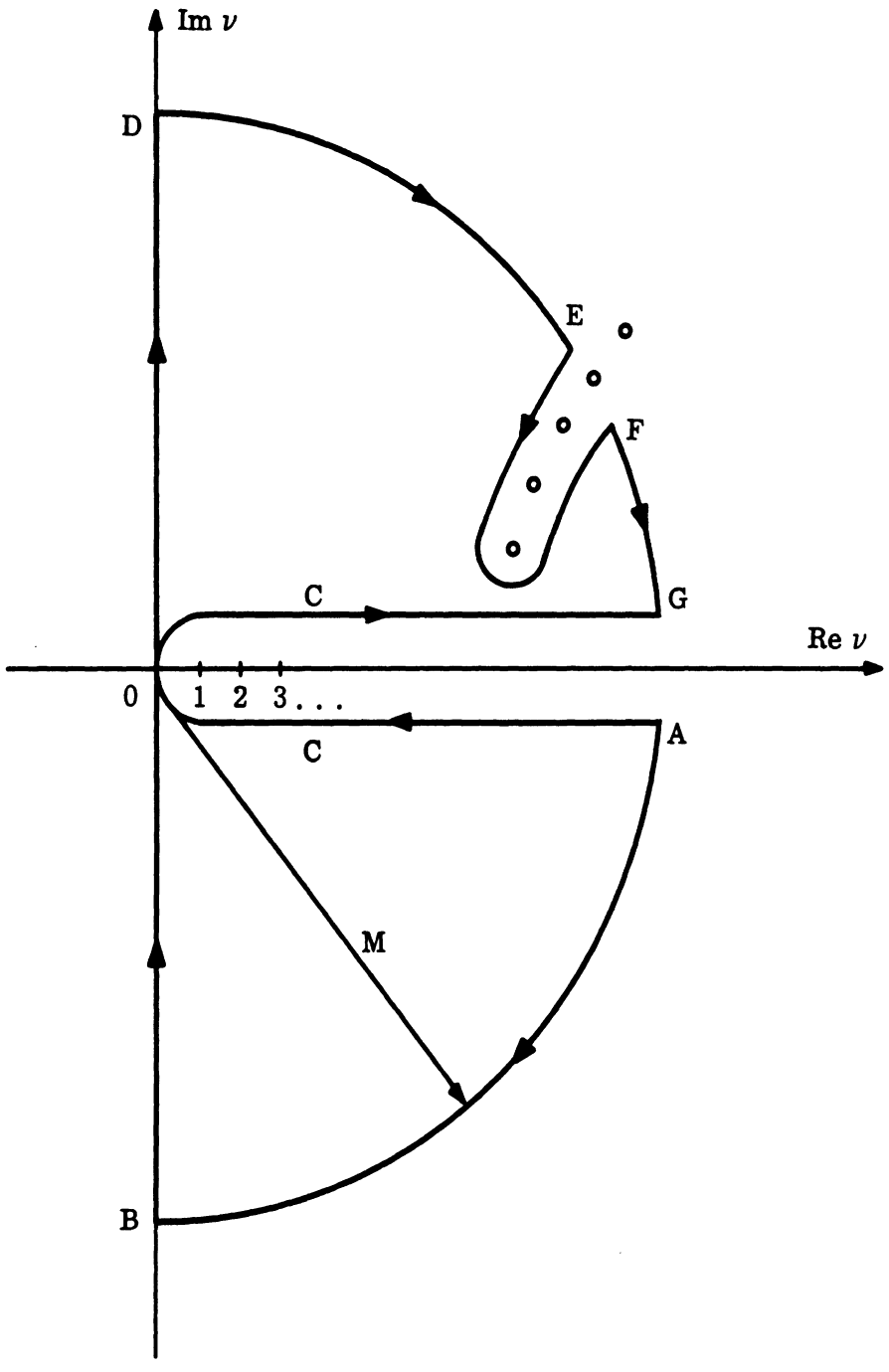

FIG. 2-3: THE COMPLEX ν-PLANE

The current density $\underline{J}$ at the surface of the conducting cylinder is given by:

$$\underline{J} = \hat{\rho} \wedge \underline{H}\Big|_{\rho=a} ,$$

so that when $\underline{E}$ is parallel to the cylinder axis

$$\underline{J} = J_z \hat{i}_z = \hat{i}_z (H_\phi^i + H_\phi^s)\Big|_{\rho=a} = \hat{i}_z \frac{2}{\pi ka} \sqrt{\epsilon/\mu} \sum_{n=0}^{\infty} \epsilon_n i^n \frac{\cos n\phi}{H_n^{(1)}(ka)} , \qquad (2.41)$$

and when $\underline{H}$ is parallel to the axis

$$\underline{J} = J_\phi \hat{\phi} = -\hat{\phi}(H_z^i + H_z^s)\Big|_{\rho=a} = -\hat{\phi} \frac{2i}{\pi ka} \sqrt{\epsilon/\mu} \sum_{n=0}^{\infty} \epsilon_n i^n \frac{\cos n\phi}{H_n^{(1)'}(ka)} . \qquad (2.42)$$

In general, for a perfectly conducting cylinder and arbitrary direction of incidence:

$$J_z = \frac{2}{\pi ka \sin\alpha} \sqrt{\epsilon/\mu}\, e^{ikz\cos\alpha} \left[\cos\beta \sum_{n=0}^{\infty} \epsilon_n \frac{i^n \cos n\phi}{H_n^{(1)}(ka\sin\alpha)} + \right.$$

$$\left. + \frac{2}{ka} \operatorname{cotg}\alpha \sin\beta \sum_{n=1}^{\infty} \frac{i^n \sin n\phi}{H_n^{(1)'}(ka\sin\alpha)} \right] , \qquad (2.41a)$$

$$J_\phi = -\frac{2i}{\pi ka} \sqrt{\epsilon/\mu} \sin\beta\, e^{ikz\cos\alpha} \sum_{n=0}^{\infty} \epsilon_n \frac{i^n \cos n\phi}{H_n^{(1)'}(ka\sin\alpha)} . \qquad (2.42a)$$

The surface current densities J_z of formula (2.41) and J_ϕ of formula (2.42) may be rewritten in the form:*

* The signs of the right hand sides of formula (13.4) in the book by King and Wu (1959) and of formulas (4) and (5) in the English translation of Goriainov's paper (1958) appear to be incorrect.

$$J_z = \frac{2i}{\pi ka}\sqrt{\epsilon/\mu}\int_C \frac{\cos\nu\phi}{H_\nu^{(1)}(ka)\sin\nu\pi}\, e^{-i\nu\frac{\pi}{2}}\, d\nu\ , \tag{2.43}$$

$$J_\phi = \frac{2}{\pi ka}\sqrt{\epsilon/\mu}\int_C \frac{\cos\nu\phi}{H_\nu^{(1)'}(ka)\sin\nu\pi}\, e^{-i\nu\frac{\pi}{2}}\, d\nu\ . \tag{2.44}$$

The path C of integration that appears in formulas (2.38), (2.39), (2.43) and (2.44) may be deformed in various ways in the complex ν plane, to give contour integrals which either can be evaluated asymptotically in a direct manner (e.g. by saddle point technique), or can be converted into a rapidly convergent residue series. Results of these approximation techniques are given in Section IV.

For example, in the case of formula (2.38) the contour C may be deformed as indicated in Fig. 2-3, so that

$$\int_C = \int_A^B + \int_B^D + \int_D^E + \int_E^F + \int_F^G\ ,$$

where the points A, B, D, E, F, G lie on a large semicircle of radius M with center at the origin $\nu = 0$, and the contour EF surrounds the zeros ν_ℓ ($\ell = 1, 2, \ldots$) of $H_\nu^{(1)}(ka)$ which lie in the first quadrant, and which are first order poles of the integrand function. When the radius M is increased to infinity, the contour integral along the semicircle vanishes:

$$\underset{(M=\infty)}{\int_A^B} = \underset{(M=\infty)}{\int_D^E} = \underset{(M=\infty)}{\int_F^G} = 0\ .$$

The remaining two integrals can be manipulated to give (for details see Imai, 1954):

$$E_z^s = \frac{1}{2}\int_{B\,(M=\infty)}^{D} \frac{H_\nu^{(2)}(ka)}{H_\nu^{(1)}(ka)} H_\nu^{(1)}(k\rho)\, e^{i\nu(\frac{\pi}{2}-\phi)}\, d\nu +$$

$$+ \int_{E\,(M=\infty)}^{F} \frac{J_\nu(ka)}{H_\nu^{(1)}(ka)} H_\nu^{(1)}(k\rho)\, \frac{e^{i\nu\phi} + e^{i\nu(2\pi-\phi)}}{e^{i\nu\pi} - e^{-i\nu\pi}}\, e^{-i\nu\frac{\pi}{2}}\, d\nu\,. \qquad (2.45)$$

Both integral representations (2.38) and (2.45) are as exact as the infinite series (2.37). If a similar calculation is performed on formula (2.40), one obtains:

$$H_z^s = \frac{1}{2}\sqrt{\epsilon/\mu}\int_{B\,(M=\infty)}^{D} \frac{H_\nu^{(2)'}(ka)}{H_\nu^{(1)'}(ka)} H_\nu^{(1)}(k\rho)\, e^{i\nu(\frac{\pi}{2}-\phi)}\, d\nu +$$

$$+ \sqrt{\epsilon/\mu}\int_{E\,(M=\infty)}^{F} \frac{J_\nu'(ka)}{H_\nu^{(1)'}(ka)} H_\nu^{(1)}(k\rho)\, \frac{e^{i\nu\phi} + e^{i\nu(2\pi-\phi)}}{e^{i\nu\pi} - e^{-i\nu\pi}}\, e^{-i\nu\frac{\pi}{2}}\, d\nu\,, \qquad (2.46)$$

where now the contour EF encloses the zeros ν_s $(s = 1, 2, \ldots)$ of $H_\nu^{(1)'}(ka)$ which lie in the first quadrant.

The scattered fields may be expressed as integrals over the surface S_1 of the cylinder, by using the vector analogue of Green's theorem (Stratton, 1941). If the cylinder is perfectly conducting, one has that

$$\underline{H}^s(\underline{r}) = \frac{1}{4\pi}\iint_{S_1} \underline{J}(\underline{r}_1) \wedge \nabla\psi_o\, dS_1\,, \qquad (2.47)$$

where $\underline{r}$ and $\underline{r}_1$ are the radius vectors for observation point and source point respectively, $\underline{J}$ is the surface current density, $dS_1 = a\, d\phi_1 dz_1$ is an element of the cylinder surface, the function $\psi_o = e^{ikR}/R$ with $R = |\underline{r} - \underline{r}_1|$ was previously intro-

duced in Section 2.1, and the gradient operates on the coordinates of the source point.

Formula (2.47) gives the scattered magnetic field as a function of the surface current density. If $\underline{J}$ is known, the determination of $\underline{H}^s$ at every point in space depends only on the evaluation of a surface integral. In the particular case of normal incidence, the double integral is easily reduced to a single integral by observing that $\underline{J}$ is independent of z_1 and that

$$\int_{-\infty}^{\infty} \psi_o \, dz_1 = i\pi H_o^{(1)}(kR_1)$$

with

$$R_1 = \left\{\rho^2 + a^2 - 2a\rho\cos(\phi - \phi_1)\right\}^{1/2} . \tag{2.48}$$

One then finds (Riblet, 1952):

$$\underline{H}^s(\rho, \phi) = -\frac{ika}{4} \int_{-\pi}^{\pi} \underline{J}(\phi_1) \wedge \hat{R}_1 H_1^{(1)}(kR_1) d\phi_1 , \tag{2.49}$$

where $\hat{R}_1 = (a\hat{\rho}_1 - \underline{\rho})/R_1$. In particular, if the incident magnetic field $\underline{H}^i$ is parallel to the cylinder axis, one has that

$$H_z^s(\rho, \phi) = \frac{ika}{4} \int_{-\pi}^{\pi} J_\phi(\phi_1) H_1^{(1)}(kR_1) \frac{a - \rho\cos(\phi - \phi)_1}{R_1} d\phi_1 \tag{2.50}$$

with J_ϕ given by formula (2.42), whereas for the other polarization ($\underline{E}^i$ parallel to the z axis) it can easily be proven that

$$E_z^s(\rho, \phi) = -\frac{ka}{4}\sqrt{\mu/\epsilon} \int_{-\pi}^{\pi} J_z(\phi_1) H_o^{(1)}(kR_1) d\phi_1 \tag{2.51}$$

with J_z given by formula (2.41). The results (2.50) and (2.51) can also be obtained by observing that we are essentially dealing with scalar problems with Neumann and Dirichlet boundary conditions, respectively, and by applying Green's theorem with $\frac{i}{4} H_o^{(1)}(kR_1)$ as Green's function. Formulas which give the scattered field as a function of the current density on the surface of the cylinder, such as (2.50) and (2.51), are especially useful when ka is large compared to unity.

An integral equation for the current density J_ϕ is obtained by adding the incident magnetic field H_z^i to both sides of equation (2.50) and by choosing the observation point on the surface of the cylinder. Since the integrand of (2.50) has a singularity at $\phi = \phi_1$ when $\rho \to a$, particular care must be taken in evaluating the limit $\rho \to a$ (Maue, 1949; Riblet, 1952). The final result is:

$$J_\phi(\phi) = -2\sqrt{\epsilon/\mu}\, e^{ika\cos\phi} - \frac{ika}{2}\int_{-\pi}^{\pi} J_\phi(\phi_1) H_1^{(1)}\left(2ka\sin\left|\frac{\phi-\phi_1}{2}\right|\right)\sin\left|\frac{\phi-\phi_1}{2}\right| d\phi_1 \tag{2.52}$$

If $\underline{E}^i$ is parallel to the z axis, the surface current $J_z(\phi)$ satisfies the integral equation: *

$$J_z(\phi) = -2\sqrt{\epsilon/\mu}\cos\phi\, e^{ika\cos\phi} + \frac{ika}{2}\int_{-\pi}^{\pi} J_z(\phi_1) H_1^{(1)}\left(2ka\sin\left|\frac{\phi-\phi_1}{2}\right|\right)\sin\left|\frac{\phi-\phi_1}{2}\right| d\phi_1 \tag{2.53}$$

If a Fourier series expansion is assumed for the surface current, the unknown coefficients of the expansion may be determined either by direct substitution of the series in the integral equation for the current, or by means of a variational principle (Papas, 1950). Of course one finds again the series (2.41) and (2.42), which were previously derived from the wave equation by separation of variables.

* Formula (28) of Riblet (1952) contains some misprints.

In order to present a qualitative discussion of the behavior of the current on the surface of a conducting cylinder, a diagram of both amplitude and phase of the surface current density $J_z = |J_z| e^{i\Phi_z}$, computed by means of formula (2.41), is shown in Fig. 2-4 for the case in which $ka = 3.1$ (King and Wu, 1959). The curves are obviously symmetric with respect to the plane of incidence. The phase velocity v_z of the surface current is given by the formula:

$$v_z/v_o = -ka/(d\Phi_z/d\phi) , \tag{2.54}$$

where $v_o = (\epsilon\mu)^{-1/2}$ is the phase velocity of the incident wave, and $d\Phi_z/d\phi$ is the slope of the phase curve in Fig. 2-4. It is then seen that the phase velocity of the current around the cylinder surface is greater than v_o in the illuminated region about $\phi = \pi$, it decreases to a value less than v_o at the shadow boundary $\phi = \pi/2$, and maintains a nearly constant value $0.7v_o$ from $\phi = \pi/2$ almost to $\phi = 0$. This means that a given phase of the surface current density creeps around the cylinder from the shadow boundary into the umbra region as a traveling wave whose velocity is sensibly constant and less than the phase velocity of the incident wave. An identical traveling wave of current exists on the other side of the cylinder. The amplitude of the surface current decreases rapidly with ϕ except near $\phi = 0$ and $\phi = \pi$, where both amplitude and phase of J_z are stationary. The behavior at $\phi = \pm\pi$ is easily understood by observing that the element of cylinder surface is there parallel to the incident wavefront. The behavior near $\phi = 0$ is a consequence of the interference of the two traveling waves which propagate in opposite directions around the cylinder and produce a standing wave. The standing wave is clearly observed only around $\phi = 0$, that is in the region where the amplitudes of the two interfering waves are of the same order of magnitude.

Analogous considerations apply to the case in which the incident magnetic field is parallel to the cylinder axis. However, the current is now in the ϕ-direction so that the waves propagating around the cylinder may be regarded as longitudinal, whereas in the case of $\underline{E}^i$ parallel to the axis, the waves are transverse to the

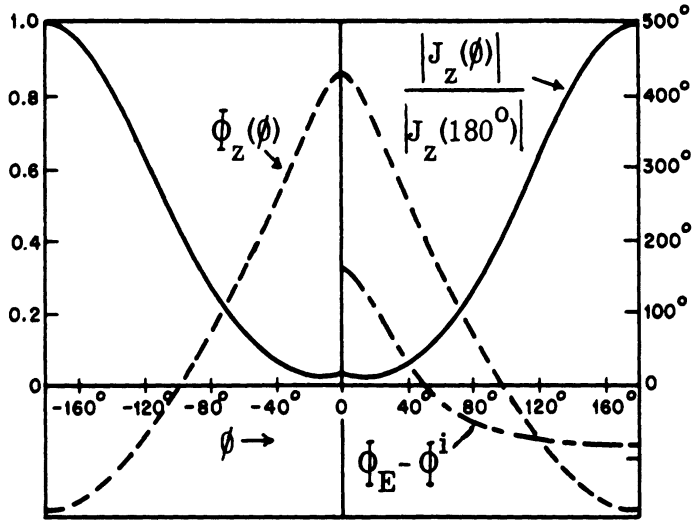

FIG. 2-4: CURRENT DENSITY $J_z = |J_z| e^{i\Phi_z}$ ON A CONDUCTING CYLINDER, WHEN $\underline{E}^i$ IS PARALLEL TO THE AXIS AND ka = 3.1 (King and Wu, 1959).

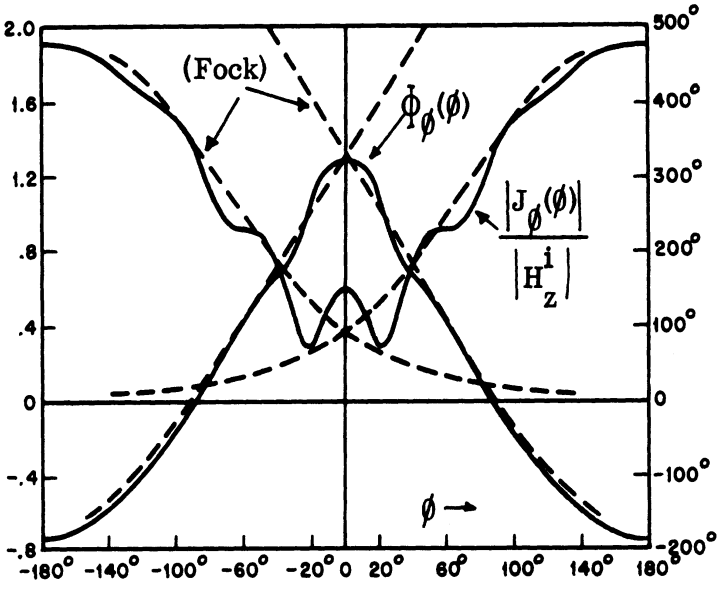

FIG. 2-5: CURRENT DENSITY $J_\phi = |J_\phi| e^{i\Phi_\phi}$ ON A CONDUCTING CYLINDER, WHEN $\underline{H}^i$ IS PARALLEL TO THE AXIS AND ka = 3.1 (King and Wu, 1959).

direction of propagation. Whenever a standing wave is produced by the interference of two longitudinal waves, regions of concentration of electric charges exist on the surface of the cylinder. Such concentrations do not occur when two transverse waves interfere. Phase and amplitude of the surface current density $J_\phi = |J_\phi| e^{i\Phi_\phi}$ for $ka = 3.1$ are given by the continuous lines of Fig. 2-5 (King and Wu, 1959). From Figs. 2-4 and 2-5 it is seen that the amplitude $|J_\phi|$ decreases more slowly than $|J_z|$, as $|\phi|$ decreases from π to zero. This explains why the standing wave pattern is much more evident in Fig. 2-5 than in Fig. 2-4.

Also represented in Fig. 2-4 is the difference $\Phi_E - \Phi^i$ between the phase Φ_E of the total electric field $E_z = |E_z| e^{i\Phi_E}$ at a point ϕ on the surface of the cylinder and the phase $\Phi^i = ka\cos\phi$ of the incident field at the same point. The broken lines of Fig. 2-5 represent amplitude and phase of the traveling waves of surface current density, as given by Fock's high frequency approximation (see chapter IV).

A detailed graphical representation and a discussion of the properties of the total electric (magnetic) field in the vicinity of the cylinder when the incident electric (magnetic) field is parallel to the axis were given by King and Wu (1957, 1959). The numerical results necessary for such discussions may be obtained easily through formulas (2.37) and (2.39), when ka is not large compared to unity. The main features of the diffraction phenomenon as well as surface current distribution for the case of $\underline{E}^i$ parallel to the cylinder axis and $a = 0.16\lambda$ are illustrated in Fig. 2-6 (Carter, 1943). The amplitude of the total electric field in the back scattering direction $|\phi| = \pi$ (Fig. 2-6a) resembles the amplitude $2|\sin k(x-a)|$ of the total field originated by the reflection of a plane wave incident perpendicularly on an infinite conducting plane at $x = -a$. In both cases, the amplitudes exhibit standing wave patterns whose maxima and minima are practically located at the same points along the negative x-axis. However, in the case of the plane ($ka = \infty$), the amplitude of the standing wave is a periodic function of x with period $\lambda/2$, whereas in the case of the cylinder, the oscillations of the amplitude pattern about the constant

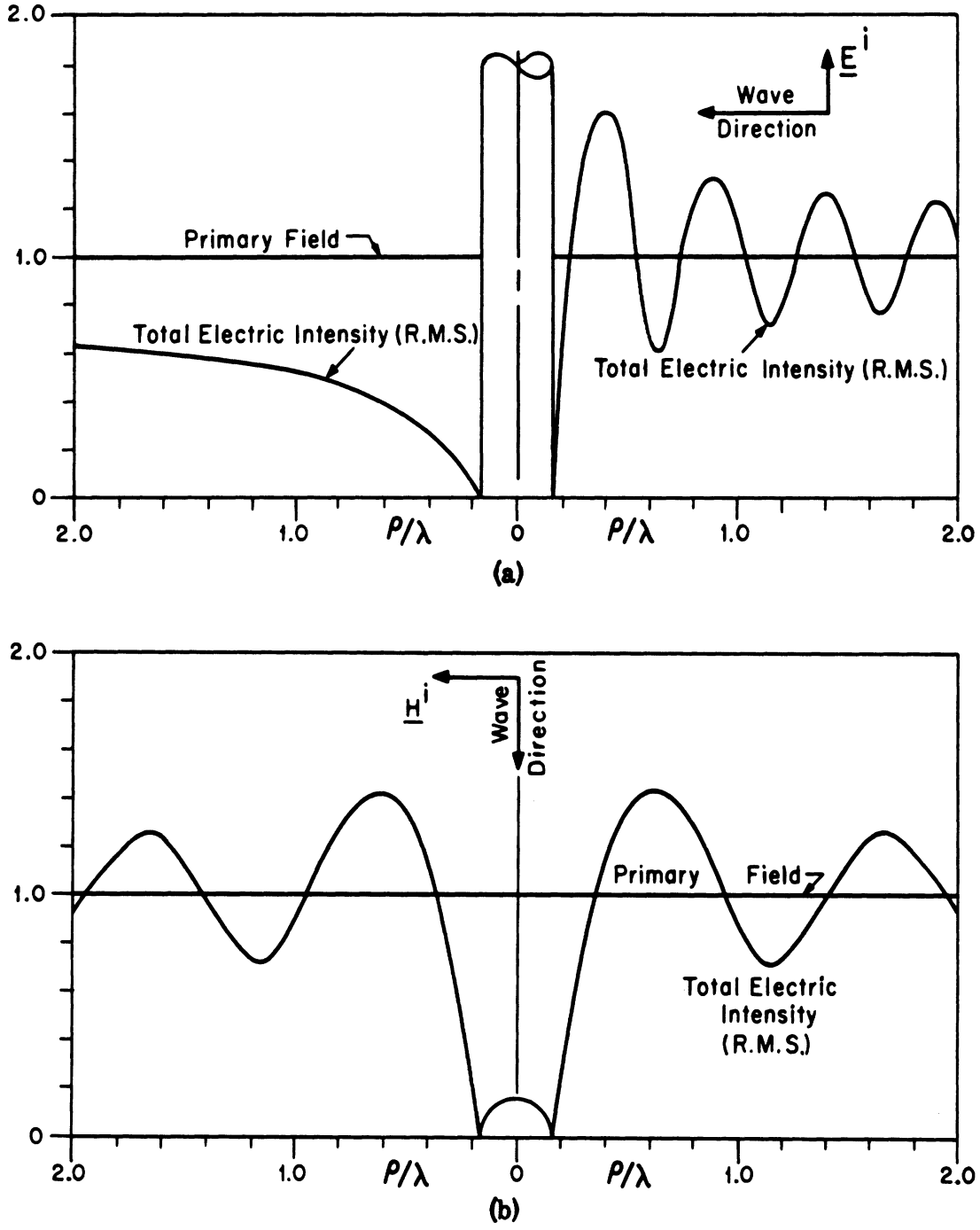

FIG. 2-6a, b: DIFFRACTION OF A PLANE WAVE BY A CONDUCTING CYLINDER, WHEN $\underline{E}^i$ IS PARALLEL TO THE AXIS AND $a = 0.16\lambda$ (Carter, 1943).

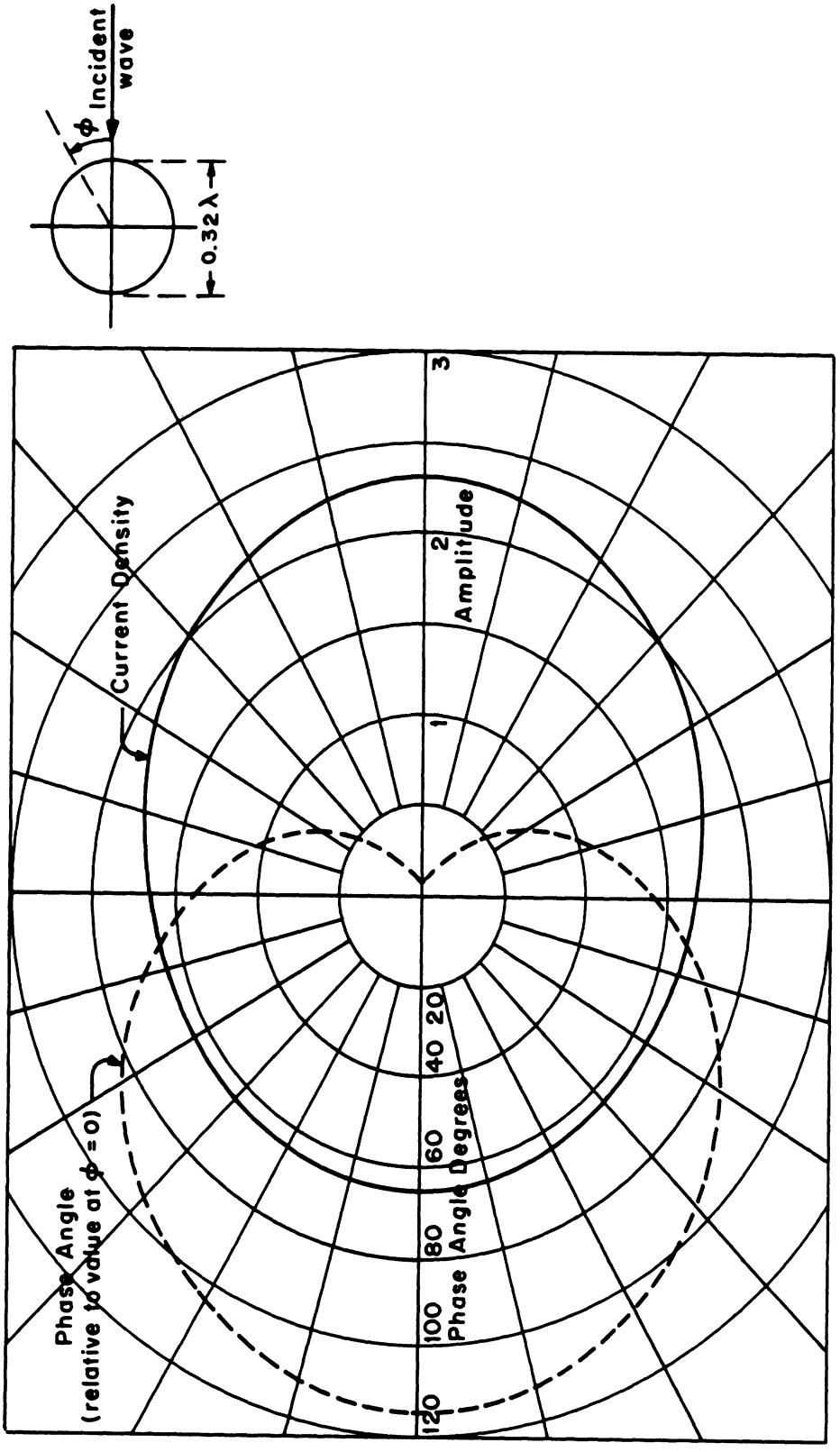

FIG. 2-6c: CURRENT DISTRIBUTION ON THE CYLINDER SURFACE (Carter, 1943).

amplitude characteristic of the incident field decrease as $|x|$ increases, and vanish at $x = -\infty$. The diffracted electric field in the back scattering direction may therefore be considered as produced by the interference of the incident wave with a cylindrical wave propagating radially outward from the cylinder (scattered wave).

Since the diffracted field very near the cylinder along the negative x-axis is very similar to the field near a conducting plane, one may try to describe the field in the illuminated region around $|\phi| = \pi$ in terms of the plane tangent to the cylinder surface at the azimuth ϕ and of the plane wave arriving at an incidence angle $\pi - |\phi|$. For a given value of ϕ, one still finds a standing wave pattern in the radial direction, which is more and more spread out as $|\phi|$ decreases from 180°; the distance between two adjacent maxima (or minima) is equal to $\lambda/(2|\cos\phi|)$. The spreading of the pattern is evident in Figs. 2-6a and 2-6b, where the cases $|\phi| = \pi$, $\pi/2$, and zero are illustrated. The agreement between this simple interpretation and the exact result (2.37) is good whenever $\cos\phi$ is bounded away from zero.

Thus we find that in the illuminated region $|\phi| \sim \pi$, the total electric field may be interpreted in terms of a standing wave in the radial direction and of a traveling wave which moves along the surface of the cylinder away from the negative z-axis with a phase velocity greater than v_0. Similar results are valid for the case in which the incident magnetic field is parallel to the axis of the cylinder (King and Wu, 1959).

The behavior of the scattered electric field near the cylinder when $\underline{E}^i$ is parallel to the axis is illustrated in Fig. 2-7, for $\phi = 0$, $\pi/2$, and π and for various values of ka (Adey, 1958). It is seen that the back scattered field amplitude never exceeds the incident field amplitude, and, for a fixed $k\rho$, increases with the cylinder radius (Fig. 2-7c). On the contrary, the amplitude of the forward scattered field sometimes exceeds the amplitude of the incident field and oscillates about that value (Fig. 2-7a), so that the scattered field in the shadow region and in the vicinity of the cylinder surface does not behave like a divergent wave.

If a plane wave is incident on an infinite cylinder perpendicularly to its generators and at an angle ϕ_0 with the x-axis, then the far scattered field components

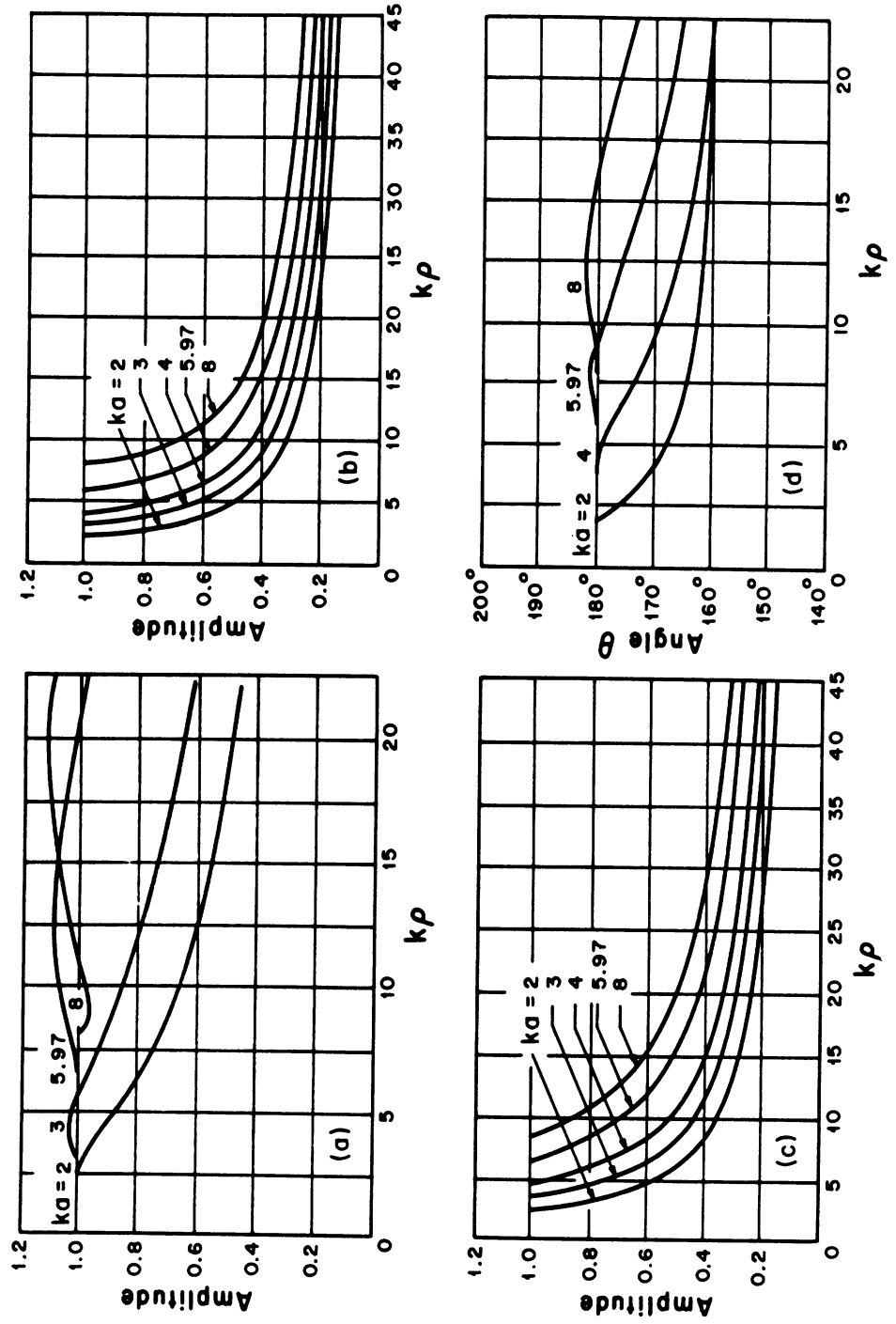

FIG. 2-7: SCATTERED FIELD $E_z^s = |E_z^s| e^{i\Phi^s}$ PRODUCED BY A PLANE WAVE INCIDENT ON A CONDUCTING CYLINDER, WHEN $\underline{E}^i$ IS PARALLEL TO THE AXIS. AMPLITUDE $|E_z^s|$ AT (a) $\phi = 0$, (b) $\phi = \pi/2$, (c) $\phi = \pi$; (d) Phase $\theta = \Phi^s - k\rho$ at $\phi = 0$ (Adey, 1958).

in the electromagnetic case, or the far scattered pressure and velocity potential in the acoustical case, may be expressed in the form

$$f(\phi, \phi_o) \sqrt{\frac{2}{\pi k \rho}}\, e^{i(k\rho - \frac{\pi}{4})}, \quad \text{as} \quad \rho \to \infty . \tag{2.55}$$

The far field amplitude function $f(\phi, \phi_o)$ has the following well known properties (see, for example, Karp, 1961):

$$f(\phi, \phi_o) = f(\phi_o + \pi, \phi + \pi) , \tag{2.56}$$

$$\int_0^{2\pi} \left| f(\phi, \phi_o) \right|^2 d\phi = -2\pi \, \mathrm{Re}\, f(\phi_o, \phi_o) . \tag{2.57}$$

Equation (2.56) may be obtained as a limiting form of the reciprocity theorem for Green's function; relation (2.57) constitutes the so-called forward amplitude theorem. In the case in which $\underline{E}^i$ is parallel to the generators of a metal cylinder (acoustically soft cylinder), it can be proven that $f(\phi, \phi_o)$ is a function of the difference $(\phi - \phi_o)$ if and only if the cylinder has a circular cross section (Karp, 1961).

The far scattered field amplitude pattern that a plane wave at normal incidence on a circular cylinder produces in the azimuthal plane depends upon the value of ka; a particular case is shown in Fig. 2-8 (Faran, 1951). For small values of ka the pattern is nearly independent of ϕ (Fig 2-8a), but lobes develop as ka increases (Fig. 2-8a, b and c).

The phase of the far scattered field is a complicated function of both ϕ and ka. In the case of electromagnetic scattering with $\underline{E}^i$ parallel to the axis of the metal cylinder, the far scattered electric field easily follows from relation (2.37):

$$(E_z^s)_{\rho \gg a} \sim -\sqrt{\frac{2}{\pi k \rho}}\, e^{ik\rho - i\frac{\pi}{4}} \sum_{n=0}^{\infty} \epsilon_n \frac{J_n(ka)}{H_n^{(1)}(ka)} \cos n\phi . \tag{2.59}$$

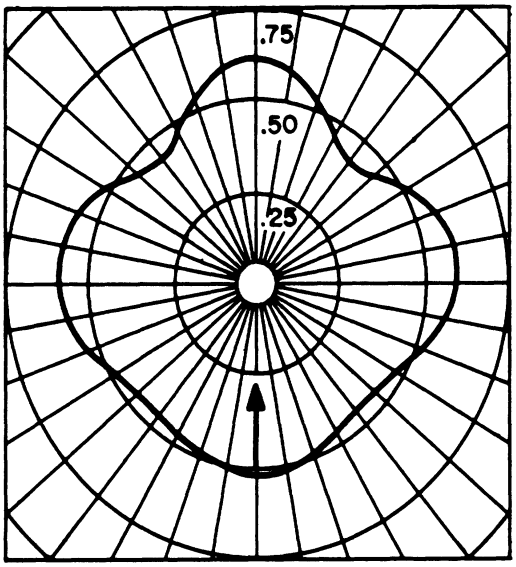

(a) ka = 1.7

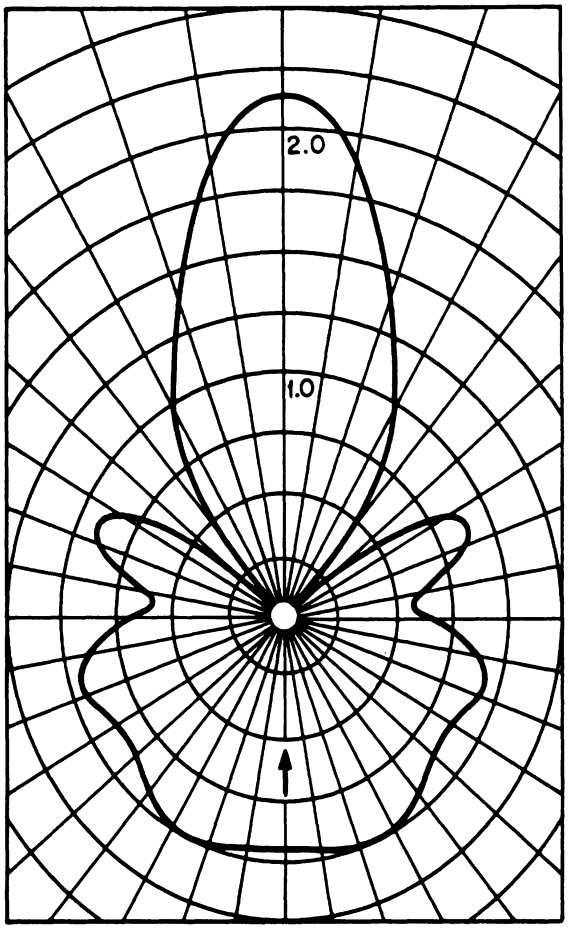

(c) ka = 5.0

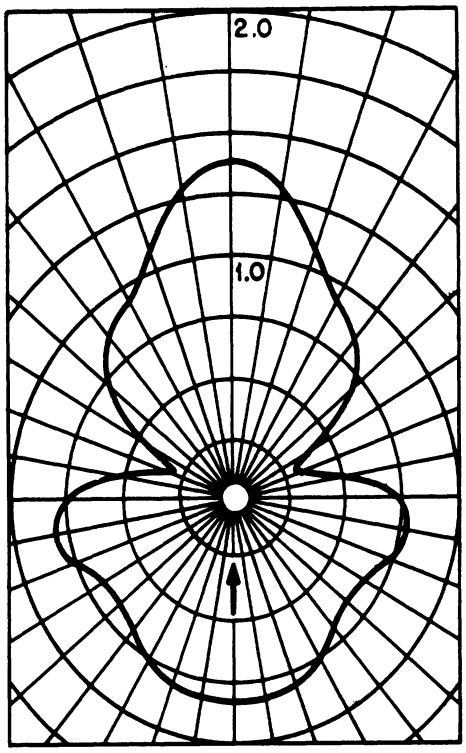

(b) ka = 3.4

FIG. 2-8: AMPLITUDE PATTERN OF THE SCATTERED PRESSURE p^s PRODUCED BY A PLANE WAVE WITH PRESSURE p^i NORMALLY INCIDENT ON A PERFECTLY RIGID CYLINDER. The scales show the quantity $\lim_{\rho \to \infty} 1/2 \, |p^s/p^i| (\pi k\rho/2)^{1/2}$ as a function of ϕ. (Faran, 1951).

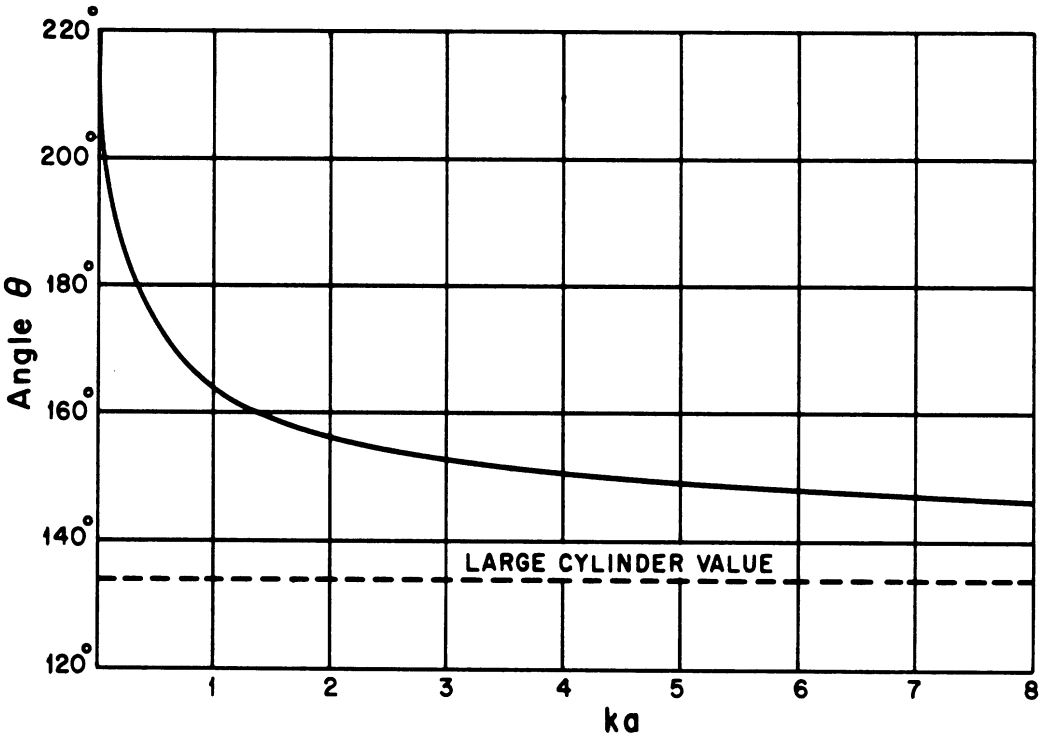

FIG. 2-9: DIFFERENCE BETWEEN THE PHASES OF THE FAR FORWARD SCATTERED FIELD AND OF THE INCIDENT FIELD, WHEN $\underline{E}^i$ IS PARALLEL TO THE AXIS OF THE PERFECTLY CONDUCTING CYLINDER. (Adey, 1958).

The difference θ between the phase of the far scattered field in the forward direction $\phi = 0$ and the phase of the incident field, both evaluated at the same point, is therefore given by:

$$\theta = \arg\left\{ - \sum_{n=0}^{\infty} \epsilon_n \frac{J_n(ka)}{H_n^{(1)}(ka)} \right\} - \frac{\pi}{4} , \tag{2.60}$$

and decreases monotonically from the value $5\pi/4$ at $ka = 0$ to the limit value $3\pi/4$ for very large cylinders, as is shown in Fig. 2-9 (Adey, 1958).

In the case of $\underline{E}^i$ parallel to the axis of the metal cylinder, the back scattering cross section σ_E per unit length, defined as

$$\sigma_E = \lim_{\rho \to \infty} 2\pi\rho \left| \frac{E_z^s}{E_z^i} \right|^2 = \lim_{\rho \to \infty} 2\pi\rho \left| \frac{\psi_1^s}{\psi_1^i} \right|^2 ,$$

is easily derived from relation (2.59). One finds that

$$\sigma_E = \frac{4}{k} A(ka) , \tag{2.61}$$

where

$$A(ka) = \left| \sum_{n=0}^{\infty} \epsilon_n (-1)^n \frac{J_n(ka)}{H_n^{(1)}(ka)} \right|^2 . \tag{2.62}$$

This is also the cross section per unit length for an acoustically soft cylinder. Similarly, in the case of $\underline{H}^i$ parallel to the axis of the conducting cylinder, the back scattering cross section σ_H per unit length defined as

$$\sigma_H = \lim_{\rho \to \infty} 2\pi\rho \left| \frac{H_z^s}{H_z^i} \right|^2 = \lim_{\rho \to \infty} 2\pi\rho \left| \frac{\psi_2^s}{\psi_2^i} \right|^2 ,$$

may be obtained from relation (2.39). One finds that

$$\sigma_H = \frac{4}{k} B(ka) , \tag{2.63}$$

where

$$B(ka) = \left| \sum_{n=0}^{\infty} \epsilon_n (-1)^n \frac{J_n'(ka)}{H_n^{(1)'}(ka)} \right|^2 . \tag{2.64}$$

This is also the cross section per unit length for an acoustically rigid cylinder. The quantities A(ka) and B(ka) are plotted in Figs. 2-10 and 2-11 for $ka \leqslant 10$ (Senior and Boynton, 1964). The broken lines show the geometrical optics approximation $\frac{\pi}{4} ka$ (see section IV). It is seen that σ_E is always larger than the geometrical optics approximation $\sigma_{g.o.} = \pi a$ and increases monotonically with ka, whereas σ_H oscillates about the geometrical optics value as ka increases. The ratios $\sigma_E/\sigma_{g.o.}$ and $\sigma_H/\sigma_{g.o.}$ are plotted in Fig. 2-12.

The total scattering cross section σ_{total} per unit length is defined by the ratio of the time averaged total scattered power per unit length of cylinder to the time averaged incident Poynting vector. In the case when $\underline{E}^i$ is parallel to the axis of the perfectly conducting cylinder, one has that

$$\sigma_{total} = \frac{1}{k} \operatorname{Re} \left\{ -i \int_{-\pi}^{\pi} \overline{E_z^s(a, \phi_1)} \left[\frac{\partial E_z^s(\rho_1, \phi_1)}{\partial \rho_1} \right]_{\rho_1 = a} a d\phi_1 \right\} \tag{2.65}$$

where the bar above E_z^s indicates the complex conjugate. Observing that $E_z^s(a, \phi_1) = -E_z^i(a, \phi_1)$, and that

$$\int_{-\pi}^{\pi} \overline{E_z^i(a, \phi_1)} \left[\frac{\partial E_z^i(\rho_1, \phi_1)}{\partial \rho_1} \right]_{\rho_1 = a} a d\phi_1 = 0 ,$$

the total scattering cross section becomes:

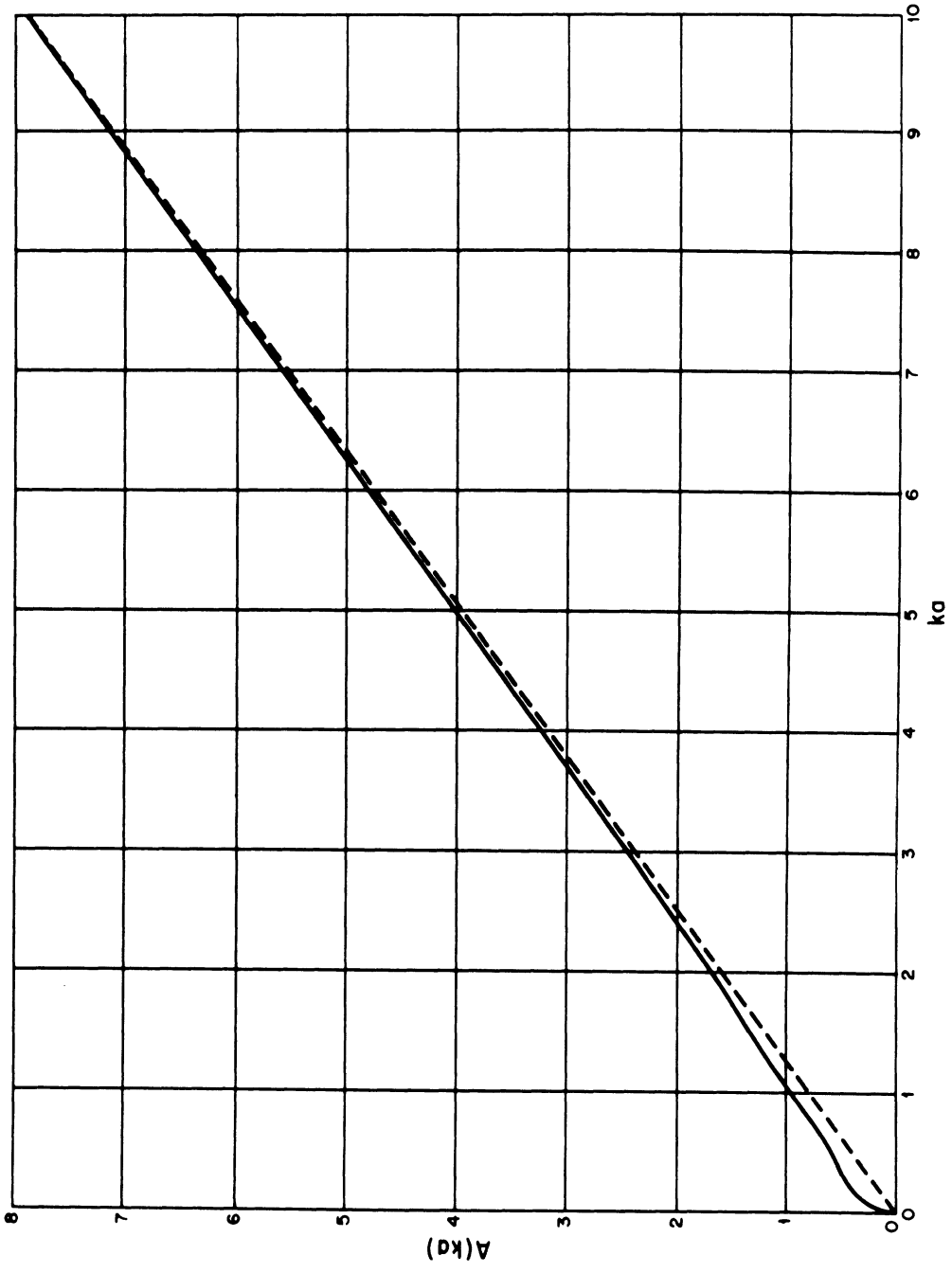

FIG. 2-10: CROSS SECTION σ_E PER UNIT LENGTH; $A(ka) = k\sigma_E/4$ (Senior and Boynton, 1964)
(– – – geometrical optics approximation).

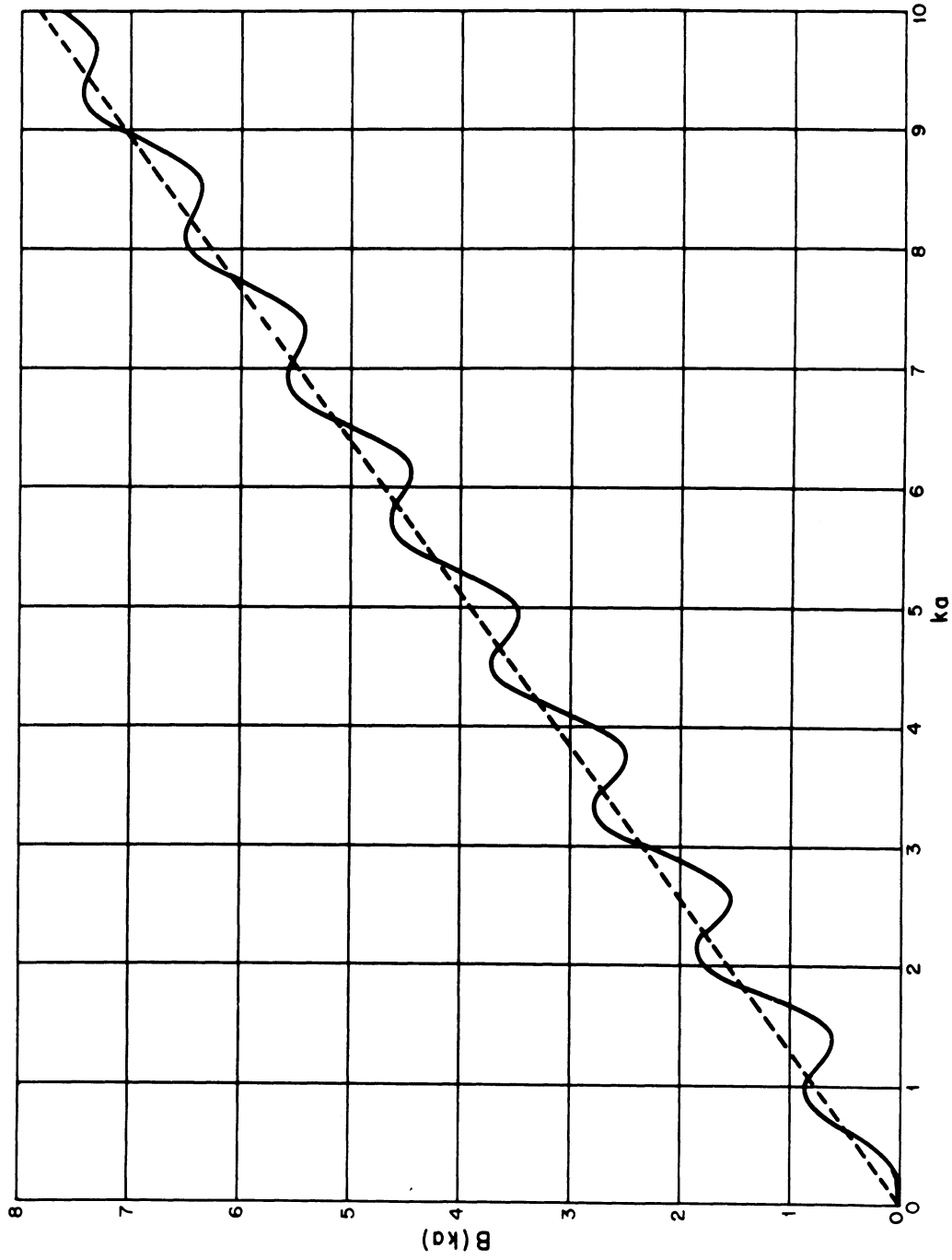

FIG. 2-11: CROSS SECTION σ_H PER UNIT LENGTH; $B(ka) = k\sigma_H/4$ (Senior and Boynton, 1964)
(- - - geometrical optics approximation).

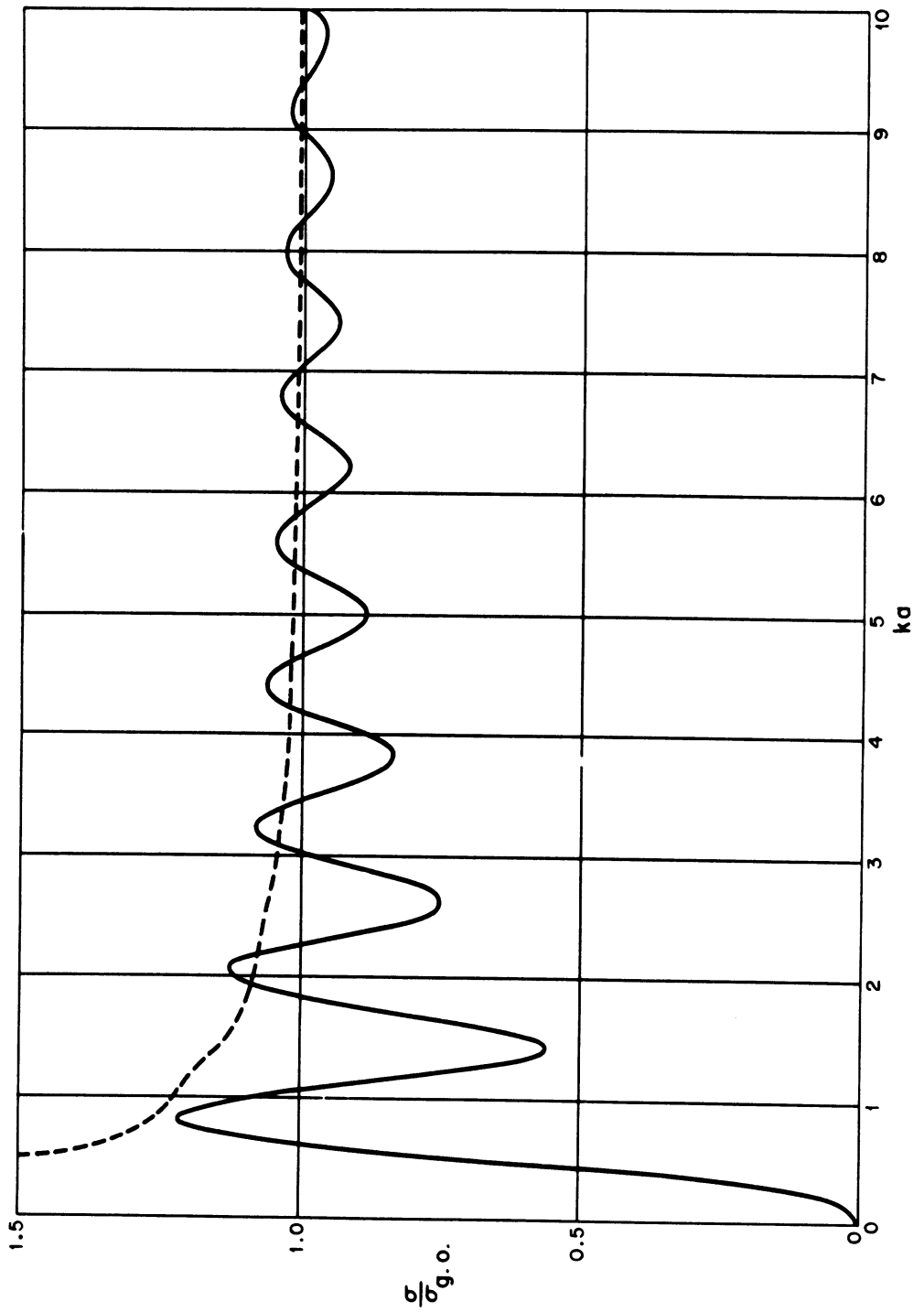

FIG. 2-12: CROSS SECTIONS σ_E (- - -) AND σ_H (——) PER UNIT LENGTH, NORMALIZED TO THEIR GEOMETRICAL OPTICS APPROXIMATION $\sigma_{g.o.}$ (Senior and Boynton, 1964).

$$\sigma_{total} = \frac{a}{k} \operatorname{Re}\left\{ i \int_{-\pi}^{\pi} \overline{E_z^i(a, \phi_1)} \left[\frac{\partial E_z(\rho_1, \phi_1)}{\partial \rho_1} \right]_{\rho_1 = a} d\phi_1 \right\}$$

$$= a\sqrt{\mu/\epsilon} \operatorname{Re}\left\{ \int_{-\pi}^{\pi} J_z(\phi_1) e^{-ika\cos\phi_1} d\phi_1 \right\}. \qquad (2.66)$$

According to notation (2.55), the scattered field E_z^s given by (2.51) may be rewritten in the form:

$$E_z^s(\rho, \phi) \sim f(\phi, 0) \sqrt{\frac{2}{\pi k\rho}}\, e^{i(k\rho - \frac{\pi}{4})}, \quad \text{as} \quad \rho \to \infty, \qquad (2.67)$$

where

$$f(\phi, 0) = -\frac{ka}{4} \sqrt{\mu/\epsilon} \int_{-\pi}^{\pi} J_z(\phi_1) e^{-ika\cos(\phi_1 - \phi)} d\phi_1 . \qquad (2.68)$$

From formulas (2.66) and (2.68) the important result follows (Papas, 1950):

$$\sigma_{total} = -\frac{4}{k} \operatorname{Re} f(0, 0) . \qquad (2.69)$$

The total scattering cross section per unit length is therefore proportional to the real part of the far field amplitude function, evaluated in the forward direction. Since the phase of $f(0, 0)$ is given by $(\theta + \pi/4)$, where θ is the angle plotted in Fig. 2-9, the real part of $f(0, 0)$ cannot be positive, and therefore one has the obvious result that σ_{total} is never negative and becomes zero for $ka = 0$. From formula (2.59) it follows that

$$f(0, 0) = -\sum_{n=0}^{\infty} \epsilon_n \frac{J_n(ka)}{H_n^{(1)}(ka)} , \qquad (2.70)$$

hence

$$\sigma_{total} = \frac{4}{k} \sum_{n=0}^{\infty} \epsilon_n \frac{J_n^2(ka)}{J_n^2(ka) + N_n^2(ka)} , \tag{2.71}$$

where $H_n^{(1)}(ka) = J_n(ka) + iN_n(ka)$.

In the case in which a finite and nonzero impedance exists at the surface of the cylinder, the calculations of far fields and cross sections become rather complicated. From the computational viewpoint it is then advantageous to use the so-called phase shift analysis. In this method the incident plane wave is expressed as a sum of modes, each of which is characterized by a certain angular dependence. The perturbation that the scattering body introduces in the field of the primary wave at large distances from the scatterer manifests itself by a shift γ_n in the phase of the radial dependence associated with the nth angular dependence. The phase shifts γ_n are entirely determined by the boundary conditions and are, in general, complex quantities. Their knowledge permits the determination of the amount of scattered radiation and of its angular distribution. The phase shift analysis is outlined in the following; further details may be found in the literature (Lowan et al, 1946; Lax and Feshbach, 1948).

It was previously found that when a plane wave $\psi^i = e^{ikx}$ propagates perpendicularly to the axis of a cylinder on whose surface an impedance boundary condition holds, then the scattered field is given by:

$$\psi^s = -\sum_{n=0}^{\infty} \epsilon_n i^n \frac{J_n'(ka) + i(C - iD)J_n(ka)}{H_n^{(1)'}(ka) + i(C - iD)H_n^{(1)}(ka)} H_n^{(1)}(k\rho) \cos n\phi , \tag{2.72}$$

where C and D are real quantities. In the acoustical case, ψ^i and ψ^s are velocity potentials and $C - iD = \omega\delta/(\zeta k)$ is the relative (or specific) acoustic admittance of the surface of the cylinder; the density δ and the normal acoustic impedance ζ were defined in section 2.1. In the electromagnetic case, if $\underline{E}^i$ is parallel to the cylinder axis then $\psi^i = E_z^i$, $\psi^s = E_z^s$, and $C - iD = Z^{-1}\sqrt{\mu/\epsilon}$ is the relative surface

admittance, whereas for $\underline{H}^i$ parallel to the axis, one has that $\psi^i = H_z^i$, $\psi^s = H_z^s$, and $C - iD = Z\sqrt{\epsilon/\mu}$ is the relative surface impedance.

Formula (2.72) may be rewritten in the form:

$$\psi^s = -\sum_{n=0}^{\infty} \epsilon_n i^{n+1} e^{-i\gamma_n} \sin\gamma_n H_n^{(1)}(k\rho) \cos n\phi \ , \tag{2.73}$$

where the phase shifts γ_n are given by:

$$\gamma_n = \delta_n - \frac{\pi}{2} + \arctan\left\{U_n - i(C - iD)T_n\right\} \ , \tag{2.74}$$

with

$$\begin{aligned} U_n &= \tan(\delta'_n - \delta_n + \tfrac{\pi}{2}) \ , & T_n &= \frac{\pi ka}{2}\left\{J_n^2(ka) + N_n^2(ka)\right\} \ , \\ \delta_n &= \arctan\left(-\frac{J_n(ka)}{N_n(ka)}\right) \ , & \delta'_n &= \arctan\left(-\frac{J'_n(ka)}{N'_n(ka)}\right) \ . \end{aligned} \tag{2.75}$$

Similarly, the diffracted field is given by

$$\psi = \psi^i + \psi^s = \sum_{n=0}^{\infty} \epsilon_n i^n e^{-i\gamma_n}\left\{\cos\gamma_n J_n(k\rho) + \sin\gamma_n N_n(k\rho)\right\} \ , \tag{2.76}$$

and the total scattering cross section per unit length by:

$$\sigma_{total} = \frac{1}{k}\sum_{n=0}^{\infty} \epsilon_n \left\{1 - 2e^{2\,\mathrm{Im}\gamma_n}\cos(2\,\mathrm{Re}\gamma_n) + e^{4\,\mathrm{Im}\gamma_n}\right\} \ . \tag{2.77}$$

In particular, when $\underline{E}^i$ is parallel to the axis of a conducting cylinder one finds that $\tan\gamma_n = \tan\delta_n$, so that relation (2.77) reduces to the form (2.71).

The quantities δ_n, U_n and T_n which appear in (2.74) can be computed without specifying the impedance at the surface of the cylinder. Lax and Feshbach (1948) published tables of T_n and U_n for the parameter values n = 0(1)20 and

ka = 0(0.1)10, whereas δ_n, δ'_n and $\sqrt{\{J_n^2(ka)+N_n^2(ka)\}}$ had been previously tabulated by Lowan and associates (1946) for the same values of n and ka. Tables of $\sqrt{\{J_n^2(ka)+N_n^2(ka)\}}$ for n = 0, 1 and ka = 0(0.2)16 may be found in the book by Watson (1922).

The phase shift analysis is obviously not limited to cylindrical scatterers. For example, Lowan (1946) and Lax and Feshbach (1948) also carried out extensive computations for absorption and scattering by spheres. Finally, the method can be applied to the more general case in which the impedance on the surface of the scatterer varies with the direction of incidence, by associating with the nth angular dependence a quantity $(C_n - iD_n)$ which is a function of the summation index n.

This section ends with a few remarks on the scattering of cylindrical and spherical waves. If a line source parallel to the cylinder axis is located at $(\rho = b, \phi = \pi)$, then the incident cylindrical wave is given by (Stratton, 1941)*:

$$\psi^i(\rho,\phi) = A H_o^{(1)}(kR)$$

$$= \begin{cases} A \sum_{n=0}^{\infty} \epsilon_n (-1)^n H_n^{(1)}(kb) J_n(k\rho) \cos n\phi , & \rho < b , \\ A \sum_{n=0}^{\infty} \epsilon_n (-1)^n J_n(kb) H_n^{(1)}(k\rho) \cos n\phi , & \rho > b , \end{cases} \qquad (2.78)$$

where $R = (\rho^2 + b^2 + 2b\rho\cos\phi)^{1/2}$. For a comparison with the case of plane wave incidence in which $\psi^i = e^{ikx}$, it is useful to choose $A = 1/H_o^{(1)}(kb)$, so that in both cases ψ^i is equal to unity along the cylinder axis. The scattered wave may be written in the form:

* Formulas (26) and (27) of Adey (1958) contain some misprints.

$$\psi^s(\rho,\phi) = -A\sum_{n=0}^{\infty} \epsilon_n (-1)^n \frac{\Omega J_n(ka)}{\Omega H_n^{(1)}(ka)} H_n^{(1)}(kb) H_n^{(1)}(k\rho)\cos n\phi \ , \qquad (2.79)$$

where

$$\Omega = 1 \quad \text{for} \quad \psi\Big|_{\rho=a} = 0 \ , \qquad \Omega = \frac{d}{d(ka)} \quad \text{for} \quad \frac{\partial\psi}{\partial\rho}\Big|_{\rho=a} = 0 \ ,$$

and the coefficients have been determined by imposing the boundary condition on the surface $\rho = a$ of the cylinder. However, these calculations are sometimes unnecessary, since many results concerning the scattering of a cylindrical wave can be derived from the known results for the scattering of a plane wave. Thus, if the field at the point ($\rho = b$, $\phi = 0^o$ ($\phi = 180^o$)) due to a plane wave propagating in the direction $\phi = 0^o$ is known, then, on the basis of the reciprocity theorem, the far field in the direction $\phi = 180^o$ due to a line source at ($\rho = b$, $\phi = 0^o$ (or 180^o)) is also known (Adey, 1958). Furthermore, it is shown by Kodis (1950, 1952) that if the line source is sufficiently far from the cylinder and this is not too large, namely if

$$a^2/(2b^2) \ll 1$$

then the scattered field is essentially equal to that produced by an incident plane wave $\psi^i = e^{ikz}$, whereas the incident field may be taken as equal to $e^{ik(R-b)}$. A few patterns of the far field amplitude of the pressure wave scattered by a rigid cylinder were computed by Faran (1953) for different values of kb. Faran concluded that one should expect little change from the plane wave scattering pattern, provided that $a/b < 0.1$. Zitron and Davis (1963) computed a quantity proportional to the amplitude of the far scattered field as a function of ϕ, for ka = 1.0 with kb = 2, 5, 10, 20; ka = 3.4 with kb = 6.8, 13.6, 17, 68; and ka = 10.0 with kb = 100, 200, 500, for both Dirichlet and Neumann boundary conditions; they also pointed out that Faran's curve for kb = 6.8 is incorrect. In the case of the hard cylinder, other results

were published by Shenderov (1961), who plotted the amplitudes of both scattered and total far fields as functions of ϕ for ka = 2, 6, 10 and b = 1.2a, and compared numerical and experimental diagrams of the amplitude of the total far field for ka = 6, 10 and b = 5.2a.

Finally, since the entire following section is devoted to the case of dipole sources, we here limit ourselves to pointing out that useful relationships exist between the current distributions on perfectly conducting cylinders of arbitrary cross section (in particular, circular), illuminated by plane or spherical waves. These relationships were established by Brick (1961), who utilized integral equations for the electromagnetic field put into an appropriate form by means of a Fourier integral operation, and obtained the leading terms of series expansions in powers of $(kR_o)^{-1}$ by the method of steepest descents. Brick's results are thus valid for $kR_o \gg 1$, where R_o is the distance between the source point and that point of the cylinder axis which belongs to the azimuthal plane containing the observation point.

2.3 Dipole Sources

In this section, we consider scattering from infinite cylinders when the excitation is an elementary source, i.e., an infinitesimal dipole, located at a finite distance from the cylinder. Although some results are included for the case when the dipole is on the surface of the cylinder, the subject of radiating slots, and the equivalence of slots and dipoles, is not treated. The reader is referred to the exhaustive treatment of Wait (1959) which also has an extensive bibliography. Our concern here is with sources off the cylinder and the limiting case is touched on only briefly for comparison.

In 1943 there appeared two independent treatments of the problem of scattering of dipole fields by cylinders, Oberhettinger's and Carter's. Oberhettinger derived the exact field scattered by a cylinder with the electric dipole oriented parallel to the cylinder axis and also presented far field asymptotic approximations. Carter used the reciprocity theorem and the results for plane wave incidence to calculate the scattered far field for dipoles and arrays of dipoles.

There are a variety of methods for deriving the expressions for the field scattered by an arbitrarily oriented dipole. Although differing in detail, they share two essential features, a representation of the field in terms of electric and magnetic Hertz vectors and, ultimately, satisfying boundary conditions on the surface by suitably matching the scattered part of the Hertz vectors with the incident field through the expansion

$$\frac{e^{ikR}}{R} = \frac{i}{2}\sum_{n=0}^{\infty} \epsilon_n \cos n(\phi - \phi_o) \int_{-\infty}^{\infty} dh \left\{ J_n(\lambda\rho_<) H_n^{(1)}(\lambda\rho_>) e^{-ih(z-z_o)} \right\} ,$$

where

$$\rho_< = \min(\rho, \rho_o) ,$$

$$\rho_> = \max(\rho, \rho_o) ,$$

$$\lambda = \sqrt{k^2 - h^2} .$$

The process is completely analogous to that employed earlier in the case of plane wave incidence (cf. Eq. 2.28) though more cumbersome due to the integration over h. Here, as before, some special cases offer inviting simplification, e.g. when the dipole is parallel to the axis of the cylinder and one Hertz vector suffices to represent the entire field (this is the case treated by Oberhettinger (1943); see also Wait (1959) and Harrington (1961)). It is also possible to construct the field due to an arbitrarily oriented dipole by suitably operating on the field scattered by an arbitrarily incident plane wave (Senior, 1953). The resulting expressions, regardless of the method used to obtain them, are cumbersome and the elegance exhibited by any particular method is usually compensated by an atrocious calculation equivalent to matching coefficients in expansions of the incident and scattered fields.

In treating scattering problems when the source is an arbitrarily oriented dipole or distribution of dipoles (e.g. current), it is now fashionable to employ the dyadic Green's function, e.g. Morse and Feshbach (1953), Van Bladel (1964) and Tai (1953, 1954a, b). This procedure enables one to formally discuss the solutions of scattering problems without actually calling into play the inevitable complicated representation of solutions of particular problems. Of course, if it is these particular solutions which are sought, then the tensor or dyadic Green's function, as a labor saving device, loses much of its value. Still it does provide a systematic way of presenting the results and a brief discussion will be given followed by the explicit representation of the dyadic Green's function for a cylinder with a number of special cases.

If the time harmonic Maxwell's equations for a current source $\underline{J}$ at a finite distance from a perfectly conducting scatterer S, are written

$$\begin{aligned} \nabla\wedge\underline{E} &= i\omega\mu\underline{H} \ , \\ \nabla\wedge\underline{H} &= -i\omega\epsilon\underline{E}+\underline{J} \ , \end{aligned} \tag{2.80}$$

then the electric field satisfies the inhomogeneous vector wave equation

$$\nabla\wedge\nabla\wedge\underline{E}-k^2\underline{E} = i\omega\mu\underline{J} \ ,$$

the boundary condition

$$\hat{n}\wedge\underline{E}\Big|_S = 0 \ ,$$

and the radiation condition

$$r\wedge\nabla\wedge\underline{E}+ik\underline{E} = o(1/r) \ . \tag{2.81}$$

If V denotes the volume exterior to S, then the solution of the problem may be written as

$$\underline{E}(\underline{r}) = i\omega\mu \int_V \underline{\underline{G}}(\underline{r}, \underline{r}_1) \cdot \underline{J}(\underline{r}_1) d\underline{r}_1 \tag{2.82}$$

where $\underline{\underline{G}}(\underline{r}, \underline{r}_1)^*$ is the dyadic Green's function and satisfies

$$\nabla \wedge \nabla \wedge \underline{\underline{G}} - k^2 \underline{\underline{G}} = \delta(\underline{r} - \underline{r}_1) \underline{\underline{I}} \ ,$$

$\underline{\underline{I}}$ is the identity dyad,

$$\hat{n} \wedge \underline{\underline{G}} \Big|_S = 0 \ ,$$

$$\underline{r} \wedge \nabla \wedge \underline{\underline{G}} + ik\underline{\underline{G}} = o(1/r) \ .$$

The nine rectangular Cartesian components of the Green's tensor are nothing else than the total electric field components for electric dipole sources oriented along the coordinate axes. That is, if $i\omega\mu\underline{J}$ is chosen to be $\hat{i}_x \delta(\underline{r}_1 - \underline{r}_o)$ then equation (2.82) yields

$$\underline{E}(\underline{r}, \underline{r}_o) = \underline{\underline{G}}(\underline{r}, \underline{r}_o) \cdot \hat{i}_x \ .$$

If we use a superscript x to denote the orientation of the dipole source, i.e.

$$\underline{E}^x(\underline{r}) = \underline{\underline{G}}(\underline{r}, \underline{r}_o) \cdot \hat{i}_x \ ,$$

then clearly

$$\underline{E}^y(\underline{r}) = \underline{\underline{G}}(\underline{r}, \underline{r}_o) \cdot \hat{i}_y \ ,$$

$$\underline{E}^z(\underline{r}) = \underline{\underline{G}}(\underline{r}, \underline{r}_o) \cdot \hat{i}_z \ .$$

Thus we see that it is possible to construct the components of the dyadic Green's

* A double underlining will be used to denote dyads.

function if we know the response of an arbitrarily oriented dipole source. In fact, these are entirely equivalent pieces of information.

For a perfectly conducting infinite cylinder the dyadic Green's function is given by Tai (1954b) as

$$\begin{aligned}\underline{\underline{G}}(\underline{r},\underline{r}_1) = \frac{i}{8\pi}\int_{-\infty}^{\infty} dh \sum_{n=0}^{\infty} \frac{\epsilon_n}{\lambda^2} \Bigg\{ &\underline{\underline{M}}_{en}^{(3)}(h,\underline{r})\left[\underline{\underline{M}}_{en}^{(1)}(-h,\underline{r}_1)+\alpha_n \underline{\underline{M}}_{en}^{(3)}(-h,\underline{r}_1)\right] + \\ &+ \underline{\underline{M}}_{on}^{(3)}(h,\underline{r})\left[\underline{\underline{M}}_{on}^{(1)}(-h,\underline{r}_1)+\alpha_n \underline{\underline{M}}_{on}^{(3)}(-h,\underline{r}_1)\right] + \\ &+ \underline{\underline{N}}_{en}^{(3)}(h,\underline{r})\left[\underline{\underline{N}}_{en}^{(1)}(-h,\underline{r}_1)+\beta_n \underline{\underline{N}}_{en}^{(3)}(-h,\underline{r}_1)\right] + \\ &+ \underline{\underline{N}}_{on}^{(3)}(h,\underline{r})\left[\underline{\underline{N}}_{on}^{(1)}(-h,\underline{r}_1)+\beta_n \underline{\underline{N}}_{on}^{(3)}(-h,\underline{r}_1)\right]\Bigg\}, \quad \text{for } \rho > \rho_1, \end{aligned} \tag{2.83}$$

where

$$\lambda^2 = k^2 - h^2 ,$$

$$\underline{\underline{M}}_{\substack{en\\o}}(h,\underline{r}) = e^{ihz}\left[\mp \frac{n}{\rho} Z_n(\lambda\rho) \begin{matrix}\sin\\\cos\end{matrix} n\phi\,\hat{\rho} - \frac{\partial}{\partial\rho} Z_n(\lambda\rho) \begin{matrix}\cos\\\sin\end{matrix} n\phi\,\hat{\phi}\right] ,$$

$$\underline{\underline{N}}_{\substack{en\\o}}(h,\underline{r}) = \frac{e^{ihz}}{k}\left[ih\frac{\partial}{\partial\rho} Z_n(\lambda\rho) \begin{matrix}\cos\\\sin\end{matrix} n\phi\,\hat{\rho} \mp \frac{inh}{\rho} Z_n(\lambda\rho) \begin{matrix}\sin\\\cos\end{matrix} n\phi\,\hat{\phi} + \right.$$

$$\left. + \lambda^2 Z_n(\lambda\rho) \begin{matrix}\cos\\\sin\end{matrix} n\phi\,\hat{z}\right] ,$$

$$\alpha_n = -\frac{J_n'(\lambda a)}{H_n^{(1)'}(\lambda a)} , \qquad \beta_n = -\frac{J_n(\lambda a)}{H_n^{(1)}(\lambda a)} .$$

The superscript (1) on $\underline{\underline{M}}_{\substack{en\\o}}$ and $\underline{\underline{N}}_{\substack{en\\o}}$ signifies that Z_n is J_n, the Bessel function of the first kind. The superscript (3) means Z_n is the Bessel function of the third kind or Hankel function $H_n^{(1)}$. When $\rho_1 > \rho$, $\underline{r}$ and $\underline{r}_1$ must be interchanged in (2.83).

Equations (2.82) and (2.83) have been employed by Tai (1964) to obtain explicit far field results for two electric dipole orientations, longitudinal and transverse (also called vertical and horizontal dipoles).

The integration in (2.82) is easily accomplished since $\underline{J}$ is always a delta function. The integration in (2.83) is carried out by the method of saddle points (e.g. Wait (1959)). In the results both cylindrical and spherical coordinates are employed, so that the familiar factor e^{ikr}/r is exhibited.

Recall that

$$r = \sqrt{\rho^2 + z^2} \quad ,$$

$$\sin\theta = \frac{\rho}{\sqrt{\rho^2 + z^2}} \quad .$$

a) Longitudinal Dipole

The current is given by

$$\underline{J} = -i\omega\epsilon A \frac{\delta(\rho-\rho_o)\delta(\phi-\phi_o)\delta(z)}{\rho} \hat{z} \, ,$$

where A is a constant ($A = p^{(1)}/\epsilon$, where $p^{(1)}$ is the dipole moment). The total far electric field is (compare with (2.29)):

$$\underline{E} = -\hat{\theta} \frac{e^{ikr}}{4\pi r} k^2 \sin\theta A \left\{ e^{-ik\rho_o \sin\theta \cos(\phi-\phi_o)} - \sum_{n=0}^{\infty} \epsilon_n (-i)^n \frac{J_n(ka\sin\theta)}{H_n^{(1)}(ka\sin\theta)} \times \right.$$

$$\left. \times H_n^{(1)}(k\rho_o \sin\theta)\cos n(\phi-\phi_o) \right\} . \qquad (2.84)$$

The far field of a longitudinal dipole in an azimuthal plane (constant θ, $0 \leqslant \phi < 2\pi$, see Fig. 2-14) is proportional to the far field of a line source (radiating at a longer wavelength) parallel to the cylinder through (ρ_o, ϕ_o) (see equations (2.78) and (2.79) where $\rho_o = b$, $\phi_o = \pi$). If the dipole radiates with wave number k, the equivalent

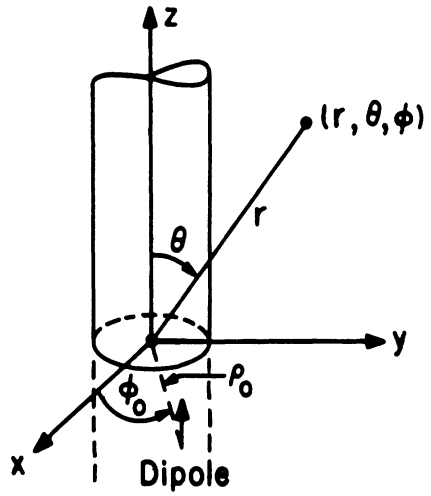

FIG. 2-13

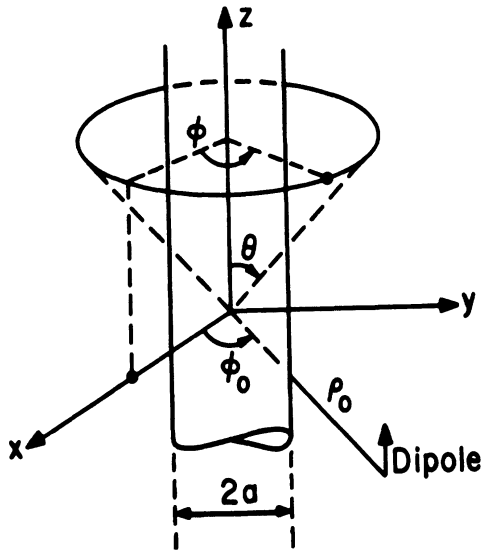

FIG. 2-14

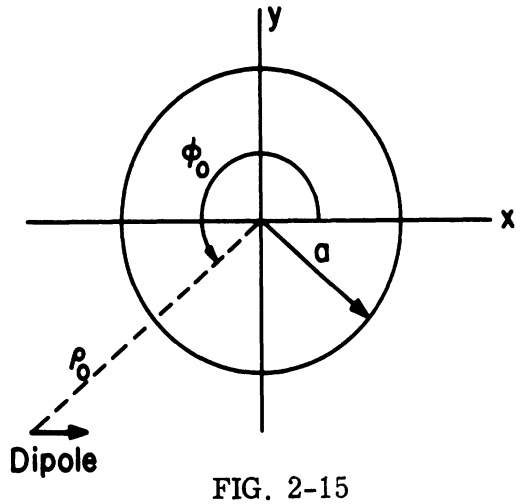

FIG. 2-15

line source radiates with wave number $k\sin\theta$. In the plane of the dipole ($\theta = \pi/2$) the wave numbers are equal. Explicitly, the far field of an electric line source parallel to the cylinder axis ($\underline{E}^i = \hat{i}_z A H_o^{(1)}(k\sqrt{\rho^2 + \rho_o^2 - 2\rho\rho_o\cos(\phi - \phi_o)}\,)$ is:

$$\underline{E} = \hat{i}_z \frac{e^{ik\rho - \frac{i\pi}{4}}}{\sqrt{k\rho}} \sqrt{2/\pi}\, A \left\{ e^{-ik\rho_o\cos(\phi-\phi_o)} - \right.$$

$$\left. - \sum_{n=0}^{\infty} \epsilon_n (-i)^n \frac{J_n(ka)}{H_n^{(1)}(ka)} H_n^{(1)}(k\rho_o)\cos n(\phi - \phi_o) \right\} . \qquad (2.84a)$$

The field of an array of longitudinal dipoles of strength A_ℓ at points (ρ_ℓ, ϕ_ℓ), all in the plane $z_o = 0$ is given by

$$\underline{E} = -\hat{\theta} \frac{e^{ikr}}{4\pi r} \sin\theta\, k^2 \sum_\ell A_\ell \left\{ e^{-ik\rho_\ell \sin\theta\cos(\phi - \phi_\ell)} - \right.$$

$$\left. - \sum_{n=0}^{\infty} \epsilon_n (-i)^n \frac{J_n(ka\sin\theta)}{H_n^{(1)}(ka\sin\theta)} H_n^{(1)}(k\rho_\ell \sin\theta)\cos n(\phi - \phi_\ell) \right\} \qquad (2.85)$$

Note that to this order in $1/r$ only E_θ is nonzero.

b) Transverse Dipole

$$\underline{J} = -i\omega\epsilon A \frac{\delta(\rho - \rho_o)\,\delta(\phi - \phi_o)\,\delta(z)}{\rho} \hat{x} .$$

The total far field in the plane of the dipole ($\theta_o = \pi/2$, $z_o = 0$) is

$$\underline{E} = A\frac{e^{ikr}}{4\pi r}k^2\hat{\phi}\left[-\sin\phi\, e^{-ik\rho_o\cos(\phi-\phi_o)} - \frac{1}{2}\sum_{n=0}^{\infty}\epsilon_n(-i)^{n+1}\frac{J_n'(ka)}{H_n^{(1)'}(ka)}\times\right.$$
$$\left.\times\left\{H_{n-1}^{(1)}(k\rho_o)\sin\left[n\phi-(n-1)\phi_o\right] + H_{n+1}^{(1)}(k\rho_o)\sin\left[n\phi-(n+1)\phi_o\right]\right\}\right] . \tag{2.86}$$

The field due to an array of such dipoles of varying strengths, A_ℓ, is

$$\underline{E} = \frac{e^{ikr}}{4\pi r}k^2\hat{\phi}\sum_{\ell}A_\ell\left[-\sin\phi\, e^{-ik\rho_\ell\cos(\phi-\phi_\ell)} - \frac{1}{2}\sum_{0}^{\infty}\epsilon_n(-i)^{n+1}\frac{J_n'(ka)}{H_n^{(1)'}(ka)}\times\right.$$
$$\left.\times\left\{H_{n-1}^{(1)}(k\rho_\ell)\sin\left[n\phi-(n-1)\phi_\ell\right] + H_{n+1}^{(1)}(k\rho_\ell)\sin\left[n\phi-(n+1)\phi_\ell\right]\right\}\right] . \tag{2.87}$$

In this case only E_ϕ is nonzero.

Note that in equations (2.84) to (2.87) the constants A or A_ℓ may be complex, $A_\ell = |A_\ell|e^{i\psi_\ell}$, thus governing both amplitude and phase of the source.

Carter (1943) has carried out a large number of calculations of far field patterns from arrays of longitudinal and transverse dipoles. The problem with which Carter was concerned was that of achieving omnidirectional azimuthal radiation patterns for arrays of dipoles around a cylinder (transmitting antenna on the Chrysler building). His approach was to calculate the radiation patterns of various symmetric arrays of dipoles with a variety of related phase differences between dipoles and then observe which pattern most closely achieved the desired shape. While this may not now be considered the most direct way of treating this problem, the patterns calculated by Carter may prove useful for other purposes.

Carter employed the reciprocity theorem and the known results for plane wave incidence to arrive at the expressions (2.84) to (2.87). This avoided the asymptotic evaluation of the integral in (2.83), since the asymptotics are in a sense already carried out for plane wave incidence. For plane wave incidence Carter has

computed the magnitude of the electric field as a function of distance from the cylinder for $\phi = 0, \pi/2, \pi, 3\pi/2$ and $ka = 1$. He also calculated surface current for this case and this has already been given in Fig. 2-6c. In the case of dipole excitation, Carter has made numerous calculations. For a single longitudinal dipole the magnitude of the electric field in the far zone is given as a function of azimuthal angle in Fig. 2-16 for a dipole .24λ from the cylinder axis and various cylinder radii ($-a/\lambda$ = .0016, .0318, .08, .16, ~.24). Also included in this figure is the pattern of a transverse dipole located .24λ from a cylinder of radius .16λ. The nearly circular pattern for the smallest radius is quite distorted, without any definite relationship between the geometrical shadow and the shape of the pattern. However, for large cylinders the pattern is quite different from the patterns of small cylinders as seen in Fig. 2-17, where the far field is plotted for a longitudinal dipole .878λ from the axis of a cylinder of radius .383λ. Carter attributes this to resonance effects.

Carter's results for arrays of dipoles include longitudinal (vertical) dipoles (1, 2, and 4 fed in phase) located .878λ from the axis of a cylinder of radius .383λ (see Fig. 2-17), and 4 transverse (horizontal) dipoles fed in phase, phase rotation, and pairs in phase, other pairs out of phase (see Figs. 2-18 to 2-20). The transverse dipoles are located .796λ from the axis of a cylinder of radius .637λ. The patterns given here are in the plane containing the dipoles; additional patterns in other planes are contained in Carter's original paper. A word of caution is called for regarding the use of Carter's analytic expressions of the far field. Numerous errors were found in these formulae, e.g. using Carter's equation numbers, terms in equation (48) should alternate in sign, equation (50) is completely incorrect, a factor j is missing from equation (51), terms in equation (55) should alternate in sign, etc. A spot check of the computed patterns, however, indicates that the correct formulas were used and the errors apparently are typographical. A complete recalculation of all the patterns was not undertaken. It is recommended that any quantitative application of Carter's results be accompanied by a suitable verification.

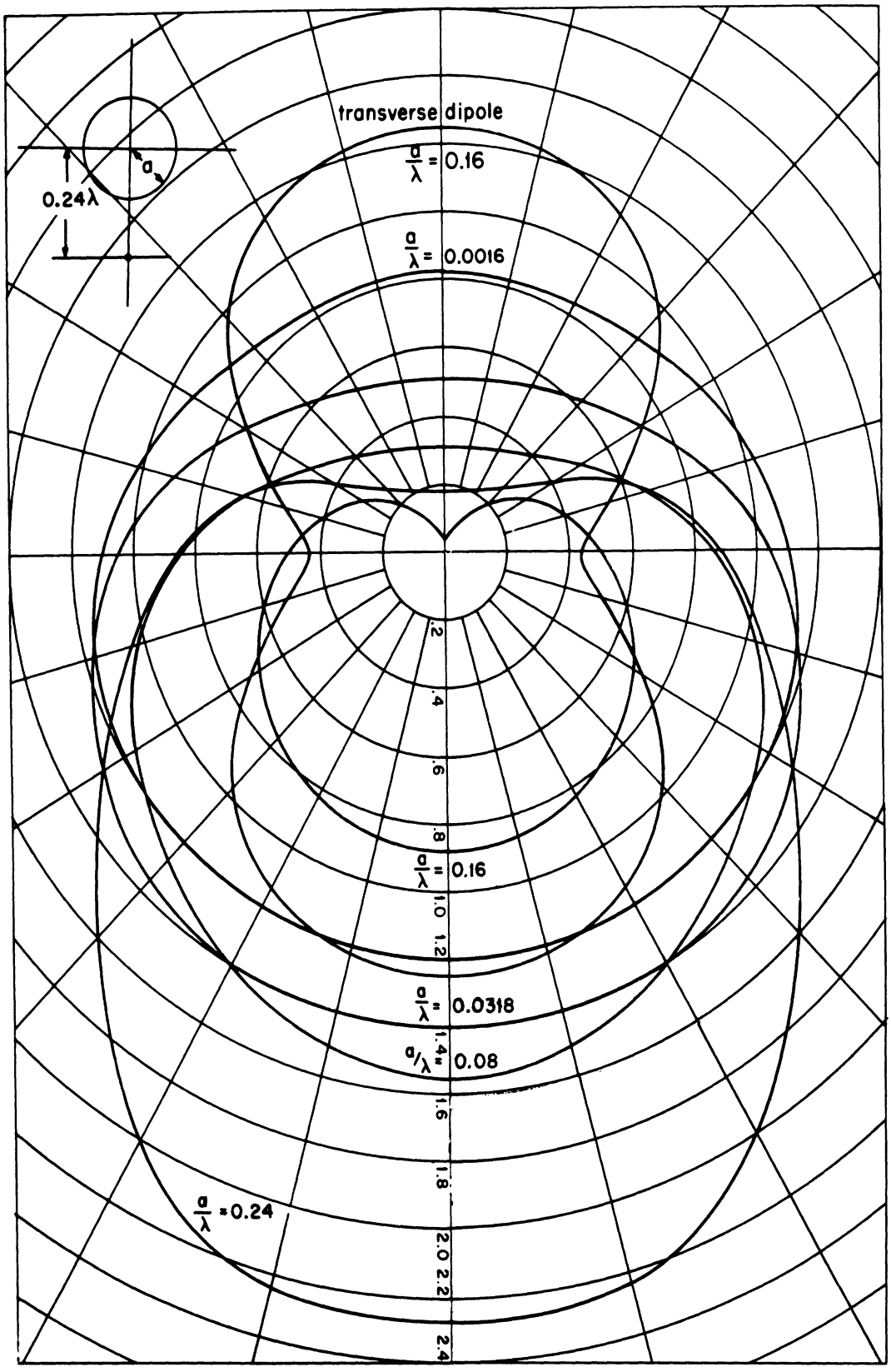

FIG. 2-16: FAR-ZONE ELECTRIC FIELD PATTERN IN THE AZIMUTHAL PLANE; All curves except one are for dipoles parallel to the cylinder axis (Carter, 1943).

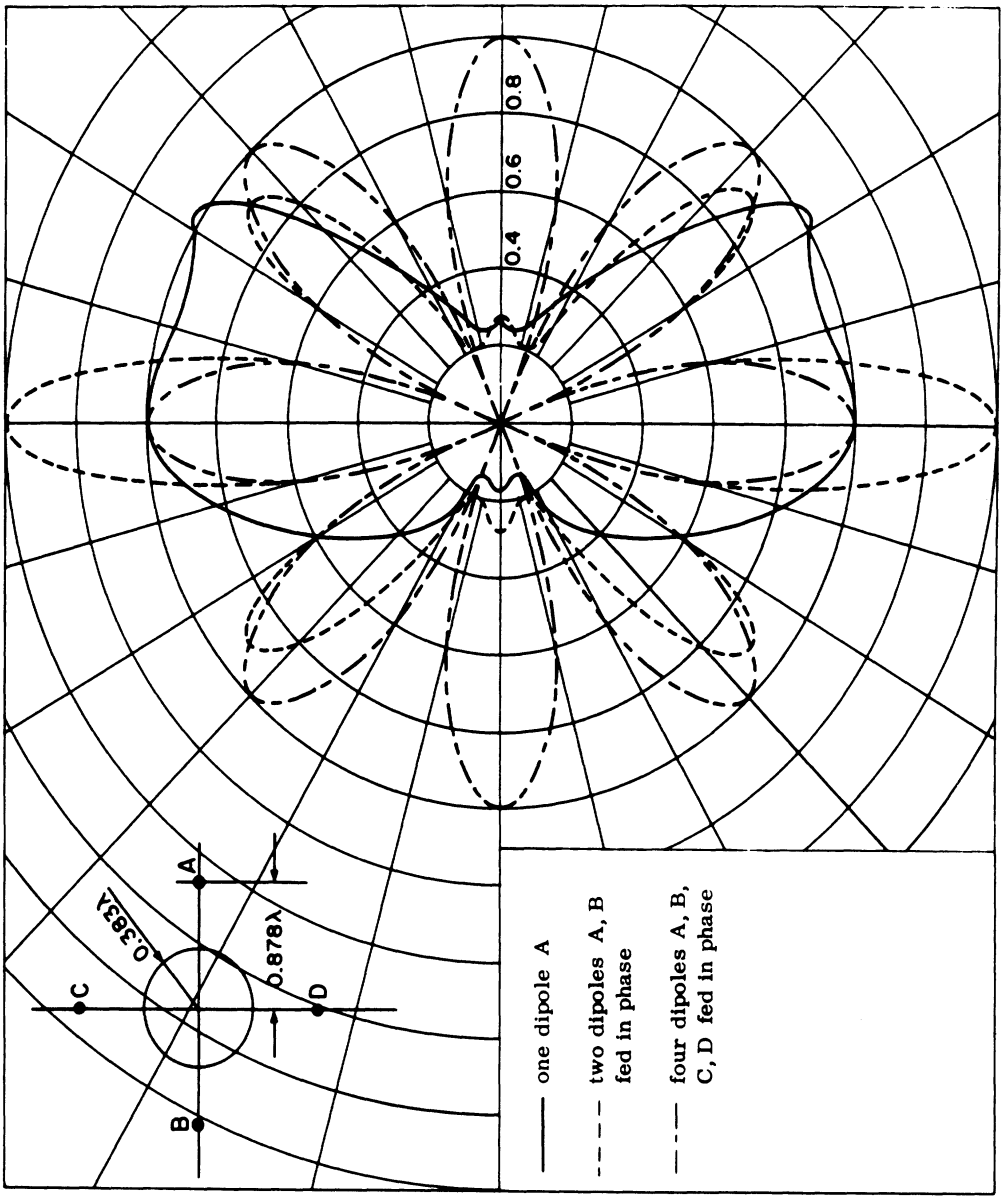

FIG. 2-17: FAR-ZONE ELECTRIC FIELD PATTERN IN THE AZIMUTHAL PLANE, FOR DIPOLES PARALLEL TO THE CYLINDER AXIS (Carter, 1943).

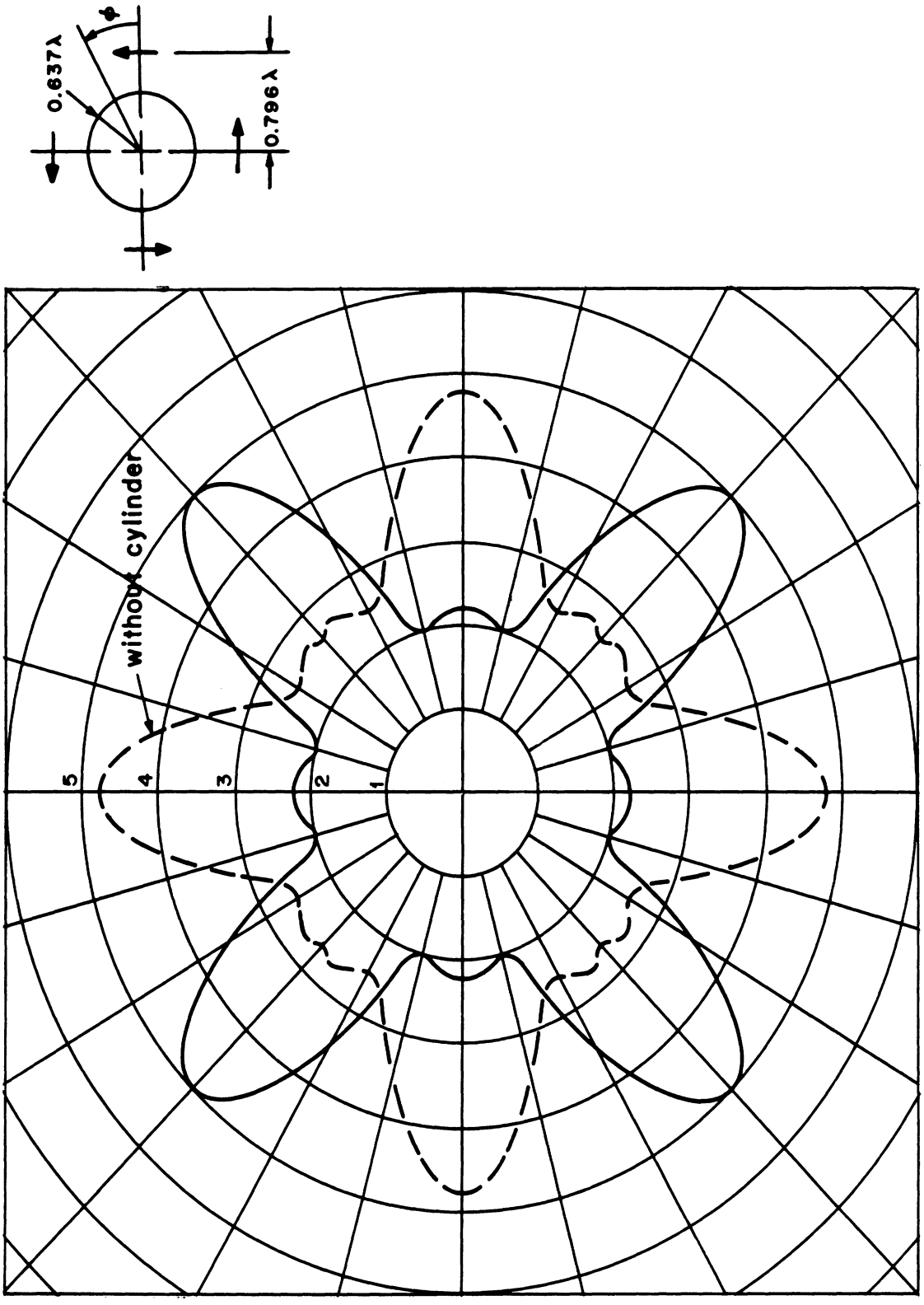

FIG. 2-18: FAR-ZONE ELECTRIC FIELD PATTERN IN THE AZIMUTHAL PLANE, FOR FOUR TRANSVERSE DIPOLES FED IN PHASE (Carter, 1943).

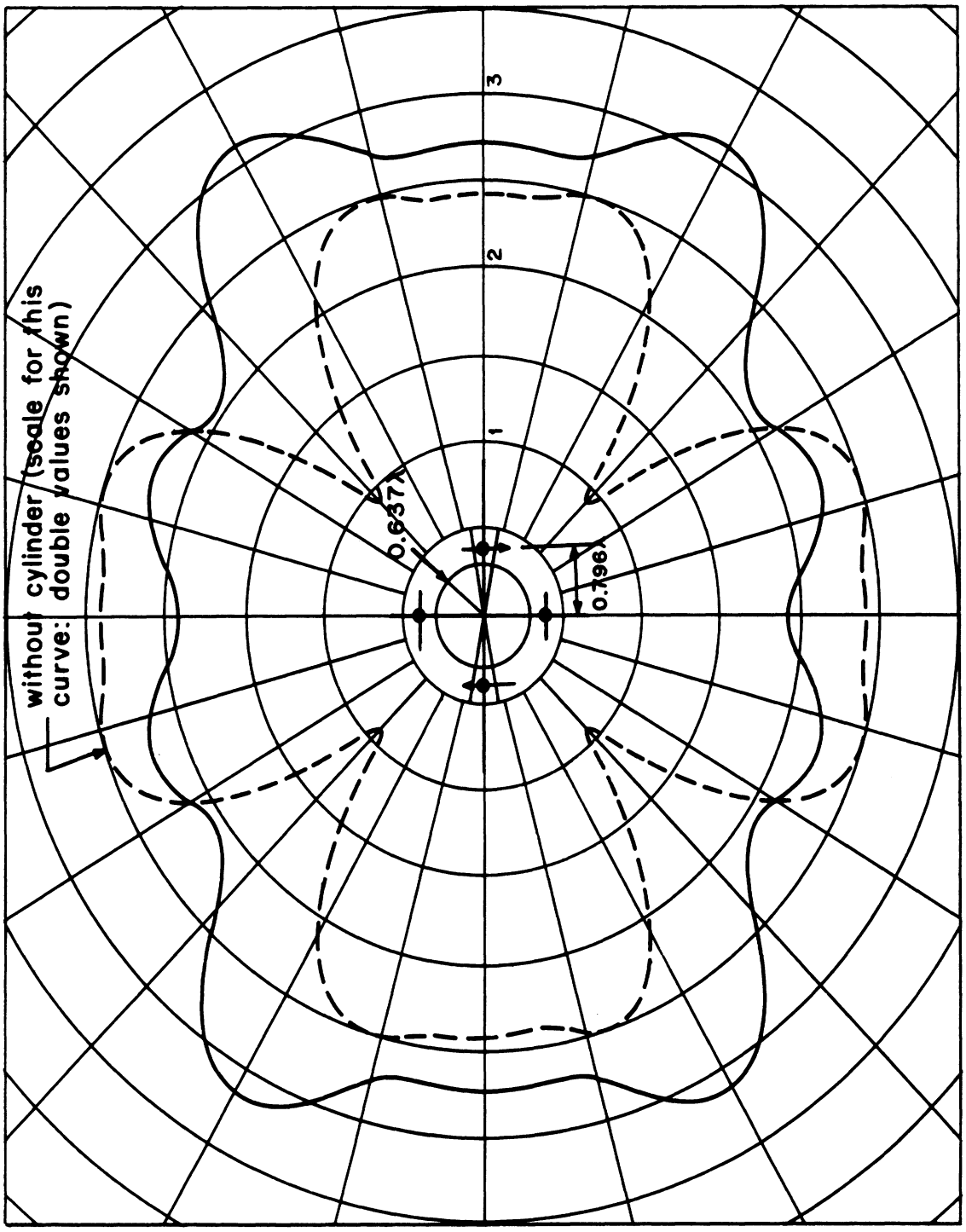

FIG. 2-19: FAR-ZONE ELECTRIC FIELD PATTERN IN THE AZIMUTHAL PLANE, FOR FOUR TRANSVERSE DIPOLES; DIAMETRICALLY OPPOSITE DIPOLES FED IN PHASE, PAIRS IN QUARTER PHASE RELATION (Carter, 1943).

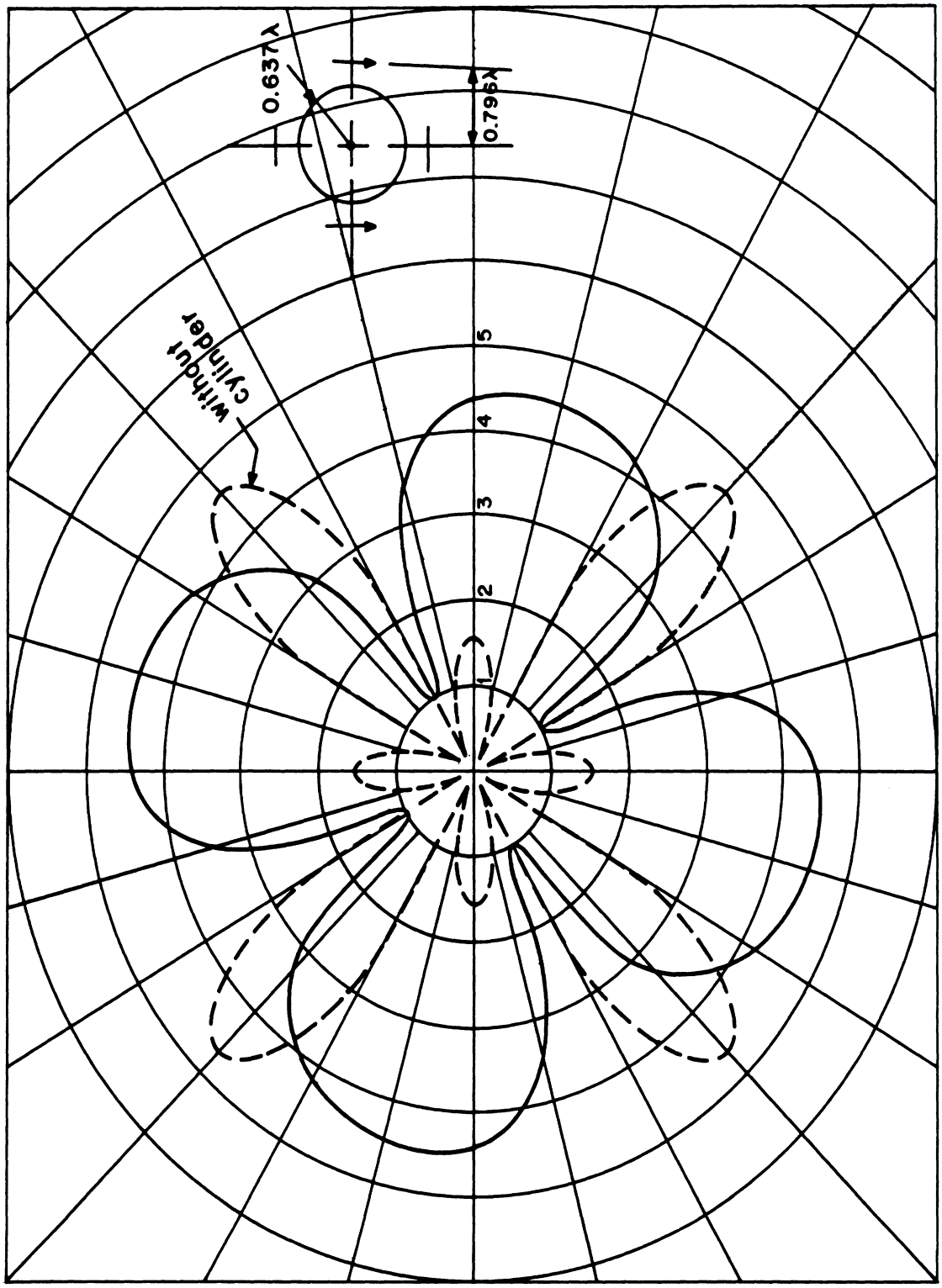

FIG. 2-20: FAR-ZONE ELECTRIC FIELD PATTERN IN THE AZIMUTHAL PLANE, FOR FOUR TRANSVERSE DIPOLES FED IN QUARTER PHASE ROTATION (Carter, 1943).

Lucke (1951) derived the Green's function for a dipole in the presence of a cylinder (both elliptic and circular). The result is contained in (2.83) and shall not be repeated. An earlier version of Lucke's work (1949) contained an error in the expression for the field but this was removed and agreement with Carter's result was obtained. Lucke calculated the scattering pattern (see Fig. 2-21) for a longitudinal dipole located .238λ from the axis of a cylinder of radius .076λ. This is almost identical with one of the cases calculated by Carter and the patterns do coincide. (Lucke's scale is a factor ka = .5 smaller than Carter's and this must be taken into account to obtain agreement).

Sinclair (1951), as Lucke, obtained some results for antennas in the presence of circular cylinders while investigating the more general case of elliptic cylinders. His results agree with Carter and are easily obtained from the expression for the Green's function given in the beginning of this section.

Wait and Okashimo (1956) have calculated radiation patterns of a radial dipole and pairs of diametrically opposite in-phase radial dipoles, located on the surface of a cylinder for cylinder radii a/λ = .0315, .125, .335, .915, 1.54. The patterns were computed from a theoretical result equivalent to (2.86) and (2.87) for special values of ϕ_ℓ ($\phi_0 = 0$ for single dipole and $\phi_0 = 0$, $\phi_1 = \pi$ for the pair). The patterns were compared, with excellent agreement, with the experimental results of Bain (1953) and are presented in Figs. 2-22 and 2-23.

Oberhettinger (1943) computed the far field pattern for an electric dipole parallel to the axis of a cylinder of radius $a = \lambda$. The dipole locations were $5/4\lambda$, $3/2\lambda$, $7/4\lambda$, 2λ from the cylinder axis and the patterns are all in the horizontal plane ($\theta = \pi/2$, see Fig. 2-24). The complexity of the pattern is seen to increase with distance of the dipole from the cylinder.

Levis (1959, 1960) has made extensive calculations of a radial dipole on a cylinder. This corresponds to a transverse dipole as defined in (2.86) when the dipole is normal to the surface of the cylinder as well as its axis, i.e., $\phi_0 = 0$. He has computed the real and imaginary parts of E_θ and E_ϕ as well as their magnitude

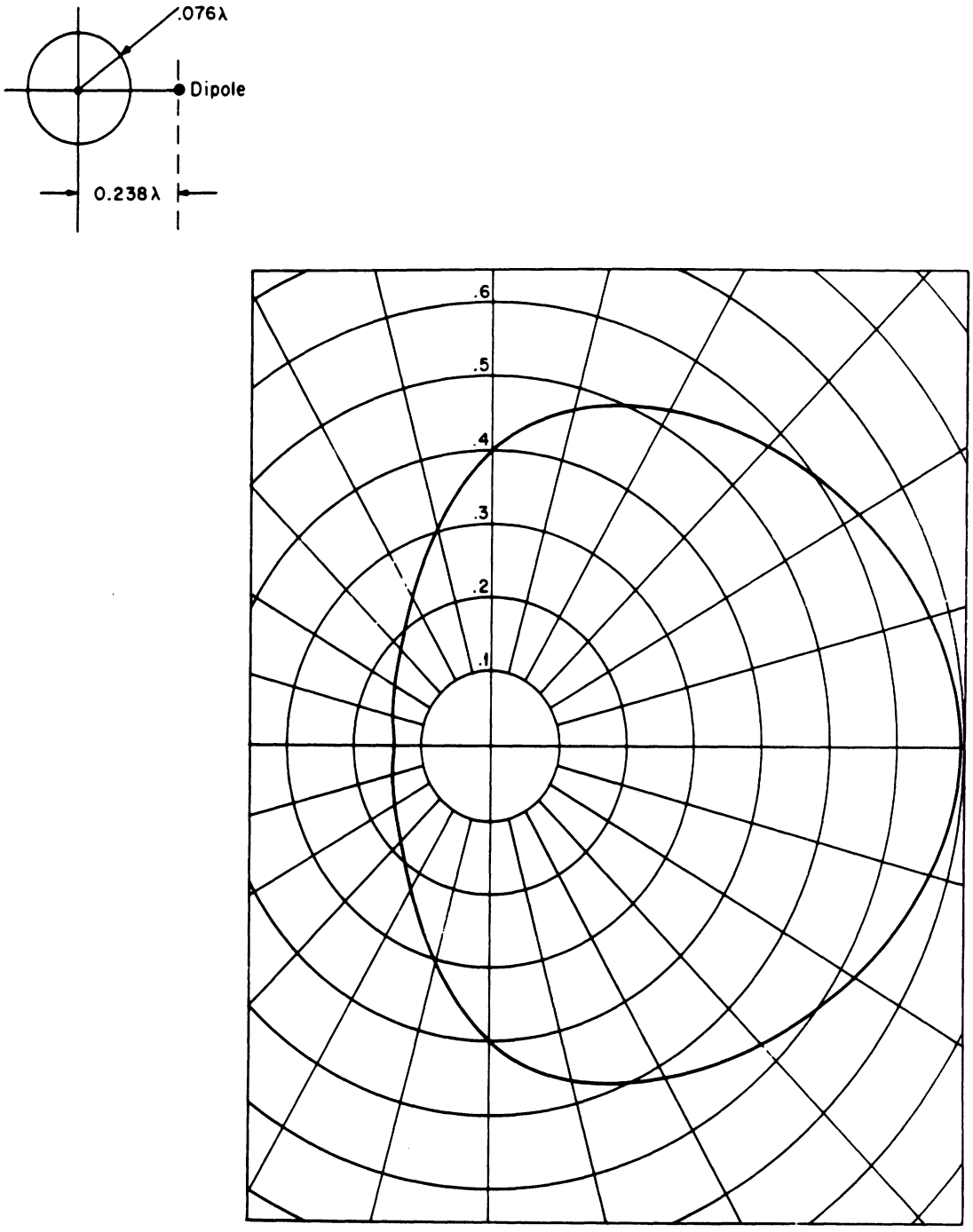

FIG. 2-21: FAR-ZONE ELECTRIC FIELD PATTERN IN THE AZIMUTHAL PLANE, FOR A DIPOLE PARALLEL TO THE CYLINDER AXIS (Lucke, 1951).

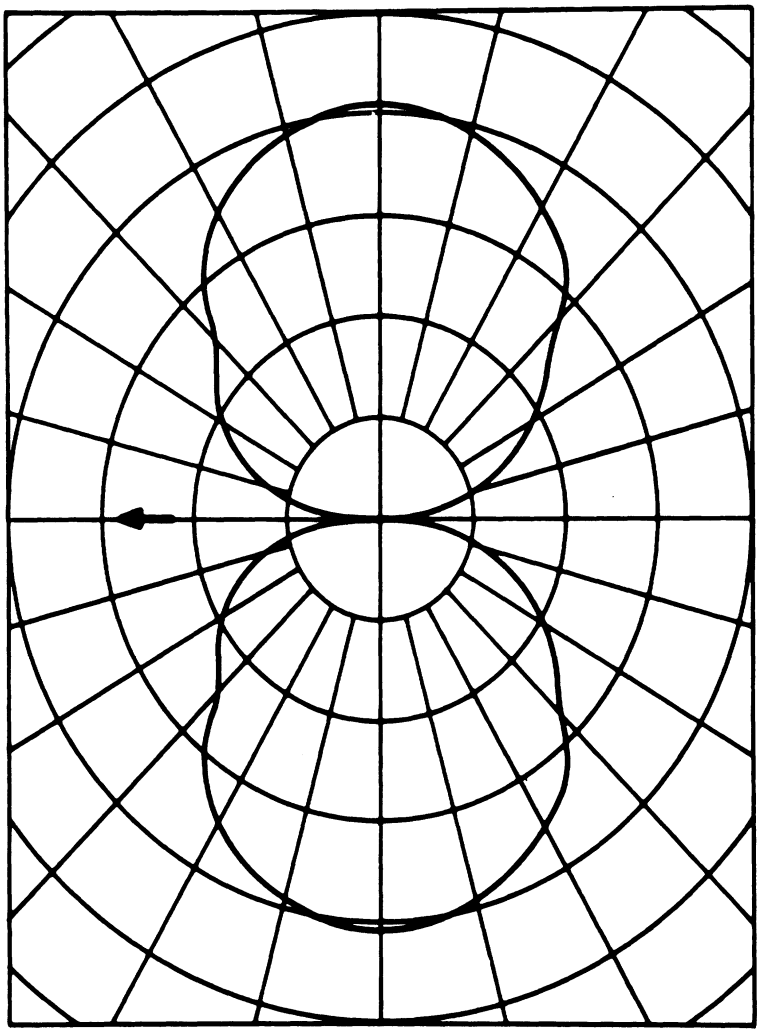

FIG. 2-22a: RADIATION PATTERN (PROPORTIONAL TO THE AMPLITUDE OF THE FAR-ZONE ELECTRIC FIELD) IN THE AZIMUTHAL PLANE, FOR A DIPOLE ON THE CYLINDER AND PERPENDICULAR TO THE CYLINDER AXIS. Case $a/\lambda = 0.0315$ (Wait and Okashimo, 1956).

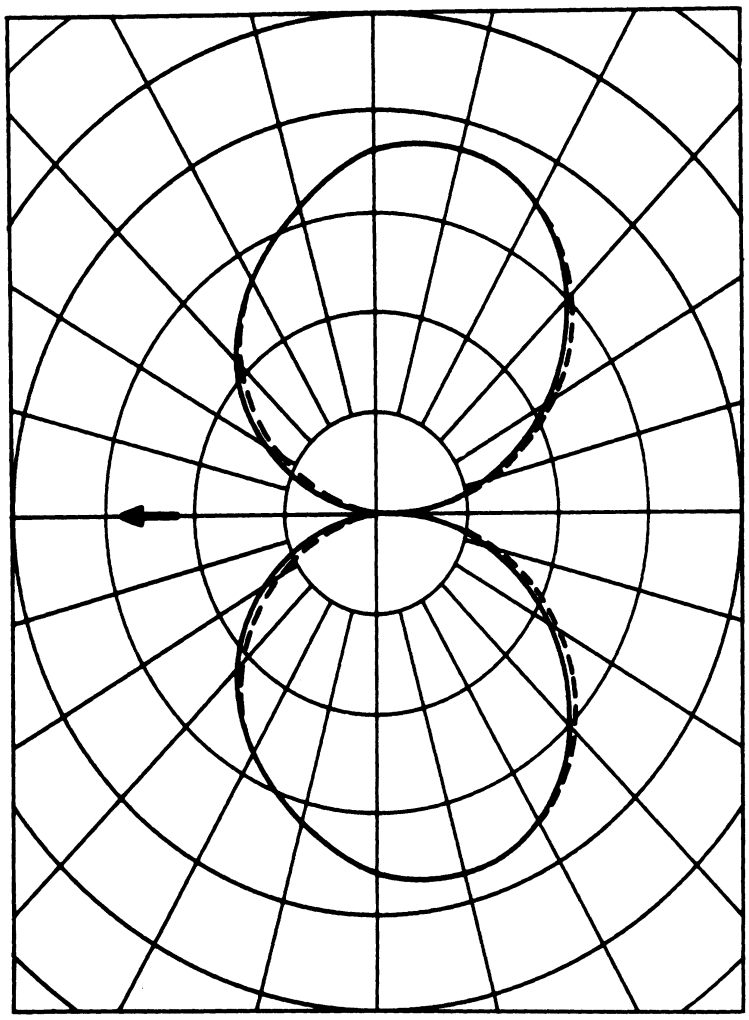

FIG. 2-22b: Case $a/\lambda = 0.125$ (Wait and Okashimo, 1956); – – – experimental (Bain, 1953).

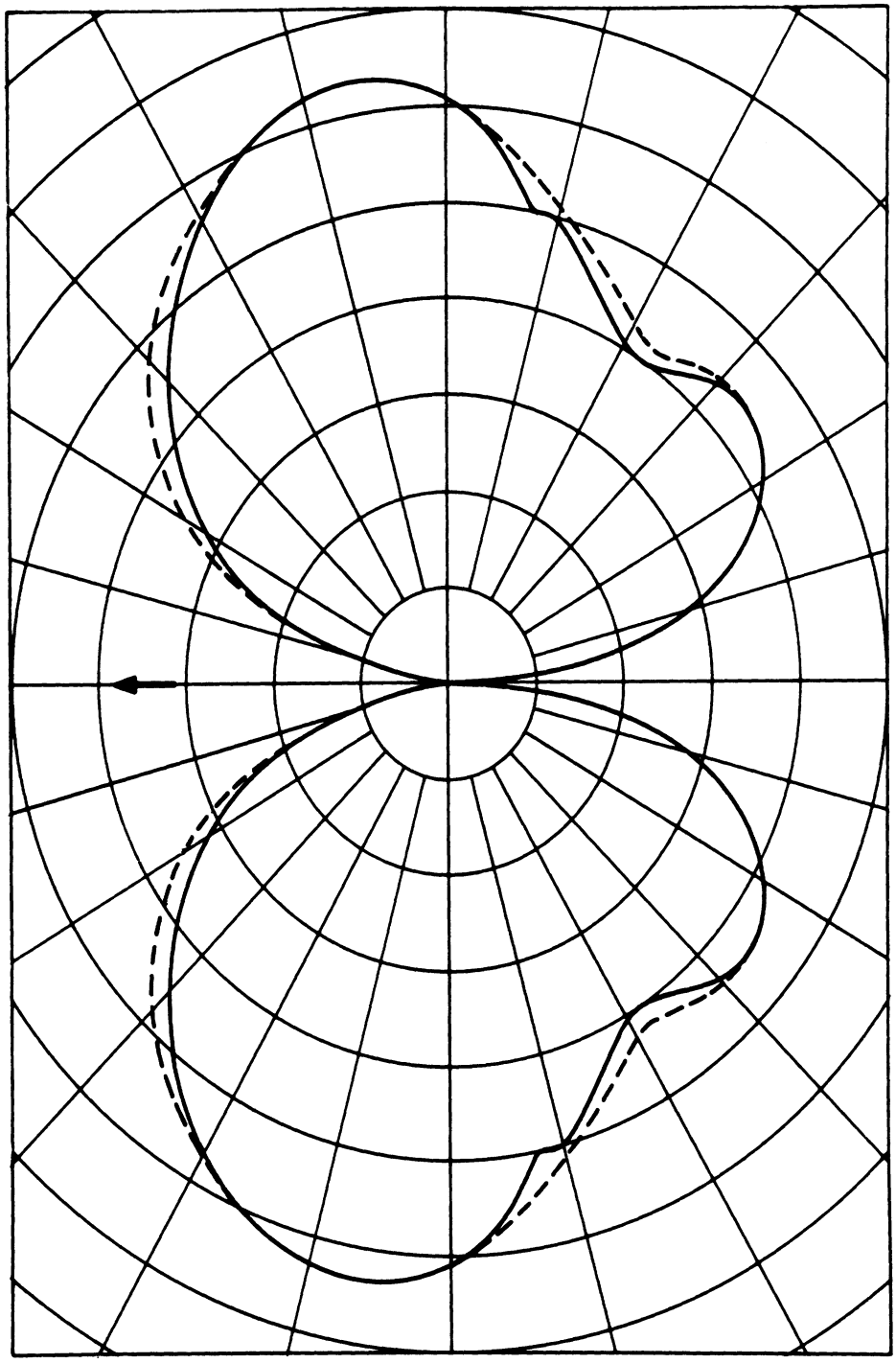

FIG. 2-22c: Case $a/\lambda = 0.335$ (Wait and Okashimo, 1956);
– – – experimental (Bain, 1953).

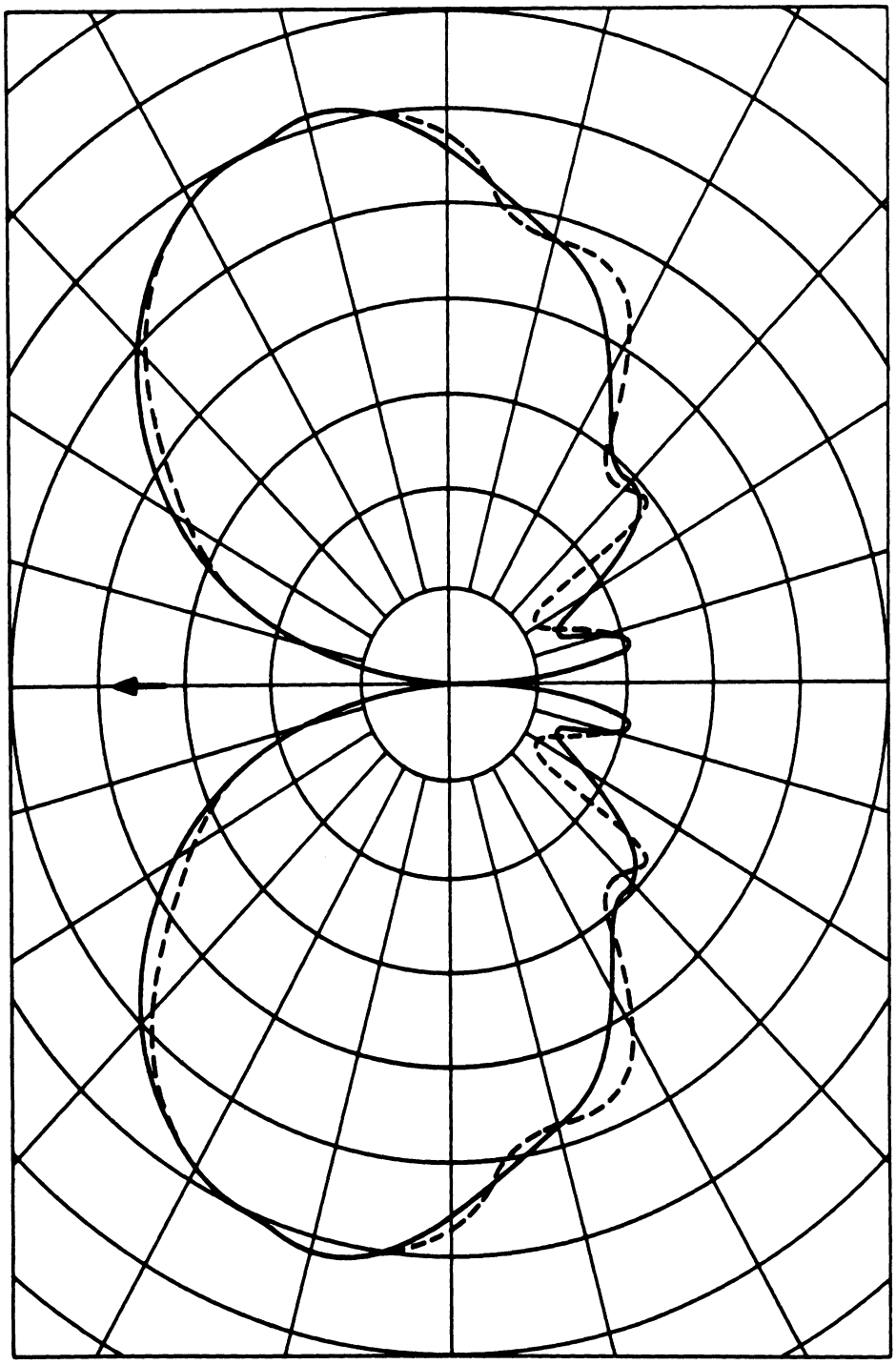

FIG. 2-22d: Case $a/\lambda = 0.915$ (Wait and Okashimo, 1956); – – – experimental (Bain, 1953).

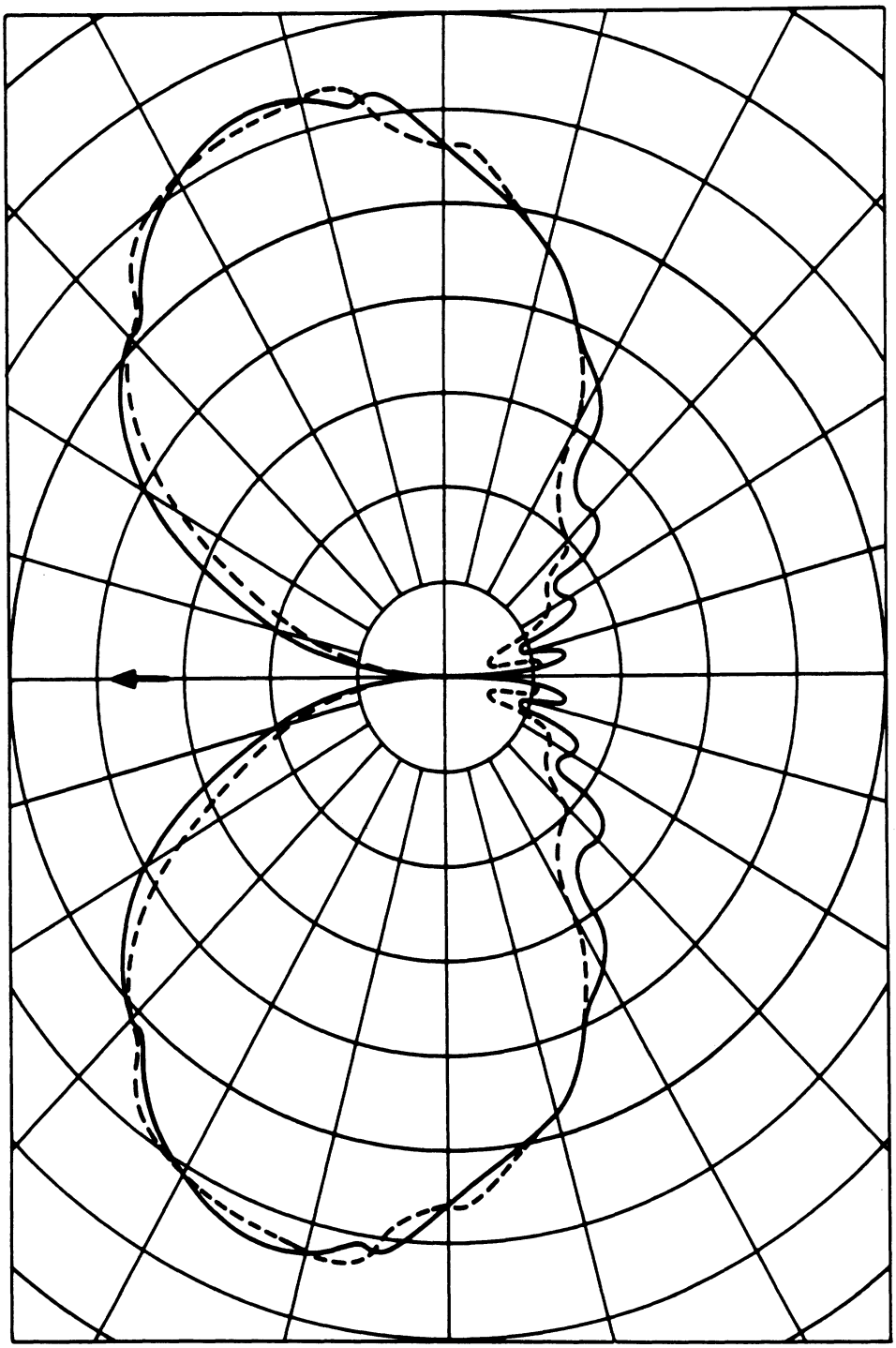

FIG. 2-22e: Case $a/\lambda = 1.54$ (Wait and Okashimo, 1956); – – – experimental (Bain, 1953).

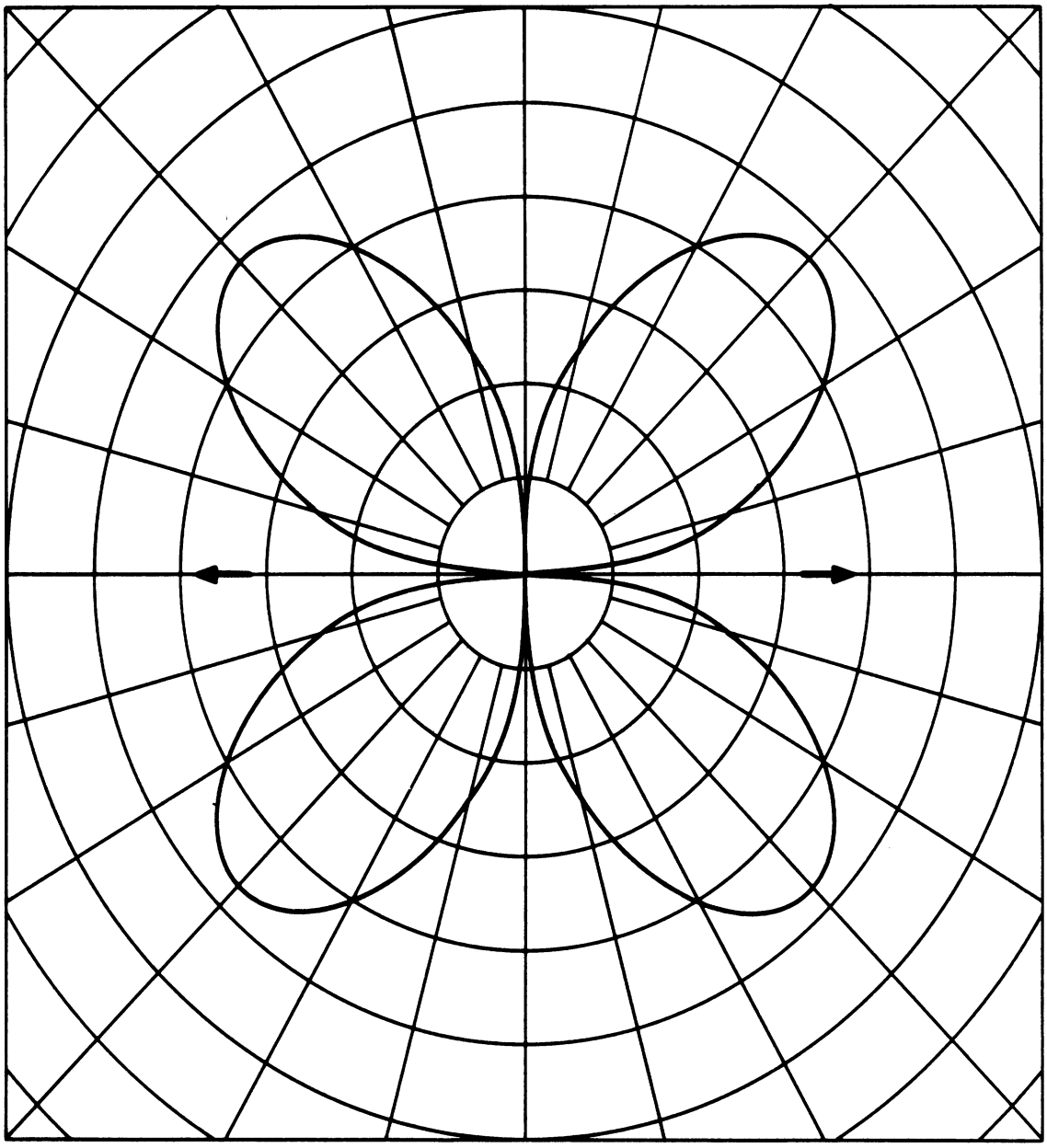

FIG. 2-23a: RADIATION PATTERN (PROPORTIONAL TO $|E_\phi|$) IN THE AZIMUTHAL PLANE, FOR TWO RADIAL DIPOLES DIAMETRICALLY OPPOSITE ON THE CYLINDER SURFACE AND FED IN PHASE.
Case $a/\lambda = 0.0315$ (Wait and Okashimo, 1956).

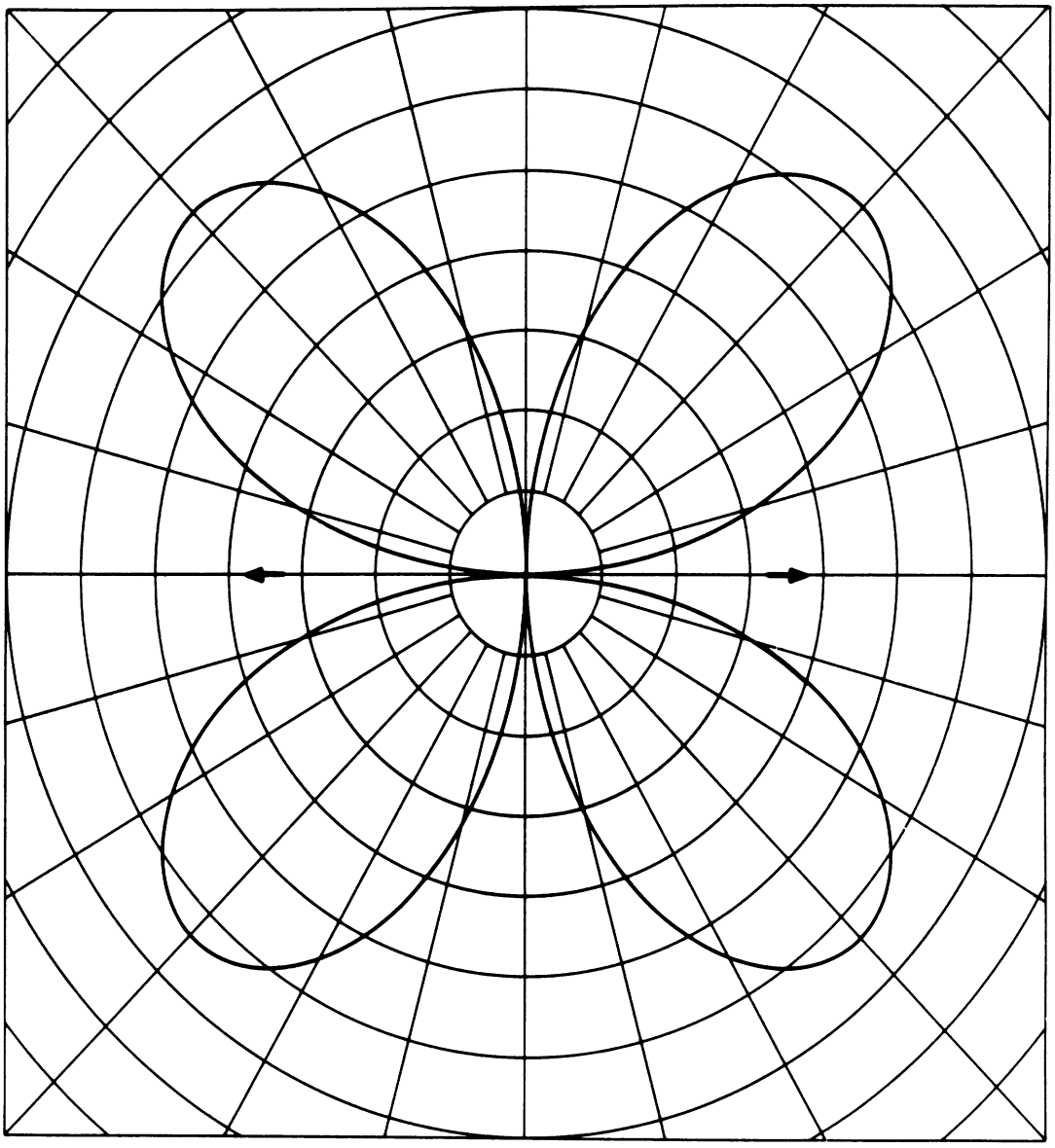

FIG. 2-23b: Case $a/\lambda = 0.125$ (Wait and Okashimo, 1956).

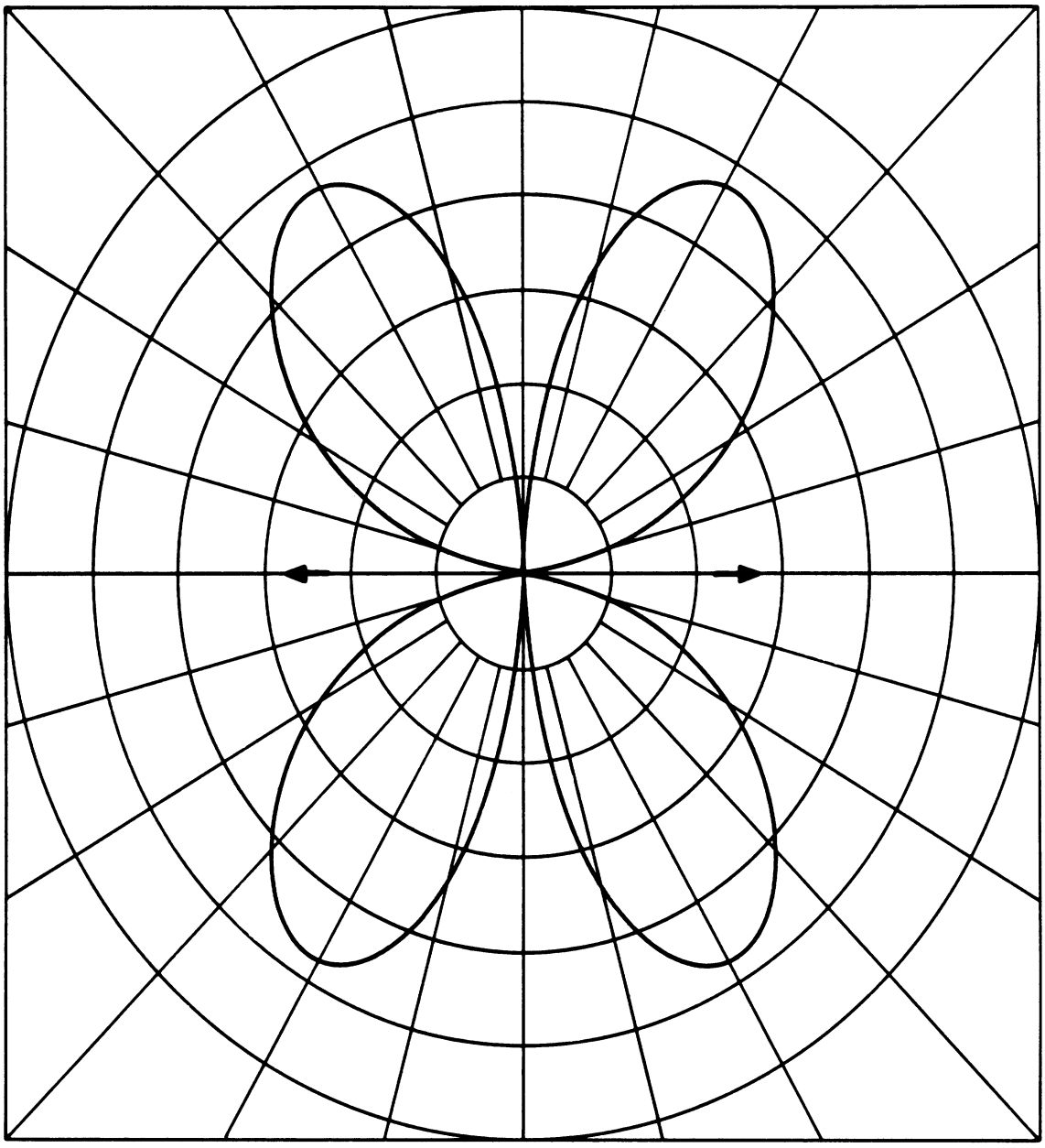

FIG. 2-23c: Case $a/\lambda = 0.335$ (Wait and Okashimo, 1956)

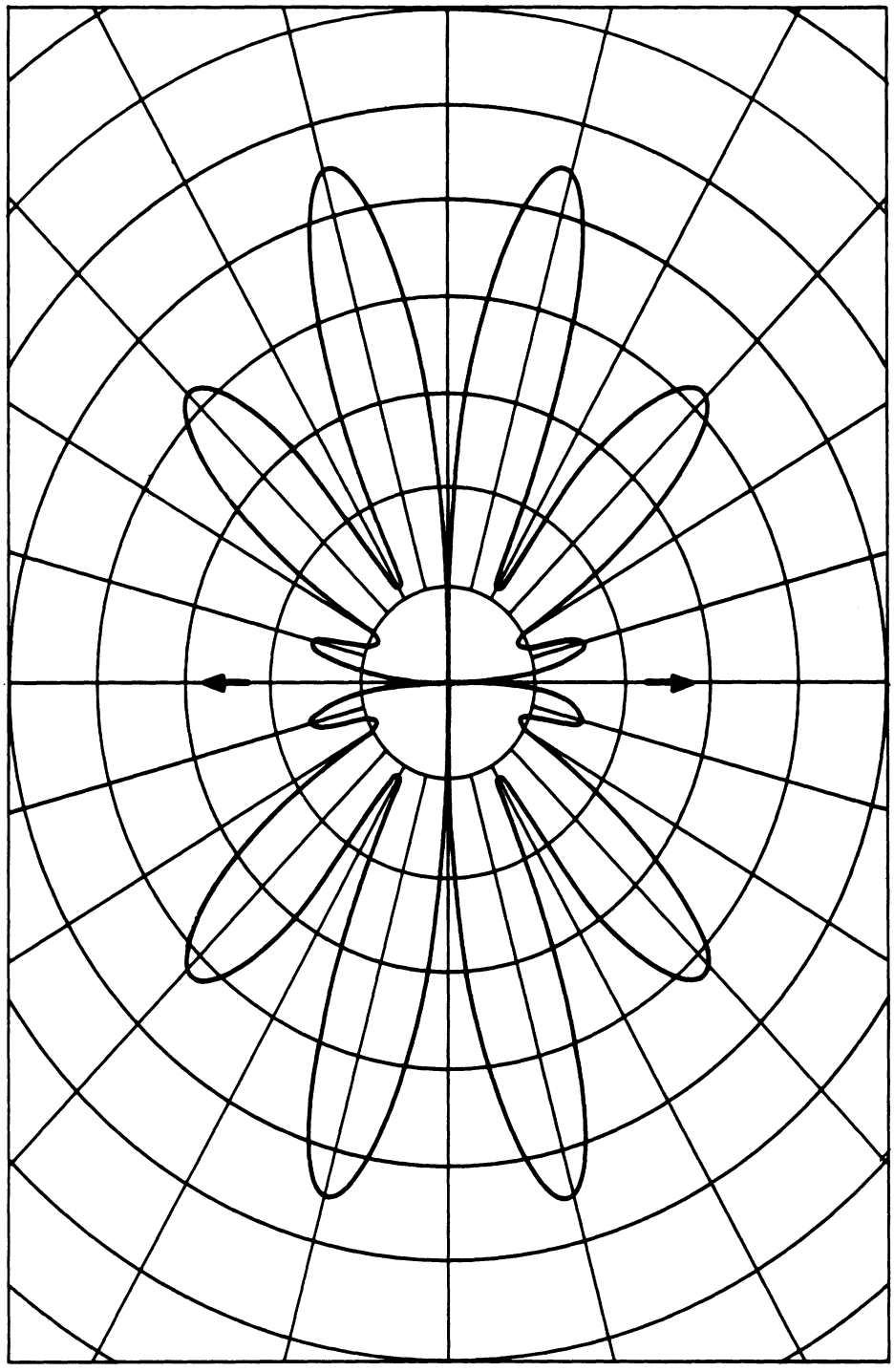

FIG. 2-23d: Case $a/\lambda = 0.915$ (Wait and Okashimo, 1956).

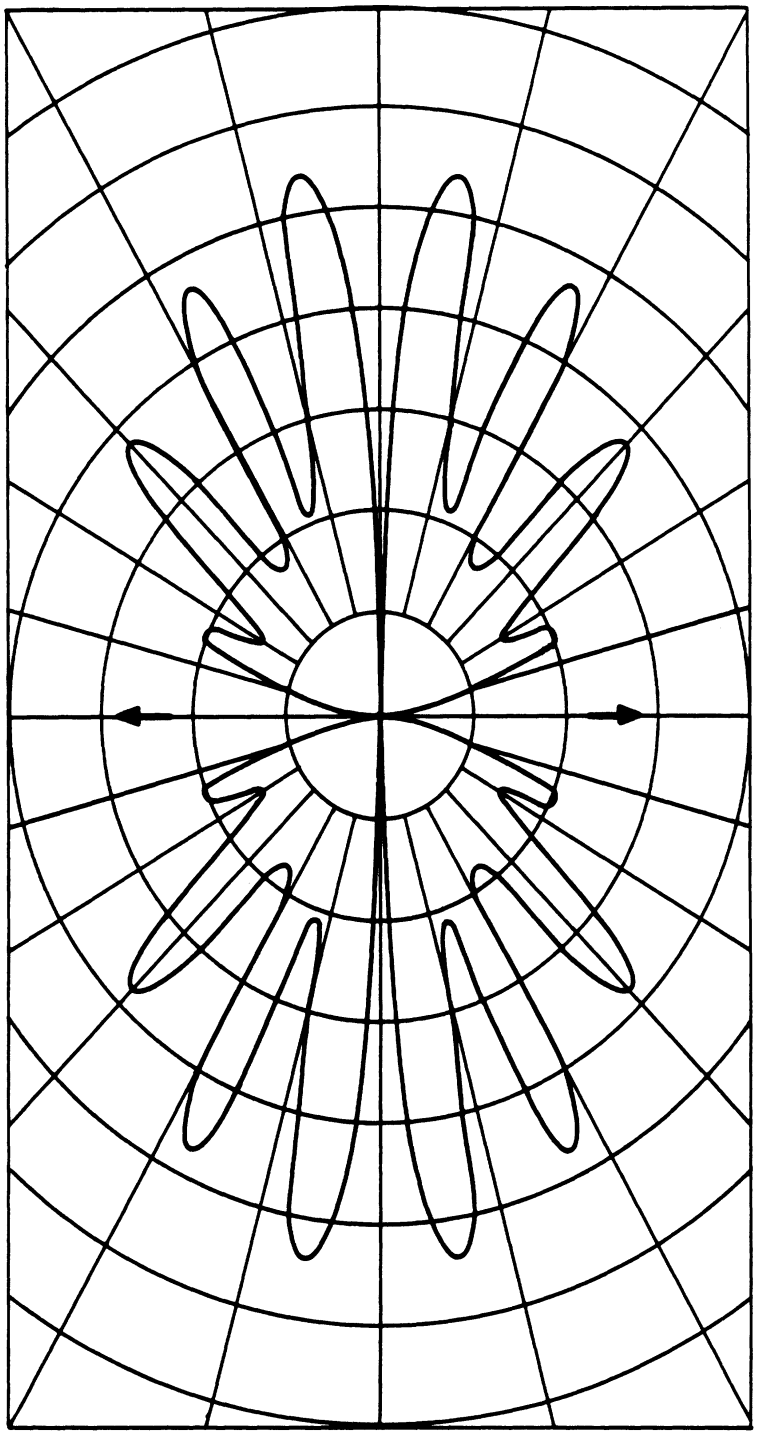

FIG. 2-23e: Case $a/\lambda = 1.54$ (Wait and Okashimo, 1956).

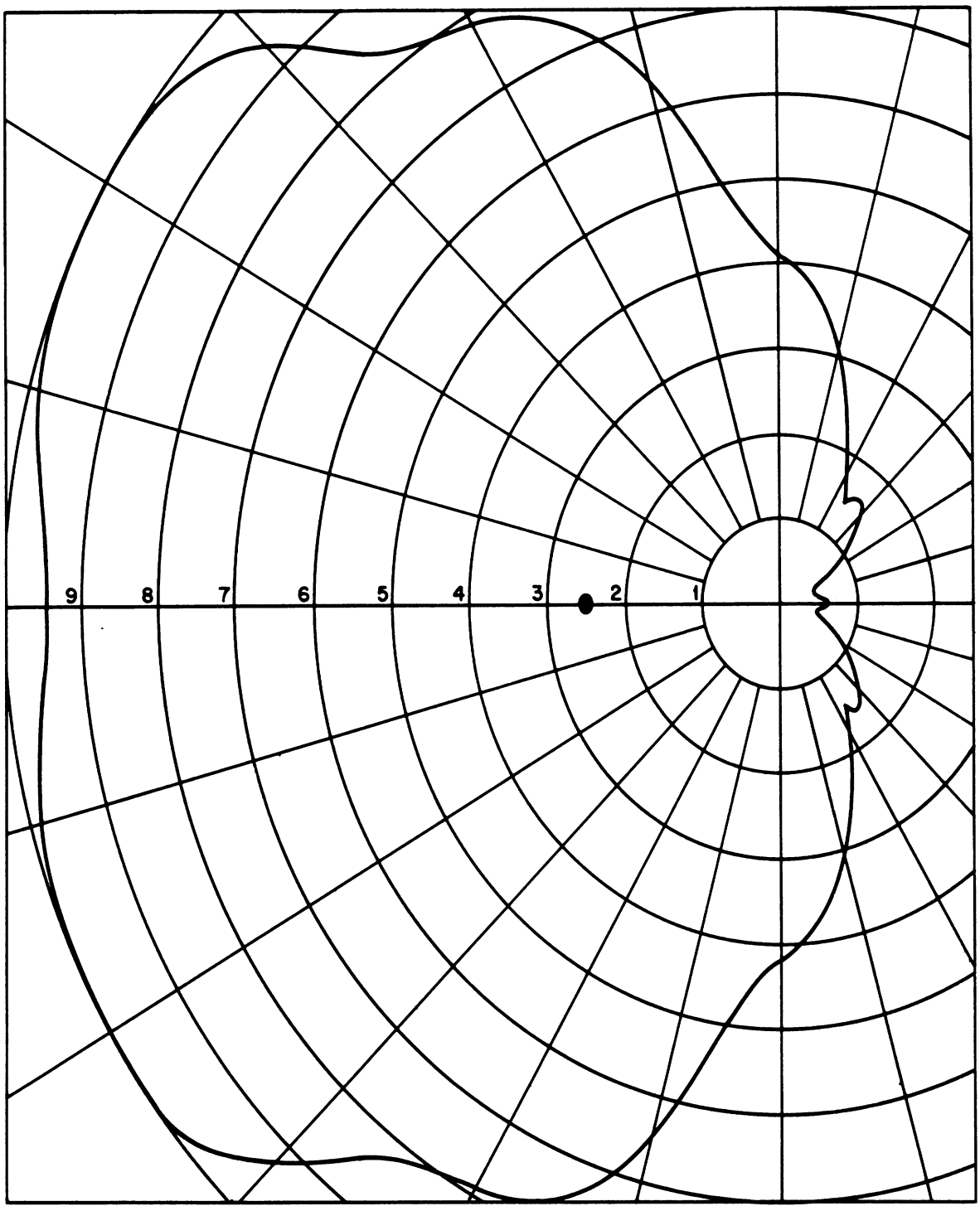

FIG. 2-24a: RADIATION PATTERN (PROPORTIONAL TO $|E_\theta|$) IN THE AZIMUTHAL PLANE OF A LONGITUDINAL DIPOLE LOCATED AT A DISTANCE d FROM THE AXIS OF A CYLINDER OF RADIUS $a = \lambda$.
Case $d = \frac{5}{4}\lambda$ (Oberhettinger, 1943).

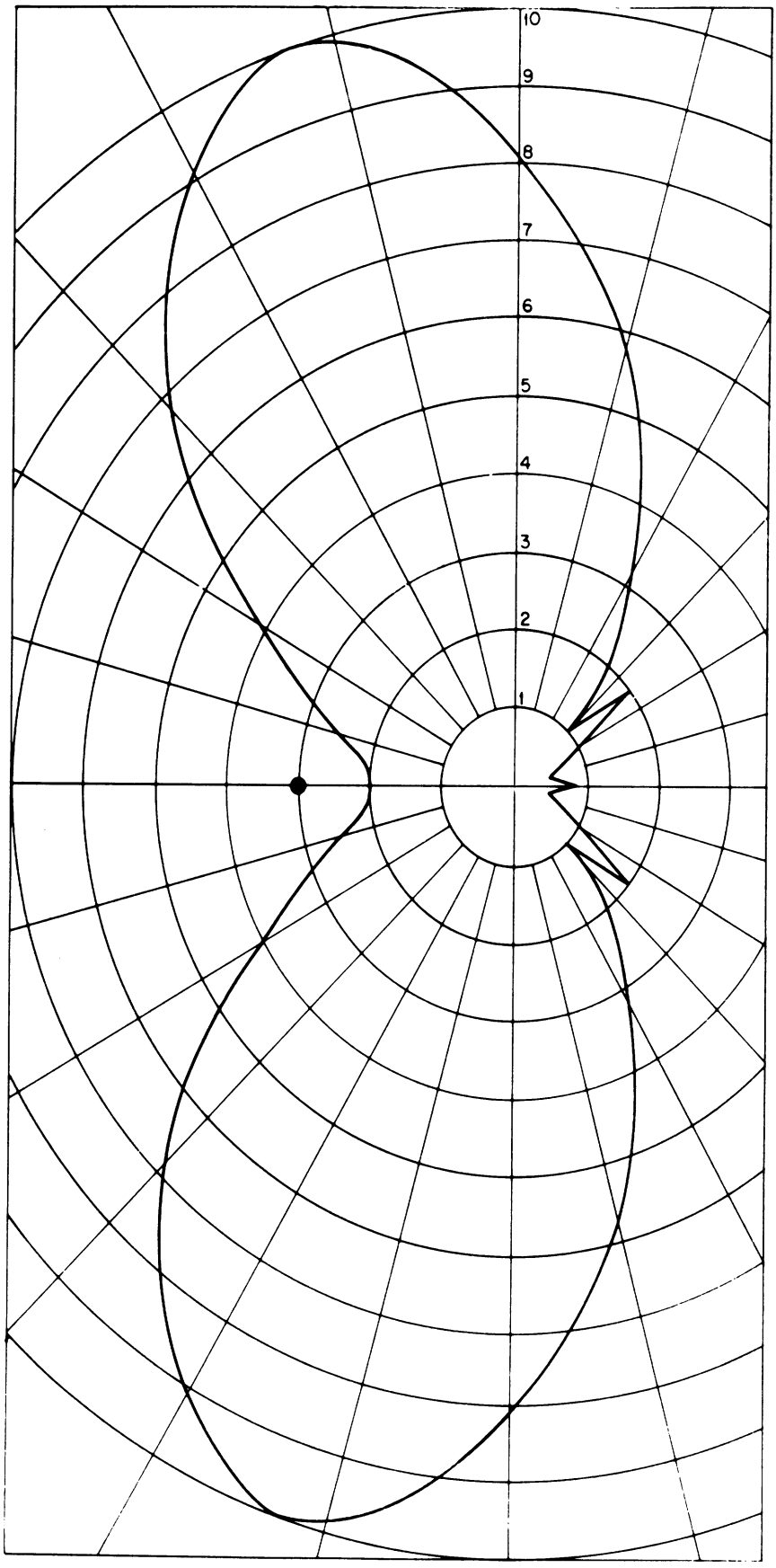

FIG. 2-24b: Case $d = \frac{3}{2}\lambda$ (Oberhettinger, 1943).

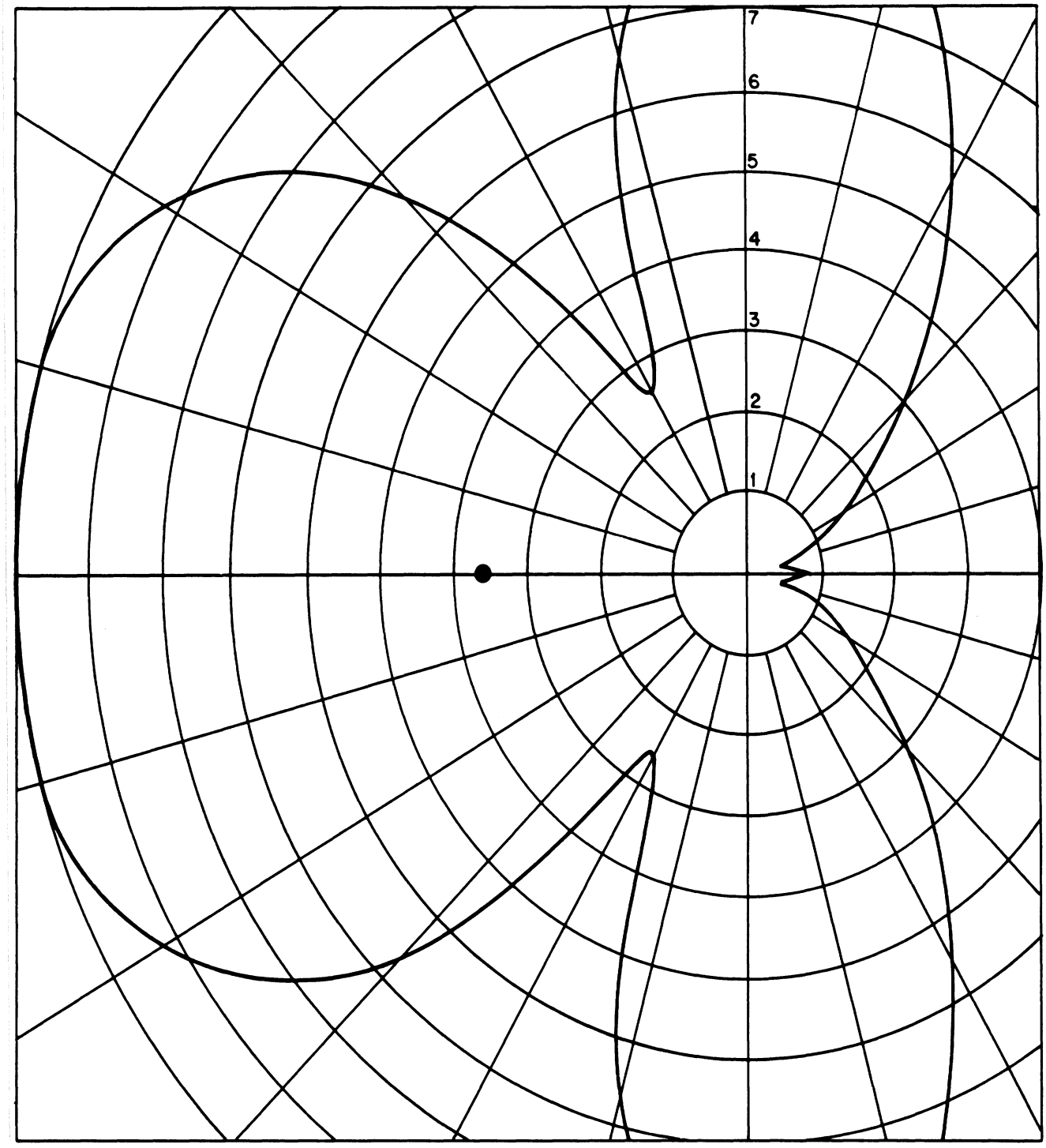

FIG. 2-24c: Case $d = \frac{7}{4}\lambda$ (Oberhettinger, 1943).

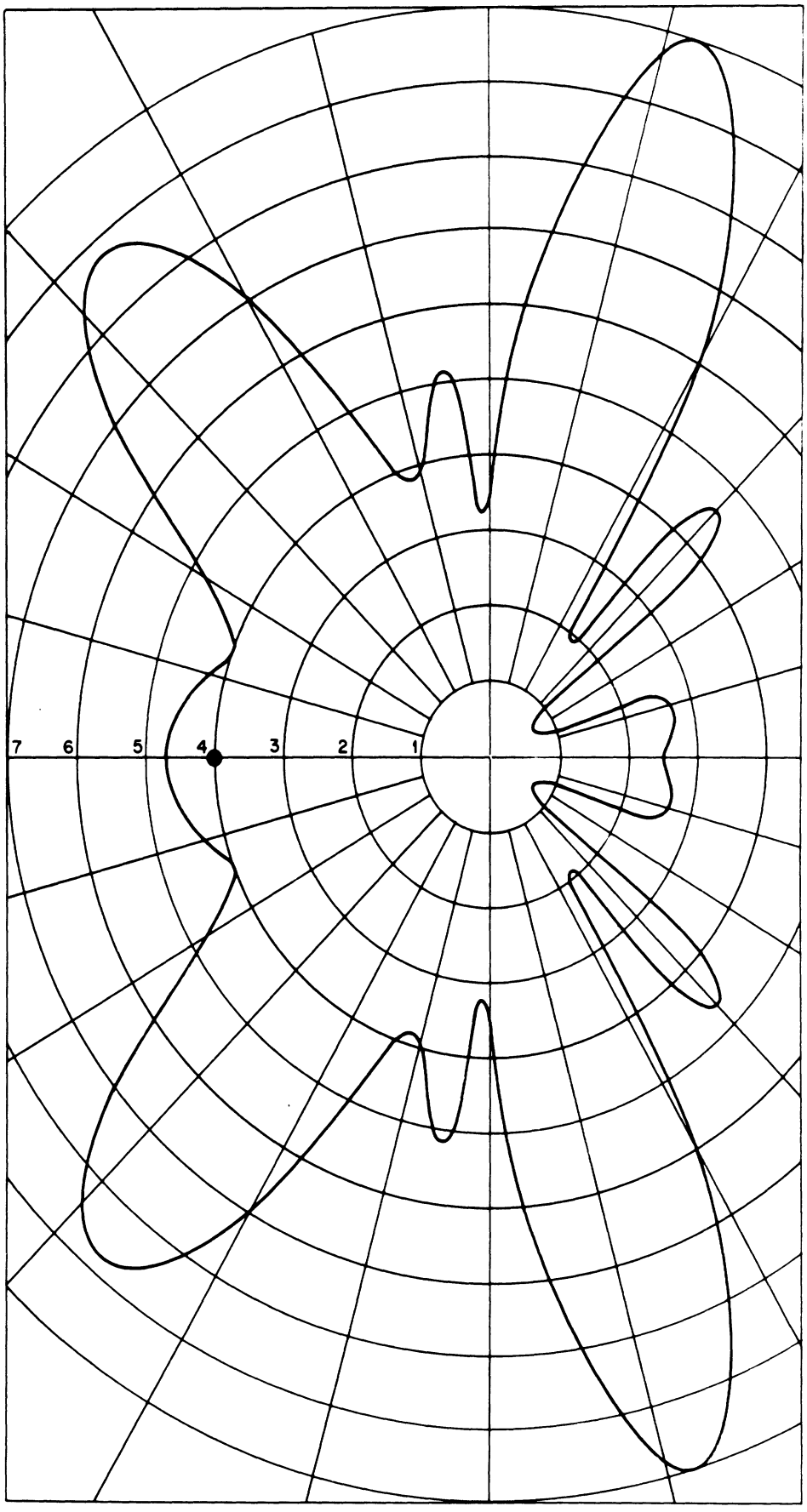

FIG. 2-24d: Case d = 2λ (Oberhettinger, 1943).

for λ varying from .05 to .5 in increments of .05. The field quantities are tabulated to five figures for the full angular range in increments of 5^{o}. It must be noted that Levis has oriented his cylinder along the x-axis, thus in order to compare his formulae and calculations with Carter, Wait and Okashimo, etc., one must rotate coordinates using the relations given explicitly by Levis.

2.4 Scattering of Evanescent Waves

In relation to certain physical phenomena, such as the Smith-Purcell effect, it is of interest to investigate theoretically the scattering of an evanescent (or surface) wave by an infinite metal cylinder. This study has been performed by Ronchi et al (1961), and is summarized in the following. Another work on this subject has recently been published by Levine (1965).

A concrete physical situation, in which this problem arises, is illustrated in Fig. 2-25. A plane electromagnetic wave is totally reflected at the plane interface A-A which separates two media with different refractive indexes, giving origin to a surface wave in the medium with smaller index of refraction. The surface wave, whose amplitude decreases exponentially as the distance from A-A linearly increases, and whose planes of constant phase are perpendicular to A-A, is scattered by the infinite metal cylinder C. It is assumed that the distance d between interface A-A and cylinder axis is so large compared to both cylinder radius and wavelength of the incident radiation, that multiple scattering effects may be neglected.

The notation of Fig. 2-2 is used, but it is now assumed that the plane of incidence $(\hat{k}, \hat{i}_z)$ forms the angle γ with the positive x-axis. According to formulas (2.16), the components of the electromagnetic field incident on the cylinder are generated by the scalar functions:

$$\psi_\ell^i = \psi_{o\ell}^i \exp\left[ik(x\cos\gamma\sin\alpha + y\sin\gamma\sin\alpha + z\cos\alpha)\right] \quad , \quad (\ell \equiv 1, 2),$$

where

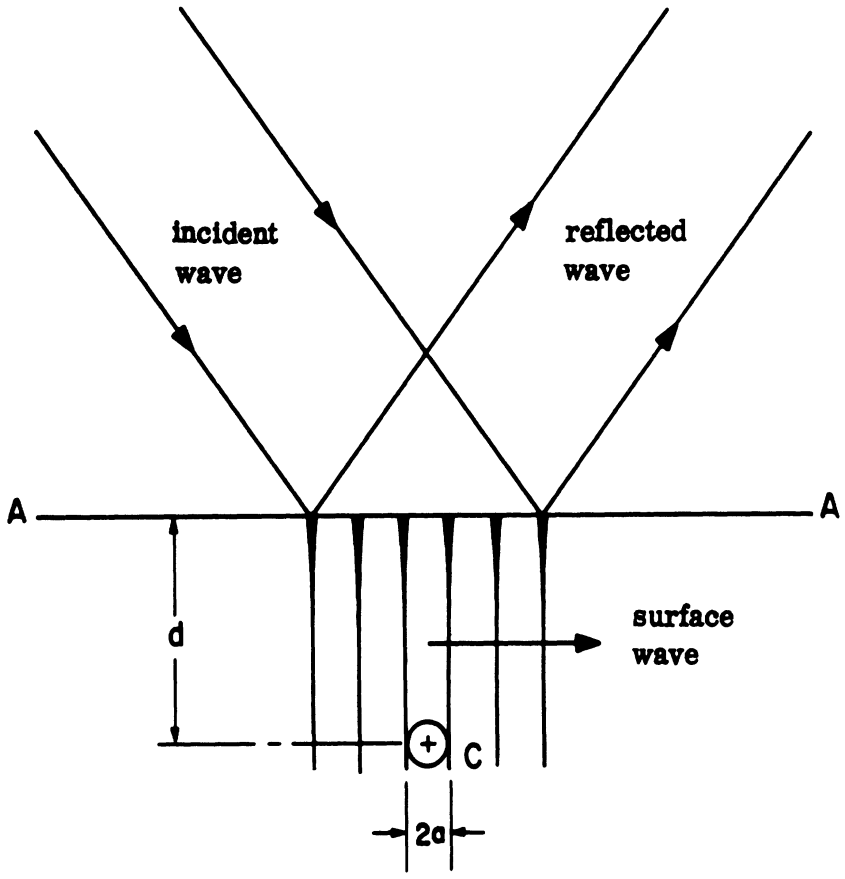

FIG. 2-25: A SURFACE WAVE IS ORIGINATED BY TOTAL REFLECTION AT A-A, AND IS SCATTERED BY THE CYLINDER C.

$$\psi^i_{o1} = \frac{\cos\beta}{k^2 \sin\alpha} \quad , \qquad \psi^i_{o2} = \sqrt{\epsilon/\mu}\, \frac{\sin\beta}{k^2 \sin\alpha} \, .$$

In order that the ψ^i_ℓ's represent an evanescent wave attenuated in the $\hat{i}_x$ direction, the quantities $\cos\alpha$ and $\sin\gamma\sin\alpha$ must be real, whereas $\cos\gamma\sin\alpha = iQ$ with Q real and positive. These conditions may be satisfied in two different ways:

Case 1: α real,

$$\gamma = \frac{\pi}{2} - i\gamma' \, , \qquad \gamma' \text{ real positive;}$$

Case 2:

$$\alpha = -i\alpha_o \, , \qquad \alpha_o \text{ real (e.g. positive),}$$

$$\gamma = \pi - i\gamma'' \, , \qquad \gamma'' \text{ real positive.}$$

Case 1 is termed the case of "small attenuation", and Case 2 the case of "large attenuation" (Ronchi et al, 1961).

The incident wave functions become, for small attenuation,

$$\psi^i_\ell = \psi^i_{o\ell} \exp(-kx \sinh\gamma' \sin\alpha) \exp\left[ik(y \cosh\gamma' \sin\alpha + z \cos\alpha)\right] \quad (\ell = 1, 2),$$

whereas for large attenuation

$$\psi^i_\ell = \psi^i_{o\ell} \exp(-kx \cosh\gamma'' \sinh\alpha_o) \exp\left[ik(y \sinh\gamma'' \sinh\alpha_o + z \cosh\alpha_o)\right] \, ,$$

$$(\ell = 1, 2).$$

Let us call δ the angle between the z-axis and the direction of propagation of the phase, which is parallel to the (y, z) plane, Then, in Case 1

$$\tan\delta = \tan\alpha \cosh\gamma' \, ,$$

and in Case 2 $$\tan\delta = \tanh\alpha_o \sinh\gamma'' \, .$$

The parameters of the evanescent wave, which have an immediate physical meaning, are the angle δ and the attenuation constant h, which equals $k\sinh\gamma' \sin\alpha$ in Case 1 and $k\cosh\gamma'' \sinh\alpha_o$ in Case 2. One can easily express α and γ', or α_o and γ'', in terms of δ and h:

Case 1

$$\begin{cases} \sin\alpha = \sqrt{\left(\sin^2\delta - \dfrac{h^2}{k^2}\cos^2\delta\right)} \\ \sinh\gamma' = \dfrac{1}{\sqrt{\left(\dfrac{k^2}{h^2}\sin^2\delta - \cos^2\delta\right)}} \end{cases}$$

Case 2

$$\begin{cases} \sinh\alpha_o = \sqrt{\left(\dfrac{h^2}{k^2}\cos^2\delta - \sin^2\delta\right)} \\ \cosh\gamma'' = \dfrac{1}{\sqrt{\left(\cos^2\delta - \dfrac{k^2}{h^2}\sin^2\delta\right)}} \end{cases}$$

It is then easily seen that Case 1 is valid for

$$h/k \ll |\tan\delta|$$

and Case 2 for

$$h/k \gg |\tan\delta|.$$

In particular, Case 1 describes the condition of normal incidence $\delta = \pi/2$.

In the case of small attenuation, one has that

$$\psi_\ell^i = \psi_{o\ell}^i \, e^{ikz\cos\alpha} \sum_{n=-\infty}^{\infty} J_n(k\rho\sin\alpha)\, e^{-n\gamma' + in\phi}, \quad (\ell = 1, 2). \qquad (2.88)$$

It is then found that the scattered field components are given by (2.16) with

$$\psi_\ell^s = \psi_{o\ell}^i e^{ikz\cos\alpha} \sum_{n=-\infty}^{\infty} a_{n\ell} H_n^{(1)}(k\rho\sin\alpha)\, e^{-n\gamma' + in\phi}, \quad (\ell = 1,2), \tag{2.89}$$

where

$$a_{n1} = -\frac{J_n(ka\sin\alpha)}{H_n^{(1)}(ka\sin\alpha)}, \qquad a_{n2} = -\frac{J_n'(ka\sin\alpha)}{H_n^{(1)'}(ka\sin\alpha)}.$$

The corresponding results for large attenuation are obtained by replacing α with $(-i\alpha_o)$ and γ' with $(\gamma'' + i\frac{\pi}{2})$ in (2.88) and (2.89). From the expressions of the field components, it can be proven that in Case 2 the radiated field vanishes. This is related to the fact that the wave number $k\cosh\alpha_o$ in the direction of the cylinder axis is larger than the wave number k in free space. Thus the scattering cross section per unit length of the cylinder, which shows some sort of resonance for increasing attenuation (Ronchi et al, 1961), vanishes for all $h \geqslant k|\tan\delta|$.

III
LOW FREQUENCY APPROXIMATIONS FOR AN INFINITE CYLINDER

In the case of an infinite circular cylinder, the low frequency or long wavelength limit ($ka \ll 1$) can be derived easily from the exact power series solution. The exact solutions for normal incidence are given in Eqs. (2.35) and (2.36). As particular cases, we shall consider the parallel ($\beta = 0$) and perpendicular ($\beta = \pi/2$) polarizations of the incident electric field.

The scattered field due to an incident wave with $\underline{E}^i$ parallel to the axis of a perfectly conducting circular cylinder is given by (2.37). Since $ka \ll 1$, we may limit our considerations to the first term of series (2.37); thus we have, in the far field:

$$\underline{E}^s \sim -\hat{i}_z \sqrt{\frac{2}{\pi k\rho}} \frac{J_o(ka)}{H_o^{(1)}(ka)} e^{i(k\rho - \frac{\pi}{4})}, \tag{3.1}$$

which is independent of the azimuthal angle ϕ. According to (2.61) and (2.62), the back scattering cross section per unit length is given by

$$\sigma_E \sim \frac{4}{k} \frac{J_o^2(ka)}{J_o^2(ka) + N_o^2(ka)} \tag{3.2}$$

and since $ka \to 0$:

$$\sigma_E \sim \frac{\pi^2}{k(\log ka)^2} . \tag{3.3}$$

In the approximation (3.1), the total scattering cross section is also given by (3.2) and (3.3):

$$\sigma_E \sim (\sigma_E)_{\text{total}} . \tag{3.4}$$

This result easily follows from Eq. (2.71).

In the case in which $\underline{H}^i$ is parallel to the cylinder axis, the bistatic cross section per unit length is given by

$$\sigma_H \sim \frac{4}{k}\left|\frac{J_o'(ka)}{H_o^{(1)'}(ka)} + \frac{2J_1'(ka)}{H_1^{(1)'}(ka)}\cos\phi\right|^2 . \tag{3.5}$$

Two terms in the exact series solution must now be considered, since they are of the same order in the limit $ka \to 0$. In particular, the back scattering cross section corresponds to $\phi = \pi$, and is given by:

$$\sigma_H \sim \frac{9\pi^2}{4k}(ka)^4 . \tag{3.6}$$

The total scattering cross section is obtained by integrating (3.5) over all values of ϕ (Panofsky and Phillips, 1956):

$$(\sigma_H)_{total} \sim \frac{3}{4}\pi^2(ka)^3 a . \tag{3.7}$$

Lord Rayleigh was the first to use potential theory solutions to construct long wavelength acoustic and electromagnetic approximations for both two-dimensional and three-dimensional problems (Strutt, 1897). The advantages of Rayleigh's method are not very evident in the case of a circular cylinder, because the exact solution is well known. Rayleigh first determined the fields in the region $a < \rho < \lambda$ by using potential theory approximations. He then introduced these intermediate fields in Green's integral in order to derive the far field form. In particular, he showed that the potential of a scatterer in a uniform field is the near field limit of the corresponding scattering problem solution, and that this yields the first term of the far field expansion.

Let a plane sound wave, whose velocity potential is given by

$$\psi^i = e^{-ik\rho\cos\phi} \tag{3.8}$$

be incident on a circular cylinder whose radius is small compared to the wavelength.

By expanding in series of Bessel functions (Strutt, 1945; sections 341, 343):

$$e^{-ik\rho\cos\phi} = J_0(k\rho) - 2iJ_1(k\rho)\cos\phi + \ldots + 2(-i)^n J_n(k\rho)\cos n\phi + \ldots \quad (3.9)$$

For small ka,

$$\psi^i\Big|_{\rho=a} = 1 - \frac{1}{4}k^2a^2 - ika\cos\theta + \ldots \quad (3.10)$$

$$\frac{d\psi^i}{dr}\Big|_{\rho=a} = -\frac{1}{2}k^2a - ik\cos\theta + \ldots \quad (3.11)$$

The velocity potential of the wave diverging from the cylindrical obstacle is given by

$$\psi^s = S_0 D_0(k\rho) + S_1 D_1(k\rho) + \ldots \quad (3.12)$$

where $S_0, S_1, \ldots$ are trigonometric functions,

$$D_0(k\rho) = \left(\gamma + \log\frac{k\rho}{2i}\right)\left\{1 - \frac{k^2\rho^2}{2^2} + \ldots\right\} + \frac{k^2\rho^2}{2^2} - \frac{3}{2}\frac{k^4\rho^4}{2^2\cdot 4^2} + \ldots$$

$$D_1(k\rho) = \frac{dD_0(k\rho)}{d(k\rho)}$$

$$= \frac{1}{k\rho}\left\{1 - \frac{k^2\rho^2}{2^2} + \ldots\right\} + \left(\gamma + \log\frac{k\rho}{2i}\right)\left\{\frac{k\rho}{2} - \frac{k^3\rho^3}{2^2\cdot 4} - \ldots\right\} +$$

$$+ \frac{k\rho}{2} - \frac{3}{2}\frac{k^3\rho^3}{2^2\cdot 4} + \ldots \quad (3.13)$$

and $\gamma = 0.577215\ldots$ is Euler's constant.

Suppose that the material of the cylinder has density δ' and compressibility m', and let δ and m be the corresponding quantities for the surrounding medium. All special cases can easily be obtained by giving appropriate values to σ' and m'. Inside the cylinder (Strutt, 1945; section 339):

$$\psi_{\text{inside}} \sim A_o \left\{ 1 - \frac{k'^2\rho^2}{2^2} + \frac{k'^4\rho^4}{2^2\cdot 4^2} \right\} + A_1\rho \left\{ 1 - \frac{k'^2\rho^2}{2\cdot 4} + \frac{k'^2\rho^2}{2\cdot 4^2\cdot 8} \cdots \right\} \cos\phi \tag{3.14}$$

where k' is the internal value of the wave number.

Outside the cylinder (Strutt, 1945; section 341):

$$\psi^s_{\text{outside}} \sim B_o \left(\gamma + \log \frac{k\rho}{2i} \right) + B_1 \frac{\cos\theta}{k\rho} \quad . \tag{3.15}$$

The conditions to be satisfied at the surface of the cylinder lead to the following equations:

$$-A_o k'^2 a^2 = -k^2 a^2 + 2B_o \ , \tag{3.16}$$

$$\frac{\sigma'}{\sigma} A \left(1 - \frac{1}{4} k'^2 a^2 \right) = 1 - \frac{1}{4} k^2 a^2 + B_o \left(\gamma + \frac{ka}{2i} \right) \ , \tag{3.17}$$

$$A_1 \left(1 - \frac{3k'^2 a^2}{8} \right) = -ik - \frac{B_1}{ka^2} \ , \tag{3.18}$$

$$\frac{\sigma'}{\sigma} A_1 a \left(1 - \frac{k'^2 a^2}{8} \right) = -ika + \frac{B_1}{ka} \quad . \tag{3.19}$$

Solving the above equations, we get

$$B_o = \frac{1}{2} k^2 a^2 \left[1 - \frac{k'^2}{k^2} \frac{\delta}{\delta'} \right] = \frac{1}{2} k^2 a^2 \frac{m' - m}{m'} \ , \tag{3.20}$$

$$B_1 = -ik^2 a^2 \frac{\delta' - \delta}{\delta' + \delta} \quad . \tag{3.21}$$

We can now write the velocity potential of the scattered wave at a large distance from the cylinder as

$$\psi^s \sim -k^2 a^2 e^{ik\rho} \left(\frac{\pi i}{2k\rho}\right)^{1/2} \cdot \left(\frac{m'-m}{2m'} + \frac{\delta'-\delta}{\delta'+\delta} \cos\phi\right) \quad . \tag{3.22}$$

The conditions $m' \to \infty$, $\delta' = \infty$ correspond to the case of a hard cylinder,

$$\psi^s \sim -\frac{2\pi^2 a^2}{\rho^{1/2}\lambda^{3/2}} \left[\frac{1}{2} + \frac{x}{\rho}\right] \cos\frac{2\pi}{\lambda}\left[vt - \rho - \frac{1}{8}\lambda\right] \quad . \tag{3.23}$$

The case $m' = 0$ gives rise to an extreme case when the zero order in circular harmonics becomes infinite and the first order term is relatively negligible. This corresponds to a boundary condition of evanescence of $(\psi^i + \psi^s)$ in which $\psi^i = 1$ (often referred to as the soft cylinder boundary condition). Therefore:

$$S_o\left(\gamma + \log\frac{k\rho}{2i}\right) + 1 = 0 \quad . \tag{3.24}$$

For large $k\rho$:

$$\psi^s \sim \frac{e^{ik\rho}}{\gamma + \log\frac{ka}{2i}} \left(\frac{\pi i}{2k\rho}\right)^{1/2} \quad . \tag{3.25}$$

The problem of electromagnetic wave scattering is analytically identical to the problem of scattering of acoustic waves in two dimensions by small cylindrical obstacles. One can identify ψ^i and ψ^s with E_z or H_z where E_z is the electromotive intensity parallel to z and H_z the magnetic force parallel to z. We also replace δ by the electrical conductivity σ and $1/m$ by μ, the permeability, and δ' and $1/m'$ by σ' and μ', the values of σ and μ inside the cylinder. The expressions for E_z and H_z are identical with (3.22) and (3.25).

Lamb (1924, section 304) has included a section on plane wave scattering by a cylindrical obstacle in his book on hydrodynamics. He has made reference to Rayleigh's contribution; the method used in Lamb's book is identical to Rayleigh's

method, for the case of normal incidence of a plane sound wave scattered by a rigid circular cylinder. He has also given the expression for the total scattering cross section for the above case in the long wavelength limit, and this agrees with our equation (3.7).

The expressions for scattering cross section in cases of E and H-polarized waves for arbitrary cylinders in two dimensions are derived by Van Bladel (1963). He has applied the low frequency limit for the Green's function in the integral equation and his results for the special case of circular cylinders agree with equations (3.3) and (3.7).

It is clear that the scattering cross sections depend markedly on the polarization of the incident waves, and this has been discussed by Kerr (1951). As ka increases, $\sigma_E/\sigma_{g.o.}$ decreases monotonically and $\sigma_H/\sigma_{g.o.}$ oscillates, departing markedly from the fourth power law (see Fig. 2-12). Some considerations on the low-frequency total scattering cross section for a cylinder with impedance boundary conditions are developed by Lax and Feshbach (1948).

IV
HIGH FREQUENCY APPROXIMATIONS FOR AN INFINITE CYLINDER

In this chapter, we consider only the cases of cylindrical and plane waves at normal incidence for both polarizations of the electric field ($\underline{E}^i$ parallel or perpendicular to the axis of the cylinder). The results obtained for a perfectly conducting cylinder by means of geometrical and physical optics approximations, of the geometrical theory of diffraction, and of asymptotic expansions of exact solutions are presented in Sections 4.1, 4.2 and 4.3, respectively. The case of a cylinder with a nonzero surface impedance is briefly examined in Section 4.4, and all results on radar cross sections are collected in Section 4.5.

4.1 Geometrical and Physical Optics Approximations

Let us assume that the wavelength λ of the incident radiation is very small compared to the radius a of the cylinder. Under this assumption, the scattered field in the illuminated region may be approximately determined by a simple ray-tracing technique. Consider a plane incident wave propagating along the x-axis, perpendicularly to the axis z of the cylinder; since the problem is essentially two-dimensional, we may restrict our considerations to the azimuthal plane of Fig. 4-1. A thin beam AA' of rays impinges on the cylinder surface at BB' where it is reflected and scattered in the angular range PP'; we want to determine amplitude and phase of the scattered field ψ^s at the point $P(\rho, \phi)$, located at a large distance from the cylinder ($\rho \to \infty$, $\phi_o \sim \phi$). The energy per unit time carried by the incident beam is proportional to

$$\left|\psi^i\right|^2(AA') = \left|\psi^i\right|^2 a\,\widehat{BOB'}\,\sin\frac{\phi}{2} \ ,$$

whereas the energy that the scattered wave carries through PP' per unit time is proportional to

$$\left|\psi^s(\rho,\phi)\right|^2(PP') = \left|\psi^s(\rho,\phi)\right|^2 2\rho\,\widehat{BOB'} \ ;$$

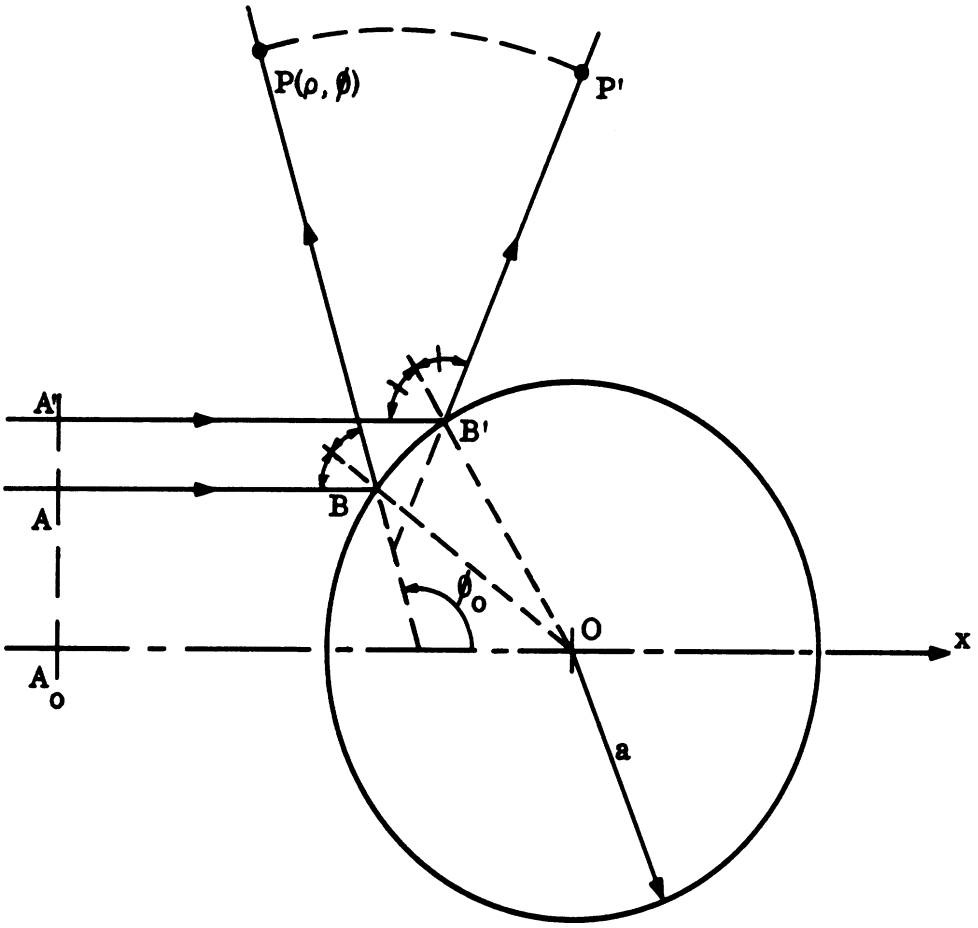

FIG. 4-1: GEOMETRICAL OPTICS APPROXIMATION

since no absorption occurs at BB', these two expressions must be equal by conservation of energy, that is

$$\left|\psi^s(\rho,\phi)\right| = \left|\psi^i\right| \sqrt{\frac{a}{2\rho}\sin\frac{\phi}{2}} \quad .$$

The phase of the scattered wave is easily determined by observing that the difference between the geometrical paths $A_o OP$ and ABP of Fig. 4-1 is given by $2a\sin\frac{\phi}{2}$. Thus

$$\arg\psi^s(\rho,\phi) = k(\rho - 2a\sin\frac{\phi}{2}) + \Phi_o \ ,$$

where Φ_o is a constant angle which depends on the boundary conditions. For an acoustically hard cylinder ($\underline{H}^s$ parallel to axis of conducting cylinder) $\Phi_o = 0$, while $\Phi_o = 180^o$ for a soft cylinder ($\underline{E}^i$ parallel to axis of conducting cylinder). Therefore, a plane electromagnetic wave normally incident on a perfectly conducting cylinder with

$$\underline{E}^i = \hat{i}_z e^{ikx}$$

produces a geometrical optics far scattered field ($\rho \to \infty$, $\phi_o \sim \phi$):

$$(E_z^s)_{g.o.} = -\sqrt{\frac{a}{2\rho}\sin\frac{\phi}{2}}\ e^{ik(\rho - 2a\sin\frac{\phi}{2})} \ , \qquad (4.1)$$

whereas a plane electromagnetic wave with the other polarization, i.e.

$$\underline{H}^i = \hat{i}_z \sqrt{\epsilon/\mu}\ e^{ikx} \ ,$$

produces a geometrical optics far scattered field

$$(H_z^s)_{g.o.} = \sqrt{\epsilon/\mu}\ \sqrt{\frac{a}{2\rho}\sin\frac{\phi}{2}}\ e^{ik(\rho - 2a\sin\frac{\phi}{2})} \ . \qquad (4.2)$$

In particular, the geometrical optics back scattered fields are:

$$(E_z^{b.s.})_{g.o.} = -\sqrt{\frac{a}{2\rho}}\, e^{ik(\rho - 2a)} \tag{4.1a}$$

for $\underline{E}^i$ parallel to the axis, and

$$(H_z^{b.s.})_{g.o.} = \sqrt{\epsilon/\mu}\,\sqrt{\frac{a}{2\rho}}\, e^{ik(\rho - 2a)} \tag{4.2a}$$

for $\underline{H}^i$ parallel to the axis. In Section 4.3 it is shown that the geometrical optics fields given by (4.1) and (4.2) are the leading terms of asymptotic expansions of the exact fields.

The physical optics approximation represents a refinement of geometrical optics. It is recalled that the physical optics approximation method consists of two steps. Firstly one obtains the total electromagnetic field on the illuminated portion of the surface of the scatterer by assuming that at every point the incident field is reflected as though an infinite plane wave were incident on the infinite tangent plane, and the field on the shadow portion of the scatterer is assumed to be zero. Then, an integration over the illuminated surface of the body gives the scattered field.

The physical optics current density $\underline{J}$ on the surface of a perfectly conducting cylinder has been given by Riblet (1952) for both polarizations of the incident plane wave. If

$$\underline{E}^i = \hat{i}_z e^{ikx} \quad ,$$

then from (2.41):

$$\underline{J} = J_z(\phi)\hat{i}_z \sim \hat{i}_z 2H_\phi^i\Big|_{\rho=a} = -\hat{i}_z 2\sqrt{\epsilon/\mu}\,\sin\frac{\phi}{2}\, e^{ikz\cos\phi} \quad , \quad \text{for } \frac{\pi}{2} < \phi < \frac{3\pi}{2} \quad , \tag{4.3}$$

$$\sim 0 \quad , \qquad \text{for } |\phi| < \frac{\pi}{2} \quad ,$$

whereas if

$$\underline{H}^i = \hat{i}_z \sqrt{\epsilon/\mu}\, e^{ikx} \quad ,$$

then from (2.42):

$$\underline{J} = J_\phi(\phi)\hat{\phi} \sim -\hat{\phi} 2H_z^i\Big|_{\rho=a} = -\hat{\phi} 2\sqrt{\epsilon/\mu}\, e^{ika\cos\phi} \quad , \quad \text{for } \frac{\pi}{2} < \phi < \frac{3\pi}{2}$$

$$\sim 0 \quad , \qquad \text{for } |\phi| < \frac{\pi}{2} \quad . \tag{4.4}$$

If the expressions (4.3) and (4.4) are substituted into formulas (2.51) and (2.50) respectively and an approximate evaluation of the integrals is carried out, the physical optics approximations to the scattered fields E_z^s and H_z^s are obtained.

Riblet (1952) considered (4.3) and (4.4) as the leading terms of asymptotic expansions of the current in inverse powers of ka. By substitution into Maxwell's equations and imposition of the boundary conditions, he was able to determine a first order correction to (4.3) and (4.4). The absolute value of the ratio between the correction terms and the leading term is equal to $\left[2ka\sin^3(\phi/2)\right]^{-1}$. These corrected physical optics currents represent an improvement with respect to the approximations (4.3) and (4.4) only in the angular range $2\pi/3 < \phi < 4\pi/3$.

Finally, we shall give a brief account of the Luneberg-Kline method (see, for example, Keller et al, 1956) for obtaining the high frequency expansion of the field reflected by an arbitrary obstacle, and shall state the explicit results for a circular cylinder. Assume that the wave function ψ, $(\nabla^2 + k^2)\psi = 0$, has an asymptotic expansion of the form

$$\psi \sim e^{ik\Phi} \sum_{n=0}^{\infty} \frac{v_n(x,y,z)}{(ik)^n} \quad , \qquad \text{as} \quad k \to \infty \quad . \tag{4.5}$$

Inserting (4.5) into the wave equation and equating to zero the coefficient of each

power of k, we find:

$$(\nabla\Phi)^2 = 1 \,, \tag{4.6}$$

$$2\nabla v_n \cdot \nabla\Phi + v_n \nabla^2\Phi = -\nabla^2 v_{n-1} \,, \tag{4.7}$$

$$(n = 0, 1, \ldots;\ v_{-1} = 0) \,.$$

The eiconal equation (4.6) determines the phase function Φ, whereas the v_n's are obtained from (4.7) by iteration. If s denotes the arc length along an optical ray (i.e. a curve orthogonal to the wavefronts Φ = constant), then the solution of (4.7) can be written in the form:

$$v_n(s) = v_n(s_o)\left[\frac{G(s)}{G(s_o)}\right]^{1/2} - \frac{1}{2}\left[G(s)\right]^{1/2}\int_{s_o}^{s}\left[G(t)\right]^{-1/2}\nabla^2 v_{n-1}(t)\,dt \,, \tag{4.8}$$

where G(s) denotes the Gaussian curvature or, in two dimensions, the ordinary curvature, of the wavefront Φ = constant at the point s on a ray. In particular, it is easily seen that v_o varies along a ray as the inverse of the square root of the cross sectional area of a narrow tube of rays, as was previously found by energy conservation.

This method has been applied by Keller et al (1956) to a variety of problems, among which is the reflection of a plane wave by a large circular cylinder. For a soft cylinder ($\psi_1\big|_{\rho=a} = 0$) and $\psi_1^i = e^{ikx}$, the reflected field at a point $P(\rho, \phi)$ is (see Fig. 4-1):

$$(\psi_1^s)_{\text{refl.}} \sim \frac{1}{2}\sqrt{\frac{a}{2s}\sin\frac{\phi_o}{2}}\,\exp\left[ik\left(s-\frac{3}{2}a\sin\frac{\phi_o}{2}\right)\right]\times$$

$$\times\sum_{n=0}^{\infty}\sum_{h=0}^{3n}\sum_{\ell=0}^{n} a_{h\ell n}\left(16\,ika\sin\frac{\phi_o}{2}\right)^{-n}(a/2)^n\left(\sin\frac{\phi_o}{2}\right)^{h-2\ell}, \qquad (4.9)$$

where the angle ϕ_o is shown in Fig. 4-1.

The coefficients $a_{h\ell n}$ satisfy the following recursion relations for $h \neq 0$:

$$\begin{aligned} a_{h\ell n} = h^{-1}\Big\{&(2h+4\ell+2n-3)(6h-4\ell-2n-1)\,a_{h-1,\ell,n-1} + \\ &+(2h-4\ell-2n+5)(2h-4\ell-2n+3)\,a_{h-1,\ell-1,n-1} + \\ &+\left[24(h-1)(h-2\ell-n)-6\right]a_{h-2,\ell,n-1} + \\ &+12(1-h)(2h-4\ell-2n+3)\,a_{h-2,\ell-1,n-1} + \\ &+9(2h-5)(1-2h)\,a_{h-3,\ell,n-1} + 9(2h-5)(2h-1)\,a_{h-3,\ell-1,n-1}\Big\}, \end{aligned} \qquad (4.10)$$

while for $h = 0$ we have:

$$a_{o\ell n} = -\sum_{h=1}^{3n} a_{h\ell n}, \qquad a_{ooo} = -2 . \qquad (4.11)$$

In particular, the first few terms of the series (4.9) are:

$$(\psi_1^s)_{\text{refl.}} \sim -\sqrt{\frac{a}{2s}\sin\frac{\phi_o}{2}}\ \exp\left[ik\left(s-\frac{3}{2}a\sin\frac{\phi_o}{2}\right)\right]\times$$

$$\times\left\{1+\frac{i}{16ka}\left[\frac{8}{\sin^3\frac{\phi_o}{2}}-\frac{3}{\sin\frac{\phi_o}{2}}+\frac{a}{2s}\left(\frac{1}{\sin^2\frac{\phi_o}{2}}-3\right)+\right.\right.$$

$$\left.\left.+\left(\frac{a}{2s}\right)^2\left(\frac{6}{\sin\frac{\phi_o}{2}}-9\sin\frac{\phi_o}{2}\right)+\left(\frac{a}{2s}\right)^3\left(15\sin^2\frac{\phi_o}{2}-15\right)\right]+\ldots\right\}\ . \tag{4.12}$$

In a plane z = constant, the family of wavefronts is a family of parallel curves with the optical rays as common normals; these rays do in general possess an envelope which is called the caustic of the wavefronts; the distance s which appears in (4.9) and (4.12) is measured along a ray from the caustic to the observation point $P(\rho, \phi)$. With reference to Fig. 4-1, we have that

$$s = BP + \frac{a}{2}\sin\frac{\phi_o}{2}\ . \tag{4.13}$$

In particular, in the far field ($\rho \to \infty$, $\phi_o \sim \phi$):

$$s \sim \rho - \frac{a}{2}\sin\frac{\phi}{2}\ , \tag{4.14}$$

so that formula (4.12) becomes:

$$(\psi_1^s)_{\text{refl.}} \sim A\sqrt{\frac{a}{2\rho}\sin\frac{\phi}{2}}\ e^{ik(\rho - 2a\sin\frac{\phi}{2})}\ , \quad (\rho\to\infty)\ , \tag{4.15}$$

where (Keller et al, 1956):

$$|A| \sim 1 + \frac{1}{(16ka)^2}\left(\frac{3477}{\sin^2\frac{\phi}{2}} - \frac{7218}{\sin^4\frac{\phi}{2}} + \frac{3817}{\sin^6\frac{\phi}{2}}\right) + \ldots \qquad (4.15a)$$

and, in particular, $A \sim -1$ as ka becomes very large.

For a hard cylinder $(\partial\psi_2/\partial\rho\big|_{\rho=a} = 0)$ and $\psi_2^i = e^{ikx}$, the reflected field at a point $P(\rho, \phi)$ is still given by (4.9) and (4.10), but (4.11) must be replaced with the following (Keller et al, 1956):

$$a_{o\ell n} = -\sum_{n=1}^{3n}\left[a_{h\ell n} + 16(2\ell + n - 1)a_{h-1,\,\ell,\,n-1} + 16(4 - 2\ell - n - 2h)a_{h-1,\,\ell-1,\,n-1}\right] \qquad (4.16)$$

$$a_{ooo} = +2 \ .$$

Explicitly, the first few terms of the expansion are:

$$(\psi_2^s)_{\text{refl.}} \sim \sqrt{\frac{a}{2s}\sin\frac{\phi_o}{2}}\ \exp\left[ik\left(s - \frac{3}{2}a\sin\frac{\phi_o}{2}\right)\right] \times$$

$$\left\{1 - \frac{i}{16ka}\left[\frac{8}{\sin^3\frac{\phi_o}{2}} + \frac{3}{\sin\frac{\phi_o}{2}} + \frac{a}{2s}\left(3 - \frac{1}{\sin^2\frac{\phi_o}{2}}\right) + \right.\right.$$

$$\left.\left. + \left(\frac{a}{2s}\right)^2\left(9\sin\frac{\phi_o}{2} - \frac{6}{\sin\frac{\phi_o}{2}}\right) + \left(\frac{a}{2s}\right)^3\left(15 - 15\sin^2\frac{\phi_o}{2}\right)\right] + \ldots\right\} \qquad (4.17)$$

where s is given by (4.13) and ϕ_o is indicated in Fig. 4-1. In the far field, approximation (4.14) applies and result (4.17) becomes:

$$(\psi_s^s)_{\text{refl.}} \sim B\sqrt{\frac{a}{2\rho}\sin\frac{\phi}{2}}\ e^{ik(\rho - 2a\sin\frac{\phi}{2})}, \quad (\rho \to \infty), \qquad (4.18)$$

where (Keller et al, 1956):

$$|B| \sim 1 + \frac{1}{(16ka)^2}\left(\frac{3477}{\sin^2\frac{\phi}{2}} - \frac{6642}{\sin^4\frac{\phi}{2}} + \frac{3049}{\sin^6\frac{\phi}{2}}\right) + \ldots \qquad (4.18a)$$

and, in particular, $B \sim 1$ as ka becomes very large.

The far fields (4.15) and (4.18) include the terms $O(k^{-2})$ in the asymptotic expansion (4.5) and they coincide to $O(k^{-1})$ with the results that Imai (1954) obtained by saddle-point evaluation of the $\int_B^D$ in the exact expressions (2.45) and (2.46), respectively. Imai did not carry his computations through $O(k^{-2})$. The leading terms in (4.15) and (4.18) are the geometrical optics fields (4.1) and (4.2), respectively. Keller et al (1956) plotted the amplitude of the back scattered fields ($\phi = \pi$) vs. ka, for both polarizations and for $1 < ka < 4$, and the amplitude of the far scattered field vs. ϕ, for both polarizations and for $ka = 4$, 40 and infinity; their diagrams are based on formulas (4.15) and (4.18).

The Luneberg-Kline method does not take into account the diffraction effects, but considers only the reflected part of the scattered field; the remaining part is the so-called creeping wave contribution, which is described in the following sections.

4.2 Geometrical Theory of Diffraction

The geometrical optics approximation does not account for the presence of nonzero scattered fields in the region of geometrical shadow, and often represents an insufficiently accurate approximation in the illuminated region. A better approximation is represented by the so-called geometrical theory of diffraction of Keller, which is an extension of geometrical optics. For a description of this theory, the reader is referred to a paper by Keller (1956), in which the extension of the laws of optics is presented in two equivalent forms. In the first form, the different situations in which diffracted rays are produced and the different kinds of diffracted rays which occur in each case are explicitly described. The second formulation is based on an extension of Fermat's principle. The equivalence of the two formulations

follows from considerations of the calculus of variations. Keller's theory assigns a field value, which includes a phase, an amplitude and, in the electromagnetic case, a polarization to each point on a ray. The total field at a point is postulated to be the sum of the fields on all rays which pass through the point.

Keller's theory has been developed for both scalar and vector fields and for objects of various shape and type (e.g., acoustically hard and soft bodies, perfect conductors, dielectrics); the results depend upon the nature of the object in an essential way. For example, a very detailed application to the diffraction of a scalar or vector wave by a smooth convex opaque object of any shape has been made by Levy and Keller (1959).

From its similarity to geometrical optics, Keller's method can be expected to yield good results when the wavelength is small compared to the obstacle dimensions. However, it has been found that in most cases the results are useful even for wavelengths as large as the relevant dimensions of the scatterer. An important advantage of the method is that it does not depend on separation of variables or any similar procedure, and it is therefore especially useful for shapes more complicated than a circular cylinder. In fact, in the case of a circular cylinder, the solution obtained by the geometrical theory of diffraction coincides with the leading terms in the asymptotic expansion of the exact solution for large ka (Levy and Keller, 1959).

If R is the distance between the observation point (ρ, ϕ, z) located off the cylinder surface $(\rho > a)$ and a line source parallel to the cylinder axis and located at $(\rho = \rho_0 > a,\ \phi = 0)$ and if

$$\psi^i = \frac{1}{4}\sqrt{\frac{2}{\pi kR}}\ e^{ikR + i\frac{\pi}{4}} \tag{4.19}$$

is the incident field, then the scattered field ψ^s may be written as

$$\psi^s \sim \psi^s_{g.o.} + \psi^s_d\ , \tag{4.20}$$

where $\psi^s_{g.o.}$ is the geometrical optics field (which, in particular, is zero in the geometrical shadow), and ψ^s_d is the diffracted field which is given by (Levy and Keller, 1959)

$$\psi^s_d(\rho,\phi) = (8\pi k)^{-1/2}\left[(\rho^2 - a^2)(\rho_o^2 - a^2)\right]^{-1/4} \times$$

$$\times \exp\left\{ik\left[(\rho^2 - a^2)^{1/2} + (\rho_o^2 - a^2)^{1/2}\right] + \frac{i\pi}{4}\right\} \times$$

$$\times \sum_\ell D_\ell^2 \frac{\exp\left[(ika - a\alpha_\ell)\phi\right] + \exp\left[(ika - a\alpha_\ell)(2\pi - \phi)\right]}{1 - \exp\left[2\pi(ika - a\alpha_\ell)\right]} \times$$

$$\times \exp\left[-(ika - a\alpha_\ell)\left(\arccos\frac{a}{\rho} + \arccos\frac{a}{\rho_o}\right)\right]. \qquad (4.21)$$

The diffraction coefficients D_ℓ and the decay exponents α_ℓ are determined by comparing (4.21) with the leading terms of the asymptotic expansions for exact solutions

$$\alpha_\ell = ik - i\nu_\ell a^{-1}, \qquad (4.22)$$

$$D_\ell = e^{i\frac{5\pi}{8}}\left(\frac{2\pi}{k}\right)^{1/4}\left[\frac{\Omega H_\nu^{(2)}(ka)}{\frac{\partial}{\partial\nu}\Omega H_\nu^{(1)}(ka)}\right]^{1/2}_{\nu=\nu_\ell}. \qquad (4.23)$$

The expressions on the right-hand sides of Equations (4.22) and (4.23) are defined below, in Section 4.3. Values of α_ℓ and D_ℓ based on these equations, and the operator Ω are given in Table I for the three types of boundary conditions considered in this report (Levy and Keller, 1959). In this table, A(q) is the special representation for the Airy integral which has been employed by Keller and Franz, and which is related to the integral Ai of Miller (1946) by the equation:

TABLE I

Boundary Conditions	$\alpha_\ell = e^{-\frac{i\pi}{6}}\left(\frac{k}{6a^2}\right)^{1/3} q_\ell$	$e^{-i\frac{5\pi}{4}}\left(\frac{k}{2\pi}\right)^{1/2} D_\ell^2$	$\Omega f(x) =$
$\psi\Big\|_{\rho=a} = 0$	$A(q_\ell) = 0$	$\frac{\pi}{6} e^{i\frac{5\pi}{6}}\left(\frac{ka}{6}\right)^{1/3}\left[A'(q_\ell)\right]^{-2}$	$f(x)$
$\frac{\partial\psi}{\partial\rho}\Big\|_{\rho=a} = 0$	$A'(q_\ell) = 0$	$\frac{\pi}{2} e^{i\frac{5\pi}{6}}\left(\frac{ka}{6}\right)^{1/3} q_\ell^{-1}\left[A(q_\ell)\right]^{-2}$	$\frac{df(x)}{dx}$
$\left(\frac{\partial}{\partial\rho} + ik\eta\right)\psi\Big\|_{\rho=a} = 0$	$\frac{A'(q_\ell)}{A(q_\ell)} = e^{i\frac{5\pi}{6}}\left(\frac{ka}{6}\right)^{1/3}\eta$	$\frac{\pi}{6} e^{i\frac{5\pi}{6}}\left(\frac{ka}{6}\right)^{1/3}\left\{\left[A'(q_\ell)\right]^2 + \frac{q_\ell}{3}\left[A(q_\ell)\right]^2\right\}^{-1}$	$\left(\frac{d}{dx} + i\eta\right) f(x)$

$$A(q) = \int_0^\infty \cos(t^3 - qt)\,dt = 3^{-1/3}\pi\,\mathrm{Ai}(-3^{-1/3}q). \qquad (4.24)$$

For a scatterer of general shape, the diffracted field is given by formulas of which (4.21) is a particular case (see, for example, formula (11) of part one in the paper by Levy and Keller (1959)). These formulas involve the incident field, various geometrical quantities, the diffraction coefficients D_ℓ and the decay exponents α_ℓ. If we assume that the leading terms in D_ℓ and α_ℓ depend only upon the radius of curvature of the scatterer's surface in the normal plane tangent to the optical ray and on no other geometrical property of the scatterer, then D_ℓ and α_ℓ can be determined from the field diffracted by any object of simple shape, e.g. a circular cylinder. Thus, the geometrical theory of diffraction is of no help in determining the high frequency behavior of the field scattered by a circulary cylinder; on the contrary, it is the knowledge of this behavior (achieved by asymptotic expansion of the exact solution) which allows us to determine in the easiest way the geometrically diffracted field for any smooth convex opaque object. Of course, small correction terms to D_ℓ and α_ℓ do involve other geometrical properties of the scattering surface, and in order to determine these additional terms it is necessary to consider the particular shape of the scatterer.

If the line source is removed to infinity and we take into account only the first term ($\ell = 0$) in the series (4.21), and if the electric field of the incident plane wave is $\underline{E}^i = \hat{i}_z e^{ikx}$, then the far back scattered field is given by (Levy and Keller, 1959):

$$E_z^{b.s.} \sim -\sqrt{\frac{a}{2\rho}}\; e^{ik(\rho - 2a)} J(ka)\,, \qquad (4.25)$$

where

$$J(ka) = 1 - 4\pi^{3/2} 6^{-4/3} \left[A'(q_o')\right]^{-2} (ka)^{-1/6} \exp\left[-\pi q_o' 6^{-1/3} (ka)^{1/3} \sin\frac{\pi}{3}\right] \times$$

$$\times \exp\left[\frac{i\pi}{12} + ika(\pi+2) + i\pi q_o' 6^{-1/3} (ka)^{1/3} \cos\frac{\pi}{3}\right], \qquad (4.26)$$

$q_o' = 3.372134$ is the smallest zero of the Airy function A(q), and $Ai(q_o') = -1.059053$. The first term on the right-hand side of (4.26) represents the geometrical optics contribution, in agreement with (4.1a). The second term in (4.26) represents the diffracted field, and may be neglected to the level of accuracy of formula (4.25). Thus $|J(ka)| = 1$, as is shown by the broken line in Fig. 4-2.

For the other polarization (rigid cylinder), such that $\underline{H}^i = \hat{i}_z \sqrt{\epsilon/\mu}\, e^{ikx}$, the far back scattered field is approximately given by (Levy and Keller, 1959):

$$H_z^{b.s.} \sim \sqrt{\epsilon/\mu}\, \sqrt{\frac{a}{2\rho}}\, e^{ik(\rho - 2a)} H(ka) , \qquad (4.27)$$

where

$$H(ka) = 1 + 2\pi^{3/2} 6^{-1/3} q_o^{-1} \left[A(q_o)\right]^{-2} (ka)^{-1/6} \exp\left[-\pi q_o 6^{-1/3} (ka)^{1/3} \sin\frac{\pi}{3}\right] \times$$

$$\times \exp\left[\frac{i\pi}{12} + ika(\pi+2) + i\pi q_o 6^{-1/3} (ka)^{1/3} \cos\frac{\pi}{3}\right] , \qquad (4.28)$$

$q_o = 1.469354$ is the smallest zero of the derivative A'(q) of the Airy function, and $A(q_o) = 1.6680$. The first term in (4.28) represents the geometrical optics contribution, in agreement with (4.2a), whereas the second term represents the diffracted field contribution. The quantity $|H(ka)|$ is plotted in Fig. 4-3.

If the geometrical optics portion of (4.25) and (4.27) is replaced by the asymptotic expansion of the reflected field in inverse powers of ka (Keller, Lewis and Seckler, 1956), then higher order corrections to the diffracted field must also be introduced. The most important of these corrections deals with the decay exponent α_ℓ, and for cylinder and sphere it was found from an analysis of the asymptotic

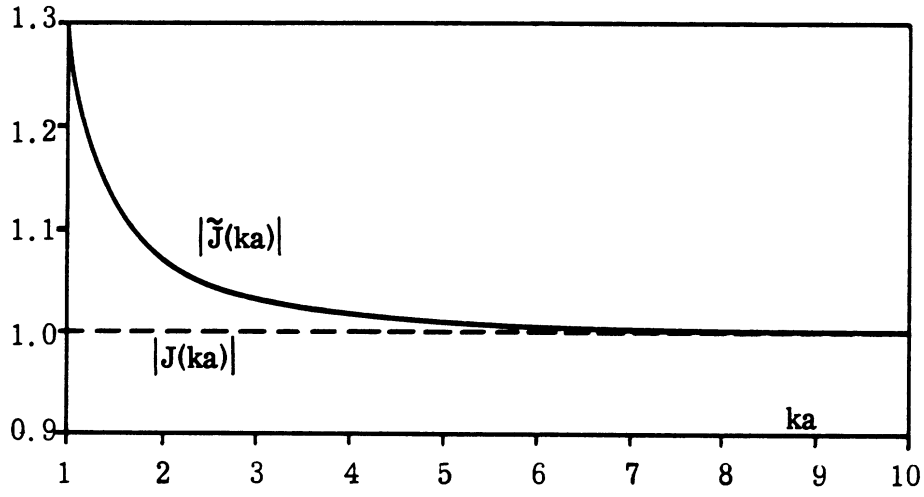

FIG. 4-2: AMPLITUDE OF FAR BACK SCATTERED FIELD FOR A SOFT CYLINDER, NORMALIZED TO THE GEOMETRICAL OPTICS VALUE $\sqrt{a/2\rho}$; THE DIFFRACTED RAYS HAVE A NEGLIGIBLE EFFECT (Levy and Keller, 1959)

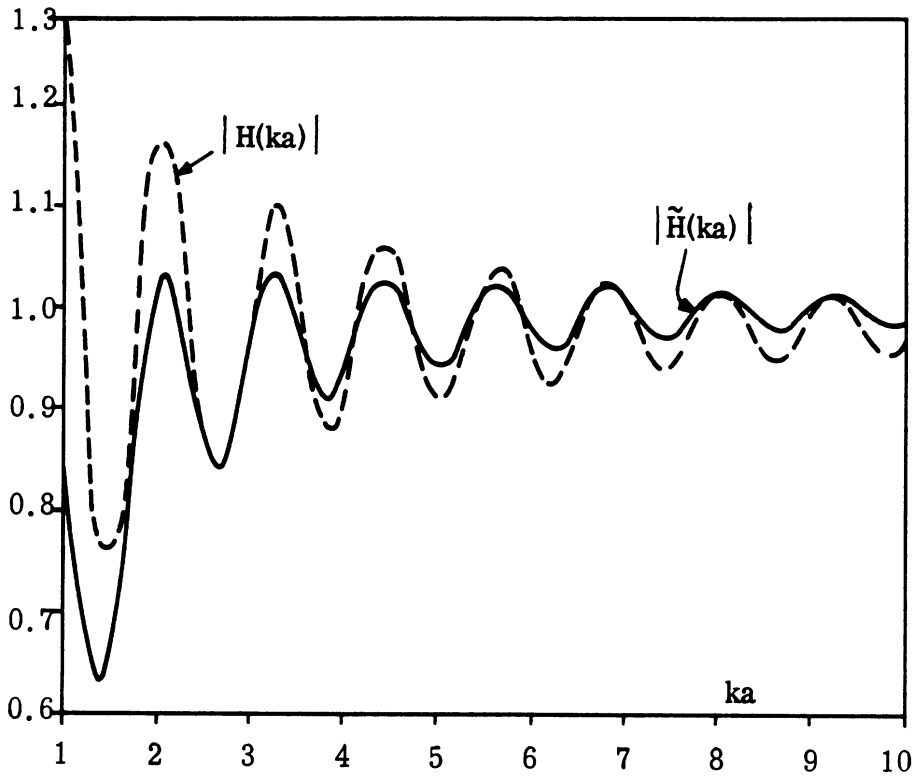

FIG. 4-3: AMPLITUDE OF FAR BACK SCATTERED FIELD FOR A RIGID CYLINDER, NORMALIZED TO THE GEOMETRICAL OPTICS VALUE $\sqrt{a/2\rho}$. (Levy and Keller, 1959).

expansion of the exact solution by Franz (1954). With these modifications, the quantities J(ka) and H(ka) in Eqs. (4.25) and (4.27) are replaced by $\tilde{J}(ka)$ and $\tilde{H}(ka)$, respectively, where (Levy and Keller, 1959):

$$\tilde{J}(ka) = 1+\frac{5i}{16ka} + \frac{127}{512(ka)^2} - $$

$$- 4\pi^{3/2} 6^{-4/3} \left[A'(q_o')\right]^{-2} (ka)^{-1/6} \frac{\exp\left[i\pi\left(\nu_2+2ka+\frac{1}{12}\right)\right]}{1-\exp(2i\pi\nu_2)}, \qquad (4.29)$$

$$\tilde{H}(ka) = 1-\frac{11i}{16ka} - \frac{353}{512(ka)^2} +$$

$$+ 2\pi^{3/2} 6^{-1/3} q_o^{-1} \left[A(q_o)\right]^{-2} (ka)^{-1/6} \frac{\exp\left[i\pi\left(\nu_1+2ka+\frac{1}{12}\right)\right]}{1-\exp(2i\pi\nu_1)}, \qquad (4.30)$$

with:

$$\nu_2 = ka + \left(\frac{ka}{6}\right)^{1/3} q_o' e^{i\frac{\pi}{3}} - \left(\frac{6}{ka}\right)^{1/3} q_o'^2 \frac{e^{-i\frac{\pi}{3}}}{180}, \qquad (4.31)$$

$$\nu_1 = ka + \left(\frac{ka}{6}\right)^{1/3} q_o e^{i\frac{\pi}{3}} - \left(\frac{6}{ka}\right)^{1/3} e^{-i\frac{\pi}{3}} \left(\frac{1}{10q_o} + \frac{q_o^2}{180}\right). \qquad (4.32)$$

The quantities $|\tilde{J}(ka)|$ and $|\tilde{H}(ka)|$ are plotted in Figs. 4-2 and 4-3, respectively.

4.3 Asymptotic Expansions of Exact Solutions

In this section, we shall review the main results obtained by Franz and his collaborators (Franz and Deppermann, 1952; Franz, 1954; Franz and Galle, 1955), Imai (1954), Wetzel (1957), and by the school of Fock (Fock, 1945, 1946; Goriainov, 1958). It is obviously impossible to give an account of the many papers written on

high frequency scattering by circular cylinders, and therefore only those works which contain new important information are explicitly mentioned, whereas many others are simply listed in the bibliography at the end of this report. We shall first consider the case of line sources parallel to the cylinder axis, and then discuss in some detail the case of plane waves at normal incidence, for both polarizations.

Let us consider a line source located at $(\rho = \rho_o, \phi = 0)$ parallel to the axis of the cylinder, and such that

$$\psi^i = \frac{i}{4} H_o^{(1)}(kR) , \tag{4.33}$$

where, as usual, R is the distance of the observation point from the line source. Then the total field ψ must satisfy the equation

$$(\nabla^2 + k^2)\psi = -\rho^{-1}\delta(\rho - \rho_o)\delta(\phi) , \quad (\rho > a) ,$$

the boundary conditions at $\rho = a$ and the radiation condition (2.19) at infinity. One has that (see Eq. (2.79) where, however, the source is at $\phi = 180^o$):

$$\psi = \frac{i}{4} \sum_{n=0}^{\infty} \epsilon_n \left[J_n(k\rho_<) - \frac{\Omega J_n(ka)}{\Omega H_n^{(1)}(ka)} H_n^{(1)}(k\rho_<) \right] H_n^{(1)}(k\rho_>) \cos n\phi , \quad (\rho \geqslant a), \tag{4.34}$$

where $\rho_<$ and $\rho_>$ are, respectively, the larger and smaller of ρ and ρ_o, and the operator Ω is given in Table I of Section 4.2 for the three types of boundary conditions considered. The sum (4.34) may be written as

$$\psi = -\frac{1}{8} \int_{C_1} \frac{e^{i\nu(\phi - \pi)}}{\sin(\pi\nu)} \frac{H_\nu^{(1)}(k\rho_>)}{\Omega H_\nu^{(1)}(ka)} \chi$$

$$\chi \left[\Omega H_\nu^{(1)}(ka) J_\nu(k\rho_<) - \Omega J_\nu(ka) H_\nu^{(1)}(k\rho_<) \right] d\nu , \tag{4.35}$$

where the contour C_1 encircles the entire real axis in the clockwise direction, or also, replacing ν with $-\nu$ on that part of C_1 for which $\mathrm{Im}\,\nu < 0$, as

$$\psi = -\frac{1}{4}\int_{C_2} \frac{\cos\left[\nu(\phi-\pi)\right]}{\sin(\pi\nu)} \frac{H_\nu^{(1)}(k\rho_>)}{\Omega H_\nu^{(1)}(ka)} \times$$

$$\times\left[\Omega H_\nu^{(1)}(ka)\, J_\nu(k\rho_<) - \Omega J_\nu(ka) H_\nu^{(1)}(k\rho_<)\right] d\nu \ , \qquad (4.36)$$

where the contour C_2 is in the upper half-plane, just above the real axis and running parallel to it. Both results (4.35) and (4.36) are as exact as the series solution (4.34).

The contour integral (4.36) has been asymptotically evaluated by Franz (1954). If the observation point (ρ, ϕ) lies in the geometrical shadow, the contour C_2 can be closed in the upper half-plane and the integral evaluated by computing the residues at the zeros ν_ℓ of $\Omega H_\nu^{(1)}(ka)$:

$$\psi = \frac{i\pi}{4}\sum_\ell \frac{\cos\left[\nu_\ell(\phi-\pi)\right]}{\sin(\pi\nu_\ell)} \left[\frac{\Omega H_\nu^{(2)}(ka)}{\frac{\partial}{\partial\nu}\Omega H_\nu^{(1)}(ka)}\right]_{\nu=\nu_\ell} H_{\nu_\ell}^{(1)}(k\rho_o) H_{\nu_\ell}^{(1)}(k\rho) \ . \qquad (4.37)$$

This residue series converges rapidly in the shadow region (source and observation point geometrically invisible to each other) and very slowly in the illuminated region. Therefore, if the field point belongs to the illuminated region, it is convenient to split the integral (4.36) into the sum of two integrals by means of the relation

$$\cos\left[\nu(\phi-\pi)\right] = e^{i\nu\pi}\cos(\nu\phi) - ie^{i\nu\phi}\sin(\nu\pi) \ , \qquad (4.38)$$

and then convert one of the two integrals into a residue series, obtaining (Franz, 1954):

$$\psi = \frac{i\pi}{4} \sum_{\ell} \frac{\cos(\nu_\ell \phi)}{\sin(\nu_\ell \pi)} e^{i\nu_\ell \pi} \left[\frac{\Omega H_\nu^{(2)}(ka)}{\frac{\partial}{\partial \nu} \Omega H_\nu^{(1)}(ka)} \right]_{\nu=\nu_\ell} H_{\nu_\ell}^{(1)}(k\rho_o) H_{\nu_\ell}^{(1)}(k\rho) +$$

$$+ \frac{i}{8} \int_{C_2} e^{i\nu\phi} \frac{H_\nu^{(1)}(k\rho_>)}{\Omega H_\nu^{(1)}(ka)} \left[\Omega H_\nu^{(1)}(ka) H_\nu^{(2)}(k\rho_<) - \Omega H_\nu^{(2)}(ka) H_\nu^{(1)}(k\rho_<) \right] d\nu \ . \quad (4.39)$$

The residue series in (4.39) converges everywhere except in the forward direction $\phi = \pi$; however, (4.39) is of interest only in the illuminated region, since in the shadow we may profitably use the simpler representation (4.37). The contour integral in (4.39) may be asymptotically evaluated by saddle point technique, and represents the sum of the primary field and the reflected part of the scattered field, whereas the residue series represents the creeping wave contribution to the scattered field. The quantities q_ℓ and

$$\left[\frac{\Omega H_\nu^{(2)}(ka)}{\frac{\partial}{\partial \nu} \Omega H_\nu^{(1)}(ka)} \right]_{\nu=\nu_\ell}$$

are given by the second and third columns of Table I in Section 4.2, and ν_ℓ is related to q_ℓ by:

$$\nu_\ell \sim ka + \left(\frac{ka}{6}\right)^{1/3} e^{i\frac{\pi}{3}} q_\ell + \ldots \quad (4.40)$$

In order to compute ψ from (4.37) or (4.39), it is necessary to know the positions of source and field point, so that the appropriate asymptotic expansions of the Hankel functions of arguments $k\rho$ and $k\rho_o$ may be used. For example, if both line source and observation point are very far from the cylinder ($\rho_o \to \infty$, $\rho \to \infty$), then (4.37) becomes:

$$\psi \sim \frac{\exp\left\{ik\left[(\rho^2 - a^2)^{1/2} + (\rho_o^2 - a^2)^{1/2}\right]\right\}}{2ik\left[(\rho^2 - a^2)(\rho_o^2 - a^2)\right]^{1/4}} \sum_{\ell} \frac{\exp(i\nu_\ell \phi) + \exp\left[i\nu_\ell(2\pi - \phi)\right]}{1 - \exp(2\pi i \nu_\ell)} \chi$$

$$\chi \exp\left[-i\nu_\ell\left(\arccos\frac{a}{\rho} + \arccos\frac{a}{\rho_o}\right)\right]\left[\frac{\Omega H_\nu^{(2)}(ka)}{\frac{\partial}{\partial\nu}\Omega H_\nu^{(1)}(ka)}\right]_{\nu=\nu_\ell} \qquad (4.41)$$

In the remaining part of this section we consider in some detail the case of a plane wave incident perpendicularly to the axis of the cylinder. The first rigorous treatment of this problem in the high frequency region is due to Franz and Deppermann (1952), who introduced the concept of creeping waves; they based their derivations on Maue's integral equation (1949). The same problem has been treated by Imai (1954) in a different way; he starts from the solution for the scattered field in the form of an infinite series and transforms it into contour integrals (see formulas (2.45) and (2.46)), which he evaluates by the saddle point method and the residue theorem obtaining the scattered field at a large distance from the cylinder. Specifically, a saddle point evaluation of the two integrals $\int_B^D$ in formulas (2.45) and (2.46) gives the reflected part of the scattered field, whereas the other integrals $\int_E^F$ are transformed into residue series whose terms correspond to the creeping waves of Franz and Deppermann. The results of Imai are not given here, because more accurate approximations were derived by Franz and Galle (1955)*.

The convergence of the asymptotic series obtained by Franz and Galle (1955) is rather poor over certain regions of the azimuthal angle ϕ. This inconvenience

* Imai (1954) pointed out some errors in the derivations of Franz and Deppermann (1952); for example, he showed that their contributions due to reflections from the shadow side do not exist. In turn, Franz (1954) remarked that the numerical values which appear in Imai's formulas (7.8), (7.18), (7.22) and (8.16) are incorrect.

has been avoided by Goriainov (1958), who has derived asymptotic expansions for both surface current and far field and for the whole range $0 \leqslant \phi < 2\pi$ by applying a technique developed by Fock (1945, 1946)*. Goriainov's results for surface current density and far field differ by at most a few percent from the exact results for $ka = 5$ and, of course, become more accurate as ka increases.

In the following, besides the azimuth ϕ, $0 \leqslant \phi < 2\pi$, we shall introduce the angle ζ, $-\pi < \zeta < \pi$, defined as

$$\zeta = \phi \ , \qquad \text{for } \phi < \pi \ ,$$

$$= \phi - 2\pi, \qquad \text{for } \phi > \pi \ .$$

Also, we shall make systematic use of the symbol m, defined as:

$$m = (ka/2)^{1/3} \ .$$

Let us consider a plane electromagnetic wave incident in the direction of the negative x-axis, such that

$$\underline{E}^i = \hat{i}_z e^{-ikx} \ , \qquad \underline{H}^i = \hat{i}_y \sqrt{\epsilon/\mu}\ e^{-ikx} \ . \tag{4.42}$$

The current density on the illuminated portion of the surface ($\rho = a$, $|\zeta| < \pi/2$) is given by (Franz and Galle, 1955):

*For a history of what is presently known as the Fock method see the first volume by Logan (1959), in which a detailed discussion of the notations employed by various authors is also given. A brief exposition of Fock's theory has been given by Goodrich (1959), and an excellent treatment of high frequency diffraction methods in general may be found, for example, in a paper by Logan and Yee (1962).

$$J_z = (H_\phi^i + H_\phi^s)_{\rho=a} \sim 2\sqrt{\epsilon/\mu}\cos\phi\, e^{-ika\cos\phi}\left[1 + \frac{i}{2ka\cos^3\phi} + \frac{1+3\sin^2\phi}{2(ka\cos^3\phi)^2} + \ldots\right] +$$

$$+ i\sqrt{\epsilon/\mu}\, e^{-i\frac{\pi}{3}} m^{-1} \sum_n D_n \frac{\exp\left[i\nu_n\left(\frac{3\pi}{2} - \zeta\right)\right] + \exp\left[i\nu_n\left(\frac{3\pi}{2} + \zeta\right)\right]}{1 - \exp(i2\pi\nu_n)}, \qquad (4.43)$$

where

$$\nu_n \sim ka + e^{i\frac{\pi}{3}} m\alpha_n - e^{-i\frac{\pi}{3}} m^{-1} \frac{\alpha_n^2}{60} - \frac{1}{70ka}\left(1 - \frac{\alpha_n^3}{10}\right) +$$

$$+ e^{i\frac{\pi}{3}} m^{-5} \frac{1}{12600}\left(29\alpha_n - \frac{281}{360}\alpha_n^4 + \ldots\right), \qquad (4.44)$$

$$D_n \sim \frac{1}{Ai'(-\alpha_n)}\left[1 + e^{i\frac{\pi}{3}} m^{-2} \frac{\alpha_n}{10} + e^{-i\frac{\pi}{3}} m^{-4} \frac{59\alpha_n^2}{12600} + \frac{1}{3150(ka)^2}\left(37 - \frac{223\alpha_n^3}{18}\right) + \ldots\right] \qquad (4.45)$$

and the α_n's $(n = 1, 2, \ldots)$ are the zeros of the Airy integral in Miller's notation (with a change in sign):

$$Ai(-\alpha_n) = 0 . \qquad (4.46)$$

The first few values of α_n and $Ai'(-\alpha_n)$ are given in Table II (Logan and Yee, 1962). The first group of terms in (4.43) represents the optics contribution to the surface current, and the first term itself is the geometrical optics current; this development is numerically useful only if $ka\cos^3\phi \gg 1$. The summation over n represents the creeping wave contribution to the surface field.

TABLE II

n	α_n	$Ai'(-\alpha_n)$
1	2.33810 74104 59767	+0.70121 08227 20691
2	4.08794 94441 30971	-0.80311 13696 54864
3	5.52055 98280 95551	+0.86520 40258 94152
4	6.78670 80900 71759	-0.91085 07370 49602
5	7.94413 35871 20853	+0.94733 57094 41568

The current density on the shadowed portion of the surface ($\rho = a$, $|\phi - \pi| < \pi/2$) is given by (Franz and Galle, 1955):

$$J_z = (H_\phi^i + H_\phi^s)_{\rho=a} \sim i\sqrt{\epsilon/\mu}\, e^{-i\frac{\pi}{3}} m^{-1} \chi$$

$$\chi \sum_n D_n \frac{\exp\left[i\nu_n\left(\phi - \frac{\pi}{2}\right)\right] + \exp\left[i\nu_n\left(\frac{3\pi}{2} - \phi\right)\right]}{1 - \exp(i2\pi\nu_n)} \qquad (4.47)$$

where ν_n and D_n are given by (4.44) and (4.45). The creeping wave series (4.47) is no longer useful for computational purposes when one approaches the shadow boundary $\zeta = \pm \pi/2$.

An alternative representation of the surface current, which is especially useful in those angular regions where (4.43) and (4.47) fail to converge rapidly, has been derived by Goriainov (1958). An expansion which may be profitably employed in the transition region about the shadow boundary

$$\left| |\zeta| - \frac{\pi}{2} \right| \lesssim m^{-1}, \qquad (4.48)$$

is the following:

$$J_z = (H_\phi^i + H_\phi^s)_{\rho=a} \sim i\sqrt{\epsilon/\mu}\; m^{-1} \sum_{\ell=0}^{\infty} \left[f^{(0)}(m\eta_\ell)\, e^{ika\eta_\ell} + f^{(0)}(m\bar{\eta}_\ell)\, e^{ika\bar{\eta}_\ell} \right] , \tag{4.49}$$

where

$$\eta_\ell = \phi - \frac{\pi}{2} + 2\pi\ell , \qquad \bar{\eta}_\ell = \frac{3\pi}{2} - \phi + 2\pi\ell . \tag{4.50}$$

The Fock function $f^{(0)}(\xi)$ is a particular case of the more general function $f^{(\ell)}(\xi)$, defined as (see, for example, Logan (1959), vol. 1):

$$f^{(\ell)}(\xi) = \frac{i^\ell}{\sqrt{\pi}} \int_\Gamma \frac{e^{i\xi t}}{w_1(t)}\, t^\ell\, dt , \qquad (-\infty < \xi < \infty) , \tag{4.51}$$

where

$$w_{\frac{1}{2}}^{1}(x) = \sqrt{\pi}\, \left[Bi(x) \pm i\, Ai(x) \right] \tag{4.52}$$

with Ai and Bi Airy integrals in Miller's notation (1946), and Γ is a contour which starts at infinity in the sector $\pi/3 < \arg t < \pi$, passes between the origin and the pole of the integrand nearest the origin, and then ends at infinity in the sector $-\pi/3 < \arg t < \pi/3$. For $\xi > 0$, one can write $f^{(\ell)}(\xi)$ as a residue series:

$$f^{(\ell)}(\xi) = e^{-i(2+7\ell)\frac{\pi}{6}} \sum_n \frac{(\alpha_n)^\ell}{Ai'(-\alpha_n)}\, e^{\xi\alpha_n e^{i\frac{5\pi}{6}}} . \tag{4.53}$$

Values of $f^{(\ell)}(\xi)$ are given by Logan (1959, vol. 2) for $\ell = -1(1)5$ and $\xi = 0.5(0.1)4.0$.*

* The values tabulated by Logan correspond to our Eq. (4.53); in the headings of his tables, a factor $(-1)^\ell$ is missing.

If, in the first approximation, we limit ourselves to the first term ($\ell = 0$) in the series (4.49), we find that after some manipulation (see Goriainov, 1958) we may write:

$$J_z \sim i\sqrt{\epsilon/\mu}\, m^{-1}\left[f^{(0)}(m\bar{\eta}_o)\, e^{ika\bar{\eta}_o} + F\left(m\cos(\pi-\phi)\right) e^{ika\cos(\pi-\phi)}\right],$$

$$(0 \leqslant \phi \leqslant \pi/2)\ , \qquad (4.54)$$

where

$$F(\xi) = f^{(0)}(\xi)\, e^{i\frac{\xi^3}{3}} \qquad (4.55)$$

Formula (4.54) provides a smooth transition between (4.49) and the geometrical optics result.

At large distances from the cylinder surface ($\rho \gg a$), the incident wave (4.42) produces the scattered field (Franz and Galle, 1955):

$$E_z^s \sim -\sqrt{\frac{a}{2\rho}\cos\frac{\zeta}{2}}\, e^{ik(\rho - 2a\cos\frac{\zeta}{2})}\left[1+i\frac{\left(2ka\sin\frac{\zeta}{2}\right)^2 - 1}{8k\rho} - \frac{3i}{16ka\cos\frac{\zeta}{2}} + \right.$$

$$\left. + \frac{i}{2ka\cos^3\frac{\zeta}{2}} + \frac{15}{512(ka\cos\frac{\zeta}{2})^2} - \frac{33}{32(ka\cos^2\frac{\zeta}{2})^2} + \frac{5}{4(ka\cos^3\frac{\zeta}{2})^2} + \ldots\right] +$$

$$+ m(2\pi k\rho)^{-1/2}\exp\left[i\left(k\rho + \frac{\pi}{12}\right)\right]\sum_n C_n \frac{\exp\left[i\nu_n(\pi+\zeta)\right] + \exp\left[i\nu_n(\pi-\zeta)\right]}{1-\exp(i2\pi\nu_n)}\, \chi$$

$$\chi\left(1+i\frac{4\nu_n^2 - 1}{8k\rho} + \ldots\right)\ , \qquad (4.56)$$

where

$$C_n \sim \left[Ai'(-\alpha_n)\right]^{-2}\left[1+e^{i\frac{\pi}{3}} m^{-2}\frac{\alpha_n}{30}+e^{-i\frac{\pi}{3}} m^{-4}\frac{3\alpha_n^2}{1400}+\right.$$

$$\left.+\frac{1}{3150(ka)^2}\left(29-\frac{281\alpha_n^2}{90}\right)+\ldots\right], \quad (4.57)$$

and ν_n is given by (4.44)*. The first group of terms in (4.56) represents the optics contribution to the far field, and the first term itself is the geometrical optics field; this development is numerically useful only if $ka\cos^3(\zeta/2) \gg 1$. The summation over n represents the creeping wave contribution to the far scattered field, and is practically applicable only for $|\phi - \pi| \gtrsim m^{-1}$. In the far field ($\rho \to \infty$) and in the back scattering direction ($\phi = 0$), equation (4.56) becomes (see (2.67), in which $f(\phi, 0)$ is now P_E):

$$E_z^s \sim P_E \sqrt{\frac{2}{\pi k\rho}}\, e^{ik\rho - i\frac{\pi}{4}}, \quad (4.58)$$

where

$$P_E \sim -\frac{1}{2}\sqrt{\pi ka}\, e^{i\frac{\pi}{4} - i2ka}\left(1+\frac{5i}{16ka}+\frac{127}{512(ka)^2}+\ldots\right)+\frac{1}{2} m e^{i\frac{5\pi}{6}} \sum_n \frac{C_n}{\sin(\pi\nu)}. \quad (4.59)$$

In the far field ($\rho \to \infty$) and in the angular region $|\phi - \pi| \ll m^{-1}$, the dominant contribution to the scattered field may be written in the form (4.58) with P_E given by (Goriainov, 1958):

*The quantity $\bar{C}_\ell$ of Franz and Galle (1955), given in their formula (17a), contains an error: the factor 3/6 in the denominator must be replaced by $6^{1/3}$.

$$P_E \sim -\frac{\sin\left[ka(\phi-\pi)\right]}{\phi-\pi} - im\sqrt{\pi}\left[p\left(m(\phi-\pi)\right)\ e^{ika(\phi-\pi)} + p\left(m(\pi-\phi)\right)\ e^{ika(\pi-\phi)}\right], \tag{4.60}$$

where

$$p(\xi) = \frac{1}{2\sqrt{\pi}\,\xi} + \frac{1}{\sqrt{\pi}} \int_{\Gamma} \exp(i\xi t)\frac{v(t)}{w_1(t)}\,dt\ , \tag{4.61}$$

with w_1 given by (4.52) and

$$v(\xi) = \frac{1}{2\sqrt{\pi}}\,\xi^{1/2}\ e^{-i\frac{\pi}{4}} \int_{-\infty}^{\infty} \exp(i\xi t)\,\frac{w_1(t)}{w_1'(t)}\,dt\ . \tag{4.62}$$

The reflection coefficient function $p(\xi)$ is tabulated in Logan (1959, vol. 2) for $\xi = -1.60(0.01)1.60$, and for $\xi = -3.0(0.1)2.0$.

In the particular case of forward scattering ($\phi = \pi$), a more refined approximation has been derived by Wu (1956); the forward scattered field is still given by (4.58) with

$$P_E \sim -ka - M_o m - \frac{1}{30}\,M_1 m^{-1} + \frac{1}{140}\left(1+\frac{3}{10}\,M_2\right)m^{-3} - \frac{1}{12600}\left(29M_o + \frac{281}{90}\,M_3\right)m^{-5} +$$

$$+\frac{1}{5821200}\left(7361M_1 + \frac{73769}{360}\,M_4\right)m^{-7} + \ldots \tag{4.63}$$

where

$$M_o = 1.2550\ 7437\ e^{i\frac{\pi}{3}}\ , \qquad M_1 = 0.5322\ 5036\ e^{i\frac{2\pi}{3}}\ ,$$

$$M_2 = 0.0935216\ , \qquad M_3 = 0.772793\ e^{i\frac{\pi}{3}}\ ,$$

$$M_4 = 1.0992\ e^{i\frac{2\pi}{3}}\ . \tag{4.64}$$

It is easily seen that for $\phi = \pi$, formula (4.60) coincides with the first two terms of the expansion (4.63). The total scattering cross section follows immediately from (4.63) and from the forward scattering theorem (2.69); the explicit result is given in Section 4.5.

The previous treatment from (4.42) to (4.64) contains the most relevant results for the case of E-polarization. We shall now investigate the case of H-polarization (hard cylinder), namely, of a plane electromagnetic wave incident in the direction of the negative x-axis, such that

$$\underline{E}^i = -\hat{i}_y \sqrt{\mu/\epsilon}\, e^{-ikx}, \qquad \underline{H}^i = \hat{i}_z\, e^{-ikx}; \tag{4.65}$$

(notice that all results from (4.65) to the end of this section are normalized with respect to the incident magnetic field).

The current density on the illuminated portion of the surface ($\rho = a$, $|\zeta| < \pi/2$) is given by (Franz and Galle, 1955):

$$J_\phi = -(H_z^i + H_z^s)_{\rho=a} \sim -2e^{-ika\cos\phi}\left[1 - \frac{i}{2ka\cos^3\phi} - \frac{1+3\sin^2\phi}{(ka\cos^3\phi)^2} + \ldots\right] +$$

$$+ \sum_n \bar{D}_n \frac{\exp\left[i\bar{\nu}_n\left(\frac{3\pi}{2} - \zeta\right)\right] + \exp\left[i\bar{\nu}_n\left(\frac{3\pi}{2} + \zeta\right)\right]}{1 - \exp(i2\pi\bar{\nu}_n)}, \tag{4.66}$$

where

$$\bar{\nu}_n \sim ka + e^{i\frac{\pi}{3}} m\beta_n - e^{-i\frac{\pi}{3}} \frac{1}{10m}\left(\beta_n^{-1} + \frac{\beta_n^2}{6}\right) + \frac{1}{100ka}\left(\beta_n^{-3} + 4 + \frac{\beta_n^3}{7}\right) -$$

$$- e^{i\frac{\pi}{3}} m^{-5} \frac{1}{2000}\left(\beta_n^{-5} - \frac{2}{3\beta_n^2} + \frac{611\beta_n}{63} + \frac{281\beta_n^4}{2268}\right) + \ldots \tag{4.67}$$

$$\bar{D}_n \sim \frac{1}{\beta_n \mathrm{Ai}(-\beta_n)} \left[1 - e^{i\frac{\pi}{3}} m^{-2} \left(\frac{1}{10\beta_n^2} + \frac{\beta_n}{30} \right) + e^{-i\frac{\pi}{3}} m^{-4} \frac{1}{200} \left(-3\beta_n^{-4} + \beta_n^{-1} - \frac{61}{63}\beta_n^2 \right) + \right.$$

$$\left. + \frac{1}{(ka)^2} \left(\frac{1}{100\beta_n^6} - \frac{3}{500\beta_n^3} - \frac{353}{7875} + \frac{\beta_n^3}{300} \right) + \ldots \right] , \tag{4.68}$$

and the β_n's ($n = 1, 2, \ldots$) are the zeros of the derivative of the Airy integral in Miller's notation (with a change in sign):

$$\mathrm{Ai}'(-\beta_n) = 0 . \tag{4.69}$$

The first few values of β_n and $\mathrm{Ai}(-\beta_n)$ are given in Table III (Logan and Yee, 1962).

TABLE III

n	β_n	$\mathrm{Ai}(-\beta_n)$
1	1.01879 29716 47471	+0.53565 66560 15700
2	3.24819 75821 79837	-0.41901 54780 32564
3	4.82009 92111 78736	+0.38040 64686 28153
4	6.16330 73556 39487	-0.35790 79437 12292
5	7.37217 72550 47770	+0.34230 12444 11624

The first group of terms in (4.66) represents the optics contribution to the surface current, and the first term itself is the geometrical optics current; this development is numerically useful only if $ka\cos^3\phi \gg 1$. The summation over n represents the creeping wave contribution to the surface field.

The current density on the shadowed portion of the surface ($\rho = a$, $|\phi - \pi| < \pi/2$) is given by (Franz and Galle, 1955):

$$J_\phi = -(H_z^i + H_z^s)_{\rho=a} \sim - \sum_n \bar{D}_n \frac{\exp\left[i\bar{\nu}_n\left(\phi - \frac{\pi}{2}\right)\right] + \exp\left[i\bar{\nu}_n\left(\frac{3\pi}{2} - \phi\right)\right]}{1 - \exp(i2\pi\bar{\nu}_n)} , \tag{4.70}$$

where $\bar{\nu}_n$ and $\bar{D}_n$ are given by (4.67) and (4.68). The creeping wave series (4.70) is no longer useful for computational purposes when one approaches the shadow boundary $\zeta = \pm \pi/2$.

An alternative representation of the surface current, which is especially useful in those angular regions where (4.66) and (4.70) fail to converge rapidly, has been derived by Goriainov (1958). An expansion which may be profitably employed in the transition region about the shadow boundary

$$\left| |\zeta| - \frac{\pi}{2} \right| \lesssim m^{-1} , \tag{4.71}$$

is the following:

$$J_\phi = -(H_z^i + H_z^s)_{\rho=a} \sim -\sum_{\ell=0}^{\infty} \left[g^{(0)}(m\eta_\ell) e^{ika\eta_\ell} + g^{(0)}(m\bar{\eta}_\ell) e^{ika\bar{\eta}_\ell} \right] , \tag{4.72}$$

where η_ℓ and $\bar{\eta}_\ell$ are given by equations (4.50). The Fock function $g^{(0)}(\xi)$ is a particular case of the more general function $g^{(\ell)}(\xi)$, defined as (see, for example, Logan (1959), vol. 1):

$$g^{(\ell)}(\xi) = \frac{i^\ell}{\sqrt{\pi}} \int_\Gamma \frac{e^{i\xi t}}{w_1'(t)} t^\ell \, dt , \qquad (-\infty < \xi < +\infty) , \tag{4.73}$$

where $w_1'(t)$ is the derivative of $w_1(t)$ given by (4.52), and Γ is the contour previously defined for (4.51). For $\xi > 0$, one can write $g^{(\ell)}(\xi)$ as a residue series:

$$g^{(\ell)}(\xi) = (-1)^\ell e^{-i\ell\frac{\pi}{6}} \sum_n \frac{(\beta_n)^{-1-\ell}}{Ai(-\beta_n)} e^{\xi\beta_n e^{i\frac{5\pi}{6}}} \tag{4.74}$$

Values of $g^{(\ell)}(\xi)$ are tabulated by Logan (1959, vol. 2) for $\ell = -5(1)5$ and $\xi = 0.5(0.1)8.0$.*

* The values tabulated by Logan correspond to our equation (4.74); in the headings of the tables, a factor $(-1)^\ell$ is missing.

If, in the first approximation, we limit ourselves to the first term ($\ell = 0$) in the series (4.72), we find that after some manipulation (see Goriainov, 1958) we may write:

$$J_\phi \sim -g^{(0)}(m\bar{\eta}_o)\, e^{ika\bar{\eta}_o} - G\left(m\cos(\pi-\phi)\right) e^{ika\cos(\pi-\phi)} \quad , \quad (0 \leqslant \phi \leqslant \pi/2) \quad , \qquad (4.75)$$

where

$$G(\xi) = g^{(0)}(\xi)\, e^{i\frac{\xi^3}{3}} \quad . \qquad (4.76)$$

Formula (4.75) provides a smooth transition between (4.72) and the geometrical optics result.

At large distances from the cylinder surface ($\rho \gg a$), the incident wave (4.65) produces the scattered field (Franz and Galle, 1955):

$$H_z^s \sim \sqrt{\frac{a}{2\rho}\cos\frac{\zeta}{2}}\, e^{ik(\rho - 2a\cos\frac{\zeta}{2})} \left[1 + i\,\frac{\left(2ka\sin\frac{\zeta}{2}\right)^2 - 1}{8k\rho} - \frac{3i}{16ka\cos\frac{\zeta}{2}} - \right.$$

$$\left. - \frac{i}{2ka\cos^3\frac{\zeta}{2}} + \frac{15}{512\left(ka\cos\frac{\zeta}{2}\right)^2} + \frac{33}{32\left(ka\cos^2\frac{\zeta}{2}\right)^2} - \frac{7}{4\left(ka\cos^3\frac{\zeta}{2}\right)^2} + \ldots \right] +$$

$$+ m(2\pi k\rho)^{-1/2} \exp\left[i\left(k\rho + \frac{\pi}{12}\right)\right] \sum_n \bar{C}_n \frac{\exp\left[i\bar{\nu}_n(\pi+\zeta)\right] + \exp\left[i\bar{\nu}_n(\pi-\zeta)\right]}{1 - \exp(i2\pi\bar{\nu}_n)} \times$$

$$\times \left(1 + i\,\frac{4\bar{\nu}_n^2 - 1}{8k\rho} + \ldots\right) \quad , \qquad (4.77)$$

where

$$\bar{C}_n \sim \beta_n^{-1}\left[Ai(-\beta_n)\right]^{-2}\left[1+e^{i\frac{\pi}{3}}m^{-2}\left(\frac{\beta_n}{30}-\frac{1}{10\beta_n^2}\right)+e^{-i\frac{\pi}{3}}m^{-4}\frac{3}{200}\left(\frac{\beta_n^2}{7}-\beta_n^{-4}\right)+\right.$$

$$\left.+\frac{1}{25(ka)^2}\left(\frac{1}{4\beta_n^6}-\frac{1}{15\beta_n^3}-\frac{611}{1260}-\frac{281\beta_n^3}{11340}\right)+\ldots\right], \quad (4.78)$$

and $\bar{\nu}_n$ is given by equation (4.67). The first group of terms in (4.77) represents the optics contribution to the far field, and the first term itself is the geometrical optics field; this development is numerically useful only if $ka\cos^3(\zeta/2) \gg 1$. The summation over n represents the creeping wave contribution to the far scattered field, and is practically applicable only for $|\phi-\pi| > m^{-1}$. In the far field ($\rho \to \infty$) and in the back scattering direction ($\phi = 0$), equation (4.77) becomes:

$$H_z^s \sim P_H\sqrt{\frac{2}{\pi k\rho}}\, e^{ik\rho - i\frac{\pi}{4}}, \quad (4.79)$$

where

$$P_H \sim \frac{1}{2}\sqrt{\pi ka}\, e^{i\frac{\pi}{4}-i2ka}\left(1-\frac{11i}{16ka}-\frac{353}{512(ka)^2}+\ldots\right)+\frac{1}{2}m e^{i\frac{5\pi}{6}}\sum_n \frac{\bar{C}_n}{\sin(\pi\bar{\nu}_n)}. \quad (4.80)$$

In the far field ($\rho \to \infty$) and in the angular region $|\phi-\pi| \ll m^{-1}$, the dominant contribution to the scattered field may be written in the form (4.79) with P_H given by (Goriainov, 1958):

$$P_H \sim -\frac{\sin\left[ka(\phi-\pi)\right]}{\phi-\pi} - im\sqrt{\pi}\left[q\left(m(\phi-\pi)\right)e^{ika(\phi-\pi)} + q\left(m(\pi-\phi)\right)e^{ika(\pi-\phi)}\right], \quad (4.81)$$

where

$$q(\xi) = \frac{1}{2\sqrt{\pi}\,\xi} + \frac{1}{\sqrt{\pi}} \int_{\Gamma} \exp(i\xi t)\, \frac{v'(t)}{w_1'(t)}\, dt \,, \tag{4.82}$$

with v and w_1 given by (4.62) and (4.52), respectively. The reflection coefficient function $q(\xi)$ is tabulated in Logan (1959, vol. 2) for $\xi = -2.00(0.01)2.00$, and for $\xi = -3.0(0.1)3.0$.

In the particular case of forward scattering ($\phi = \pi$), a more refined approximation has been derived by Wu (1956); the forward scattered field is still given by (4.79) with

$$P_H \sim -ka - \bar{M}_o m - \frac{1}{10}\left(\bar{M}_{-2} + \frac{\bar{M}_1}{3}\right) m^{-1} + \frac{1}{50}\left(1 - \frac{3}{4}\bar{M}_{-4} + \frac{3}{28}\bar{M}_2\right) m^{-3} -$$

$$- \frac{1}{100}\left(\frac{281}{11340}\bar{M}_3 - \frac{611}{1260}\bar{M}_o + \frac{1}{15}\bar{M}_{-3} + \frac{1}{4}\bar{M}_{-6}\right) m^{-5} + \frac{1}{400}\left(\frac{73769}{5239080}\bar{M}_4 -$$

$$- \frac{56299}{31185}\bar{M}_1 + \frac{1679}{2772}\bar{M}_{-2} - \frac{7}{75}\bar{M}_{-5} - \frac{7}{40}\bar{M}_{-8}\right) m^{-7} + \ldots \tag{4.83}$$

where

$$\bar{M}_o = -1.088874119\, e^{i\frac{\pi}{3}}, \qquad \bar{M}_1 = -0.93486491\, e^{i\frac{2\pi}{3}},$$

$$\bar{M}_2 = -0.1070199, \qquad \bar{M}_3 = -0.757663\, e^{i\frac{\pi}{3}},$$

$$\bar{M}_4 = -1.1574\, e^{i\frac{2\pi}{3}}, \qquad \bar{M}_{-2} = -3.70409389\, e^{-i\frac{\pi}{3}},$$

$$\bar{M}_{-3} = 0.41682138\, e^{-i\frac{2\pi}{3}}, \qquad \bar{M}_{-4} = 3.17579652,$$

$$\bar{M}_{-5} = 2.55965945 + 3.12247506\, e^{-i\frac{\pi}{3}}, \quad \bar{M}_{-6} = 2.06575721\, e^{-i\frac{2\pi}{3}},$$

$$\bar{M}_{-8} = -1.36515171 - 2.94764528\, e^{-i\frac{\pi}{3}}. \tag{4.84}$$

It is easily seen that for $\phi = \pi$, formula (4.81) coincides with the first two terms of the expansion (4.83)*. The total scattering cross section follows at once from (4.83) and from the forward scattering theorem; the explicit result is given in Section 4.5.

4.4 Impedance Boundary Conditions

Some considerations on the case of impedance boundary conditions have already been developed in Sections 4.2 and 4.3 (see, for example, Table I in Section 4.2 and the discussion on line sources in Section 4.3). Most authors limit their considerations to the scattering cross section (Lax and Feshbach, 1948; Rubinow and Keller, 1961; Sharples, 1962). An asymptotic evaluation of the reflected field for plane wave incidence can be found in Keller et al (1956).

The far back scattered field, produced by a plane wave at normal incidence with the electric field parallel to the cylinder axis, may be obtained as a particular case of the results given by Uslenghi (1964). If the incident field is such that

$$\underline{E}^i = \hat{i}_z e^{ikx} , \tag{4.85}$$

and the impedance boundary condition (2.4) is valid, where $Z = \eta\sqrt{\mu/\epsilon}$ is the surface impedance, then the far back scattered field may be written in the form

$$E_z^{b.s.} \sim \sqrt{\frac{2}{\pi k\rho}}\, e^{ik\rho - i\frac{\pi}{4}} \left[\tilde{A}_o + 2\sum_{n=1}^{\infty} (-1)^n A_n\right] , \tag{4.86}$$

with the coefficient $\tilde{A}_n$ $(n = 0, 1, 2, \ldots)$ given by the first of relations (2.36). Treating the summation over n as a residue series, the summation is replaced by a contour integral C in the complex ν plane taken in the clockwise direction around the poles at $\nu = 1, 2, \ldots$; following a Watson transformation, the contour C is then deformed to include the poles of the integrand which lie in the first quadrant (see Fig. 2-3). Thus, the far back scattered field is obtained as a sum of two contributions:

* The diagram of $\tilde{g}(\zeta)$ in Fig. 3 of Goriainov (1958) appears to be incorrect.

$$E_z^{b.s.} \sim (E_z^{b.s.})_{refl.} + (E_z^{b.s.})_{cr.w.} ; \tag{4.87}$$

the reflected field arises from an asymptotic evaluation of the term containing $\tilde{A}_o$ in (4.86) and from a saddle point evaluation of the line integral, whereas the creeping wave field is represented by the residue series due to the complex poles of the integrand. One finds that

$$(E_z^{b.s.})_{refl.} \sim \frac{\eta-1}{\eta+1}\sqrt{\frac{a}{2\rho}}\, e^{ik\rho - i2ka}\left\{1+\frac{i}{2ka}\left[\frac{5}{8}+\frac{\eta}{\eta^2-1}(1-2\eta-2\eta^2)\right]\right\} . \tag{4.88}$$

The leading term in (4.88) is the geometrical optics field; the "reflection coefficient" is given by $(\eta-1)/(\eta+1)$ and becomes (-1) for a perfectly conducting cylinder $(\eta=0)$. The case in which the relative surface impedance is close to unity is of considerable interest in applications to absorbers; for $\eta=1$, formula (4.88) becomes:

$$(E_z^{b.s.})_{\substack{refl.\\ \eta=1}} \sim -\sqrt{\frac{a}{2\rho}}\, e^{ik\rho - i2ka}\left(\frac{3i}{8ka}\right) = \frac{3i}{8ka}\,(E_z^{b.s.})_{\substack{g.o.\\ \eta=0}} . \tag{4.89}$$

The creeping wave contribution is given by

$$(E_z^{b.s.})_{cr.w.} \sim 2\sqrt{2\pi}\, m^{-1} e^{-i\frac{3\pi}{4}} \frac{e^{ik\rho}}{\sqrt{k\rho}} \sum_n \left[\sin(\pi\nu_n) w_1^2(t_n)\left(\eta^{-2}+\frac{t_n}{m^2}\right)\right]^{-1} , \tag{4.90}$$

where w_1 is given by (4.52),

$$\nu_n = ka + mt_n , \qquad m = (ka/2)^{1/3} , \tag{4.91}$$

and the t_n's are the roots of the equation

$$\frac{w_1'(t_n)}{w_1(t_n)} = im\eta^{-1} , \tag{4.92}$$

which may be obtained from the values of $w_1'(t)/w_1(t)$ that were computed by Logan and Yee (1962) when t lies in the first quadrant. A similar analysis of the far back scattered field may be carried out for the H-polarization.

An approximate expression of the forward scattered field (and of the total scattering cross section) has been found by Sharples (1962) who used an extended form of the Kirchhoff-Fresnel theory of diffraction, and arrived at numerical results for values of the relative surface impedance either large or small compared to unity. The method of Sharples is an extension of a previous work on soft cylinders by Jones and Whitham (1957), and leads to more accurate results than the variational technique developed by Kodis (1958).

The quantities ν_n of (4.91), and the corresponding quantities for the H-polarization, are the roots of the equation

$$H_\nu^{(1)'}(ka)+i\xi H_\nu^{(1)}(ka) = 0 , \quad \begin{cases} \xi = \eta^{-1}, & \text{for E-polarization,} \\ \xi = \eta , & \text{for H-polarization,} \end{cases} \tag{4.93}$$

which have a positive imaginary part; in the particular case $\eta = 0$, the ν_n's are given by the asymptotic expansions (4.44) and (4.67) of Section 4.3. The roots of equation (4.93) have been studied in detail by Streifer (1964), for the two cases in which $\xi = O(m^{-2})$ and $\xi \geqslant O(1)$. If we indicate with α_n and β_n the opposites of the roots of Ai and Ai', which are given in Tables II and III of Section 4.3, then (Streifer, 1964):

$$\nu_n \sim ka + e^{i\frac{\pi}{3}} m\alpha_n - e^{-i\frac{\pi}{3}} m^{-1} \frac{\alpha_n^2}{60} - \frac{1}{70ka}\left(1-\frac{\alpha_n^3}{10}\right) - i\xi^{-1} -$$

$$- \frac{i}{3\xi} e^{i\frac{\pi}{3}} \left(\frac{1}{2} - \xi^{-2}\right) \alpha_n m^{-2} - \frac{1}{2ka}\xi^{-2}(1-\xi^{-2}) - \frac{i}{5\xi} e^{-i\frac{\pi}{3}} \left(\frac{1}{72} + \frac{13}{18\xi^2} - \xi^{-4}\right) \times$$

$$\times \alpha_n^2 m^{-4} + O(m^{-5}) , \quad \text{for } \xi \geqslant O(1) , \tag{4.94}$$

whereas:

$$\nu_n \sim ka + e^{i\frac{\pi}{3}} m\beta_n - \frac{e^{-i\frac{\pi}{3}}}{10}\left(\beta_n^{-1} + \frac{\beta_n^2}{6}\right) m^{-1} + \frac{1}{25ka}\left(1 + \frac{1}{4\beta_n^3} + \frac{\beta_n^3}{28}\right) +$$

$$+ i\xi e^{-i\frac{\pi}{3}} \beta_n^{-1} m - \frac{\xi^2}{4}\beta_n^{-3} ka - \frac{i\xi}{10}(1+\beta_n^{-3}) + i\xi^3 e^{i\frac{\pi}{3}}\left(\frac{1}{3\beta_n^2} - \frac{1}{2\beta_n^5}\right) m^4 -$$

$$- \frac{\xi^2}{10} e^{i\frac{\pi}{3}}\left(\frac{1}{\beta_n^2} - \frac{3}{2\beta_n^5}\right) m + \frac{\xi^4}{4} e^{-i\frac{\pi}{3}}\left(\frac{7}{3\beta_n^4} - \frac{5}{2\beta_n^7}\right) m^5 -$$

$$- \frac{i\xi}{20} e^{i\frac{\pi}{3}}\left(\frac{1}{5\beta_n^2} - \frac{41\beta_n}{126} - \frac{3}{10\beta_n^5}\right) m^{-2} + \frac{i}{2}\xi^3 e^{-i\frac{\pi}{3}} \chi$$

$$\chi\left(\frac{11}{45\beta_n} + \frac{7}{15\beta_n^4} - \frac{1}{2\beta_n^7}\right) m^2 - i\xi^5\left(\frac{1}{5\beta_n^3} - \frac{21}{20\beta_n^6} + \frac{7}{8\beta_n^9}\right) m^6 + O(m^{-5}),$$

$$\text{for } \xi = O(m^{-2}). \qquad (4.95)$$

If the radius of the cylinder is very large compared to the wavelength, then only the first creeping wave, corresponding to that root ν_1 of either (4.94) or (4.95) which has the smallest imaginary part (hereafter called the "first root"), gives a sizeable contribution to the scattered field. The position of the forst root ν_1 in the complex ν-plane is indicated in Fig. 4-4 for $\xi = 0$, 1, and infinity, and for various values of ka. The position of ν_1 for two fixed values of ka and for ξ varying from zero to infinity is plotted in Fig. 4-5. Finally, values of ν_1 for different values of ka and $\xi = 1$ are given in Table IV (Streifer, 1964); these values are in good agreement with those obtained by Weston (1963).

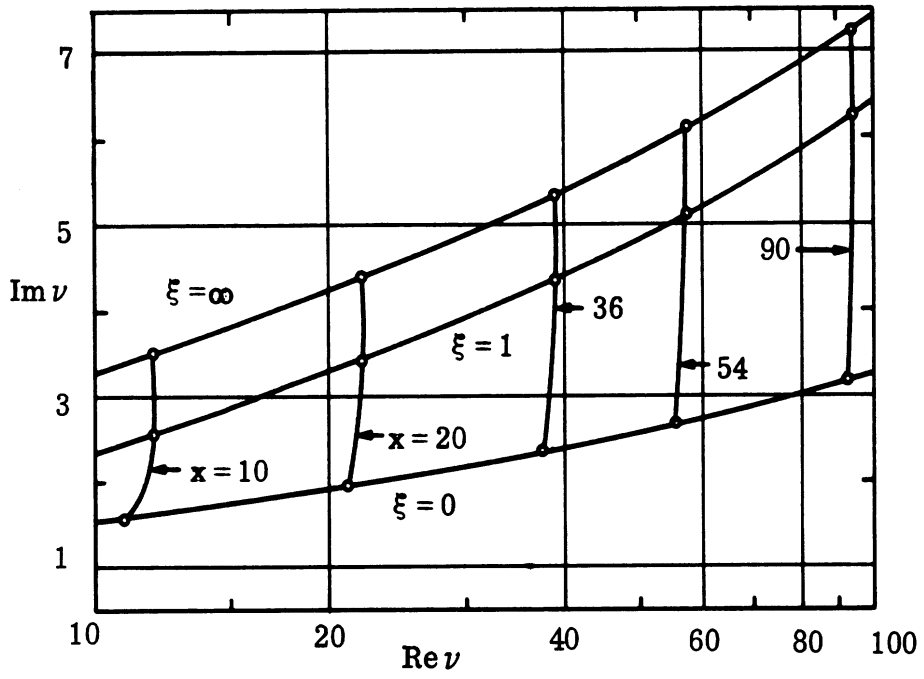

FIG. 4-4: THE FIRST ROOT ν_1 OF (4.93) FOR THREE VALUES OF ξ AND VARIOUS VALUES OF x = ka (Streifer, 1964).

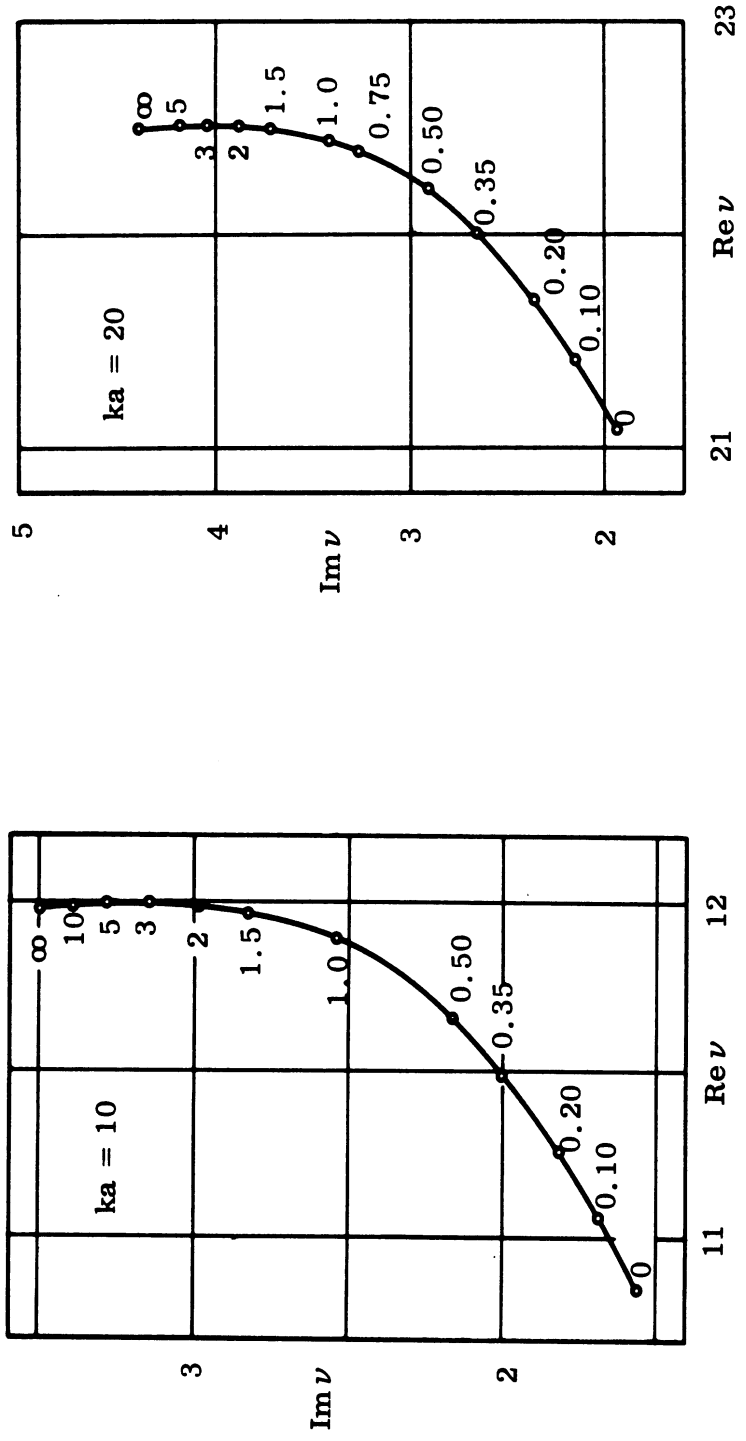

FIG. 4-5: THE FIRST ROOT ν_1 OF (4.93) AS A FUNCTION OF ξ, FOR (a) ka = 10 AND (b) ka = 20. (Streifer, 1964)

TABLE IV

The First Root ν_1 of $H_\nu^{(1)'}(ka) + iH_\nu^{(1)}(ka) = 0$. (Streifer, 1964).

ka	$\left[(\nu_1 - ka)m^{-1}\right]_{\xi=1}$	ka	$\left[(\nu_1 - ka)m^{-1}\right]_{\xi=1}$
4	1.051 + i1.300	14	1.118 + i1.542
5	1.064 + i1.355	16	1.123 + i1.561
6	1.075 + i1.394	18	1.128 + i1.578
7	1.084 + i1.425	20	1.131 + i1.592
8	1.092 + i1.450	30	1.142 + i1.643
9	1.098 + i1.471	40	1.148 + i1.675
10	1.103 + i1.489	50	1.151 + i1.699
12	1.112 + i1.518		

4.5 Radar Cross Sections

In this section, we shall state the principal results on high frequency back scattering and total scattering cross sections for a perfectly conducting cylinder, and mention briefly the various techniques which have been used in the case of impedance boundary conditions.

The geometrical optics approximation to the back scattering cross section per unit length of the cylinder is given by

$$\sigma_{g.o.} = \pi a \ , \tag{4.96}$$

and is the same for both polarizations. The agreement of (4.96) with the exact results is excellent even for relatively small ka in the case of E-polarization (see Fig. 2-10), whereas it is unsatisfactory for H-polarization (see Fig. 2-11). A more refined approximation to the back scattering cross section is obtained by computing the far back scattered field with the aid of the formulas given in Sections 4.3 and 4.4.*

* The formulas of Section 4.3 may be used to compute the bistatic cross section.

For many practical purposes, it is sufficient to determine only certain average characteristics of the scatterer, such as, for example, the total scattering cross section. According to the forward scattering theorem of formula (2.69), which holds for both polarizations, σ_{total} can be easily derived from the forward scattered field. Thus, in the case of the E-polarization, it follows from (4.63) that (Wu, 1956):

$$(\sigma_{total})_E \sim 4a \left[1+0.49807659(ka)^{-2/3} - 0.01117656(ka)^{-4/3} - 0.01468652(ka)^{-2} + \right.$$
$$\left. + 0.00488945(ka)^{-8/3} + 0.00179345(ka)^{-10/3} + \ldots\right] , \qquad (4.97)$$

whereas for the H-polarization, it follows from (4.83) that (Wu, 1956):

$$(\sigma_{total})_H \sim 4a \left[1 - 0.43211998(ka)^{-2/3} - 0.21371236(ka)^{-4/3} + 0.05573255(ka)^{-2} - \right.$$
$$\left. - 0.00055534(ka)^{-8/3} + 0.02324932(ka)^{-10/3} + \ldots\right] . \qquad (4.98)$$

In particular, the geometrical optics σ_{total} is given by

$$(\sigma_{total})_{g.o.} = 4a , \qquad (4.99)$$

for both polarizations. The total scattering cross section, normalized to its geometrical optics value (4.99), is shown in Fig. 4-6 for E-polarization and in Fig. 4-7 for H-polarization. In both figures, the exact value computed from the exact series solution (such as (2.71) for E-polarization) is shown in full line; the approximate values given by the first few terms of (4.97) and (4.98) are shown in broken lines. It is seen that the first three terms of (4.97) give an excellent approximation to the exact value of σ_{total} for all $ka \gtrsim 1$, whereas in the case of (4.98), the first three terms represent a good approximation for all $ka \gtrsim 4$.

The technique employed by Wu (1956) to arrive at (4.97) and (4.98) allows us to find any finite number of terms in the asymptotic series. It consists in solving

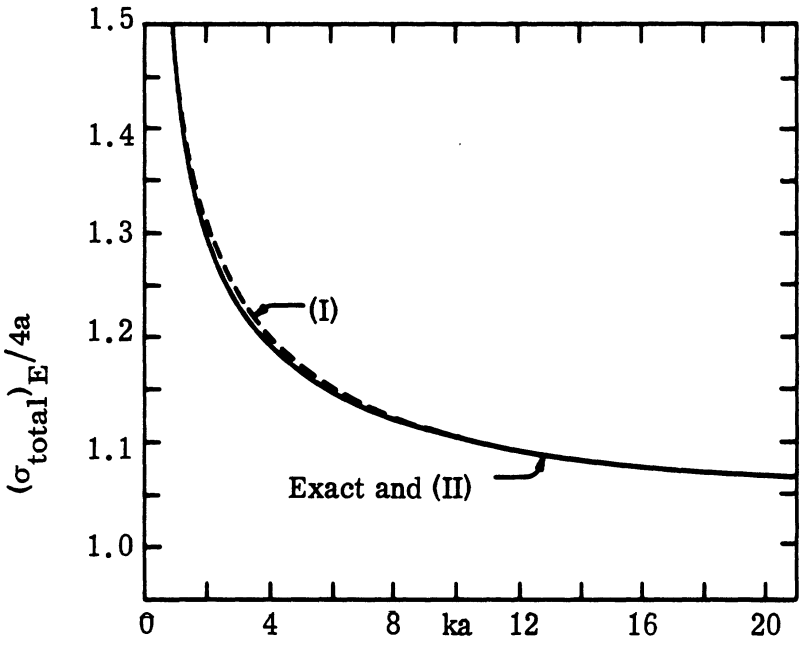

FIG. 4-6: NORMALIZED TOTAL SCATTERING CROSS SECTION $\sigma_{total}/(4a)$ AS A FUNCTION OF ka, FOR ELECTRIC FIELD PARALLEL TO AXIS; (I) GEOMETRICAL OPTICS WITH ONE CORRECTION TERM, (II) GEOMETRICAL OPTICS WITH TWO CORRECTION TERMS. (King and Wu, 1959)

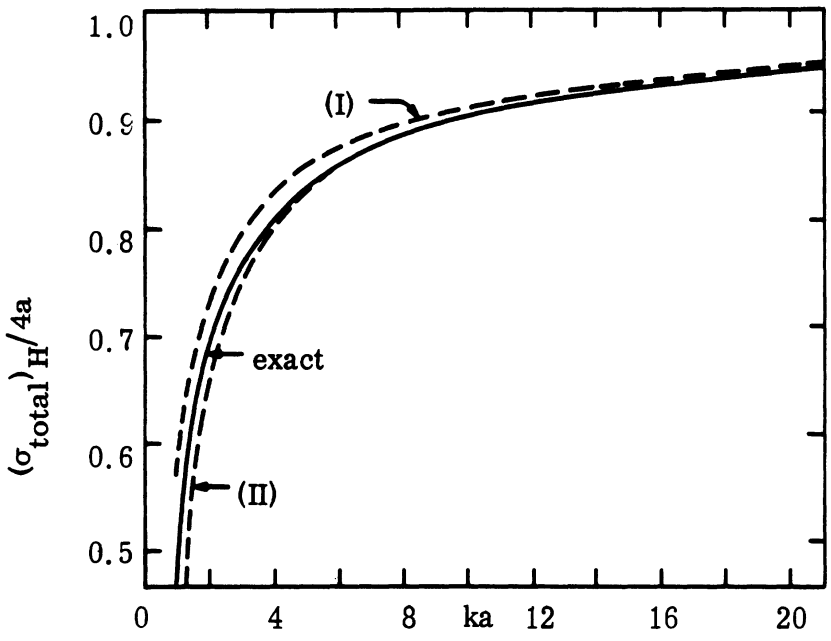

FIG. 4-7: NORMALIZED TOTAL SCATTERING CROSS SECTION $\sigma_{total}/(4a)$ AS A FUNCTION OF ka, FOR MAGNETIC FIELD PARALLEL TO AXIS; (I) GEOMETRICAL OPTICS WITH ONE CORRECTION TERM, (II) GEOMETRICAL OPTICS WITH TWO CORRECTION TERMS. (King and Wu, 1959)

the reduced wave equation in the region outside the cylinder by considering this region as a Riemann surface with infinitely many sheets; this procedure is essentially different from that given by Franz and Deppermann (1952). A different approach to obtain (4.97) and (4.98) has been developed by Beckmann and Franz (1957).

Before the 1956 paper by Wu, various attempts were made to obtain a high frequency expansion for σ_{total}, following essentially two different ways. Wu and Rubinow (1955) performed very extensive transformations on the exact series solution for the forward scattered field, and succeeded in determining the first correction term to geometrical optics for both polarizations; their method was, however, too cumbersome to permit the determination of higher-order terms. An entirely different approach was adopted by Papas (1950), who used the variational method of Levine and Schwinger. For example, for the E-polarization, Papas finds that

$$\sigma_{total} \sim 4a\left[1-\left(\frac{4}{ka}\right)^2\right]^{-1/2} \quad ; \tag{4.100}$$

although the leading term of this formula has the correct value 4a, the higher order terms are incorrect. Subsequent works by Wetzel (1957) and Kodis (1958) proved that it is very difficult for the variational method to provide even the first correction term to geometrical optics. Kodis, for example, finds that

$$(\sigma_{total})_E \sim 4a\left[1+0.746(ka)^{-2/3}\right] , \tag{4.101}$$

and it is seen by comparison with (4.97) that the numerical coefficient of the second term of (4.101) is in error by about 30 percent.

Finally, we mention a few works on the determination of σ_{total} for a cylinder with impedance boundary conditions. The phase shift analysis procedure which was described in Section 2.2 permits to calculate the approximate high frequency cross section; however, Lax and Feshbach (1948) give explicit results only for the sphere. The determination of the scattering cross section (and of the shift of the shadow

boundary) for a cylinder with impedance boundary conditions was performed by Rubinow and Keller (1961), who also extended their results to any smooth two- or three-dimensional object. A different approximation method was developed by Sharples in 1962 (see remarks in Section 4.4).

V
SCATTERING FROM A SEMI-INFINITE CYLINDER

This section is devoted to the scattering of electromagnetic and acoustic waves by a semi-infinite cylinder of circular cross section. Both a thin-walled tube and a solid cylinder are considered. The boundary conditions are $\frac{\partial u}{\partial \rho} = 0$ (rigid cylinder) or $u = 0$ (soft cylinder) for the scalar case and it is assumed that the cylinder is perfectly conducting in the electromagnetic case. When the scattering body is a thin-walled semi-infinite tube the sources can be located either inside or outside the tube. In the former case we assume the solution of the corresponding infinite waveguide problem to be known. That is, the amplitude and phase of all modes are known at the point corresponding to the end of the tube.

The semi-infinite cylinder problems are solved by employing the method of Weiner and Hopf (1931) for treatment of integral equations in the interval $(0, \infty)$. However, the calculations will be somewhat more straightforward if one does not formulate the problem as an integral equation but instead takes the Fourier transform of all quantities before applying the boundary conditions. This approach has been used by Wainstein (1949) and Jones (1952), among others.

To illustrate the method we will treat the problem of electromagnetic scattering from a semi-infinite rod (i.e. a solid cylinder with a plane end surface). The corresponding scalar problem for plane wave incidence has been treated by Jones (1955) and as in that case the final expressions contain the solution for the semi-infinite thin-walled tube plus additional terms which make the solution fulfill the boundary condition on the end surface. These additional terms are not expressed explicitly but only given as the solution of an infinite system of linear equations. Contrary to the infinite cylinder case, the solution of the electromagnetic scattering problem for the solid or tube-shaped semi-infinite cylinder cannot be constructed from the scalar problems with boundary conditions $u = 0$ and $\frac{\partial u}{\partial \rho} = 0$ respectively by taking the incident scalar waves as the component along the cylinder axis of the incident electric

and magnetic field. The scattering field due to an incident TE field, for example, consists of both a TE and a TM part.

5.1 Electromagnetic Scattering from a Perfectly Conducting Semi-Infinite Solid Cylinder

Let (ρ, ϕ, z) be cylindrical coordinates as in Fig. 2-1 and let the semi-infinite circular cylinder occupy the space $\rho \leqslant a$, $z \geqslant 0$. As before, the time dependence $e^{-i\omega t}$ will be suppressed throughout.

We write the total electromagnetic fields as

$$\underline{E} = \underline{E}^i + \underline{E}^s \tag{5.1}$$

$$\underline{H} = \underline{H}^i + \underline{H}^s$$

where $\underline{E}^i$ and $\underline{H}^i$ denote the incident field (the field obtained if the rod were absent). The scattered fields $\underline{E}^s$ and $\underline{H}^s$ satisfy the Helmholtz equations

$$(\nabla^2 + k^2)\underline{E}^s = 0 \tag{5.3}$$

$$(\nabla^2 + k^2)\underline{H}^s = 0 \tag{5.4}$$

outside the rod ($k = \omega\sqrt{\epsilon\mu} = 2\pi/\lambda$) and the following additional conditions:

(i) $E_\phi^s = -E_\phi^i$, $E_z^s = -E_z^i$ $\rho = a,\ z > 0$

$E_\rho^s = -E_\rho^i$, $E_\phi^s = -E_\phi^i$ $\rho < a,\ z = 0$

(ii) $\underline{E}^s$, $\underline{H}^s$ satisfy a radiation condition at infinity

(iii) $E_z^s(a, \phi_o, z) \sim O(z^{-1/3})$, $E_\phi^s(a, \phi_o, z) \sim O(z^{2/3})$

$H_z^s(a, \phi_o, z) \sim O(z^{-1/3})$, $H_\phi^s(a, \phi_o, z) \sim O(1)$

as $z \to -0$ where ϕ_o is an arbitrary fixed angle.

Condition (iii) is the edge condition, necessary to ensure uniqueness of the solution (Bouwkamp, 1946; Meixner, 1949; Heins and Silver, 1955; Van Bladel, 1964).

We assume temporarily that $k = k_r + ik_i$ ($k_r > 0$, $k_i > 0$) and allow $k_i \to 0$ in the final results. This assumption is equivalent to introducing losses in the surrounding medium and consequently the Fourier transform of all field quantities related to the (outgoing) scattered wave will exist in the ordinary sense. We expand all field components in a Fourier series with respect to ϕ and take the Fourier transform with respect to z. Thus, for example

$$\mathcal{E}_{zn}(\rho,\alpha) = \frac{1}{2\pi}\int_0^{2\pi}\int_{-\infty}^{\infty} E_z(\rho,\phi,z)\, e^{-i(\alpha z + n\phi)}\, d\phi dz \tag{5.5}$$

from which the original field is obtained as

$$E_z(\rho,\phi,z) = \frac{1}{2\pi}\sum_{n=-\infty}^{\infty} e^{in\phi}\int_{-\infty}^{\infty} \mathcal{E}_{zn}(\rho,\alpha)\, e^{i\alpha z}\, d\alpha \ . \tag{5.6}$$

If we associate an imaginary part to k it follows that the fields are exponentially decreasing as $|z| \to \infty$ and that their Fourier transforms are analytic functions of α in the strip $-k_i < \mathrm{Im}\alpha < k_i$.

Let F(z) be a function, exponentially decreasing as $|z| \to \infty$, and $\mathcal{F}(\alpha)$ its Fourier transform. We introduce the following notations

$$F^+(z) = \begin{cases} F(z), & z > 0 \\ 0, & z < 0 \end{cases}$$

$$F^-(z) = \begin{cases} 0, & z > 0 \\ F(z), & z < 0 \end{cases}$$

Denoting the Fourier transform of $F^+(z)$ and $F^-(z)$ by $\mathcal{F}^+(\alpha)$ and $\mathcal{F}^-(\alpha)$ respectively, we have

$$\mathcal{F}^{+}(\alpha) = -\frac{1}{2\pi i}\int_{-\infty}^{\infty}\frac{\mathcal{F}(\gamma)}{\gamma-\alpha}\,d\gamma \tag{5.7}$$

$$\mathcal{F}^{-}(\alpha) = \frac{1}{2\pi i}\int_{-\infty}^{\infty}\frac{\mathcal{F}(\gamma)}{\gamma-\alpha}\,d\gamma \tag{5.8}$$

where the path of integration passes above the pole $\gamma = \alpha$ in (5.7) and below it in (5.8). Equations (5.7) and (5.8) are easily obtained from application of the Cauchy integral formula to $\mathcal{F}(\alpha)$ in its strip of analyticity. $\mathcal{F}^{+}(\alpha)$ is analytic in the lower half-plane ($\mathrm{Im}\alpha < 0$) and $\mathcal{F}^{-}(\alpha)$ in the upper one.

The z-component of (5.3) in cylindrical coordinates reads

$$\frac{1}{\rho}\frac{\partial}{\partial\rho}\left(\rho\frac{\partial E_z^s}{\partial\rho}\right) + \frac{1}{\rho^2}\frac{\partial^2 E_z^s}{\partial\phi^s} + \frac{\partial^2 E_z^s}{\partial z^2} + k^2 E_z^s = 0 \tag{5.9}$$

and the same equation is valid for H_z^s. The corresponding equation for $\mathcal{E}_{zn}^s$ and $\mathcal{H}_{zn}^s$ is

$$\left[\frac{1}{\rho}\frac{\partial}{\partial\rho}\left(\rho\frac{\partial}{\partial\rho}\right) + k^2 - \alpha^2 - \frac{n^2}{\rho^2}\right]\begin{Bmatrix}\mathcal{E}_{zn}^s(\rho,\alpha)\\ \\ \mathcal{H}_{zn}^s(\rho,\alpha)\end{Bmatrix} = 0\,. \tag{5.10}$$

This is Bessel's differential equation and the solution valid for $\rho > a$ and satisfying the radiation condition is

$$\mathcal{E}_{zn}^s(\rho,\alpha) = \mathcal{E}_{zn}^s(a,\alpha)\frac{H_n^{(1)}\left(\rho\sqrt{k^2-\alpha^2}\right)}{H_n^{(1)}\left(a\sqrt{k^2-\alpha^2}\right)}, \quad \rho > a \tag{5.11}$$

$$\mathcal{H}_{zn}^s(\rho,\alpha) = \mathcal{H}_{zn}^s(a,\alpha)\frac{H_n^{(1)}\left(\rho\sqrt{k^2-\alpha^2}\right)}{H_n^{(1)}\left(a\sqrt{k^2-\alpha^2}\right)}, \quad \rho > a \tag{5.12}$$

The solution for the region $\rho < a$, $z < 0$ satisfying the boundary conditions on the plane end surface can be obtained by use of images. We use the superscript I to denote quantities related to the field in this region and define

$$\mathcal{E}_{zn}^{I-}(\rho,\alpha)+\mathcal{E}_{zn}^{I-}(\rho,-\alpha) = \left[\mathcal{E}_{zn}^{I-}(a,\alpha)+\mathcal{E}_{zn}^{I-}(a,-\alpha)\right]\frac{J_n\left(\rho\sqrt{k^2-\alpha^2}\right)}{J_n\left(a\sqrt{k^2-\alpha^2}\right)}, \qquad \rho<a \tag{5.13}$$

$$\mathcal{H}_{zn}^{I-}(\rho,\alpha)-\mathcal{H}_{zn}^{I-}(\rho,-\alpha) = \mathcal{H}_{zn}^{I-}(a,\alpha)-\mathcal{H}_{zn}^{I-}(a,-\alpha)\frac{J_n\left(\rho\sqrt{k^2-\alpha^2}\right)}{J_n\left(a\sqrt{k^2-\alpha^2}\right)}, \qquad \rho<a\ . \tag{5.14}$$

The fields obtained by inserting these $\mathcal{E}_{zn}$ and $\mathcal{H}_{zn}$ in (5.6) are the total fields in the region $\rho < a$, $z < 0$ if there is no source of the incident fields in $\rho < a$. If there are sources for $\rho < a$ we have to add the incident field plus its reflection by a perfectly conditing infinite plane at $z = 0$ to obtain the total field. Thus, for $\rho < a$,

Source at $\rho_o < a$,

$$\mathcal{E}_{zn}^{I-}(\rho,\alpha) = \mathcal{E}_{zn}^{s-}(\rho,\alpha)-\mathcal{E}_{zn}^{i+}(\rho,-\alpha) \tag{5.15}$$

$$\mathcal{H}_{zn}^{I-}(\rho,\alpha) = \mathcal{H}_{zn}^{s-}(\rho,\alpha)+\mathcal{H}_{zn}^{i+}(\rho,-\alpha) \tag{5.16}$$

Source at $\rho_o > a$,

$$\mathcal{E}_{zn}^{I-}(\rho,\alpha) = \mathcal{E}_{zn}^{s-}(\rho,\alpha)+\mathcal{E}_{zn}^{i-}(\rho,\alpha) \tag{5.17}$$

$$\mathcal{H}_{zn}^{I-}(\rho,\alpha) = \mathcal{H}_{zn}^{s-}(\rho,\alpha)+\mathcal{H}_{zn}^{i-}(\rho,\alpha) \tag{5.18}$$

where the + and - superscripts denote a division according to (5.7) and (5.8). That the fields obtained from (5.13) and (5.14) satisfy the boundary condition for $z = 0$ follows from the fact that the pertinent E_ϕ and E_ρ are both odd continuous functions of z and thus vanish at $z = 0$.

If E_z and H_z are known for $\rho = a$, $-\infty < z < \infty$, they can be obtained everywhere from equations (5.11) - (5.14). The remaining field components can then be derived from Maxwell's equations. As a special case we obtain the following equations between the field components at $\rho = a$:

$$\mathcal{H}^{s}_{zn}(a,\alpha) = \frac{i H^{(1)}_n(a\kappa)}{\omega\mu\kappa H^{(1)'}_n(a\kappa)} \left[\kappa^2 \mathcal{E}^{s}_{\phi n}(a,\alpha) + \frac{\alpha n}{a} \mathcal{E}^{s}_{zn}(a,\alpha)\right] \tag{5.19}$$

$$\mathcal{H}^{s}_{\phi n}(a,\alpha) = -\frac{\alpha n}{a\kappa^2} \mathcal{H}^{s}_{zn}(a,\alpha) + \frac{i\omega\epsilon H^{(1)'}_n(a\kappa)}{\kappa H^{(1)}_n(a\kappa)} \mathcal{E}^{s}_{zn}(a,\alpha) \tag{5.20}$$

$$\mathcal{H}^{I-}_{zn}(a,\alpha) - \mathcal{H}^{I-}_{zn}(a,-\alpha) = \frac{i J_n(a\kappa)}{\omega\mu\kappa J'_n(a\kappa)} \left[\kappa^2 \left(\mathcal{E}^{I-}_{\phi n}(a,\alpha) - \mathcal{E}^{I-}_{\phi n}(a,-\alpha)\right) + \right.$$
$$\left. + \frac{\alpha n}{a} \left(\mathcal{E}^{I-}_{zn}(a,\alpha) + \mathcal{E}^{I-}_{zn}(a,-\alpha)\right)\right] \tag{5.21}$$

$$\mathcal{H}^{I-}_{\phi n}(a,\alpha) + \mathcal{H}^{I-}_{\phi n}(a,-\alpha) = -\frac{\alpha n}{a\kappa^2} \left(\mathcal{H}^{I-}_{zn}(a,\alpha) - \mathcal{H}^{I-}_{zn}(a,-\alpha)\right) + \frac{i\omega\epsilon J'_n(a\kappa)}{\kappa J_n(a\kappa)} \times$$
$$\times \left(\mathcal{E}^{I-}_{zn}(a,\epsilon) + \mathcal{E}^{I-}_{zn}(a,-\alpha)\right) \tag{5.22}$$

where $\kappa = \sqrt{k^2 - \alpha^2}$ (the branch whose real part is positive when $\alpha = 0$) and $H^{(1)'}_n$ and J'_n denote the derivative with respect to the argument. We define

$$e_n(\alpha) = \kappa^2 a^2 \mathcal{E}_{\phi n}(a,\alpha) + \alpha n a \mathcal{E}_{zn}(a,\alpha) \tag{5.23}$$

$$h_n(\alpha) = \kappa^2 a^2 \mathcal{H}_{\phi n}(a,\alpha) + \alpha n a \mathcal{H}_{zn}(a,\alpha) \ . \tag{5.24}$$

For the incident field we have

$$\mathcal{H}^{i}_{zn}(a,\alpha) = \frac{i H^{(1)}_{n}(a\kappa)}{\omega\mu\kappa a^{2} H^{(1)'}_{n}(a\kappa)}\, e^{i}_{n}(\alpha) \tag{5.25}$$

$$h^{i}_{n}(\alpha) = \frac{i\omega\epsilon\kappa a^{2} H^{(1)'}_{n}(a\kappa)}{H^{(1)}_{n}(a\kappa)}\, \mathcal{E}^{i}_{zn}(a,\alpha) \tag{5.26}$$

if the source is at $\rho_o < a$, and

$$\mathcal{H}^{i}_{zn}(a,\alpha) = \frac{i J_{n}(a\kappa)}{\omega\mu\kappa a^{2} J'_{n}(a\kappa)}\, e^{i}_{n}(\alpha) \tag{5.27}$$

$$h^{i}_{n}(\alpha) = \frac{i\omega\epsilon\kappa a^{2} J'_{n}(a\kappa)}{J_{n}(a\kappa)}\, \mathcal{E}^{i}_{zn}(a,\alpha) \tag{5.28}$$

if the same source is at $\rho_o > a$. Combining (5.19) - (5.28) and using the fact that $\mathcal{E}^{+}_{zn}(a,\alpha) \equiv \mathcal{E}^{+}_{\phi n}(a,\alpha) \equiv 0$ (total field) we obtain

$$\mathcal{H}^{+}_{zn}(a,\alpha) + \mathcal{H}^{-}_{zn}(a,-\alpha) = \frac{i}{\omega\mu\kappa a^{2}}\left\{\left(\frac{H^{(1)}_{n}(a\kappa)}{H^{(1)'}_{n}(a\kappa)} - \frac{J_{n}(a\kappa)}{J'_{n}(a\kappa)}\right)\left(e^{-}_{n}(\alpha) - e^{i}_{n}(\alpha)\right) + \frac{J_{n}(a\kappa)}{J'_{n}(a\kappa)}\, e^{-}_{n}(-\alpha)\right\} \tag{5.29}$$

$$h^{+}_{n}(\alpha) - h^{-}_{n}(-\alpha) = i\omega\epsilon\kappa a^{2}\left\{\left(\frac{H^{(1)'}_{n}(a\kappa)}{H^{(1)}_{n}(a\kappa)} - \frac{J'_{n}(a\kappa)}{J_{n}(a\kappa)}\right)\left(\mathcal{E}^{-}_{zn}(a,\alpha) - \mathcal{E}^{i}_{zn}(a,\alpha)\right) - \frac{J'_{n}(a\kappa)}{J_{n}(a\kappa)}\, \mathcal{E}^{-}_{zn}(a,-\alpha)\right\} \tag{5.30}$$

where all quantities except $e^{i}_{n}(\alpha)$ and $\mathcal{E}^{i}_{zn}(\alpha)$ are related to the total fields. Equations

(5.29) and (5.30) are valid if the source of the incident field is at $\rho_o > a$. If the source is at $\rho_o < a$ the corresponding relations are obtained by replacing $e^i_n(\alpha)$ by $e^i_n(\alpha) - e^i_n(-\alpha)$ in (5.29) and $\xi^i_{zn}(\alpha)$ by $\xi^i_{zn}(\alpha) + \xi^i_{zn}(-\alpha)$ in (5.30).

Employing the Wronskian we can write

$$\frac{H_n^{(1)}(a\kappa)}{H_n^{(1)'}(a\kappa)} - \frac{J_n(a\kappa)}{J_n'(a\kappa)} = \frac{-2i}{\pi a\kappa J_n'(a\kappa) H_n^{(1)'}(a\kappa)} \tag{5.31}$$

$$\frac{H_n^{(1)'}(a\kappa)}{H_n^{(1)}(a\kappa)} - \frac{J_n'(a\kappa)}{J_n(a\kappa)} = \frac{2i}{\pi a\kappa J_n(a\kappa) H_n^{(1)}(a\kappa)} \quad . \tag{5.32}$$

We now perform a factorization such that

$$L_n(\alpha) L_n(-\alpha) = \pi i J_n(a\kappa) H_n^{(1)}(a\kappa) \tag{5.33}$$

$$M_n(\alpha) M_n(-\alpha) = \pi i J_n'(a\kappa) H_n^{(1)'}(a\kappa) \tag{5.34}$$

where, for $\mathrm{Im}\alpha > -k_i$, $L_n(\alpha)$ and $M_n(\alpha)$ are analytic, have no zeros and behave as $O(1/\sqrt{\alpha})$ as $|\alpha| \to \infty$. We define

$$L_{-n}(\alpha) \equiv L_n(\alpha) \tag{5.35}$$

$$M_{-n}(\alpha) \equiv M_n(\alpha) \tag{5.36}$$

$$M_o(\alpha) \equiv L_1(\alpha) \quad . \tag{5.37}$$

Further details about the functions L_n and M_n are given in Section 5.6. Equations (5.29) and (5.30) can now be rewritten as

$$(-i\omega\mu a)\left(\mathcal{H}_z^+(a,\alpha)+\mathcal{H}_z^-(a,-\alpha)\right) M_n(-\alpha) - F_n^+(\alpha)+f_n^+(\alpha) - \frac{e_n^-(k)}{a^2k(k-\alpha)M_n(k)}$$

$$= \frac{2e_n^-(\alpha)}{a^2\kappa^2 M_n(\alpha)} - \frac{e_n^-(k)}{a^2k(k-\alpha)M_n(k)} + F_n^-(\alpha) - f_n^-(\alpha) \tag{5.38}$$

$$i\frac{h_n^+(\alpha)-h_n^-(-\alpha)}{\omega\epsilon(k+\alpha)a^2} L_n(-\alpha) - G_n^+(\alpha)+g_n^+(\alpha) - i\frac{h_n^+(-k)-h_n^-(k)}{\omega\epsilon(k+\alpha)a^2} L_n(k)$$

$$= \frac{2\mathcal{E}_{zn}^-(a,\alpha)}{a(k+\alpha)L_n(\alpha)} - i\frac{h_n^+(-k)-h_n^-(k)}{\omega\epsilon(k+\alpha)a^2} L_n(k)+G_n^-(\alpha)-g_n^-(\alpha) \tag{5.39}$$

where

$$F_n(\alpha) = \frac{J_n(a\kappa)M_n(-\alpha)}{\kappa a J_n'(a\kappa)} e_n^-(-\alpha) \tag{5.40}$$

$$G_n(\alpha) = \frac{\kappa J_n'(a\kappa)L_n(-\alpha)}{(k+\alpha)J_n(a\kappa)} \mathcal{E}_{zn}^-(a,-\alpha) \tag{5.41}$$

and

$$f_n(\alpha) = \frac{2}{a^2\kappa^2 M_n(\alpha)} \begin{cases} e_n^i(\alpha), & \text{source at } \rho_o > a \\ e_n^i(\alpha) - e_n^i(-\alpha), & \text{source at } \rho_o < a \end{cases} \tag{5.42}$$

$$g_n(\alpha) = \frac{2}{a(k+\alpha)L_n(\alpha)} \begin{cases} \mathcal{E}_{zn}^i(a,\alpha), & \text{source at } \rho_o > a \\ \mathcal{E}_{zn}^i(a,\alpha) + \mathcal{E}_{zn}^i(a,-\alpha), & \text{source at } \rho_o < a \end{cases} \tag{5.43}$$

The left hand side in (5.38) and (5.39) is analytic when $\mathrm{Im}\alpha < k_i$ and the right hand side is analytic when $\mathrm{Im}\alpha > -k_i$. They consequently represent a function analytic in the whole α-plane. The behavior of the Fourier transforms of the field components when $|\alpha| \to \infty$ is given by the edge conditions and $L_n(\alpha)$ and $M_n(\alpha)$ are $O(1/\sqrt{\alpha})$ as $|\alpha| \to \infty$. From this it can be concluded that both sides tend to zero at infinity and the common analytic function is consequently identically zero. The constants $e_n^-(k)$ and $h_n^+(-k) - h_n^-(k)$ in (5.38) and (5.39) can be determined by putting $\alpha = -k$ in (5.38) and $\alpha = k$ in (5.39) and using the relations $e_n^-(k) = kna\mathcal{E}_{zn}^-(a,k)$ and $h_n^+(-k) - h_n^-(k) = -kna\left[\mathcal{H}_{zn}^+(a,-k) + \mathcal{H}_{zn}^-(a,k)\right]$ obtained from (5.23) and (5.24). Performing this we end up with the following expressions:

$$e_n^-(\alpha) = a(k+\alpha)M_n(\alpha)\left\{\frac{aknL_n(k)}{4k^2a^2M_n^2(k) - n^2L_n^2(k)}\left[2k^2a^2M_n(k)\left(g_n^-(k) - G_n^-(k)\right) - \right.\right.$$

$$\left.\left. -nL_n(k)\left(f_n^+(-k) - F_n^+(-k)\right)\right] + \frac{a(k-\alpha)}{2}\left(f_n^-(\alpha) - F_n^-(\alpha)\right)\right\} \tag{5.44}$$

$$\mathcal{E}_{zn}^-(a,\alpha) = L_n(\alpha)\left\{\frac{aknL_n(k)}{4k^2a^2M_n^2(k) - n^2L_n^2(k)}\left[nL_n(k)\left(g_n^-(k) - G_n^-(k)\right) - \right.\right.$$

$$\left.\left. -2M_n(k)\left(f_n^+(-k) - F_n^+(-k)\right)\right] + \frac{a(k+\alpha)}{2}\left(g_n^-(\alpha) - G_n^-(\alpha)\right)\right\} . \tag{5.45}$$

Employing equations (5.8), (5.40) and (5.41) we obtain

$$F_n^-(\alpha) = \frac{1}{2\pi i}\int_{-\infty}^{\infty} \frac{J_n\left(a\sqrt{k^2-\gamma^2}\right)M_n(-\gamma)e_n^-(-\gamma)}{a\sqrt{k^2-\gamma^2}\,J_n'\left(a\sqrt{k^2-\gamma^2}\right)(\gamma-\alpha)}\,d\gamma \tag{5.46}$$

$$G_n^-(\alpha) = \frac{1}{2\pi i} \int_{-\infty}^{\infty} \frac{\sqrt{k^2-\gamma^2}\, J_n'\left(a\sqrt{k^2-\gamma^2}\right) L_n(-\gamma)\, \mathcal{E}_{zn}^-(a,-\gamma)}{(k+\gamma)\, J_n\left(a\sqrt{k^2-\gamma^2}\right)(\gamma-\alpha)}\, d\gamma \qquad (5.47)$$

where the path of integration passes below the pole $\gamma=\alpha$.

Thus, equations (5.44) and (5.45) are in fact a system of integral equations. The only singularities of the integrands in (5.46) and (5.47) in the lower half-plane are simple poles and by completing the contour of integration by a large semi-circle in the lower half-plane $F_n^-(\alpha)$ and $G_n^-(\alpha)$ can be calculated by means of residues. We write

$$F_n^-(\alpha) = \sum_{m=1}^{\infty} \frac{A_{nm}}{\alpha+\alpha'_{nm}} \qquad (5.48)$$

$$G_n^-(\alpha) = \sum_{m=0}^{\infty} \frac{B_{nm}}{\alpha+\alpha_{nm}} \qquad (5.49)$$

where

$$A_{nm} = \frac{1}{a^2} \frac{M_n(\alpha'_{nm})\, e_n^-(\alpha'_{nm})\, j'^2_{nm}}{\alpha'_{nm}(n^2 - j'^2_{nm})} \qquad (5.50)$$

$$B_{nm} = \frac{L_n(\alpha_{nm})\, j^2_{nm}\, \mathcal{E}_{zn}^-(a,\alpha_{nm})}{a^3 \alpha_{nm}(k-\alpha_{nm})} \qquad m \geqslant 1$$

$$B_{no} = \frac{n}{a} L_n(k)\, \mathcal{E}_{zn}^-(a,k) \qquad (5.51)$$

and

$$J_n'(j'_{nm}) = 0\,, \qquad 0 = j'_{no} < j'_{n1} < \ldots$$

$$\alpha'_{nm} = \sqrt{k^2 - \frac{j'^2_{nm}}{a^2}}\,, \qquad \mathrm{Im}\alpha'_{nm} > 0$$

$$J_n(j_{nm}) = 0\,, \qquad 0 = j_{no} < j_{n1} < \ldots$$

$$\alpha_{nm} = \sqrt{k^2 - \frac{j^2_{nm}}{a^2}}\,, \qquad \mathrm{Im}\alpha_{nm} > 0$$

(we define $j_{oo} = j'_{1o} = 0$ although they are not zeros of J_o and J'_1.)

Inserting $\alpha = \alpha'_{nm}$ and $\alpha = \alpha_{nm}$ respectively in (5.44) and (5.45) we obtain the following infinite system of linear equations for the coefficients A_{nm} and B_{nm}:

$$\frac{a\alpha'_{n\ell}(n^2 - j'^2_{n\ell})}{M_n^2(\alpha'_{n\ell})j'^2_{n\ell}(k+\alpha'_{n\ell})} A_{n\ell} =$$

$$= \frac{akn\,L_n(k)\left[nL_n(k)\left(\sum_{m=1}^{\infty}\frac{A_{nm}}{\alpha'_{nm}-k} + f_n^+(-k)\right) - 2a^2k^2M_n(k)\left(g_n^-(k) - \sum_{m=0}^{\infty}\frac{B_{nm}}{k+\alpha_{nm}}\right)\right]}{nL_n^2(k)\left(n+2a^2k^2M_n^2(k)\right) - 4a^2k^2M_n^2(k)}$$

$$- \frac{a(k-\alpha'_{n\ell})}{2}\left(\sum_{m=1}^{\infty}\frac{A_{nm}}{\alpha'_{n\ell}+\alpha'_{nm}} - f_n^-(\alpha'_{n\ell})\right) \qquad \begin{matrix} n = 0,1,2,\ldots \\ \ell = 1,2,3,\ldots \end{matrix}$$

(5.52)

$$\frac{a^3\alpha_{n\ell}(k-\alpha_{n\ell})}{L_n^2(\alpha_{n\ell})j_{nm}^2}B_{n\ell} = \frac{akn\,L_n(k)\left[L_n(k)\left(\sum_{m=0}^{\infty}\frac{B_{nm}}{k+\alpha_{nm}} - g_n^-(k)\right)\left(n+2a^2k^2M_n^2(k)\right) + 2M_n(k)\left(\sum_{m=1}^{\infty}\frac{A_{nm}}{\alpha'_{nm}-k} + f_n^+(-k)\right)\right]}{nL_n^2(k)\left(n+2a^2k^2M_n^2(k)\right) - 4a^2k^2M_n^2(k)}$$

$$+ \frac{a(k+\alpha_{n\ell})}{2}\left(g_n^-(\alpha_{n\ell}) - \sum_{m=0}^{\infty}\frac{B_{nm}}{\alpha_{n\ell}+\alpha_{nm}}\right) \qquad \begin{matrix} n = 0, 1, 2, \ldots \\ \ell = 1, 2, 3, \ldots \end{matrix}$$

$$B_{no} = \frac{2nk\,L_n^2(k)\,M_n(k)\left[2a^2k^2M_n(k)\left(\sum_{m=0}^{\infty}\frac{B_{nm}}{k+\alpha_{nm}} - g_n^-(k)\right) + nL_n(k)\left(\sum_{m=1}^{\infty}\frac{A_{nm}}{\alpha'_{nm}-k} + f_n^+(-k)\right)\right]}{nL_n^2(k)\left(n+2a^2k^2M_n^2(k)\right) - 4a^2k^2M_n^2(k)}$$

(5.53)

When A_{nm} and B_{nm} are calculated, the solution to the problem is obtained by inserting in (5.44) and (5.45) $F_n^-(\alpha)$ from (5.48) and $G_n^-(\alpha)$ from (5.49) and

$$F_n^+(-k) = \frac{2a^2k^2M_n^2(k)L_n(k)\left[nL_n(k)\left(\sum_{m=1}^{\infty}\frac{A_{nm}}{\alpha'_{nm}-k}+f_n^+(-k)\right)-2a^2k^2M_n(k)\left(g^-(k)-\sum_{m=0}^{\infty}\frac{B_{nm}}{k+\alpha_{nm}}\right)\right]}{nL_n^2(k)\left(n+2a^2k^2M_n^2(k)\right)-4a^2k^2M_n^2(k)}$$

$$-\sum_{m=1}^{\infty}\frac{A_{nm}}{\alpha'_{nm}-k} \qquad n = 1, 2, 3, \ldots \qquad (5.54)$$

The functions $F_n(\alpha)$ and $G_n(\alpha)$ affect only the boundary values on the plane end surface. $E_z(a, z)$ and $E_\phi(a, z)$ vanish for $z > 0$ for every choice of F_n and G_n. In particular, by taking $G_n(\alpha) = F_n(\alpha) = 0$, (5.44) and (5.45) express the solution for a semi-infinite thin-walled tube. In this case, the $f_n(\alpha)$ and $g_n(\alpha)$ are defined by the upper alternatives in (5.42) and (5.43) regardless of the position of the source of the incident field.

The field components at an arbitrary point can now be calculated as a summation over $n = -\infty$ to ∞ and an integration over α from $-\infty$ to ∞ of expressions containing the quantities $e_n^-(\alpha)$ and $\mathcal{E}_{zn}^-(a,\alpha)$ of (5.44) and (5.45). We write

$$X(\rho, \phi, z) = X^i(\rho, \phi, z) + \frac{1}{2\pi} \sum_{n=-\infty}^{\infty} e^{in\phi} \int_\Gamma \left[A(\alpha)H_n^{(1)}(\rho\kappa) + B(\alpha)H_n^{(1)'}(\rho\kappa)\right] e^{i\alpha z}\, d\alpha \tag{5.55}$$

$$\rho > a, \quad -\infty < z < \infty$$

where X stands for an arbitrary field component. The path of integration Γ is as indicated in Fig. 5-1 after the imaginary part of k is put to zero. When $\rho < a$ and

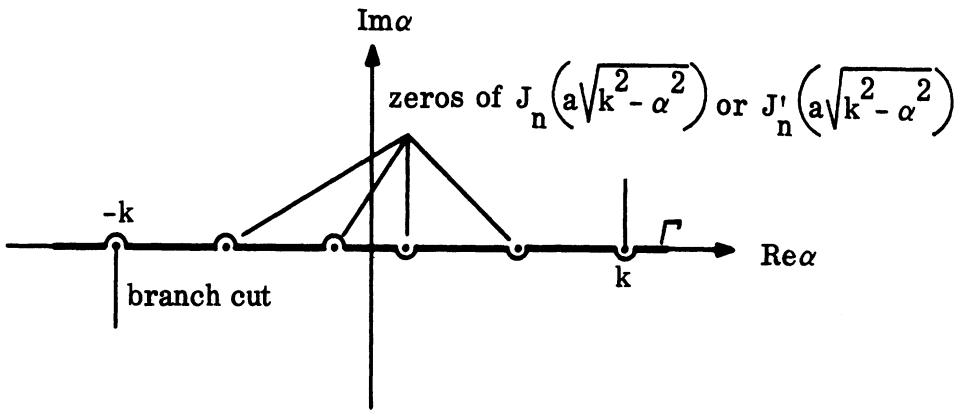

FIG. 5-1: PATH OF INTEGRATION FOR THE INVERSE FOURIER TRANSFORM

the source of the incident field is located at $\rho_o > a$ we have

$$X(\rho,\phi,z) = \frac{1}{2\pi}\sum_{n=-\infty}^{\infty} e^{in\phi}\int_{\Gamma}\left[A(\alpha)J_n(\rho\kappa)+B(\alpha)J_n'(\rho\kappa)\right]e^{i\alpha z}\,d\alpha \qquad (5.56)$$

$$\rho < a,\ -\infty < z < 0$$

If the source is at $\rho_o < a$ we write

$$X(\rho,\phi,z) = X^i(\rho,\phi,z)+X^r(\rho,\phi,z)+\frac{1}{2\pi}\sum_{n=-\infty}^{\infty} e^{in\phi}\int_{\Gamma}\left[A(\alpha)J_n(\rho\kappa)+B(\alpha)J_n'(\rho\kappa)\right]e^{i\alpha z}\,d\alpha$$

$$\rho < a,\ -\infty < z < 0 \qquad (5.57)$$

where X^r is the incident field reflected by a perfectly conducting infinite plane at $z = 0$. The expressions for $A(\alpha)$ and $B(\alpha)$ in (5.55) - (5.57) are given in Table V.

The radiation far field can be obtained from (5.55) by estimating the integral by the method of steepest descent. If we introduce spherical coordinates (r,θ,ϕ) such that $z = r\cos\theta$, $\rho = r\sin\theta$ we get

$$X(r,\theta,\phi) \sim X^i + \frac{e^{ikr}}{r}\frac{1}{\pi}\sum_{n=-\infty}^{\infty} e^{in\phi}(-i)^n\left[-iA(k\cos\theta)+B(k\cos\theta)\right] \qquad (5.58)$$

when $kr\to\infty$ is $kr\sin^2\theta \gg 1$.

Equation (5.58) is obtained under the assumption that the source of the incident field is located at a finite distance. For plane wave incidence, the scattered field in the region $\theta < \theta_o$, where θ_o is the angle between the direction of propagation of the plane wave and the positive z-axis, contains an additional part equal to the field reflected by an infinite cylinder. A and B in (5.58) are still given by Table V with $b(\alpha)$ and $c(\alpha)$ belonging to $\rho > a$. The terms containing ρ in the denominator then contribute only to higher order terms and should be disregarded.

TABLE V
Relation Between the Field Components and the Quantity X
of Equations (5.55) - (5.58)

X	A(α)	B(α)
E_ρ	$-\frac{in}{\rho\kappa^3 a^2} b(\alpha)$	$\frac{i\alpha}{\kappa} c(\alpha)$
E_ϕ	$-\frac{\alpha n}{\rho\kappa^2} c(\alpha)$	$\frac{1}{\kappa^2 a^2} b(\alpha)$
E_z	$c(\alpha)$	0
H_ρ	$\frac{\omega\epsilon n}{\rho\kappa^2} c(\alpha)$	$-\frac{\alpha}{\omega\mu\kappa^2 a^2} b(\alpha)$
H_ϕ	$-\frac{in\alpha}{\rho\omega\mu\kappa^3 a^2} b(\alpha)$	$\frac{i\omega\epsilon}{\kappa} c(\alpha)$
H_z	$\frac{i}{\omega\mu\kappa a^2} b(\alpha)$	0

where $b(\alpha) = \dfrac{e_n^-(\alpha) - e_n^i(\alpha)}{H_n^{(1)'}(a\kappa)}$ $\qquad$ $b(\alpha) = \dfrac{e_n^-(\alpha) - e_n^-(-\alpha)}{J_n'(a\kappa)}$

$$c(\alpha) = \frac{\mathcal{E}_{zn}^-(a,\alpha) - \mathcal{E}_{zn}^i(a,\alpha)}{H_n^{(1)}(a\kappa)} \qquad c(\alpha) = \frac{\mathcal{E}_{zn}^-(a,\alpha) + \mathcal{E}_{zn}^-(a,-\alpha)}{J_n(a\kappa)}$$

when $\rho > a$ $\qquad$ when $\rho < a$

$$\kappa^2 = k^2 - \alpha^2 \ .$$

5.2 Scattering of a Scalar Plane Wave by a Semi-Infinite Cylinder

The case when the cylinder is solid, i.e. a rod of circular cross section, has been treated by Jones (1955) (cf. also Matsui, 1960) for both the boundary condition $\frac{\partial u}{\partial \rho} = 0$ and $u = 0$. His results also contain in principle the solution for a thin-walled tube and therefore we will not treat that case separately. Since the problem under consideration can be treated in a way quite analogous to that given in the previous section, the results will be given without derivation. As noted before, if the solution to the electromagnetic scattering problem is known, $u_1 = H_z$ and $u_2 = E_z$ do not yield the solution to the scalar problems with boundary conditions $\partial u_1/\partial \rho = 0$ and $u_2 = 0$ for the incident waves $u_1^i = H_z^i$ and $u_2^i = E_z^i$ respectively. The reason is that u_1 and u_2 so constructed do not satisfy the correct edge condition at the open end of the tube.

This section contains essentially the results given in Jones' paper, written in conformity with our earlier notations (time dependence $e^{-i\omega t}$).

Let the cylinder occupy the space $\rho < a$, $z > 0$ and the incident plane wave be given by

$$u^{(0)} = \exp(ik\rho \sin\theta_i \cos\phi + ikz \cos\theta_i) \tag{5.59}$$

i.e., the angle between the direction of propagation and the positive z-axis is θ_i.

5.2.1 The Boundary Condition $\partial u/\partial \rho = 0$ when the Angle of Incidence is Neither 0 Nor π

Let the total field be given by

$$u^{(0)} + u^{(1)} + u(\rho, \phi, z) \quad \text{in} \quad \rho > a$$

$$u(\rho, \phi, z) \quad \text{in} \quad \rho < a, \; z < 0$$

$$0 \quad \text{in} \quad \rho < a, \; z > 0$$

where

$$u^{(1)} = -e^{ikz\cos\theta_i} \sum_{n=-\infty}^{\infty} e^{in\frac{\pi}{2}} \frac{J_n'(ka\sin\theta_i)}{H_n^{(1)'}(ka\sin\theta_i)} H_n^{(1)}(k\rho\sin\theta_i)\, e^{in\phi} \tag{5.60}$$

is the field reflected by an infinite cylinder (cf. Eq. 2.34).

We have

$$u(\rho,\phi,z) = \begin{cases} \dfrac{1}{2\pi}\displaystyle\sum_{n=-\infty}^{\infty} e^{in\phi}\int_\Gamma \frac{P_n(\alpha)}{\kappa H_n^{(1)'}(\kappa a)} H_n^{(1)}(\kappa\rho)\, e^{i\alpha z}\, d\alpha\,, & \rho > a \\ \dfrac{1}{2\pi}\displaystyle\sum_{n=-\infty}^{\infty} e^{in\phi}\int_\Gamma \left[\frac{P_n(\alpha)}{\kappa J_n'(\kappa a)} J_n(\kappa\rho) + i\alpha \sum_{m=0}^{\infty} \frac{f_{nm} J_n\left(\frac{j'_{nm}\rho}{a}\right)}{\alpha^2 - \alpha'^2_{nm}}\right] e^{i\alpha z}\, d\alpha\,, & \rho < a \end{cases} \tag{5.61}$$

where

$$f_{nm} = \frac{2i j'^2_{nm} P_n(\alpha'_{nm})}{a\alpha'_{nm}(j'^2_{nm} - n^2)J_n(j'_{nm})}, \qquad m \geq 1$$

$$f_{no} = \frac{2i\delta_{on} P_o(k)}{ak} \qquad (\delta_{mn} = 0,\ n \neq m;\ = 1,\ n = m)$$

and as before

$$\kappa^2 = k^2 - \alpha^2$$

$$J_n'(j'_{nm}) = 0 \qquad 0 = j'_{no} < j'_{n1} < \ldots \quad \text{(we define } j'_{10} = 0 \text{ although it is not a zero of } J_1')$$

$$\alpha'_{nm} = \sqrt{k^2 - \frac{j'^2_{nm}}{a^2}}\,, \qquad \text{positive real or imaginary .}$$

The path of integration is given by Fig. 5-1 and passes above all poles of $P_n(\alpha)$. The equation for $P_n(\alpha)$ is

$$\frac{\pi i P_n(\alpha)}{(\alpha+k)M_n(\alpha)} = \frac{G_n}{\alpha - k\cos\theta_i} - \frac{\delta_{on} G_o a_{oo}}{a+k} - \sum_{m=1}^{\infty} \frac{G_n a_{nm}}{\alpha + \alpha'_{nm}} \tag{5.62}$$

where

$$G_n = \frac{i^{n+1}(1-\cos\theta_i)M_n(-k\cos\theta_i)}{\sin\theta_i H_n^{(1)'}(ka\sin\theta_i)}$$

and $M_n(\alpha)$ is the split function defined by (5.34). The constants a_{nm} are determined by the following equations:

$$a'_{nr}a_{nr} = \frac{1}{\alpha'_{nr} - k\cos\theta_i} - \frac{\delta_{on}a_{oo}}{a'_{nr}+k} - \sum_{m=1}^{\infty} \frac{a_{nm}}{\alpha'_{nr}+\alpha'_{nm}}, \qquad r = 0, 1, \ldots \tag{5.63}$$

where

$$a'_{nr} = \frac{2\alpha'_{nr}(j'^2_{nr} - n^2)}{\left[j'_{nr}(\alpha'_{nr}+k)M_n(\alpha'_{nr})\right]^2}$$

$$\alpha'_{oo} = \frac{1}{2kL_1^2(k)} .$$

The edge condition requires that $a_{nm} \sim m^{-7/6}$ as $m \to \infty$ and we must also have

$$\delta_{on}a_{oo} + \sum_{m=1}^{\infty} a_{nm} = 1 . \tag{5.64}$$

The solution for a semi-infinite thin-walled tube is obtained by putting $f_{nm} = 0$ in (5.61) and $a_{nm} = 0$ in (5.62) for all n and m. Inside the tube, i.e., $\rho < a$, $z > 0$, the integral in equation (5.61) can be calculated by residues. Thus,

$$u(\rho,\phi,z) = \frac{iP_o(k)}{ka} e^{ikz} + i \sum_{n=-\infty}^{\infty} e^{in\phi} \sum_{m=1}^{\infty} \frac{j'^2_{nm} P_n(\alpha'_{nm}) J_n(j'_{nm}\frac{\rho}{a})}{a\alpha'_{nm}(j'^2_{nm} - n^2) J_n(j'_{nm})} e^{i\alpha'_{nm} z}$$

$$\rho < a, \quad z > 0 \qquad (5.65)$$

5.2.2 The Boundary Condition $\partial u/\partial\rho = 0$ when the Angle of Incidence is 0

Here we take the incident wave to be e^{ikz}. The total field is assumed to be

$$e^{ikz} + u \qquad \text{in } \rho < a$$

$$e^{ikz} + e^{-ikz} + u \qquad \text{in } \rho < a, \quad z < 0$$

$$0 \qquad \text{in } \rho < a, \quad z > 0 \ .$$

The result is

$$u(\rho,\phi,z) = \begin{cases} \dfrac{1}{2\pi} \displaystyle\int_\Gamma \frac{P(\alpha)}{\kappa H_o^{(1)'}(\kappa a)} H_o^{(1)}(\kappa\rho) e^{i\alpha z} d\alpha & \rho > a \\ \dfrac{1}{2\pi} \displaystyle\int_\Gamma \left[\frac{P(\alpha)}{\kappa J'_o(\kappa a)} J_o(\kappa\rho) + i\alpha \sum_{m=0}^{\infty} \frac{h_m J_o\left(\frac{j'_{om}\rho}{a}\right)}{\alpha^2 - \alpha'^2_{nm}} \right] e^{i\alpha z} d\alpha \ , & \rho < a \end{cases} \qquad (5.66)$$

where

$$h_m = \frac{2iP(\alpha'_{om})}{a\alpha'_{nm} J_o(j'_{om})} \ , \qquad m \neq 0$$

$$h_o = \frac{2i\,P(k)}{ak} \ .$$

The equation for $P(\alpha)$ is

$$\frac{\pi i P(\alpha)}{\beta'_o(\alpha+k)L_1(\alpha)} = \frac{1-\beta_o}{a+k} - \sum_{m=1}^{\infty} \frac{\beta_m}{\alpha+\alpha'_{om}} \qquad (5.67)$$

where $\beta'_o = -\pi akL_1(k)$.

The equations for the constants β_m are

$$\frac{2\alpha'_{or}\beta_r}{\left[(\alpha'_{or}+k)L_1(\alpha'_{or})\right]^2} = \frac{1-\beta_o}{\alpha'_{or}+k} - \sum_{m=1}^{\infty}\frac{\beta_m}{\alpha'_{or}+\alpha'_{om}}\ , \qquad r = 0, 1, \ldots \tag{5.68}$$

5.2.3 The Boundary Condition u = 0

We assume the angle of incidence to be neither 0 nor π and write the total field as

$$\begin{cases} u^{(0)} + u^{(2)} + u(\rho, \phi, z) & \text{in } \rho \geqslant a \\ u(\rho, \phi, z) & \text{in } \rho \leqslant a,\ z \leqslant 0 \\ 0 & \text{in } \rho \leqslant a,\ z \geqslant 0 \end{cases}$$

where $u^{(0)}$ is the incident wave given by (5.59) and

$$u^{(2)} = -e^{ikz\cos\theta_i}\sum_{n=-\infty}^{\infty} e^{in\frac{\pi}{2}}\frac{J_n(ka\sin\theta_i)}{H_n^{(1)}(ka\sin\theta_i)}H_n^{(1)}(k\rho\sin\theta_i)e^{in\phi} \tag{5.69}$$

is the field reflected by an infinite cylinder (cf Eq. 2.29). We obtain

$$u(\rho, \phi, z) = \begin{cases} \dfrac{1}{2\pi}\displaystyle\sum_{n=-\infty}^{\infty} e^{in\phi}\int_\Gamma \frac{R_n(\alpha)}{H_n^{(1)}(\kappa a)}H_n^{(1)}(\kappa\rho)e^{i\alpha z}\,d\alpha\ , & \rho > a \\ \dfrac{1}{2\pi}\displaystyle\sum_{n=-\infty}^{\infty} e^{in\phi}\int_\Gamma \left[\frac{R_n(\alpha)}{J_n(\kappa a)}J_n(\kappa\rho) - \sum_{m=1}^{\infty}\frac{g_{nm}J_n\left(\frac{j_{nm}\rho}{a}\right)}{\alpha^2-\alpha_{nm}^2}\right]e^{i\alpha z}\,d\alpha\ , & \rho < a \end{cases} \tag{5.70}$$

where

$$g_{nm} = \frac{2j_{nm} R_n(\alpha_{nm})}{a^2 J_{n+1}(j_{nm})}$$

and as before

$$\kappa^2 = k^2 - \alpha^2$$

$$J_n(j_{nm}) = 0 \qquad 0 < j_{n1} < j_{n2} < \ldots$$

$$\alpha_{nm} = \sqrt{k^2 - \frac{j_{nm}^2}{a^2}} \qquad \text{positive real or imaginary .}$$

The equation for $R_n(\alpha)$ becomes

$$\frac{\pi R_n(\alpha)}{L_n(\alpha)} = \frac{\gamma_n}{\alpha - k\cos\theta_i} - \sum_{m=1}^{\infty} \frac{\gamma_n \gamma_{nm}}{\alpha + \alpha_{mn}} \tag{5.71}$$

where

$$\gamma_n = \frac{(i)^n L_n(-k\cos\theta_i)}{k\sin\theta_i H_n^{(1)}(ka\sin\theta_i)}$$

and $L_n(\alpha)$ is defined by (5.33). The γ_{nm} are determined from

$$\frac{-2a^2\alpha_{nr}\gamma_{nr}}{j_{nr}^2 L_n^2(\alpha_{nr})} = \frac{1}{\alpha_{nr} - k\cos\theta_i} - \sum_{m=1}^{\infty} \frac{\gamma_{nm}}{\alpha_{nr} + \alpha_{nm}}, \qquad r = 1, 2, \ldots \tag{5.72}$$

We also have

$$\gamma_{nm} = O(m^{-7/6}) \qquad \text{as} \qquad m \to \infty$$

and

$$\sum_{m=1}^{\infty} \gamma_{mn} = 1 \quad . \tag{5.73}$$

The solution for a semi-infinite thin-walled tube can be obtained by putting $g_{nm} = 0$ in (5.70) and $\gamma_{nm} = 0$ in (5.71) for all n and m. Inside the tube the field can be expressed as

$$u(\rho, \phi, z) = -i \sum_{n=-\infty}^{\infty} e^{in\phi} \sum_{m=1}^{\infty} \frac{j_{nm} R_n(\alpha_{nm}) J_n(j_{nm} \frac{\rho}{a})}{a^2 \alpha_{nm} J'_n(j_{nm})} e^{i\alpha_{nm} z} \tag{5.74}$$

$$\rho < a, \quad z > 0$$

5.2.4 The Far Field

For points at large distances from the origin the integrals in equations (5.61), (5.66) and (5.70) may be evaluated by the method of steepest descent. The integrand has a pole at $\alpha = k\cos\theta_i$ which for certain points of observation will be close to the saddle point. To overcome this difficulty a method by Van der Waerden (1951) is used. We introduce spherical coordinates (r, θ, ϕ) $\rho = r\sin\theta$, $z = r\cos\theta$ and following Bowman (1963b) we write the field in the far zone $kr\sin^2\theta \gg 1$ as

$$u \sim U(\theta, \phi) \frac{e^{ikr}}{r} + H(\theta - \theta_i) A(\phi) \frac{e^{ikr\cos(\theta - \theta_i)}}{\sqrt{kr\sin\theta}} -$$

$$- \frac{1}{2} \mathrm{sgn}(\theta - \theta_i) A(\phi) T(r, \theta - \theta_i) \frac{e^{ikr}}{\sqrt{kr\sin\theta}} \tag{5.75}$$

where

$$U(\theta, \phi) = \frac{1}{\pi} \sum_{n=-\infty}^{\infty} (-i)^{n+1} \frac{P_n(k\cos\theta)}{k\sin\theta H_n^{(1)'}(ka\sin\theta)} e^{in\phi} \tag{5.76}$$

$$A(\phi) = \sqrt{\frac{2}{\pi}}\, e^{-i\frac{\pi}{4}} \sum_{n=-\infty}^{\infty} \frac{J_n'(ka\sin\theta_i)}{\sqrt{\sin\theta_i}\, H_n^{(1)'}(ka\sin\theta_i)} e^{in\phi} \tag{5.77}$$

when the boundary condition is $\frac{\partial u}{\partial \rho} = 0$ and

$$U(\theta,\phi) = \frac{1}{\pi} \sum_{n=-\infty}^{\infty} (-i)^{n+1} \frac{R_n(k\cos\theta)}{H_n^{(1)}(ka\sin\theta)} e^{in\phi} \tag{5.78}$$

$$A(\phi) = \sqrt{\frac{2}{\pi}}\, e^{-i\frac{\pi}{4}} \sum_{n=-\infty}^{\infty} \frac{J_n(ka\sin\theta_i)}{\sqrt{\sin\theta_i}\, H_n^{(1)}(ka\sin\theta_i)} e^{in\phi} \tag{5.79}$$

when the boundary condition is $u = 0$. The total field is obtained as before by adding the incident and reflected waves to u. The functions $H(\theta-\theta_i)$ and $\mathrm{sgn}(\theta-\theta_i)$ are the Heaviside step function and the signum step function defined by

$$H(x) = \begin{cases} 1, & x > 0 \\ 0, & x < 0 \end{cases} \qquad \mathrm{sgn}\, x = \begin{cases} 1, & x > 0 \\ -1, & x < 0 \end{cases} \tag{5.80}$$

The function $T(r, \theta-\theta_i)$ is given by

$$T(r,\theta-\theta_i) = e^{-i2w^2}\, \mathrm{erfc}\left[(1-i)w\right] - \frac{e^{i\frac{\pi}{4}}}{w\sqrt{2\pi}} \tag{5.81}$$

where $w = \sqrt{kr}\left|\sin\frac{\theta-\theta_i}{2}\right|$ and the error function is defined by

$$\mathrm{erfc}\, z = \frac{2}{\sqrt{\pi}} \int_z^{\infty} e^{-t^2}\, dt \tag{5.82}$$

The second term in (5.75) removes the reflected wave $u^{(1)}$ and $u^{(2)}$ respectively in the region $\theta > \theta_i$. The last term can be interpreted as a transition contribution which assures a continuous field across the shadow boundary $\theta = \theta_i$. Thus it compensates for both the jump in the reflected field and the singularity of the first term at $\theta = \theta_i$. For fixed $\theta \neq \theta_i$ the transition term is asymptotically smaller than the other two; in practice it can usually be neglected when $w > 4$.

For $ka \ll 1$ and the boundary condition $u = 0$ the only term in (5.70) which must be considered is that for $n = 0$. For values of α such that $|\alpha a| \ll 1$ we can write the equation for $R_o(\alpha)$, (5.71), as

$$\frac{\pi R_o(\alpha)}{L_o(\alpha)} = \gamma_o \left(\frac{1}{\alpha - k\cos\theta_i} - \sum_{m=1}^{\infty} \frac{\gamma_{om}}{\alpha + \alpha_{om}} \right)$$

$$\approx \frac{\gamma_o}{\alpha - k\cos\theta_i} \left[1 + i(\alpha - k\cos\theta_i)\zeta \right]$$

$$\approx \frac{\pi R^{(0)}(\alpha)}{\gamma_o L_o(\alpha)} e^{i(\alpha - k\cos\theta_i)\zeta} \qquad (5.83)$$

where $\zeta = i \sum_{m=1}^{\infty} \frac{\gamma_{om}}{\alpha_{om}}$ and $R^{(0)}(\alpha)$ is the value of $R_o(\rho)$ when $\gamma_{om} = 0$ (all m), i.e. the case of a tube-shaped cylinder. Near the saddle point we have $|\alpha a| \ll 1$ and in estimating the far field we can consequently replace $R_o(\alpha)$ in the integral of (5.70) by the expression given in (5.83). This integral is then just that which occurs in the diffraction by a semi-infinite thin-walled tube at the positions $\rho = a$, $-\zeta \leqslant z \leqslant \infty$.

Thus, the far field for the semi-infinite rod is the same as that produced by a semi-infinite thin-walled tube of the same diameter, but longer by ζ, subject to the same incident field.

Under the assumption that $\gamma_{om} = 0$, $m > 2$, Jones calculated ζ to be $0.087a$ and he estimates the correct value to be close to $0.1a$.

There is no corresponding result for the boundary condition $\frac{\partial u}{\partial \rho} = 0$.

5.2.5 Numerical Computations for the Boundary Condition $\partial u/\partial \rho = 0$

Jones shows that when the angle of incidence is zero,

$$\frac{2}{a^2}\int_0^a t(u+2)_{z=0}\,dt = 2(1-\beta_o) \ . \tag{5.84}$$

The modulus of the left hand side of (5.84) represents the average pressure amplitude on the end of the rod if u stands for the velocity potential of a small-amplitude sound wave. The constant β_o is obtained from (5.68). Jones solves this equation approximately by assuming successively

(i) $\beta_m = 0, \ m > 0$ (ii) $\beta_m = 0, \ m > 1$ (iii) $\beta_m = 0, \ m > 2$.

The average pressure amplitude as a function of ka for the range $0 \leqslant ka \leqslant 10$ is given in Fig. 5-2. The plotted curves correspond to the third and seventh ($\beta_m = 0$, $m > 6$) approximation, the latter calculated by Matsui (1960) for $ka \leqslant 3$.

When the incident wave is propagating along the axis of the cylinder it satisfies the boundary condition along the cylindrical surface $\rho = a$. The scattered energy is consequently finite and can be obtained by integration over the end surface only. The scattering coefficient c_o is related to the constant β_o by

$$c_o = 1 - 2\,\mathrm{Re}\{\beta_o\} \tag{5.85}$$

c_o is defined as $c_o = c_1/\pi a^2$ where c_1 is the scattering cross section defined as the quotient of the scattered energy and the incident energy per unit area. The scattering coefficient is plotted against ka in Fig. 5-3.

For small ka ($ka < 2$) we can use the approximation

$$c_o \approx \frac{1}{4}(ka)^2 \ . \tag{5.86}$$

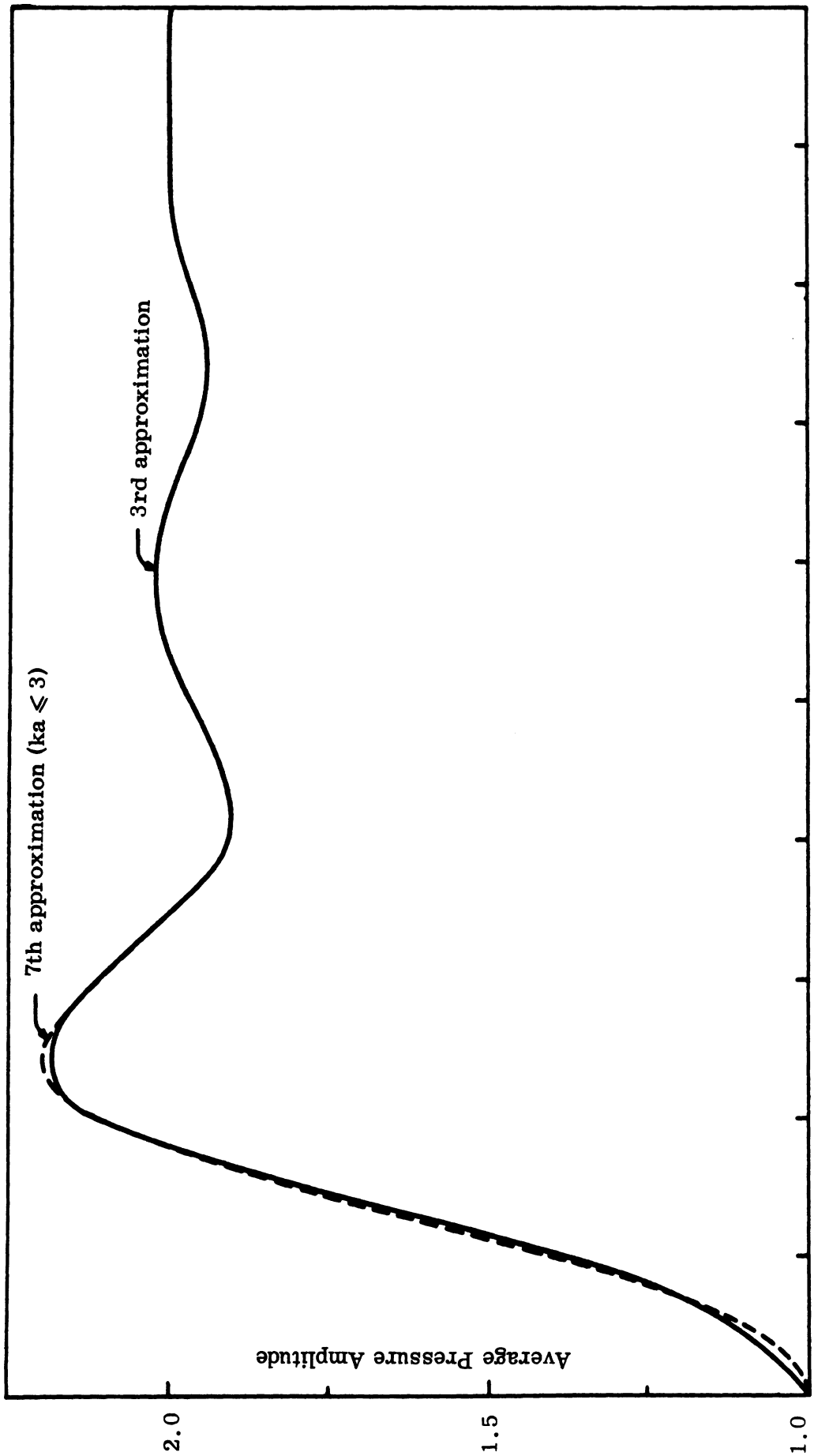

FIG. 5-2: THE AVERAGE PRESSURE AMPLITUDE ON THE END OF THE ROD WHEN THE ANGLE OF INCIDENCE IS ZERO. (— Jones, 1955; - - - Matsui, 1960).

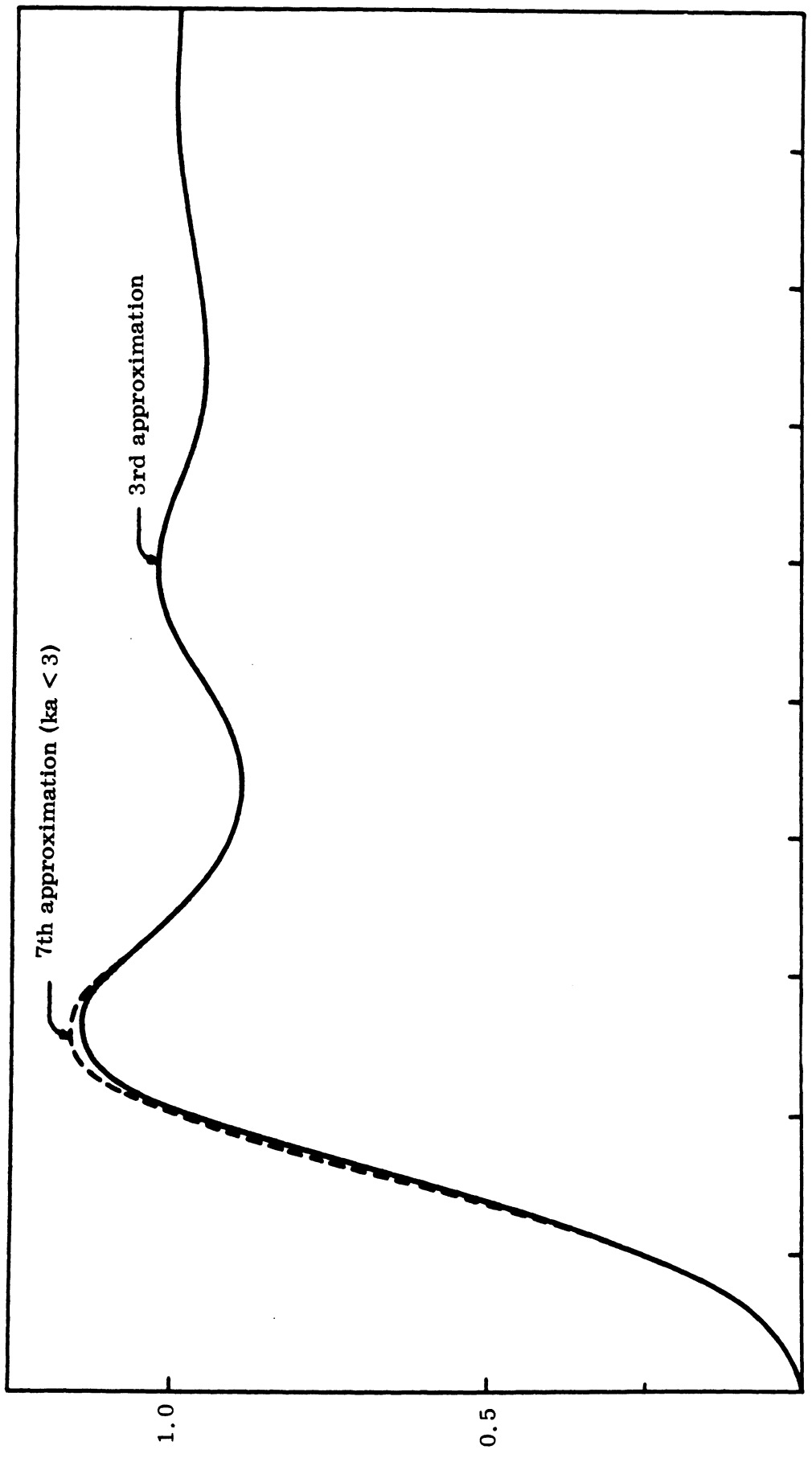

FIG. 5-3: THE SCATTERING COEFFICIENT WHEN THE ANGLE OF INCIDENCE IS ZERO. (—— Jones, 1955; – – – Matsui, 1960)

When the angle of incidence is not 0, Jones shows that, to a first approximation (which is better the smaller ka), the average pressure amplitude on the end of the cylinder is the product of the average pressure amplitude when the angle of incidence is 0 and the amplitude of the symmetric wave that is produced in a hollow semi-infinite cylinder occupying the same position as the rod. The results given by Jones are reproduced in Fig. 5-4.

Jones also calculates the pressure on the end of the rod due to a pressure pulse when the angle of incidence is zero. Let the pressure of the incident sound pulse be given by

$$p_o(t,z) = H\left(t-\frac{z}{a_o}\right) = -\frac{1}{2\pi i}\int_{-\infty+i\epsilon}^{\infty+i\epsilon}\frac{e^{-ik(v_o t-z)}}{k}\,dk \qquad (5.87)$$

where v_o is the speed of sound, t is the time and $H(x)$ is the Heaviside step function defined by (5.80). According to (5.84) the average pressure (i.e. total pressure/end area) due to the incident wave e^{ikz} is $2(1-\beta_o)$. The average pressure due to $p_o(t,z)$ is consequently

$$p(t) = -\frac{1}{\pi i}\int_{-\infty+i\epsilon}^{\infty+i\epsilon}\frac{e^{-ikv_o t}}{k}\left[1-\beta_o(k)\right]dk\,. \qquad (5.88)$$

The integrand has a simple pole at $k=0$ with residue $1/2$ since $\beta_o = 1/2$ when $ka=0$. Thus the above integral may be written as

$$p(t) = 1-\frac{1}{2\pi i}\int_{-\infty}^{\infty}\frac{1-2\beta_o(k)}{k}e^{-ikv_o t}\,dk$$

$$= 1+\frac{1}{\pi}\int_{-\infty}^{\infty}\left[\left(F(k)-1\right)\sin(kv_o t)+G(k)\cos(kv_o t)\right]\frac{dk}{k} \qquad (5.89)$$

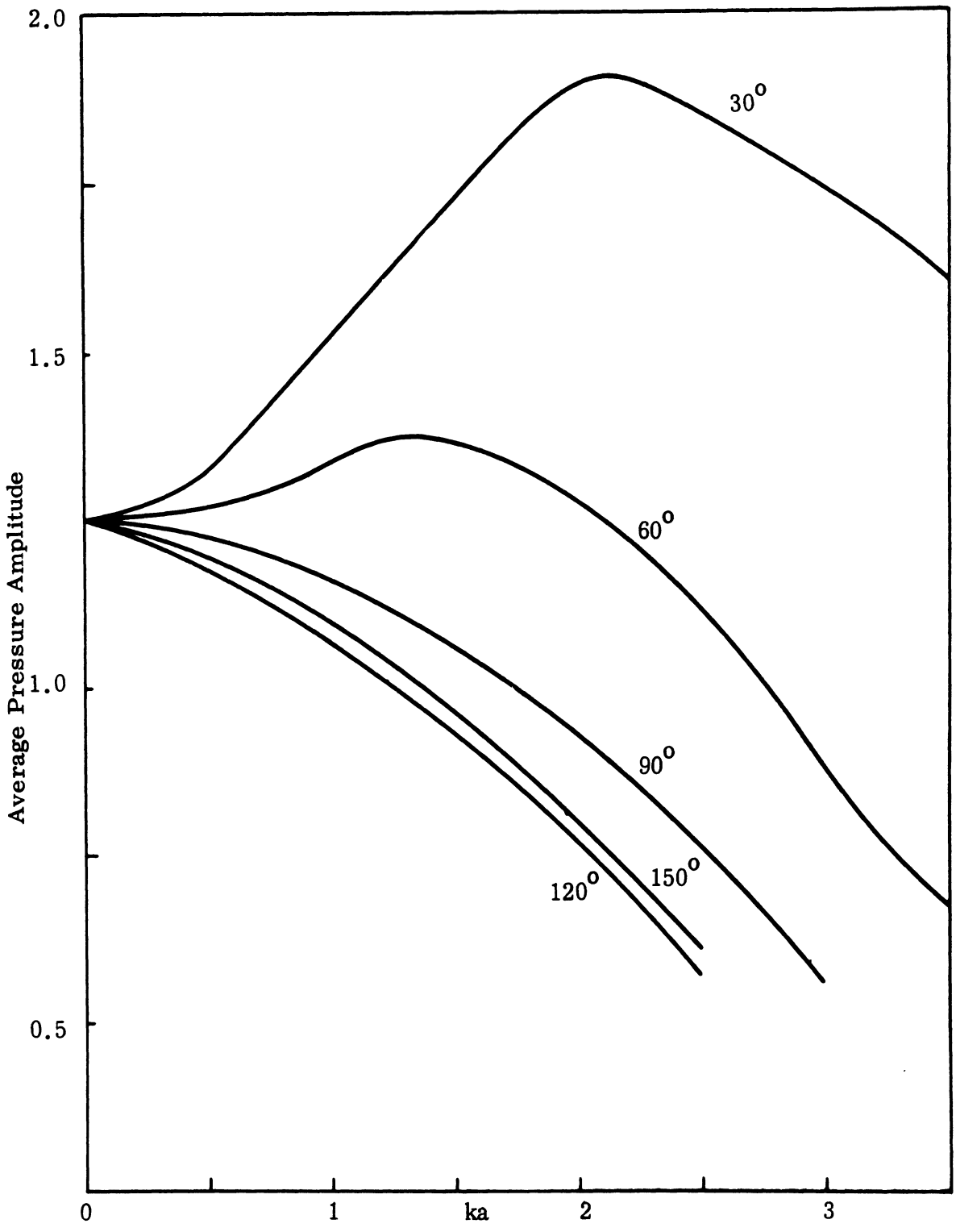

FIG. 5-4: THE AVERAGE PRESSURE AMPLITUDE ON THE END OF THE ROD FOR VARIOUS ANGLES OF INCIDENCE (Jones, 1955).

where $2\left[1-\beta_o(k)\right] = F(k)+iG(k)$ and we used the fact that $\beta_o(-k)$ is the complex conjugate of $\beta_o(k)$. Jones computes the integral in (5.89) from the earlier values of $\beta_o(k)$ (third approximation) by replacing F and G by parabolic approximation over the intervals $(0, 1/2), (1/2, 1), \ldots$. The result is shown in Fig. 5-5. The curve given there is within 1 percent of

$$\left[0.915+0.745\left(2-\frac{v_o t}{a}\right)^2\right]^{1/2}$$

Jones also constructs expressions for the distant fields and for β_o whose first variations are zero for small variations of a_{nm}, γ_{nm} and β_m about their correct values. However, he does not use these expressions in the numerical computations.

5.3 Radiation of Sound from a Source Inside a Semi-Infinite Thin-Walled Tube

5.3.1 General Solution

The problem of scalar diffraction when the source of the incident field is located inside the tube has been treated by Levine and Schwinger (1948) and independently by Wainstein (1949) for the boundary condition $\frac{\partial u}{\partial \rho} = 0$ (rigid tube).

We assume that the tube is located at $\rho = a$, $z > 0$ and that a single arbitrary mode is propagated in the negative z-direction. The velocity potential of this incident mode can be written as

$$u^{(0)} = A_{nm}\frac{J_n(j'_{nm}\frac{\rho}{a})}{J_n(j'_{nm})}\cos n\phi\, e^{-i\alpha'_{nm} z} \qquad (5.90)$$

$$m \geqslant 0 \text{ when } n = 0, \quad m \geqslant 1 \text{ when } n \geqslant 1$$

where $J'_n(j'_{nm}) = 0$, $0 = j'_{no} < j'_{n1} < \ldots$ and

$$\alpha'_{nm} = \sqrt{k^2 - \frac{j'^2_{nm}}{a^2}}$$

is positive or positive imaginary. The field inside an infinite tube for arbitrary excitation can always be written as an infinite sum of cylindrical modes. The solution

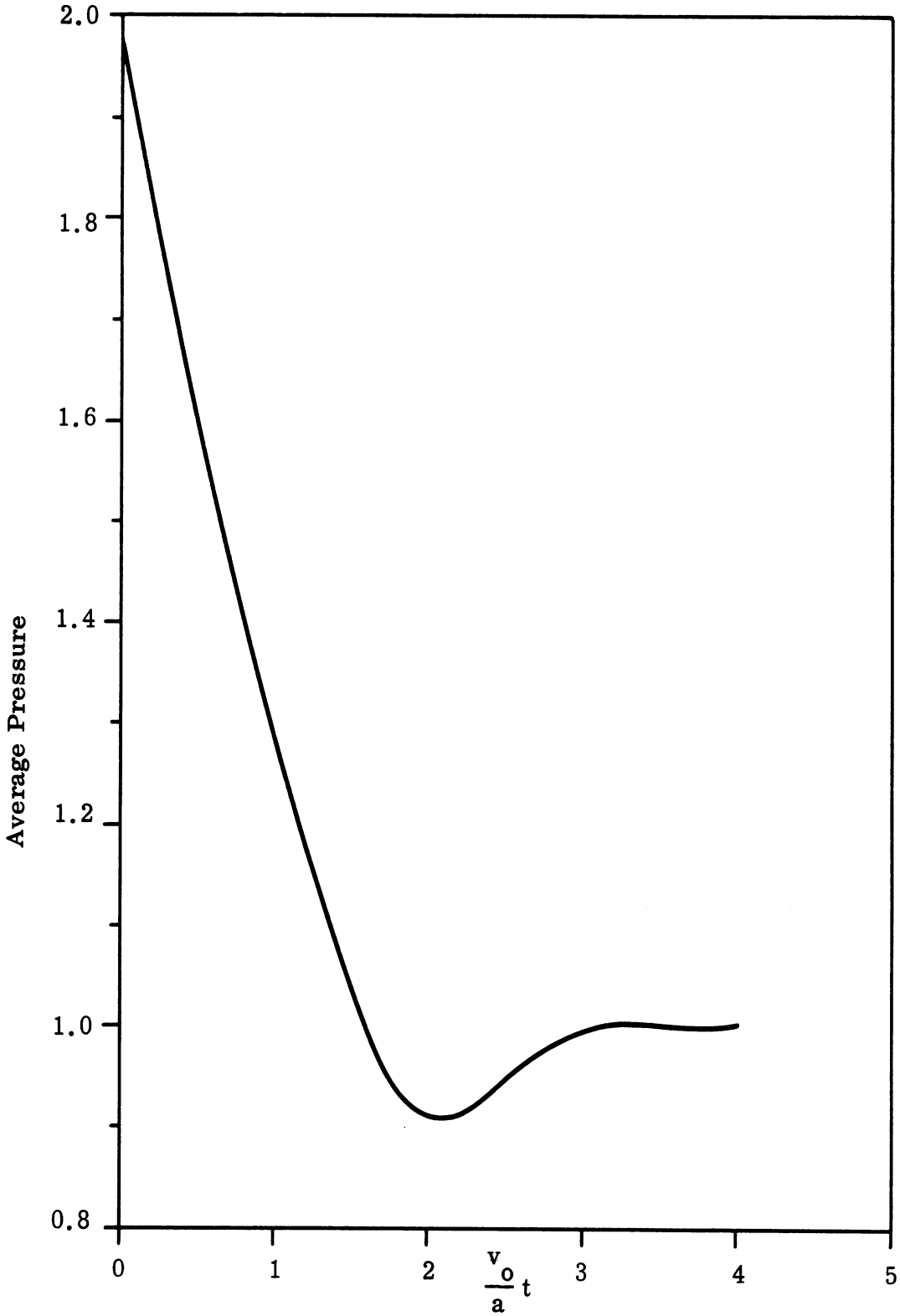

FIG. 5-5: THE AVERAGE PRESSURE ON THE END OF THE ROD DUE TO AN INCIDENT UNIT PRESSURE PULSE. v_o IS THE SPEED OF SOUND (Jones, 1955)

of the corresponding diffractionproblem for the same excitation inside a semi-infinite tube is then obtained by summing up the contributions from all modes.

The total field due to the incident mode of (5.90) is

$$u(\rho,\phi,z) = \begin{cases} \dfrac{1}{2\pi}\cos n\phi \displaystyle\int_\Gamma \frac{F_n(\alpha)}{\kappa H_n^{(1)'}(\kappa a)} H_n^{(1)}(\kappa\rho)\, e^{i\alpha z}\, d\alpha\,, & \rho > a \\ u^{(0)} + \dfrac{1}{2\kappa}\cos n\phi \displaystyle\int_\Gamma \frac{F_n(\alpha)}{\kappa J_n'(\kappa a)} J_n(\kappa\rho)\, e^{i\alpha z}\, d\alpha\,, & \rho < a \end{cases} \tag{5.91}$$

where, as before, $\kappa^2 = k^2 - \alpha^2$ and the path of integration is given in Fig. 5-1, passing above all real poles of the integrand when $\mathrm{Re}\,\alpha < 0$ and below them when $\mathrm{Re}\,\alpha > 0$. We have

$$F_n(\alpha) = \frac{ia}{2} A_{nm}(k+\alpha'_{nm}) M_n(\alpha'_{nm}) \frac{(k+\alpha)M_n(\alpha)}{\alpha+\alpha'_{nm}} \tag{5.92}$$

where the split function $M_n(\alpha)$, as before, is defined by (5.35).

5.3.2 Field Inside the Tube

When $\rho < a$, $z > 0$, evaluation of the integral in (5.91) by means of residues yields

$$u(\rho,\phi,z) = A_{nm}\cos n\phi \left\{ \frac{J_n(j'_{nm}\frac{\rho}{a})}{J_n(j'_{nm})} e^{-i\alpha'_{nm}z} + \sum_{\ell=0}^{\infty} R_{m\ell}^{(n)} \frac{J_n(j'_{n\ell}\frac{\rho}{a})}{J_n(j'_{n\ell})} e^{i\alpha'_{n\ell}z} \right\} \tag{5.93}$$

where

$$R_{mm}^{(n)} = -\frac{j'^2_{nm}}{4(j'^2_{nm} - n^2)} \left[\frac{(k+\alpha'_{nm})M_n(\alpha'_{nm})}{\alpha'_{nm}} \right]^2 \tag{5.94}$$

is the reflection coefficient of the incident mode and

$$R_{m\ell}^{(n)} = -\frac{j'^{2}_{n\ell}}{2(j'^{2}_{n\ell} - n^{2})} \frac{(k+\alpha'_{nm})(k+\alpha'_{n\ell})M_n(\alpha'_{nm})M_n(\alpha'_{n\ell})}{\alpha'_{n\ell}(\alpha'_{n\ell}+\alpha'_{nm})} \qquad m \neq \ell \tag{5.95}$$

can be called the conversion coefficient of mode A_{nm} into mode $A_{n\ell}$.

We write the coefficients $R_{m\ell}^{(n)}$ as

$$R_{m\ell}^{(n)} = -\left|R_{m\ell}^{(n)}\right| e^{i\Theta_{m\ell}^{(n)}} \quad . \tag{5.96}$$

The moduli and the phases of these coefficients for a symmetric incident wave (A_{oo}, A_{o1}) as functions of ka in the range $0 < ka < j'_{o2}$ $(j'_{o2} = 7.016)$ are given in Figs. 5-6 and 5-7. The modulus of the reflection coefficient of mode A_{11} for $j'_{11} < ka < j'_{12}$ $(j'_{11} = 1.841,\ j'_{12} = 5.331)$ is shown in Fig. 5-8.

If we introduce some auxiliary functions connected with the split,function, the quantities in Figs. 5-6 through 5-8 can be expressed as

$$\left|R_{oo}^{(0)}\right| = e^{ka\,\mathrm{Re}\,P_1(k)}, \qquad 0 < ka < j'_{o1} = 3.832 \ ; \tag{5.97}$$

and

$$\left|R_{oo}^{(0)}\right| = \frac{k+\alpha_{11}}{k-\alpha_{11}} e^{ka\,\mathrm{Re}\,P_1(k)}, \qquad \left|R_{11}^{(0)}\right| = \frac{k+\alpha_{11}}{k-\alpha_{11}} e^{a\alpha_{11}\,\mathrm{Re}\,P_1(\alpha_{11})}$$

$$\left|R_{o1}^{(0)}\right| = \frac{2k}{k-\alpha_{11}} e^{\frac{a}{2}\left[k\,\mathrm{Re}\,P_1(k)+\alpha_{11}\,\mathrm{Re}\,P_1(\alpha_{11})\right]}$$

$$\left|R_{1o}^{(0)}\right| = \frac{2\alpha_{11}}{k-\alpha_{11}} e^{\frac{a}{2}\left[k\,\mathrm{Re}\,P_1(k)+\alpha_{11}\,\mathrm{Re}\,P_1(\alpha_{11})\right]} \tag{5.98}$$

for $j'_{o1} \leqslant ka < j'_{o2}$;

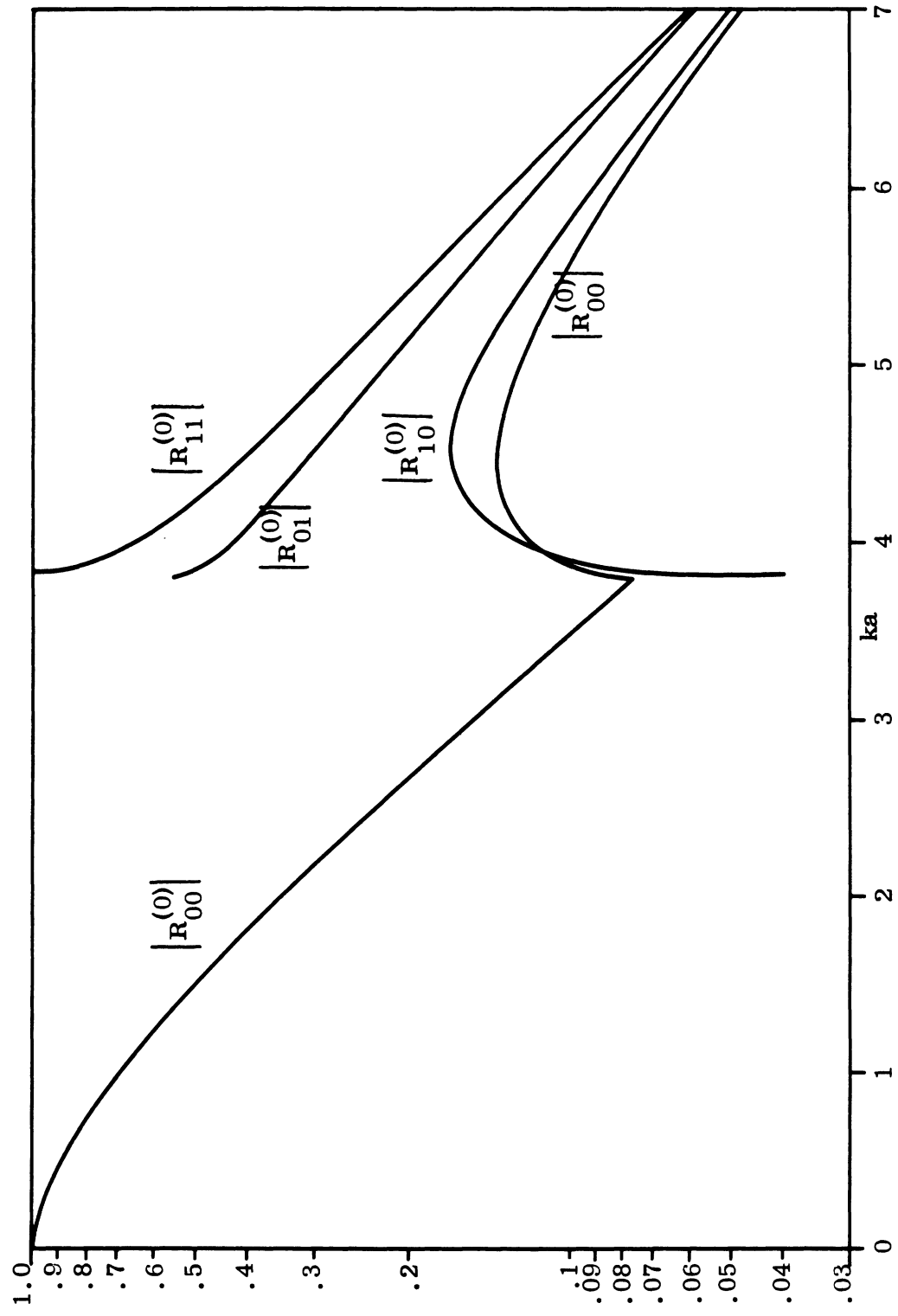

FIG. 5-6: MODULI OF REFLECTION AND CONVERSION COEFFICIENTS FOR SYMMETRIC MODES A_{oo}, A_{o1}. (Wainstein, 1949; $|R_{oo}^{(0)}|$ for ka < 3.832 is also given by Levine and Schwinger, 1948).

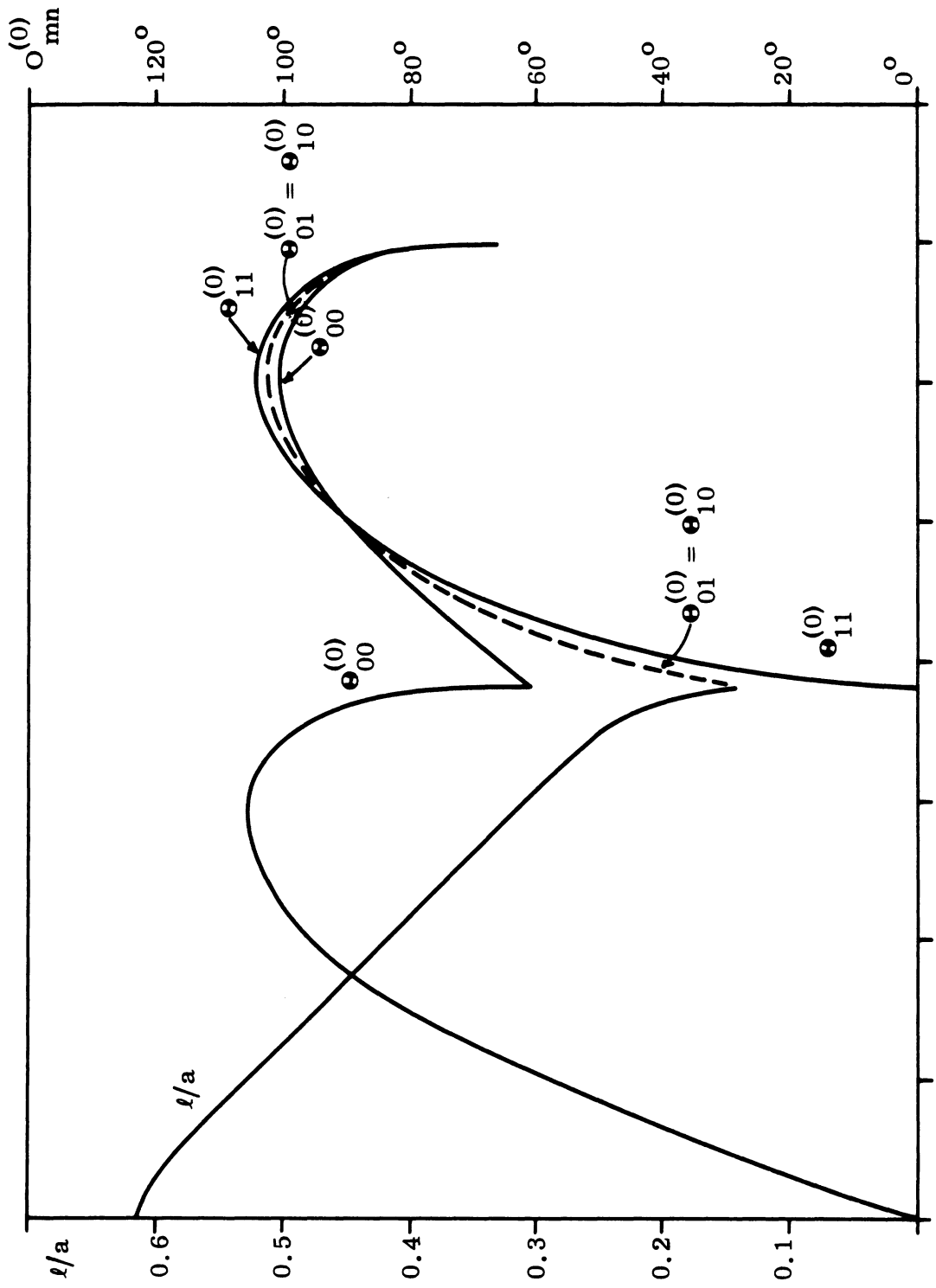

FIG. 5-7: PHASES OF REFLECTION AND CONVERSION COEFFICIENTS FOR SYMMETRIC MODES A_{00}, A_{01} AND END CORRECTION FOR MODE A_{00}. (Wainstein, 1949; ℓ/a is also given by Levine and Schwinger, 1948).

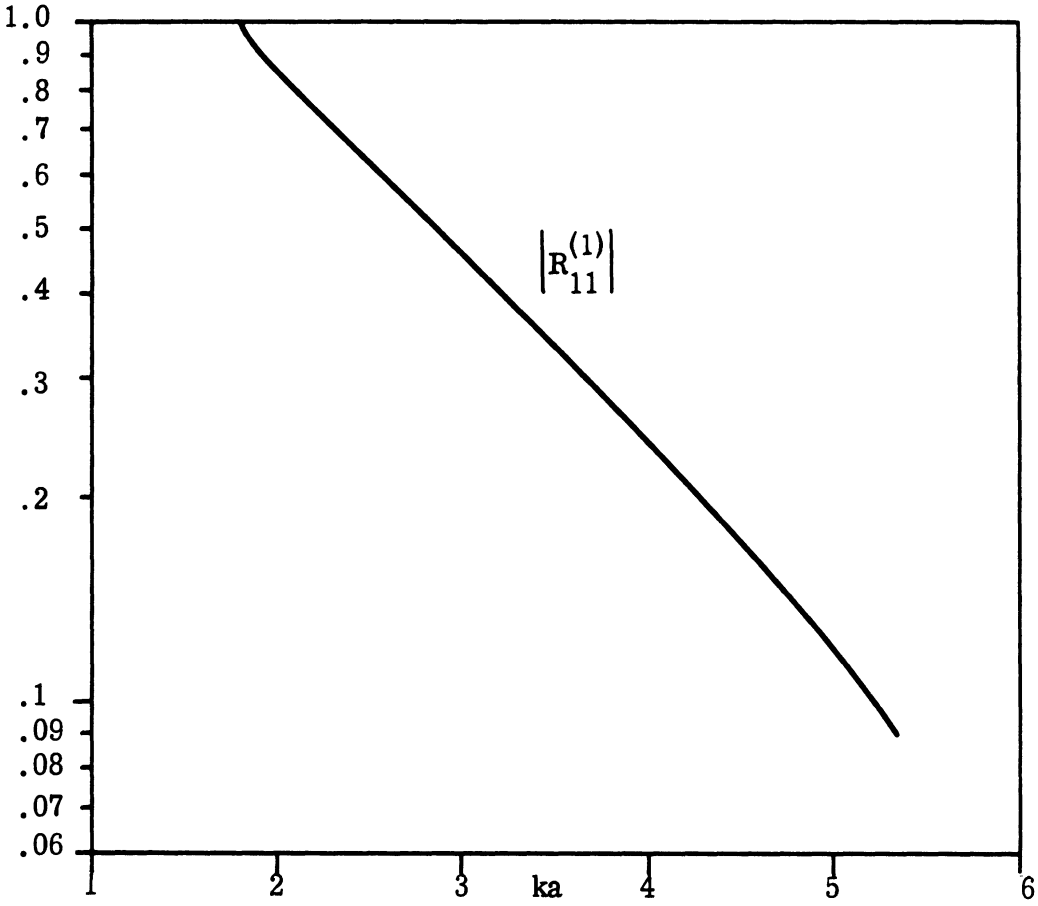

FIG. 5-8: MODULUS OF THE REFLECTION COEFFICIENT FOR MODE A_{11} (Wainstein, 1949).

$$\left|R_{11}^{(1)}\right| = \frac{k+\alpha'_{11}}{k-\alpha'_{11}}\, e^{a\alpha'_{11}\,\mathrm{Re}\,S_1(\alpha'_{11})} \quad , \qquad \text{for } j'_{11} \leqslant ka < j'_{12} \; ; \tag{5.99}$$

$$\Theta_{oo}^{(1)} = ka\,\mathrm{Im}\,P_1(k), \quad \Theta_{11}^{(0)} = a\alpha_{11}\,\mathrm{Im}\,P_1(\alpha_{11}), \quad \Theta_{1o}^{(0)} = \Theta_{o1}^{(0)} = \frac{\Theta_{oo}^{(0)} + \Theta_{11}^{(0)}}{2} \; , \tag{5.100}$$

where the functions P_1 and S_1 are defined by equations (5.222) - (5.223).

Using the approximate formulas (5.233) and (5.252) we find

$$\left|R_{oo}^{(0)}\right| \approx e^{-\frac{(ka)^2}{2}} \left[1+\frac{(ka)^4}{6}\left(\log\frac{1}{\gamma_1 ka}+\frac{19}{12}\right)\right] \quad , \; ka<1 \tag{5.101}$$

where $\log\gamma_1 = 0.5772$ in Euler's constant, and

$$\left|R_{oo}^{(0)}\right| \approx \sqrt{\pi ka}\; e^{-ka}\left(1+\frac{3}{32}\,\frac{1}{(ka)^2}\right) \quad , \qquad 1 < ka < j'_{o1} = 3.832. \tag{5.102}$$

At $ka = 1$, (5.101) and (5.102) yield values larger and smaller respectively than the correct one by about 3 percent.

If the incident mode is A_{oo} and the frequency is so low that all the higher modes are exponentially damped, the field inside the tube for large z is given by

$$u = A_{oo}\left[e^{-ikz} + R_{oo}^{(0)}\, e^{ikz}\right] \; . \tag{5.103}$$

Equation (5.103) represents a standing wave of amplitude

$$|u| = A_{oo}\sqrt{1+\left|R_{oo}^{(0)}\right|^2 - 2\left|R_{oo}^{(0)}\right|\cos(2kz+\Theta_{oo}^{(0)})} \; . \tag{5.104}$$

The first node is consequently located at $z = -\ell$, where

$$2k\ell = \Theta_{oo}^{(0)} \; . \tag{5.105}$$

The length ℓ is called the end correction and it determines the resonant frequencies of cylindrical resonantors open at one end. When $ka \to 0$ the end correction tends to the limit

$$\lim_{ka\to 0} \frac{\ell}{a} = \frac{1}{\pi}\int_0^\infty \frac{1}{x^2} \arctan\left(-\frac{J_1(x)}{Y_1(x)}\right) dx = \frac{1}{\pi}\int_0^\infty \frac{1}{x^2} \log \frac{1}{2I_1(x)K_1(x)}\, dx = 0.6128^* \tag{5.106}$$

The quantity ℓ/a is plotted in Fig. 5-7, and some numerical values, together with those of $-\frac{1}{ka} \ln \left|R_{oo}^{(0)}\right|$, are given in Table VI.

TABLE VI

End Correction and a Function Related to the Absolute Value of the Reflection Coefficient for Mode A_{oo}^{+}

ka	ℓ/a	$-\frac{\ln \left\|R_{oo}^{(0)}\right\|}{ka}$ ++	ka	ℓ/a	$-\frac{\ln \left\|R_{oo}^{(0)}\right\|}{ka}$
0	.613	0	.55	.576	.235
.05	.612	.0245	.60	.571	.251
.10	.611	.0485	.65	.565	.266
.15	.608	.0719	.70	.560	.281
.20	.604	.0948	.75	.554	.290
.25	.610	.117	.80	.549	.311
.30	.598	.139	.85	.544	.325
.35	.594	.160	.90	.538	.333
.40	.590	.180	.95	.533	.351
.45	.586	.200	1.00	.527	.364
.50	.581	.219			

+ Wainstein (1949)

++ The phase of $R_{oo}^{(0)}$ is given by $\Theta_{oo}^{(0)} = 2ka\frac{\ell}{a}$.

When $ka > j'_{nm}$, i.e. above cut-off, the power transported by the mode A_{nm} of (5.90) is

* This value was obtained by Brooker and Turing as reported by Jones (1955) and independently by Matsui (1961). Levine and Schwinger (1948) give 0.6133 and Wainstein (1949) 0.613.

$$P_{nm} = \frac{\pi}{2\epsilon_n} \rho_o v_o ka^2 \alpha'_{nm} \left(1 - \frac{n^2}{j'^2_{nm}}\right) |A_{nm}|^2 \qquad (5.107)$$

where ρ_o is the density of the surrounding medium, v_o the velocity of sound and $\epsilon_o = 1$, $\epsilon_1 = \epsilon_2 = \ldots = 2$ are the Neumann numbers. Thus, the fraction of the power of the incident wave A_{nm} which is converted into the mode $A_{n\ell}$ and propagated towards $z = \infty$ is

$$r^{(n)}_{m\ell} = \frac{\alpha'_{n\ell}\left(1 - \frac{n^2}{j'^2_{n\ell}}\right)}{\alpha'_{nm}\left(1 - \frac{n^2}{j'^2_{nm}}\right)} \left|R^{(n)}_{m\ell}\right|^2 . \qquad (5.108)$$

From (5.95) it follows that

$$r^{(n)}_{m\ell} = r^{(n)}_{\ell m} \qquad (5.109)$$

which is a consequence of reciprocity. The total power reflection coefficient for the mode A_{nm} is

$$r^{(n)}_{m} = \sum_{\ell=0}^{\ell_o} r^{(n)}_{m\ell} \qquad (5.110)$$

where the summation is taken over all propagated modes. In Fig. 5-9 the power reflection and conversion coefficients together with the total power reflection coefficient are given for the symmetric modes A_{oo}, A_{o1}.

5.3.3 The Far Field

If we introduce spherical coordinates (r, θ, ϕ) such that $z = r\cos\theta$, $\rho = r\sin\theta$, and evaluate the upper integral in (5.91) by the method of steepest descent, we obtain

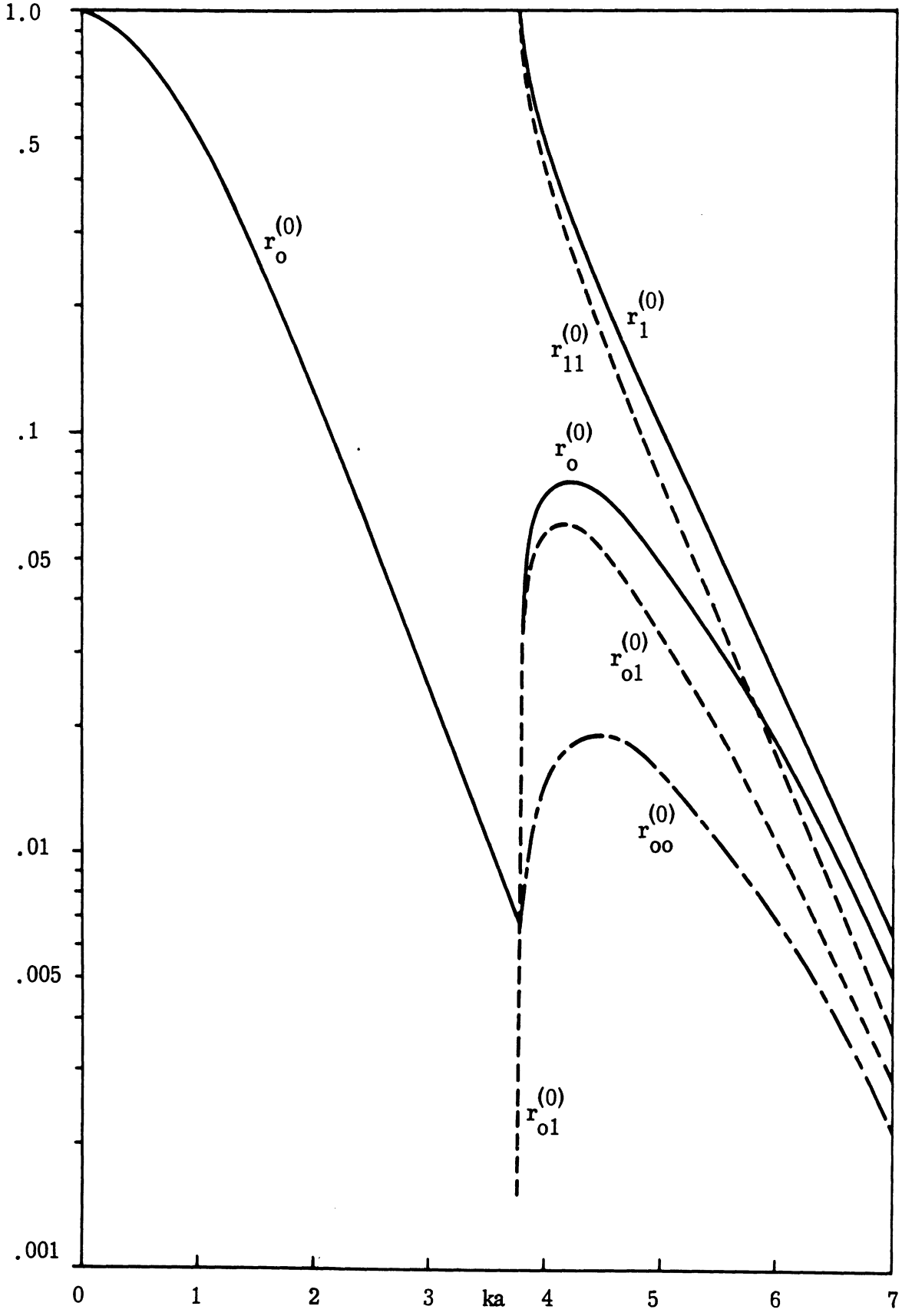

FIG. 5-9: POWER REFLECTION AND CONVERSION COEFFICIENTS OF SYMMETRIC MODES A_{oo} AND A_{o1} (Wainstein, 1949).

the total far field*

$$u(r,\theta,\phi) \sim A_n \cos n\phi \, \frac{e^{ikr}}{r} \, \frac{(-i)^n}{2\pi} \, \frac{a(k+\alpha'_{nm})(1+\cos\theta)M_n(\alpha'_{nm})M_n(k\cos\theta)}{\sin\theta(k\cos\theta+\alpha'_{nm})H_n^{(1)'}(ka\sin\theta)} \, . \qquad (5.111)$$

The power radiated per unit solid angle about the direction (θ,ϕ) is given by

$$p(\theta,\phi) = \frac{1}{2}\rho_o v_o k^2 |u|^2 r^2 \, . \qquad (5.112)$$

This quantity divided by the power of the incident A_{nm} mode is called the <u>power pattern</u> $f_{nm}(\theta,\phi)$. Using (5.111) and (5.107) we get

$$f_{nm}(\theta,\phi) = \frac{\epsilon_n k(k+\alpha'_{nm})^2 \left|M_n(\alpha'_{nm})\right|^2 (1+\cos\theta)^2 \left|M_n(k\cos\theta)\right|^2}{4\pi^3 \alpha'_{nm}\left(1-\frac{n^2}{j'^2_{nm}}\right)\sin^2\theta(k\cos\theta+\alpha'_{nm})^2\left|H_n^{(1)'}(ka\sin\theta)\right|^2} \cos^2 n\phi \qquad (5.113)$$

where as before, $\epsilon_o = 1$, $\epsilon_1 = \epsilon_2 = \ldots = 2$ and $ka > j'_{nm}$. The relation between $f_{nm}(\theta,\phi)$ and the power gain function, i.e. the radiated power related to an isotropically radiating source, is

$$G_{nm}(\theta,\phi) = \frac{p(\theta,\phi)}{P_{rad}/4\pi} = 4\pi \, \frac{f_{nm}(\theta,\phi)}{1-r_m^{(n)}} \qquad (5.114)$$

where $r_m^{(n)}$ is the total power reflection coefficient given by (5.110).

If we insert in (5.113) the expression given by (5.215) for $M_o(\alpha) \equiv L_1(\alpha)$, we obtain

---

* As pointed out by Noble (1958), the sign for the far field in the directions $\theta = 0$ and $\theta = \pi$ when $n = m = 0$ as given by Levine and Schwinger (1948) (Eq. III, 12, 13) and by Morse and Feshbach (1953) (Eq. 11.4.33) seems to be in error.

$$f_{oo}(\theta) = \frac{J_1(ka\sin\theta)}{\pi^2\sin^2\theta\left|H_1^{(1)}(ka\sin\theta)\right|}\exp\left[ka\left(\mathrm{Re}\,P_1(ka)+\cos\theta\,\mathrm{Re}\,P_1(k\cos\theta)\right)\right] \tag{5.115}$$

when $0 < ka < j'_{o1} = 3.832$, and

$$f_{oo}(\theta) = \frac{1}{\pi^2}\prod_{m=1}^{m_o}\left(\frac{k+\alpha_{1m}}{k-\alpha_{1m}}\,\frac{k\cos\theta+\alpha_{1m}}{k\cos\theta-\alpha_{1m}}\right)\frac{J_1(ka\sin\theta)}{\sin^2\theta\left|H_1^{(1)}(ka\sin\theta)\right|}\times$$

$$\times\exp\left[ka\left(\mathrm{Re}\,P_1(k)+\cos\theta\,\mathrm{Re}\,P_1(k\cos\theta)\right)\right] \tag{5.116}$$

when $j'_{om_o} \leqslant ka < j'_{o(m_o+1)}$. For the lowest mode with ϕ-dependence $\cos n\phi$ (also including ${}^{o}A_{o1}$) the corresponding expression is*

$$f_{n1}(\theta,\phi) = \frac{\epsilon_n\alpha'_{n1}}{\pi^2 k}\left(\frac{\tan\frac{\theta_{n1}}{2}}{\tan\frac{\theta}{2}}\right)^2\frac{J'_n(ka\sin\theta)}{\left|H_n^{(1)'}(ka\sin\theta)\right|}\times$$

$$\times\frac{\exp\left[\alpha'_{n1}\,\mathrm{Re}\,S_n(\alpha'_{n1})+k\cos\theta\,\mathrm{Re}\,S_n(k\cos\theta)\right]}{\cos^2\theta-\cos^2\theta_{n1}}\cos^2 n\phi \tag{5.117}$$

when $j'_{n1} < ka < j'_{n2}$, where θ_{n1} is defined by

$$k\cos\theta_{nm} = -\alpha'_{nm} \tag{5.118}$$

The power patterns of the mode A_{oo} for different values of ka in the range $0 < ka < 4.023$ is given in Fig. 5-10 and for modes A_{oo} and A_{o1} for $ka = 4.023$ in Fig. 5-11. The power gain function in the forward direction ($\theta = \pi$) for mode A_{oo} is

* The factor $\left(\tan\frac{\theta_{n1}}{2}\Big/\tan\frac{\theta}{2}\right)^2$ is missing from the corresponding formula (Eq. 81) in Wainstein (1949).

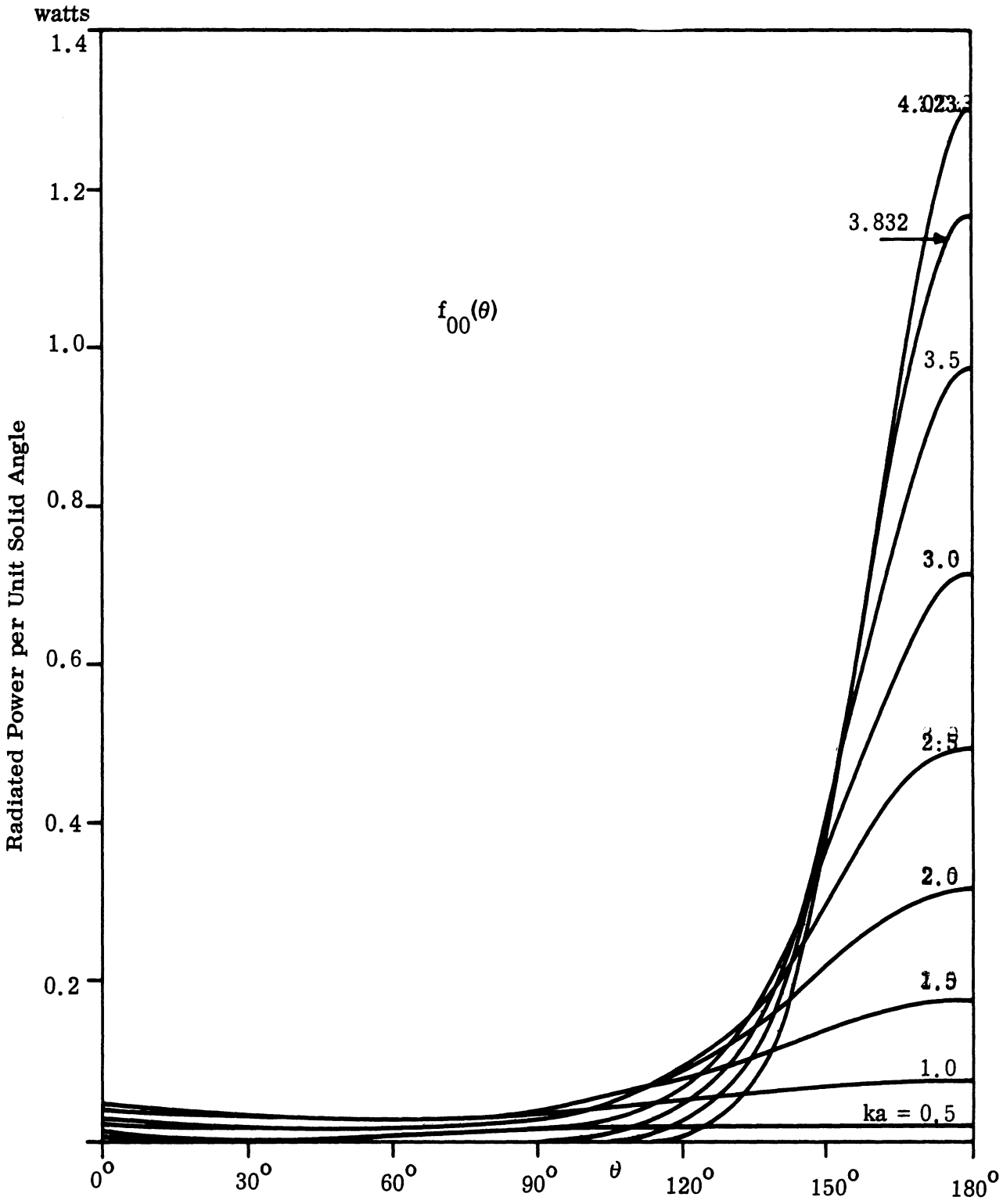

FIG. 5-10: RADIATED POWER PER UNIT SOLID ANGLE FOR INCIDENT MODE A_{00} CARRYING THE POWER 1 WATT. (Levine and Schwinger, 1948 ($ka \leqslant 3.832$) and Wainstein, 1949 ($ka = 4.023$))

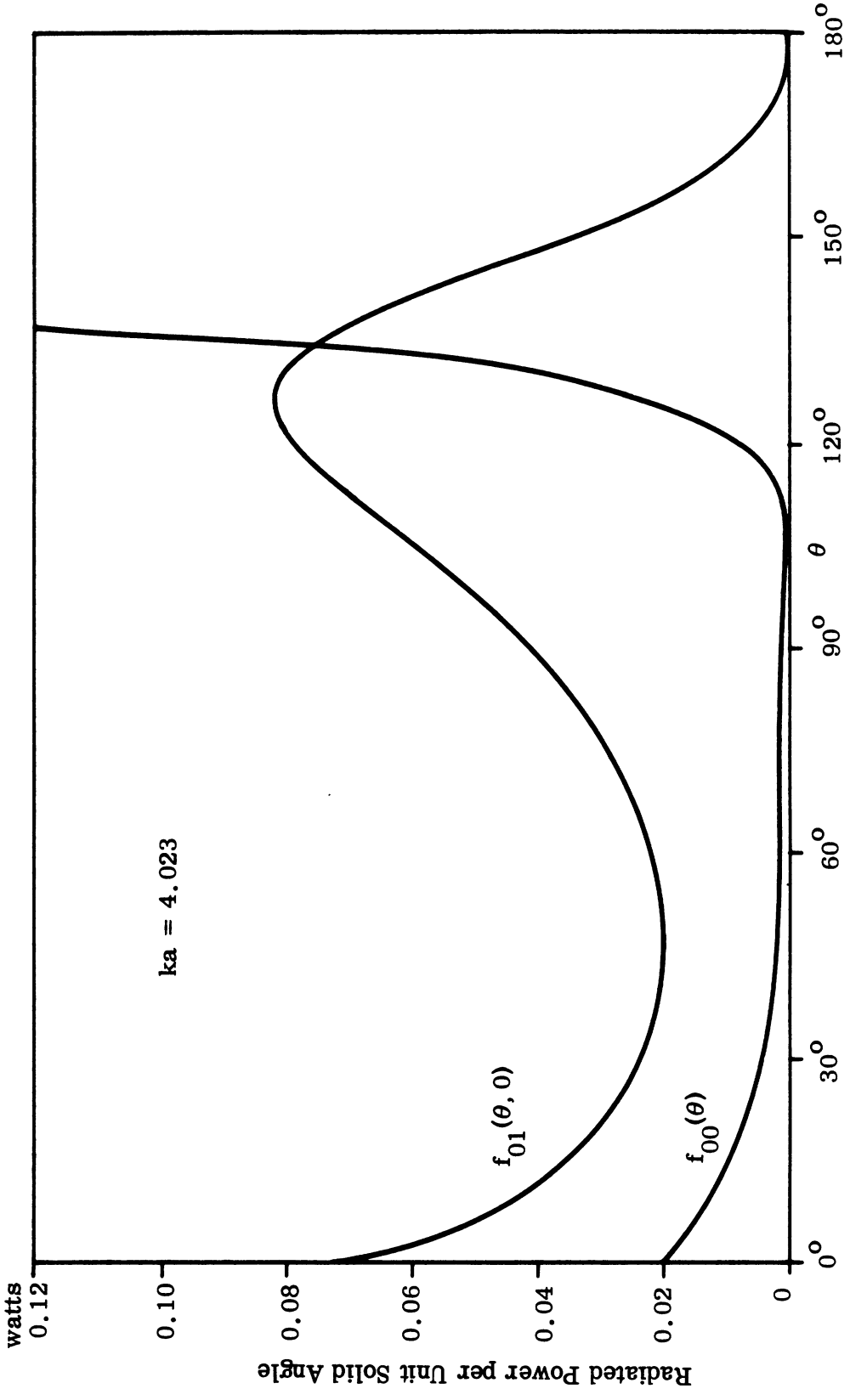

FIG. 5-11: RADIATED POWER PER UNIT SOLID ANGLE FOR INCIDENT MODES A_{00} AND A_{01} CARRYING THE POWER 1 WATT FOR ka = 4.023 (Wainstein, 1949).

$$G_{oo}(\pi) = \frac{(ka)^2}{1 - \left|R_{oo}^{(0)}\right|^2} \quad . \tag{5.119}$$

This function is plotted against ka for $ka < j'_{01} = 3.832$ in Fig. 5-12.

The exact power patterns of Figs. 5-9 and 5-10 can be compared with the Kirchhoff approximation, in which the radiation field is calculated from the incident field and its normal derivative at the open end.

The radiated power per unit solid angle for the incident mode A_{nm} carrying 1 watt of power obtained from the Kirchhoff approximation is

$$f_{nm}^{K}(\theta,\phi) = \frac{\epsilon_n k}{4\pi\alpha'_{nm}\left(1 - \frac{n^2}{j'^2_{nm}}\right)}\left[\frac{\sin\theta J'_n(ka\sin\theta)}{\cos\theta - \cos\theta_{nm}}\right]^2 \cos^2 n\phi \tag{5.120}$$

where θ_{nm} is defined by (5.118). If we compare (5.120) with the exact expression of (5.113) we find that

$$f_{nm}(\theta_{nm},\phi) = f_{nm}^{K}(\theta_{nm},\phi = \frac{\epsilon_n (ka)^2 \alpha'_{nm}}{4\pi}\left(1 - \frac{n^2}{j'^2_{nm}}\right)\left[J_n(j'_{nm})\right]^2 \cos^2 n\phi \quad . \tag{5.121}$$

The Kirchhoff approximation therefore gives the correct value for the radiated power in the direction $\theta = \theta_{nm}$ $(\pi/2 < \theta_{nm} \leqslant \pi)$. It also gives correctly the directions of zero radiation if $\theta > \pi/2$.

From (5.113) we obtain the special cases

$$\begin{aligned} f_{om}(0) &= \frac{(ka)^3}{4\pi a\alpha'_{om}}\left|R_{mo}^{(0)}\right|^2 \qquad m = 0, 1, 2, \ldots \\ f_{nm}(0,\phi) &= 0 \qquad\qquad n \geqslant 1 \end{aligned} \tag{5.122}$$

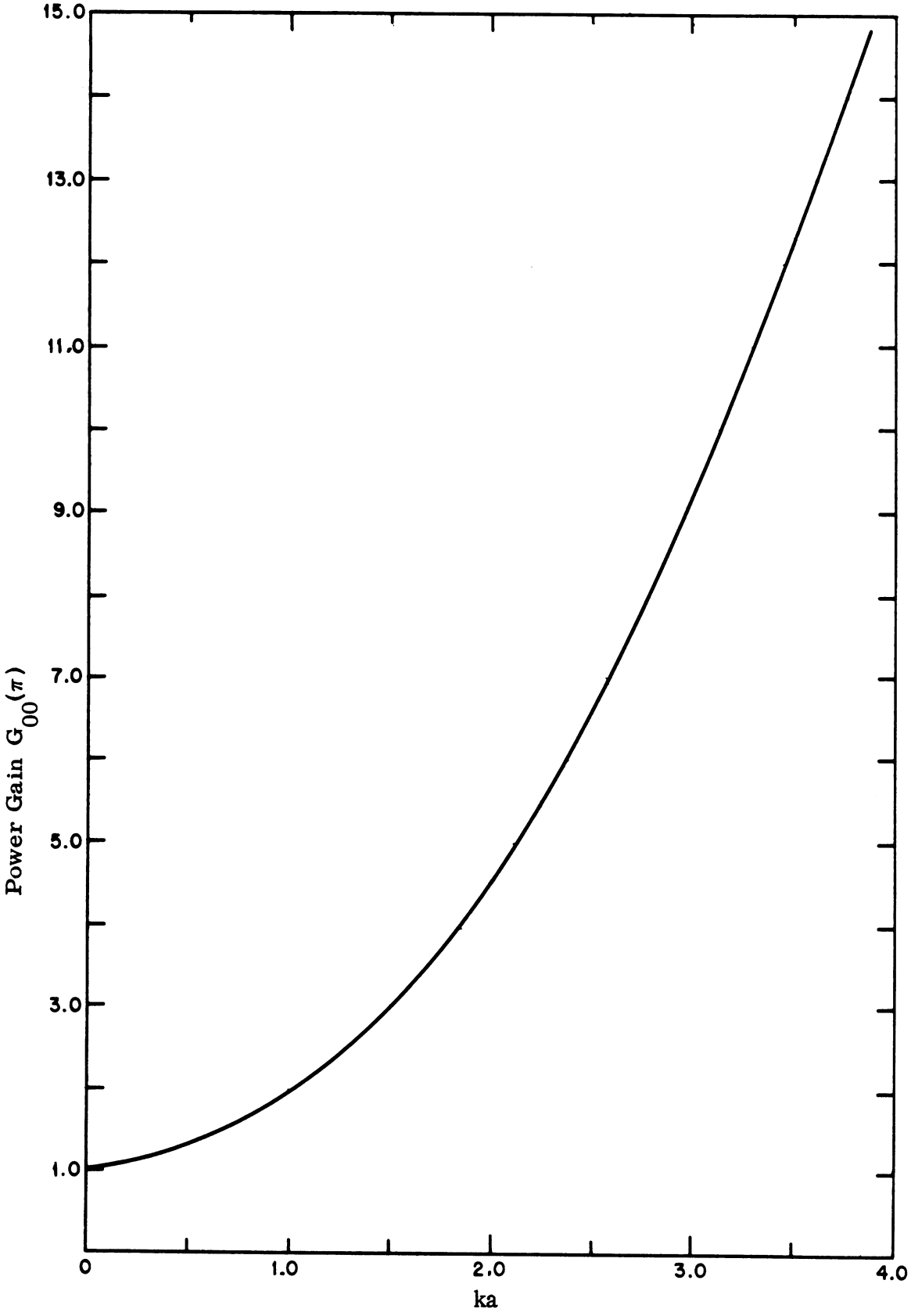

FIG. 5-12: THE POWER GAIN IN THE FORWARD DIRECTION ($\theta = \pi$)
(Levine and Schwinger, 1948)

$$f_{nm}(\pi/2,\phi) = \frac{\epsilon_n k}{\pi^2 \alpha'_{nm}} \left| \frac{J'_n(ka)}{H_n^{(1)'}(ka)} \right| \left| R_{mm}^{(n)} \right| \cos^2 n\phi \tag{5.123}$$

$$f_{oo}(\pi) = \frac{(ka)^2}{4\pi}$$

$$f_{nm}(\pi,\phi) = 0 \qquad n \geq 0\,, \qquad m \geq 1 \tag{5.124}$$

The corresponding values for the Kirchhoff approximation for the mode A_{oo} are

$$f_{oo}^K(0) = 0\,, \qquad f_{oo}^K(\pi/2) = \frac{J_1^2(ka)}{4\pi}\,, \qquad f_{oo}^K(\pi) = \frac{(ka)^2}{4\pi} \tag{5.125}$$

$f_{oo}(0)$, $f_{oo}(\pi/2)$ and $f_{oo}^K(\pi/2)$ are plotted against ka in Fig. 5-13.

For low frequencies the Kirchhoff approximation can be improved if we add the reflected A_{oo} mode to the incident field. This modified Kirchhoff formula for incident A_{oo} mode reads

$$f_{oo}^{K'}(\theta) = \frac{1}{4\pi}\left(\frac{J_1(ka\sin\theta)}{\sin\theta}\right)^2 \left[(1-\cos\theta)^2 + \left|R_{oo}^{(0)}\right|^2 (1+\cos\theta)^2 - 2\sin^2\theta\, \mathrm{Re}\left\{R_{oo}^{(0)}\right\}\right] \tag{5.126}$$

A comparison with (5.122) shows that this expression yields the correct value not only for $\theta = \pi$ but also for $\theta = 0$. A comparison of the exact and approximate power patterns for $ka = 1.0$ is given in Fig. 5-14.

As our problem is self-adjoint, there is a reciprocity relation between the results of this section with those obtained for scattering of a scalar plane wave in Section 5.2. The principle of reciprocity can be stated as follows. To the incident mode A_{nm} of equation (5.90) we relate the far field $\cos n\phi \frac{e^{ikr}}{r} g_{nm}(\theta)$ and from an incident plane wave given by (5.59) (i.e. propagating in the direction $(\theta_i, 0)$) we assume the excitation inside the tube to be

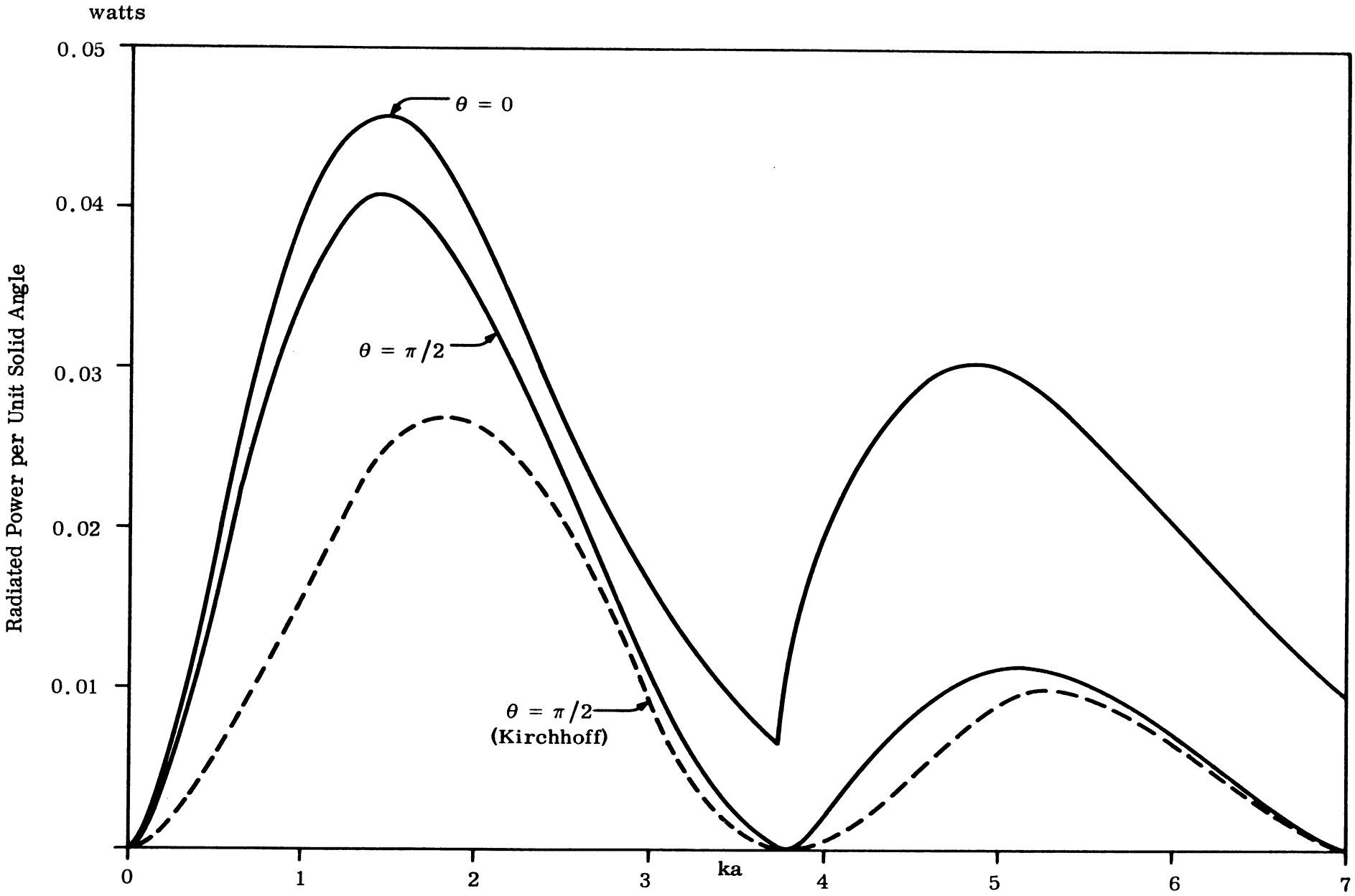

FIG. 5-13: RADIATED POWER PER UNIT SOLID ANGLE IN THE DIRECTIONS $\theta = 0$ AND $\theta = \pi/2$ FOR INCIDENT MODE A_{oo} CARRYING 1 WATT OF POWER (Wainstein, 1949).

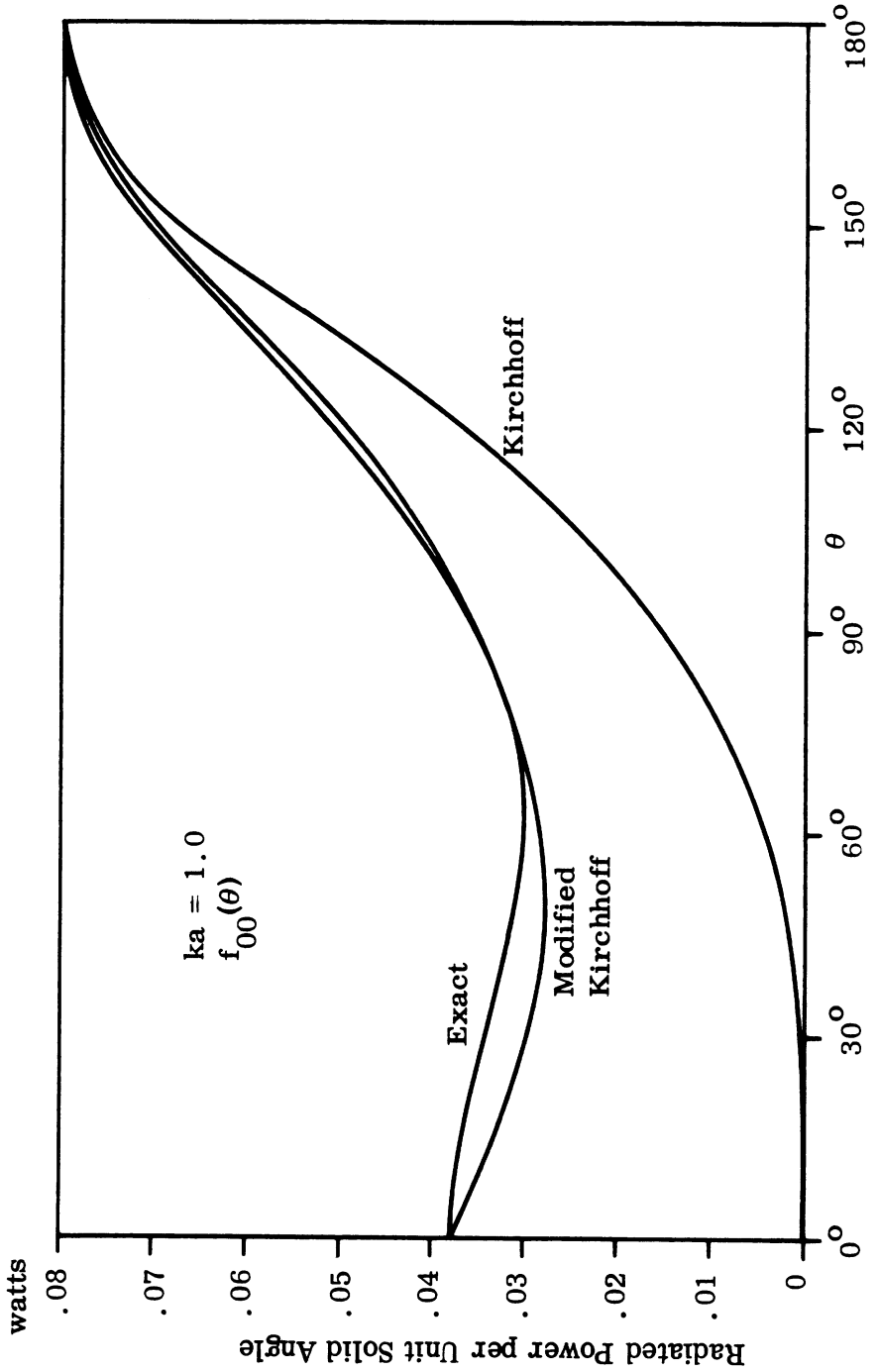

FIG. 5-14: COMPARISON OF EXACT AND APPROXIMATE EXPRESSIONS FOR RADIATED POWER PER UNIT SOLID ANGLE FOR INCIDENT MODE A_{00} CARRYING THE 1 WATT OF POWER AT ka = 1.0 (Levine and Schwinger, 1948).

$$u(\rho, \phi, z) = \sum_{n=0}^{\infty} \sum_{m=1}^{\infty} B_{nm} \frac{J_n(j'_{nm} \frac{\rho}{a})}{J_n(j'_{nm})} \cos n\phi \, e^{i\alpha'_{nm} z} .$$

Then

$$A_{nm} B_{nm} = (-1)^n \frac{2\epsilon_n i j'^2_{nm}}{(j'^2_{nm} - n^2) a^2 \alpha'_{nm}} g_{nm}(\pi - \theta_i) \tag{5.127}$$

It is readily checked that (5.127) conforms to (5.65) and (5.111). It may be noted that if we want to use the principle of reciprocity to calculate the field at an arbitrary point inside the tube due to an incident plane wave, we must know the far field excited also be all evanescent modes. Equation (5.111) is still valid for a mode below cut-off, but the quantity $f_{nm}(\theta, \phi)$ of (5.113) has lost its physical meaning as there is no energy transported by the incident mode in that case.

For $ka < 1.841$ the absorption cross section for an incident plane wave, defined as the ratio of the power transmitted into the tube to the power incident per unit area, is related to the power pattern of mode A_{oo} by

$$\sigma_a(\theta_i) = \lambda^2 f_{oo}(\pi - \theta_i) \tag{5.128}$$

where $\lambda = 2\pi/k$ is the free-space wavelength.

5.3.4 Cylindrical Resonators with an Open End

We assume the resonator to consist of a tube of length L closed at one end by a rigid wall and open at the other end (Fig. 5-15). The resonator is excited by a plane wave propagating along the positive z-axis

$$u^{(0)} = A e^{ikz} . \tag{5.129}$$

If we neglect all higher modes, the field inside the tube is represented by the mode A_{oo} alone, reflected with reflection coefficient 1 at the closed end and with reflection coefficient $R^{(0)}_{oo}$ of (5.94) at the open end. Summing up all these traveling waves

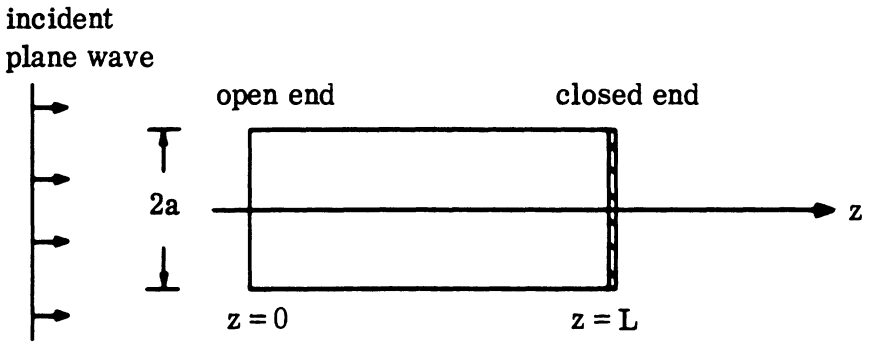

FIG. 5-15: CYLINDRICAL RESONATOR WITH AN OPEN END.

we obtain the velocity potential

$$u(z) = A \frac{e^{ikz} + e^{ik(2L-z)}}{1 - Re^{i2kL}} \quad . \tag{5.130}$$

As a measure of resonance we take the quantity

$$g = \left| \frac{u(L)}{2A} \right| \tag{5.131}$$

which is equal to the ratio of the pressure amplitude at the closed end to the pressure at an infinite plane screen located at $z = L$. Introducing the end correction ℓ defined by (5.105) we obtain

$$g = \frac{1}{\sqrt{1 + |R|^2 + 2|R| \cos 2k(L+\ell)}} \tag{5.132}$$

Fig. 5-16 shows g as a function of ka for a resonator with $L/a = 7.82$.

5.4 Scattering of a Plane Electromagnetic Wave from a Semi-Infinite Thin-Walled Tube

5.4.1 General Solution

Let the semi-infinite tube occupy the space $\rho = a$, $z \geqslant 0$ and the incident plane wave be given by

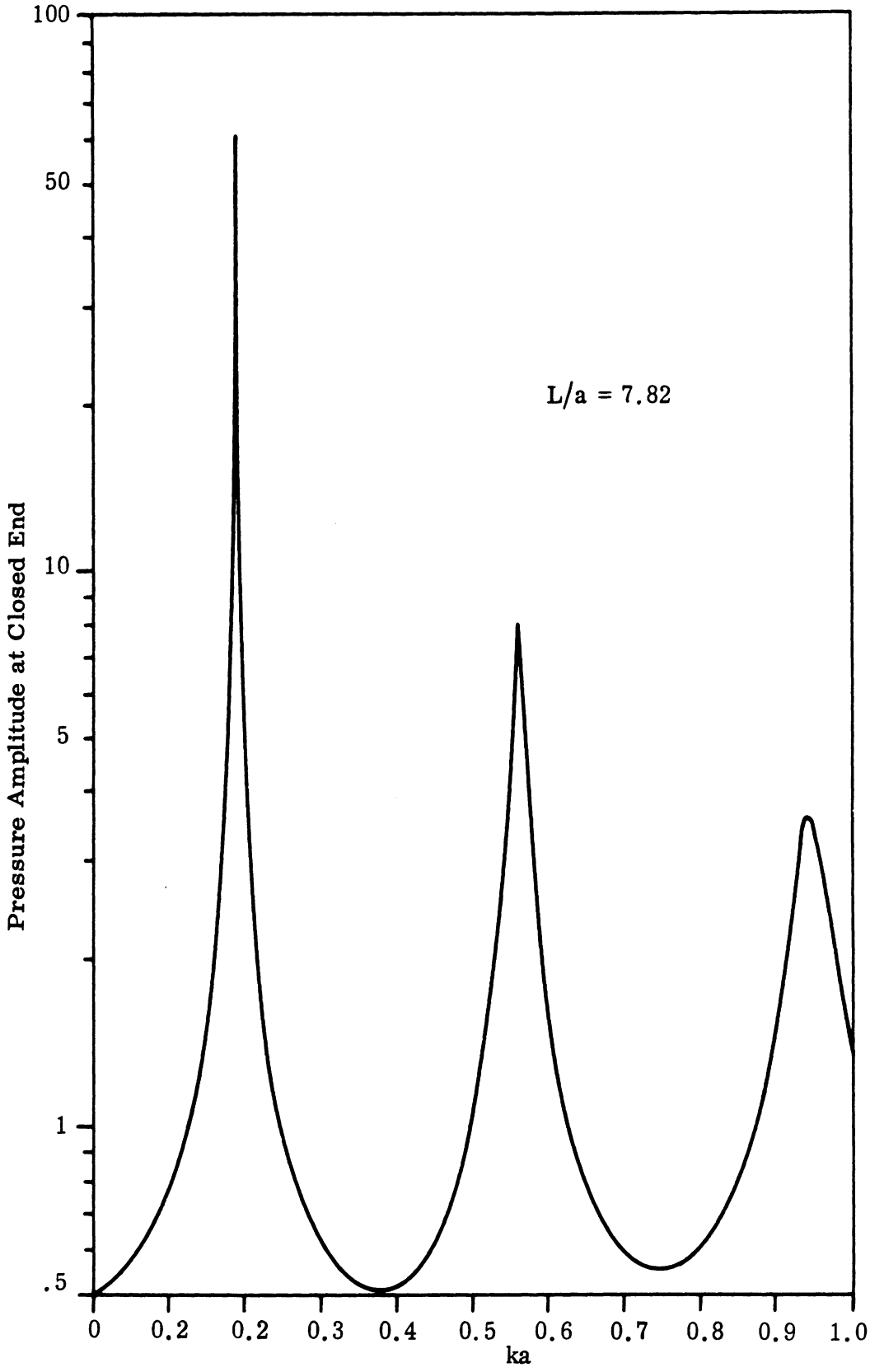

FIG. 5-16: RESONANCE CURVE FOR A CYLINDRICAL RESONATOR WITH LENGTH TO RADIUS RATIO 7.82 (Wainstein, 1949)

$$\underline{E}^i = (-\cos\theta_i \cos\beta \hat{i}_x + \sin\beta \hat{i}_y + \sin\theta_i \cos\beta \hat{i}_z)\, e^{ik(x\sin\theta_i + z\cos\theta_i)} \tag{5.133}$$

$$\underline{H}^i = \sqrt{\frac{\epsilon_o}{\mu_o}}\, (-\cos\theta_i \sin\beta \hat{i}_x - \cos\beta \hat{i}_y + \sin\theta_i \sin\beta \hat{i}_z)\, e^{ik(x\sin\theta_i + z\cos\theta_i)}$$

i.e., its direction of propagation is parallel to the (x, z)-plane and makes an angle θ_i with the (y, z)-plane. The configuration is given by Fig. 2-2 with θ_i exchanged for α.

The problem has been treated by Pearson (1953) for the special case $\beta = 0$ (incident TM-wave)* and by Bowman (1963a, b, c, d) in a series of unpublished memoranda. Its solution is, in principle, given in Section 5.1 as soon as the functions $f_n(\alpha)$ and $g_n(\alpha)$ of (5.42) and (5.43) are determined from the incident field. Inserting $x = \rho\cos\phi$ in (5.133) and using

$$e^{ik\rho\sin\theta_i\cos\phi} = \sum_{n=-\infty}^{\infty} i^n J_n(k\rho\sin\theta_i)\, e^{in\phi} \tag{5.134}$$

we obtain

$$E_z^i(a, \phi, z) = \sin\theta_i \cos\beta\, e^{ikz\cos\theta_i} \sum_{n=-\infty}^{\infty} i^n J_n(ka\sin\theta_i)\, e^{in\phi} \tag{5.135}$$

$$E_\phi^i(a, \phi, z) = -e^{ikz\cos\theta_i} \sum_{n=-\infty}^{\infty} \left[\frac{\cos\theta_i \cos\beta}{ka\sin\theta_i}\, n J_n(ka\sin\theta_i) + i\sin\beta J_n'(ka\sin\theta_i) \right] i^n e^{in\phi} .$$

From the definitions of $f_n(\alpha)$ and $g_n(\alpha)$ in (5.42) and (5.43) we get

* The sign after 1 in the quantity $N^n(ik)$ defined in connection with equation (2) in Pearson's paper seems to be incorrect.

$$f_n^-(\alpha) = \frac{2i^n \sin\beta J_n'(ka\sin\theta_i)}{M_n(k\cos\theta_i)(\alpha - k\cos\theta_i)}$$

$$f_n^+(-k) = \frac{2i^n \sin\beta J_n'(ka\sin\theta_i)}{M_n(k\cos\theta_i)\, k(1+\cos\theta_i)} \tag{5.136}$$

$$g_n^-(\alpha) = \frac{2i^{n+1} \sin\theta_i \cos\beta J_n(ka\sin\theta_i)}{ka(1+\cos\theta_i)L_n(k\cos\theta_i)(\alpha - k\cos\theta_i)}$$

$$g_n^-(k) = \frac{2i^{n+1} \cos\beta J_n(ka\sin\theta_i)}{k^2 a\sin\theta_i L_n(k\cos\theta_i)} \tag{5.137}$$

where $M_n(\alpha)$ and $L_n(\alpha)$ are the split functions defined by (5.33) and (5.34). Inserting (5.136) and (5.137) in (5.44) and (5.45) and putting $F_n(\alpha) = G_n(\alpha) = 0$ yields the solution to the problem. In accordance with (5.55) and (5.56) we write

$$X(\rho,\phi,z) = X^i(\rho,\phi,z) + \frac{1}{2\pi}\sum_{n=-\infty}^{\infty} e^{in\phi}\int_\Gamma \left[A(\alpha)H_n^{(1)}(\rho\kappa) + B(\alpha)H_n^{(1)'}(\rho\kappa)\right] e^{i\alpha z}\, d\alpha\,, \tag{5.138}$$

$$\rho > a,\quad -\infty < z < \infty$$

$$X(\rho,\phi,z) = X^i(\rho,\phi,z) + \frac{1}{2\pi}\sum_{n=-\infty}^{\infty} e^{in\phi}\int_\Gamma \left[A(\alpha)J_n(\rho\kappa) + B(\alpha)J_n'(\rho\kappa)\right] e^{i\alpha z}\, d\alpha\,, \tag{5.139}$$

$$\rho < a,\quad -\infty < z < \infty$$

where as before $\kappa = \sqrt{k^2 - \alpha^2}$ and the path of integration Γ is as indicated in Fig. 5-1 with the addition requirement that it passes below the pole $\alpha = k\cos\theta_i$. X stands for an arbitrary component of the total field, and X^i is the corresponding component of the incident field. The functions $A(\alpha)$ and $B(\alpha)$ are given in Table V if we take

$$b(\alpha) = \frac{e_n^-(\alpha)}{H_n^{(1)'}(a\kappa)} \quad , \qquad c(\alpha) = \frac{\mathcal{E}_{zn}^-(a,\alpha)}{H_n^{(1)}(a\kappa)} \quad \text{when } \rho > a$$

$$b(\alpha) = \frac{e_n^-(\alpha)}{J_n'(a\kappa)} \quad , \qquad c(\alpha) = \frac{\mathcal{E}_{zn}^-(a,\alpha)}{J_n(a\kappa)} \quad \text{when } \rho < a \tag{5.140}$$

where, from (5.44) and (5.45) and (5.136) and (5.137),

$$e_n^-(\alpha) = i^n a(k+\alpha) M_n(\alpha) \left\{ \frac{2akn\, L_n(k)}{4k^2a^2M_n^2(k) - n^2L_n^2(k)} \left(\frac{2ia\cos\beta\, M_n(k)\, J_n(ka\sin\theta_i)}{\sin\theta_i L_n(k\cos\theta_i)} - \right.\right.$$

$$\left.\left. - \frac{n\sin\beta\, L_n(k)\, J_n'(ka\sin\theta_i)}{k(1+\cos\theta_i)M_n(k\cos\theta_i)} \right) + \frac{a\sin\beta\, J_n'(ka\sin\theta_i)(k-\alpha)}{M_n(k\cos\theta_i)(\alpha - k\cos\theta_i)} \right\} \tag{5.141}$$

$$\mathcal{E}_{zn}^-(a,\alpha) = i^n L_n(\alpha) \left\{ \frac{2akn\, L_n(k)}{4k^2a^2M_n^2(k) - n^2L_n^2(k)} \left(\frac{in\cos\beta\, L_n(k)\, J_n(ka\sin\theta_i)}{ak^2\sin\theta_i L_n(k\cos\theta_i)} - \right.\right.$$

$$\left.\left. - \frac{2\sin\beta\, M_n(k) J_n'(ka\sin\theta_i)}{k(1+\cos\theta_i)M_n(k\cos\theta_i)} \right) + \frac{i\cos\beta\sin\theta_i\, J_n(ka\sin\theta_i)(k+\alpha)}{k(1+\cos\theta_i)L_n(k\cos\theta_i)(\alpha - k\cos\theta_i)} \right\} . \tag{5.142}$$

As a special case of (5.138) and (5.139), the curreng flowing in the wall of the tube is given by

$$-j_\phi(\phi, z) = H_z(a+0, \phi, z) - H_z(a-0, \phi, z)$$

$$= \frac{i}{\pi}\sqrt{\frac{\epsilon_o}{\mu_o}} \sum_{n=-\infty}^{\infty} e^{in\phi} \int_\Gamma \frac{e_n^-(\alpha)}{a^3k\kappa^2 M_n(\alpha)M_n(-\alpha)} e^{i\alpha z}\, d\alpha \tag{5.143}$$

$$j_z(\phi, z) = H_\phi(a+0, \phi, z) - H_\phi(a-0, \phi, z)$$

$$= \frac{i}{\pi}\sqrt{\frac{\epsilon_o}{\mu_o}} \sum_{n=-\infty}^{\infty} e^{in\phi} \int_\Gamma \left(\frac{n\alpha \bar{e}_n(\alpha)}{k\kappa^4 a^4 M_n(\alpha) M_n(-\alpha)} - \frac{k \bar{\mathcal{E}}_{zn}(a,\alpha)}{a\kappa^2 L_n(\alpha) L_n(-\alpha)} \right) e^{i\alpha z} d\alpha \,. \tag{5.144}$$

5.4.2 Field Inside the Tube

For the interior of the tube, i.e. $\rho < a$, $z > 0$, the integral in (5.139) can be calculated by means of residues. The contribution from the pole $\alpha = k\cos\theta_i$ cancels the incident field and we obtain the H_z and E_z components of the total field expressed as infinite sums of TE- and TM-modes respectively:

$$H_z(\rho, \phi, z) = \sum_{n=-\infty}^{\infty} \sum_{m=1}^{\infty} A_{nm} e^{in\phi} \frac{J_n(j'_{nm} \frac{\rho}{a})}{J_n(j'_{nm})} e^{i\alpha'_{nm} z} \tag{5.145}$$

$$E_z(\rho, \phi, z) = \sum_{n=-\infty}^{\infty} \sum_{m=1}^{\infty} B_{nm} e^{in\phi} \frac{J_n(j_{nm} \frac{\rho}{a})}{J'_n(j_{nm})} e^{i\alpha_{nm} z} \tag{5.146}$$

where as before $J'_n(j'_{nm}) = 0$, $0 < j'_{n1} < j'_{n2} < \ldots$

$$J_n(j_{nm}) = 0, \quad 0 < j_{n1} < j_{n2} < \ldots \quad \text{and} \quad \alpha'_{nm} = \sqrt{k^2 - \frac{j'^2_{nm}}{a^2}}, \quad \alpha_{nm} = \sqrt{k^2 - \frac{j^2_{nm}}{a^2}}$$

are positive or positive imaginary. The constants A_{nm} and B_{nm} are given by

$$A_{nm} = -\sqrt{\frac{\epsilon_o}{\mu_o}} \frac{\bar{e}_n(\alpha'_{nm})}{ka^3 \alpha'_{nm} \left(1 - \frac{n^2}{j'^2_{nm}}\right)} \tag{5.147}$$

and

$$B_{nm} = -i \frac{j_{nm} \mathcal{E}_{zn}(a, \alpha_{nm})}{a^2 \alpha_{nm}} \quad . \tag{5.148}$$

The remaining field components are readily obtained from (5.139) in the same manner, or by Maxwell's equations, from the knowledge of H_z and E_z. Specifically the surface currents on the inside of the wall of the tube are

$$j^i_\phi(\phi, z) = H_z(a, \phi, z) = \sum_{n=-\infty}^{\infty} \sum_{m=1}^{\infty} A_{nm} e^{in\phi} e^{i\alpha'_{nm} z} \tag{5.149}$$

$$j^i_z(\phi, z) = -H_\phi(a, \phi, z) = \sum_{n=-\infty}^{\infty} \sum_{m=1}^{\infty} e^{in\phi} \left(\frac{na\alpha'_{nm}}{j'^2_{nm}} A_{nm} e^{i\alpha'_{nm} z} - i \sqrt{\frac{\epsilon_o}{\mu_o}} \frac{ka}{j_{nm}} B_{nm} e^{i\alpha_{nm} z} \right) .$$

5.4.3 The Far Field

When $kr \sin^2\theta \gg 1$, where r, θ are spherical coordinates such that $\rho = r \sin\theta$, $z = r \cos\theta$, the integral in (5.138) can be estimated by the method of steepest descent. When $\theta > \theta_i$ we have to cross over the pole $\alpha = k \cos\theta_i$ to deform the contour of integration into the path of steepest descent. The contribution from the integral along the path of steepest descent when $\theta \neq \theta_i$ is given by (5.58) and for $\theta > \theta_i$ the residue at $\alpha = k \cos\theta_i$ yields an additional term which removes the reflected wave X^r. As in the scalar case we use the method of Van der Waerden (1951) to obtain an expression continuous at $\theta = \theta_i$ (cf. Section 5.2.4). We write the E_z and H_z components of the total fields in the far zone $kr \sin^2\theta \gg 1$ as

$$\left.\begin{matrix} E_z \\ H_z \end{matrix}\right\} \sim \left\{\begin{matrix} E_z^i \\ H_z^i \end{matrix}\right. + U_{E,H}(\theta,\phi)\frac{e^{ikr}}{r} - H(\theta_i-\theta)A_{E,H}(\phi)\frac{e^{ikr\cos(\theta-\theta_i)}}{\sqrt{kr\sin\theta}}$$

$$+ \frac{1}{2}\,\mathrm{sgn}(\theta_i-\theta)A_{E,H}(\phi)\,T(r,\theta-\theta_i)\,\frac{e^{ikr}}{\sqrt{kr\sin\theta}} \qquad (5.150)$$

where

$$U_E(\theta,\phi) = \frac{1}{\pi}\sum_{n=-\infty}^{\infty}(-i)^{n+1}\frac{\mathcal{E}_{zn}(a,k\cos\theta)}{H_n^{(1)}(ak\sin\theta)}\,e^{in\phi} \qquad (5.151)$$

$$A_E(\phi) = \sqrt{\frac{2}{\pi}}\,e^{-i\frac{\pi}{4}}\cos\beta\sum_{n=-\infty}^{\infty}\frac{\sqrt{\sin\theta_i}\,J_n(ka\sin\theta_i)}{H_n^{(1)}(ka\sin\theta_i)}\,e^{in\phi} \qquad (5.152)$$

and

$$U_H(\theta,\phi) = \frac{1}{\pi}\sqrt{\frac{\epsilon_o}{\mu_o}}\sum_{n=-\infty}^{\infty}(-i)^n\frac{e_n^-(k\cos\theta)}{(ak)^2\sin\theta\,H_n^{(1)'}(ak\sin\theta)}\,e^{in\phi} \qquad (5.153)$$

$$A_H(\phi) = \sqrt{\frac{\epsilon_o}{\mu_o}}\sqrt{\frac{2}{\pi}}\,e^{-i\frac{\pi}{4}}\sin\beta\sum_{n=-\infty}^{\infty}\frac{\sqrt{\sin\theta_i}\,J_n'(ka\sin\theta_i)}{H_n^{(1)'}(ka\sin\theta_i)}\,e^{in\phi}\,. \qquad (5.154)$$

The functions $H(\theta_i-\theta)$ and $\mathrm{sgn}(\theta_i-\theta)$ are the Heaviside step function and the signum function defined by (5.80) and $T(r,\theta-\theta_i)$ is given by (5.81). If $\theta > \theta_i$, i.e. the observation angle is outside the domain of cylindrical waves, the scattered field is a spherical wave given by

$$E_\theta^s(r,\theta,\phi) = \sqrt{\frac{\mu_o}{\epsilon_o}}\, H_\phi^s = -\frac{E_z^s}{\sin\theta} \sim -\frac{U_E(\theta,\phi)}{\sin\theta}\,\frac{e^{ikr}}{r}$$

$$E_\phi^s(r,\theta,\phi) = -\sqrt{\frac{\mu_o}{\epsilon_o}}\, H_\theta^s = \sqrt{\frac{\mu_o}{\epsilon_o}}\,\frac{H_z^s}{\sin\theta} \sim \sqrt{\frac{\mu_o}{\epsilon_o}}\,\frac{U_H(\theta,\phi)}{\sin\theta}\,\frac{e^{ikr}}{r}\ . \tag{5.155}$$

In the negative z-direction, i.e., $\theta=\pi$, we can still use (5.155) in spite of the fact that the condition $kr\sin^2\theta \gg 1$ is not satisfied. In the sums for U_E and U_H only the terms $n=\pm 1$ will contribute and we get:

$$E_x^s(0,0,z) = -\sqrt{\frac{\mu_o}{\epsilon_o}}\, H_y^s \sim \frac{e^{ik|z|}}{|z|}\,\frac{2ia\cos\beta\, L_1(k)\, J_1(ka\sin\theta_i)}{\left[4k^2a^2M_1^2(k) - L_1^2(k)\right]\sin\theta_i L_1(k\cos\theta_i)} \tag{5.156}$$

$$E_y^s(0,0,z) = \sqrt{\frac{\mu_o}{\epsilon_o}}\, H_x^s \sim -\frac{e^{ik|z|}}{|z|}\,\frac{4ika^2\sin\beta\, M_1(k)\, J_1'(ka\sin\theta_i)}{\left[4k^2a^2M_1^2(k) - L_1^2(k)\right](1+\cos\theta_i)M_1(k\cos\theta_i)} \tag{5.157}$$

as as $z\to-\infty$. Along the outer surface of the tube, $\rho=a+0$, the fields when $z\to\infty$ can be estimated from the integrals of (5.138) by deforming the path of integration in the upper half-plane into a U-shaped contour around a branch cut from k to $k+i\infty$. The symmetric term $n=0$ is dominant, and due to the boundary condition the components E_ϕ, E_z and H_ρ of the total field are identically zero. For the remaining components of the total field, representing surface charges and surface current, the results are:

$$E_\rho(a+0,\phi,z) \sim -\frac{2i}{\pi} e^{ikz\cos\theta_i} \sum_{n=-\infty}^{\infty} i^n e^{in\phi} \left(\frac{i\cos\beta\cos\theta_i}{ka\sin\theta_i H_n^{(1)}(ka\sin\theta_i)} + \right.$$

$$\left. + \frac{n\sin\beta}{(ka\sin\theta_i)^2 H_n^{(1)}(ka\sin\theta_i)} \right) - \frac{2i\cos\beta J_o(ka\sin\theta_i) L_o(k)}{ka\sin\theta_i L_o(k\cos\theta_i)} \frac{e^{ikz}}{\ell n \frac{2z}{\gamma_1 ka^2} + i\frac{\pi}{2}} ,$$

(5.157)

$$\sqrt{\frac{\mu_o}{\epsilon_o}} H_\phi(a+0,\phi,z) \sim -\frac{2i}{\pi} e^{ikz\cos\theta_i} \sum_{n=-\infty}^{\infty} i^n e^{in\phi} \left(\frac{i\cos\beta}{ka\sin\theta_i H_n^{(1)}(ka\sin\theta_i)} + \right.$$

$$\left. + \frac{n\sin\beta\cos\theta_i}{(ka\sin\theta_i)^2 H_n^{(1)'}(ka\sin\theta_i)} \right) - \frac{2i\cos\beta J_o(ka\sin\theta_i) L_o(k)}{ka\sin\theta_i L_o(k\cos\theta_i)} \frac{e^{ikz}}{\ell n \frac{2z}{\gamma_1 ka^2} + i\frac{\pi}{2}} ,$$

$$\sqrt{\frac{\mu_o}{\epsilon_o}} H_z(a+0,\phi,z) \sim \frac{2i}{\pi} e^{ikz\cos\theta_i} \sum_{n=-\infty}^{\infty} i^n e^{in\phi} \frac{\sin\beta}{ka H_n^{(1)'}(ka\sin\theta_i)} -$$

$$- \left(\frac{L_1(k)\sin\beta J_o'(ka\sin\theta_i)}{L_1(k\cos\theta_i)(1-\cos\theta_i)} + k e_1^-(k) e^{i\phi} + k e_{-1}^-(k) e^{-i\phi} \right) \frac{a e^{ikz}}{kz^2}$$

as $z \to \infty$, where $\ell n\, \gamma_1 = 0.5772156649...$ is Euler's constant. The terms containing the summation over n from $-\infty$ to ∞ are the fields pertaining to an infinite cylinder (cf. equations 2.41 and 2.42).

5.4.4 Axial Incidence

The case of axial incidence, i.e. $\theta_i = 0$, is of some interest because in that case the sum over n only contains the terms for $n = \pm 1$. Thus, we need to know only the split functions $M_1(\alpha)$ and $L_1(\alpha)$ ($\equiv M_o(\alpha)$) to solve the problem.

The solution is obtained as a special case of the previous results if we put $\theta_i = 0$. It is no restriction to assume the incident field to be polarized in the x-direction, i.e. the incident field is

$$\underline{E}^i = \hat{i}_x e^{ikz} ,$$
$$\underline{H}^i = \sqrt{\epsilon_o/\mu_o}\, \hat{i}_y e^{ikz} . \tag{5.158}$$

The components of the total field are then

$$E_\rho(\rho,\phi,z) = E_\rho^i + \frac{i}{\pi}\cos\phi \int_\Gamma \left(\frac{\alpha \bar{\mathcal{E}}_{z1}(a,\alpha)}{\kappa} \frac{H_1^{(1)'}(\kappa\rho)}{H_1^{(1)}(\kappa a)} - \frac{\bar{e}_1(\alpha)}{a^2\rho\kappa^3} \frac{H_1^{(1)}(\kappa\rho)}{H_1^{(1)'}(\kappa\rho)} \right) e^{i\alpha z}\, d\alpha$$

$$E_\phi(\rho,\phi,z) = E_\phi^i + \frac{i}{\pi}\sin\phi \int_\Gamma \left(\frac{\bar{e}_1(\alpha)}{a^2\kappa^2} \frac{H_1^{(1)'}(\kappa\rho)}{H_1^{(1)'}(\kappa a)} - \frac{\alpha \bar{\mathcal{E}}_{z1}(a,\alpha)}{\rho\kappa^2} \frac{H_1^{(1)}(\kappa\rho)}{H_1^{(1)}(\kappa a)} \right) e^{i\alpha z}\, d\alpha$$

$$E_z(\rho,\phi,z) = \frac{\cos\phi}{\pi} \int_\Gamma \bar{\mathcal{E}}_{z1}(a,\alpha) \frac{H_1^{(1)}(\kappa\rho)}{H_1^{(1)}(\kappa a)} e^{i\alpha z}\, d\alpha \tag{5.159a}$$

$$H_\rho(\rho,\phi,z) = H_\rho^i + \sqrt{\frac{\epsilon_o}{\mu_o}} \frac{i}{\pi}\sin\phi \int_\Gamma \left(\frac{k\bar{\mathcal{E}}_{z1}(a,\alpha) H_1^{(1)}(\kappa\rho)}{\rho\kappa^2 H_1^{(1)}(\kappa a)} - \frac{\alpha \bar{e}_1(\alpha)}{a^2 k\kappa^2} \frac{H_1^{(1)'}(\kappa\rho)}{H_1^{(1)'}(\kappa a)} \right) \times$$
$$\times\, e^{i\alpha z}\, d\alpha$$

$$H_\phi(\rho,\phi,z) = H_\phi^i + \sqrt{\frac{\epsilon_o}{\mu_o}} \frac{i}{\pi}\cos\phi \int_\Gamma \left(\frac{k\bar{\mathcal{E}}_{z1}(a,\alpha) H_1^{(1)'}(\kappa\rho)}{\kappa H_1^{(1)}(\kappa a)} - \frac{\alpha \bar{e}_1(\alpha)}{\rho a^2 k\kappa^3} \frac{H_1^{(1)}(\kappa\rho)}{H_1^{(1)'}(\kappa a)} \right) \times$$
$$\times e^{i\alpha z}\, d\alpha$$

$$H_z(\rho,\phi,z) = -\sqrt{\frac{\epsilon_o}{\mu_o}}\,\frac{\sin\phi}{\pi}\int_\Gamma \frac{e_1^-(\alpha)}{a^2 k\kappa}\,\frac{H_1^{(1)}(\kappa\rho)}{H_1^{(1)'}(\kappa a)}\,e^{i\alpha z}\,d\alpha \qquad (5.159b)$$

when $\rho > a$, where $e_1^-(\alpha)$ and $\mathcal{E}_{z1}^-(a,\alpha)$ are obtained from (5.141) and (5.142) by putting $n=1$, $\theta_i = 0$ and $\beta = \pi$. Thus,

$$e_1^-(\alpha) = \frac{2a^4k^2M_1(k)}{4k^2a^2M_1^2(k) - L_1^2(k)}\,(k+\alpha)M_1(\alpha)\,,$$

$$\mathcal{E}_{z1}^-(a,\alpha) = \frac{aL_1(k)}{4k^2a^2M_1^2(k) - L_1^2(k)}\,L_1(\alpha)\,. \qquad (5.160)$$

The field components for $\rho < a$ are given by expressions identical to those of (5.159) with $H_n^{(1)}$ and $H_n^{(1)'}$ exchanged for J_n and J_n' respectively.

The H_z and E_z components of the field inside the tube ($\rho < a$, $z > 0$) are

$$H_z(\rho,\phi,z) = -2i\sqrt{\frac{\epsilon_o}{\mu_o}}\sin\phi\sum_{m=1}^{\infty}\frac{j_{1m}'^2\,e_1^-(\alpha_{1m}')}{ka^3\alpha_{1m}'(j_{1m}'^2-1)}\,\frac{J_1(j_{1m}'\frac{\rho}{a})}{J_1(j_{1m}')}\,e^{i\alpha_{1m}'z}\,,$$

$$E_z(\rho,\phi,z) = -2i\cos\phi\sum_{m=1}^{\infty}\frac{j_{1m}\,\mathcal{E}_{z1}^-(a,\alpha_{1m})}{a^2\alpha_{nm}}\,\frac{J_1(j_{1m}\frac{\rho}{a})}{J_1'(j_{1m})}\,e^{i\alpha_{1m}z}\,. \qquad (5.161)$$

The far-zone scattered field is

$$E_\theta^s = \sqrt{\frac{\mu_o}{\epsilon_o}}\,H_\phi^s \sim \frac{2}{\pi}\,\frac{e^{ikr}}{r}\,\frac{\mathcal{E}_{z1}^-(a,k\cos\theta)}{\sin\theta\,H_1^{(1)}(ak\sin\theta)}\cos\phi$$

$$E_\phi^s = -\sqrt{\frac{\mu_o}{\epsilon_o}}\,H_\theta^s \sim \frac{2}{\pi}\,\frac{e^{ikr}}{r}\,\frac{e_1^-(k\cos\theta)}{(ak\sin\theta)^2\,H_1^{(1)'}(ak\sin\theta)}\sin\phi \qquad (5.162)$$

when $kr\sin^2\theta \gg 1$. In the back scattering direction $\theta = \pi$ the polarization is the same as that of the incident field, and from (5.156) we obtain

$$E_x^s(0,0,z) \sim -\frac{e^{ik|z|}}{|z|} \frac{ia^2k}{4k^2a^2M_1^2(k) - L_1^2(k)}, \qquad z \to -\infty \tag{5.163}$$

Along the outer surface of the tube the asymptotic forms of the nonvanishing components of the total field are

$$E_\rho(a+0,\phi,z) \sim \sqrt{\frac{\mu_o}{\epsilon_o}}\, H_\phi(a+0,\phi,z) \sim \cos\phi\, e^{ikz}\left(1+\frac{ika^2}{z}\,\frac{4k^2a^2M_1^2(k)+L_1^2(k)}{4k^2a^2M_1^2(k)-L_1^2(k)}\right) \tag{5.164}$$

$$H_z(a+0,\phi,z) \sim -\sin\phi\sqrt{\frac{\epsilon_o}{\mu_o}}\,\frac{8ia^5k^3M_1^2(k)}{4k^2a^2M_1^2(k)-L_1^2(k)}\,\frac{e^{ikz}}{z^2}$$

as $z \to \infty$.

5.5 Electromagnetic Radiation from a Source Inside a Semi-Infinite Thin-Walled Tube

5.5.1 General Solution

We assume that the tube is located at $\rho = a$, $z > 0$ and that a single waveguide mode is propagated in the negative z-direction. The incoming mode can be either a TM mode with the axial component of the electrical field strength

$$E_z^i = E_{nm}\,\frac{J_n(j_{nm}\frac{\rho}{a})}{J_n'(j_{nm})}\cos n\phi\, e^{-i\alpha_{nm}z} \tag{5.165}$$

or a TE mode with the H_z-component

$$H_z^i = H_{nm}\,\frac{J_n(j'_{nm}\frac{\rho}{a})}{J_n(j'_{nm})}\cos n\phi\, e^{-i\alpha'_{nm}z} \tag{5.166}$$

$n \geqslant 0$, $m \geqslant 1$

where $J_n(j_{nm}) = 0$, $0 < j_{n1} < j_{n2} < \ldots$

$J'_n(j'_{nm}) = 0$, $0 < j'_{n1} < j'_{n2} < \ldots$

and

$$\alpha_{nm} = \sqrt{k^2 - \frac{j_{nm}^2}{a^2}} \quad , \qquad \alpha'_{nm} = \sqrt{k^2 - \frac{j'^2_{nm}}{a^2}}$$

are positive or positive imaginary. For arbitrary excitation inside the tube we have to calculate the field in a corresponding infinite waveguide at $z = 0$ expressed as an infinite sum of waveguide modes and then sum up the results from each mode.

The problem has been studied in detail by L. A. Wainstein (1948c; 1950a, b). We can obtain its solution from the results of Section 5.1 by proper choice of the functions $f_n(\alpha)$ and $g_n(\alpha)$ in (5.44) and (5.45). For that purpose it is suitable to decompose the total field into the field obtained from the surface current at $\rho = a$, $0 < z < \infty$, connected with the incoming waveguide mode, plus the scattering of this field from the semi-infinite cylinder. For the scattering problem so formulated the expressions of Section 5.1 are directly applicable and

$$e_n^i(\alpha) = H_{nm} \frac{\omega\mu_o \kappa^2 a^3}{2\epsilon_n(\alpha + \alpha'_{nm})} M_n(\alpha) M_n(-\alpha)$$

$$\mathfrak{E}_{zn}^i(a,\alpha) = -\frac{1}{2\epsilon_n} L_n(\alpha) L_n(-\alpha) \left\{ E_{nm} \frac{i\kappa^2 a^2}{j_{nm}(\alpha + \alpha_{nm})} + nH_{nm} \frac{\kappa^2 a^2 \alpha'_{nm} + j'^2_{nm} \alpha}{\omega\epsilon_o j'^2_{nm} (\alpha + \alpha'_{nm})} \right\} \tag{5.167}$$

where $\epsilon_o = 1$, $\epsilon_1 = \epsilon_2 = \ldots = 2$. The only singularities of $e_n^i(\alpha)$ and $\mathfrak{E}_{zn}^i(\alpha)$ are at $\alpha = \pm k$. Inserting the expressions of (5.167) into (5.42) and (5.43) and separating the result according to (5.7) and (5.8) we get

$$\epsilon_n f_n^-(\alpha) = H_{nm} \frac{\omega\mu_o a M_n(\alpha'_{nm})}{(\alpha+\alpha'_{nm})}$$

$$\epsilon_n f_n^+(-k) = H_{nm} \frac{\omega\mu_o a\left[M_n(\alpha'_{nm}) - M_n(k)\right]}{k-\alpha'_{nm}}$$

$$\epsilon_n g_n^-(\alpha) = -E_{nm} \frac{ia(k+\alpha_{nm})L_n(\alpha_{nm})}{j_{nm}(\alpha+\alpha_{nm})} - H_{nm} \frac{nkL_n(k)}{a\omega\epsilon_o(k+\alpha)(k-\alpha'_{nm})} \tag{5.168}$$

$$\epsilon_n g_n^-(k) = -E_{nm} \frac{iaL_n(\alpha_{nm})}{j_{nm}} - H_{nm} \frac{nL_n(k)}{2a\omega\epsilon_o(k-\alpha'_{nm})}$$

The quantities $e_n^-(\alpha)$ and $\mathcal{E}_{zn}^-(a,\alpha)$, related to the Fourier transforms of the tangential components of the total electric field strength at $\rho = a$, $-\infty < z < 0$, are obtained from (5.44) and (5.45) on putting $G_n(\alpha) = F_n(\alpha) \equiv 0$. We write an arbitrary component of the total field as

$$X(\rho,\phi,z) = \frac{1}{2\pi}\int_\Gamma \left[A(\alpha,\phi)H_n^{(1)}(\rho\kappa) + B(\alpha,\phi)H_n^{(1)'}(\rho\kappa)\right] e^{i\alpha z}\, d\alpha\,, \tag{5.169}$$

$$\rho > a,\quad -\infty < z < \infty$$

$$X(\rho,\phi,z) = X^i(\rho,\phi,z) + \frac{1}{2\pi}\int_\Gamma \left[A(\alpha,\phi)J_n(\rho\kappa) + B(\alpha,\phi)J_n'(\rho\kappa)\right] e^{i\alpha z}\, d\alpha\,, \tag{5.170}$$

$$\rho > a,\quad -\infty < z < \infty$$

where as before $\kappa = \sqrt{k^2-\alpha^2}$ and the path of integration Γ is as indicated in Fig. 5-1. X^i xtands for a component of the fields of the incoming waveguide mode and the functions $A(\alpha,\phi)$ and $B(\alpha,\phi)$ are given in Table VII if we define

$$P_E(\alpha) = \frac{2k^3a^5 n M_n(k)L_n(k)L_n(\alpha_{nm})}{j_{nm}N}(k+\alpha)M_n(\alpha)$$

$$P_H(\alpha) = \sqrt{\frac{\mu_o}{\epsilon_o}}\, a^3 k M_n(\alpha'_{nm})\left(\frac{k-\alpha}{2(\alpha+\alpha'_{nm})} - \frac{n^2 k L_n^2(k)}{(k-\alpha'_{nm})N}\right)(k+\alpha)M_n(\alpha) \tag{5.171}$$

$$Q_E(\alpha) = \frac{a^2}{j_{nm}}L_n(\alpha_{nm})\left(\frac{(k+\alpha_{nm})(k+\alpha)}{2(\alpha+\alpha_{nm})} + \frac{n^2 k L_n^2(k)}{N}\right)L_n(\alpha)$$

$$Q_H(\alpha) = -\sqrt{\frac{\mu_o}{\epsilon_o}}\,\frac{2a^2k^2 n L_n(k)M_n(k)M_n(\alpha'_{nm})}{(k-\alpha'_{nm})N}L_n(\alpha)$$

where $N = 4k^2a^2M_n^2(k) - n^2L_n^2(k)$.

As a special case of (5.169) and (5.170), the current flowing in the wall of tne tube is given as

$$-j_\phi(\phi, z) = H_z(a+0, \phi, z) - H_z(a-0, \phi, z)$$

$$= -H_{nm}\cos n\phi\, e^{-i\alpha'_{nm}z} +$$

$$+\sqrt{\frac{\epsilon_o}{\mu_o}}\,\frac{i}{\pi a^3 k}\int_\Gamma \frac{H_{nm}P_H(\alpha)\cos n\phi + E_{nm}P_E(\alpha)\sin n\phi}{\kappa^2 M_n(\alpha)M_n(-\alpha)}\, e^{i\alpha z}\, d\alpha \tag{5.172}$$

TABLE VII

Relation Between the Field Components and the Quantity X of Equations (5.169) and (5.170)

X	$A(\alpha, \phi)$	$B(\alpha, \phi)$
E_ρ	$\frac{-n}{\rho\kappa^3 a^2}\left[b_E(\alpha)\cos n\phi - b_H(\alpha)\sin n\phi\right]$	$\frac{\alpha}{\kappa}\left[c_E(\alpha)\cos n\phi - c_H(\alpha)\sin n\phi\right]$
E_ϕ	$\frac{-\alpha n}{\rho\kappa^2}\left[c_H(\alpha)\cos n\phi + c_E(\alpha)\sin n\phi\right]$	$\frac{1}{\kappa^2 a^2}\left[b_H(\alpha)\cos n\phi + b_E(\alpha)\sin n\phi\right]$
E_z	$-i\left[c_E(\alpha)\cos n\phi - c_H(\alpha)\sin n\phi\right]$	0
H_ρ	$\frac{\omega\epsilon_o n}{\rho\kappa^2}\left[c_H(\alpha)\cos n\phi + c_E(\alpha)\sin n\phi\right]$	$\frac{-\alpha}{\omega\mu_o\kappa^2 a^2}\left[b_H(\alpha)\cos n\phi + b_E(\alpha)\sin n\phi\right]$
H_ϕ	$\frac{-n\alpha}{\rho\omega\mu_o\kappa^3 a^2}\left[b_E(\alpha)\cos n\phi - b_H(\alpha)\sin n\phi\right]$	$\frac{\omega\epsilon_o}{\kappa}\left[c_E(\alpha)\cos n\phi - c_H(\alpha)\sin n\phi\right]$
H_z	$\frac{i}{\omega\mu_o\kappa a^2}\left[b_H(\alpha)\cos n\phi + b_E(\alpha)\sin n\phi\right]$	0

where

for $\rho > a$:

$$b_E(\alpha) = \frac{E_{nm} P_E(\alpha)}{H_n^{(1)'}(a\kappa)}$$

$$b_H(\alpha) = \frac{H_{nm} P_H(\alpha)}{H_n^{(1)'}(a\kappa)}$$

$$c_E(\alpha) = \frac{E_{nm} Q_E(\alpha)}{H_n^{(1)}(a\kappa)}$$

$$c_H(\alpha) = \frac{H_{nm} Q_H(\alpha)}{H_n^{(1)}(a\kappa)}$$

for $\rho < a$:

$$b_E(\alpha) = \frac{E_{nm} P_E(\alpha)}{J_n'(a\kappa)}$$

$$b_H(\alpha) = \frac{H_{nm} P_H(\alpha)}{J_n'(a\kappa)}$$

$$c_E(\alpha) = \frac{E_{nm} Q_E(\alpha)}{J_n(a\kappa)}$$

$$c_H(\alpha) = \frac{H_{nm} Q_H(\alpha)}{J_n(a\kappa)}$$

$$j_z(\phi, z) = H_\phi(a+0, \phi, z) - H_\phi(a-0, \phi, z)$$

$$= \sqrt{\frac{\epsilon_o}{\mu_o}} \frac{ka}{ij_{nm}} E_{nm} \cos n\phi\, e^{-\alpha_{nm} z} + \frac{na\alpha'_{nm}}{ij'^2_{nm}} H_{nm} \sin n\phi\, e^{-\alpha'_{nm} z} +$$

$$+ \sqrt{\frac{\epsilon_o}{\mu_o}} \frac{1}{\pi a} \int_\Gamma \left[\frac{n\alpha \left[H_{nm} P_H(\alpha) \sin n\phi - E_{nm} P_E(\alpha) \cos n\phi \right]}{a^3 k \kappa^4 M_n(\alpha) M_n(-\alpha)} + \right.$$

$$\left. + \frac{k \left[H_{nm} Q_H(\alpha) \sin n\phi - E_{nm} Q_E(\alpha) \cos n\phi \right]}{\kappa^2 L_n(\alpha) L_n(-\alpha)} \right] e^{i\alpha z} d\alpha \,. \qquad (5.173)$$

5.5.2 Field Inside the Tube

When $\rho < a$, $z > 0$ the integral in (5.170) can be evaluated by means of residues. Thus, the E_z and H_z components of the field can be written as

$$E_z(\rho, \phi, z) = E_{nm} \cos n\phi \left\{ \frac{J_n(j_{nm} \frac{\rho}{a})}{J'_n(j_{nm})} e^{-i\alpha_{nm} z} + \sum_{\ell=0}^{\infty} R^{nE}_{m\ell} \frac{J_n(j_{n\ell} \frac{\rho}{a})}{J'_n(j_{n\ell})} e^{i\alpha_{n\ell} z} \right\} +$$

$$+ H_{nm} \sin n\phi \sum_{\ell=0}^{\infty} T^{nH}_{m\ell} \frac{J_n(j_{n\ell} \frac{\rho}{a})}{J'_n(j_{n\ell})} e^{i\alpha_{n\ell} z} \qquad (5.174)$$

$$H_z(\rho, \phi, z) = H_{nm} \cos n\phi \left\{ \frac{J_n(j'_{nm} \frac{\rho}{a})}{J_n(j'_{nm})} e^{-i\alpha'_{nm} z} + \sum_{\ell=0}^{\infty} R^{nH}_{m\ell} \frac{J_n(j'_{n\ell} \frac{\rho}{a})}{J_n(j'_{n\ell})} e^{i\alpha'_{n\ell} z} \right\} +$$

$$+ E_{nm} \sin n\phi \sum_{\ell=0}^{\infty} T^{nE}_{m\ell} \frac{J_n(j'_{n\ell} \frac{\rho}{a})}{J_n(j'_{n\ell})} e^{i\alpha'_{n\ell} z} \qquad (5.175)$$

where

$$R_{m\ell}^{nE} = -\left|R_{m\ell}^{nE}\right| e^{i\Theta_{m\ell}^{nE}} = -\frac{j_{n\ell}}{a^2 \alpha_{n\ell}} Q_E(\alpha_{n\ell})$$

$$R_{m\ell}^{nH} = -\left|R_{m\ell}^{nH}\right| e^{i\Theta_{m\ell}^{nH}} = -\sqrt{\frac{\epsilon_o}{\mu_o}} \frac{j'^2_{n\ell}}{a^3 k\alpha'_{n\ell}(j'^2_{n\ell} - n^2)} P_H(\alpha'_{n\ell}) \tag{5.176}$$

$$T_{m\ell}^{nH} = \frac{j_{n\ell}}{a^2 \alpha_{n\ell}} Q_H(\alpha_{n\ell})$$

$$T_{m\ell}^{nE} = -\sqrt{\frac{\epsilon_o}{\mu_o}} \frac{j'^2_{n\ell}}{a^3 k\alpha'_{n\ell}(j'^2_{n\ell} - n^2)} P_E(\alpha'_{n\ell})$$

For symmetric modes $(n=0)$, $T_{m\ell}^{nE} = T_{m\ell}^{nH} = 0$ and the reflection and conversion coefficients are easily expressible in terms of the auxiliary functions $P_n(\alpha)$ and $S_n(\alpha)$, connected with the split functions, of equations (5.220) and (5.225). Thus, for the reflection coefficients we have

$$\left.\begin{aligned} \left|R_{11}^{oE}\right| &= \frac{k+\alpha_{o1}}{k-\alpha_{o1}} e^{a\alpha_{o1}\,\mathrm{Re}\,P_o(\alpha_{o1})} \\ \Theta_{11}^{oE} &= a\alpha_{o1}\,\mathrm{Im}\,P_o(\alpha_{o1}) \end{aligned}\right\} j_{o1} \leqslant ka < j_{o2} \tag{5.177}$$

$$\left.\begin{aligned} \left|R_{11}^{oH}\right| &= e^{a\alpha_{11}\,\mathrm{Re}\,P_1(\alpha_{11})} \\ \Theta_{11}^{oH} &= a\alpha_{11}\,\mathrm{Im}\,P_1(\alpha_{11}) \end{aligned}\right\} j_{11} \leqslant ka < j_{12} \tag{5.178}$$

Approximate expressions for the reflection and conversion coefficients of arbitrary E_{nm} or H_{nm} modes can be obtained using the function U(s, g) defined by (5.258). The absolute value of reflection and conversion coefficients of the symmetric modes H_{o1}, H_{o2} and of the reflection coefficient of mode H_{11} as functions of ka in the range $j'_{11} < ka < j'_{o3}$ ($j'_{11} = 1.841$, $j'_{o3} = 10.173$) are given in Fig. 5-17 and the corresponding phase functions of symmetric modes H_{o1}, H_{o2} are shown in Fig. 5-18. The absolute value and phase of reflection and conversion coefficients of symmetric modes E_{o1}, E_{o2} for $j_{o1} < ka < j_{o3}$ ($j_{o1} = 2.405$, $j_{o3} = 8.654$) are shown in Figs. 5-19 and 5-20.

When the incident mode is E_{o1} and $j_{o1} < ka < j_{o2}$, or when it is H_{n1} and $j'_{o1} < ka < j'_{o2}$, $n = 0$, or $j'_{n1} < ka < j_{n1}$, $n \geq 1$, the only undamped mode traveling in the positive z-direction is the reflected incident mode. For large z the z-dependence of all components of the field is given by

$$Z(z) = e^{-ihz} \pm R\, e^{ihz} \tag{5.179}$$

where h is the wave number of the incident mode and R is the reflection coefficient given by (5.176). Equation (5.179) represents a standing wave of amplitude

$$\left|Z(z)\right| = \sqrt{1+|R|^2 \pm 2|R|\cos(2hz+\Theta)} \quad . \tag{5.180}$$

Thus the first node or antinode is located at $z = -\ell$ where

$$2\alpha_{o1}\ell = \Theta_{11}^{oE} \tag{5.181}$$

for an incident E_{o1} mode and

$$2\alpha'_{n1}\ell = \Theta_{11}^{nH} \tag{5.182}$$

for an incident H_{n1} mode. As in the scalar case we call the length ℓ the <u>end correction</u> related to the pertinent mode. In Figs. 5-18 and 5-20 the quantity ℓ/a is plotted for incident modes H_{o1} and E_{o1} respectively.

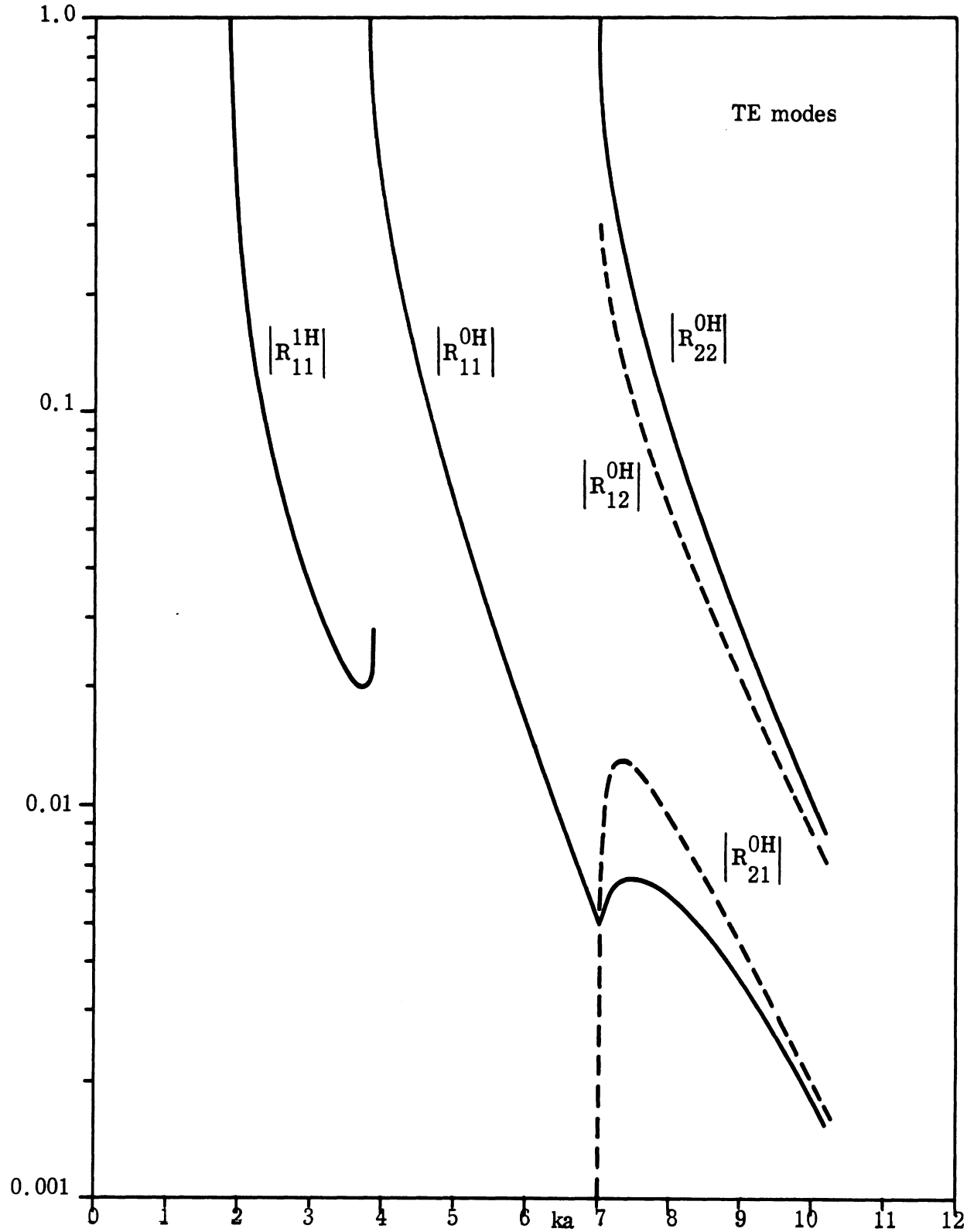

FIG. 5-17: ABSOLUTE VALUE OF REFLECTION AND CONVERSION COEFFICIENTS OF SYMMETRIC MODES H_{01}, H_{02} AND OF THE REFLECTION COEFFICIENT OF THE MODE H_{11}. (Wainstein, 1948c; 1950a).

This page is blank

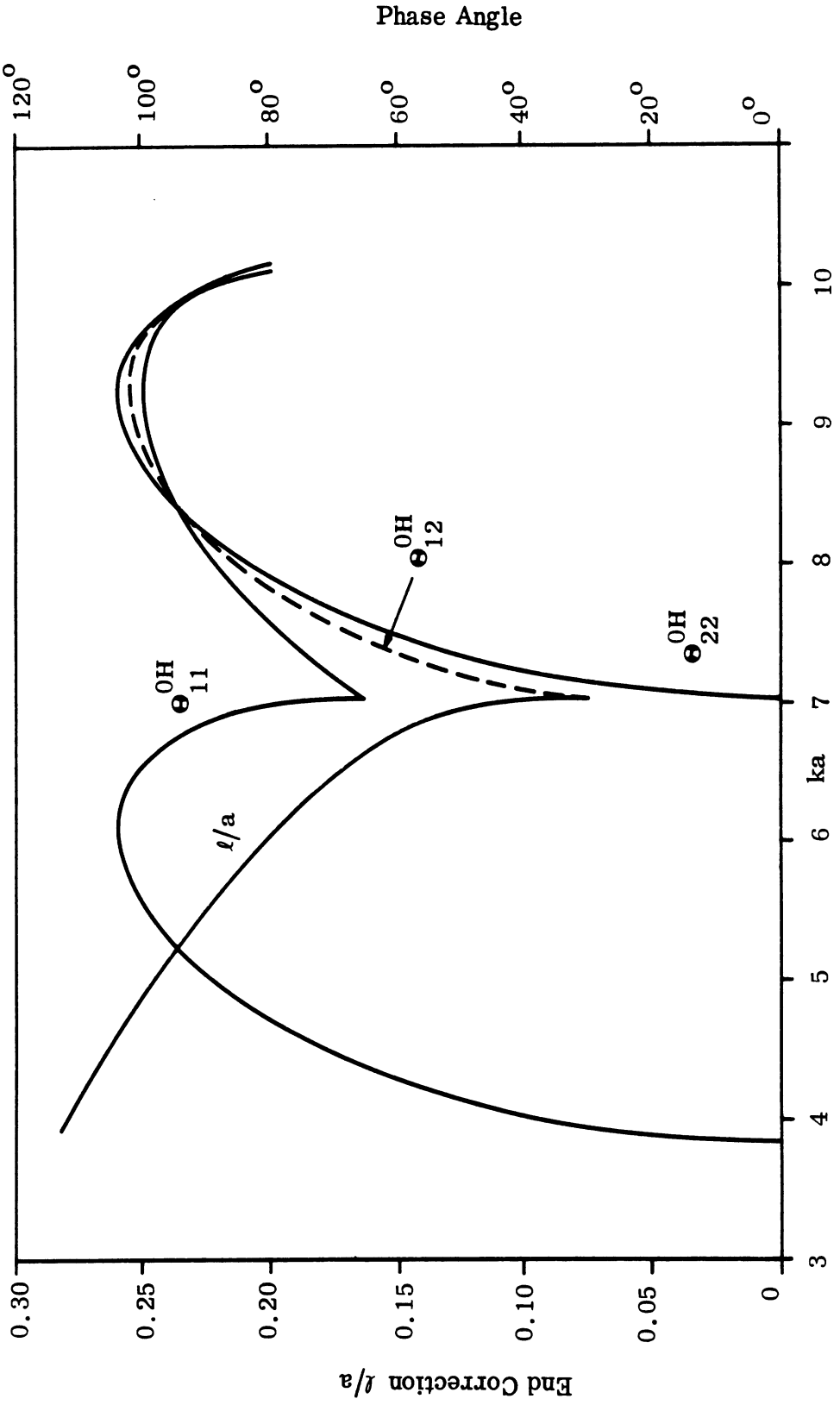

FIG. 5-18: PHASE OF REFLECTION AND CONVERSION COEFFICIENTS OF SYMMETRIC MODES H_{01}, H_{02} AND END CORRECTION. (Wainstein, 1948c)

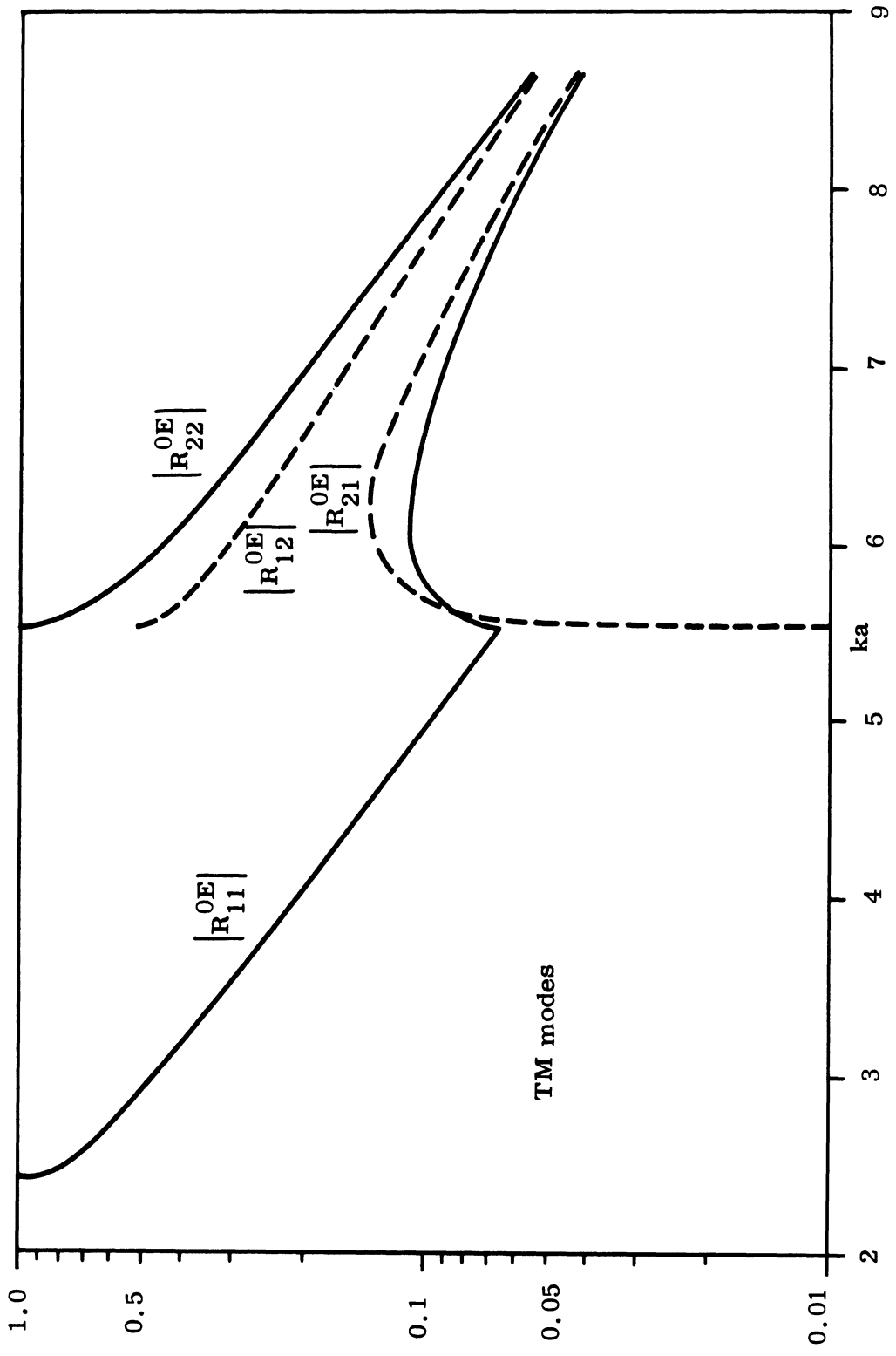

FIG. 5-19: ABSOLUTE VALUE OF REFLECTION AND CONVERSION COEFFICIENTS OF SYMMETRIC MODES E_{01}, E_{02}. (Wainstein, 1948c)

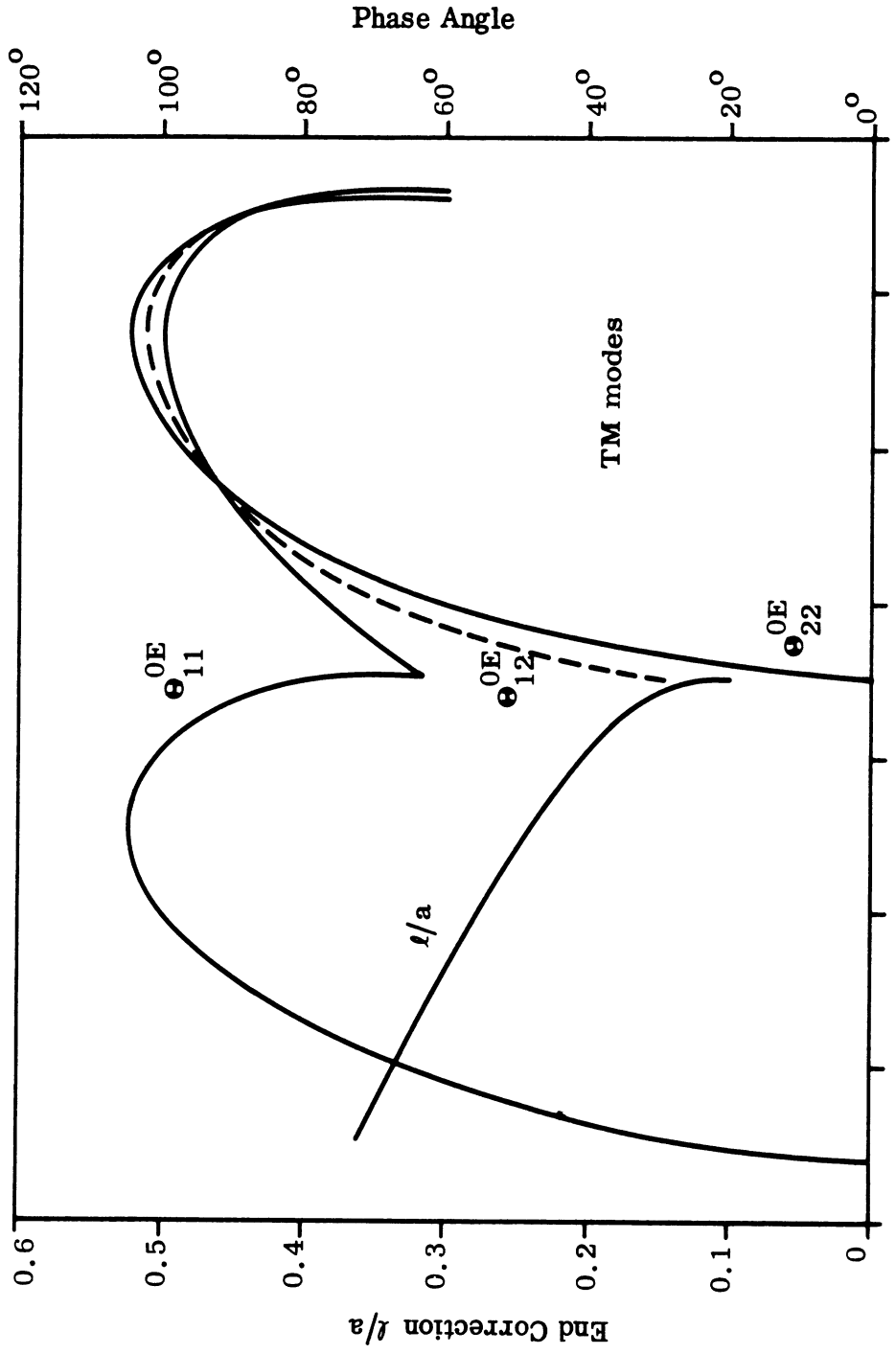

FIG. 5-20: PHASE OF REFLECTION AND CONVERSION COEFFICIENTS OF SYMMETRIC MODES E_{01}, E_{02} AND END CORRECTION. (Wainstein, 1948c)

There exist some symmetry relations for the coefficients $R^{nE}_{m\ell'}$, $R^{nH}_{m\ell'}$, $T^{nE}_{m\ell'}$, $T^{nH}_{m\ell}$. From (5.171) and (5.176) we obtain

$$\frac{\alpha_{nm}}{j^2_{nm}} R^{nE}_{\ell m} = \frac{\alpha_{n\ell}}{j^2_{n\ell}} R^{nE}_{m\ell}$$

$$\frac{\alpha'_{nm}(j'^2_{nm} - n^2)}{j'^4_{nm}} R^{nH}_{\ell m} = \frac{\alpha'_{n\ell}(j'^2_{n\ell} - n^2)}{j'^4_{n\ell}} R^{nH}_{m\ell} \tag{5.183}$$

$$\frac{\alpha_{nm}}{j^2_{nm}} T^{nH}_{\ell m} = \frac{\mu_o}{\epsilon_o} \frac{\alpha'_{n\ell}(j'^2_{n\ell} - n^2)}{j'^4_{n\ell}} T^{nE}_{m\ell} \quad .$$

Furthermore, for symmetric modes ($n = 0$) and $ka \geqslant j_{om} > j_{o\ell}$,

$$\Theta^{oE}_{\ell m} = \Theta^{oE}_{m\ell} = \frac{\Theta^{oE}_{\ell\ell} + \Theta^{oE}_{mm}}{2} \quad . \tag{5.184}$$

The same relation is true for $\Theta^{oH}_{m\ell}$ if $ka \geqslant j'_{om} > j'_{o\ell}$.

The power flow connected with the modes of (5.165) and (5.166) if $ka > j_{nm}$ or $ka > j'_{nm}$ is

$$P^E_{nm} = \sqrt{\frac{\epsilon_o}{\mu_o}} \frac{\pi a^4 k \alpha_{nm}}{2\epsilon_n j^2_{nm}} |E_{nm}|^2,$$

$$P^H_{nm} = \sqrt{\frac{\mu_o}{\epsilon_o}} \frac{\pi a^4 k \alpha'_{nm}(j'^2_{nm} - n^2)}{2\epsilon_n j'^4_{nm}} |H_{nm}|^2 . \tag{5.185}$$

If $ka > j_{n\ell}, j'_{ns}$ the fraction of the power of an incoming undamped E_{nm} mode converted into the $E_{n\ell}$ and H_{ns} modes respectively is

$$r_{m\ell}^{nE} = \frac{j_{nm}^2 \alpha_{n\ell}}{j_{n\ell}^2 \alpha_{nm}} \left| R_{m\ell}^{nE} \right|^2 ,$$

$$t_{ms}^{nE} = \frac{\mu_o}{\epsilon_o} \frac{j_{nm}^2 \alpha'_{ns} (j'^2_{ns} - n^2)}{j'^4_{ns} \alpha_{nm}} \left| T_{ms}^{nE} \right|^2 . \qquad (5.186)$$

Similarly, the fraction of the power of an incoming undamped H_{nm} mode converted into the $H_{n\ell}$ and E_{ns} modes respectively if $ka > j'_{n\ell}, j_{ns}$ is

$$r_{m\ell}^{nH} = \frac{j'^4_{nm} \alpha'_{n\ell} (j'^2_{n\ell} - n^2)}{j'^4_{n\ell} \alpha'_{nm} (j'^2_{nm} - n^2)} \left| R_{m\ell}^{nH} \right|^2 ,$$

$$t_{ms}^{nH} = \frac{\epsilon_o}{\mu_o} \frac{j'^4_{nm} \alpha_{ns}}{j_{ns}^2 \alpha'_{nm} (j'^2_{nm} - n^2)} \left| T_{ms}^{nH} \right|^2 . \qquad (5.187)$$

Using (5.183) we see that

$$\begin{aligned} r_{\ell m}^{nE} &= r_{m\ell}^{nE} \\ r_{\ell m}^{nH} &= r_{m\ell}^{nH} \\ t_{\ell m}^{nE} &= t_{m\ell}^{nH} \end{aligned} \qquad (5.188)$$

The total power reflection coefficients of the modes E_{nm} and H_{nm} are

$$r_m^{nE} = \sum_{\ell=1}^{\ell_o} r_{m\ell}^{nE} + \sum_{s=1}^{s_o} t_{ms}^{nH}$$

$$r_m^{nH} = \sum_{\ell=1}^{\ell_o} r_{m\ell}^{nH} + \sum_{s=1}^{s_o} t_{ms}^{nH} \qquad (5.189)$$

where the summation is to be taken over all undamped modes.

5.5.3 The Far Field

We introduce spherical coordinates r, θ such that $\rho = r\sin\theta$ and $z = r\cos\theta$ and assume that $kr^2\sin^2\theta \gg 1$. The integral in (5.169) can then be estimated by the method of steepest descent. According to (5.58) the result is

$$E_\theta(r,\theta,\phi) = \sqrt{\frac{\mu_o}{\epsilon_o}}\, H_\phi = -\frac{E_z}{\sin\theta}$$

$$\sim \frac{(-i)^n}{\pi\sin\theta\, H_n^{(1)}(ka\sin\theta)}\left[E_{nm}Q_E(k\cos\theta)\cos n\phi - H_{nm}Q_H(k\cos\theta)\sin n\phi\right]\frac{e^{ikr}}{r},$$

(5.190)

$$E_\phi(r,\theta,\phi) = -\sqrt{\frac{\mu_o}{\epsilon_o}}\, H_\theta = \sqrt{\frac{\mu_o}{\epsilon_o}}\,\frac{H_z}{\sin\theta}$$

$$\sim \frac{(-i)^n}{\pi(ka\sin\theta)^2 H_n^{(1)'}(ka\sin\theta)}\left[H_{nm}P_H(k\cos\theta)\cos n\phi + E_{nm}P_E(k\cos\theta)\sin n\phi\right]\frac{e^{ikr}}{r}.$$

Equation (5.190) is still valid in the negative z-direction ($\theta = \pi$) in spite of the fact that the condition $kr\sin^2\theta \gg 1$ is not satisfied. It is readily checked that the far field of order $1/r$ in that direction vanishes except when $n = 1$ in which case the result is

$$E_x(0,0,z) = -\sqrt{\frac{\mu_o}{\epsilon_o}}\, H_y \sim -E_{1m}\, \frac{k^2 a^3 L_1(\alpha_{1m})\, L_1(k)}{2j_{1m}\left[4k^2a^2M_1^2(k) - L_1^2(k)\right]}\, \frac{e^{ik|z|}}{|z|}$$

$$H_x(0,0,z) = \sqrt{\frac{\epsilon_o}{\mu_o}}\, E_y \sim -H_{1m}\, \frac{k^3 a^3 M_1(\alpha'_{1m}) M_1(k)}{(k-\alpha'_{1m})\left[4k^2a^2M_1^2(k) - L_1^2(k)\right]}\, \frac{e^{ik|z|}}{|z|} \qquad (5.191)$$

$$z \to -\infty \ .$$

When z tends to infinity along the outer surface of the tube ($\rho = a+0$) the integral in (5.169) can be estimated by deforming the path of integration into a U-shaped contour around a branch cut from k to $k+i\infty$. The asymptotic behavior of the nonvanishing components of fields representing surface charge and current so obtained are, for $n=0$,

$$E_\rho(a+0,z) = \sqrt{\frac{\mu_o}{\epsilon_o}}\, H_\phi \sim E_{om}\, \frac{ika\, L_o(\alpha_{om}) L_o(k)}{j_{om}\left(\ln\frac{2z}{\gamma_1 ka^2} + i\frac{\pi}{2}\right)}\, e^{ikz}$$

$$H_z(a+0,z) \sim -H_{nm}\, \frac{ka^2 L_1(\alpha'_{om}) L_1(k)}{2(k+\alpha'_{om})}\, \frac{e^{ikz}}{z^2} \qquad (5.192)$$

as $z \to \infty$, where $\ln\gamma_1 = 0.5772156649\ldots$ is Euler's constant. For $n \geqslant 1$ we have

$$E_p(a+0,\phi,z) = \sqrt{\frac{\mu_o}{\epsilon_o}}\, H_\phi \sim \frac{2^{2-n}(-i)^{n-1} a^{2n+1} k^{n+2} L_n(k) M_n(k)}{(n-1)!\left[4k^2a^2M_n^2(k) - n^2L_n^2(k)\right]}\, \frac{e^{ikz}}{z^n} \times$$

$$\times \left[E_{nm}\, \frac{2ka^2 M_n(k) L_n(\alpha_{nm})}{j_{nm}} \cos n\phi + \sqrt{\frac{\mu_o}{\epsilon_o}}\, H_{nm}\, \frac{n M_n(\alpha'_{nm}) L_n(k)}{k-\alpha'_{nm}} \sin n\phi \right] \qquad (5.193a)$$

$$H_z(a+0,\phi,z) \sim \frac{2^{2-n}(-i)^{n-1}a^{2n+2}k^{n+2}L_n(k)M_n(k)}{(n-1)!\left[4k^2a^2M_n^2(k)-n^2L_n^2(k)\right]}\frac{e^{ikz}}{z^{n+1}}\chi$$

$$\chi\left[H_{nm}\frac{nM_n(\alpha'_{nm})L_n(k)}{k-\alpha'_{nm}}\cos n\phi - \sqrt{\frac{\epsilon_o}{\mu_o}}E_{nm}\frac{2ka^2M_n(k)L_n(\alpha_{nm})}{j_{nm}}\sin n\phi\right] \tag{5.193b}$$

as $z\to\infty$.

By a well-known formula, the field outside the tube can be expressed as a surface integral of the field components over the opening and the outer cylindrical surface. In the Kirchhoff approximation the field over the opening is assumed to be that of an infinite waveguide and the field on the outer cylindrical surface to be zero. It is readily shown that the field obtained from this approximation (in Kottler's formulation, cf. Stratton (1941), p. 468) is identical with the field calculated from a surface current in the wall of the semi-infinite tube equal to that of an infinite waveguide. Thus, the field of the Kirchhoff approximation is what we called the "incident field" in our formulation of the problem as a scattering problem. The components of this field are obtained from (5.169), (5.170) and Table VII if we put $P_E^K(\alpha)=0$ and define $P_H^K(\alpha)$, $Q_E^K(\alpha)$ and $Q_H^K(\alpha)$ such that

$$\begin{aligned} H_{nm}P_H^K(\alpha) &= \epsilon_n e_n^i(\alpha) \\ H_{nm}Q_H^K(\alpha) - iE_{nm}Q_E^K(\alpha) &= \epsilon_n \mathcal{E}_{zn}^i(a,\alpha) \end{aligned} \tag{5.194}$$

where $e_n^i(\alpha)$ and $\mathcal{E}_{zn}^i(a,\alpha)$ are given by (5.167). Thus the far field according to (5.190) is

$$E_\theta^K(r,\theta,\phi) \sim \frac{(-i)^{n-1} J_n(ka\sin\theta)}{2\sin\theta}\left[E_{nm}\frac{a^2k^2\sin^2\theta}{j_{nm}(k\cos\theta+\alpha_{nm})}\cos n\phi + \right.$$

$$\left. + \sqrt{\frac{\mu_o}{\epsilon_o}} H_{nm} n \frac{a^2 k\alpha'_{nm}\sin^2\theta + j'^2_{nm}\cos\theta}{j'^2_{nm}(k\cos\theta+\alpha'_{nm})}\sin n\phi\right]\frac{e^{ikr}}{r} \quad ,$$

(5.195)

$$E_\phi^K(r,\theta,\phi) \sim \sqrt{\frac{\mu_o}{\epsilon_o}}\frac{(-i)^{n-1} ka J'_n(ka\sin\theta)}{2(k\cos\theta+\alpha'_{nm})} H_{nm}\cos n\phi\frac{e^{ikr}}{r} \quad .$$

Comparing (5.195) with the exact expression in (5.190) we find

$$E_\theta(r,\theta_{nm},\phi) \sim E_\theta^K(r,\theta_{nm},\phi) \sim \frac{(i)^{n-1}a^3 k\alpha_{nm} J'_n(j_{nm})}{2j_{nm}} E_{nm}\cos n\phi\frac{e^{ikr}}{r}$$

(5.196)

$$E_\phi(r,\theta'_{nm},\phi) \sim E_\phi^K(r,\theta'_{nm},\phi) \sim \sqrt{\frac{\mu_o}{\epsilon_o}}\frac{(-i)^{n+1}a^3 k\alpha'_{nm}(j^2_{nm}-n^2)J_n(j'_{nm})}{2j^3_{nm}} \times$$

$$\times H_{nm}\cos n\phi\frac{e^{ikr}}{r}$$

where θ_{nm} and θ'_{nm} are defined by

$$k\cos\theta_{nm} = -\alpha_{nm}$$

$$k\cos\theta'_{nm} = -\alpha'_{nm} \qquad (5.197)$$

The power radiated into a unit solid angle about the direction (θ,ϕ) is

$$p(\theta,\phi) = \frac{1}{2}\sqrt{\frac{\epsilon_o}{\mu_o}}\left(|E_\theta|^2 + |E_\phi|^2\right)r^2 \; . \qquad (5.198)$$

We call this quantity divided by the power of the incident E_{nm} or H_{nm} mode the power pattern $f^{E}_{nm}(\theta,\phi)$ and $f^{H}_{nm}(\theta,\phi)$ respectively. Thus, using (5.185) and (5.190) we get

$$f^{E}_{nm}(\theta,\phi) = \frac{\epsilon_n j^2_{nm}}{\pi^3 a^4 k\alpha_{nm}}\left(\left|\frac{Q_E(k\cos\theta)}{\sin\theta H^{(1)}_n(ka\sin\theta)}\right|^2 \cos^2 n\phi + \left|\frac{P_E(k\cos\theta)}{(ka\sin\theta)^2 H^{(1)'}_n(ka\sin\theta)}\right|^2 \sin^2 n\phi\right), \tag{5.199}$$

$$f^{H}_{nm}(\theta,\phi) = \frac{\epsilon_o}{\mu_o}\frac{\epsilon_n j'^4_{nm}}{\pi^3 a^4 k\alpha'_{nm}(j'^2_{nm}-n^2)}\left(\left|\frac{Q_H(k\cos\theta)}{\sin\theta H^{(1)}_n(ka\sin\theta)}\right|^2 \sin^2 n\phi + \left|\frac{P_H(k\cos\theta)}{(ka\sin\theta)^2 H^{(1)'}_n(ka\sin\theta)}\right|^2 \cos^2 n\phi\right).$$

From (5.196) we see that

$$f^{E}_{nm}(\theta_{nm},0) = f^{EK}_{nm}(\theta_{nm},0) = \frac{\epsilon_n ka}{4\pi} J'^2_n(j_{nm})\sqrt{k^2a^2 - j^2_{nm}} \tag{5.200}$$

$$f^{H}_{nm}(\theta'_{nm},0) = f^{HK}_{nm}(\theta'_{nm},0) = \frac{\epsilon_n ka}{4\pi}\frac{j'^2_{nm}-n^2}{j'^2_{nm}} J^2_n(j'_{nm})\sqrt{k^2a^2 - j'^2_{nm}}$$

where as before $\epsilon_o = 1$, $\epsilon_1 = \epsilon_2 = \ldots = 2$. Thus for E_{nm} modes the Kirchhoff approximation gives the correct value of the radiated power in the direction $(\theta_{nm}, 0)$ where θ_{nm}, $\pi/2 < \theta_{nm} < \pi$, is given by (5.197). If another mode $E_{n\ell}$ can propagate undamped in the waveguide the power pattern vanishes in the direction $(\theta_{n\ell}, 0)$ which also is correctly given by the Kirchhoff approximation. The same is true for H_{nm} modes in the directions $(\theta'_{nm}, 0)$ and $(\theta'_{n\ell}, 0)$ respectively.

The relation between $f_{nm}(\theta, \phi)$ and the power gain function, i.e. the radiated power related to an isotropically radiating source, is

$$G_{nm}(\theta, \phi) = \frac{p(\theta, \phi)}{P_{rad}/4\pi} = 4\pi \frac{f_{nm}(\theta, \phi)}{1 - r_m^n} , \tag{5.201}$$

where r_m^n is the total power reflection coefficient given by (5.189). The fraction of the incident power which is radiated into the space outside the tube for H_{o1} mode is $1 - r_1^{oH} = p - \left|R_{11}^{oH}\right|^2$ when $j'_{o1} < ka < j'_{o2}$. This quantity is shown in Fig. 5-21 as a function of ka/j'_{o1} compared with the result obtained from the Kirchhoff approximation.

The power pattern for modes H_{o1}, E_{o1} and H_{11} are shown in Fig. 5-22, together with the results from the Kirchhoff approximation.

When $ka \gg 1$ we can use the function $U(s, g)$ of (5.238) to obtain an approximate expression of the far field. For example, inserting (5.257) and (5.261) into (5.190) yields, for H_{om} and E_{om} modes respectively

$$E_\phi(r, \theta) \quad \sqrt{\frac{\mu_o}{\epsilon_o}}\, H_{om}\, \frac{e^{ikr}}{r}\, \frac{\exp\left[U(s, q_H) + U(s'_{om}, q_H)\right]}{i4\pi(k\cos\theta + \alpha'_{om})} \times$$

$$\times \begin{cases} \dfrac{1}{H_1^{(1)}(ka\sin\theta)\sin\dfrac{\theta'_{om}}{2}\cos\dfrac{\theta}{2}} , & 0 < \theta < \pi/2 \\ \dfrac{2\pi ak J_1(ka\sin\theta)\sin\dfrac{\theta}{2}}{\sin\dfrac{\theta'_{om}}{2}} , & \pi/2 < \theta < \pi \end{cases} \tag{5.202}$$

where $s = \sqrt{2ka}\cos\theta$, $\quad s'_{om} = \sqrt{\dfrac{2a}{k}}\,\alpha'_{om}$, $\quad q_H = \left(ka - \dfrac{\pi}{4} + \dfrac{3}{8ka}\right)$;

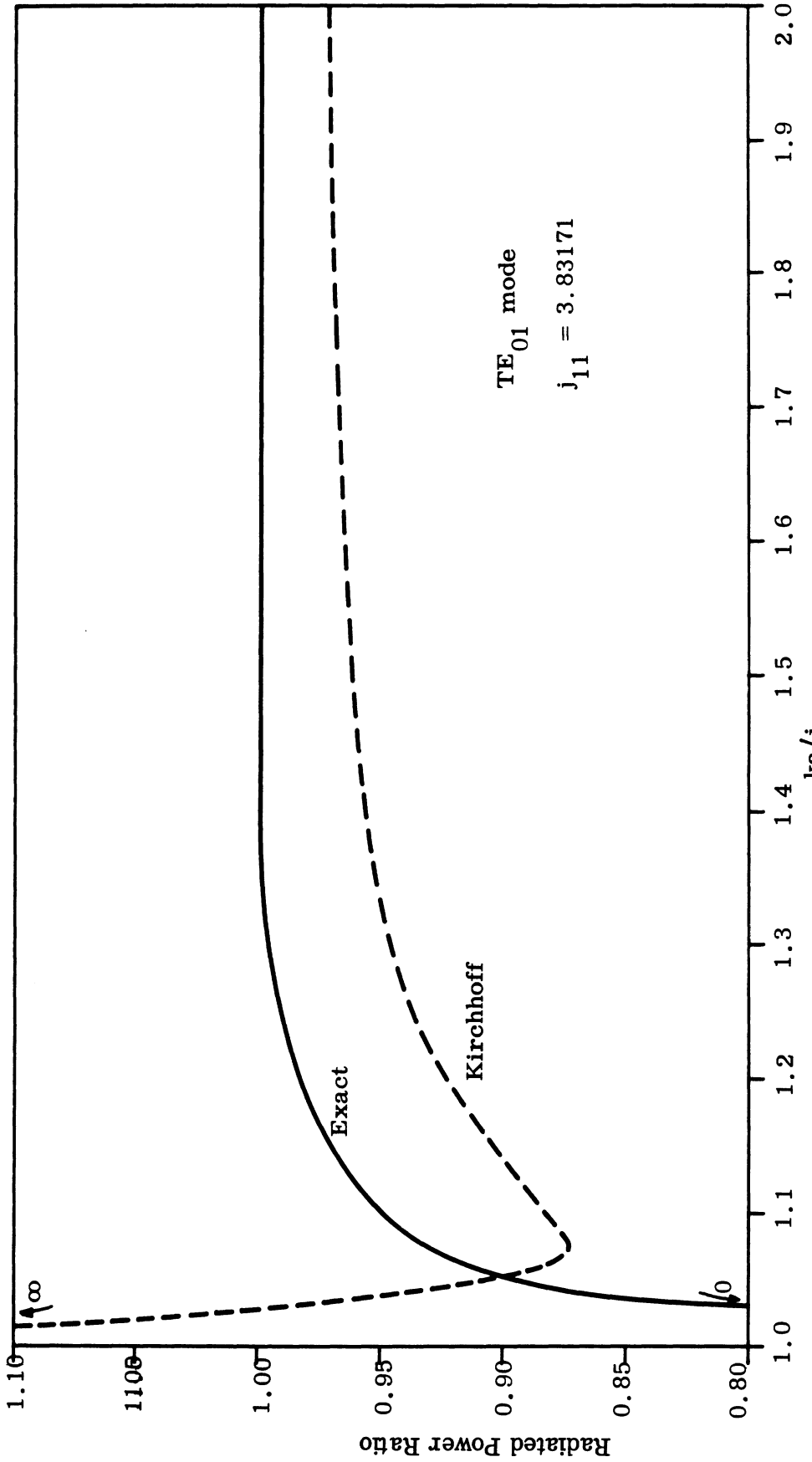

FIG. 5-21: RADIATED POWER FOR INCIDENT H_{01} MODE CARRYING 1 WATT OF POWER ($j_{11} = 3.83171\ldots$) (Wainstein, 1948c).

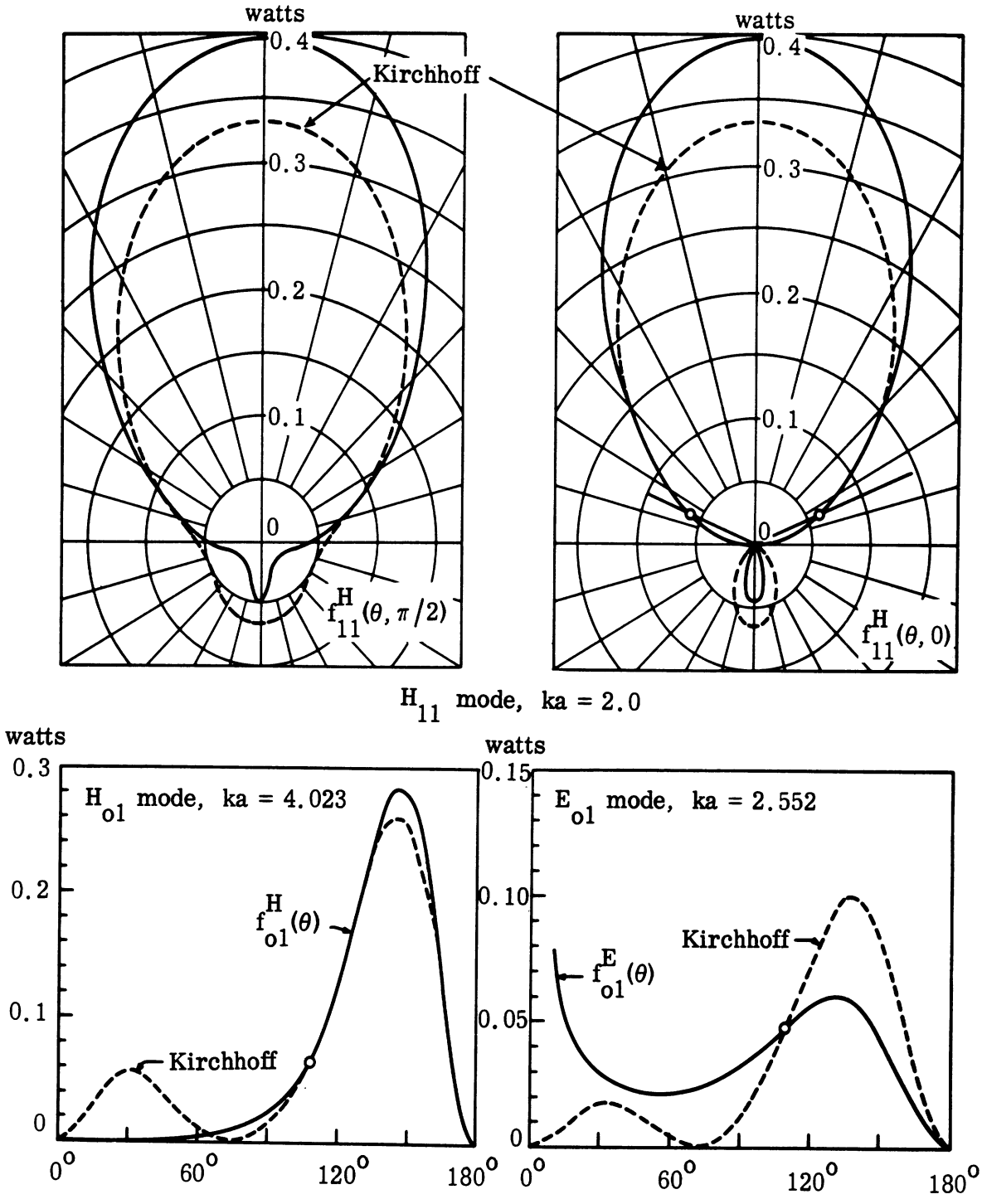

FIG. 5-22: RADIATED POWER PER UNIT SOLID ANGLE FOR INCIDENT MODES EACH CARRYING 1 WATT OF POWER (Wainstein, 1948c, 1950a).
(The solid curves for H_{11} mode are renormalized by using the fact that the Kirchhoff approximation gives the exact value at θ'_{11} (113.0^{o}). Consequently their absolute magnitude is rather uncertain.)

$$E_\theta(r,\theta) \sim E_{om} \frac{e^{ikr}}{r} \frac{iak \exp\left[U(s,q_E)+U(s_{om},q_E)\right]}{j_{om}(k\cos\theta+\alpha_{om})} \chi$$

$$\chi \begin{cases} \dfrac{\sin\dfrac{\theta_{om}}{2}}{2\pi H_o^{(1)}(ka\sin\theta)\sin\dfrac{\theta}{2}}, & 0<\theta<\pi/2 \\ ak J_o(ka\sin\theta)\sin\dfrac{\theta_{om}}{2}\cos\dfrac{\theta}{2}, & \pi/2<\theta<\pi \end{cases} \qquad (5.203)$$

where $s = \sqrt{2ka}\cos\theta$, $s_{om} = \sqrt{\frac{2a}{k}}\alpha_{om}$, $q_E = \left(ka+\frac{\pi}{4}-\frac{1}{8ka}\right)$,

and the angle θ_{om} and θ'_{om} are defined by (5.197). Wainstein (1948c) reports that for H_{o1} and E_{o1} modes and ka equal to that of Fig. 5-22 (higher than the cut-off frequency by 6 percent and 5 percent respectively), the difference between the exact power patterns and the approximate ones obtained from (5.202) and (5.203) does not exceed 2-3 percent. This indicates that for practical purposes the condition $ka \gg 1$ is fulfilled as soon as the incident mode is above cut-off. For general H_{nm} and E_{nm} modes, somewhat more complicated approximate expressions are obtainable in the same manner. As $j_{nm} > j'_{nm} > n$, when $n > 1$, those formulas should also be useful as soon as the incident mode is above cut-off. As pointed out in Section 5.6, the approximate expressions of $M_n(\alpha)$ and $L_n(\alpha)$ obtained by using the function U(s, g) have a small jump at $\alpha = 0$. Consequently the approximate radiation patterns display a small jump at $\theta = \pi/2$, the amount of which is a measure of the accuracy of the approximation.

When $ka\sin\theta \gg 1$ is satisfied along with the condition $ka \gg 1$, we can replace the Bessel and Hankel functions of (5.202) and (5.203) by their asymptotic forms. For an E_{om} mode with $0 < \theta < \pi/2$, the result is

$$E_\theta(r,\theta) \sim E_{om} \frac{i\sqrt{2}ak}{2\sqrt{\pi}\, j_{om}} \frac{\sin\frac{\theta_{om}}{2}\cos\frac{\theta}{2}}{\cos\theta - \cos\theta_{om}} \frac{\exp\left[i(kr - ka\sin\theta + \frac{\pi}{4}) + U(s_{om}, q_E)\right]}{\sqrt{kr}} F(r,\theta) \tag{5.204}$$

where

$$F(r,\theta) = \sqrt{\frac{a}{r\sin\theta}} \exp\left[U(s, q_E)\right]$$

The factor before the function $F(r,\theta)$ is the field of an incident plane wave propagating in the direction θ_{om} scattered by a half-plane tangent to the tube. If we express the incident waveguide mode as a superposition of plane waves repeatedly reflected at the wall of the tube, the direction of propagation of these plane waves is also given by θ_{om}. Thus the first factor of (5.204) can be interpreted as the geometrical optics contribution to the far field. The factor $\sqrt{\frac{a}{r\sin\theta}}$ "expands" the cylindrical half-plane waves into spherical waves as the distance from the edge increases.

When $\pi/2 < \theta < \pi$, substitution of the asymptotic form for J_o in (5.203) yields the expressions of (5.204) plus an identical wave originating from the opposite edge of the wall of the tube.

The function $U(s, q_E)$ tends to zero as $ka \to \infty$ for every fixed $\theta \neq \pi/2$. At $\theta = \pi/2$ it is discontinuous in such a manner that it compensates for the jump in the geometrical optics approximation. This also means that the term $U(s_{om}, q_E)$ is approximately zero for ka so large that the incident mode is not close to cut-off.

As in the scalar case the principle of reciprocity can be used to relate the results of this section to those obtained in Section 5.4 for the scattering of a plane electromagnetic wave. We assume that the plane wave is that of (5.133) (i.e., is propagating in the direction $(\theta_i, 0)$) and write the field inside the tube due to this wave as

$$H_z = \sum_{n=0}^{\infty}\sum_{m=1}^{\infty}(A_{nm}\cos n\phi + B_{nm}\sin n\phi)\,\frac{J_n(j'_{nm}\frac{\rho}{a})}{J_n(j'_{nm})}\,e^{i\alpha'_{nm}z}$$

$$E_z = \sum_{n=0}^{\infty}\sum_{m=1}^{\infty}(C_{nm}\cos n\phi + D_{nm}\sin n\phi)\,\frac{J_n(j_{nm}\frac{\rho}{a})}{J'_n(j_{nm})}\,e^{i\alpha_{nm}z} \qquad (5.205)$$

To an H_{mn} mode incident from $z=\infty$ given by (5.166) we relate the radiated far field

$$E_\theta \sim F^H_{nm}(\theta)\sin n\phi\,\frac{e^{ikr}}{r} \quad ,$$

$$E_\phi \sim G^H_{nm}(\theta)\cos n\phi\,\frac{e^{ikr}}{r} \quad .$$

In the same manner the far field pertinent to an E_{nm} mode (5.165) is taken as

$$E_\theta \sim F^E_{nm}(\theta)\cos n\phi\,\frac{e^{ikr}}{r} \quad ,$$

$$E_\phi \sim G^E_{nm}(\theta)\sin n\phi\,\frac{e^{ikr}}{r} \quad .$$

We then have

$$A_{nm}H_{nm} = (-1)^n\,\frac{\epsilon_o}{\mu_o}\,\frac{i2\epsilon_n j'^4_{nm}}{k^2a^4\alpha'_{nm}(j'^2_{nm}-n^2)}\,G^H_{nm}(\pi-\theta_i)\sin\beta$$

$$B_{nm}H_{nm} = (-1)^{n+1}\,\frac{\epsilon_o}{\mu_o}\,\frac{4i\,j'^4_{nm}}{k^2a^4\alpha'_{nm}(j'^2_{nm}-n^2)}\,F^H_{nm}(\pi-\theta_i)\cos\beta$$

$$C_{nm}E_{nm} = (-1)^{n+1}\,\frac{i2\epsilon_n j^2_{nm}}{k^2a^4\alpha_{nm}}\,F^E_{nm}(\pi-\theta_i)\cos\beta$$

$$D_{nm}E_{nm} = (-1)^n \frac{i4j_{nm}^2}{k^2a^2\alpha_{nm}} G_{nm}^E(\pi-\theta_i)\sin\beta \qquad (5.206)$$

where $\epsilon_o = 1$, $\epsilon_1 = \epsilon_2 = \ldots = 2$. It is readily checked that equations (5.206) conform to equations (5.145), (5.146) and (5.190). From (5.206) the absorption cross section, defined as the ratio of the power transmitted into the tube to the power incident per unit area, can be related to the power patterns of the modes above cut-off. Thus, for $j'_{11} < ka < j_{01}$ ($j'_{11} = 1.841$, $j_{01} = 2.405$) where only the H_{11} mode is above cut-off, we have

$$\sigma_a(\theta_i) = \lambda^2\left(\frac{ka}{j'_{11}}\right)^4\left[f_{11}^H(\pi-\theta_i, 0)\sin^2\beta + f_{11}^H(\pi-\theta_i, \pi/2)\cos^2\beta\right] \qquad (5.207)$$

where $\lambda = 2\pi/k$ is the free-space wavelength. The absorption cross section for $ka = 2$ can consequently be constructed from Fig. 5-22.

5.6 The Wiener-Hopf Factorization

5.6.1 Explicit Expressions

The fundamental step in the Wiener-Hopf technique is to find the split functions $L_n(\alpha)$ and $M_n(\alpha)$ analytic in the upper half-plane and such that

$$L_n(\alpha)L_n(-\alpha) = \pi i J_n(a\kappa)H_n^{(1)}(a\kappa) \qquad (5.208 = 5.33)$$

$$M_n(\alpha)M_n(-\alpha) = \kappa i J'_n(a\kappa)H_n^{(1)'}(a\kappa) \qquad (5.209 = 5.34)$$

where $\kappa = \sqrt{k^2 - \alpha^2}$ and where $L_n(\alpha)$ and $M_n(\alpha)$ behave as $O(1/\sqrt{\alpha})$ as $|\alpha| \to \infty$. (See Wiener and Hopf, 1931; and Paley and Wiener, 1934.) These conditions determine the split functions completely except for a factor ± 1 but all physical quantities are independent of the choice of this sign. As we have defined $L_{-n}(\alpha) \equiv L_n(\alpha)$, $M_{-n}(\alpha) \equiv M_n(\alpha)$ and $M_o(\alpha) \equiv L_1(\alpha)$, it is only necessary to determine $L_n(\alpha)$ for

$n \geqslant 0$ and $M_n(\alpha)$ for $n \geqslant 1$. In the following we will give formulas only for $L_n(\alpha)$ in those cases where the corresponding expression for $M_n(\alpha)$ is obtained by just replacing the Bessel functions by their derivatives.

An explicit expression for the function $\log L_n(\alpha)$ is obtained by applying (5.8) to $\log\left[\pi i J_n(a\kappa)H_n^{(1)}(a\kappa)\right]$. Thus,

$$L_n(\alpha) = \exp\left\{\frac{1}{2\pi i} P \int_{-\infty}^{\infty} \frac{\log\left[\pi i J_n\left(a\sqrt{k^2-\gamma^2}\right)H_n^{(1)}\left(a\sqrt{k^2-\gamma^2}\right)\right]}{\gamma-\alpha} d\gamma\right\} \tag{5.210}$$

where the path of integration passes below the pole $\gamma = \alpha$ and where P designates the Cauchy principal value as $|\gamma| \to \infty$. Wainstein (1948c; 1949; 1950a, b) factorizes the functions $\pi\kappa J_n(a\kappa)H_n^{(1)}(a\kappa)$ in which case the integral corresponding to (5.210) exists in the ordinary sense. The split function, analytic in the upper half-plane, is then instead $\sqrt{-ia(k+\alpha)}\,L_n(\alpha)$. Multiplying both numerator and denominator of the integrand of (5.210) by $\gamma+\alpha$ and observing that the logarithm is an even function of γ we get

$$L_n(\alpha) = \exp\left\{\frac{\alpha}{2\pi i} \int_{\Lambda_1} \frac{\log\left[\pi i J_n\left(a\sqrt{k^2-\gamma^2}\right)H_n^{(1)}\left(a\sqrt{k^2-\gamma^2}\right)\right]}{\gamma^2-\alpha^2} d\gamma\right\} \tag{5.211}$$

where the path of integration is indicated in Fig. 5-23a for the case when α is real and $|\alpha| < k$. To determine the field quantities everywhere, it is sufficient to know $L_n(\alpha)$ and $M_n(\alpha)$ for positive real values of α such that $0 < \alpha \leqslant k$ and for all positive imaginary values. $L_n(\alpha)$ and $M_n(\alpha)$ are continuous and different from zero at those points.

The integrand in (5.211) is an even function of γ and we can therefore integrate only over the interval $(0, \infty)$. Change of the variable of integration to v defined by $v = a\sqrt{k^2-\gamma^2}$ for $0 \leqslant \gamma < k$ and $v = a\sqrt{\gamma^2-k^2}$ for $k < \gamma$ yields

$$L_n(\alpha) = \sqrt{\pi i J_n(a\kappa)H_n^{(1)}(a\kappa)} \times$$

$$\times \exp\left\{-\frac{\alpha a}{\pi}\left[P\int_0^{ka} \frac{v\left[\frac{\pi}{2}+\arctan\frac{Y_n(v)}{J_n(v)}-i\log\left(\pi\left|J_n(v)H_n^{(1)}(v)\right|\right)\right]}{(v^2-a^2\kappa^2)\sqrt{a^2k^2-v^2}}\,dv + \right.\right.$$

$$\left.\left. + i\int_0^{\infty} \frac{v\log\left[2I_n(v)K_n(v)\right]}{(a^2\kappa^2+v^2)\sqrt{a^2k^2+v^2}}\,dv\right]\right\} \quad (5.212)$$

$$M_n(\alpha) = \sqrt{\pi i J_n'(a\kappa)H_n^{(1)'}(a\kappa)} \times$$

$$\times \exp\left\{-\frac{\alpha a}{\pi}\,P\int_0^{ka} \frac{v\left[\frac{\pi}{2}+\arctan\frac{Y_n'(v)}{J_n'(v)}-i\log\left(\pi\left|J_n'(v)H_n^{(1)'}(v)\right|\right)\right]}{(v^2-a^2\kappa^2)\sqrt{a^2k^2-v^2}}\,dv + \right.$$

$$\left. + i\int_0^{\infty} \frac{v\log\left[-2I_n'(v)K_n'(v)\right]}{(a^2\kappa^2+v^2)\sqrt{a^2k^2+v^2}}\,dv\right]\right\} \quad (5.213)$$

where $-\pi/2 < \arctan\phi \leqslant \pi/2$ and $I_n(v) = i^{-n}J_n(iz)$, $K_n(v) = \frac{\pi i^{n+1}}{2}H_n^{(1)}(iz)$ are modified Bessel functions.

These expressions are valid if α is real and $-k < \alpha < k$. However, $L_n(\alpha_{n\ell})$ and $M_n(\alpha'_{n\ell})$ take the form $0\cdot\infty$ for real $\alpha_{n\ell}$ and $\alpha'_{n\ell}$ respectively, where as before

$$J_n(j_{nm}) = 0 \qquad J_n'(j'_{nm}) = 0\,, \qquad 0 = j_{no} < j_{n1} < \ldots, \quad 0 = j'_{no} < j'_{n1} < \ldots$$

(we define $j_{oo} = j'_{1o} = 0$ although they are not zeros of J_o and J_1') and

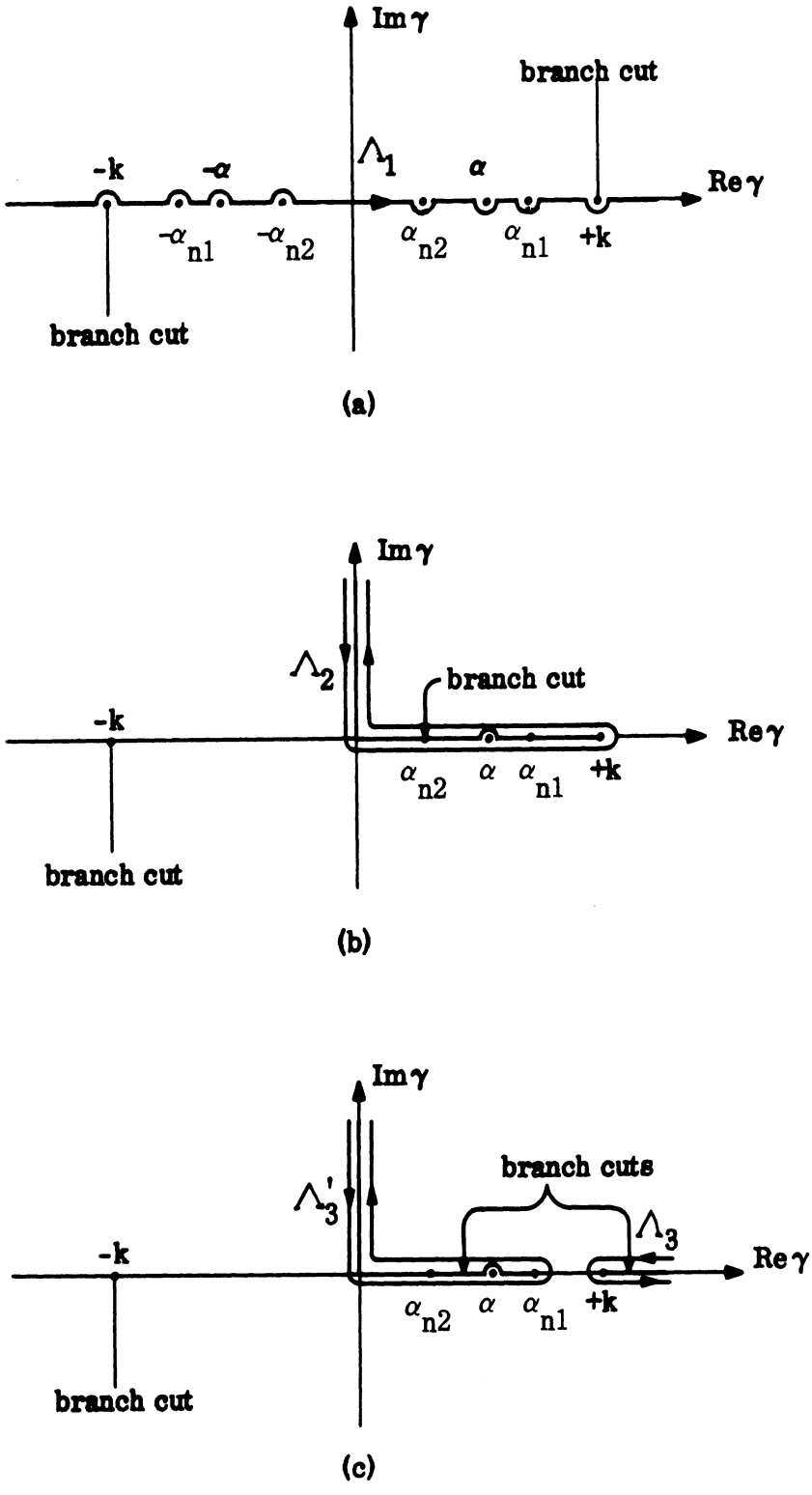

FIG. 5-23: PATHS OF INTEGRATION FOR THE SPLIT FUNCTIONS

$$\alpha_{nm} = \sqrt{k^2 - \frac{j_{nm}^2}{a^2}}, \qquad \alpha'_{nm} = \sqrt{k^2 - \frac{j'^2_{nm}}{a^2}}$$

are real and positive real or imaginary. Equations (5.202) and (5.213) are also valid for an arbitrary positive imaginary value of α if the square root factor is substituted by 1. In that case the use of principal value is no longer necessary. $L_1(k)$ can also be obtained from (5.212) by putting $\kappa = 0$. Thus

$$L_1(k) = \exp\left\{-\frac{ka}{\pi}\left[\int_0^{ka} \frac{\frac{\pi}{2} + \arctan\frac{Y_1(v)}{J_1(v)} - i\log\left(\pi\left|J_1(v)H_1^{(1)}(v)\right|\right)}{v\sqrt{a^2k^2 - v^2}}\,dv\right.\right.$$
$$\left.\left. + i\int_0^{\infty} \frac{\log\left[2I_1(v)K_1(v)\right]}{v\sqrt{a^2k^2 + v^2}}\,dv\right]\right\}. \qquad (5.214)$$

A different expression for $L_n(\alpha)$ and $M_n(\alpha)$ is obtained if the contour of integration is deformed according to Fig. 5-23b. This scheme has been employed by Wainstein (1948c; 1949; 1950a, b) and what follows is a generalization of his work. We write

$$L_n(\alpha) = \sqrt{\pi i J_n(a\kappa)H_n^{(1)}(a\kappa)\prod_{m=1}^{m_o}\frac{\alpha_{nm}+\alpha}{\alpha_{nm}-\alpha}}\; e^{\frac{\alpha a}{2}} P_n(\alpha) \qquad (5.215)$$

$$M_n(\alpha) = \sqrt{\pi i J'_n(a\kappa)H_n^{(1)'}(a\kappa)\prod_{m=1}^{m'_o}\frac{\alpha'_{nm}+\alpha}{\alpha'_{nm}-\alpha}}\; e^{\frac{\alpha a}{2}} S_n(\alpha) \qquad (5.216)$$

where m_o and m'_o are the smallest non-negative integers such that $j_{n(m_o+1)} > \kappa a$, $j_{n(m_o+1)} > ka$ and $j'_{n(m'_o+1)} > \kappa a$, $j'_{n(m'_o+1)} > ka$. If $m_o = 0$, i.e. $j_{n1} > ka$ or $j'_{n1} > ka$, the product should be disregarded.

If we combine the integrals along both sides of the branch cut in Fig. 5-23b, observing that the small indention around $\gamma = k$ gives no contribution if $\alpha \neq k$, we get

$$P_n(\alpha) = \frac{2}{\pi a}(P)\int_0^k \frac{\frac{\pi}{2} + \arctan \frac{Y_n\left(a\sqrt{k^2-\gamma^2}\right)}{J_n\left(a\sqrt{k^2-\gamma^2}\right)}}{\gamma^2 - \alpha^2} d\gamma -$$

$$- \frac{2}{\pi a}(P)\int_0^{i\infty} \frac{\frac{\pi}{2} + \arctan \frac{Y_n\left(a\sqrt{k^2-\gamma^2}\right)}{J_n\left(a\sqrt{k^2-\gamma^2}\right)}}{\gamma^2 - \alpha^2} d\gamma - \frac{i}{\alpha a}\left(\frac{\pi}{2} + \arctan \frac{Y_n(a\kappa)}{J_n(a\kappa)}\right) -$$

$$- \frac{1}{\alpha a}\sum_{m=1}^{m_o} \log \frac{\alpha_{nm} + \alpha}{\alpha_{nm} - \alpha} \quad . \tag{5.217}$$

The functions

$$\frac{\pi}{2} + \arctan \frac{Y_n(x)}{J_n(x)} \qquad \text{and} \qquad \frac{\pi}{2} + \arctan \frac{Y_n'(x)}{J_n'(x)}$$

are discontinuous and jump by π at the zeros of $J_n(x)$ and $J_n'(x)$ respectively. We introduce instead the continuous functions

$$\Omega_n(x) = \frac{\pi}{2} + \arg H_n^{(1)}(x) = \arctan \frac{Y_n(x)}{J_n(x)} + \frac{\pi}{2} + m\pi \tag{5.218}$$

$$\text{if } j_{nm} < x < j_{n(m+1)}$$

$$\Omega_n'(x) = \frac{\pi}{2} + \arg H_n^{(1)'}(x) = \arctan \frac{Y_n'(x)}{J_n'(x)} + \frac{\pi}{2} + m\pi \tag{5.219}$$

$$\text{if } j'_{nm} < x < j'_{n(m+1)}$$

Thus, we have

$$\Omega_n(j_{n\ell}) = \ell\pi \ , \qquad \ell \geqslant 0, \ n \geqslant 0$$

$$\Omega_n'(0) = \pi \ , \qquad \Omega_n'(j'_{n\ell}) = \ell\pi \ , \qquad \ell \geqslant 1, \ n \geqslant 1$$

Insertion of $\Omega_n(x)$ into (5.217) gives a divergent integral which is compensated by a similarly divergent series. By subtracting the divergent part from both the integral and the series, the result can be written as

$$\mathrm{Re}\, P_n(\alpha) = \frac{2}{\pi}\int_0^{ka} \frac{v\Omega_n(v) - a\kappa\Omega_n(a\kappa)}{(a^2\kappa^2 - v^2)\sqrt{a^2k^2 - v^2}}\, dv \ , \tag{5.220}$$

$$\mathrm{Im}\, P_n(\alpha) = -\frac{\Omega_n(a\kappa)}{\alpha a} + \frac{2}{\pi}\left\{1 + \log\frac{2\pi}{ka} - \sum_{m=m_o+1}^{\infty}\left(\frac{\pi}{\alpha a}\arctan\frac{\alpha a}{\sqrt{j_{nm}^2 - a^2k^2}} - \frac{1}{m}\right) + \right.$$

$$\left. + \psi(m_o+1) + \int_{ka}^{\infty}\frac{v\left[\Omega_n(v) - v\right]}{(v^2 - a^2\kappa^2)\sqrt{v^2 - a^2k^2}}dv + \frac{\kappa}{\alpha}\arccos\frac{\alpha}{k}\right\} \tag{5.221}$$

for α real, $0 < \alpha < k$. Here m_o is zero or an integer such that $j_{nm_o} < ka < j_{n(m_o+1)}$ and $\psi(m_o+1) = 1 + \frac{1}{2} + \frac{1}{3} + \ldots + \frac{1}{m_o} - \gamma$, $(\gamma = 0.577216\ldots)$ is the logarithmic derivative of the gamma function.

When α is positive imaginary, the expressions take the form

$$\mathrm{Re}\, P_n(i\eta) = \frac{2}{\pi}\int_0^{ka}\frac{v\Omega_n(v)}{(a^2\kappa^2 - v^2)\sqrt{a^2k^2 - v^2}}\, dv - \frac{\Omega_n(a\kappa)}{\eta a} \tag{5.222}$$

$$\operatorname{Im} P_n(i\eta) = \frac{2}{\pi}\left\{1+\log\frac{2\pi}{ka} - \left[\Omega_n(a\kappa)-a\kappa\right]\log\frac{\kappa+\eta}{k} + \psi(m_o+1) - \right.$$

$$- \sum_{m=m_o+1}^{\infty}\left(\frac{\pi}{2\eta a}\log\frac{\sqrt{j_{nm}^2 - a^2k^2}+\eta}{\sqrt{j_{nm}^2 - a^2k^2}-\eta} - \frac{1}{m}\right) +$$

$$\left. + \int_{ka}^{\infty} \frac{v\left[\Omega_n(v)-v\right] - a\kappa\left[\Omega_n(a\kappa)-a\kappa\right]}{(v^2-a^2\kappa^2)\sqrt{v^2-a^2k^2}}\,dv + \frac{\kappa}{\eta}\log\left(\frac{\kappa-\eta}{2k^2a}\right)\right\} \qquad (5.223)$$

for $0<\eta<\infty$. Here m_o iz zero or an integer such that $j_{nm_o} < \kappa a < j_{n(m_o+1)}$, where as before $\kappa a = a\sqrt{k^2+\eta^2}$.

In the same manner, the expressions for $\operatorname{Re} S_n(\alpha)$ and $\operatorname{Im} S_n(\alpha)$ are obtained from (5.220) and (5.223) by substitution of $\Omega_n'(x)$ and j_{nm}' for $\Omega_n(x)$ and j_{nm} respectively*.

When $\alpha \to k$ the integral in (5.220) defining $\operatorname{Re} P_o(\alpha)$ and $\operatorname{Re} S_n(\alpha)$, $n>1$, diverges, but this is compensated by a contribution from the indentation around $\gamma = k$ in Fig. 5.23b. Thus, we have

$$L_o(k) = \sqrt{\prod_{m=1}^{m_o}\frac{\alpha_{om}+k}{\alpha_{om}-k}}\,\exp\left\{-\int_0^b\left(\frac{\frac{ka}{\pi}\Omega_o(v)}{v\sqrt{a^2k^2-v^2}} + \frac{1}{2v\log v}\right)dv - \right.$$

$$\left. - \frac{ka}{\pi}\int_b^{ka}\frac{\Omega_o(v)}{v\sqrt{a^2k^2-v^2}}\,dv + \frac{1}{2}\log\left(2\log\frac{1}{b}\right) + i\frac{ka}{2}\operatorname{Im} P_o(k)\right\} \qquad (5.224)$$

* Wainstein (1949) indicates that $\Omega_n'(x)$ should be defined as $\Omega_n'(x) = \arg H_n^{(1)'}(x) - \frac{\pi}{2}$, which seems to be incorrect.

where $b < 1$ if $ka \geqslant 1$ and $b = ka$ if $ka < 1$,

$$L_n(k) = \sqrt{\frac{1}{n} \prod_{m=1}^{m_o} \frac{\alpha_{nm} + k}{\alpha_{nm} - k}} \exp\left\{\frac{ka}{2} P_n(k)\right\} \qquad n \geqslant 1 \qquad (5.225)$$

$$M_n(k) = \frac{1}{ak} \sqrt{n \prod_{m=1}^{m_o} \frac{\alpha'_{nm} + k}{\alpha'_{nm} - k}} \exp\left\{-\frac{ka}{\pi} \int_0^{ka} \frac{\Omega'_n(v) - \pi}{v\sqrt{a^2k^2 - v^2}}\, dv + \frac{i}{2}\left[ka \operatorname{Im} S_n(k) + \pi\right]\right\}$$

$$n \geqslant 1 \qquad (5.226)$$

As before, m_o or m'_o is an integer or zero such that $j_{nm_o} < ka < j_{n(m_o+1)}$ and $j'_{nm'_o} < ka < j'_{n(m'_o+1)}$ respectively, and the product should be put equal to 1 if $m_o = 0$ or $m'_o = 0$.

5.6.2 Low Frequency Approximations

A low frequency expansion of $L_n(\alpha)$ and $M_n(\alpha)$ can be obtained from (5.220) through (5.226) by using the power series expansions of J_n and Y_n or J'_n and Y'_n respectively. Since $\Omega_o(v)$ behaves as

$$\frac{-\pi}{2(\gamma + \log\frac{v}{2})}$$

when $v \to 0$, the expansion for $L_o(\alpha)$ contains a series of inverse powers of $\log(ka)$ and consequently it can be expected to give accurate results only when $\log ka \gg 1$. The expression for $L_o(\alpha)$ is

$$L_o(\alpha) \approx L_o(k)\left\{1 - A^{-1}\log(1-\xi) + A^{-2}\mathcal{L}_2(\xi) - \right.$$

$$\left. - A^{-3}\left[\frac{\pi^2}{3}\log(1-\xi) - \int_0^{\xi} \frac{2-3u}{u(1-u)}\,\mathcal{L}_2(u)\,du\right]\right\} \qquad (5.227)$$

where

$$A = -2\log ak - 2\gamma + i\pi \ , \quad \xi = \frac{k-\alpha}{2k} \ , \quad \gamma = 0.577216\ldots \text{(Euler's constant)}$$

$$\mathcal{L}_2(x) = -\int_0^x \frac{\log(1-t)}{t}\,dt \quad \text{(the Dilogarithm)} \tag{5.228}$$

and

$$L_o(k) \approx \sqrt{A}\left(1 - \frac{\pi^2}{12}A^{-2} - 2\zeta(3)A^{-3}\right) \tag{5.229}$$

$$\zeta(3) = \sum_{n=1}^{\infty}\frac{1}{n^3} = 1.2020569\ldots \tag{5.230}$$

Equations (5.227) and (5.229) are given by Hallen (1961) in connection with his treatment of cylindrical antennas. We also give only the results for $L_1(\alpha)$ and $M_1(\alpha)$ which are the ones most easily obtained.

$$\mathrm{Re}\,P_1(\alpha) \approx -\frac{a(k^2-\alpha^2)}{4\alpha}\log\frac{k+\alpha}{k-\alpha} - \frac{ka}{2} \quad \text{for } \alpha \text{ real, } 0<\alpha<k \tag{5.231}$$

$$\mathrm{Re}\,P_1(i\eta) \approx \frac{a(k^2+\eta^2)}{2\eta}\arctan\frac{k}{\eta} - \frac{ka}{2} \quad \text{for } 0<\eta<\infty$$

$$\mathrm{Re}\,S_1(\alpha) \approx \frac{a^2(k^2-\alpha^2)-4}{4a\alpha}\log\frac{k+\alpha}{k-\alpha} + \frac{ka}{2} \quad \text{for } \alpha \text{ real, } 0<\alpha<k \tag{5.232}$$

$$\mathrm{Re}\,S_1(i\eta) \approx -\frac{a^2(k^2+\eta^2)-4}{2a\eta}\arctan\frac{k}{\eta} + \frac{ka}{2} \quad \text{for } 0<\eta<\infty$$

$$\left|L_1(k)\right| \approx \exp\left\{-\frac{a^2k^2}{4}\left[1+\frac{a^2k^2}{3}\left(\gamma - \frac{19}{12} + \log ka\right)\right]\right\} \tag{5.233}$$

$$|M_1(k)| \approx \exp\left\{\frac{a^2k^2}{4}\left[1-\frac{a^2k^2}{3}\left(\gamma+\frac{5}{12}+\log ka\right)\right]\right\} \tag{5.234}$$

The expression for $|L_1(k)|$ is given by Levine and Schwinger (1948) and they report that it gives values in excess of the correct value by less than 3 percent if $ka < 1$.

5.6.3 High Frequency Approximations

A high frequency expansion of $\operatorname{Im} P_n(\alpha)$ and $\operatorname{Im} S_n(\alpha)$ is obtained by employing instead the asymptotic series

$$\Omega_n(v) \underset{v\to\infty}{\sim} v-\left(\frac{n}{2}-\frac{1}{4}\right)\pi+\frac{\mu-1}{2(4v)}+\frac{(\mu-1)(\mu-25)}{6(4v)^3}+\frac{(\mu-1)(\mu^2-114\mu+1073)}{5(4v)^5}$$

$$+\frac{(\mu-1)(5\mu^3-1535\mu^2+54703\mu-375733)}{14(4v)^7}+\cdots \tag{5.235}$$

$$\Omega_n'(v) \underset{v\to\infty}{\sim} v-\left(\frac{n}{2}-\frac{3}{4}\right)\pi+\frac{\mu+3}{2(4v)}+\frac{\mu^2+46\mu-63}{6(4v)^3}+\frac{\mu^3+185\mu^2-2053\mu+1899}{5(4v)^5}+\cdots \tag{5.236}$$

where $\mu = 4n^2$. Hence

$$\operatorname{Im} P_n(\alpha) \underset{ka\to\infty}{\sim} -\frac{\Omega_n(a\kappa)}{\alpha a} + \frac{2}{\pi}\left\{1+\log\frac{2\pi}{ka} - \sum_{m=m_o+1}^{\infty}\left(\frac{\pi}{\alpha a}\arctan\frac{\alpha a}{\sqrt{j_{nm}^2 - a^2k^2}} - \frac{1}{m}\right) + \right.$$

$$+ \psi(m_o+1) + \frac{\kappa}{\alpha}\arccos\frac{\alpha}{k} - \frac{\left(\frac{n}{2}-\frac{1}{4}\right)\pi^2}{2\alpha a} + \frac{(\mu-1)\arccos\frac{\alpha}{k}}{8\alpha a^2\kappa}$$

$$+ \frac{(\mu-1)(\mu-25)}{384}\left(\frac{\arccos\frac{\alpha}{k}}{\alpha a(\kappa a)^3} - \frac{1}{(\kappa a^2 k)^2}\right) + \ldots + A_{-\ell}\left[\frac{\arccos\frac{\alpha}{k}}{\alpha a(\kappa a)^{\ell}} - \right.$$

$$\left.\left. - \sum_{\nu=0}^{\frac{\ell-3}{2}} \frac{\nu!\,2^{\nu}}{(\kappa a)^{\ell-2\nu-1}(ka)^{2(\nu+1)}\,1\cdot 3\cdots(2\nu+1)}\right] + \ldots\right\} \qquad (5.237)$$

for α real, $0 < \alpha \leqslant k$, where $A_{-\ell}$ is the coefficient of $v^{-\ell}$ in (5.235).

$$\operatorname{Im} P_n(i\eta) \underset{ka\to\infty}{\sim} \frac{2}{\pi}\left\{1+\log\frac{2\pi}{ka} - \sum_{m=m_o+1}^{\infty}\left(\frac{\pi}{2\eta a}\log\frac{\sqrt{j_{nm}^2 - a^2k^2}+\eta}{\sqrt{j_{nm}^2 - a^2k^2}-\eta} - \frac{1}{m}\right) + \psi(m_o+1) - \right.$$

$$\left. - \frac{\kappa}{\eta}\log\left(\frac{\kappa-\eta}{k}\right) - \frac{\left(\frac{n}{2}-\frac{1}{4}\right)\pi}{\eta a} - \frac{(\mu-1)\log\frac{\kappa-\eta}{k}}{8\eta a^2\kappa} + \ldots\right\} \qquad (5.238)$$

for $\alpha = i\eta$, $\eta > 0$. The corresponding expressions for $\operatorname{Im} S_n(\alpha)$ are obtained by substitution of the coefficients of (5.235) against those of (5.236).

To obtain an approximate expression for $\operatorname{Re} P_n(\alpha)$ and $\operatorname{Re} S_n(\alpha)$ valid for large values of ka, we deform the contour of integration in (5.211) according to Fig. 5-23c. Apart from the integrals along Λ_3 and Λ_3' we get contributions from the pole at $\gamma = \alpha$ and from the first quadrant of the large circle used to complete the contour. The integral along Λ_3' is readily performed. It only contributes to the imaginary parts of $P_n(\alpha)$ and $S_n(\alpha)$ and is essentially equal to the series term of (5.222) or

(5.223). The real parts of $P_n(\alpha)$ and $S_n(\alpha)$ are given by

$$\mathrm{Re}\, P_n(\alpha) = -1 - \frac{(-1)^n}{\pi} \int_0^\infty \frac{\frac{\pi}{2} - \arctan \frac{K_n(u)}{\pi I_n(u)}}{(u^2 + a^2\kappa^2)\sqrt{a^2k^2 + u^2}}\, u\,du \tag{5.239}$$

$$\mathrm{Re}\, S_n(\alpha) = -1 + \frac{(-1)^n}{\pi} \int_0^\infty \frac{\frac{5\pi}{2} - \arctan \frac{-K_n'(u)}{\pi I_n'(u)}}{(u^2 + a^2\kappa^2)\sqrt{a^2k^2 + u^2}}\, u\,du \tag{5.240}$$

where α is real and $0 < \alpha < k$.

Consider the formula

$$\int_{-\infty}^{\infty} \frac{u}{u^2+\beta^2} \log \left\{ \sqrt{\frac{2u}{\pi}}\, e^u K_n(u) \prod_{m=0}^{M} \frac{u}{u-\gamma_m} \right\} du$$

$$= -\pi i \log \left\{ -\sqrt{\frac{\pi\beta}{2}}\, i^n e^{i\left(\frac{\pi}{4}-\beta\right)} H_n^{(1)}(\beta) \prod_{m=0}^{M} \frac{\beta}{\beta - i\gamma_m} \right\} \tag{5.241}$$

where β is real and positive and the line of integration lies below the branch cuts. The quantities $\gamma_1, \gamma_2, \ldots \gamma_M$ are the complex zeros of $K_n(u)$ in the third quadrant, and we put $\gamma_o = 0$. The number of zeros is $M = \frac{n}{2} - \frac{1}{4}\left[1 - (-1)^n\right]$ and they are distributed close to the curve indicated in Fig. 5-24. Equation (5.241) is a generalization of a formula given by Jones (1955). By changing the sign of the variable of integration in the range $(-\infty, 0)$, and separating out the term containing the product over M which can be easily integrated, we get

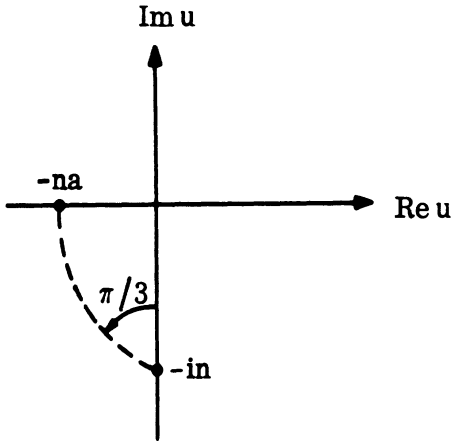

$$a = t_o^2 - 1 = 0.66274,$$

where t_o is the positive root of $\cosh t = t$.

FIG. 5-24: LOCATION OF THE ZEROS OF $K_n(u)$ AND $K_n'(u)$ IN THE THIRD QUADRANT.

$$\int_0^\infty \frac{u}{u^2+\gamma^2} \log\left(\frac{e^{2u}K_n(u)}{\pi I_n(u) - i(-1)^n K_n(u)}\right) du =$$

$$= -\pi i \log\left\{-\sqrt{\frac{\pi\beta}{2}}\, i^n e^{i\left(\frac{\pi}{4}-\beta\right)} H_n^{(1)}(\beta) \prod_{m=1}^{M} \frac{\beta^2}{\beta^2+\gamma_m^2}\right\} \tag{5.242}$$

Taking the imaginary part of both sides, we have

$$(-1)^{n+1} \int_0^\infty \frac{u}{u^2+\beta^2} \arctan\frac{K_n(u)}{\pi I_n(u)}\, du$$

$$= \frac{\pi}{2}\left\{\log\left[\frac{\pi\beta}{2}\left(J_n^2(\beta)+Y_n^2(\beta)\right)\right] - 2\sum_{m=0}^{M} \log\frac{\left|\beta^2+\gamma_m^2\right|}{\beta^2}\right\} \tag{5.243}$$

and in particular, by letting $\beta \to \infty$,

$$(-1)^{n+1} \int_0^\infty u \arctan \frac{K_n(u)}{\pi I_n(u)}\, du = \pi \left\{ \frac{4n^2-1}{16} - \sum_{m=0}^{M} \mathrm{Re}\left\{ \gamma_m^2 \right\} \right\} \tag{5.244}$$

By an identical procedure we obtain

$$(-1)^{n+1} \int_0^\infty \frac{u}{u^2+\beta^2} \arctan \frac{K_n'(u)}{\pi I_n'(u)}\, du$$

$$= \frac{\pi}{2} \left\{ \log \frac{\pi\beta}{2} \left[\left(J_n'^2(\beta) + Y_n'^2(\beta) \right) \right] - 2 \sum_{m=0}^{M'} \log \frac{\left| \beta^2 + \gamma_m'^2 \right|}{\beta^2} \right\} \tag{5.245}$$

$$(-1)^{n+1} \int_0^\infty u \arctan \frac{K_n'(u)}{\pi I_n'(u)}\, du = -\pi \left\{ \frac{4n^2-3}{16} + \sum_{m=0}^{M'} \mathrm{Re}\left\{ \gamma_m'^2 \right\} \right\} \tag{5.246}$$

where γ_m' are the complex zeros of $K_n'(u)$ in the third quadrant and $\gamma_o' = 0$, $M' = \frac{n}{2} + \frac{1}{4}\left[1-(-1)^n\right]$.

We have

$$\arctan \frac{K_n(u)}{\pi I_n(u)} = O(e^{-2u}) \quad \text{as} \quad u \to \infty \tag{5.247}$$

and the same is true for

$$\arctan \frac{-K_n'(u)}{\pi I_n'(u)} \quad .$$

We therefore obtain an asymptotic expression as $ka \to \infty$ from (5.239) and (5.240) by replacing $(a^2k^2+u^2)^{-1/2}$ by

$$\frac{1}{ak} - \frac{u^2}{2a^3k^3} \quad ,$$

and thus

$$\operatorname{Re} P_n(\alpha) \underset{ka\to\infty}{\sim} -1 - \frac{1+\frac{\kappa^2}{2k^2}}{2ak} \log\left[\frac{\pi a\kappa}{2}\left(J_n^2(a\kappa)+Y_n^2(a\kappa)\right)\prod_{m=0}^{M}\frac{\beta^2}{|\beta^2+\gamma_m^2|^2}\right] +$$

$$+\frac{1}{2a^3k^3}\left(\frac{4n^2-1}{16} - \sum_{m=0}^{M}\operatorname{Re}\left\{\gamma_m^2\right\}\right) - (-1)^n f(\alpha) \qquad (5.248)$$

$$\operatorname{Re} S_n(\alpha) \underset{ka\to\infty}{\sim} -1 - \frac{1+\frac{\kappa^2}{2k^2}}{2ak} \log\left[\frac{\pi a\kappa}{2}\left(J_n'^2(a\kappa)+Y_n'^2(a\kappa)\right)\prod_{m=0}^{M'}\frac{\beta^4}{|\beta^2+\gamma_m'^2|^2}\right] -$$

$$-\frac{1}{2a^3k^3}\left(\frac{4n^2-3}{16} + \sum_{m=0}^{M'}\operatorname{Re}\left\{\gamma_m'^2\right\}\right) + \left((-1)^n-4\right) f(\alpha) \qquad (5.249)$$

where $\kappa = \sqrt{k^2-\alpha^2}$ and

$$f(\alpha) = \begin{cases} \dfrac{1}{a\alpha}\log\dfrac{\kappa}{k-\alpha} & 0<\kappa<k \quad (\alpha \text{ real}) \\ \dfrac{1}{a|\alpha|}\arctan\dfrac{|\alpha|}{k} & k<\kappa \quad (\alpha \text{ imaginary}) \end{cases} \qquad (5.250)$$

The divergence of the integrals in (5.239) and (5.240) when $\alpha \to k$ is compensated by a contribution from the indentation around $\alpha = k$ of the path of integration, so that

$$L_o(k) \underset{ka\to\infty}{\sim} \sqrt{\prod_{m=1}^{m_o}\frac{k+\alpha_{om}}{k-\alpha_{om}}}\ \exp\left\{-\frac{ka}{2} - \frac{1}{4}\log\frac{ka}{\pi} - \frac{1}{64a^2k^2}\right\} \qquad (5.251)$$

$$\left|L_n(k)\right| \underset{ka\to\infty}{\sim} \sqrt{\frac{1}{n}\prod_{m=1}^{m_o}\frac{k+\alpha_{om}}{k-\alpha_{om}}}\ \exp\left\{-\frac{ka}{2}-\frac{1}{4}\log\frac{\left[(n-1)!\,2^n\right]^2}{2\pi}-\right.$$

$$\left.-\frac{(-1)^n}{4}\log(2ka)+\frac{1}{2}\sum_{m=1}^{M}\log\left|\gamma_m\right|^2+\frac{1}{4a^2k^2}\left(\frac{4n^2-1}{16}+\sum_{m=0}^{M}\mathrm{Re}\left\{\gamma_m^2\right\}\right)\right\},$$

$$n\geqslant 1 \qquad (5.252)$$

$$\left|M_n(k)\right| \underset{ka\to\infty}{\sim} \frac{1}{ak}\sqrt{n\prod_{m=1}^{m'_o}\frac{k+\alpha'_{nm}}{k-\alpha'_{nm}}}\ \exp\left\{-\frac{ka}{2}-\frac{1}{4}\log\frac{\left[n(n-1)!\,2^n\right]^2}{2\pi}+\right.$$

$$\left.+\frac{(-1)^n}{4}\log(2ka)+\frac{1}{2}\sum_{m=1}^{M'}\log\left|\gamma'_m\right|^2-\frac{1}{4a^2k^2}\left(\frac{4n^2-3}{16}-\sum_{m=0}^{M'}\mathrm{Re}\left\{\gamma'^2_m\right\}\right)\right\},$$

$$n>1 \qquad (5.253)$$

where, as before, m_o or m'_o is an integer or zero such that $j_{nm_o}\leqslant ka<j_{n(m_o+1)}$ or $j'_{nm_o}\leqslant ka<j'_{n(m_o+1)}$. Jones (1955) reports that (5.248) and (5.252) for $\mathrm{Re}\,P_1(\alpha_{1\ell})$ ($\ell>0$) and $\left|L_1(k)\right|$ respectively yield values differing from the exact ones by less than one percent when $ka\geqslant 2$.

Wainstein (1948c) has derived an asymptotic approximation to $L_o(\alpha)$ and $L_1(\alpha)$ in terms of a universal function $U(s,g)$. Bowman (1963c) shows that both $L_n(\alpha)$ and $M_n(\alpha)$ can be represented asymptotically in terms of the same function for all values of n. The function $U(s,g)$ was introduced by Wainstein in connection with the problem of diffraction by two parallel half-planes.

We start from the formula

$$\log\left(\sqrt{-ia(k+\alpha)}\,L_n(\alpha)\right)=\frac{1}{2\pi i}\int_{-\infty}^{\infty}\frac{\log\left[\pi a\sqrt{k^2-\gamma^2}\,J_n\left(a\sqrt{k^2-\gamma^2}\right)H_n^{(1)}\left(a\sqrt{k^2-\gamma^2}\right)\right]}{\gamma-\alpha}d\gamma$$

(2.254)

where the path of integration passes below the pole $\gamma = \alpha$. We change the variable of integration in (5.254) by $\gamma = k \sin\tau$ and obtain

$$\log\left(\sqrt{-ia(k+\alpha)}\, L_n(\alpha)\right) = \frac{k}{2\pi i} \int_C \cos\tau \, \frac{\log\left[\pi ak \cos\tau \, J_n(ak\cos\tau) H_n^{(1)}(ak\cos\tau)\right]}{k\sin\tau - \alpha} \, d\tau \tag{5.255}$$

The path C goes from $\tau = -\frac{\pi}{2} + i\infty$ to $\tau = \frac{\pi}{2} - i\infty$ and below the point $\tau = \arcsin\alpha$. If we introduce into (5.255) the asymptotic approximation

$$\pi x J_n(x) H_n^{(1)}(x) \underset{x\to\infty}{\sim} \left[1 - e^{2i\Omega_n(x)}\right]\left(1 + \frac{4n^2-1}{8x^2} + \ldots\right) \tag{5.256}$$

where $\Omega_n(x)$ is given by (5.235), we can deform the contour C into a path of steepest descent C_o. From (5.256) and (5.235) it follows that C_o goes through a saddle point at $\tau = 0$ at an angle $-\pi/4$ with the real axis. Thus, we may replace the exact integral in (5.255) by the usual steepest descent approximation and we can write

$$L_n(\alpha) \underset{ka\to\infty}{\sim} \frac{1}{\sqrt{a(k+\alpha)}} e^{i\frac{\pi}{4} + U(s, q_L)} \tag{5.257}$$

if α is real and $0 < \alpha < k$ or if α is positive imaginary, where

$$U(s,g) = \frac{1}{2\pi i} \int_{-\infty}^{\infty} \log\left(1 - e^{2iq - \frac{t^2}{2}}\right) \frac{dt}{t - s e^{i\frac{\pi}{4}}} \tag{5.258}$$

and where $s = \alpha\sqrt{\frac{2a}{k}}$, $q_L = \Omega(ak)$. We have

$$U(0+, q) = \frac{1}{2}\log(1 + e^{2iq}) \, . \tag{5.259}$$

By comparing the corresponding value of $L_n(0)$ with the exact value

$$L_n(0) = \sqrt{\pi i J_n(ak) H_n^{(1)}(ak)} , \tag{5.260}$$

and indication of the error in (5.257) can be obtained.

In an analogous manner we have

$$M_n(\alpha) \underset{ka \to \infty}{\sim} \frac{1}{\sqrt{a(k+\alpha)}} e^{i\frac{\pi}{4} + U(s, q_M)} \tag{5.261}$$

if α is real and $0 < \alpha \leqslant k$ or if α is positive imaginary where

$$s = \alpha\sqrt{\frac{2a}{k}} , \qquad q_M = \Omega_n'(ak) .$$

It should be noted that all approximate formulas for $ka \to \infty$ given here are obtained from the ordinary asymptotic expansion for the Bessel functions, i.e. the order is kept fixed as the argument tends to infinity. This means that we have to require $ka \gg n$, when $n \geqslant 1$ in order to apply the formulas. Consequently, a high frequency approximation for scattering of a plane wave at nonaxial incidence cannot be obtained because in that case functions of order 2 or 3 ka are needed to obtain sufficient accuracy.

We have given formulas for $L_n(\alpha)$ and $M_n(\alpha)$ valid if α is real and $0 \leqslant \alpha \leqslant k$, or if α is positive imaginary. As we have seen in the preceeding sections of this chapter, the physical quantities of interest are given as inverse Fourier transforms of functions involving $L_n(\alpha)$ and $M_n(\alpha)$. When $z > 0$ we can deform the path of integration for the inverse Fourier transform (Fig. 5-1) into Λ_2 of Fig. 5-23b, and when $z < 0$, into a corresponding contour around a branch cut from -k to -i∞. As $L_n(\alpha)$ and $M_n(\alpha)$ are regular in the upper half-plane they take the same values on both sides of the branch cut in Fig. 5-23b. When $z < 0$ and the branch cut goes from -k to -i∞ we get the values on the upper and right side of the branch cut $\alpha+$ and on

the left and lower side $\alpha-$ from

$$L_n(\alpha+) = \frac{\pi i J_n(a\kappa)H_n^{(1)}(a\kappa)}{L_n(-\alpha)} \tag{5.262}$$

$$L_n(\alpha-) = -\frac{\pi i J_n(a\kappa)H_n^{(2)}(a\kappa)}{L_n(-\alpha)} \tag{5.263}$$

where $a\kappa = a\sqrt{k^2 - \alpha^2}$, as before, is the branch that is positive when $\alpha = 0$. The corresponding formulas for $M_n(\alpha+)$ and $M_n(\alpha-)$ are obtained by replacing the Bessel functions by their derivatives.

5.6.4 Numerical Computations

Numerical computations of $L_1(\alpha_{1\ell})$, $\ell = 0, 1 \ldots 6$ have been performed by Matsui (1960) for $0 \leqslant ka \leqslant 3$ using (5.212) and (5.214). Jones (1955) reports numerical computations of $L_1(\alpha_{1\ell})$, $- = 0, 1, 2$, for $0 \leqslant ka \leqslant 10$ by Brooker and Turing. They use a formula obtained by deforming the path of integration into Λ_3 of Fig. 5-23 (cf. equation 5.239). The numerical values are shown in Table VIII*.

For $ka < 0.5$, using a formula similar to (5.226), Hallén (1956) has computed the end admittance of a tube-shaped antenna, which admittance is equal to the complex conjugate of the quantity

$$4\pi \sqrt{\frac{\epsilon_o}{\mu_o}} \left[\frac{1}{L_o(k)}\right]^2$$

His results, converted into a graph of $L_o(k)$, are shown in Fig. 5-25.

*Brooker, Turing and Matsui use the time factor $e^{i\omega t}$. Their split function is therefore the complex conjugate of $L_1(\alpha)$.

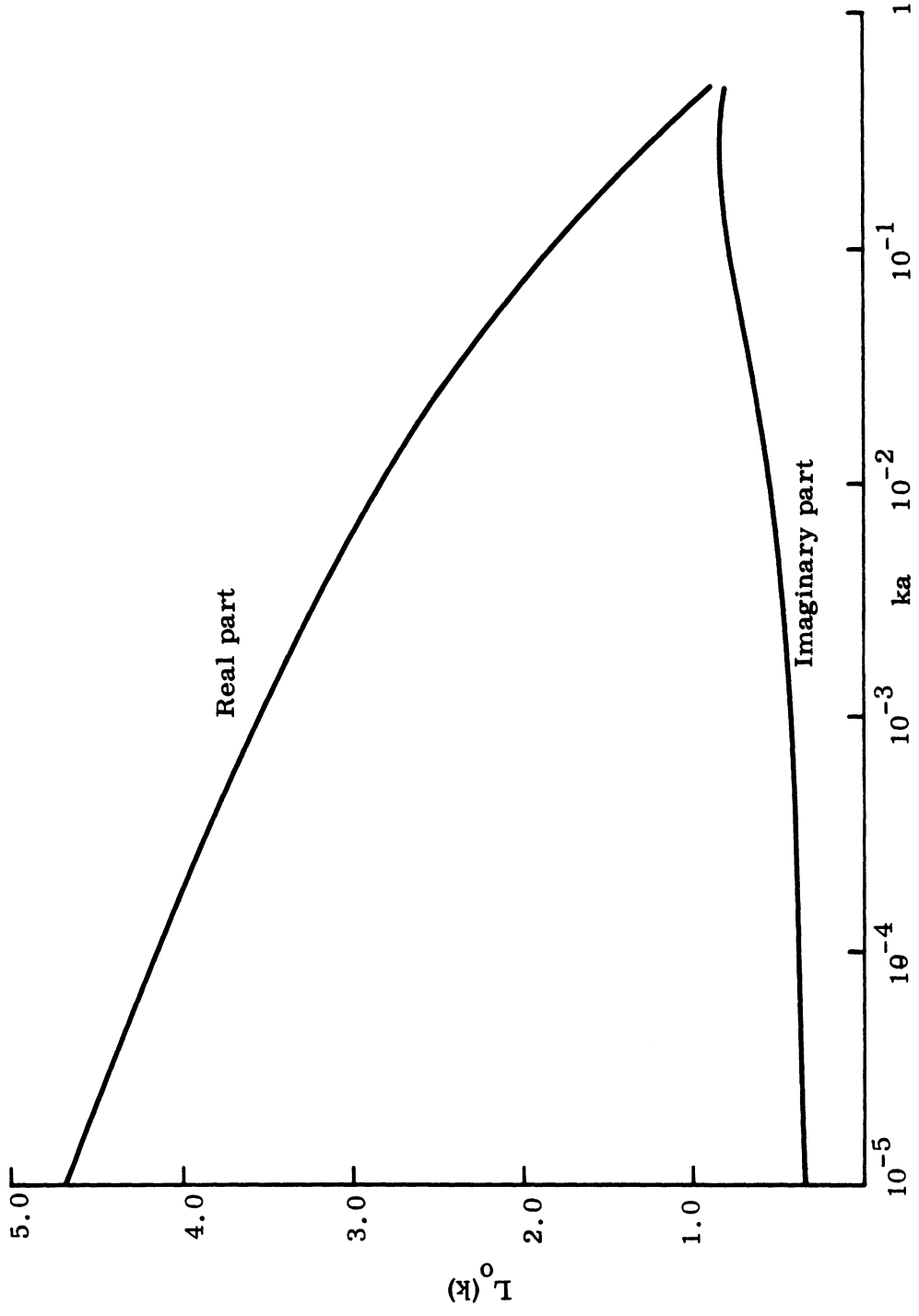

FIG. 5-25: REAL AND IMAGINARY PARTS OF $L_o(k)$ AS A FUNCTION OF ka. (Hallén, 1956)
(The diagram is constructed from Eq. 5.229 for small values of ka and due to the conversion from Hallén's curve, the accuracy for large values of ka is rather poor.)

TABLE VIII

Real and Imaginary Parts of $L_1(\alpha_{1\ell})$ *

ka	$\mathrm{Re}\{L_1(k)\}$		$\mathrm{Im}\{L_1(k)\}$	
	M	J	M	J
.0	1.0000	1.0000	.0000	.0000
.1	.9957		.0609	
.2	.9831		.1198	
.25		.9747		.1501
.3	.9633		.1752	
.4	.9375		.2259	
.5	.9070	.9078	.2716	.2747
.6	.8730		.3117	
.7	.8364		.3464	
.75		.8180		.3654
.8	.7983		.3757	
.9	.7595		.4000	
1.0	.7205	.7206	.4196	.4235
1.1	.6818		.4348	
1.2	.6440	.	.4460	
1.25		.6252		.4541
1.3	.6073		.4536	
1.4	.5719		.4580	
1.5	.5382	.5375	.4595	.4634
1.6	.5060		.4586	
1.7	.4757		.4554	
1.75		.4601		.4568
1.8	.4471		.4504	
1.9	.4204		.4437	
2.0	.3955	.3942	.4356	.4391
2.1	.3724		.4264	
2.2	.3510		.4161	
2.25		.3394		.4139
2.3	.3313		.4050	
2.4	.3133		.3932	
2.5	.2969	.2952	.3808	.3839
2.6	.2820		.3680	
2.7	.2686		.3549	
2.75		.2606		.3510
2.8	.2566		.3414	
2.9	.2459		.3276	

* Matsui (1960), Jones (1955) M = Matsui
J = Jones

Table VIII (cont'd)

ka	$\mathrm{Re}\{L_1(k)\}$		$\mathrm{Im}\{L_1(k)\}$	
	M	J	M	J
3.0	.2366	.2348	.3136	.3163
3.25		.2173		.2799
3.5		.2086		.2405
3.75		.2145		.1888
4.0		.2867		.1903
4.25		.2900		.2208
4.5		.2790		.2391
4.75		.2625		.2493
5.0		.2439		.2532
5.25		.2253		.2518
5.5		.2078		.2464
5.75		.1922		.2376
6.0		.1789		.2260
6.25		.1684		.2119
6.5		.1612		.1954
6.75		.1588		.1750
7.0		.1705		.1388
7.25		.2068		.1640
7.5		.2054		.1801
7.75		.1982		.1901
8.0		.1884		.1957
8.25		.1776		.1978
8.5		.1668		.1970
8.75		.1565		.1937
9.0		.1473		.1882
9.25		.1395		.1809
9.5		.1334		.1717
9.75		.1298		.1604
10.0		.1305		.1452

$\alpha_{10} = k$ and $\alpha_{1\ell} = \sqrt{k^2 - \frac{j_{1\ell}^2}{a^2}}$ $\ell \geq 1$ is real and positive or positive imaginary.

Table VIII (cont'd)

ka	Re $\{L_1(\alpha_{11})\}$		Im $\{L_1(\alpha_{11})\}$	
	M	J	M	J
.0	.4533	.4533	.0000	.0000
.1	.4537		.0000	
.2	.4547		.0002	
.25		.4556		.0003
.3	.4564		.0005	
.4	.4588		.0011	
.5	.4618	.4618	.0022	.0021
.6	.4653		.0036	
.7	.4693		.0055	
.75		.4715		.0066
.8	.4737		.0080	
.9	.4785		.0111	
1.0	.4836	.4836	.0148	.0147
1.1	.4890		.0193	
1.2	.4947		.0245	
1.25		.4976		.0272
1.3	.5006		.0305	
1.4	.5065		.0373	
1.5	.5125	.5124	.0451	.0449
1.6	.5184		.0539	
1.7	.5243		.0637	
1.75	.	.5270		.0687
1.8	.5298		.0746	
1.9	.5350		.0866	
2.0	.5397	.5395	.0999	.0996
2.1	.5436		.1145	
2.2	.5467		.1304	
2.25	.	.5476		.1385
2.3.	.5487		.1476	
2.4	.5494		.1662	
2.5	.5483	.5480	.1862	.1858
2.6	.5453		.2075	
2.7	.5398		.2301	
2.75		.5356		.2413
2.8	.5313		.2537	
2.9	.5193		.2782	

Table VIII (cont'd)

ka	$\mathrm{Re}\{L_1(\alpha_{11})\}$		$\mathrm{Im}\{L_1(\alpha_{11})\}$	
	M	J	M	J
3.0	.5031	.5028	.3031	.3026
3.25		.4378		.3624
3.5		.3206		.3982
3.75		.1101		.3080
4.0		.3440		.1148
4.25		.3761		.2052
4.5		.3553		.2531
4.75		.3223		.2768
5.0		.2880		.2851
5.25		.2562		.2831
5.5		.2286		.2742
5.75		.2055		.2606
6.0		.1870		.2437
6.25		.1733		.2244
6.5		.1644		.2026
6.75		.1616		.1770
7.0		.1749		.1328
7.25		.2202		.1614
7.5		.2194		.1809
7.75		.2111		,1930
8.0		.1997		.1998
8.25		.1872		.2024
8.5		.1748		.2015
8.75		.1631		.1977
9.0		.1527		.1915
9.25		.1439		.1832
9.5		.1372		.1730
9.75		.1332		,1604
10.0		.1338		.1437

$$\alpha_{11} = \sqrt{k^2 - \frac{j_{11}^2}{a^2}} \quad \text{where} \quad j_{11} = 3.83171\ldots$$

Table VIII (cont'd)

ka	Re $\{L_1(\alpha_{12})\}$		Im $\{L_1(\alpha_{12})\}$	
	M	J	M	J
.0	.3526	.3594	.0000	.0000
.1	.3527		.0000	
.2	.3532		.0001	
.25		.3604		.0001
.3	.3539		.0002	
.4	.3549		.0005	
.5	.3562	.3631	.0009	.0009
.6	.3576		.0015	
.7	.3593		.0023	
.75		.3671		.0028
.8	.3611		.0033	
.9	.3631		.0046	
1.0	.3652	.3721	.0060	.0061
1.1	.3674		.0078	
1.2	.3697		.0098	
1.25		.3778		.0110
1.3	.3720		.0121	
1.4	.3744		.0146	
1.5	.3768	.3837	.0175	.0177
1.6	.3791		.0207	
1.7	.3815		.0242	
1.75		.3894		.0264
1.8	.3837		.0280	
1.9	.3859		.0321	
2.0	.3879	.3946	.0366	.0371
2.1	.3897		.0414	
2.2	.3913		.0466	
2.25		.3986		.0500
2.3	.3926		.0521	
2.4	.3937		.0579	
2.5	.3943	.4008	.0641	.0649
2.6	.3945		.0706	
2.7	.3942		.0773	
2.75		.4001		.0819
2.8	.3934		.0844	
2.9	.3919		.0917	

Table VIII (cont'd)

ka	$\mathrm{Re}\{L_1(\alpha_{12})\}$		$\mathrm{Im}\{L_1(\alpha_{12})\}$	
	M	J	M	J
3.0	.3896	.3954	.0991	.1004
3.25		.3850		.1196
3.5		.3657		.1376
3.75		.3275		.1483
4.0		.3145		.0196
4.25		.3331		.0884
4.5		.3488		.0902
4.75		.3628		.0989
5.0		.3748		.1137
5.25		.3837		.1344
5.5		.3878		.1608
5.75		.3846		.1929
6.0		.3705		.2294
6.25		.3399		.2676
6.5		.2842		.2997
6.75		.1886		.3030
7.0		.0167		.1197
7.25		.2805		.1131
7.5		.2921		.1750
7.75		.2750		.2088
8.0		.2507		.2256
8.25		.2258		.2313
8.5		.2020		.2295
8.75		.1831		.2225
9.0		.1666		.2119
9.25		.1536		.1987
9.5		.1443		.1832
9.75		.1391		.1654
10.0		.1398		.1426

$$\alpha_{12} = \sqrt{k^2 - \frac{j_{12}^2}{a^2}} \qquad \text{where} \quad j_{12} = 7.01559\ldots$$

Table VIII (cont'd)

ka	$\mathrm{Re}\{L_1(\alpha_{13})\}$ M	$\mathrm{Im}\{L_1(\alpha_{13})\}$ M	$\mathrm{Re}\{L_1(\alpha_{14})\}$ M	$\mathrm{Im}\{L_1(\alpha_{14})\}$ M
.0	.2988	.0000	.2640	.0000
.1	.2989	.0000	.2641	.0000
.2	.2992	.0000	.2643	.0000
.3	.2996	.0001	.2645	.0001
.4	.3002	.0003	.2649	.0002
.5	.3009	.0005	.2654	.0004
.6	.3018	.0009	.2660	.0006
.7	.3027	.0013	.2666	.0009
.8	.3038	.0019	.2674	.0013
.9	.3049	.0026	.2681	.0018
1.0	.3061	.0035	.2689	.0023
1.1	.3074	.0045	.2698	.0030
1.2	.3087	.0056	.2707	.0037
1.3	.3101	.0069	.2716	.0046
1.4	.3114	.0083	.2725	.0056
1.5	.3128	.0099	.2734	.0066
1.6	.3142	.0117	.2743	.0078
1.7	.3155	.0136	.2752	.0091
1.8	.3168	.0158	.2761	.0104
1.9	.3181	.0180	.2769	.0119
2.0	.3193	.0205	.2777	.0135
2.1	.3204	.0231	.2785	.0153
2.2	.3213	.0259	.2792	.0171
2.3	.3222	.0289	.2798	.0190
2.4	.3229	.0321	.2803	.0211
2.5	.3234	.0354	.2807	.0232
2.6	.3237	.0389	.2809	.0255
2.7	.3238	.0425	.2811	.0279
2.8	.3236	.0463	.2810	.0303
2.9	.3230	.0502	.2807	.0329
3.0	.3221	.0543	.2803	.0355

$\alpha_{13} = \sqrt{k^2 - \frac{j_{13}^2}{a^2}}$ where $j_{13} = 10.17347\ldots$ $\alpha_{14} = \sqrt{k^2 - \frac{j_{14}^2}{a^2}}$ where $j_{14} = 13.3236$

Table VIII (cont'd)

ka	$\mathrm{Re}\{L_1(\alpha_{15})\}$ M	$\mathrm{Im}\{L_1(\alpha_{15})\}$ M	$\mathrm{Re}\{L_1(\alpha_{16})\}$ M	$\mathrm{Im}\{L_1(\alpha_{16})\}$ M
.0	.2391	.0000	.2201	.0000
.1	.2391	.0000	.2202	.0000
.2	.2393	.0000	.2203	.0000
.3	.2395	.0001	.2204	.0000
.4	.2398	.0001	.2207	.0001
.5	.2401	.0003	.2209	.0002
.6	.2406	.0004	.2213	.0003
.7	.2410	.0007	.2216	.0005
.8	.2415	.0009	.2220	.0007
.9	.2421	.0013	.2225	.0010
1.0	.2427	.0017	.2229	.0013
1.1	.2433	.0022	.2234	.0017
1.2	.2440	.0027	.2239	.0021
1.3	.2446	.0033	.2244	.0026
1.4	.2453	.0040	.2249	.0031
1.5	.2460	.0048	.2254	.0037
1.6	.2466	.0057	.2259	.0043
1.7	.2473	.0066	.2265	.0050
1.8	.2479	.0076	.2270	.0058
1.9	.2486	.0086	.2274	.0066
2.0	.2491	.0098	.2279	.0075
2.1	.2497	.0110	.2283	.0085
2.2	.2502	.0124	.2287	.0095
2.3	.2506	.0137	.2291	.0105
2.4	.2510	.0152	.2294	.0116
2.5	.2513	.0168	.2296	.0128
2.6	.2516	.0184	.2298	.0141
2.7	.2517	.0201	.2299	.0154
2.8	.2517	.0219	.2299	.0167
2.9	.2515	.0237	.2298	.0181
3.0	.2512	.0256	.2296	.0196

$$\alpha_{15} = \sqrt{k^2 - \frac{j_{15}^2}{a^2}} \text{ where } j_{15} = 16.47063\ldots \qquad \alpha_{16} = \sqrt{k^2 - \frac{j_{16}^2}{a^2}} \text{ where } j_{16} = 19.61586\ldots$$

VI
EXPERIMENTAL DATA

This chapter contains the experimental data for scattering by circular cylinders. Most of the material is relevant to scattering by infinite cylinders, but some results for finite cylinders are included. Scattering of a plane acoustic wave by an infinite cylinder is presented in view of the direct correspondence to scattering of an electromagnetic wave. The details of the measuring techniques will not be discussed here, but appropriate reference are given in each case.

The infinite cylinder is considered first, followed by the finite cylinders. The excitation is by a plane wave or point source. The notation used is given in the following diagram:

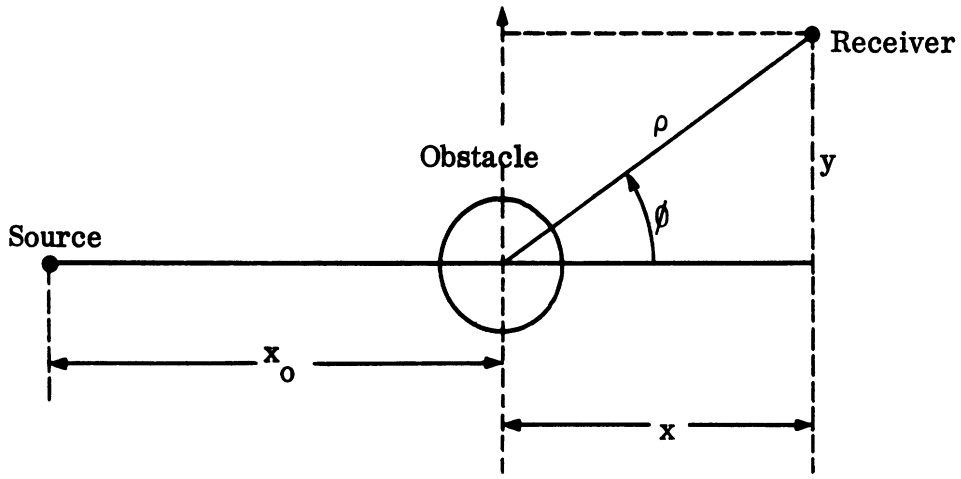

6.1 Scattering of Plane Waves by an Infinite Circular Cylinder

Using the parallel plate technique, Adey (1955) measured the amplitude and phase of the diffracted electric field for perfectly conducting circular cylinders with ka = 2, 3.4 and 5.97. The incident radiation was a plane wave propagating perpendicular to the cylinder axis with the electric vector in the axial direction and wavelength 3.28 cm. Figures 6-1 through 6-3 are plots of the amplitudes and phases of the back and forward scattered fields.

Current distribution measurements on conducting cylinders for a plane wave incident perpendicular to the axis of the cylinder with the magnetic vector parallel have been performed by Wetzel and Brick (1955). The image plane technique was used, and the normalized amplitude and phase of the surface current, as functions of the angle measured from the center of the illuminated side, are presented in Figs. 6-4 and 6-5. The cylinder was perfectly conducting with $ka = 12$ (cf. Eq. 2.42).

Cook and Chrzanowski (1946) studied the absorption and scattering of a plane sound wave by a simulated infinitely long circular cylinder whose axis was perpendicular to the direction of incidence. Figure 6-6(a) shows the absorption cross section for a Fiberglas cylinder of radius 2.88 in. over the frequency range 100-5000 Hz. Figures 6-6(b) and (c) correspond to the cylinders having one and two layers respectively of cattle felt of thickness 7/8 in. wrapped around them. Theoretical curves are given for comparison purposes.

Acoustic scattering by circular cylinders of infinite length immersed in a liquid medium has been treated by Faran (1951). He measured the amplitudes of waves scattered by metal cylinders in water. Figures 6-7(a) and (b) show the scattering amplitude patterns for brass and steel cylinders respectively with $ka = 1.7$. The direction of the incident plane wave is indicated by the arrow in each diagram. Figures 6-8(a), (b) and 6-9(a) give the scattering patterns for brass, copper and steel cylinders, respectively with $ka = 3.4$ and Figs. 6-9(b), 6-10(a), (b) show the corresponding quantities for $ka = 5.0$.

6.2 Scattering of a Point Source Field by an Infinite Circular Cylinder

Kodis (1950) used the image plane technique to measure the scattering of electromagnetic waves by conducting and dielectric cylinders. The electric field was directed along the cylinder axis and the source was a horn antenna operating at 24 GHz ($\lambda = 1.25$ cm). Figures 6-11 through 6-22 show the amplitude and phase of the diffracted field for brass cylinders with $ka = 3.1$, 6.3 and 10 respectively. The theoretical values for point source excitation are related to those for a line source parallel to the axis.

Wiles and McLay (1954) employed a technique similar to that of Kodis (1950) to measure the diffracted electromagnetic field amplitudes for brass cylinders of infinite length. The incident cylindrical wave had a wavelength of 3.2 cm and electric vector parallel to the cylinder axis. Figure 6-23 shows the relative intensity of the axial component of total diffracted electric field for $ka = 2.494$, measured in the range $5 < ky < 25$.

Bauer, Tamarkin and Lindsay (1948) used ultrasonic waves at 1145 kHz ($\lambda = 1.3$ mm) to measure the scattering by steel cylinders in water. Relative pressure distributions at different points at right angles to the direction of propagation, for various distances of the obstacle and the receiver from the source are plotted in Figs. 6-24 through 6-31. The models used were 1/4 and 1/2 in. steel rods and 5/8 in. polystyrene tubes.

6.3 Finite Cylinders

Measurements of scattered pressure for finite cylinders using acoustic waves have been made by Wiener (1947). The wooden cylinders had length and diameter equal, and the results were compared with theoretical values for an infinite cylinder.

The scattering of electromagnetic waves ($\lambda = 3.13$ cm) by brass cylinders of length-to-width ratios 4.44, 8.89 and 13.32 has been determined by Giese and Siedenthopf (1962). The measurements were confined to the far fields as a function of the scattering angle (angle between the radius vector to the point of observation and the cylinder axis).

Meyer, Kuttruff and Severin (1959) used the Doppler method to measure the electromagnetic back scattering cross sections of finite cylinders at a wavelength of $\lambda = 3.2$ cm. Figures 6-32 through 6-39 give plots of the differential cross section as a function of the scattering angle θ. The maximum back scattering cross section (in the plane $\theta = 90^{\circ}$) is presented as a function of ℓ/λ in Fig. 6-40, and the corresponding quantity for $\theta = 0^{\circ}$ or 180° is plotted in Fig. 6-41.

6.4 Thin Cylinders

Figure 6-42 shows a set of measurements reported by Van Vleck, Bloch and Hammermesh (1947) for a thin cylinder (ℓ = 900 a) at broadside incidence. The normalized back scattering cross section is compared with theoretical values calculated by Lindroth (1955).

Figure 6-43 shows the results of measurements made by Liepa and Chang (1965) on the back scattering cross section of a silver-plated stainless steel cylinder 1/16 in. in diameter. The frequency of the incident electromagnetic wave was maintained at 2.370 GHz (corresponding to ka = 0.0394), and the length of the cylinder was varied from 30 in. to 1.5 in. (Note that this curve is not directly comparable to Fig. 6-42 because ℓ/a is kept constant in the latter, whereas ka is constant in the former.)

A similar set of data for a silver plated stainless steel cylinder with ka = .0222 is given by King and Wu (1959) in Fig. 6-44. The values are compared with data for a cylinder with ka = .0202 (Liepa, 1964) and are in good agreement.

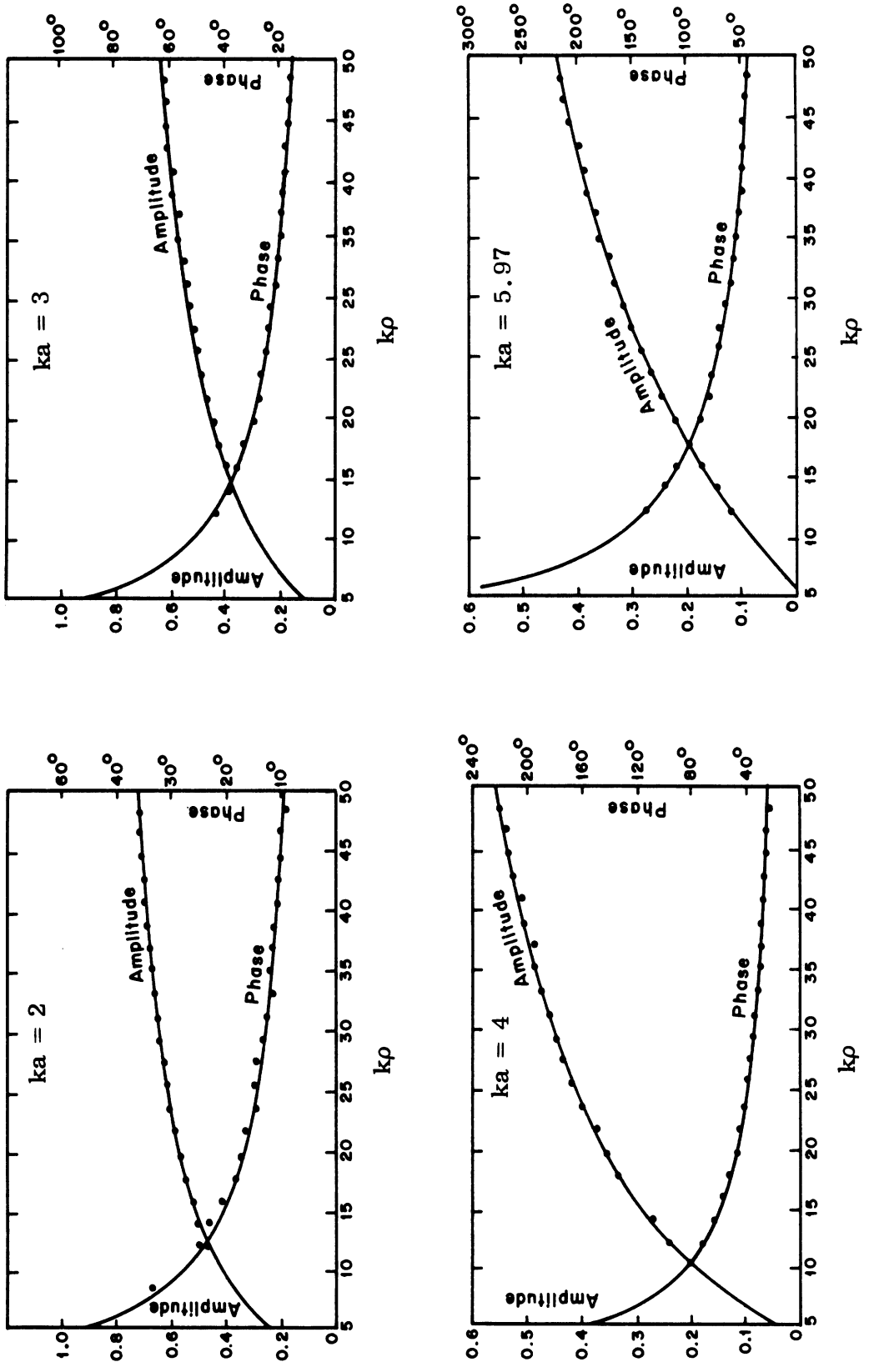

FIG. 6-1: MEASURED (· · ·) AND THEORETICAL (——) AMPLITUDE AND PHASE OF TOTAL ELECTRIC FIELD IN THE FORWARD DIRECTION ($\phi = 0$) FOR A METALLIC CYLINDER WITH $\underline{E}^i$ PARALLEL TO THE AXIS (Adey, 1955).

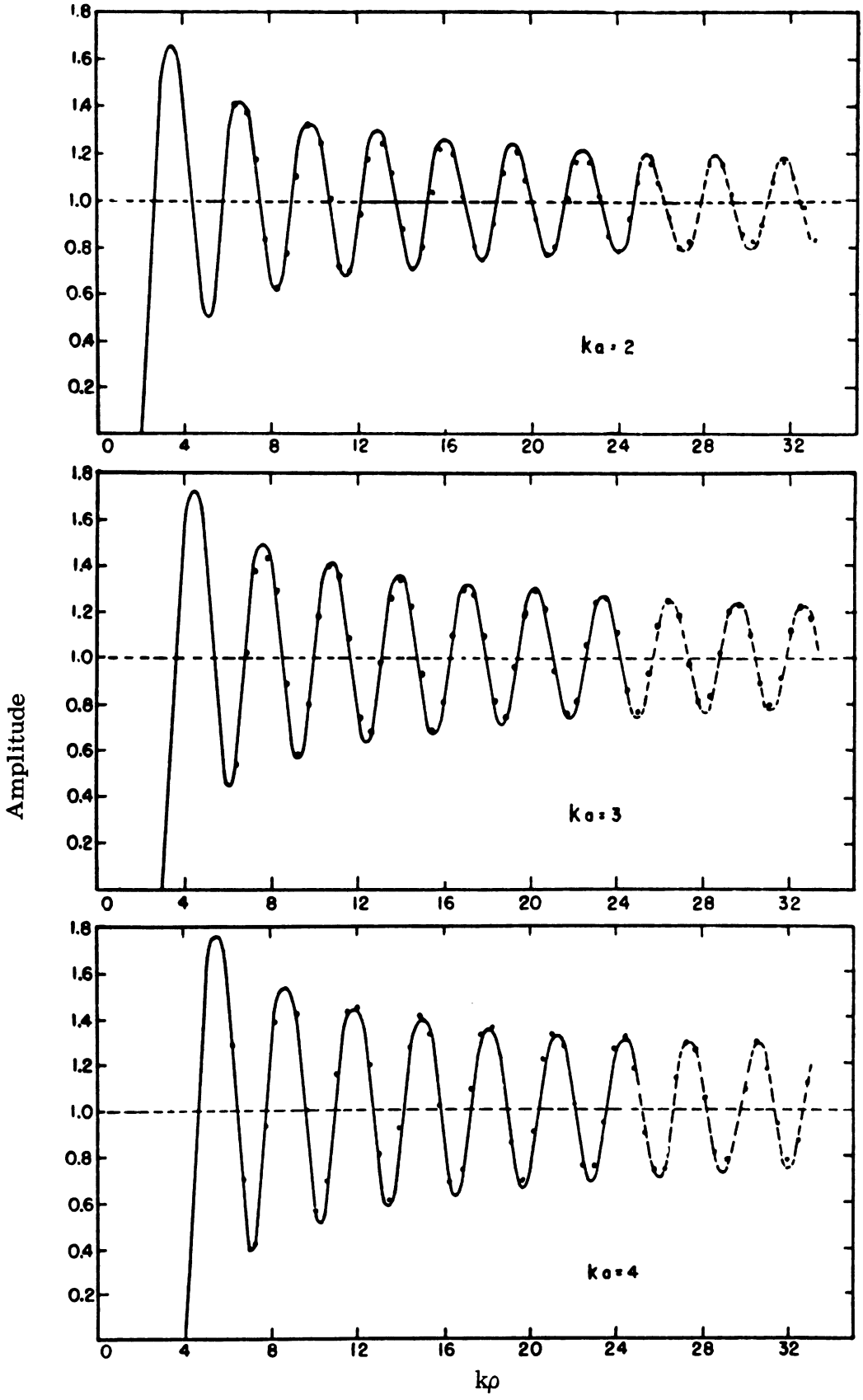

FIG. 6-2: MEASURED (· · ·) AND THEORETICAL (——) AMPLITUDE OF TOTAL ELECTRIC FIELD IN THE BACKWARD DIRECTION ($\phi = \pi$) FOR A METALLIC CYLINDER WITH $\underline{E}^i$ PARALLEL TO THE AXIS (Adey, 1955).

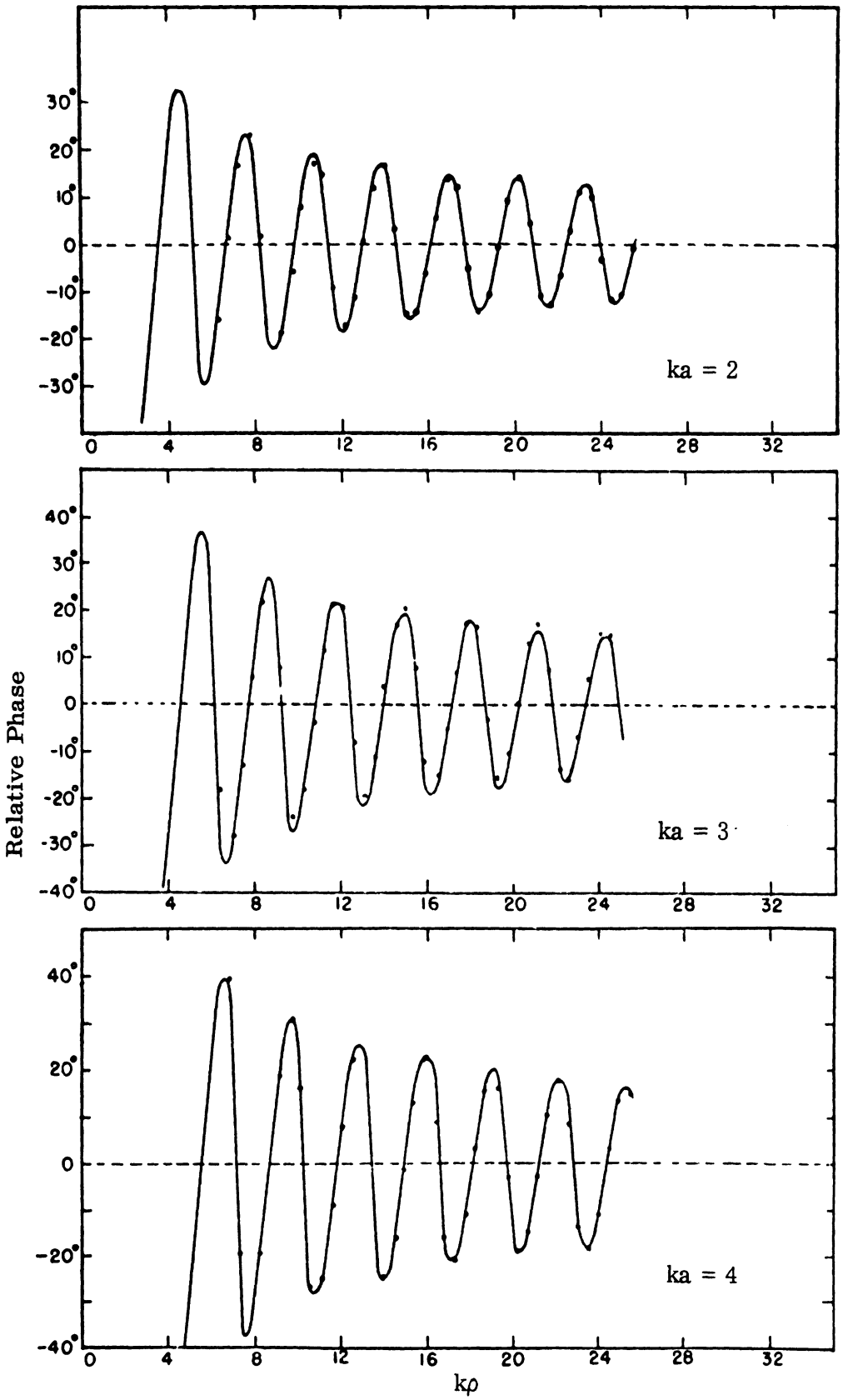

FIG. 6-3: MEASURED (· · ·) AND THEORETICAL (—) RELATIVE PHASE OF TOTAL ELECTRIC FIELD IN THE BACKWARD DIRECTION ($\phi = \pi$) FOR A METALLIC CYLINDER WITH $\underline{E}^i$ PARALLEL TO THE AXIS (Adey, 1955).

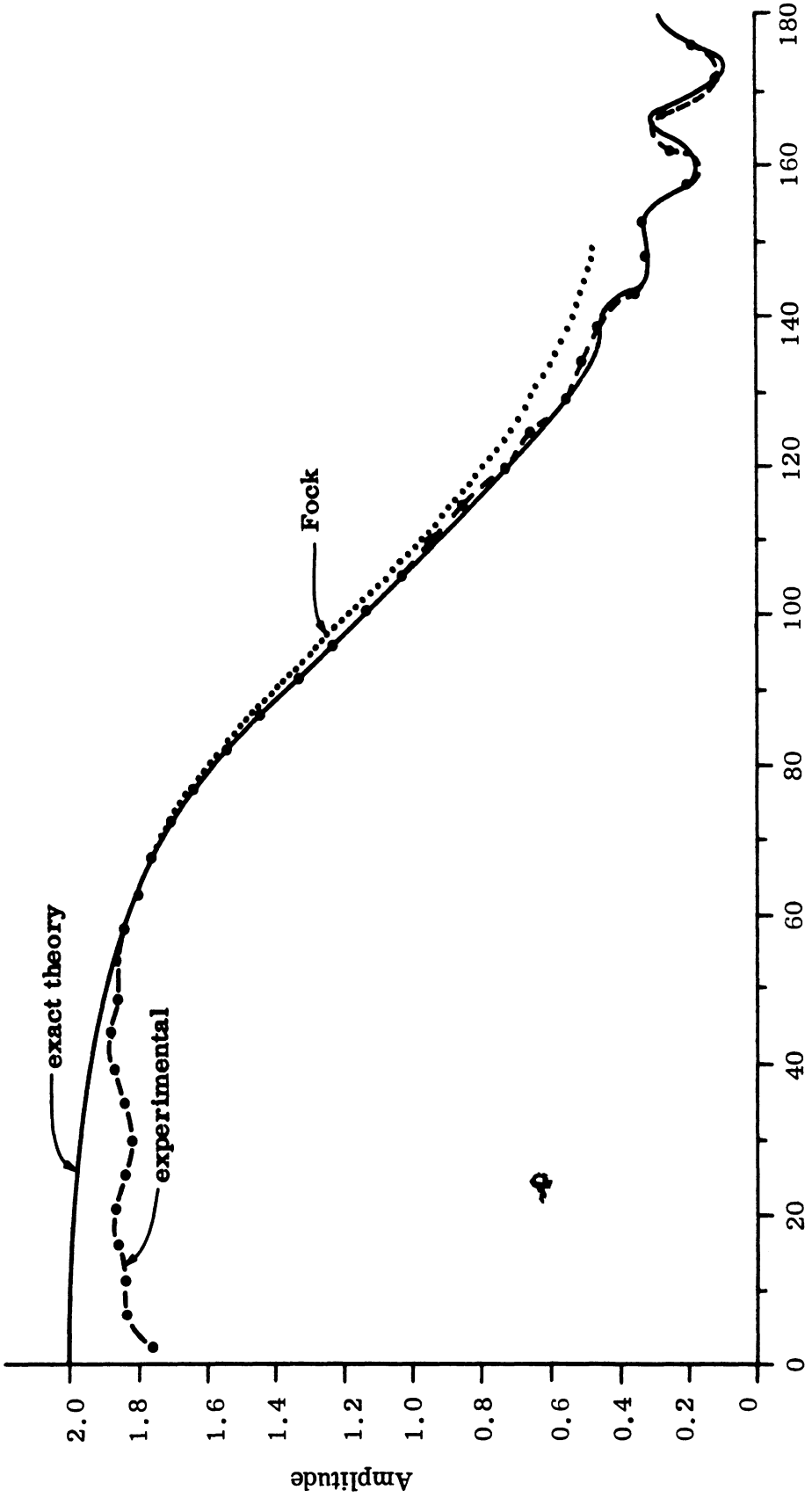

FIG. 6-4: AMPLITUDE OF CURRENT DENSITY J_ϕ ON A METALLIC CYLINDER FOR ka = 12 WITH $\underline{H}^i$ PARALLEL TO THE AXIS (Wetzel and Brick, 1955).

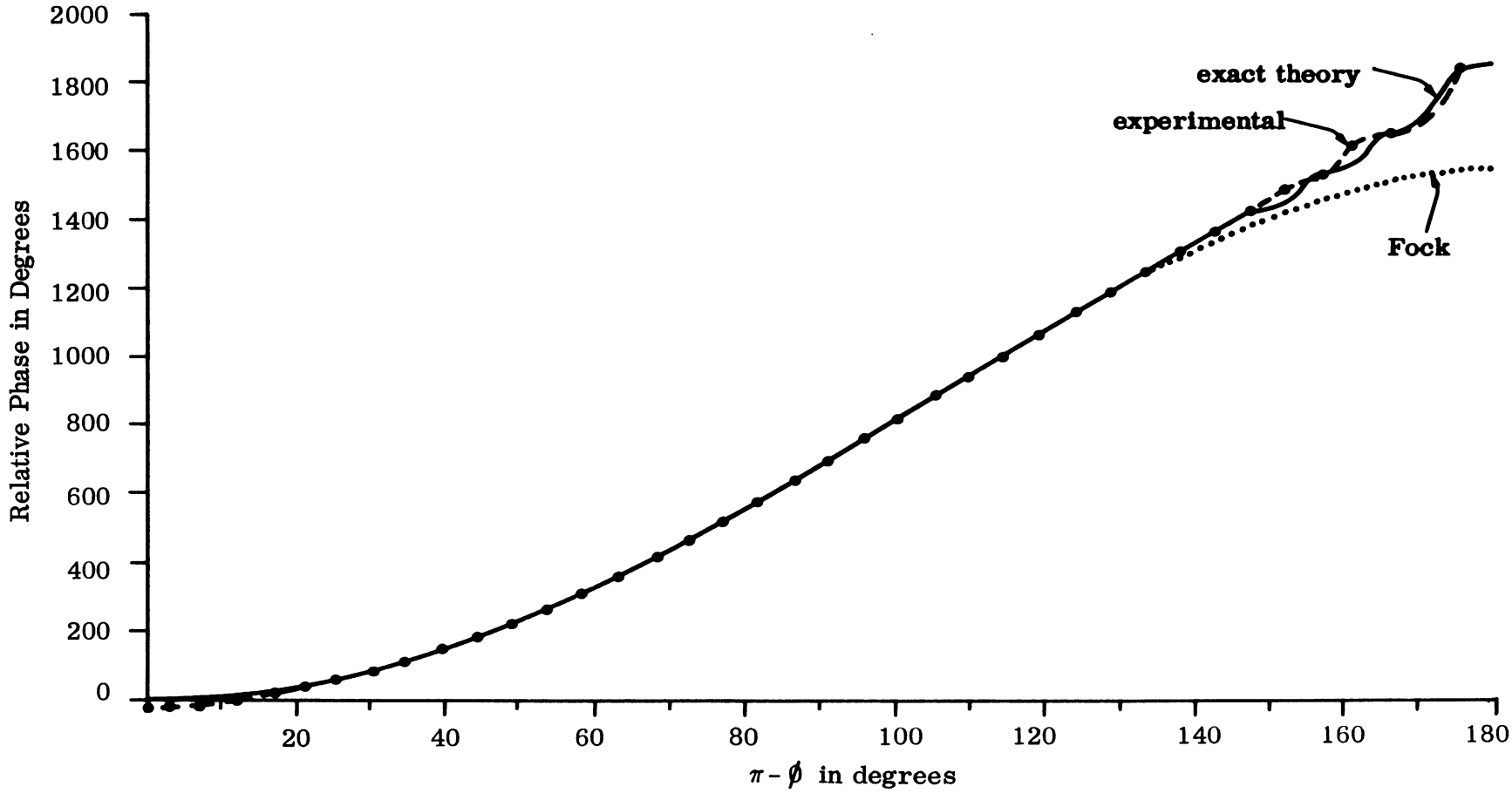

FIG. 6-5: RELATIVE PHASE OF CURRENT DENSITY J_ϕ ON A METALLIC CYLINDER FOR ka = 12 WITH $\underline{H}^i$ PARALLEL TO THE AXIS (Wetzel and Brick, 1955).

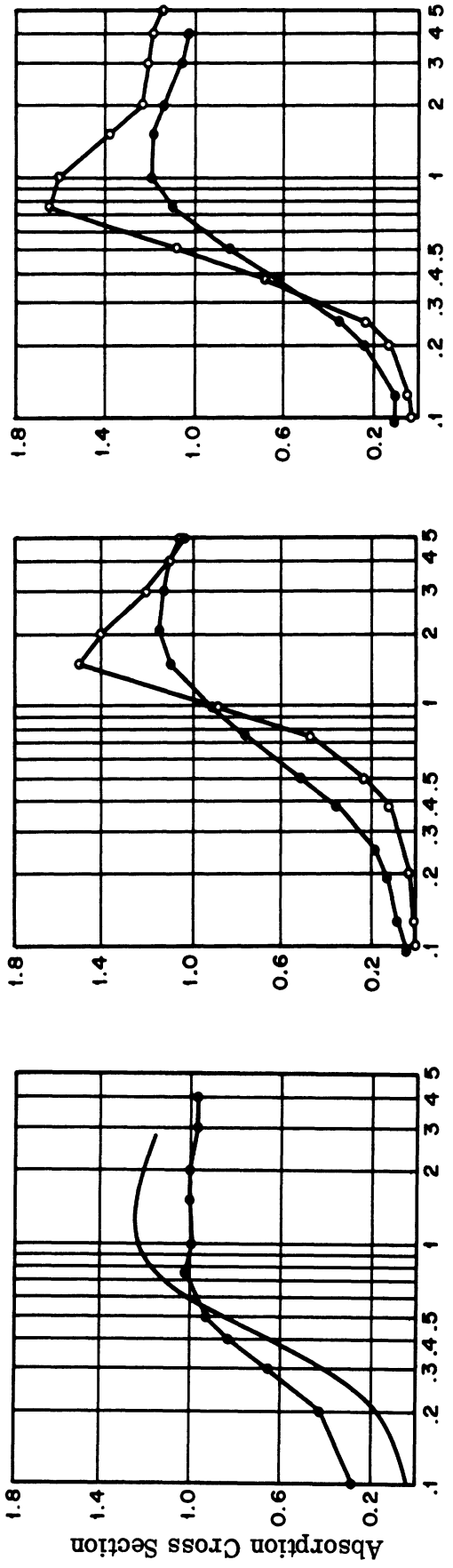

FIG. 6-6: MEASURED (• • •) AND THEORETICAL (∘ ∘ ∘ , ——) ABSORPTION CROSS SECTION FOR A FIBERGLAS CYLINDER: (a) BARE, (b) WITH ONE LAYER OF HAIR FELT, (c) WITH TWO LAYERS OF HAIR FELT (Cook and Chrzanowski, 1948).

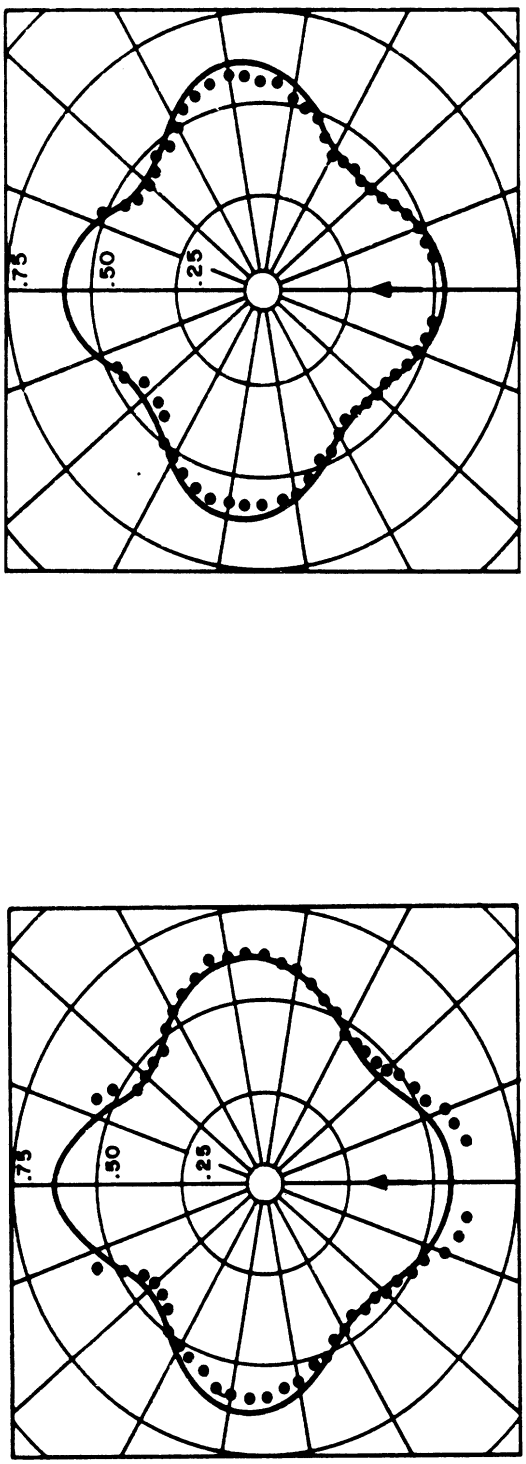

FIG. 6-7: MEASURED (• • •) AND THEORETICAL (——) SCATTERED PRESSURE AMPLITUDE FOR PLANE WAVE INCIDENCE: (a) BRASS CYLINDER, ka = 1.7; (b) STEEL CYLINDER, ka = 1.7 (Faran, 1951).

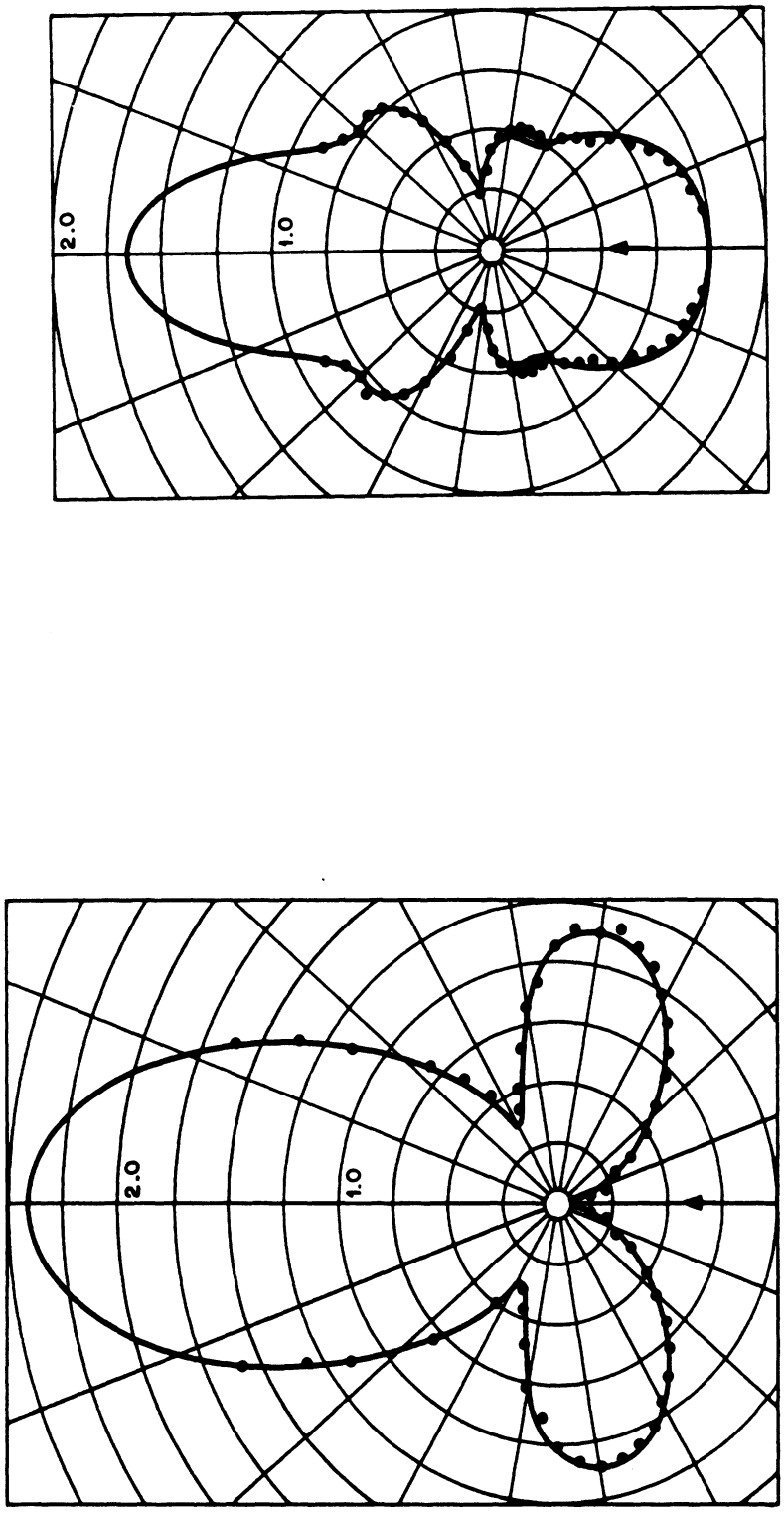

FIG. 6-8: MEASURED (• • •) AND THEORETICAL (——) SCATTERED PRESSURE AMPLITUDE FOR PLANE WAVE INCIDENCE: (a) BRASS CYLINDER, ka = 3.4; (b) COPPER CYLINDER, ka = 3.4 (Faran, 1951).

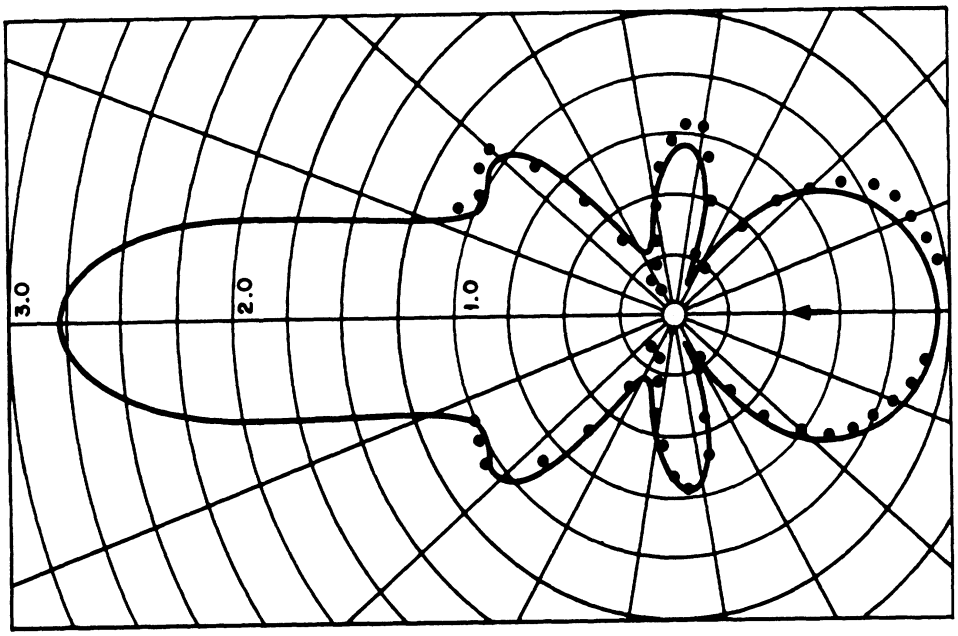

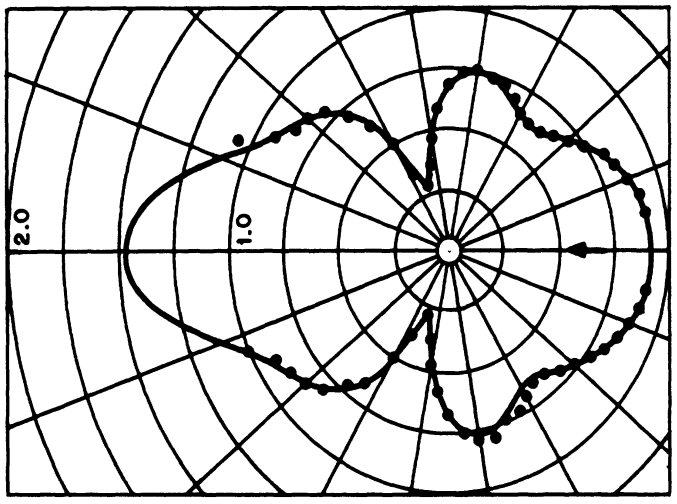

FIG. 6-9: MEASURED (• • •) AND THEORETICAL (——) SCATTERED PRESSURE AMPLITUDE FOR PLANE WAVE INCIDENCE: (a) STEEL CYLINDER, ka = 3.4; (b) BRASS CYLINDER, ka = 5.0 (Faran, 1951).

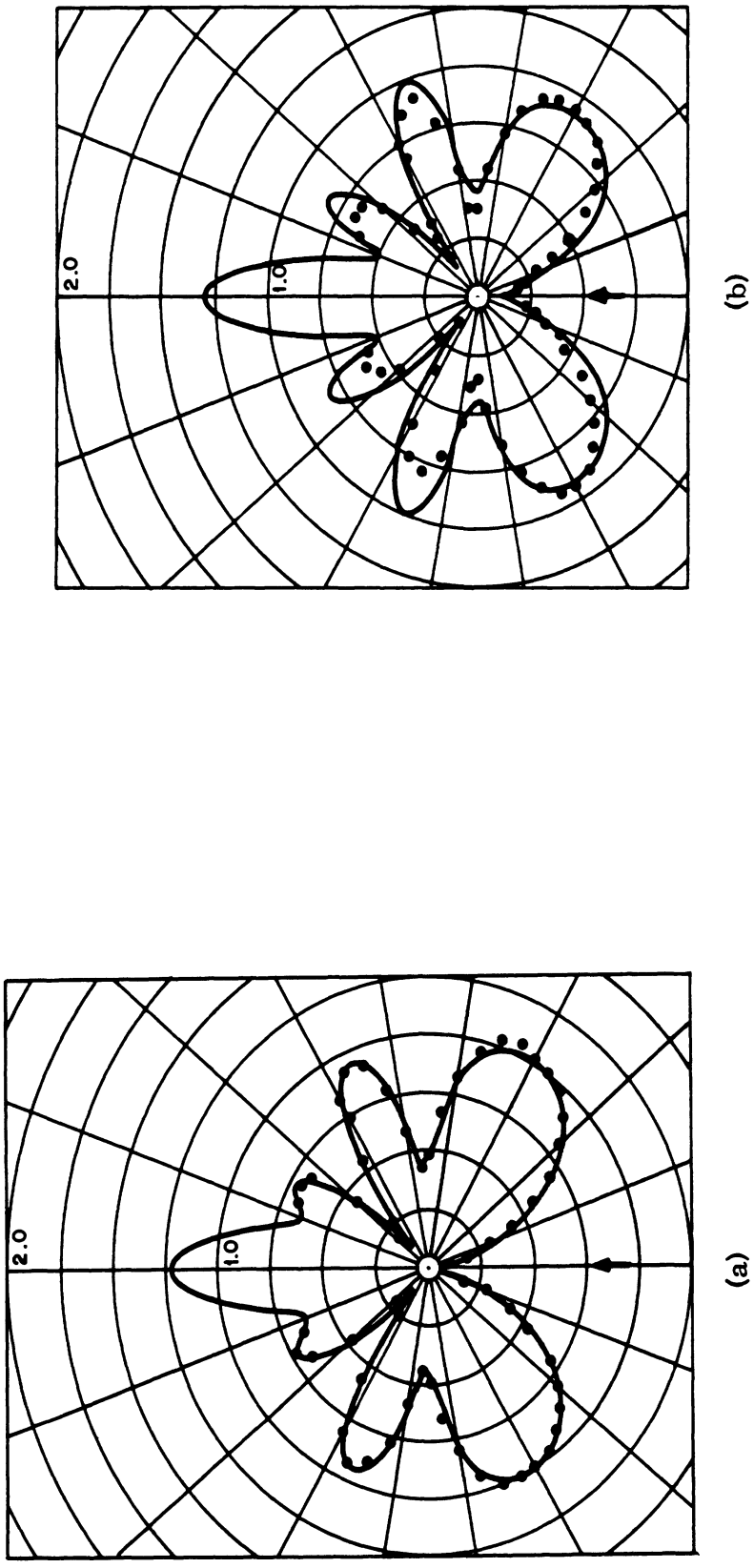

FIG. 6-10: MEASURED (• • •) AND THEORETICAL (——) SCATTERED PRESSURE AMPLITUDE FOR PLANE WAVE INCIDENCE: (a) STEEL CYLINDER, ka = 5.0; (b) ALUMINUM CYLINDER, ka = 5.0 (Faran, 1951).

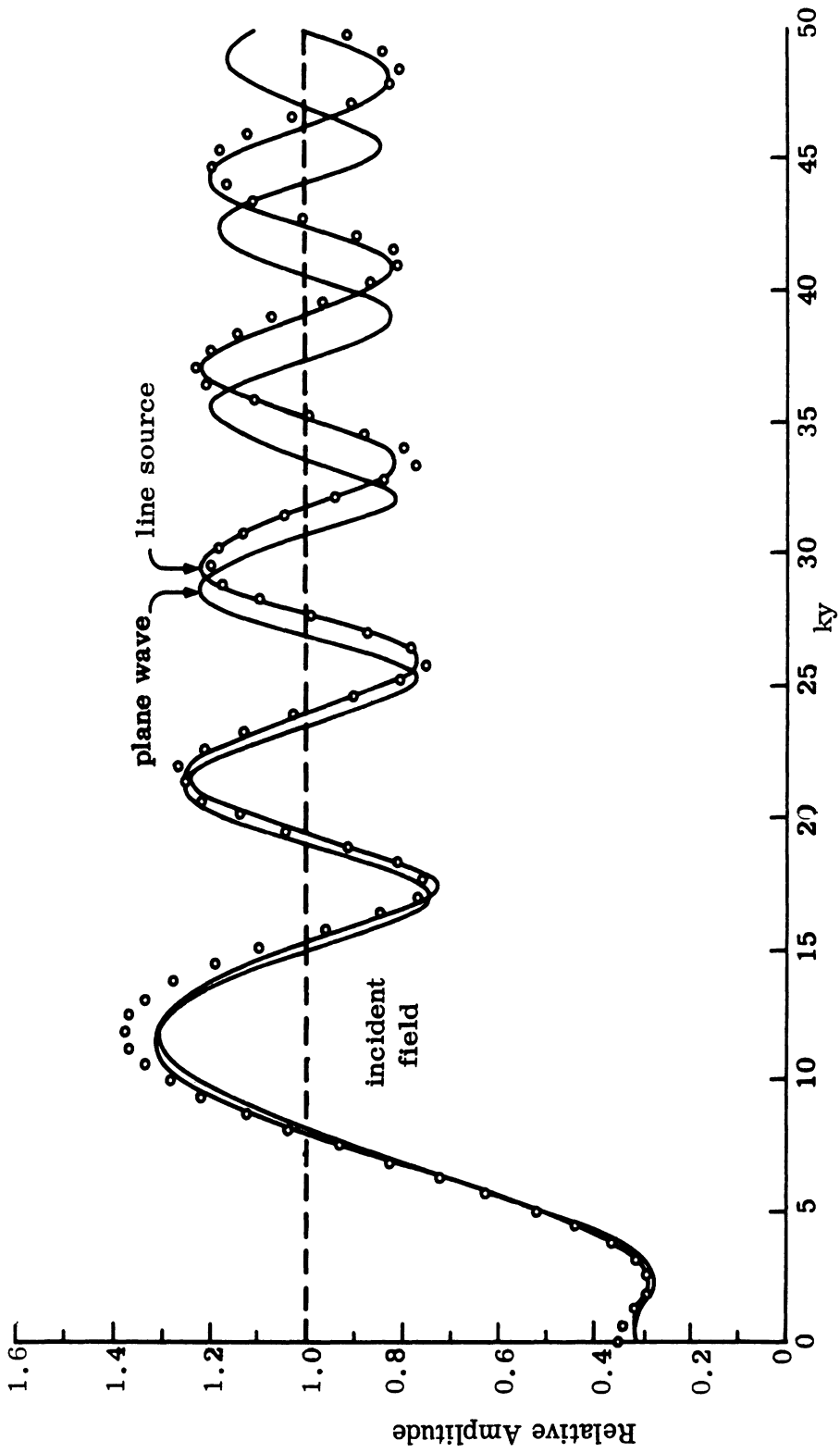

FIG. 6-11: MEASURED (∘ ∘∘) AND THEORETICAL (——) AMPLITUDE $|E_z|$ FOR ka = 3.1 AND kx = 4π (Kodis, 1950).

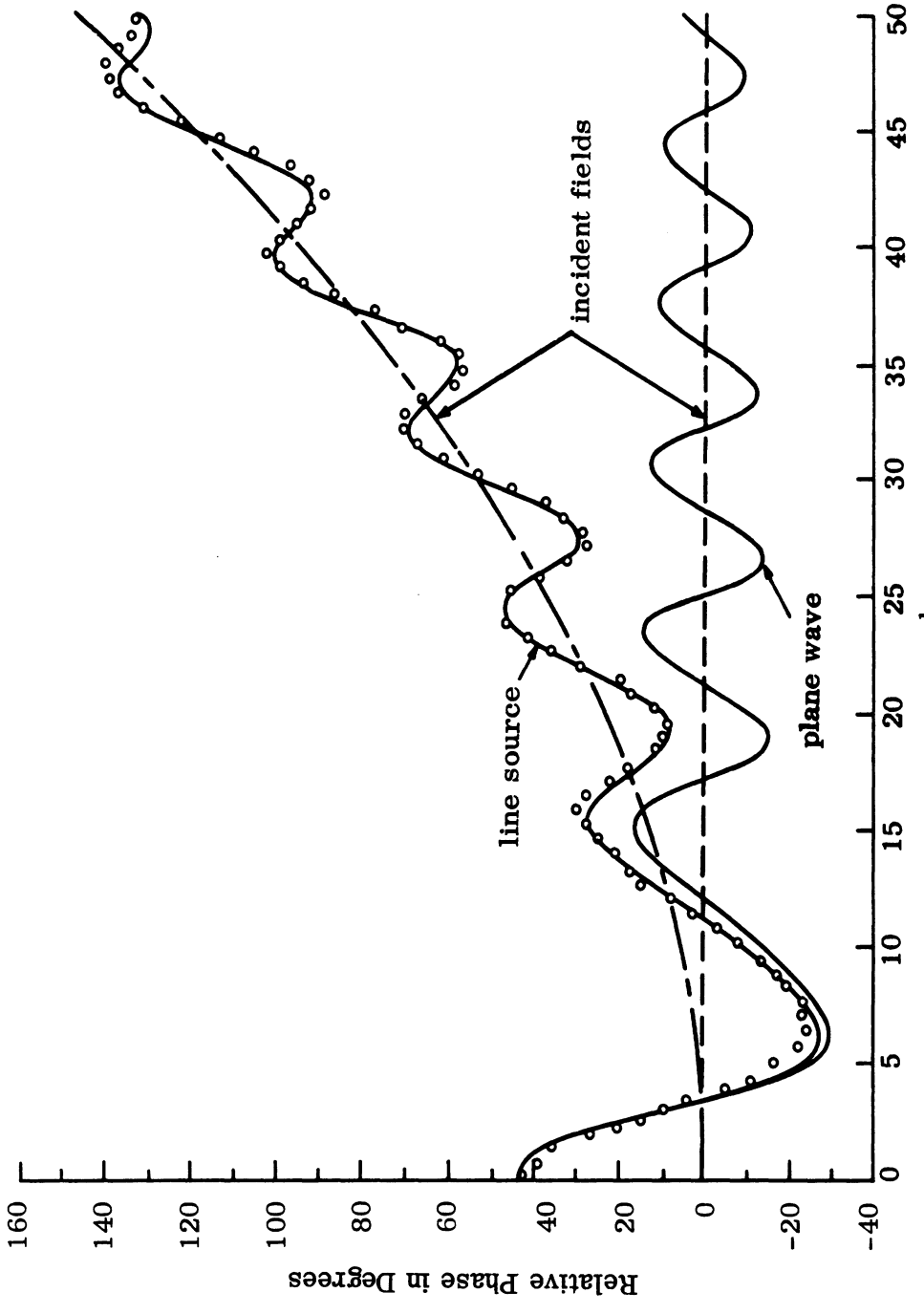

FIG. 6-12: MEASURED (• • •) AND THEORETICAL (——) PHASE OF E_z FOR ka = 3.1 AND kx = 4π (Kodis, 1950).

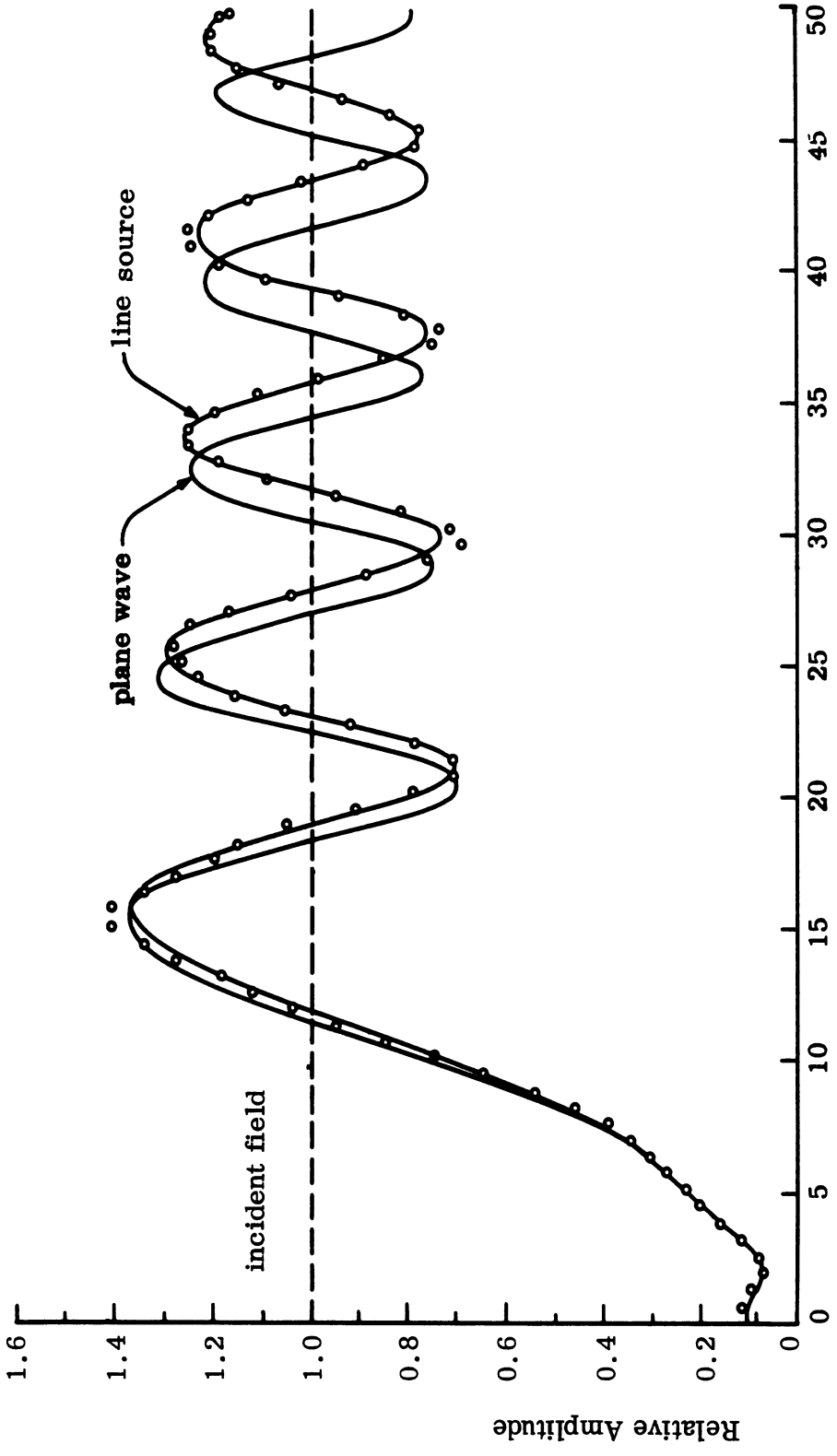

FIG. 6-13: MEASURED (∘ ∘ ∘) AND THEORETICAL (——) AMPLITUDE $|E_z|$ FOR ka = 6.3 AND kx = 4π (Kodis, 1950).

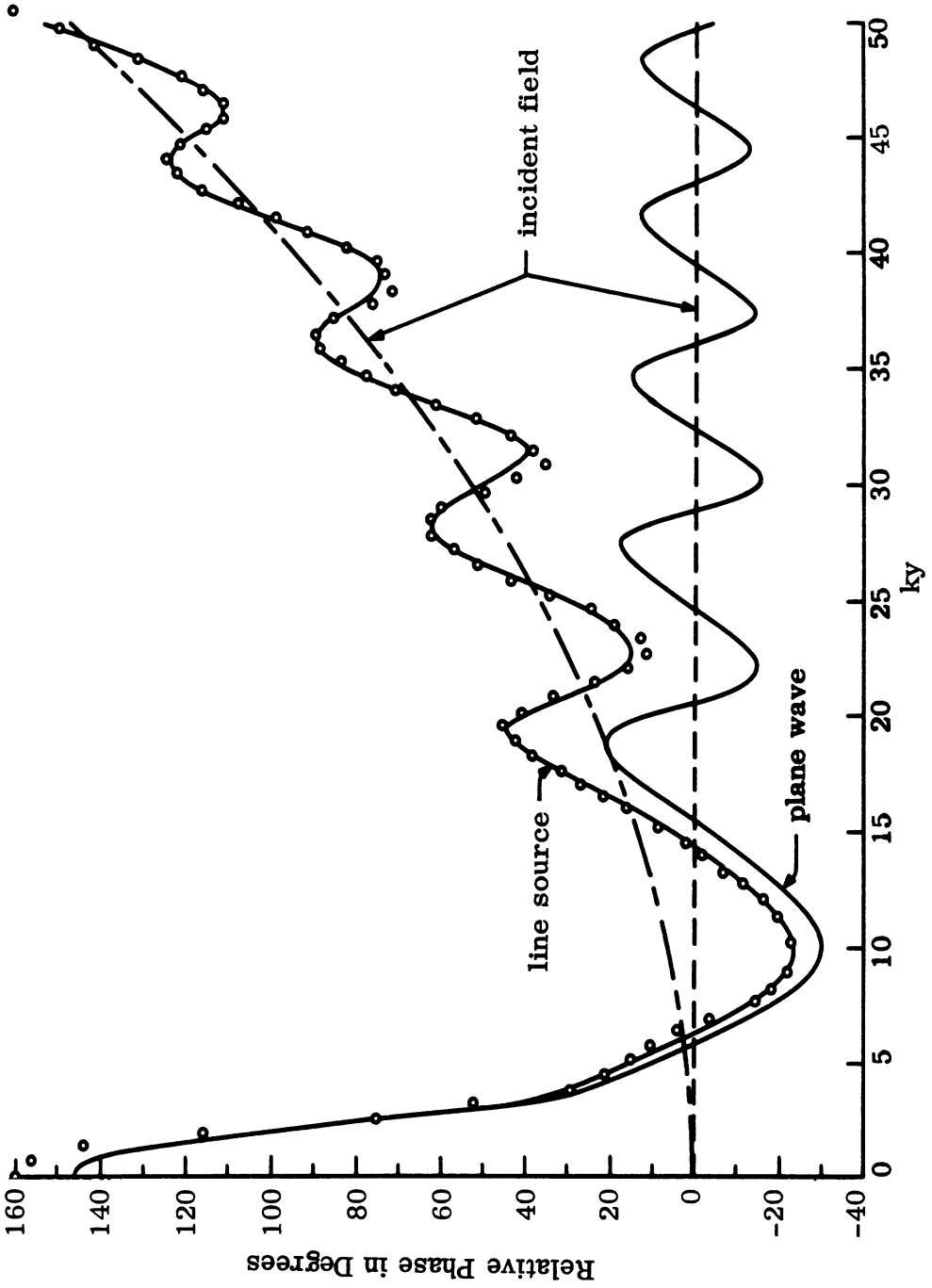

FIG. 6-14: MEASURED (o o o) AND THEORETICAL (—) PHASE OF E_z FOR ka = 6.3 AND kx = 4π (Kodis, 1950).

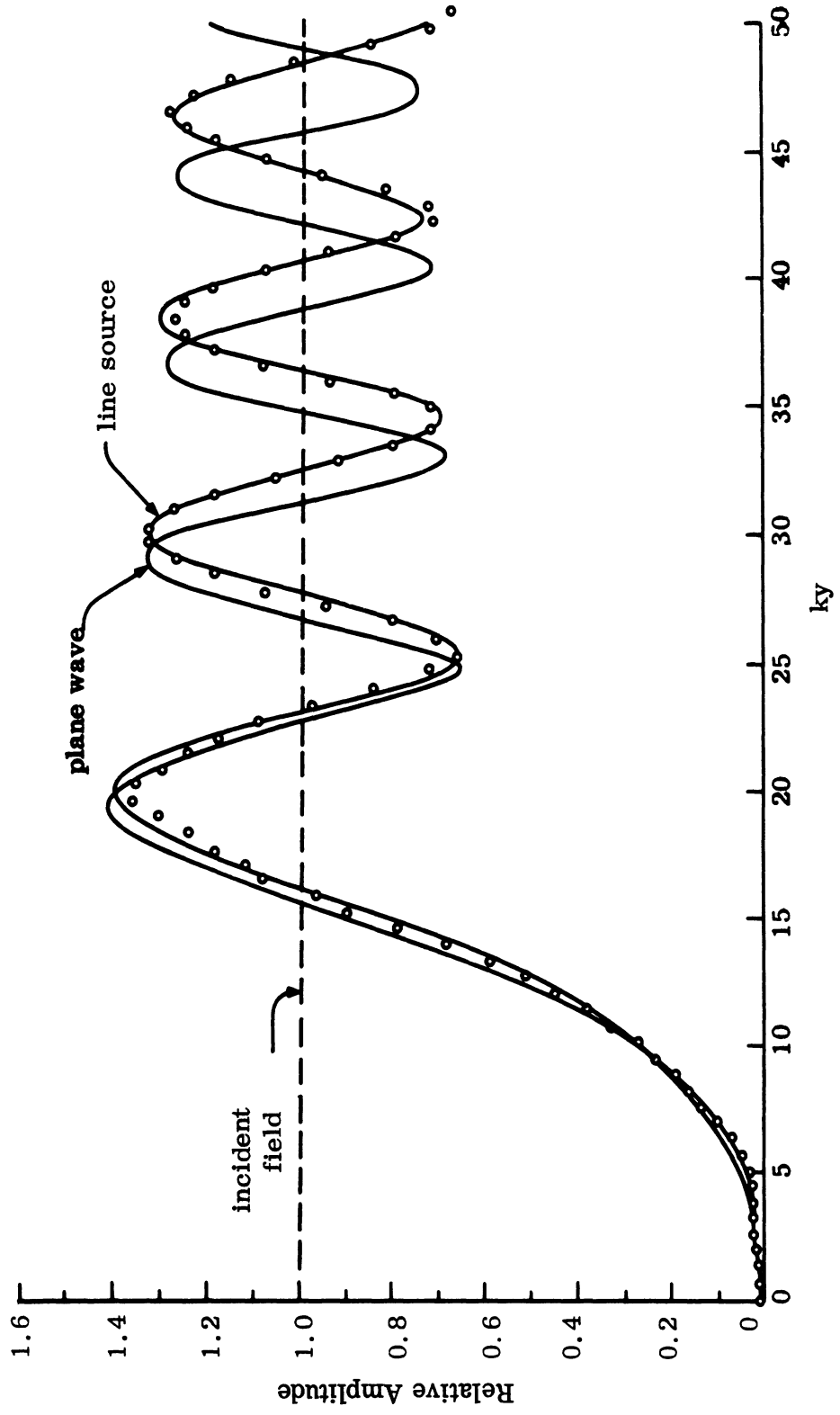

FIG. 6-15: MEASURED (o o o) AND THEORETICAL (——) AMPLITUDE $|E_z|$ FOR ka = 10 AND kx = 4π (Kodis, 1950).

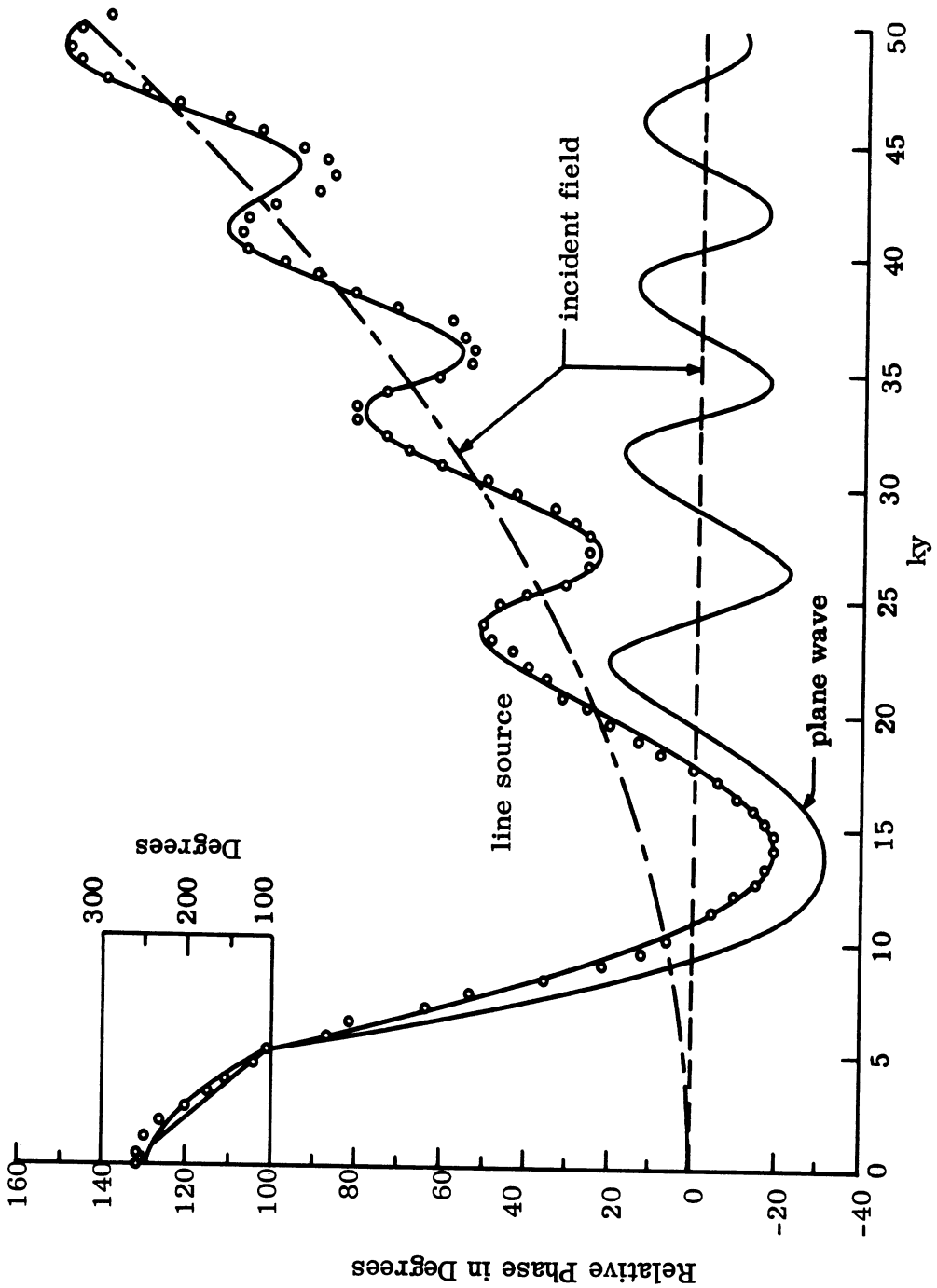

FIG. 6-16: MEASURED (• • •) AND THEORETICAL (——) PHASE OF E_z FOR ka = 10 AND kx = 4π (Kodis, 1950).

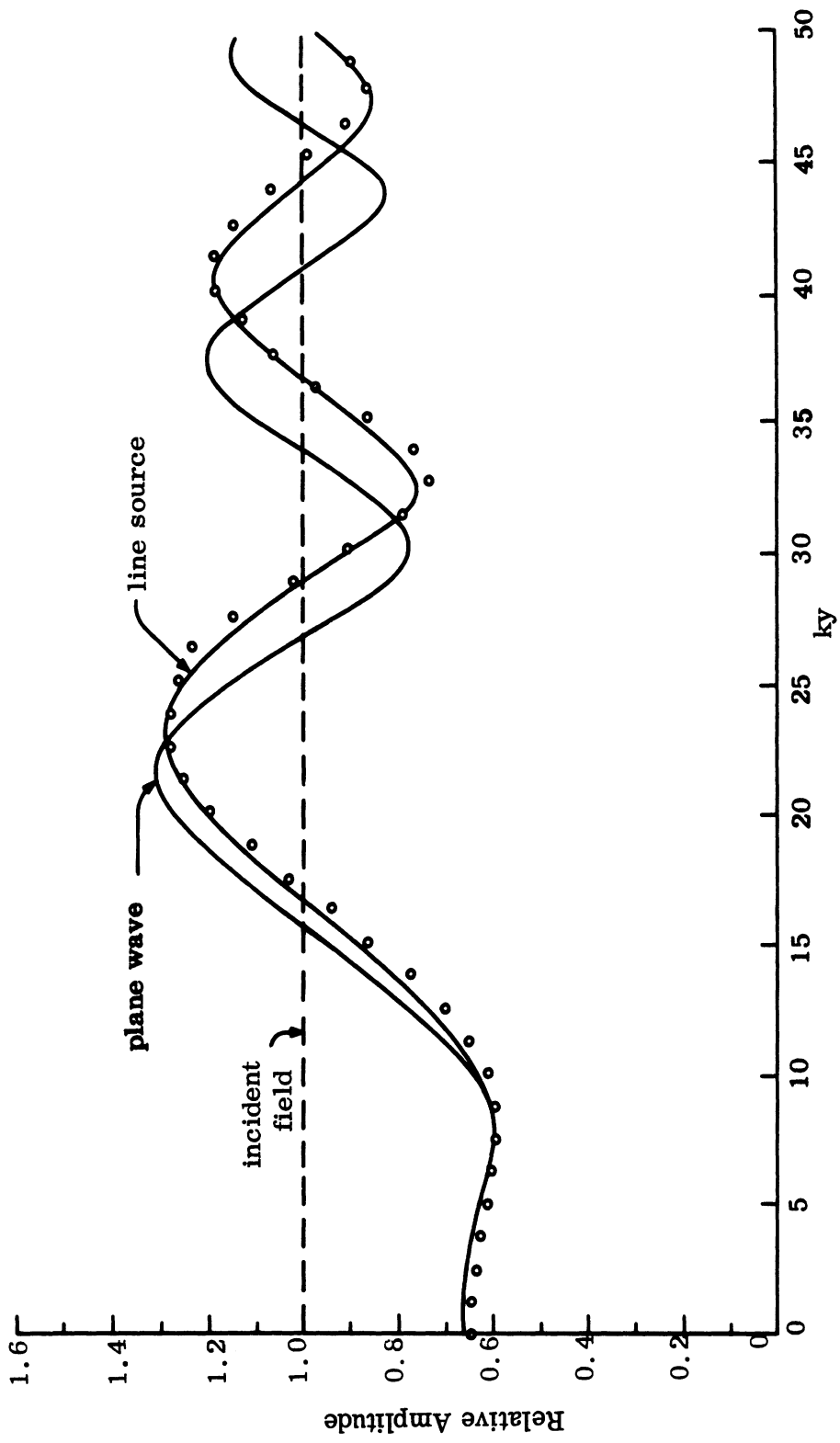

FIG. 6-17: MEASURED (∘ ∘ ∘) AND THEORETICAL (——) AMPLITUDE $|E_z|$ FOR ka = 3.1 AND kx = 20π (Kodis, 1950).

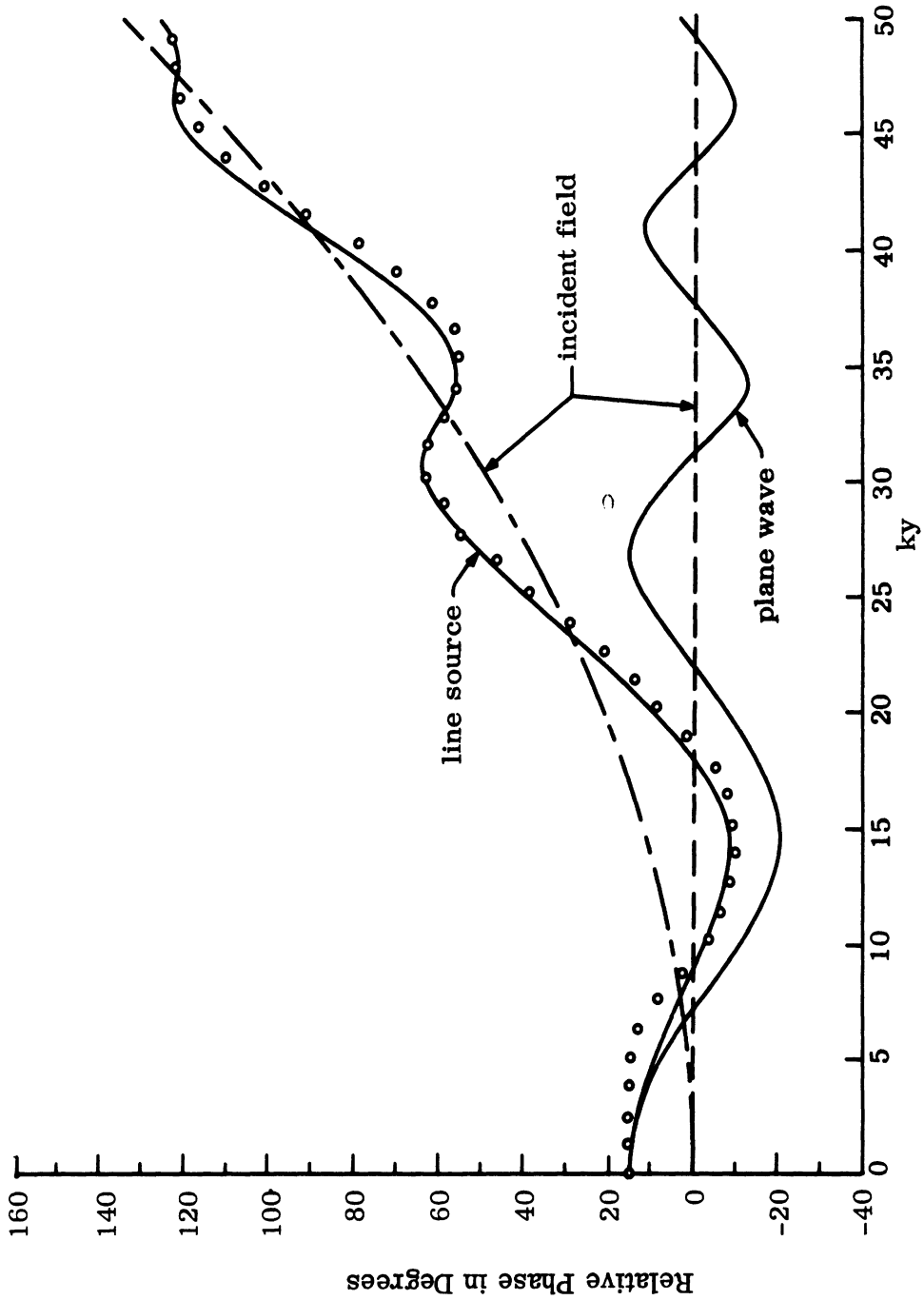

FIG. 6-18: MEASURED (• • •) AND THEORETICAL (——) PHASE OF E_z FOR ka = 3.1, kx = 20π (Kodis, 1950).

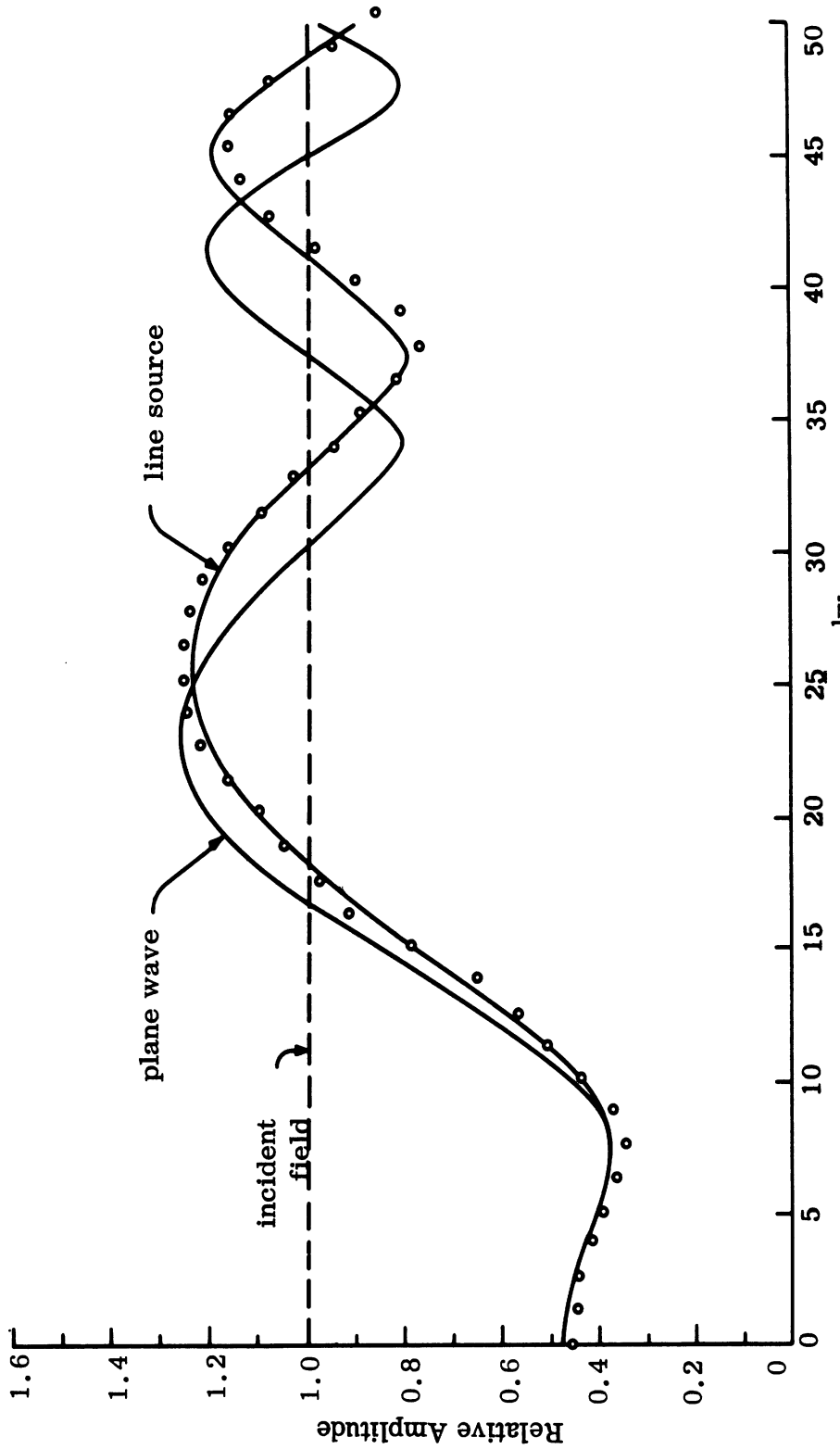

FIG. 6-19: MEASURED (∘ ∘ ∘) AND THEORETICAL (——) AMPLITUDE $|E_z|$ FOR ka = 6.3 AND kx = 20π (Kodis, 1950).

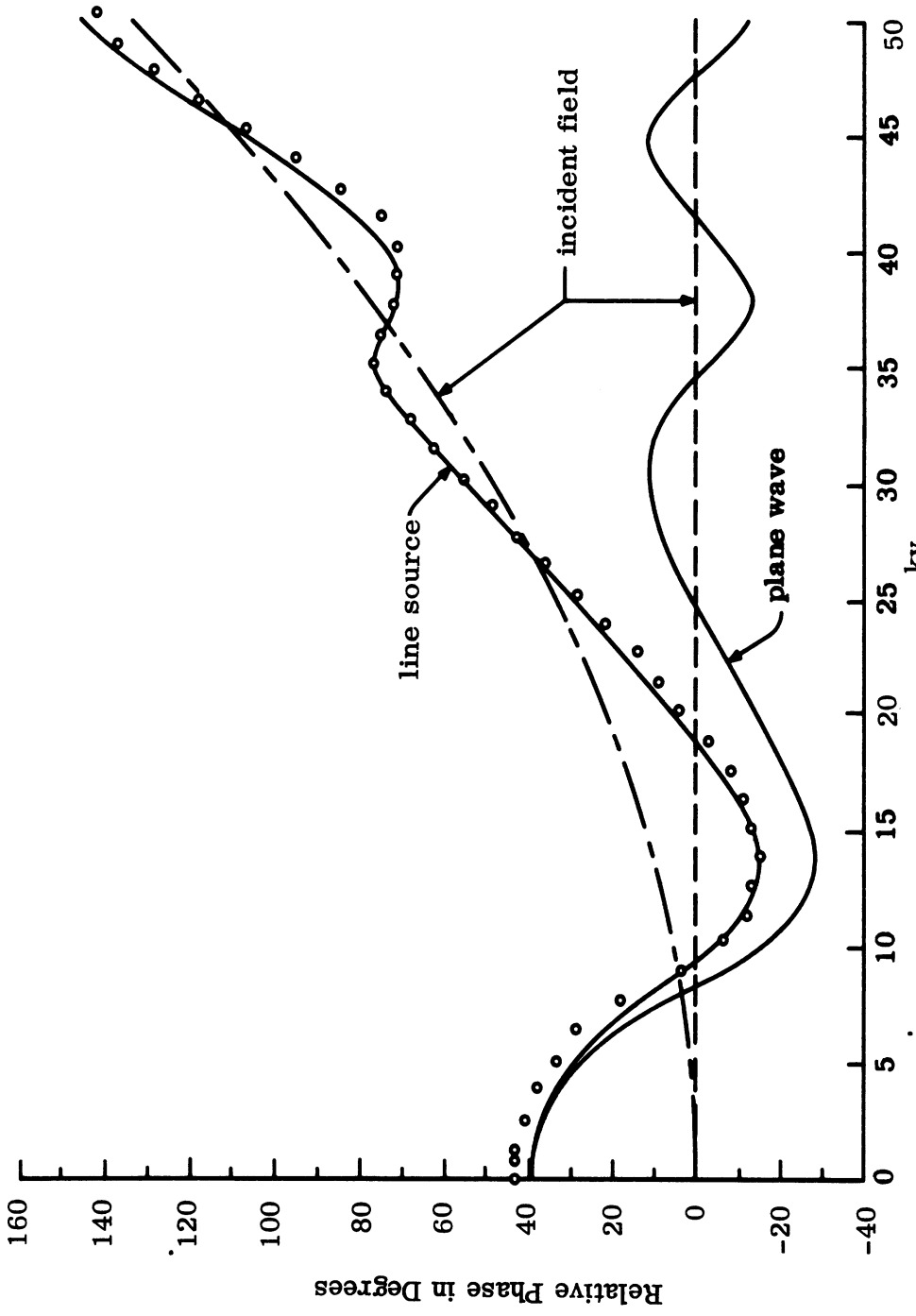

FIG. 6-20: MEASURED (•••) AND THEORETICAL (——) PHASE OF E_z FOR ka = 6.3 AND kx = 20π (Kodis, 1950).

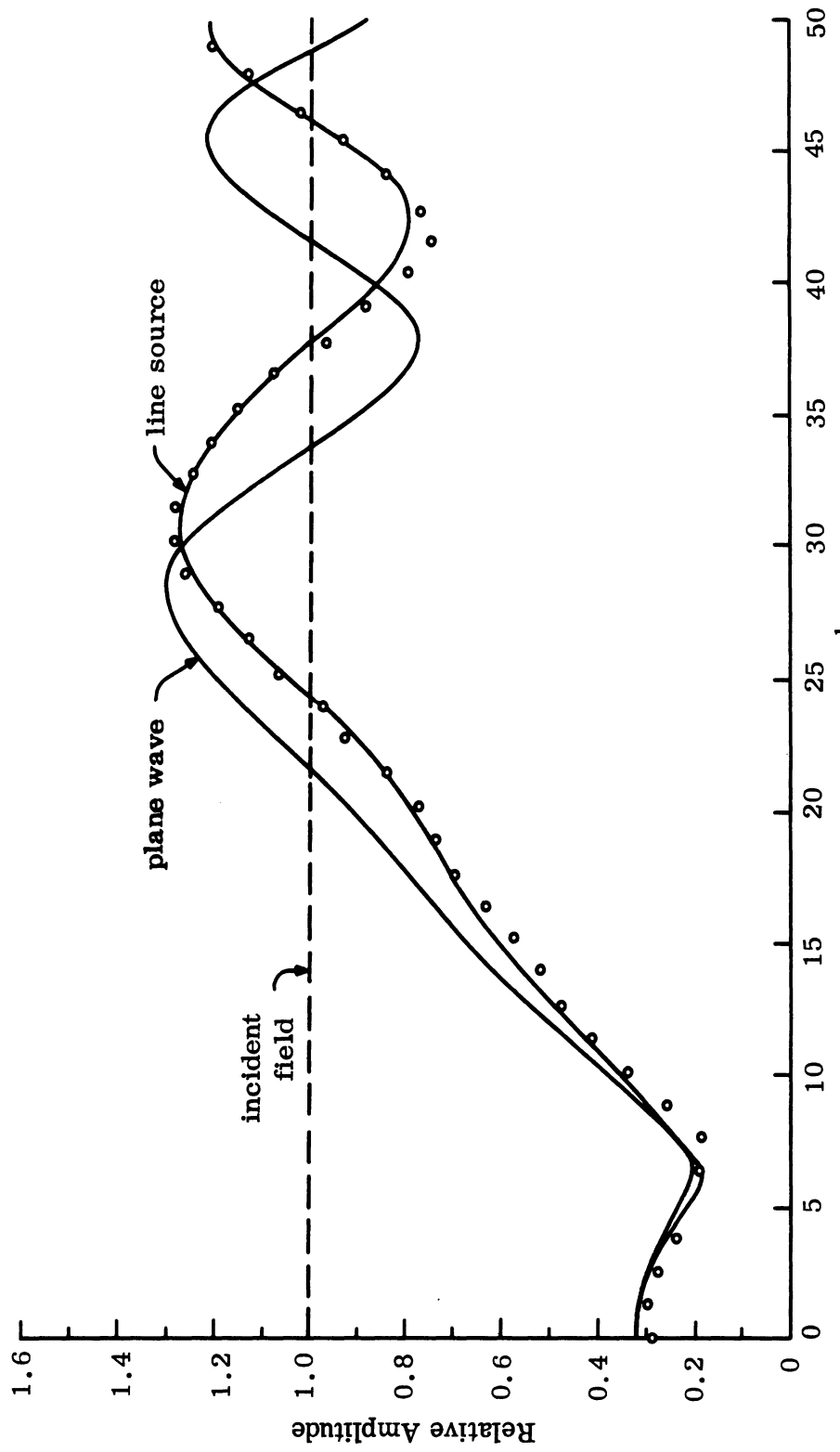

FIG. 6-21: MEASURED (∘ ∘ ∘) AND THEORETICAL (——) AMPLITUDE $|E_z|$ FOR ka = 10 AND kx = 20π (Kodis, 1950).

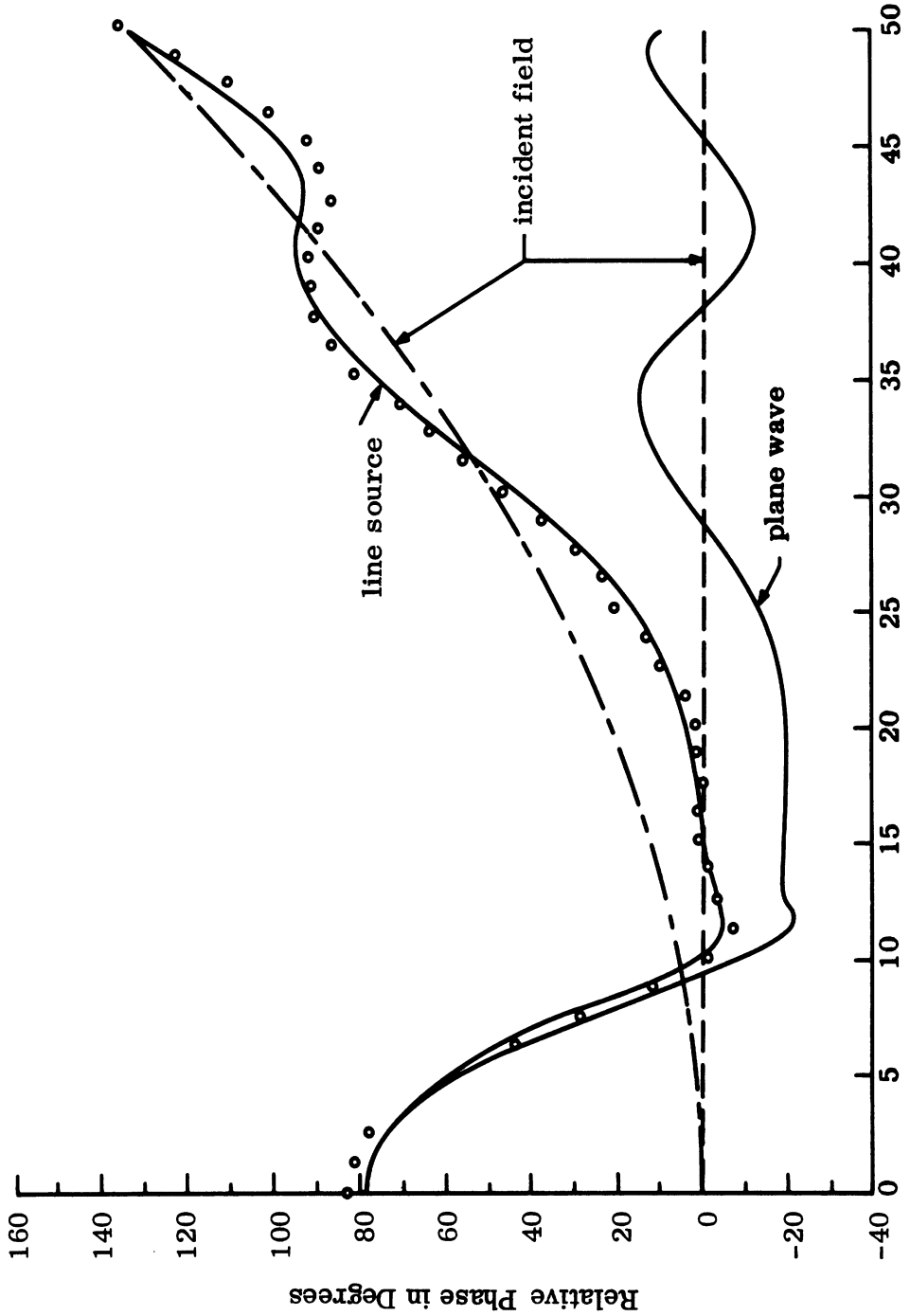

FIG. 6-22: MEASURED (• • •) AND THEORETICAL (—) PHASE OF E_z FOR ka = 10 AND kx = 20π (Kodis, 1950).

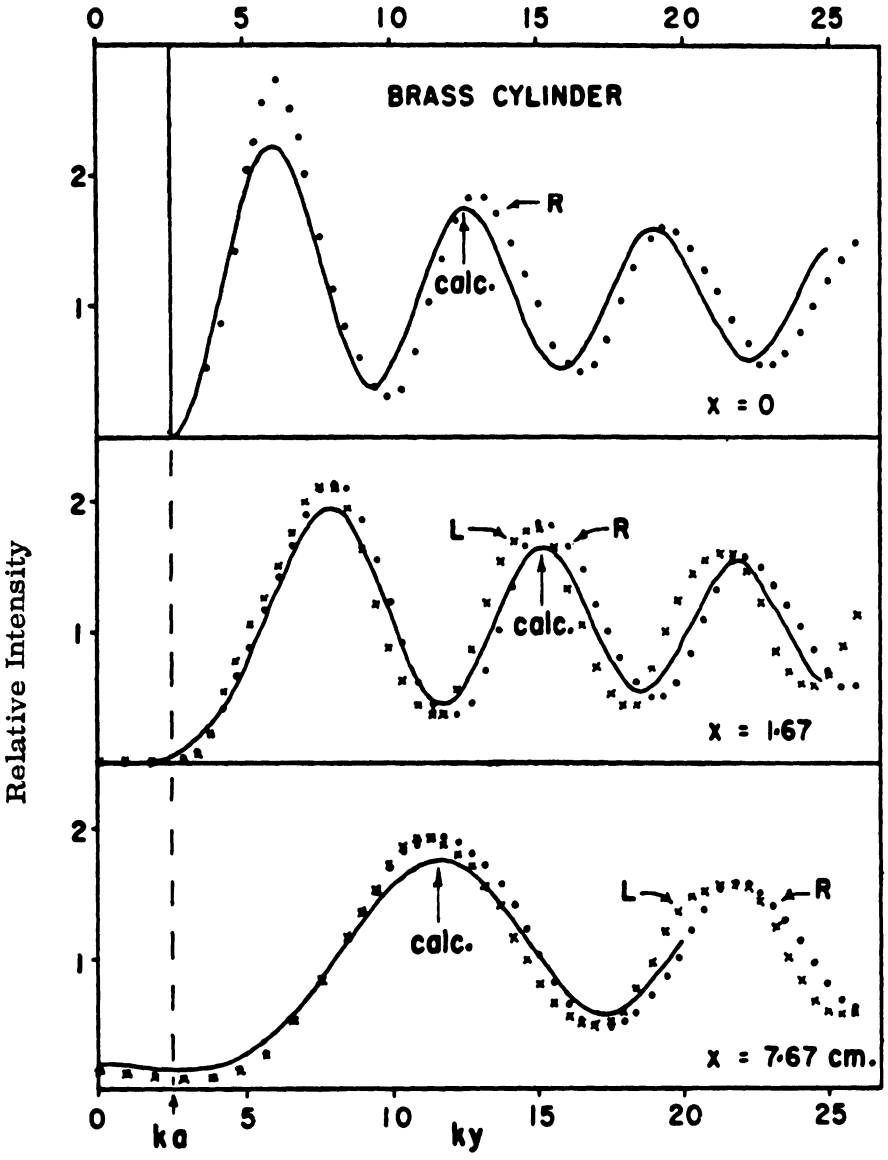

FIG. 6-23: MEASURED (o o o, x x x) AND THEORETICAL (——) RELATIVE INTENSITY OF THE TOTAL DIFFRACTED FIELD E_z FOR A BRASS CYLINDER; ka = 2.494 (L - left of the cylinder, R - right of the cylinder) (Wiles and McLay, 1954).

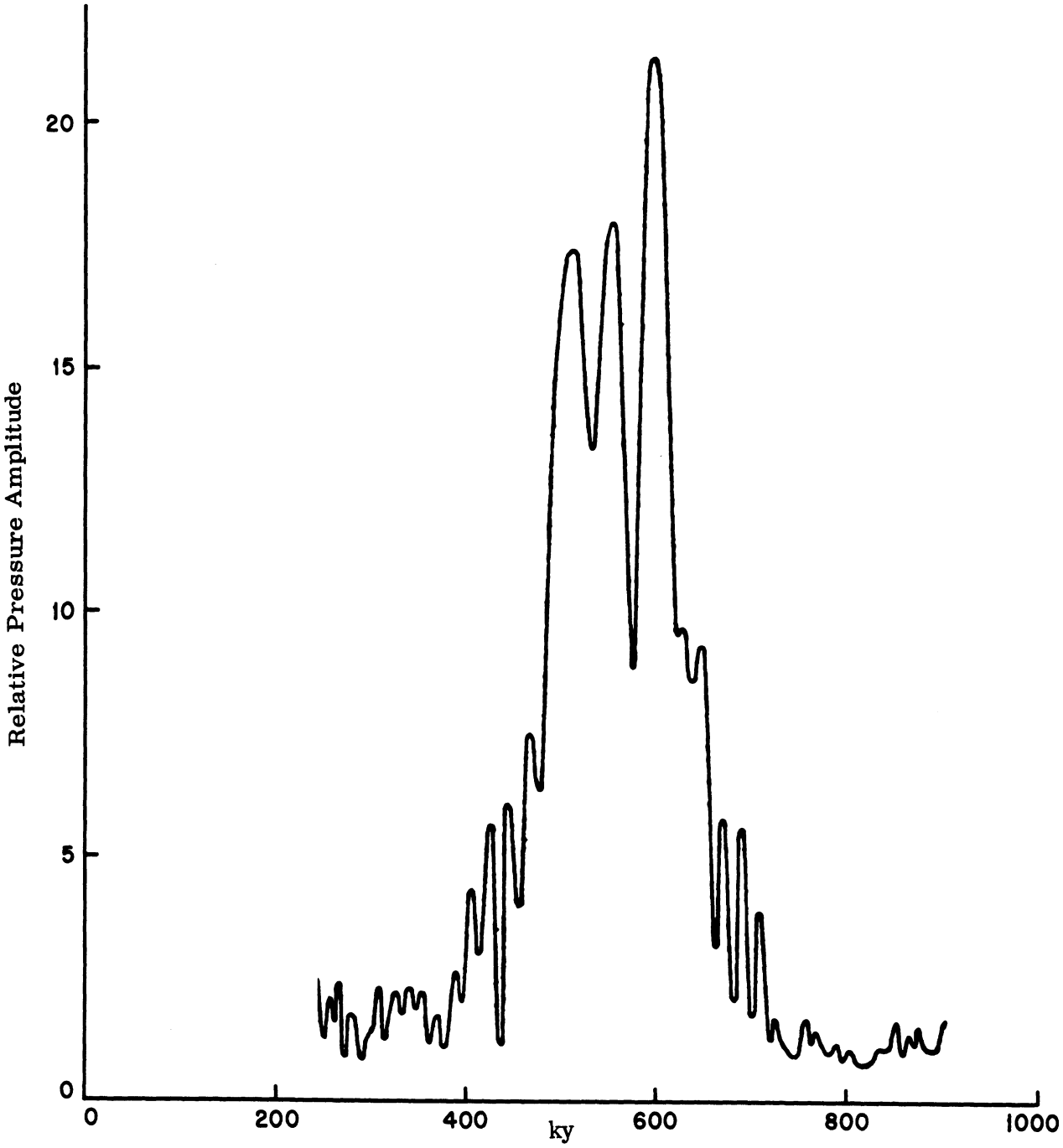

FIG. 6-24: RELATIVE SCATTERED PRESSURE AMPLITUDE FOR A 1/4 IN. STEEL ROD RITH ka = 14.4, x_o = 12.7 cm AND x = 6.6 cm (Bauer et al, 1948).

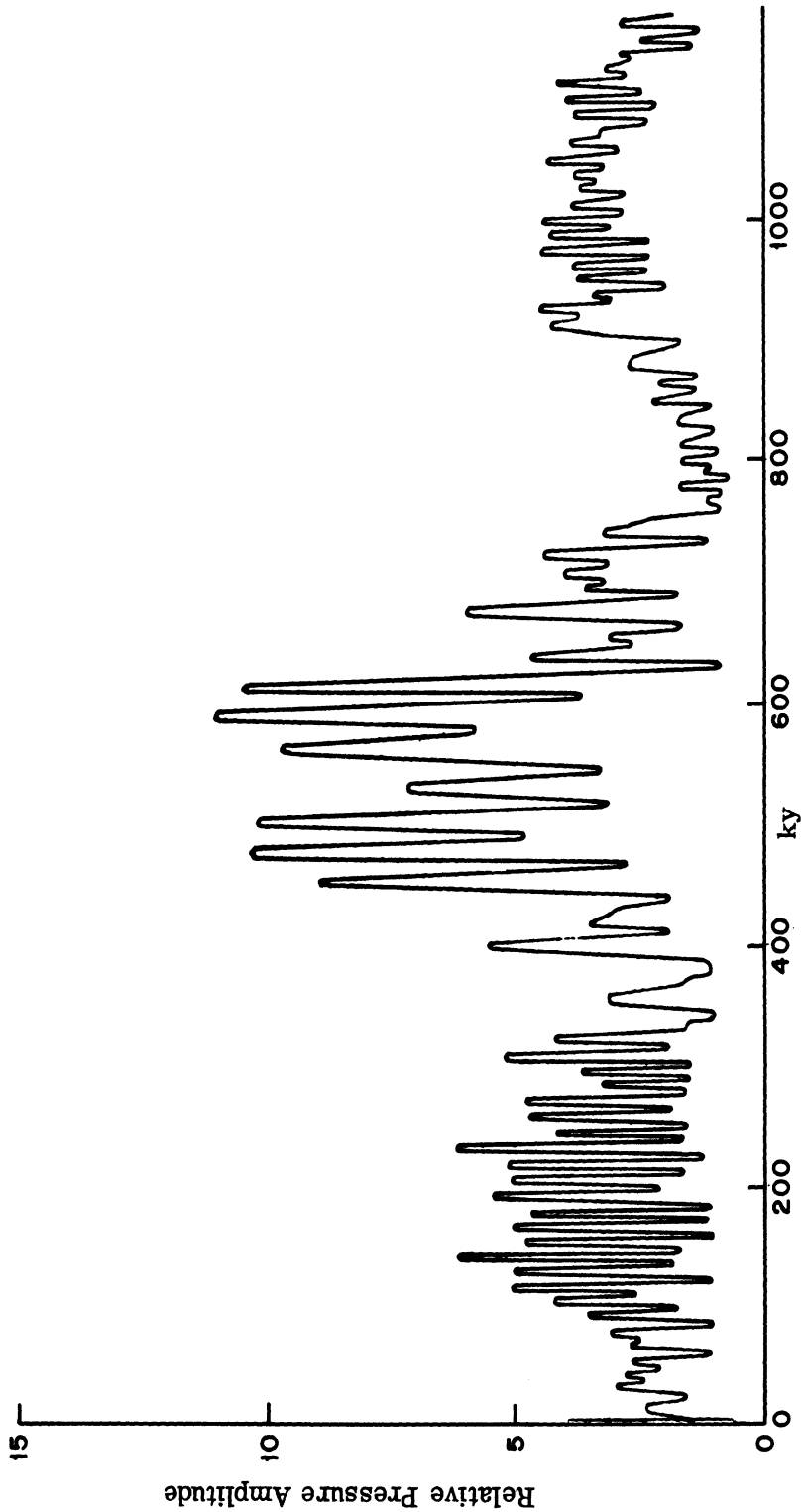

FIG. 6-25: RELATIVE SCATTERED PRESSURE AMPLITUDE FOR A 1/2 IN. STEEL ROD WITH ka = 28.8, x_o = 12.7 cm AND x = 6.6 cm (Bauer et al, 1948).

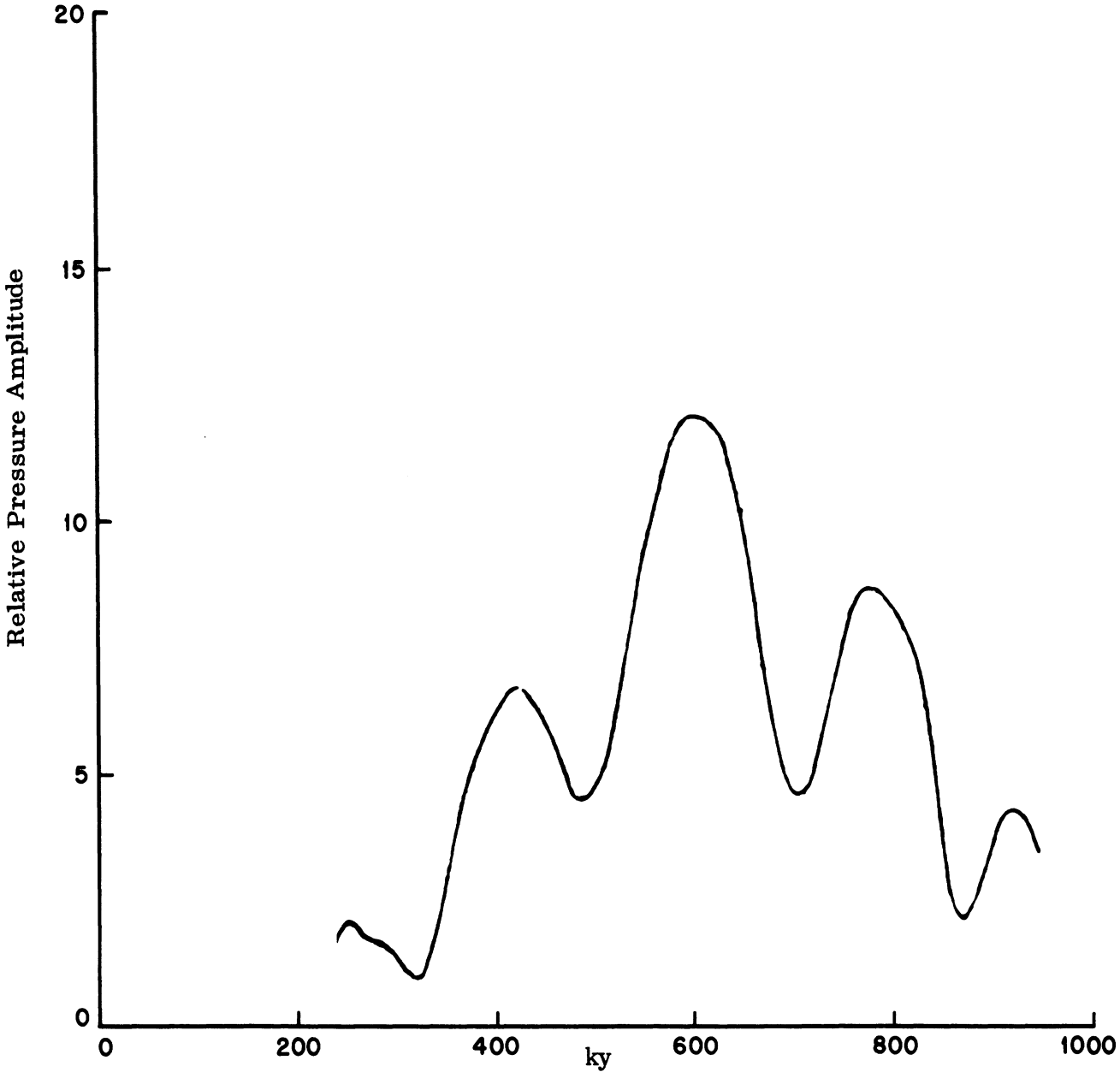

FIG. 6-26: RELATIVE SCATTERED PRESSURE AMPLITUDE FOR A 1/4 IN. STEEL ROD WITH ka = 14.4, x_o = 12.7 cm AND x = 46.6 cm (Bauer et al, 1948).

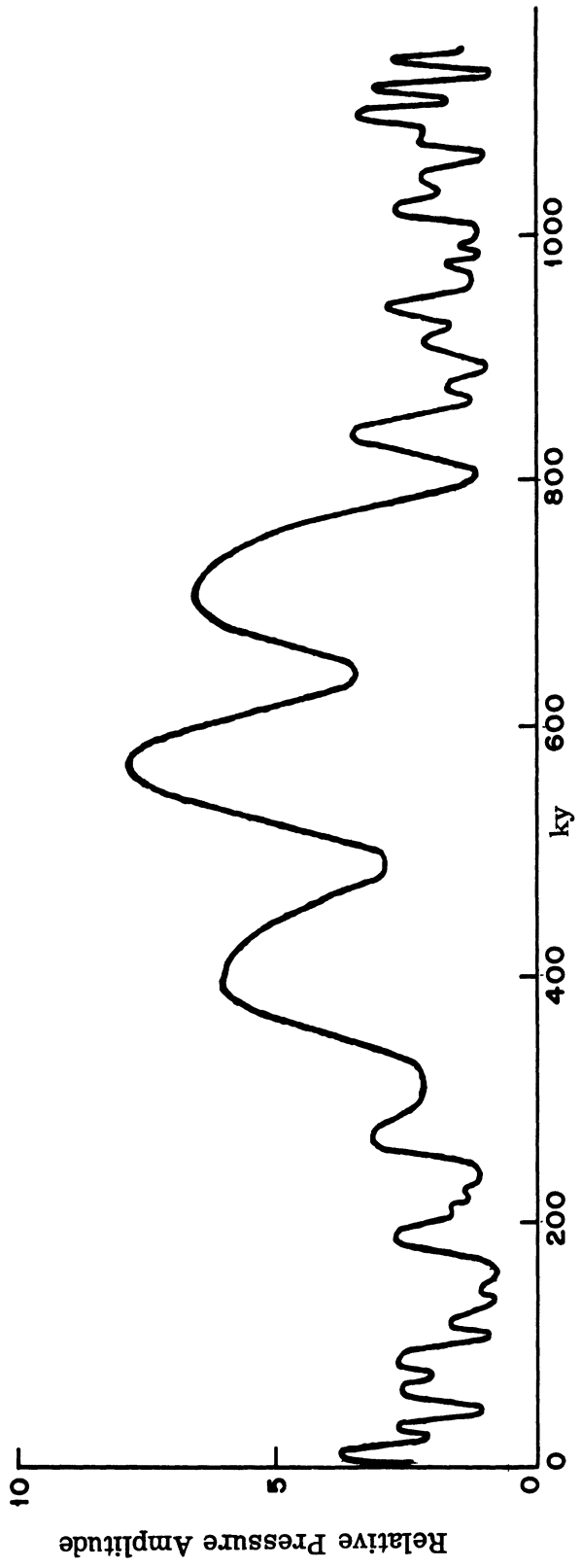

FIG. 6-27: RELATIVE SCATTERED PRESSURE AMPLITUDE FOR A 1/2" IN. STEEL ROD WITH ka = 28.8, x_o = 12.7 cm AND x = 46.6 cm (Bauer et al, 1948).

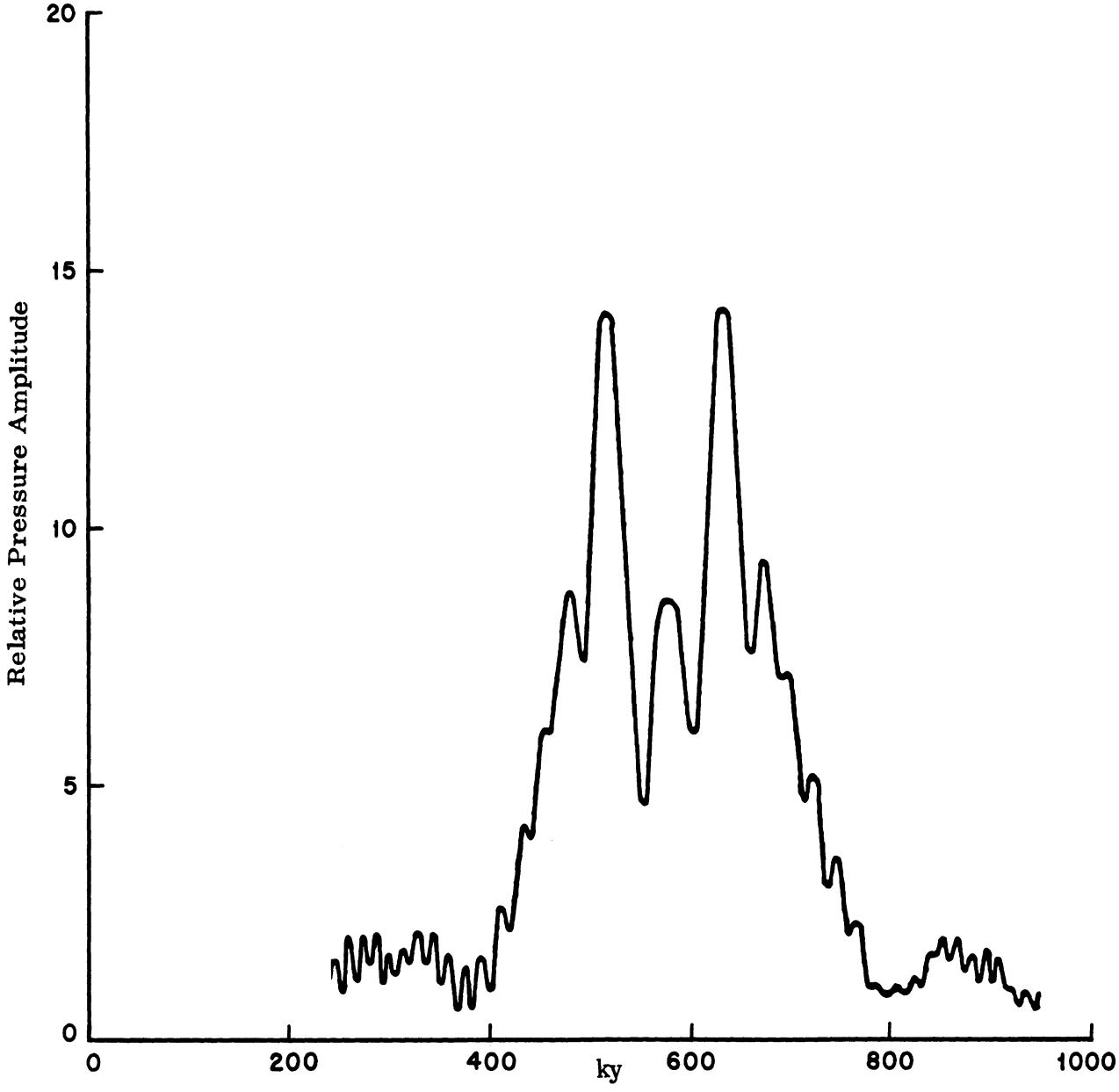

FIG. 6-28: RELATIVE SCATTERED PRESSURE AMPLITUDE FOR A 1/4 IN. STEEL ROD WITH ka = 14.4, x_o = 54.3 cm AND x = 10 cm (Bauer et al, 1948).

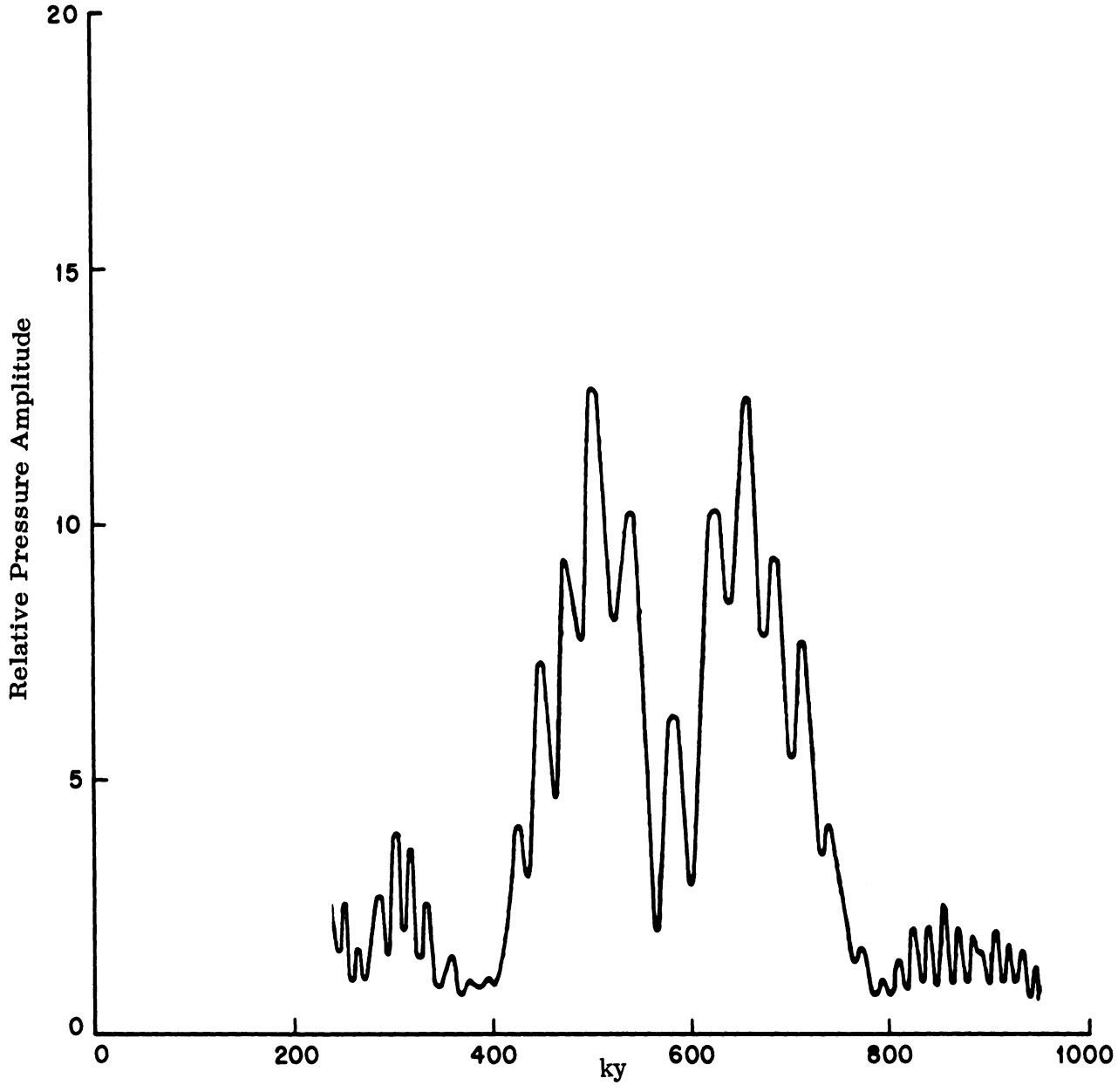

FIG. 6-29: RELATIVE SCATTERED PRESSURE AMPLITUDE FOR A 1/2 IN. STEEL ROD WITH ka = 28.8, x_o = 54.3 cm AND x = 10 cm (Bauer et al, 1948).

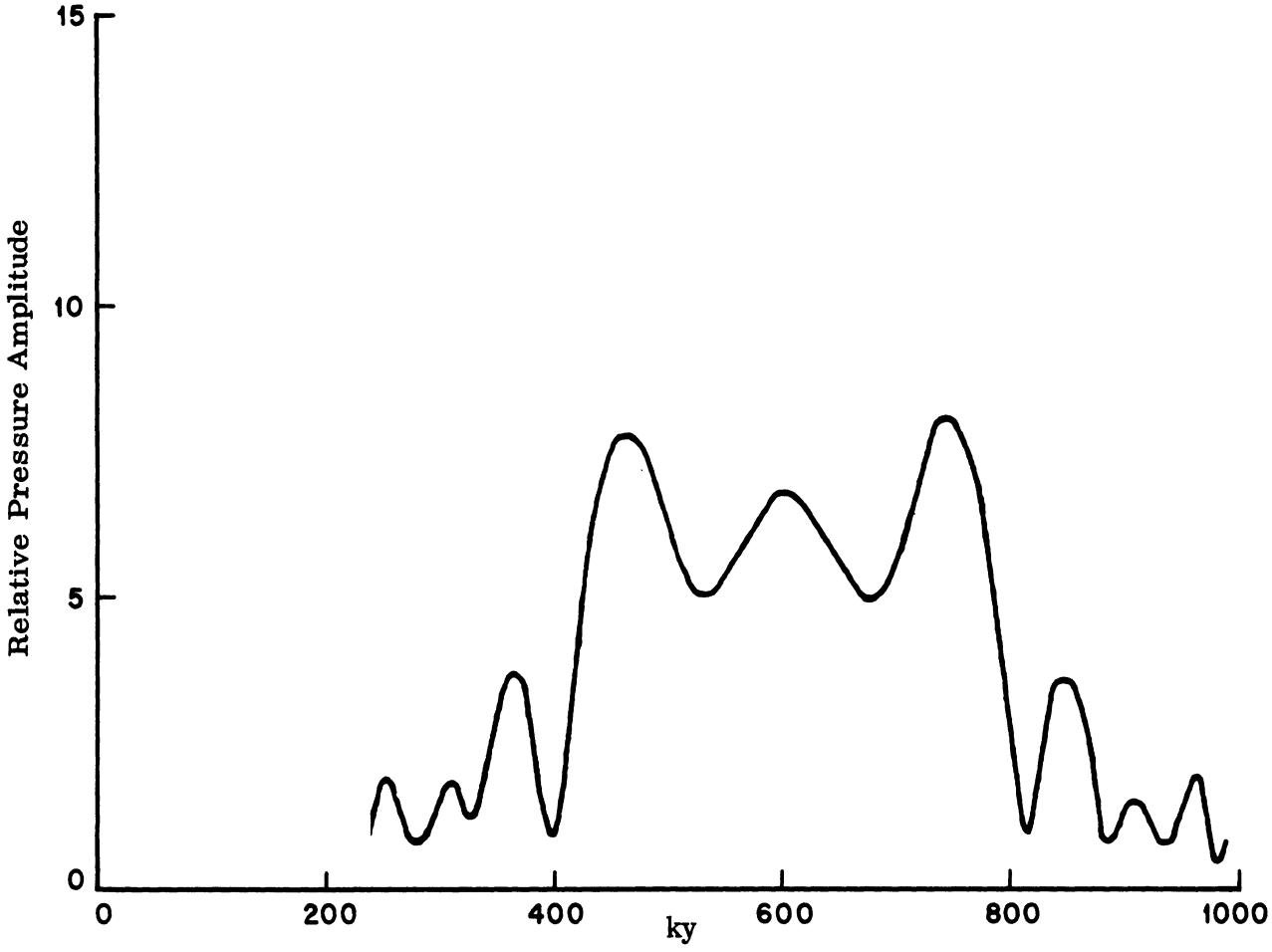

FIG. 6-30: RELATIVE SCATTERED PRESSURE AMPLITUDE FOR A 1/4 IN. STEEL ROD WITH ka = 14.4, x_o = 54.3 cm AND x = 40 cm (Bauer et al, 1948).

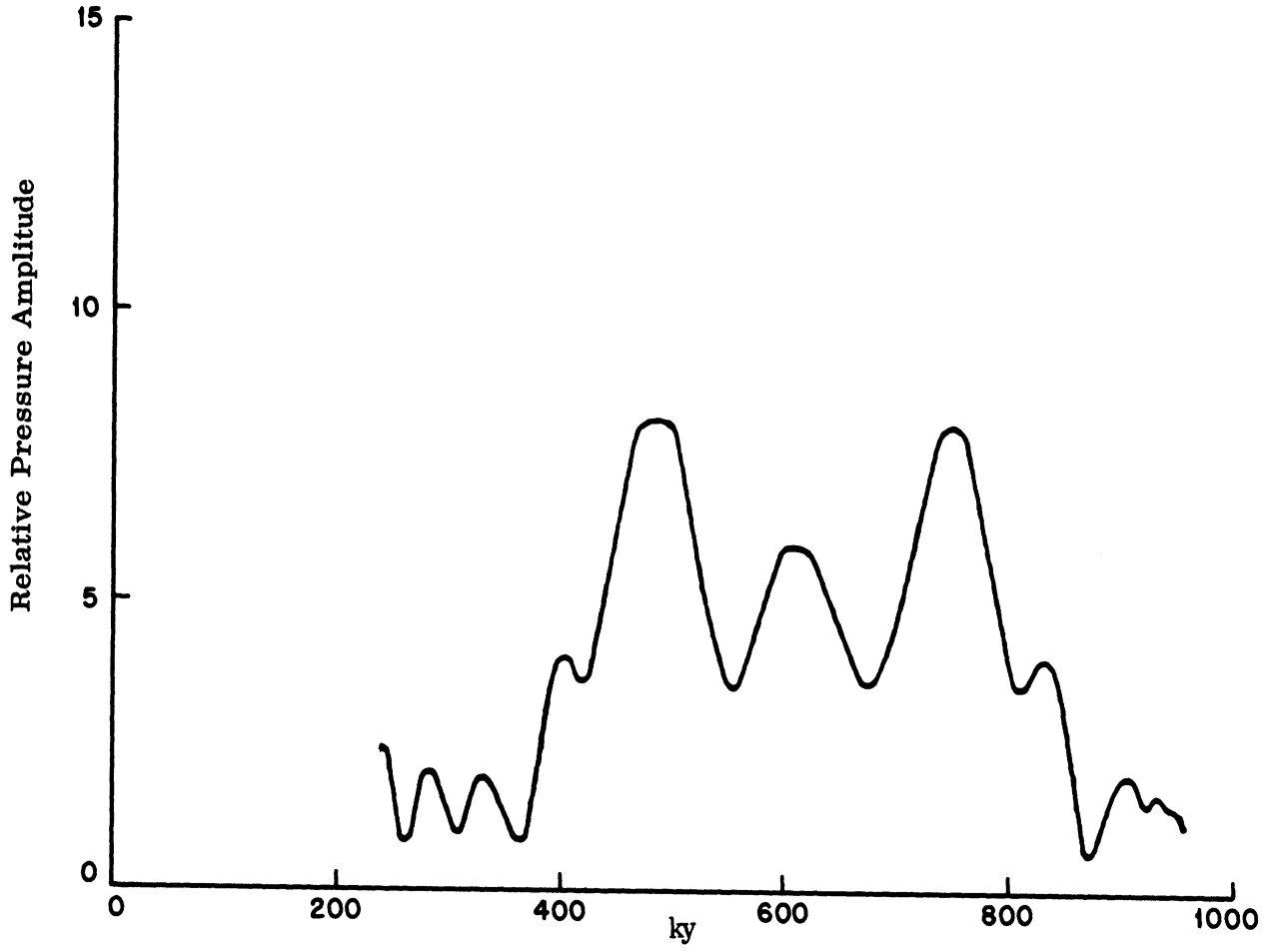

FIG. 6-31: RELATIVE SCATTERED PRESSURE AMPLITUDE FOR A 1/2 IN. STEEL ROD WITH ka = 28.8, x_o = 54.3 cm AND x = 40 cm (Bauer et al, 1948).

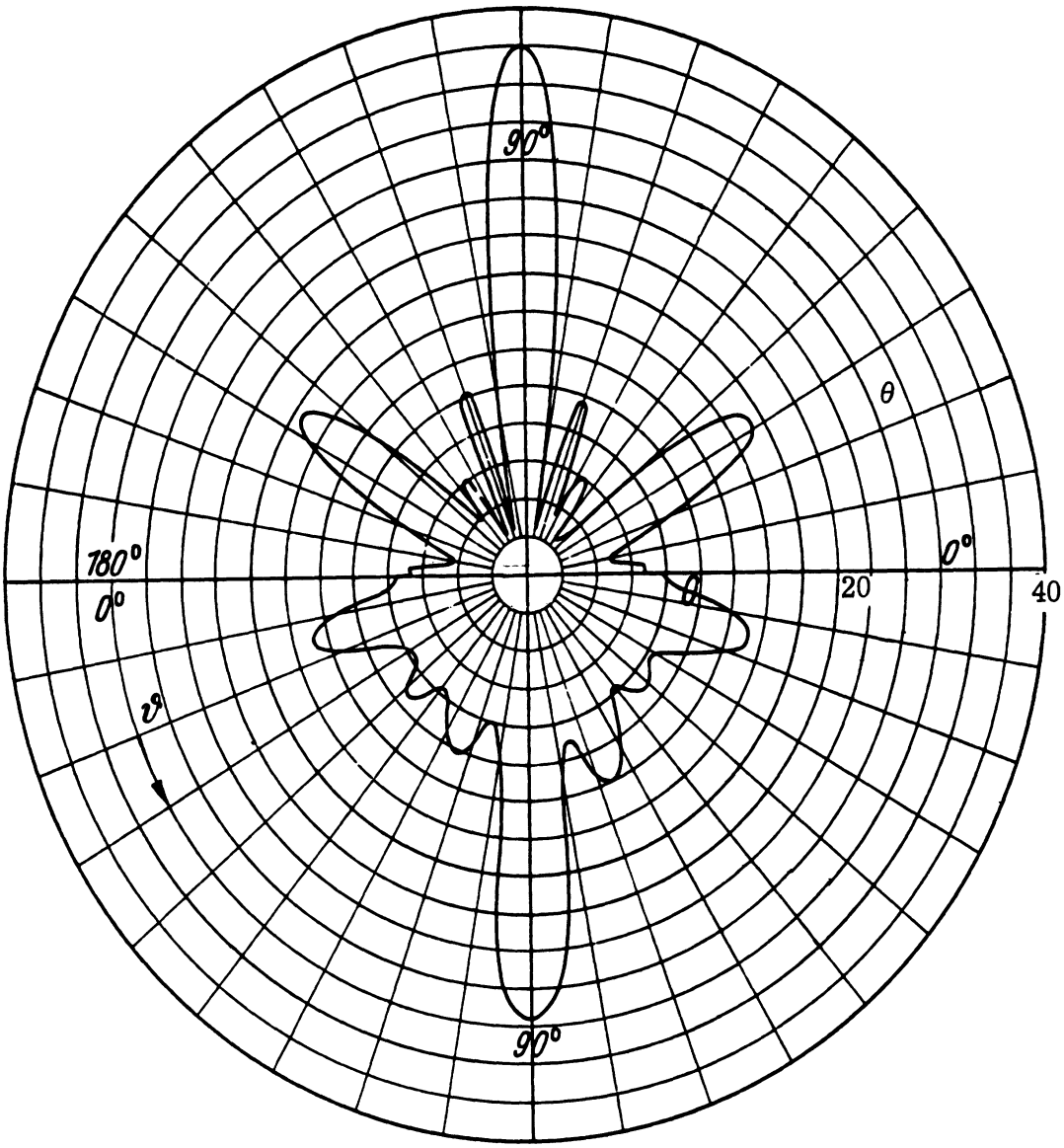

FIG. 6-32: BACK SCATTERING CROSS SECTION (IN db/cm^2) FOR INCIDENCE AT ANGLE θ TO CYLINDER AXIS. UPPER HALF: $\sigma_{||}$ ($\underline{E}^i$ PARALLEL TO AXIS); LOWER HALF: $\sigma_{\perp}$ ($\underline{E}^i$ PERPENDICULAR TO AXIS); ℓ = 6 cm, λ = 3.2 cm, ka = 0.588 (Meyer et al, 1959).

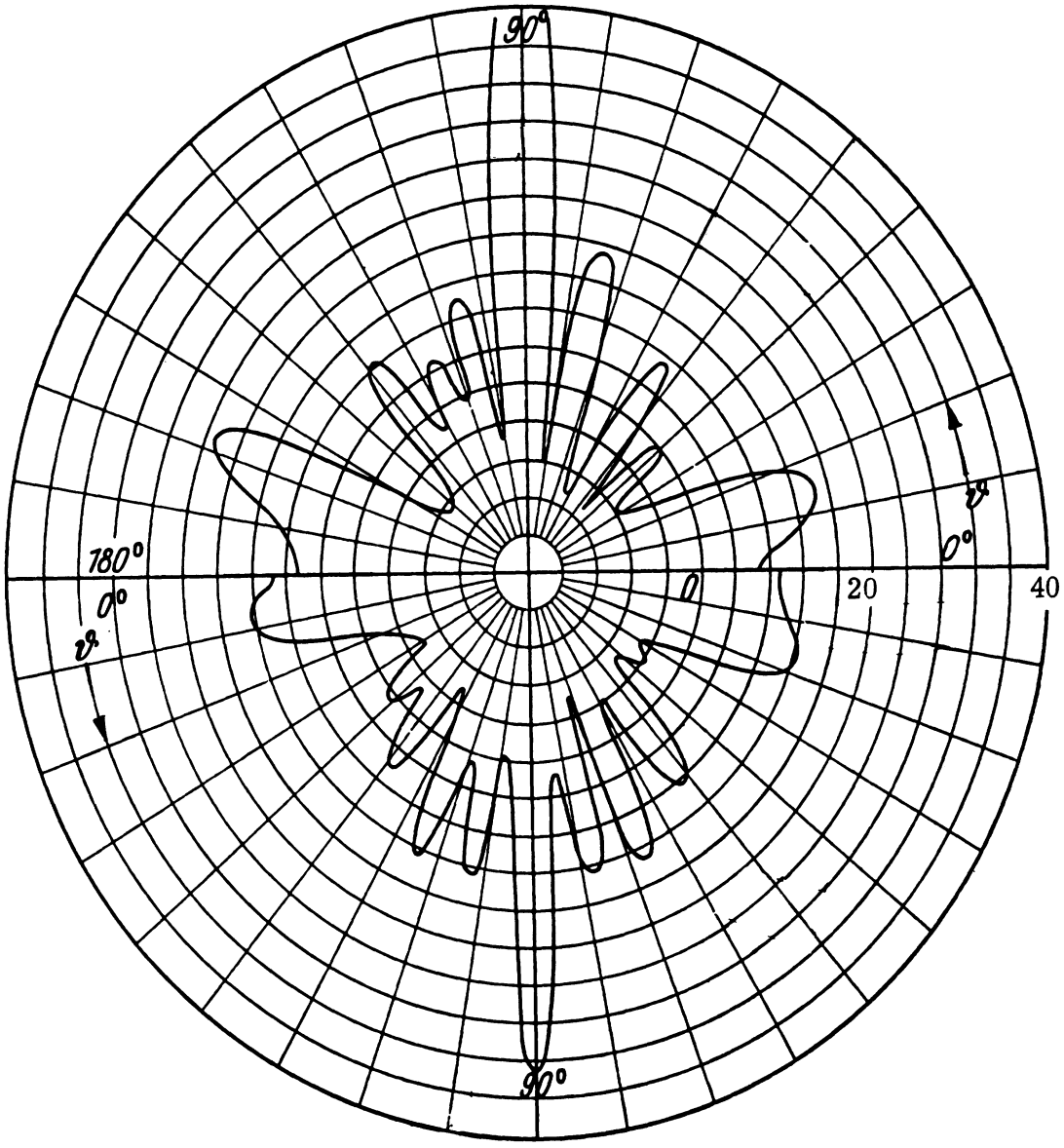

FIG. 6-33: BACK SCATTERING CROSS SECTION (IN db/cm^2) FOR INCIDENCE AT ANGLE θ TO CYLINDER AXIS. UPPER HALF: $\sigma_{||}$ ($\underline{E}^i$ PARALLEL TO AXIS); LOWER HALF: $\sigma_{\perp}$ ($\underline{E}^i$ PERPENDICULAR TO AXIS); $\ell = 9$ cm, $\lambda = 3.2$ cm, ka = .882 (Meyer et al, 1959).

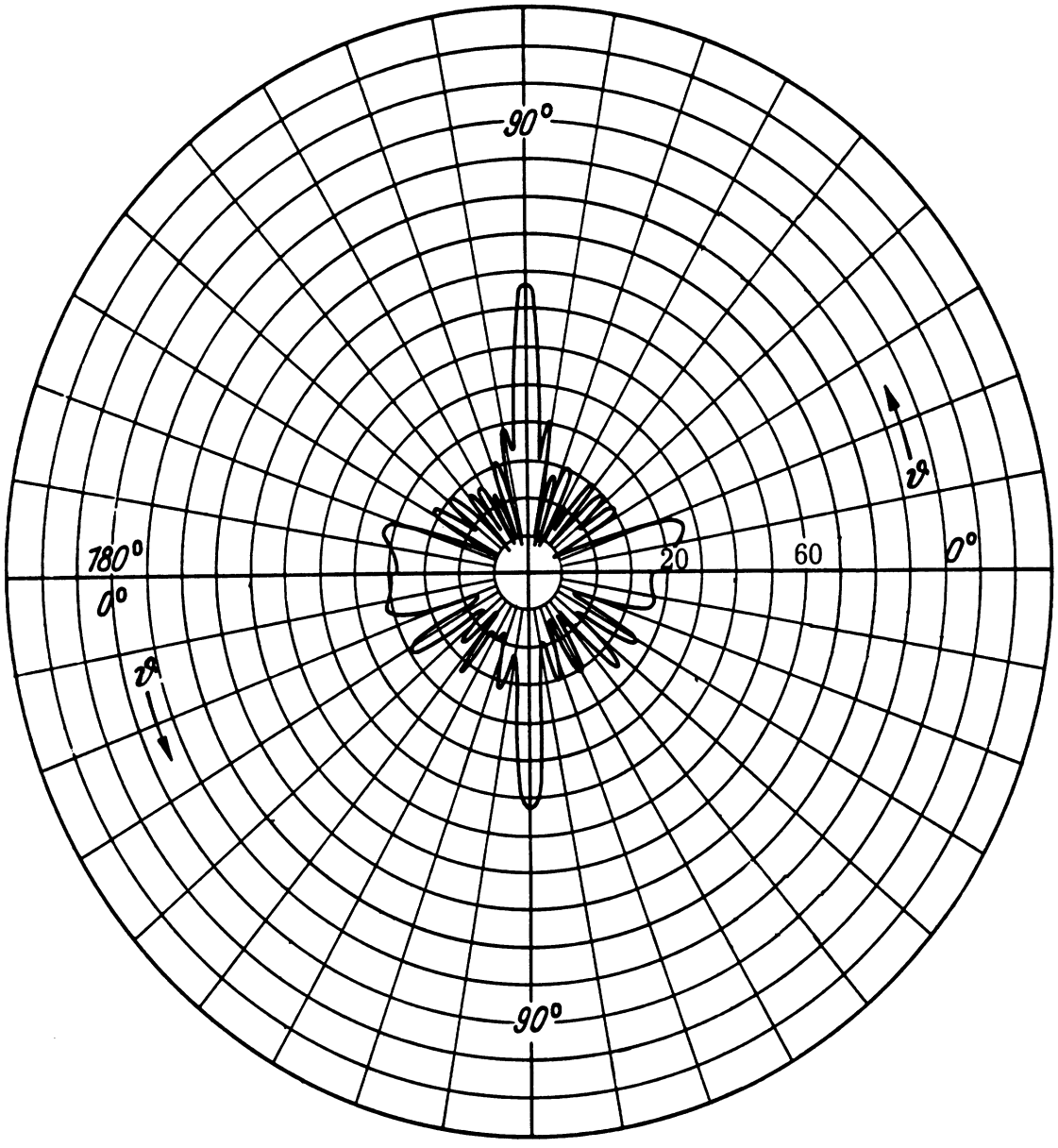

FIG. 6-34: BACK SCATTERING CROSS SECTION (IN db/cm^2) FOR INCIDENCE AT ANGLE θ TO CYLINDER AXIS. UPPER HALF: $\sigma_{||}$ ($\underline{E}^i$ PARALLEL TO AXIS); LOWER HALF: $\sigma_{\perp}$ ($\underline{E}^i$ PERPENDICULAR TO AXIS; ℓ = 14 cm, λ = 3.2 cm, ka = 1.375 (Meyer et al, 1959).

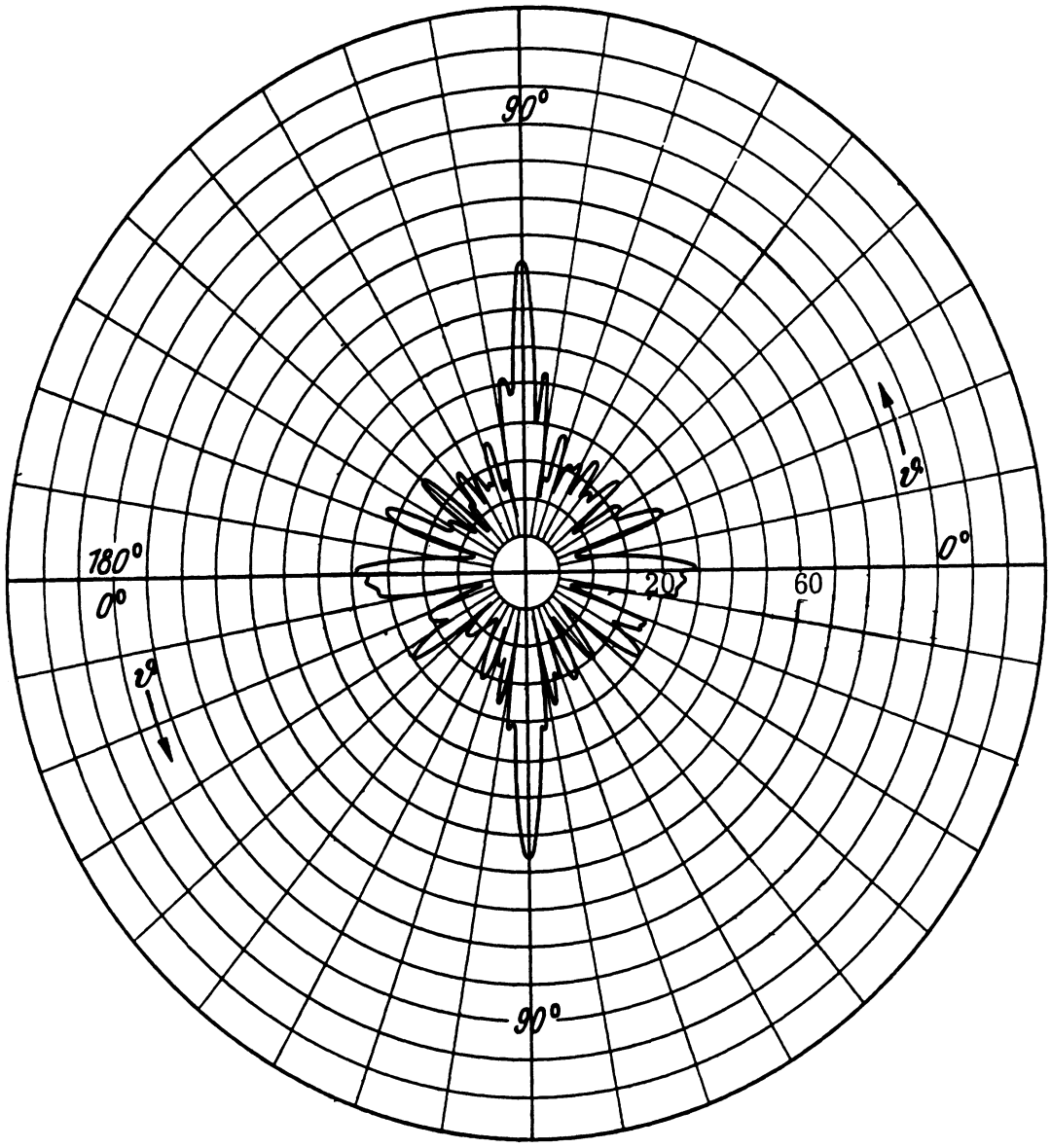

FIG. 6-35: BACK SCATTERING CROSS SECTION (IN db/cm^2) FOR INCIDENCE AT ANGLE θ TO CYLINDER AXIS. UPPER HALF: $\sigma_{||}$ ($\underline{E}^i$ PARALLEL TO AXIS); LOWER HALF: $\sigma_{\perp}$ ($\underline{E}^i$ PERPENDICULAR TO AXIS); ℓ = 18 cm, λ = 3.2 cm AND ka = 1.766 (Meyer et al, 1959).

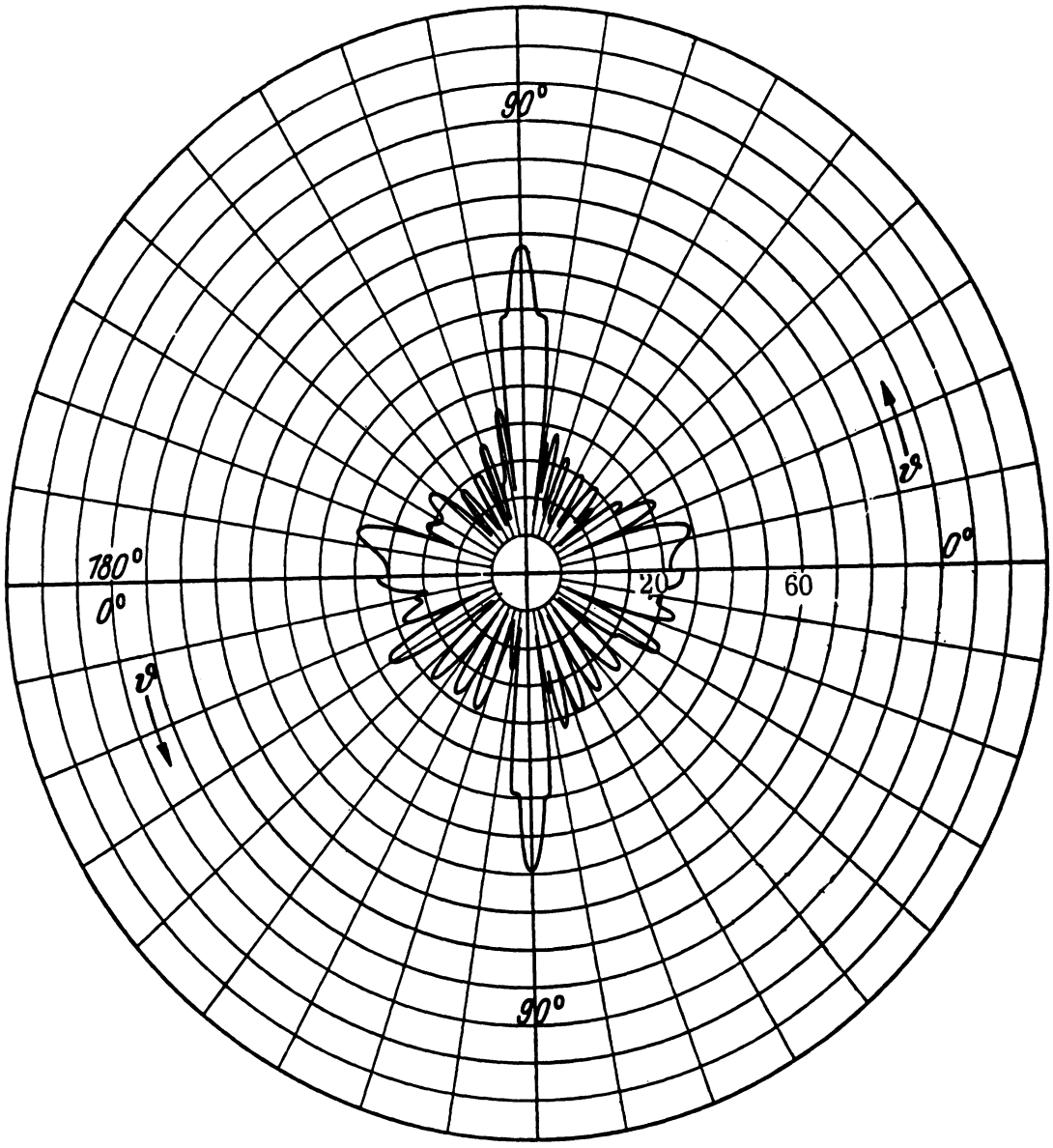

FIG. 6-36: BACK SCATTERING CROSS SECTION (IN db/cm^2) FOR INCIDENCE AT ANGLE θ TO CYLINDER AXIS. UPPER HALF: $\sigma_{\parallel}$ ($\underline{E}^i$ PARALLEL TO AXIS; LOWER HALF: $\sigma_{\perp}$ ($\underline{E}^i$ PERPENDICULAR TO AXIS); ℓ = 22 cm, λ = 3.2 cm, ka = 2.16 (Meyer et al, 1959).

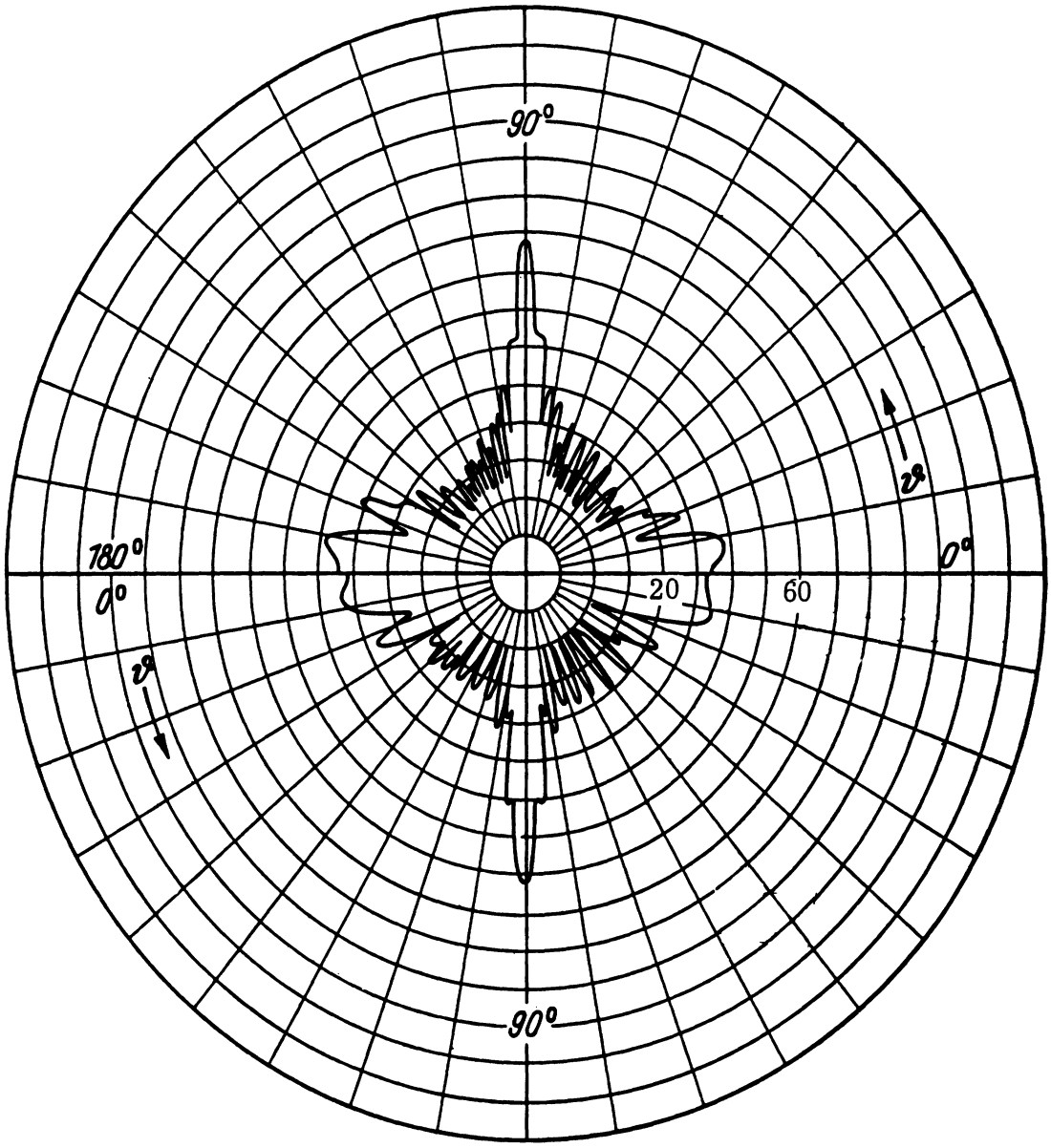

FIG. 6-37: BACK SCATTERING CROSS SECTION (IN db/cm^2) FOR INCIDENCE AT ANGLE θ TO CYLINDER AXIS. UPPER HALF: $\sigma_{||}$ ($\underline{E}^i$ PARALLEL TO AXIS; LOWER HALF: $\sigma_{\perp}$ ($\underline{E}^i$ PERPENDICULAR TO AXIS); ℓ = 28 cm, λ = 3.2 cm, ka = 2.74 (Meyer et al, 1959).

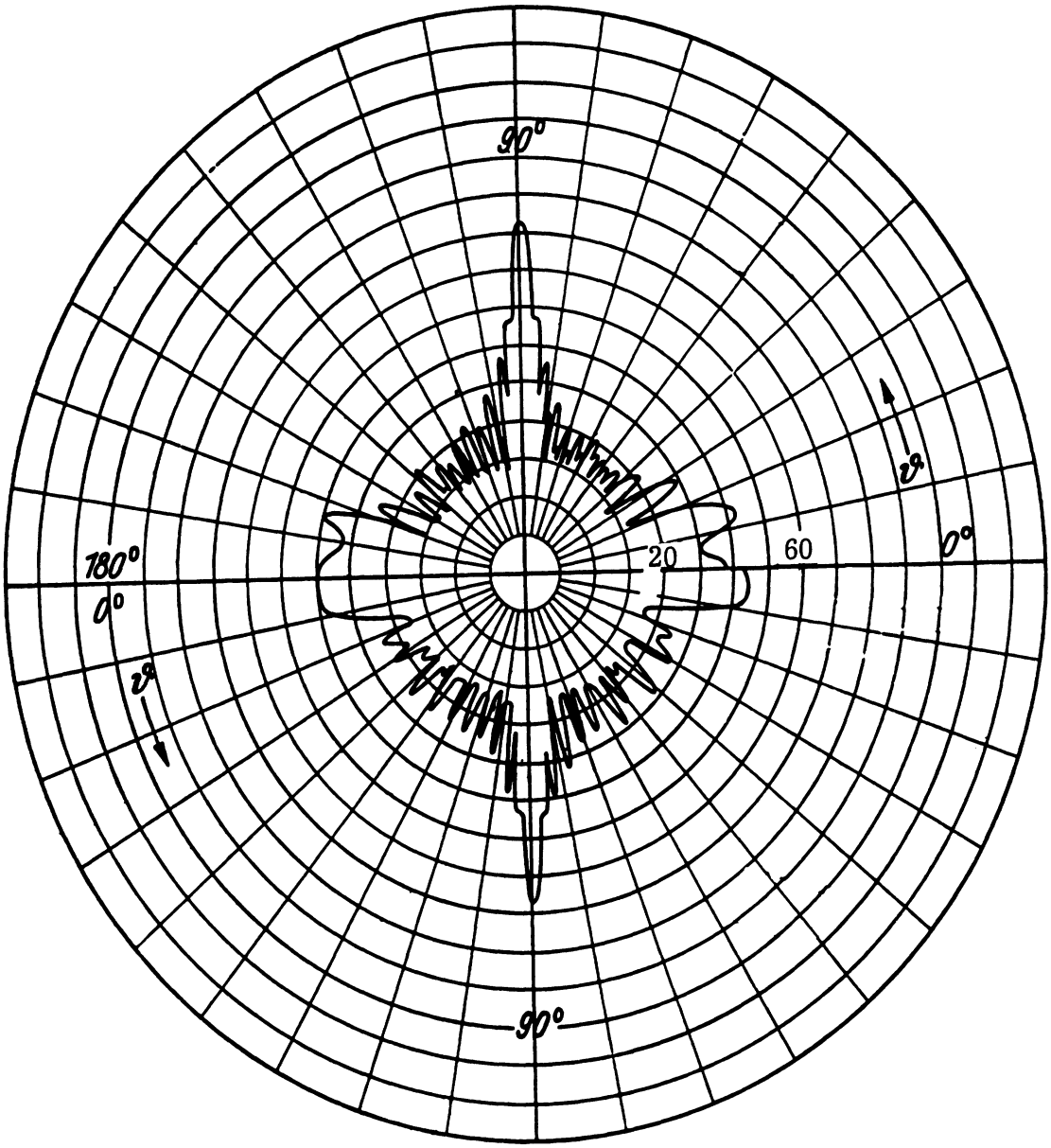

FIG. 6-38: BACK SCATTERING CROSS SECTION (IN db/cm^2) FOR INCIDENCE AT ANGLE θ TO CYLINDER AXIS. UPPER HALF: $\sigma_{||}$ ($\underline{E}^i$ PARALLEL TO AXIS); LOWER HALF: $\sigma_{\perp}$ ($\underline{E}^i$ PERPENDICULAR TO AXIS); ℓ = 32 cm, λ = 3.2 cm, ka = 3.14 (Meyer et al, 1959).

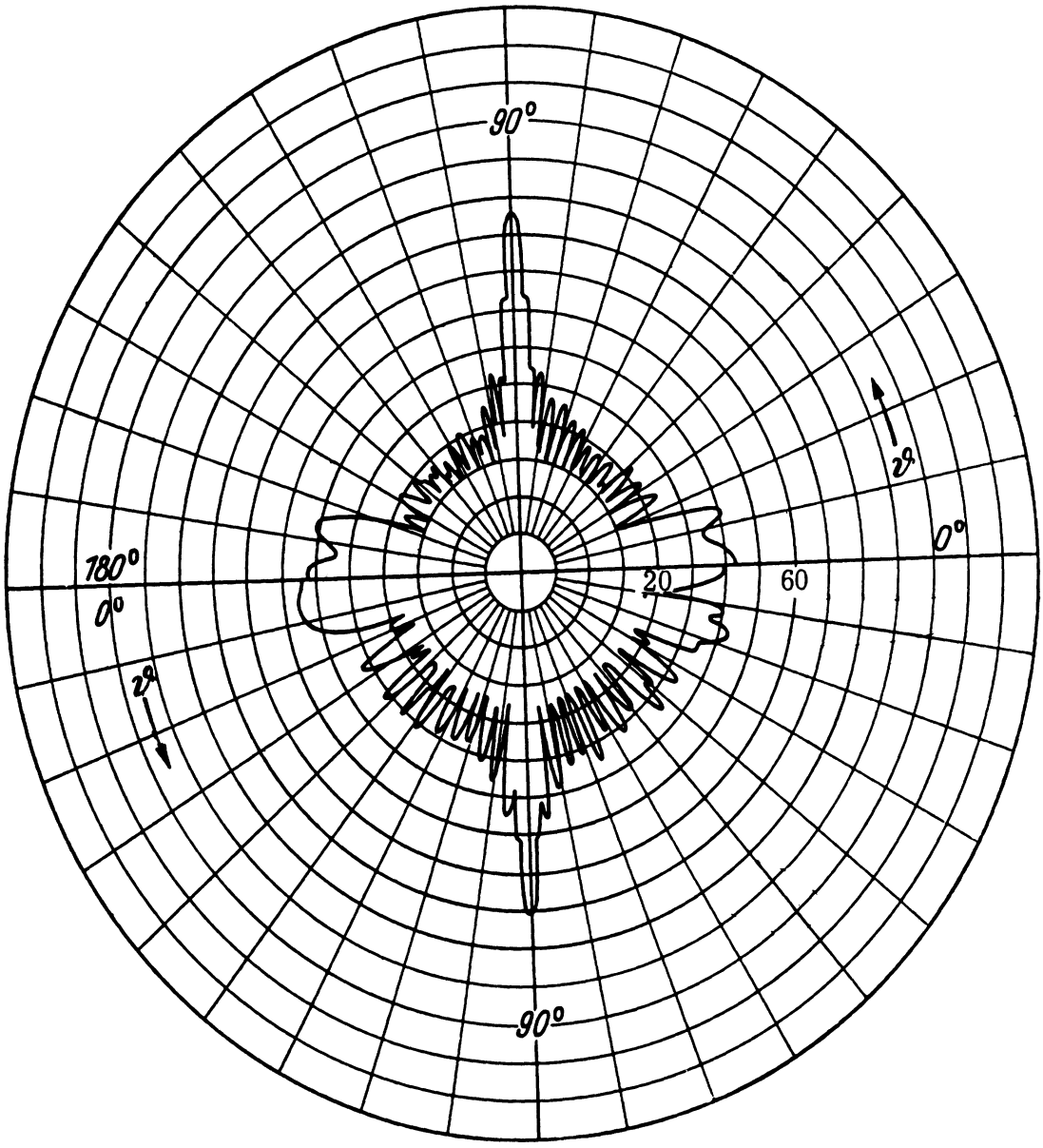

FIG. 6-39: BACK SCATTERING CROSS SECTION (IN db/cm^2) FOR INCIDENCE AT ANGLE θ TO CYLINDER AXIS. UPPER HALF: $\sigma_{||}$ ($\underline{E}^i$ PARALLEL TO AXIS); LOWER HALF: $\sigma_{\perp}$ ($\underline{E}^i$ PERPENDICULAR TO AXIS); ℓ = 40 cm, λ = 3.2 cm, ka = 3.92 (Meyer et al, 1959).

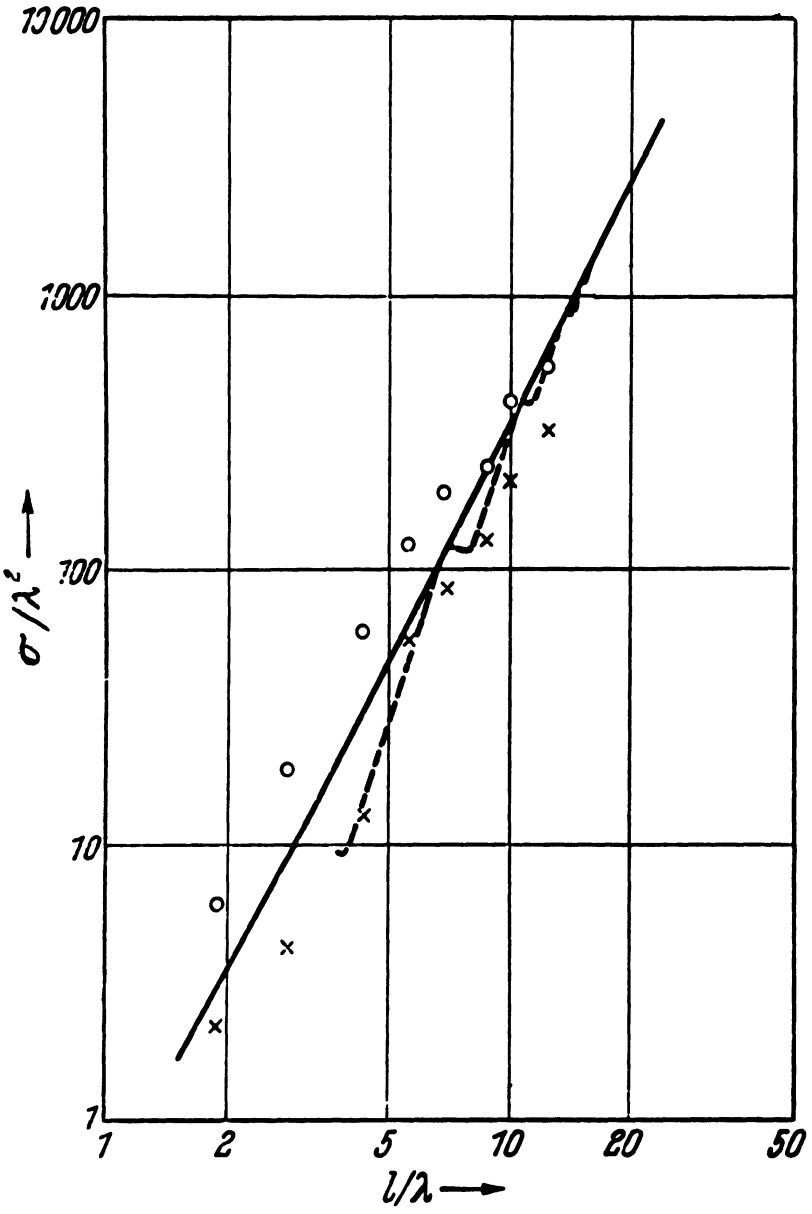

FIG. 6-40: MAXIMUM BACK SCATTERING CROSS SECTION ($\theta = 90^{o}$) OF A CYLINDER AS A FUNCTION OF LENGTH. MEASURED (o o o) AND THEORETICAL (——) $\sigma_{||}$; MEASURED (x x x) AND THEORETICAL (– – –) $\sigma_{\perp}$ (Meyer et al, 1959).

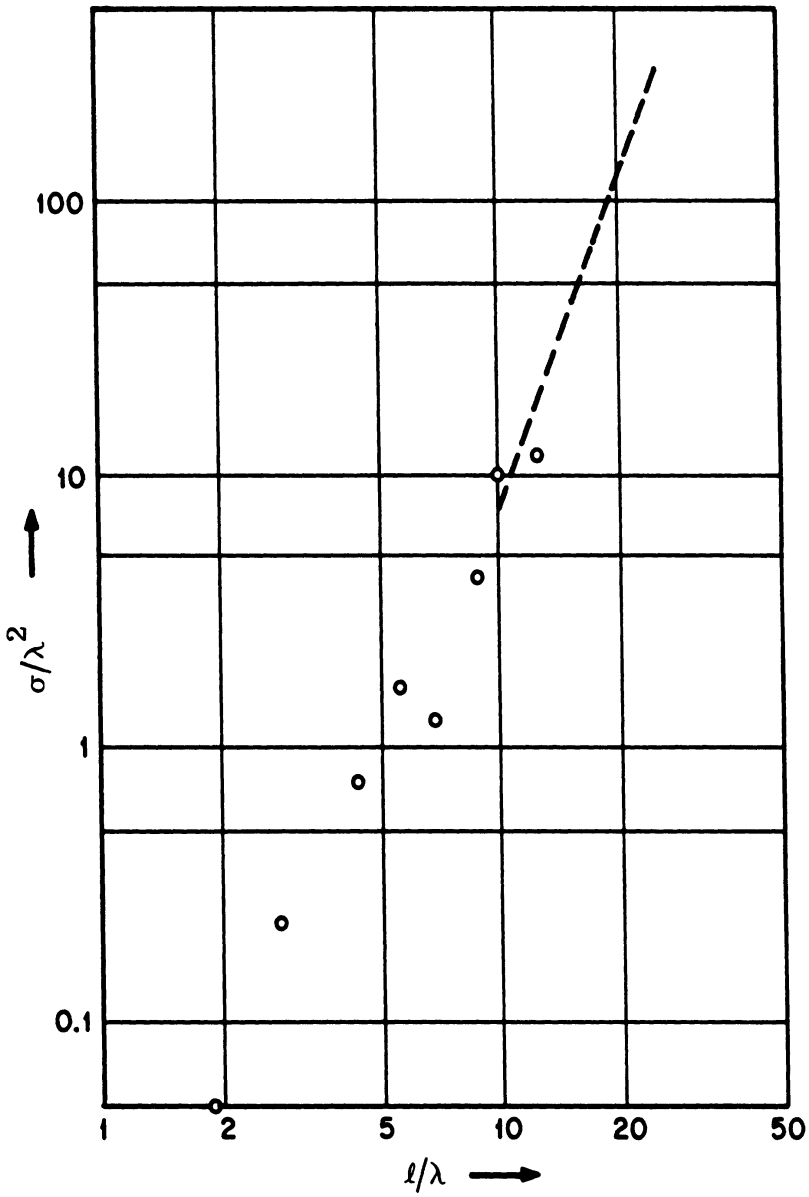

FIG. 6-41: MEASURED (∘ ∘ ∘) AND PHYSICAL OPTICS (– – –) BACK SCATTERING CROSS SECTION IN THE AXIAL DIRECTION ($\theta = 0^o$ or 180^o) (Meyer et al, 1959).

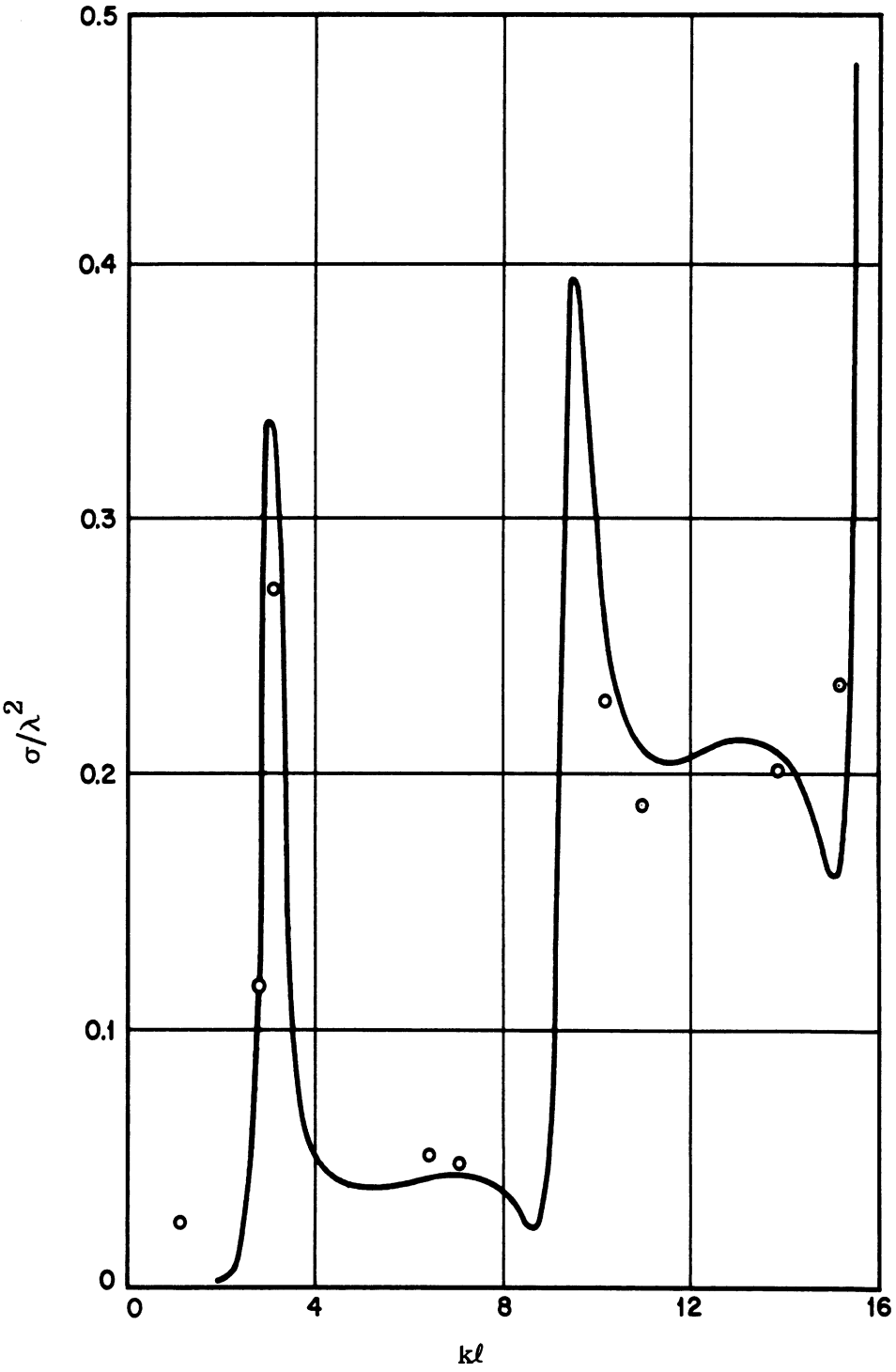

FIG. 6-42: BACK SCATTERING CROSS SECTION OF THIN WIRE AT BROADSIDE INCIDENCE FOR ℓ/a = 900; EXPERIMENTAL (o o o) (Van Vleck et al, 1947); THEORETICAL (——) (Lindroth, 1955).

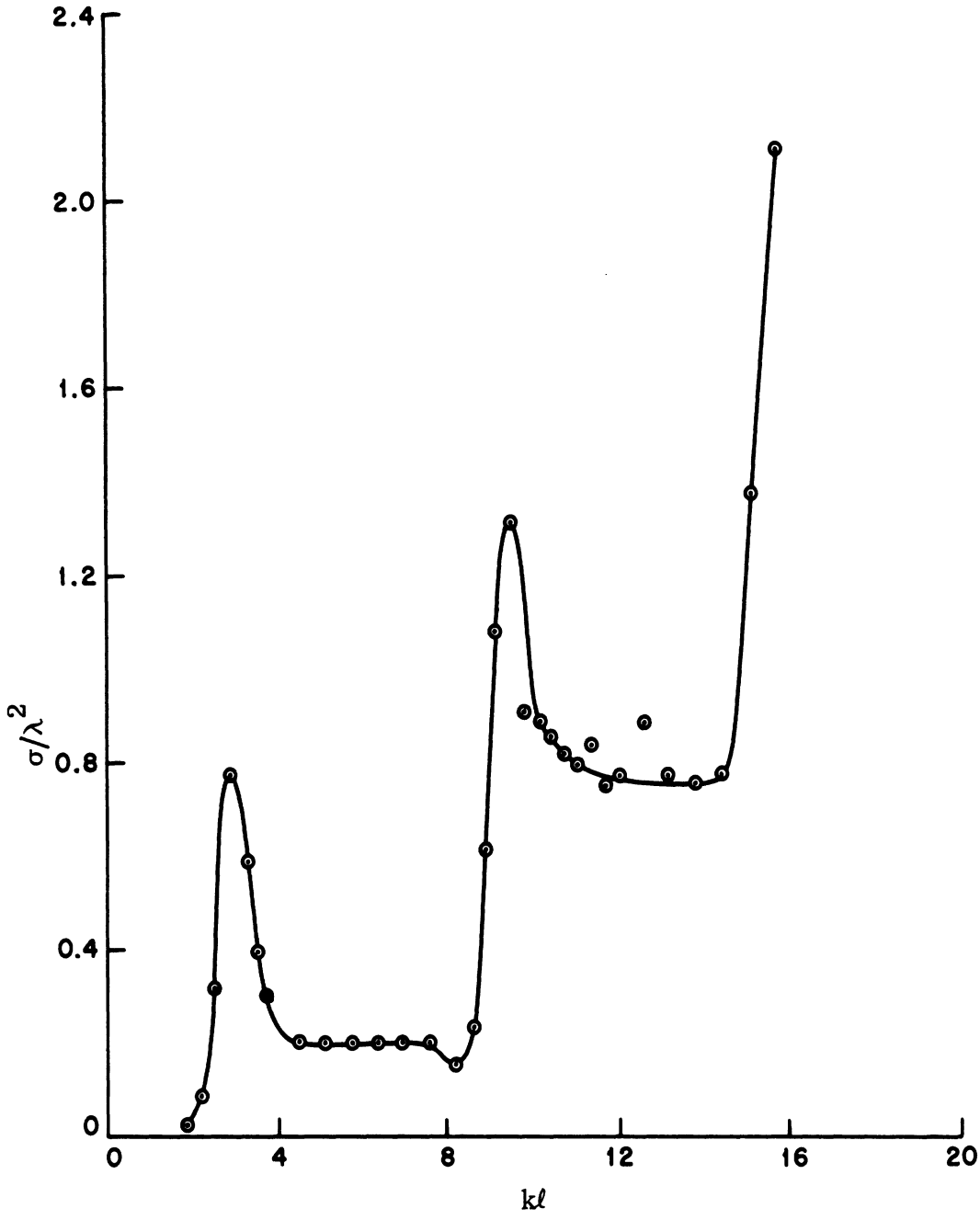

FIG. 6-43: MEASURED BACK SCATTERING CROSS SECTION OF STAINLESS STEEL CYLINDER AT BROADSIDE INCIDENCE; ka = 0.0395 (Liepa and Chang, 1965).

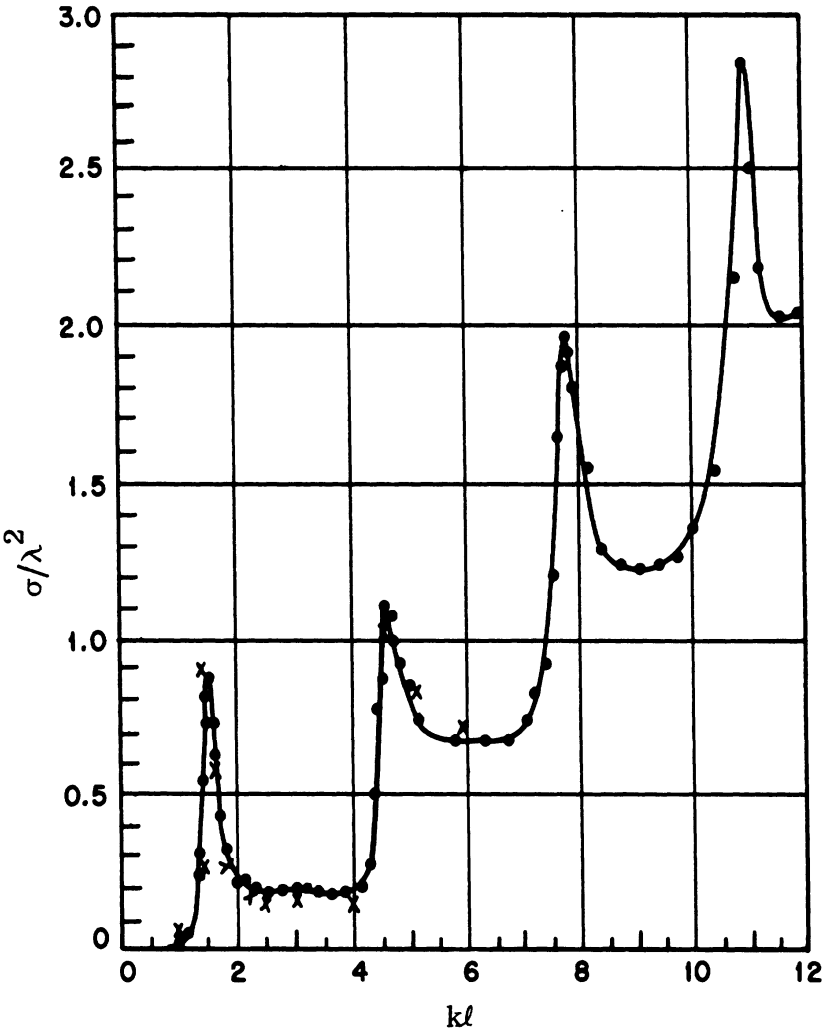

FIG. 6-44: MEASURED BACK SCATTERING CROSS SECTION OF SILVER PLATED STEEL CYLINDER AT BROADSIDE INCIDENCE; ∘ ∘ ∘FOR ka = 0.022 (King and Wu, 1959); × × ×FOR ka = 0.0202 (Liepa, 1964).

REFERENCES

Adey, A.W. (1955) "Diffraction of Microwaves by Long Metal Cylinders," Can. J. Phys., 33, 407-419.

Adey, A.W. (1958) "Scattering of Electromagnetic Waves by Long Cylinders," Electronic and Radio Engineer, 149-158.

Bain, J.D. (1953) "Radiation Pattern Measurements of Stub and Slot Antennas on Spheres and Cylinders," Stanford Research Institute Tech. Rep. No. 42, Stanford, California.

Barakat, R.G. (1961) "Propagation of Acoustic Pulses from a Circular Cylinder," J. Acous. Soc. Am. 33, 1759-1764.

Barakat, R.G. (1965) "Diffraction of a Plane Step Pulse by a Perfectly Conducting Circular Cylinder," J. Opt. Soc. Am. 55, 998-1002.

Bauer, L., P. Tamarkin and R.B. Lindsay (1948) "The Scattering of Ultrasonic Waves in Water by Cylindrical Obstacles," J. Acous. Soc. Am. 20, 858-868.

Beckmann, P. and W. Franz (1957) "Computation of the Scattering Cross Sections of the Sphere and Cylinder by Application of a Modified Watson Transformation," Z. für Naturforschung 12a, 533-537 (in German).

Blacksmith, P., R.E. Hiatt and R.B. Mack (1965) "Introduction to Radar Cross Section Measurements," Proc. IEEE 53, 901-919.

Bouwkamp, C.J. (1946) "A Note on Singularities Occurring at Sharp Edges in Electromagnetic Diffraction Theory," Physica 12, 467-474.

Bouwkamp, C.J. (1954) "Diffraction Theory," Reports on Progress in Physics 17, 35-100.

Bowman, J.J. (1963a) "Scattering of Plane Electromagnetic Waves from a Semi-Infinite Hollow Circular Pipe (Axial Incidence)"Internal Memorandum No. D 0620-125-M41-10, Conductron Corporation, Ann Arbor, Michigan.

Bowman, J.J. (1963b) "Scattering of Plane Electromagnetic Waves from a Semi-Infinite Hollow Circular Pipe (Off-Axis Incidence)"Internal Memorandum No. D 0620-127-M41-13, Conductron Corporation, Ann Arbor, Michigan.

Bowman, J.J. (1963c) "On the Vainshtein Factorization Functions," Internal Memorandum No. D 0620-135-M41-20, Conductron Corporation, Ann Arbor, Michigan.

Bowman, J.J. (1963d) "Far Scattered Fields Due to Thin Semi-Infinite Cones and Cylinders," Internal Memorandum No. D 0620-162-M, P0047-23-M, Conductron Corporation, Ann Arbor, Michigan.

Brick, D.B. (1961) "Current Distributions on Cylinders Excited by Spherical Electromagnetic Waves," IRE Trans. AP-9, 315-317.

Bromwich, T.J. I'A. (1919) "Electromagnetic Waves," Phil. Mag. 38, 143-163.

Brysk, H. (1960) "The Radar Cross Section of a Semi-Infinite Body," Can. J. Phys. 38, 48-56.

Carter, P.S. (1943) "Antenna Arrays Around Cylinders," Proc. IRE 31, 671-693.

Clemmow, P.C. (1959a) "Infinite Integral Transforms in Diffraction Theory," IRE Trans. AP-7, S7-S11.

Clemmow, P.C. (1959b) "On the Theory of the Diffraction of a Plane Wave by a Large Perfectly Conducting Circular Cylinder," The University of Michigan Radiation Laboratory Rep. No. 2778-3-T, Ann Arbor, Michigan.

Cook, R.K. and P. Chrzanowski (1946) "Absorption and Scattering by Sound Absorbent Cylinders," J. Acous. Soc. Am. 17, 315-325.

Debye, P. (1908) "Das elektromagnetische Feld um einen Zylinder und die Theorie des Regenbogens," Physik. Z. 9, 775-778.

Duncan, R.H. and F.A. Hinchey (1960) "Cylindrical Antenna Theory," J. Res. NBS 64D, 569-584.

Faran, J.J. (1951) "Sound Scattering by Solid Cylinders and Spheres," J. Acous. Soc. Am. 23, 405-418.

Faran, J.J. (1953) "Scattering of Cylindrical Waves by a Cylinder," J. Acous. Soc. Am. 25, 155-156.

Fock, V. (1945) "Diffraction of Radio Waves Around the Earth's Surface," J. Phys. USSR 9, 255-266.

Fock, V. (1946) "The Distribution of Currents Induced by a Plane Wave on the Surface of a Conductor," J. Phys. USSR 10, 130-136.

Franz, W. (1954) "On the Green's Functions of the Cylinder and the Sphere," Z. für Naturforschung 9a, 705-716 (in German).

Franz, W. and K. Deppermann (1952) "Theory of Diffraction by a Cylinder as Affected by the Surface Wave," Ann. der Physik 10, 361-373 (in German).

Franz, W. and R. Galle (1955) "Semiasymptotic Series for the Diffraction of a Plane Wave by a Cylinder," Z. für Naturforschung 10a, 374-378 (in German).

Friedlander, F.G. (1954) "Diffraction of Pulses by a Circular Cylinder," Comm. Pure Appl. Math. 7, 705-732

Friedlander, F.G. (1958) Sound Pulses (Cambridge University Press, Cambridge, England).

Giese, R.H. and H. Siedentopf (1962) "Ein Modellversuch zur Bestimmung der Streufunktionen Nicht Kugelförmiger Teilchen mit 3 cm Wellen," Zeit. für Naturforschung 17a, 817-819.

Goodrich, R.F. (1958) "Fock Theory," The University of Michigan Radiation Laboratory Rep. No. 2591-3-T, Ann Arbor, Michigan.

Goodrich, R.F. (1959) "Fock Theory—An Appraisal and Exposition," IRE Trans. AP-7, S28-S36.

Goodrich, R.F., B.A. Harrison, R.E. Kleinman and T.B.A. Senior (1961) "Studies in Radar Cross Sections XLVII - Diffraction and Scattering by Regular Bodies I: The Sphere," The University of Michigan Radiation Laboratory Rep. No. 3648-1-T, Ann Arbor, Michigan.

Goriainov, A.S. (1956) "Diffraction of Plane Electromagnetic Waves on a Conducting Cylinder," Doklady, AN SSSR 109, 477-480 (English translation by M.D. Friedman, ASTIA Document No. AD 110165).

Goriainov, A.S. (1958) "An Asymptotic Solution of the Problem of Diffraction of a Plane Electromagnetic Wave by a Conducting Cylinder," Radio Engr. and Electr. Phys. 3, 23-39 (English translation of Radiotekhnica i Elektronica 3).

Govorun, N.N. (1962) "The Numerical Solution of an Integral Equation of the First Kind for the Current Density in an Antenna Body of Revolution," USSR Computational Math. and Math. Phys. 3, 779-799.

Gray, M.C. (1944) "A Modification of Hallén's Solution of the Antenna Problem," J. Appl. Phys. 15, 61-65.

Grib, A.A. (1955) "On a Particular Solution of the Equations of Plane, Cylindrical and Spherical Waves," Doklady, AN SSSR 102, 225-228.

Hallén, E. (1938) "Theoretical Investigations into the Transmitting and Receiving Qualities of Antennas," Nova Acta Regiae Societatis Scientiarum Upsaliensis, Ser. IV, II, No. 4.

Hallén, E. (1956) "Exact Treatment of Antenna Current Wave Reflection at the End of a Tube-Shaped Cylindrical Antenna," IRE Trans. AP-4, 479-491.

Hallén, E. (1961) "Exact Solution of the Antenna Equation," Trans. Roy. Inst. Techn. 183.

Harrington, R.F. (1961) Time-Harmonic Electromagnetic Fields (McGraw-Hill Book Co., Inc., New York).

Heins, A.E. and S. Silver (1955) "The Edge Conditions and Field Representation Theorems in the Theory of Electromagnetic Diffraction," Proc. Cambridge Phil. Soc. 51, 149-161.

Hochstadt, H. (1959) "Some Diffraction by Convex Bodies," Arch. Rational Mech. Anal. 3, 422-438.

Imai, I. (1954) "The Diffraction of Electromagnetic Waves by a Circular Cylinder," Zeit. Physik 137, 31-48 (in German).

Jones, D.S. (1952) "A Simplifying Technique in the Solution of a Class of Diffraction Problems," Quart. J. Math. 3, 189-196.

Jones, D.S. (1955) "The Scattering of a Scalar Wave by a Semi-Infinite Rod of Circular Cross Section," Phil. Trans. Roy. Soc. London, Ser. A 247 p. 499.

Jones, D.S. (1957) "High-Frequency Scattering of Electromagnetic Waves," Proc. Roy. Soc. 240A, 206-213.

Jones, D.S. and G.B. Whitham (1957) "An Approximate Treatment of High-Frequency Scattering," Proc. Cambridge Phil. Soc. 53, 691-701.

Junger, M.C. (1953) "The Physical Interpretation of the Expression for an Outgoing Wave in Cylindrical Coordinates," J. Acous. Soc. Am. 25, 40-47.

Kapitsa, P.L., V.A. Fok and L.A. Vainshtein (1960) "Symmetric Electric Oscillation of an Ideally Conducting Hollow Cylinder of Finite Length," Soviet Phys. 4, 1089-1105.

Karp, S.N. (1961) "Far Field Amplitudes and Inverse Diffraction Theory," in Electromagnetic Waves, ed. R.E. Langer (University of Wisconsin Press, Madison, Wisconsin) 291-300.

Keller, J.B. (1955) "Diffraction by a Convex Cylinder," IRE Trans. AP-4, 312-321.

Keller, J.B. (1956) "A Geometrical Theory of Diffraction," in Calculus of Variations and Its Applications, ed. L.W. Graves (McGraw-Hill Book Co., Inc., New York, 1958) 27-52.

Keller, J.B., R.M. Lewis and B.D. Seckler (1956) "Asymptotic Solution of Some Diffraction Problems," Comm. Pure Appl. Math. 9, 207-265 .

Kerr, D.E. (1951) Propagation of Short Radio Waves (McGraw-Hill Book Co., Inc., New York).

Kieburtz, R. (1963) "Scattering by a Finite Cylinder," in Electromagnetic Theory and Antennas, ed. E.C. Jordan (Pergamon Press, New York) Part I, 145-156.

Kieburtz, R. (1965) "Construction of Asymptotic Solutions to Scattering Problems in the Fourier Transform Representation," Appl. Sci. Res. 12B, 221-234.

King, R.W.P. (1956) The Theory of Linear Antennas (Harvard University Press, Cambridge, Massachusetts).

King, R.W. P. and D. Middleton (1946) "The Cylindrical Antenna; Current and Impedance," Quart. Appl. Math. 3, 302-335.

King, R.W.P. and T.T. Wu (1957) "The Reflection of Electromagnetic Waves from Surfaces of Complex Shape - II Theoretical Studies," Cruft Laboratory Sci. Rep. 13, Harvard University, Cambridge, Massachusetts.

King, R.W.P. and T.T. Wu (1959) The Scattering and Diffraction of Waves, (Harvard University Press, Cambridge, Massachusetts).

Kleinman, R.E. and T.B.A. Senior (1963) "Studies in Radar Cross Sections XLVII - Diffraction and Scattering by Regular Bodies II: The Cone," The University of Michigan Radiation Laboratory Rep. No. 3648-2-T, Ann Arbor, Michigan.

Kline, M. (1955) "Asymptotic Solutions of Maxwell's Equations Involving Fractional Powers of the Frequency," Comm. Pure Appl. Math. 8, 595-614.

Kodis, R.D. (1950) "An Experimental Investigation on Microwave Diffraction," Cruft Laboratory Tech. Rep. No. 105, Harvard University, Cambridge, Massachusetts.

Kodis, R.D. (1952) "Diffraction Measurements at 1.25 Centimeters," J. Appl. Phys. 23, 249-255.

Kodis, R.D. (1957) "On the Green's Function for a Cylinder," Scientific Rep. No. 1391/8, Brown University, Providence, Rhode Island.

Kodis, R.D. (1958) "Variational Principles in High-Frequency Scattering," Proc. Camb. Phil. Soc. 54, 512-529.

Lamb, H. (1924) Hydrodynamics (Cambridge University Press, Cambridge, England).

Lax, M.(1950) "On a Well-Known Cross-Section Theorem," Phys. Rev. 78, 306-307.

Lax, M. and H. Feshbach (1948) "Absorption and Scattering for Impedance Boundary Conditions on Spheres and Circular Cylinders," J. Acous. Soc. Am. 20, 108-124.

Levine, H. (1965) "Scattering of Surface Waves by a Submerged Circular Cylinder," J. Math. Phys. 6, 1231-1243.

Levine, H. and J. Schwinger (1948) "On the Radiation of Sound from an Unflanged Circular Pipe," Phys. Rev. 73, p. 383.

Levine, H. and J. Schwinger (1950) "On the Theory of Electromagnetic Wave Diffraction by an Aperture in an Infinite Plane Conducting Screen," Comm. Pure Appl. Math. 3, 355-391.

Levis, C.A. (1959) "Patterns of a Radial Dipole on an Infinite Circular Cylinder: Numerical Values," The Ohio State University Antenna Laboratory Rep. No. 667-51, Columbus, Ohio.

Levis, C.A. (1960) "Patterns of a Radial Dipole on an Infinite Circular Cylinder: Numerical Values," IRE Trans. AP-8, 218-222.

Levy, B.R. and J.B. Keller (1959) "Diffraction by a Smooth Object," Comm. Pure Appl. Math. 12, 159-209.

Liepa, V. (1964) The University of Michigan Radiation Laboratory, unpublished data.

Liepa, V. and S. Chang (1965) University of Michigan Radiation Laboratory, unpublished data.

Lindroth, Kristen (1955) "Reflection of Electromagnetic Waves from Thin Metal Strips (Passive Antennas)," Trans. Roy. Inst. Tech. No. 91, Stockholm, Sweden.

Logan, N.A. (1959) "General Research in Diffraction Theory," Vols. 1 and 2, Lockheed Tech. Reps. LMSD-288087/8, Sunnyvale, California (AD 241228 and AD 243182).

Logan, N.A. (1965) "Survey of Some Early Studies of the Scattering of Plane Waves by a Sphere," Proc. IEEE 53, 773-785.

Logan, N.A. and K.S. Yee (1962) "A Mathematical Model for Diffraction by Convex Surfaces," in Electromagnetic Waves, ed. R.E. Langer (University of Wisconsin Press, Madison, Wisconsin) 139-180.

Lowan, A.N., P.M. Morse, H. Feshbach and M. Lax (1946) Scattering and Radiation from Circular Cylinders and Spheres (Tables of Amplitudes and Phase Angles), U.S. Navy Office of Research and Inventions, Washington, D.C.

Lucke, W.S. (1949) "Electric Dipoles in the Presence of Elliptic and Circular Cylinders," Stanford Research Institute Tech. Rep. No. 1, Contract AF 19(122)-78, Stanford, California.

Lucke, W.S. (1951) "Electric Dipoles in the Presence of Elliptic and Circular Cylinders," J. Appl. Phys. 22, 15-19.

Matsui, E. (1960) "On the Free-Field Correction for Laboratory Standard Microphones Mounted on a Semi-Infinite Rod," NBS Rep. No. 7038.

Maue, A.W. (1949) "On the Formulation of a General Diffraction Problem through an Integral Equation," Zeit. f. Phys. 126, 601-618 (in German).

Meixner, J. (1949) "Die Kantenbedingung in der Theorie der Beugung Elektromagnetischer Wellen an Vollkommen Leitenden Ebenen Schirmen," Ann. der Phys. 6, 2-7.

Mentzer, J.R. (1955) Scattering and Diffraction of Radio Waves (Pergamon Press, London and New York).

Meyer, E., H. Kuttruff and H. Severin (1959) "Experimentelle Bestimmung des Radar-Streuquerschnittes Zylindrischer Metallkorper," Zeitschrift für Angewandte Physik 11, 1-6.

Miller, J.C.P. (1946) The Airy Integral, Giving Tables of Solutions of the Differential Equation y'' = xy (Cambridge University Press, Cambridge, England).

Mindlin, I.A. (1946) "Propagation of Waves over the Surface of a Circular Cylinder of Infinite Length," Doklady AN SSSR 52, 107-110.

Mindlin, I.A. (1947) "Mixed Problem of the Wave Equation for the Circle and the Sphere," Doklady AN SSSR 56, 141-144.

Morse, P.M. (1948) Vibration and Sound (McGraw-Hill Book Co., Inc., New York).

Morse, P.M. and H. Feshbach (1946) Methods of Theoretical Physics (MIT Technology Press, Cambridge, Massachusetts).

Morse, P.M. and H. Feshbach (1953) Methods of Theoretical Physics (McGraw-Hill Book Co., Inc., New York).

Moullin, E.B. (1949) Radio Aerials (Oxford University Press, Oxford, England) Chapter 6.

Moullin, E.B. and L.G. Reynolds (1941) "Expression for the Echoing Power of a Cylinder," Admiralty Signal Establishment (Great Britain) Rep. No. M.397.

Neff, H.P., C.E. Hickman and J.D. Tillman (1964) "Circular Arrays Around Cylinders," Sci. Rep. No. 7, Contract AF 19(628)-288, Department of Electrical Engineering, University of Tennessee, Knoxville, Tennessee.

Nicholson, J.W. (1912) "The Pressure of Radiation on a Cylindrical Obstacle," Proc. London Math. Soc. 11, 104-126.

Nisbet, A. (1955) "Hertzian Electromagnetic Potentials and Associated Gauge Transformations," Proc. Roy. Soc. London 231, 250-263.

Noble, B. (1958) The Wiener-Hopf Technique (Pergamon Press, New York).

Noble, B. (1962) "Integral Equation Perturbation Methods in Low-Frequency Diffration," in Electromagnetic Waves, ed. R.E. Langer (University of Wisconsin Press, Madison, Wisconsin) 323-360.

Oberhettinger, F. (1943) "Über ein Radnwetproblem der Wellengleichung in Zylinderkoordinaten," Ann. der Phys. 43, 136-160.

Paley, R.E.A.C. and N. Wiener (1934) "Fourier Transforms in the Complex Domain," Am. Math. Soc. Colloquium Publications XIX.

Panofsky, W.K.H. and M. Phillips (1956) Classical Electricity and Magnetism (Addison-Wesley, Reading, Massachusetts).

Papas, C.H. (1950) "Diffraction by a Cylindrical Obstacle," J. Appl. Phys. 21, 318-325.

Pearson, J.D. (1953) "The Diffraction of Electromagnetic Waves by a Semi-Infinite Circular Wave Guide," Proc. Cambridge Phil. Soc. 49, 659-667.

Riblet, H.J. (1952) "Geometric-Optical Currents," Microwave Development Laboratories Report, Contract AF 19(122)-167, Waltham, Massachusetts.

Ronchi, L., V. Russo, G. Toraldo di Francia, and C. Zaccagnini (1961) "Scattering of Evanescent Waves by Cylindrical Structures," Optica Acta 8, 281-299.

Rubinow, S.I. and J.B. Keller (1961) "Shift of the Shadow Boundary and Scattering Cross Section of an Opaque Object," J. Appl. Phys. 32, 814-820.

Schwinger, J. (1943) MIT Radiation Laboratory Report No. 43-44, Cambridge, Massachusetts.

Seitz, W. (1905) "Die Wirkung eines unendlich langen Metallzylinders auf Hertzsche Wellen," Ann. der Phys. 16, 746-772.

Seitz, W. (1906) "Die Wirkung eines unendlich langen Metallzylinders auf Hertzsche Wellen. II," Ann. der Phys. 19, 554-566.

Senior, T.B.A. (1953) "The Diffraction of a Dipole Field by a Perfectly Conducting Half-Plane," J. Mech. Appl. Math. VI, Pt. 1, 101-113.

Senior, T.B.A. and T. Boynton (1964) "The Back Scattering Cross Section of a Circular Cylinder," The University of Michigan Internal Memorandum No. 6677-507-M, Ann Arbor, Michigan.

Sharples, A. (1962) "An Approximate Method in High-Frequency Scattering," Proc. Cambridge Phil. Soc. 58, Pt. 4, 662-670.

Shenderov, E.L. (1961) "Diffraction of a Cylindrical Sound Wave by a Cylinder," Akusticheskii Zhurnal 7, 370-374 (English translation in Soviet Physics - Acoustics 7, 293-296).

Sinclair, G. (1951) "The Patterns of Antennas Located Near Cylinders of Elliptical Cross Section," Proc. IRE 39, 660-668.

Sinclair, G., E.C. Jordan and E.W. Vaughan (1947) "Measurement of Aircraft-Antenna Patterns Using Models," Proc. IRE 35, 1451-1462.

Sleator, F.B. (1964) "Studies in Radar Cross Sections XLIX - Diffraction and Scattering by Regular Bodies III: The Prolate Spheroid," The University of Michigan Radiation Laboratory Rep. No. 3648-6-T, Ann Arbor, Michigan.

Stöckel, H. (1962) "Herleitung dreidimensionaler Beugunglösungen für Ebene elektromagnetische Wellen aus zweidimensionalen Lösungen," Optik 19, 3-7.

Storer, S.E. (1951) "Solution of Thin Wire Antenna Problems by Variation Methods," Dissertation, Harvard University, Cambridge, Massachusetts.

Stratton, J.A. (1941) Electromagnetic Theory (McGraw-Hill Book Co., Inc., New York).

Streifer, W. (1964) "Creeping Wave Propagation Constants for Impedance Boundary Conditions," IEEE Trans. AP-12, 764-766.

Strutt, J.W., Lord Rayleigh (1881) "On the Electromagnetic Theory of Light," Phil. Mag. 12, 81-101.

Strutt, J.W., Lord Rayleigh (1897) "On the Incidence of Aerial and Electric Waves Upon Small Obstacles in the Form of Ellipsoids or Elliptic Cylinders, and on the Passage of Electric Waves Through a Circular Aperture in a Conducting Screen," Phil. Mag. 44, 28-52.

Strutt, J.W., Lord Rayleigh (1918) "The Dispersal of Light by a Dielectric Cylinder," Phil. Mag. 36, 365-376.

Strutt, J.W., Lord Rayleigh (1945) The Theory of Sound (Dover Publications, New York).

Tai, C-T (1951) "Radar Response from Thin Wires," Stanford Research Institute Tech. Rep. No. 18, Stanford, California.

Tai, C-T (1953) "Some Electromagnetic Problems Involving a Sphere," Stanford Research Institute Tech. Rep. No. 41, Contract AF 19(604)-266, Stanford, California.

Tai, C-T (1954a) "Radiation from Current Elements and Apertures in the Presence of a Perfectly Conducting Plane Sheet," Stanford Research Institute Tech. Rep. No. 45, Contract AF 19(604)-266, Stanford, California.

Tai, C-T (1954b) "A Glossary of Dyadic Green's Functions," Stanford Research Institute Tech. Rep. No. 46, Contract AF 19(604)-266, Stanford, California.

Tai, C-T (1964) private communication.

Thomson, J.J. (1893) Recent Researches in Electricity and Magnetism (Oxford University Press, Oxford, England).

Twersky, V. (1964) "Rayleigh Scattering," Appl. Optics 3, 1150-1162.

Uslenghi, P.L.E. (1964) "High-Frequency Scattering by a Coated Cylinder," Can. J. Phys. 42, 2121-2128.

Van Bladel, J. (1963) "Low-Frequency Scattering by Cylindrical Bodies," Appl. Sci. Res. 10B, 195-202.

Van Bladel, J. (1964) Electromagnetic Fields (McGraw-Hill Book Co., Inc., New York).

van der Waerden, B.L. (1950) "On the Method of Saddle Points," Appl. Sci. Res. 2B, 33-45.

Van Vleck, J.H., F. Bloch and M. Hamermesh (1947) "Theory of Radar Reflection from Wires or Thin Metallic Strips," J. Appl. Phys. 18, 274-294.

Wainstein, L.A. (1948a) "Rigorous Solution of the Problem of an Open-Ended Parallel Plate Waveguide," Izv. Akad. Nauk. Ser. Fiz. 12, 144-165. (See also New York University Report No. EM-63 (1954) for an English translation.)

Wainstein, L.A. (1948b) "On the Theory of Diffraction by Two Parallel Half-Planes," Izv. Akad. Nauk.Ser. Fiz. 12, 166-180. (See also New York University Report No. EM-63.)

Wainstein, L.A. (1948c) "Theory of Symmetric Waves in a Cylindrical Waveguide with an Open End," Zhurnal Tekh. Fiz. 18, 1543-1564. (See also New York University Report No. EM-63))

Wainstein, L.A. (1949) "The Theory of Sound Waves in Open Tubes," Zhurnal Tech. Fiz. 19, 911-930. (See also New York University Report No. EM-63.)

Wainstein, L.A. (1950a) "Radiation of Asymmetric Electromagnetic Waves from the Open End of a Circular Waveguide," Doklady Ak. Nauk 74, 485-488. (See also New York University Report No. EM-63.)

Wainstein, L.A. (1950b) "Diffraction at the Open End of a Circularly Cylindrical Waveguide Whose Diameter is Much Greater than Wavelength," Doklady Ak. Nauk. 74, 909-912. (See also New York University Report No. EM-63.)

Wait, J.R. (1955) "Scattering of a Plane Wave from a Circular Dielectric Cylinder at Oblique Incidence," Can. J. Phys. 33, 189-195.

Wait, J.R. (1959) Electromagnetic Radiation from Cylindrical Structures (Pergamon Press, New York).

Wait, J.R. and K. Okashimo (1956) "Patterns of Stub Antennas on Cylindrical Structures," Can. J. Phys. 34, 190-202.

Watson, G.N. (1922) A Treatise on the Theory of Bessel Functions (Cambridge University Press, Cambridge, England).

Weston, V.H. (1963) "Theory of Absorbers in Scattering," IEEE Trans. AP-11, 578-584.

Wetzel, L. (1957) "High Frequency Current Distributions on Conducting Obstacles," Scientific Rep. No. 10, Cruft Laboratory, Harvard University, Cambridge, Massachusetts.

Wetzel, L. and D.B. Brick (1955) "An Experimental Investigation of High Frequency Current Distributions on Conducting Cylinders," Scientific Rep. No. 4, Harvard University, Cambridge, Massachusetts.

Wiener, F.M. (1947) "Sound Diffraction by Rigid Spheres and Circular Cylinders," J. Acous. Soc. Am. 19, 444-451.

Wiener, N. and E. Hopf (1931) "Über eine Klasse singulärer Integralgleichungen," Sitz. Berlin Akad. Wiss., 696-706.

Wilcox, C. (1955) "The Scattering of Electromagnetic Radiation by a Cylindrical Shell of Finite Length," Doctoral Dissertation, Harvard University, Cambridge, Massachusetts.

Wiles, S.T. and A.B. McLay (1954) "Diffraction of 3.2 cm Electromagnetic Waves by Cylindrical Objects," Can. J. Phys. 32, 372-380.

Williams, W.E. (1956) "Diffraction by a Cylinder of Finite Length," Proc. Cambridge Phil. Soc. 52, Pt. 2, 322-335.

Wu, T.T. (1956a) "High Frequency Scattering," Phys. Rev. 104, 1201-1212.

Wu, T.T. (1956b) "High Frequency Scattering," Technical Rep. No. 232, Cruft Laboratory, Harvard University, Cambridge, Massachusetts.

Wu, T.T. and S.I. Rubinow (1955) "The Correction to Geometrical-Optical Cross Sections of Circular Cylinders and Spheres," Scientific Rep. No. 3, Cruft Laboratory, Harvard University, Cambridge, Massachusetts.

Zanderer, E. (1964) "Wave Propagation Around a Convex Cylinder," J. Math. and Mech. 13, 171-186.

Zitron, N. and J. Davis (1963) "A Numerical Investigation of Scattering of Radiation for an Asymmetric Source by Circular Cylinder," Math. Res. Center Tech. Summary Rep. No. 365, University of Wisconsin, Madison, Wisconsin.